

Geological Controls on the Engineering Properties of Mudrocks of the North Lisbon Area

Filipe Telmo Santos Alcobia Alves Jeremias



Submitted in fulfilment of the
requirements for the degree
of Doctor of Philosophy

Department of Civil and Structural Engineering
University of Sheffield
June 2000

**ALL MISSING
PAGES ARE
BLANK IN THE
ORIGINAL**

IMAGING SERVICES NORTH

Boston Spa, Wetherby

West Yorkshire, LS23 7BQ

www.bl.uk

**CONTAINS
PULLOUT**

**This research project was partially funded by Junta
Nacional de Investigação Científica e Tecnológica**

ACKNOWLEDGEMENTS

I would like to express my gratitude to the Laboratório Nacional de Engenharia Civil, in the person of its Director, Eng. Rui Correia, for all the resources and facilities offered.

I would like to thank particularly to,

Doctor John Cripps, my supervisor, for his support, knowledge of mudrocks imparted, patience during this work and principally the friendship shown during my staying in Sheffield;

Research Officer António Gomes Coelho, for the constant encouragement and help, sharing of knowledge and friendship shown, since I began my career at LNEC;

Research Officer Luís Fialho Rodrigues for the innumerable and fruitful suggestions and advice given to me during the passed twelve years;

JNICT for funding the periods spent at the Sheffield University;

BRISA for having made it possible to use the samples collected during the site investigation works carried out for the Feasibility Study of the motorway A10 Bucelas-Carregado;

Geocontrole for the facilities given to access to the samples used in this work;

LNEC's colleagues Maria João, João Marcelino, Bilé Serra and António Santos Silva, for their help and patience during this work;

Mourice Czerewko for his support, help, assistance and friendship during the periods spent at the University of Sheffield;

All the staff within Site Investigation Division, who have, in one way or another, assisted in this work, particularly Eng. Natércia Silva, Daniel Filipe, Rosado Fernandes, Artur Santos and Catarino Paulo;

The staff of other divisions within LNEC, namely, António Cardoso and Lemos Costa in assisting with the compaction tests, Suzete Lavareda and António Carvalho in

assisting with the organic matter analysis, Paula Melo in assisting with the electron microscope and Luís Nunes in assisting with the mercury porosimetry;

All the staff within the former Department of Earth Sciences for their assistance during the research, especially Dr. R. Soutirou for help with XRD and XRF analysis and Pat Mellor and Paul Higham for helping me in settling down;

Fernando Ribeiro for his patience in working some illustrations and the Editorial staff of LNEC for all their efforts in printing this thesis.

ABSTRACT

The purpose of this work is mainly to contribute towards the characterization of fine-grained sedimentary rocks (mudrocks). The influence of the mineralogical and textural aspects of these rocks on their geotechnical properties is given particular emphasis, so that the performance of these materials, when involved in engineering works, *i.e.* in cut slopes and embankments as a construction material, can be predicted. A wide ranging programme of laboratory characterization of Jurassic mudrocks collected in the Arruda and Óbidos areas (north Lisbon area) was carried out.

The geological and geotechnical classifications usually used to describe and classify mudrocks were reviewed as part of the studies made. It is considered that the distinction between the various lithotypes, that comprise mudrocks, should be based on the grain size and stratification of these materials. A field and laboratory classification is presented, based on the following parameters: strength, colour, stratification thickness, Rock Name, discontinuity spacing, other characteristics (when applicable) and weathering state.

The rocks studied are basically composed of quartz, feldspars (potassium feldspar and plagioclase), carbonates (calcite and dolomite), clay minerals (kaolinite, illite, chlorite, smectite and mixed-layer clays), pyrite and organic material. The microtextural characterization of the rocks was undertaken mainly by using scanning electron microscopy (SEM). The samples are described according to the following features: particle orientation, grain to grain relations, clay fabric and carbonate occurrence mode.

The geotechnical characterization of the mudrocks studied comprised mainly the following properties: swelling, strength and slaking (durability). The results obtained confirm that the performance of these materials is mainly affected by the importance of the total void space (pores and fissures) and by the expandable clay mineral content. It is accordingly found that increased porosity and swelling correspond, in the materials studied, to lower strength and durability characteristics. The compaction and strength characteristics of rock mixtures were also determined. The results reflect the durability and lithological composition of the materials used to make up these mixtures. It was

noted that mixtures formed by rocks with coarser lithological composition (siltstones and sandstones) and with a high slaking durability have higher dry density and strength values.

It was also found, by natural exposure and simulated ageing tests, in addition to the influence of the above mentioned factors on the behaviour of mudrocks, that the presence of carbonate cements has a short term effect on the durability of these materials. Accordingly, rocks with a carbonate content of more than 10% (classified as calcareous) have greater disintegration at the end of a 4 to 6 month test period, while materials with a very low carbonate content have a rapid disintegration rate, so that the weathering of the samples basically occurs during the first two months of the test period. The dissolution of carbonate cements allows greater water access into the materials and can lead to physical disintegration of rocks caused by air compression in voids and micro-discontinuities and clay mineral expansion.

The detailed characterization of mudrocks in order to evaluate their durability in engineering works, involves the use of complex laboratory resources and high costs, which may not be justified in feasibility studies of materials, the aim of that is merely to distinguish between potentially problematic and non-problematic materials. It was therefore sought to evaluate the durability of the materials using index tests that can be determined rapidly and cheaply. The durability index - DI - was proposed for this purpose. Dry density, methylene blue adsorption and the percentage of material retained in the second cycle of the slake durability test were adopted as the parameters of this index, because they evaluate distinct characteristics of the material, *i.e.* the pore space, the content and importance of clay minerals (particularly expandable clay minerals) and slaking susceptibility. The index is calculated from the sum of the ranking coefficients attributed to the classes defined for each of the parameters selected. The results obtained using DI index for the rocks studied, show that it has potential for use in soft mudrocks in order to distinguish between non-durable materials and materials with medium and high durability.

Finally some comments are made on the information obtained in the experimental work carried out on the behaviour of mudrocks in natural and cut slopes and in fills as construction material.

NOTATION

Although the meaning of the symbols and abbreviations used is stated in the text it was considered worthwhile to provide a list of the most important ones.

Symbol Meaning

Å	Ångstrom (10^{-10} m)
AIV	Aggregate impact value
APD	Average pore diameter
c	Cohesion
c'	Effective cohesion
Carb	Carbonate content
CBR	California Bearing Ratio
CCV	Chalk crushing value
CI _(0,23)	Cone indenter number determined for a steel blade deflection of 0.23 mm
CI _(0,635)	Cone indenter number determined for a steel blade deflection of 0.635 mm
C _{uo}	Initial undrained shear strength
d	Lattice spacing
DI	Durability index
DKC	Degree of kaolinite crystallinity
E _{sec}	Secant modulus
E _t	Tangent modulus
F _{CBR(10 mm)}	Force corresponding to a penetration of 10 mm of a CBR plunger
F _{CBR(25 mm)}	Force corresponding to a penetration of 25 mm of a CBR plunger
G _s	Grain specific gravity
I	Intensity
IC	Index of crushing

Symbol Meaning

I_{d1}	Percentage of retained material in slake durability test after 200 rotations
I_{d2}	Percentage of retained material in slake durability test after 400 rotations
I_{d3}	Percentage of retained material in slake durability test after 600 rotations
I_{d5}	Percentage of retained material in slake durability test after 1,000 rotations
I_{d_d}	Percentage of retained material in slake durability test using dry samples
I_{d_s}	Percentage of retained material in slake durability test using soaked samples
I_j	Jar slake index
I_{mf}	Microfracture frequency index
I_s	Soundness index test
I_s	Point load strength
I_{s50}	Point load strength for 50 mm standard-sized specimen
$K\alpha$	Characteristic radiation generated due to the transfer of electrons from L shell into the K shell
L_0	Initial length of the test specimen used in swelling tests
LI	Liquidity index
LL	Liquid limit
LOI	Loss on ignition
MBA	Methylene blue adsorption value
MCV	Moisture condition value
MLC	Mixed-layer clay content
MO	Organic matter content
N	Effective porosity
PI	Plasticity index
PL	Plastic limit
Q+F	Sum of percentages of quartz plus feldspar
r	correlation coefficient
R^2	Goodness-of-fit

Symbol Meaning

RI	Reference intensity
RIR	Reference intensity ratio
RV	Rank values of the DI index
S_u	Undrained shear strength
UCS	Uniaxial compressive strength
TCM	Total clay mineral content
TECM	Total expandable clay mineral content
TNCA	Total non-clay constituents content
w	Water content
w_{ad95}	Water adsorption at 95%RH
w_{opt}	Optimum moisture content
ΔC_u	Undrained shear strength loss during softening
ΔL	Change in length after swelling
ΔV	Volumetric strain
Δw_{96h}	water content increment after soaking during 96 h
ε	Swelling strain
ε_a	Axial strain
ε_s	Swelling strain measured on remoulded specimens
$\varepsilon_{x,y}$	Swelling strain measured on intact specimens parallel to bedding/lamination
ε_z	Swelling strain measured on intact specimens perpendicular to bedding/lamination
ϕ	Angle of friction
ϕ'_p	Peak effective angle of friction
ϕ'_r	Residual effective angle of friction
ϕ'_s	Fully softened effective angle of friction
γ_{dmax}	Maximum dry density
λ	Wavelength of the X-rays

Symbol Meaning

θ	Angle of diffraction
ρ_d	Dry density
σ_a	Axial stress
σ_c	Ultimate compressive strength

Abbreviations

AASHTO	American Association of State Highway and Transportation Officials
ASTM	American Society for Testing and Materials
BEI	Backscattered electron image
BGD	Basical Geotechnical Classification
BS	British Standards
BSE	Backscattered electron mode
EDS	Energy dispersive system
EE	Edge-to-edge association mode
EF	Edge-to-face association mode
FF	Face-to-face association mode
HS	Natural weathering test with treatment of the samples with a acid solution
HT	Ageing test in an environmental chamber with temperature and relative humidity control
IAEG	International Association of Engineering Geology
ISRM	International Society of Rock Mechanics
LNEC	Laboratório Nacional de Engenharia Civil
MRDE	Mining Research Development Establishment
N	Natural exposure test
NCB	National Coal Board

NP	Portuguese standard
PPL	Plane-polarized light
RH	Relative humidity
r.p.m.	Rotations per minute
SC	Ageing test in a salt spray chamber
SE	Secondary electron mode
SEI	Secondary electron image
SEM	Scanning electron microscope(y)
SR	Slaking rate
WDS	Wavelength dispersive system
WR	Whole rock sample (material not subjected to the natural exposure and ageing tests)
XPL	Crossed polars
<i>e.g.</i>	exempli gratia
<i>et al.</i>	et alia
<i>ibid.</i>	ibidem
<i>id.</i>	idem
<i>i.e.</i>	id est
<i>op. cit.</i>	opere citato

CONTENTS

1 - INTRODUCTION	1
2 - DESCRIPTION AND LABORATORY INVESTIGATION OF MUDROCKS	7
2.1 - INTRODUCTION	7
2.2 - GEOLOGICAL CHARACTERIZATION OF MUDROCKS	8
2.2.1 - <i>Terminology and definitions</i>	8
2.2.2 - <i>Mineralogical composition of mudrocks</i>	10
2.2.3 - <i>Textural and structural characterization of mudrocks</i>	14
2.2.4 - <i>Colour</i>	18
2.2.5 - <i>Laboratory Techniques</i>	19
2.3 - COMPACTION AND WEATHERING OF MUDROCK	22
2.4 - GEOTECHNICAL CHARACTERIZATION OF MUDROCKS	24
2.4.1 - <i>Geotechnical properties</i>	24
2.4.2 - <i>Laboratory tests</i>	32
2.4.2.1 - <i>Identification tests</i>	32
2.4.2.2 - <i>Strength tests</i>	35
2.4.2.3 - <i>Swelling tests</i>	40
2.4.2.4 - <i>Durability tests</i>	42
2.4.2.5 - <i>Compaction tests</i>	44
2.5 - SUMMARY	49
3 - MUDROCK CLASSIFICATIONS	51
3.1 - INTRODUCTION	51
3.2 - GEOLOGICAL CLASSIFICATIONS	53
3.2.1 - <i>Geological criteria used for classification of mudrocks</i>	53
3.2.2 - <i>Classifications</i>	55
3.3 - CLASSIFICATIONS OF MUDROCKS FOR ENGINEERING PROPOSES	61
3.3.1 - <i>Engineering definition of mudrock</i>	61
3.3.2 - <i>Classifications</i>	63
3.4 - ENGINEERING GEOLOGICAL MUDROCK DESCRIPTION SCHEME ADOPTED IN THE STUDY	74
3.4.1 - <i>Strength</i>	74
3.4.2 - <i>Colour</i>	75
3.4.3 - <i>Stratification thickness</i>	75
3.4.4 - <i>Rock Name</i>	76
3.4.5 - <i>Discontinuity spacing</i>	77

3.4.6 - <i>Other characteristics</i>	78
3.4.7 - <i>Weathering state</i>	79
3.5 - SUMMARY.....	81
4 - GEOLOGICAL SETTING AND SAMPLING.....	83
4.1 - INTRODUCTION	83
4.2 - GEOLOGICAL SETTING.....	84
4.2.1 - <i>Geological description of the Arruda dos Vinhos area</i>	84
4.2.2 - <i>Geological setting of the man-made slopes in IC1 motorway</i>	87
4.3 - SAMPLING	88
4.3.1 - <i>Methods</i>	88
4.3.2 - <i>Sample descriptions</i>	90
4.3.3 - <i>Preparation of the samples</i>	100
5 - MINERALOGICAL AND TEXTURAL CHARACTERIZATION	103
5.1 - INTRODUCTION	103
5.2 - MINERALOGICAL CHARACTERIZATION	104
5.2.1 - <i>X-ray diffraction: mineral identification and clay mineral and feldspar abundances</i>	104
5.2.1.1 - X-ray diffraction theory.....	105
5.2.1.2 - Preparation of the samples.....	108
5.2.1.3 - Mineral identification	112
5.2.1.4 - Determination of the relative percentage of clay minerals.....	115
5.2.1.5 - Feldspar determination	119
5.2.2 - <i>X-ray fluorescence analysis</i>	122
5.2.2.1 - X-ray fluorescence theory.....	122
5.2.2.2 - Preparation of fused disks.....	122
5.2.2.3 - Determination of bulk rock geochemistry	123
5.2.2.4 - Determination of apatite and rutile	124
5.2.3 - <i>Mineralogical determinations by wet chemical analysis techniques</i>	126
5.2.3.1 - Quartz determination	126
5.2.3.2 - Determination of carbonates - calcite and dolomite.....	129
5.2.3.3 - Determination of pyrite.....	132
5.2.3.4 - Determination of organic matter.....	134
5.2.4 - <i>Discussion of the results determined in mineralogical characterization</i>	136
5.2.4.1 - Errors introduced in the determination of the mineralogical composition of the rocks	136
5.2.4.2 - Calculation of the mineralogical composition of the mudrocks studied	140
5.3 - TEXTURAL CHARACTERIZATION	145
5.3.1 - <i>Experimental techniques used</i>	145
5.3.2 - <i>Study method</i>	148

5.3.3 - <i>Sample descriptions</i>	151
5.4 - FINAL COMMENTS.....	166
6 - GEOTECHNICAL CHARACTERIZATION.....	169
6.1 - INTRODUCTION.....	169
6.2 - IDENTIFICATION TESTS	171
6.2.1 - <i>Grain specific gravity</i>	171
6.2.2 - <i>Dry density</i>	173
6.2.3 - <i>Porosity</i>	175
6.2.4 - <i>Water Adsorption in a controlled-humidity atmosphere</i>	177
6.2.5 - <i>Methylene blue adsorption determined by the spot method</i>	180
6.2.6 - <i>Atterberg limits</i>	182
6.3 - STRENGTH AND DEFORMABILITY.....	185
6.3.1 - <i>Uniaxial compression tests</i>	185
6.3.2 - <i>NCB Cone Indenter tests</i>	189
6.4 - SWELLING.....	192
6.4.1 - <i>Swelling test performed on a radially confined remoulded specimens</i>	192
6.4.2 - <i>Unconfined triaxial free swelling test</i>	194
6.5 - SLAKING.....	197
6.5.1 - <i>Jar slake test</i>	198
6.5.2 - <i>Slake durability test</i>	200
6.6 - COMPACTION OF MIXTURES OF CRUSHED ROCKS.....	204
6.6.1 - <i>Compaction test</i>	204
6.6.2 - <i>Evaluation of the strength of compacted mixtures of crushed rocks to penetration of a 'CBR plunger'</i>	207
6.7 - DISCUSSION OF RESULTS	209
7 - EVALUATION OF DURABILITY: NATURAL EXPOSURE AND SIMULATED AGEING TESTS	229
7.1 - INTRODUCTION.....	229
7.2 - METHODOLOGY AND DESCRIPTION OF THE WEATHERING EXPERIMENTS	230
7.2.1 - <i>Outline of the test methodology</i>	230
7.2.2 - <i>Description of the weathering experiments</i>	232
7.3 - VISUAL, MINERALOGICAL, GEOCHEMICAL AND MECHANICAL MONITORING OF THE ROCK MATERIALS SUBJECTED TO THE WEATHERING EXPERIMENTS	236
7.3.1 - <i>Visual description of the extent of sample slaking</i>	236
7.3.2 - <i>Mineralogical analysis by XRD of the weathered samples</i>	241
7.3.3 - <i>Geochemical analysis of the weathered samples by XRF</i>	254
7.3.4 - <i>NCB cone indenter tests</i>	262
7.4 - DISCUSSION.....	267

8 - GEOLOGICAL CONTROLS ON THE ENGINEERING PROPERTIES OF MUDROCKS...	271
8.1 - INTRODUCTION	271
8.2 - CHARACTERIZATION OF THE VARIOUS LITHOTYPES STUDIED	272
8.2.1 - <i>Assessment of non-indurated materials durability</i>	274
8.2.2 - <i>Assessment of weathered mudrocks durability</i>	274
8.2.3 - <i>Assessment of mudstone durability</i>	275
8.2.4 - <i>Assessment of mudshale durability</i>	279
8.2.5 - <i>Assessment of siltstone and siltshale durability</i>	284
8.3 - CLASSIFICATION OF THE MUDROCKS STUDIED	287
8.4 - APPLICATION OF DURABILITY CLASSIFICATION TO MUDROCK BEHAVIOUR IN NATURAL AND CUT SLOPES	300
8.5 - CHARACTERIZING STUDIED MUDROCKS BEHAVIOUR IN FILLS AS CONSTRUCTION MATERIAL.....	304
9 - CONCLUSIONS AND SUGGESTIONS FOR FUTURE RESEARCH	309
9.1 - GENERAL CONCLUSIONS	309
9.1.1 - <i>Overview</i>	309
9.1.2 - <i>Classification and description of mudrocks</i>	310
9.1.3 - <i>Mineralogical studies</i>	311
9.1.4 - <i>Textural characterization</i>	312
9.1.5 - <i>Geotechnical characterization</i>	313
9.1.6 - <i>Natural exposure and simulated ageing tests</i>	316
9.1.7 - <i>Assessment of mudrock durability</i>	317
9.2 - SUGGESTIONS FOR FUTURE RESEARCH	318
REFERENCES	321
APPENDIX I - MINERALOGY AND GEOCHEMISTRY	341
APPENDIX I.1 - WHOLE ROCK AND LESS THAN 2 MM FRACTION XRD SCANS	343
APPENDIX I.2 - XRF RAW DATA	377
APPENDIX II - GEOTECHNICAL CHARACTERIZATION TESTS	381
APPENDIX II.1 - UNIAXIAL COMPRESSIVE STRENGTH TEST PLOTS	383
APPENDIX II.2 - SWELLING TESTS PLOTS	387
APPENDIX II.3 - RESULTS FOR THE SLAKE DURABILITY TESTS - PARTICLE SIZE DISTRIBUTION PLOTS AND PHOTOGRAPHIC RECORD OF THE FRAGMENTS RETAINED IN THE DRUM	401
APPENDIX II.4 - RESULTS FOR THE COMPACTION TESTS - PARTICLE SIZE DISTRIBUTION AND FORCE-PENETRATION PLOTS	435
APPENDIX III - SLAKING BEHAVIOUR - PHOTOGRAPHIC RECORD OF SAMPLES SUBJECTED TO NATURAL EXPOSURE AND SIMULATED AGEING TESTS	443

LIST OF FIGURES

Fig. 2.1 – Schematic representation of the structure and composition of the main clay minerals (after Taylor & Cripps, 1984).	11
Fig. 2.2 - Schematic representation of the evolution of the fabric of respectively originally flocculated and dispersed textured mudrocks with the depth of burial (after Moon & Hurst, 1983).	15
Fig. 2.3 - Thickness classes of stratification and fissility (adapted from McKee & Weir, 1953; Ingram, 1954; Campbell, 1967; Potter et. al., 1980).	16
Fig. 2.4 - Different types of lamination in mudrock (after Lundegard & Samuels, 1980).	18
Fig. 2.5 - Schematic geological history of an overconsolidated clay or mudrock: (A) compaction and unloading; (B) effect of compaction and unloading on shear strength; (C) variation of horizontal and vertical stresses due to compaction and unloading (after Cripps & Taylor, 1981).	23
Fig. 2.6 - Moisture uptake by clay minerals: (a) intercrystalline absorption of water in a non-expanding lattice; (b) intracrystalline absorption of water in an expanding lattice (after Gillott, 1987).	27
Fig. 2.7 - Model proposed to explain osmotic swelling mechanism between two clay platelets (after Taylor & Smith, 1986).	28
Fig. 2.8 - Plasticity chart.	35
Fig. 2.9 - Relationship between peak, fully softened and residual shear strength of an overconsolidated fissured clay (after Taylor & Spears, 1981).	39
Fig. 2.10 - Equipment used to measure axial swelling stress of an undisturbed radially confined rock specimen (after Jeremias, 1993).	41
Fig. 2.11 - Initial and final aggregate size distributions for New Providence shale (after Hale et al., 1981).	47
Fig. 2.12 - Moisture condition apparatus (after BS 1377: Part 4, 1990).	48
Fig. 2.13 - Relation between change in penetration and number of blows (after BS 1377: Part 4, 1990).	49
Fig. 3.1 - Classification of detrital sedimentary rocks (adapted from IAEG, 1979).	52
Fig. 3.2 - Comparison of the grain size limits defined by the Wentworth (1922), BS 5930 (1981) and ASTM D422 (1998) scales.	54
Fig. 3.3 - Textural classification of sedimentary rocks of sand-silt-clay grain sizes (after Picard, 1971).	57
Fig. 3.4 - Classification of mudrocks proposed by Potter et al. (1980).	59
Fig. 3.5 - Definitions of weak rock according to various standards (adapted de ISRM, 1981; IAEG, 1981 e BS 5930, 1981).	63

Fig. 3.6 - Engineering classification of intact rock showing fields for igneous, sedimentary and metamorphic rocks (after Deere & Miller, 1966).....	65
Fig. 3.7 -Durability-plasticity chart of Gamble (1971).	66
Fig. 3.8 - Classification of mudrocks for embankment construction (after Deo et al., 1974).	67
Fig. 3.9 - Olivier's geodurability classification developed for strong mudrocks and arenaceous types of the Karoo Supergrup (after Olivier, 1976).....	68
Fig. 3.10 - Criterion for evaluating embankment construction on the basis of slaking behaviour of materials (after Lutton, 1977).	69
Fig. 3.11 - Mudrock rating chart (after Franklin, 1981).....	70
Fig. 3.12 - Grainger's (1984) mudrock classification for engineering purposes.....	71
Fig. 3.13 - Proposed abacus for the geotechnical classification of carbonates rocks (after Rodrigues, 1988).	72
Fig. 3.14 - Mudrock durability classification system based on lithological characteristics (after, Dick et al., 1994).	73
Fig. 4.1 - Geological Map at 1/50,000 scale of Arruda dos Vinhos area (based on the sheets 30D - Alenquer and 34B - Loures) with the location of the sampling points.	85
Fig. 4.2 - (A) Upper Jurassic stratigraphy of the Lusitanian Basin in the Arruda and Alcobaça areas (adapted from Fürsich, 1987); (B) Stratigraphic column for the Arruda Area (adapted from Coelho, 1979).	87
Fig. 4.3 - Borehole 34 sampling between 8.00 and 16.40 m depth.	91
Fig. 4.4 - Borehole 44 sampling between 8.50 and 18.30 m depth.	92
Fig. 4.5 - Log of borehole 5 with the description of samples 51 and 52.	93
Fig. 4.6 - Log of borehole 8 with the description of samples 81 and 83.	94
Fig. 4.7 - Log of borehole 11 with the description of samples 111, 112 and 114.	94
Fig. 4.8 - Log of borehole 15 with the description of samples 151, 152, 153, 154 and 156.	95
Fig. 4.9 - log of borehole 16 with the description of samples 162 and 163.	95
Fig. 4.10 - Log of borehole 28 with the description of samples 283, 285 and 286.	96
Fig. 4.11 - Log of borehole 29 with the description of samples 294 and 296.	96
Fig. 4.12 - Log of borehole 33 with the description of samples 332, 333, 334 and 336.	97
Fig. 4.13 - Log of borehole 34 with the description of samples 342 and 345.	97
Fig. 4.14 - Log of borehole 43 with the description of samples 431 and 436.	98
Fig. 4.15 - Geological profile of borehole 44 with the description of samples 441 and 445.	98
Fig. 5.1 - Schematic representation of the geometry of a typical diffractometer (adapted from Hardy & Tucker, 1988).	106

Fig. 5.2 - Geometry of the X-ray diffraction by more than one row of atoms illustrating Bragg's law.....	107
Fig. 5.3 - Filtration apparatus (after Moore & Reynolds, 1989).....	111
Fig. 5.4 - Application of a wet clay film onto a glass substrate (after Moore & Reynolds, 1989).	112
Fig. 5.5 - Flow chart used for clay mineral identification (adapted from Starkey et al., 1984).	113
Fig. 5.6. - Experimental curve deduced by Schultz (1960) for mixtures of various types of kaolinite with equal amounts of the same illite sample in which the degree of kaolinite crystallinity is related to the ratio of the 7 Å/10 Å peak areas.	118
Fig. 5.7 - Flow sheet for the quantitative determination of quartz (after Chapman et al., 1969).....	128
Fig. 5.8 - Flow sheet used for the quantification of pyrite.....	133
Fig. 5.9 - Mineralogical distribution along borehole 11.	141
Fig. 5.10 - Mineralogical distribution along borehole 15.	143
Fig. 5.11 - Mineralogical distribution along borehole 28.	143
Fig. 5.12 - Mineralogical distribution along borehole 33.	144
Fig. 5.13 - Mineralogical distribution along borehole 44.	144
Fig. 5.14 - Schematic diagram of the elements of a SEM. (Sá, 1993).	146
Fig. 5.15 - Schematic diagram of the different types of radiation emitted by the specimen and of the position of the detectors (White et al., 1984).	148
Fig. 5.16 - Non-indurated materials: (A) Photomicrograph of sample 332, XPL; (B) Secondary electron image (SEI) of sample 111 (thin section); (C) Backscattered electron image (BEI) of sample 151, (q) quartz, (fk) K-feldspar, (ca) calcite, (ch) chlorite, (I) illite/mica, (om) organic matter, (py) pyrite; (D) Backscattered electron image (BEI) of sample 111, (q) quartz, (fk) K-feldspar, (p) plagioclase, (I) illite/mica, (om) organic matter.	153
Fig. 5.17 - Sandstone (sample 83); (A) Photomicrograph, PPL; (B) Photomicrograph, XPL, (q) quartz, (p) plagioclase, (m) muscovite, (ca) calcite, (om) organic matter; (C) Secondary electron image (SEI) of a freshly-fractured surface, (q) quartz, (m) muscovite, (cmt) presence of calcite on matrix; (D) Backscattered electron image (BEI), (q) quartz, (fk) K-feldspar, (ca) calcite, (d) dolomite, (I) illite/mica, (om) organic matter, (py) pyrite.....	154
Fig. 5.18 - Siltstones and siltshales: (A) Photomicrograph of sample 163 (siltstone), XPL, (om) organic matter; (B) Photomicrograph of sample OB2 (siltstone), XPL; (C) Photomicrograph of sample 334 (siltshale), XPL, (om) organic matter; (D) Photomicrograph of sample 431 (siltshale), XPL, (om) organic matter.....	156
Fig. 5.19 - Siltstones and siltshales (cont.); (A) Backscattered electron image (BEI) of sample 114 (siltstone), (q) quartz, (ca) calcite, (I) illite/mica, (om) organic matter; (B) Backscattered electron image (BEI) of sample OB2 (siltstone), (q) quartz, (fk) K-feldspar, (p) plagioclase, (ca) calcite, (I) illite/mica, (om) organic matter, (py) pyrite; (C) Backscattered electron image (BEI) of sample 334 (siltshale), (q) quartz, (fk) K-feldspar, (p) plagioclase, (d) dolomite, (I) illite/mica, (k) kaolinite, (ch) chlorite, (om) organic matter; (D) Backscattered electron image (BEI) of sample 431 (siltshale), (q) quartz, (ca) calcite, (I) illite/mica, (om) organic matter.	158

Fig. 5.20 - Mudstones and mudshales; (A) Photomicrograph of sample 286 (mudstone), XPL, (sf) shell fragment, (om) organic matter; (B) Photomicrograph of sample 336 (mudstone), XPL; (C) Photomicrograph of sample 154 (mudshale), PPL, (om) organic matter; (D) Photomicrograph of sample 445 (mudshale), XPL.	160
Fig. 5.21 - Mudstones and mudshales (cont.); (A) Backscattered electron image (BEI) of sample 336 (mudstone), (q) quartz, (fk) K-feldspar, (ca) calcite, (d) dolomite, (I) illite/mica, (ch) chlorite, (om) organic matter; (B) Backscattered electron image (BEI) of sample 436 (mudstone), (q) quartz, (fk) K-feldspar, (ca) calcite, (d) dolomite, (I) illite/mica, (ch) chlorite, (om) organic matter; (C) Backscattered electron image (BEI) of sample 52 (mudshale), (q) quartz, (fk) K-feldspar, (ca) calcite, (I) illite/mica, (py) pyrite; (D) Backscattered electron image (BEI) of sample 154 (mudshale), (q) quartz, (fk) K-feldspar, (p) plagioclase, (ca) calcite, (d) dolomite, (I) illite/mica, (ch) chlorite, (k) kaolinite, (om) organic matter.	161
Fig. 5.22 - Claystone and clayshale; (A) Photomicrograph of sample 294 (claystone), PPL, (om) organic matter; (B) Photomicrograph of sample 152 (clayshale), PPL, (om) organic matter; (C) Secondary electron image (SEI) of a freshly-fractured surface (sample 294); (D) Backscattered electron image (BEI) of sample 152, (q) quartz, (fk) K-feldspar, (ca) calcite, (I) illite/mica, (om) organic matter.	163
Fig. 5.23 - Oolitic limestone (sample 345); (A) Photomicrograph, PPL, (oc) ooid with concentric structure, (or) ooid with radial structure; (B) Photomicrograph, XPL, (plq) polycrystalline quartz with undulose extinction, (m) muscovite, (scc) sparry calcite cement; (C) Secondary electron image (SEI) of a freshly-fractured surface, (fk) K-feldspar, (m) muscovite, (ca) calcite; (D) Backscattered electron image (BEI), (q) quartz, (ca) calcite, (I) illite/mica, (ch) chlorite, (py) pyrite, (om) organic matter.	165
Fig. 6.1 - A comparison of average grain specific gravities of the various samples studied.	173
Fig. 6.2 - A comparison of average dry densities of the various samples studied.	174
Fig. 6.3 - A comparison of average effective porosities of the various samples studied.	177
Fig. 6.4 - A comparison of average water adsorptions of the various samples studied.	179
Fig. 6.5 - Flow sheet used in the determination of the methylene blue adsorption.	181
Fig. 6.6 - A comparison of average methylene blue adsorption values of the various samples studied.	183
Fig. 6.7 - Casagrande's plasticity chart showing composition of the rocks studied with respect to the soil type.	184
Fig. 6.8 - A comparison of average uniaxial compressive strengths of the various samples studied.	186
Fig. 6.9 - Apparatus used to measure axial strains (right hand specimen showing brass gauge points and left hand specimen monitoring frame and gauge).	188
Fig. 6.10 - Diagrammatic illustration of NCB cone indenter (after Stacey et al., 1988).	190
Fig. 6.11 - Relative strength of the rocks studied in terms of cone indenter number (standard procedure).	191
Fig. 6.12 - Diagrammatic illustration of the equipment used to carry out swelling tests on remoulded specimens (after LNEC, 1967d).	193
Fig. 6.13 - A comparison of average swelling strains measured on remoulded specimens of the various samples studied.	194

Fig. 6.14 - Diagrammatic illustration of the equipment used to measure swelling strain in three directions (after ISRM, 1979b).	196
Fig. 6.15 - A comparison of the results obtained for swelling strain as measured in rock specimens perpendicular to bedding/lamination of the various samples studied.	197
Fig. 6.16 - A comparison of the values of I_{42} index of the various samples studied.	203
Fig. 6.17 - A comparison of the values of I_{45} index of the various samples studied.	204
Fig. 6.18 - Apparatus used during the stage of penetration of a 'CBR plunger'	209
Fig. 6.19 - Relationship between uniaxial compressive strength (σ_c) and porosity (N).	211
Fig. 6.20 - Relationship between methylene blue adsorption (MBA) and water adsorption at 95%RH (w_{ad95}).....	212
Fig. 6.21 - Relationship between methylene blue adsorption (MBA) and swelling strain measured on remoulded specimens (ϵ_r).....	213
Fig. 6.22 - Relationship between methylene blue adsorption (MBA) and plasticity index (PI).	213
Fig. 6.23 - Correlation between the cone indenter numbers measured according to the standard ($CI_{(0.635)}$) and soft rock ($CI_{(0.23)}$) versions.	214
Fig. 6.24 - Correlation between uniaxial compressive strength and cone indenter number measured according to the soft rock version ($CI_{(0.23)}$).....	215
Fig. 6.25 - Correlation between uniaxial compressive strength and cone indenter number measured according to the standard version ($CI_{(0.635)}$).	216
Fig. 6.26 - Relationship between swelling strain measured on remoulded specimens and cone indenter number measured according to the soft rock version ($CI_{(0.23)}$).	216
Fig. 6.27 - Relationship between swelling strain measured on remoulded specimens (ϵ_r) and on intact specimens perpendicular to bedding/lamination (ϵ_p).....	218
Fig. 6.28 - Relationship between porosity (N) and swelling strain measured on intact specimens perpendicular to bedding/lamination (ϵ_p).	219
Fig. 6.29 - Relationship between I_j index results and swelling strain measured on intact specimens perpendicular to bedding/lamination (ϵ_p).	220
Fig. 6.30 - Relationship between I_j index results and porosity (N).	220
Fig. 6.31 - Relationship between I_j index results and cone indenter number measured according to the standard version ($CI_{(0.635)}$).	221
Fig. 6.32 - Relationship between the results of I_{42} and I_{45} indexes.....	222
Fig. 6.33 - Relationship between the I_{42} index and cone indenter number measured according to the soft rock version ($CI_{(0.23)}$).	224
Fig. 6.34 - Relationship between I_j and I_{42} indexes.	225
Fig. 7.1 - Schematic representation of the weathering sample test cell design used in the outdoor weathering experiments.	233

Fig. 7.2 -View of the weathering experiments performed outdoors.....	234
Fig. 7.3 - Cycle used in the RH/T ageing process.	234
Fig. 7.4 - Cycle used in the ageing tests conducted in the salt spray chamber.	235
Fig. 7.5 - XRD traces of sample 83 referring to whole rock (WR) and to the materials subjected to natural exposure (N) and simulated ageing tests (HS, HT and SC).....	243
Fig. 7.6 - XRD traces of sample 114 referring to whole rock (WR) and to the materials subjected to natural exposure (N) and simulated ageing tests (HS, HT and SC).....	244
Fig. 7.7 - XRD traces of sample 283 referring to whole rock (WR) and to the materials subjected to natural exposure (N) and simulated ageing tests (HS, HT and SC).....	245
Fig. 7.8 - XRD traces of sample 286 referring to whole rock (WR) and to the materials subjected to natural exposure (N) and simulated ageing tests (HS, HT and SC).....	246
Fig. 7.9 - XRD traces of sample 333 referring to whole rock (WR) and to the materials subjected to natural exposure (N) and simulated ageing tests (HS, HT and SC).....	247
Fig. 7.10 - XRD traces of sample 336 referring to whole rock (WR) and to the materials subjected to natural exposure (N) and simulated ageing tests (HS, HT and SC).....	248
Fig. 7.11 - XRD traces of sample 342 referring to whole rock (WR) and to the materials subjected to natural exposure (N) and simulated ageing tests (HS, HT and SC).....	249
Fig. 7.12 - XRD traces of sample 431 referring to whole rock (WR) and to the materials subjected to natural exposure (N) and simulated ageing tests (HS, HT and SC).....	250
Fig. 7.13 - XRD traces of sample 441 referring to whole rock (WR) and to the materials subjected to natural exposure (N) and simulated ageing tests (HS, HT and SC).....	251
Fig. 7.14 - XRD traces of sample OB2 referring to whole rock (WR) and to the materials subjected to natural exposure (N) and simulated ageing tests (HS, HT and SC).....	252
Fig. 7.15 - Sample 83 weathering experiment XRF data plot.	257
Fig. 7.16 - Sample 114 weathering experiment XRF data plot.	258
Fig. 7.17 - Sample 283 weathering experiment XRF data plot.	258
Fig. 7.18 - Sample 286 weathering experiment XRF data plot.	259
Fig. 7.19 - Sample 333 weathering experiment XRF data plot.	259
Fig. 7.20 - Sample 336 weathering experiment XRF data plot.	260
Fig. 7.21 - Sample 342 weathering experiment XRF data plot.	260
Fig. 7.22 - Sample 431 weathering experiment XRF data plot.	261
Fig. 7.23 - Sample 441 weathering experiment XRF data plot.	261
Fig. 7.24 - Sample OB2 weathering experiment XRF data plot.....	261
Fig. 7.25 - Comparison of the cone indenter test results determined for sandstone and siltstone samples.	264

Fig. 7.26 - Comparison of the cone indenter test results determined for mudstone samples.....	265
Fig. 8.1 - Plot of I_{d2} versus Carb (%). Fig. 8.2 - Plot of I_{d2} versus w_{ad95}	277
Fig. 8.3 - Plot of I_{d5} versus TECM (%). Fig. 8.4 - Plot of I_{d5} versus MBA.....	277
Fig. 8.5 - Plot of I_{d5} versus PI. Fig. 8.6 - Plot of I_j versus Carb (%)......	277
Fig. 8.7 - Plot of I_j versus TCM (%). Fig. 8.8 - Plot of I_j versus ρ_d	277
Fig. 8.9 - Plot of I_j versus w_{ad95} . Fig. 8.10 - Plot of I_j versus $CI_{(0.635)}$	278
Fig. 8.11 - Plot of $CI_{(0.23)}$ versus TECM (%). Fig. 8.12 - Plot of $CI_{(0.23)}$ versus ρ_d	278
Fig. 8.13 - Plot of $CI_{(0.23)}$ versus N. Fig. 8.14 - Plot of $CI_{(0.23)}$ versus MBA.....	278
Fig. 8.15 - Plot of $CI_{(0.23)}$ versus PI. Fig. 8.16 - Plot of $CI_{(0.635)}$ versus w_{ad95}	278
Fig. 8.17 - Plot of I_{d2} versus TECM (%). Fig. 8.18 - Plot of I_{d2} versus ρ_d	281
Fig. 8.19 - Plot of I_{d2} versus N. Fig. 8.20 - Plot of I_{d2} versus MBA.....	281
Fig. 8.21 - Plot of I_{d5} versus Q+F (%). Fig. 8.22 - Plot of I_{d5} versus $CI_{(0.635)}$	281
Fig. 8.23 - Plot of I_j versus Q+F (%). Fig. 8.24 - Plot of I_j versus TECM (%).	281
Fig. 8.25 - Plot of I_j versus ρ_d . Fig. 8.26 - Plot of I_j versus N.....	282
Fig. 8.27 - Plot of I_j versus w_{ad95} . Fig. 8.28 - Plot of I_j versus MBA.....	282
Fig. 8.29 - Plot of I_j versus PI. Fig. 8.30 - Plot of ϵ_s versus TECM (%).....	282
Fig. 8.31 - Plot of $CI_{(0.635)}$ versus ρ_d . Fig. 8.32 - Plot of $CI_{(0.635)}$ versus N.....	282
Fig. 8.33 - Plot of I_{d5} versus ϵ_r . Fig. 8.34 - Plot of I_j versus w_{ad95}	286
Fig. 8.35 - Plot of I_j versus $CI_{(0.635)}$. Fig. 8.36 - Plot of ϵ_s versus MBA.....	286
Fig. 8.37 - Plot of σ_c versus N. Fig. 8.38 - Plot of $CI_{(0.23)}$ versus ρ_d	286
Fig. 8.39 - Plot of $CI_{(0.635)}$ versus Q+F (%). Fig. 8.40 - Plot of $CI_{(0.635)}$ versus w_{ad95}	286
Fig. 8.41 - Relationship between porosity and dry density.....	290
Fig. 8.42 - Relationship between the expansive clay minerals content and the methylene blue adsorption value.....	293
Fig. 8.43 - Classification of the samples studied using the durability-plasticity chart of Gamble (1971).....	296
Fig. 8.44 - Typical grain size distributions and materials structure for soil, soil and rockfill mixture and rockfill (after Maranha das Neves, 1993).....	304
Fig. 8.45 - Criteria for evaluating embankment construction based on mudrock durability classes defined for I_{d2} values (adapted from Lutton, 1977).....	306

Fig. AIII.1 - Natural exposure test (N): (A) initial breakdown state of sample 83; (B) final breakdown state of sample 83; (C) initial breakdown state of sample 114; (D) final breakdown state of sample 114.	445
Fig. AIII.2 - Natural exposure test (N): (A) initial breakdown state of sample 283; (B) final breakdown state of sample 283; (C) initial breakdown state of sample 286; (D) final breakdown state of sample 286.	446
Fig. AIII.3 - Natural exposure test (N): (A) initial breakdown state of sample 333; (B) final breakdown state of sample 333; (C) initial breakdown state of sample 336; (D) final breakdown state of sample 336.	447
Fig. AIII.4 - Natural exposure test (N): (A) initial breakdown state of sample 342; (B) final breakdown state of sample 342; (C) initial breakdown state of sample 431; (D) final breakdown state of sample 431.	448
Fig. AIII.5 - Natural exposure test (N): (A) initial breakdown state of sample 441; (B) final breakdown state of sample 441; (C) initial breakdown state of sample OB2; (D) final breakdown state of sample OB2.	449
Fig. AIII.6 - Simulated ageing test with treatment of the samples with a acid solution (HS): (A) initial breakdown state of sample 83; (B) final breakdown state of sample 83; (C) initial breakdown state of sample 114; (D) final breakdown state of sample 114.	450
Fig. AIII.7 - Simulated ageing test with treatment of the samples with a acid solution (HS): (A) initial breakdown state of sample 283; (B) final breakdown state of sample 283; (C) initial breakdown state of sample 286; (D) final breakdown state of sample 286.	451
Fig. AIII.8 - Simulated ageing test with treatment of the samples with a acid solution (HS): (A) initial breakdown state of sample 333; (B) final breakdown state of sample 333; (C) initial breakdown state of sample 336; (D) final breakdown state of sample 336.	452
Fig. AIII.9 - Simulated ageing test with treatment of the samples with a acid solution (HS): (A) initial breakdown state of sample 342; (B) final breakdown state of sample 342; (C) initial breakdown state of sample 431; (D) final breakdown state of sample 431.	453
Fig. AIII.10 - Simulated ageing test with treatment of the samples with a acid solution (HS): (A) initial breakdown state of sample 441; (B) final breakdown state of sample 441; (C) initial breakdown state of sample OB2; (D) final breakdown state of sample OB2.	454
Fig. AIII.11 - Simulated ageing in an environmental chamber (HT): (A) initial breakdown state of sample 83; (B) final breakdown state of sample 83; (C) initial breakdown state of sample 114; (D) final breakdown state of sample 114.	455
Fig. AIII.12 - Simulated ageing in an environmental chamber (HT): (A) initial breakdown state of sample 283; (B) final breakdown state of sample 283; (C) initial breakdown state of sample 286; (D) final breakdown state of sample 286.	456
Fig. AIII.13 - Simulated ageing test in an environmental chamber (HT): (A) initial breakdown state of sample 333; (B) final breakdown state of sample 333; (C) initial breakdown state of sample 336; (D) final breakdown state of sample 336.	457
Fig. AIII.14 - Simulated ageing test in an environmental chamber (HT): (A) initial breakdown state of sample 342; (B) final breakdown state of sample 342; (C) initial breakdown state of sample 431; (D) final breakdown state of sample 431.	458

Fig. AIII.15 - Simulated ageing test in an environmental chamber (HT): (A) initial breakdown state of sample 441; (B) final breakdown state of sample 441; (C) initial breakdown state of sample OB2; (D) final breakdown state of sample OB2.....	459
Fig. AIII.16 - Simulated ageing test in a salt spray chamber (SC): (A) initial breakdown state of sample 83; (B) final breakdown state of sample 83; (C) initial breakdown state of sample 114; (D) final breakdown state of sample 114.	460
Fig. AIII.17 - Simulated ageing test in a salt spray chamber (SC): (A) initial breakdown state of sample 283; (B) final breakdown state of sample 283; (C) initial breakdown state of sample 286; (D) final breakdown state of sample 286.	461
Fig. AIII.18 - Simulated ageing test in a salt spray chamber (SC): (A) initial breakdown state of sample 333; (B) final breakdown state of sample 333; (C) initial breakdown state of sample 336; (D) final breakdown state of sample 336.	462
Fig. AIII.19 - Simulated ageing test in a salt spray chamber (SC): (A) initial breakdown state of sample 342; (B) final breakdown state of sample 342; (C) initial breakdown state of sample 431; (D) final breakdown state of sample 431.	463
Fig. AIII.20 - Simulated ageing test in a salt spray chamber (SC): (A) initial breakdown state of sample 441; (B) final breakdown state of sample 441; (C) initial breakdown state of sample OB2; (D) final breakdown state of sample OB2.	464

LIST OF TABLES

Table 2.1 - The terminology adopted to describe fine-grained detrital sedimentary rocks.....	9
Table 2.2 - Average mineral composition of mudrocks.....	10
Table 2.3 - Classification of plasticity in terms of liquid limit and plasticity index (adapted from IAEG, 1981).....	34
Table 2.4 - Variables investigated in slake-durability testing procedures.	43
Table 3.1 - Classifications of fine-grained sedimentary rocks containing more than 50% grains less than 63 μm (silt and/or clay) suggested by Ingram (1953), Folk (1968) Blatt et al. (1980) and Stow (1981).....	58
Table 3.2 - Mudrock classification based on quartz percentage (after Spears, 1980).....	60
Table 3.3 - Classification of fine-grained rocks based on proportion of phyllosilicates (after Weaver, 1980; 1989).....	61
Table 3.4 - Soil and rock characteristics used in engineering geological classifications of mudrocks.....	64
Table 3.5 - Classification adopted to evaluate rock strength based on UCS values and/or on field criteria.	75
Table 3.6 - Classification adopted to bedding and lamination thickness.	76
Table 3.7 - Classification adopted to the fine-grained rocks of the north Lisbon area.	77
Table 3.8 - Classification adopted to describe discontinuity spacing.	78
Table 3.9 - Classification adopted to describe fissility.	79
Table 3.10 - Classification adopted to describe weathering state.	80
Table 4.1 - Classification and sampling depth.	93
Table 4.2 - Distribution of the samples collected according to the rock types identified.	99
Table 5.1 - Relative proportions of clay minerals identified in the samples and the factors used to recalculate them.	119
Table 5.2 - Recalculated geochemical composition of the mudrocks studied.	125
Table 5.3 - Quartz percentages of the mudrock samples determined by the method proposed by Chapman et al. (1965).....	129
Table 5.4 - Percentages of CO_2 , calcite and dolomite present in the rocks studied.	131
Table 5.5 - Results of pyrite determinations.	134
Table 5.6 - Results of organic matter content determinations.....	136
Table 5.7 - Coefficients of variation calculated for the results of wet geochemical determinations.	139

Table 5.8 - Mineralogical composition of the mudrocks studied	142
Table 5.9 - Description of the microtextural features observed in the rocks studied.	150
Table 5.10 - Microtextural characteristics of the rocks studied.....	151
Table 6.1 - Results (average values) of the identification tests and soil classification of the samples studied.....	172
Table 6.2 - Strength parameters and secant modulus of the samples studied.....	187
Table 6.3 - Swelling tests results.	195
Table 6.4 - Jar slake classification.....	199
Table 6.5 - Jar slake test results.....	200
Table 6.6 - Descriptive scheme of the material retained in drum mesh during the slake durability test.....	201
Table 6.7 - Results of slake durability test and mudrock durability classification.	202
Table 6.8 - Samples used to make the mixtures tested.	206
Table 6.9 - Results of the compaction tests and of CBR plunger penetration tests.	207
Table 7.1 - Geological characteristics of the samples used in the weathering experiments.	230
Table 7.2 - Weathering sample descriptions using the jar slake classification scheme.	237
Table 7.3 - Recalculated geochemical composition of whole rock samples (WR) and of weathered materials (N, HS, HT and SC).	256
Table 7.4 - Cone indenter test results for the 'original' rock and for the tested materials (N; HS; HT and SC).....	263
Table 7.5 - Selected mineralogical and physical characteristics of the materials subjected to the weathering experiments.	268
Table 8.1 - Correlation coefficient matrix between the main mineralogical, physical and geotechnical parameters determined for mudstones.	276
Table 8.2 - Correlation coefficient matrix between the main mineralogical, physical and geotechnical parameters determined for mudshales.	280
Table 8.3 - Correlation coefficient matrix between the main mineralogical, physical and geotechnical parameters determined for siltstones and siltshales.	285
Table 8.4 - Intervals of values adopted for each index test selected as classification parameter and corresponding rank values.	294
Table 8.5 - Determination of the DI index for sample 431.	294
Table 8.6 - Classification of the samples according to the DI index proposed and the corresponding durability classes.....	295
Table 8.7 - Comparison of the durability classes adopted for the samples studied, applying various classification schemes.....	297

Table 8.8 - Czerewko mudrock's data and comparison of the durability classes adopted for the samples applying the DI index and the Czerewko's classification.	299
Table 8.9 - Types of slope instability which according to mudrock durability are more probable to occur (adapted from Dick & Shakoor, 1995).....	301

1 - INTRODUCTION

The objective of this thesis is to contribute towards the study and characterization of mudrocks, particularly with regard to the influence geological controls have on their engineering properties. Special emphasis has been given to the mineralogical, geochemical and structural aspects of these rocks in the study of their engineering properties.

Research on properties of mudrocks commenced in the United Kingdom in the nineteen-fifties on the initiative of the coal industry because of problems associated with the variable slaking properties of these rocks in the coal washing process (Taylor, 1988). The research carried out improved the understanding of the breakdown behaviour of mudrocks in water. Particularly worthy of mention are the works of Badger *et al.* (1956) and Berkovitch *et al.* (1959). Subsequent studies centred on the evaluation of slaking of mudrocks leading to the development of specific tests, such as the 'slake durability test' (Franklin & Chandra, 1972), and geotechnical classifications (Gamble, 1971; Deo *et al.*, 1974; Morgenstern & Eigenbrod, 1974; Olivier, 1976; Deen, 1981; Franklin, 1981; Taylor, 1988). At the same time, the research in this area led to the elaboration of recommendations for testing (ISSMFE, 1993) and to describe these materials for engineering purposes (Taylor & Spears, 1981; Grainger, 1984; Hawkins & Pinches, 1992; Spink, & Norbury, 1993).

In addition, specific studies were performed particularly in the USA, on the suitability of mudrocks in embankments as a construction material (Deo *et al.*, 1974; Shamburger

et al., 1975; Lutton, 1977; Strohm *et al.*, 1978; Hale *et al.*, 1981) and on the behaviour of these rocks in slopes in which the works of Skempton (1964), Chandler & Skempton (1974), Taylor & Cripps (1987), Shakoor & Webster (1988) and Dick & Shakoor (1995) merit mention.

The engineering properties of mudrocks including durability, are related to their composition, geological history and degree of weathering (Cripps & Taylor, 1981; Shakoor & Brock, 1987). The influence of these aspects on the breakdown behaviour of mudrocks has been investigated by various authors who based their studies on specific formations (Spears & Taylor, 1972; Chandler, 1974; Seedsman, 1980; Russel, 1982; Steward & Cripps, 1983; Okagbue, 1984; Taylor, 1988; Campbell, 1993; Bell *et al.*, 1997, Venter, 1998) and on a suite of mudrocks of different geological ages and geographical localities (Gamble, 1971; Dick & Shakoor, 1992). The results of these studies demonstrated that the main processes involved in the breakdown of mudrocks are due to the stress relief of the geological materials, to physical disintegration and mineralogical effects on contact with water and to chemical weathering involving pyrite breakdown. These studies also showed that the development of the above mentioned processes is influenced by diagenetic bonds, by the presence of sedimentary structures, tectonic discontinuities, fabric and composition (mainly of the content of expansive clay minerals) of mudrocks.

Existing experience with mudrocks indicates that in many cases, they are subject to rapid degradation in engineering timescales in response to environmental changes both during and after the construction of civil engineering works. This usually involves the modification of the geotechnical parameters, such as strength and deformability, determined for design purposes. The degradation of engineering properties of mudrocks has, in many cases, led to numerous costly failures of structures requiring expenditure on re-construction and/or maintenance and costly additional unanticipated works during construction. Depending on the situation, problems can arise even where mudrocks constitute only a minor part of a formation. In some cases ignorance about the engineering behaviour of these materials gives rise to a tendency to use conservative design parameters, involving extra costs, which are unjustified where the materials do not display problematic forms of behaviour.

This work is intended to contribute to the existing body of research on the engineering properties of mudrocks. In its existing methods of predicting mudrock behaviour are extended to a class of soft mudrocks characterized by high porosity values and high carbonate content taking into account the climatic conditions prevailing in the north Lisbon area. It is also intended to compare the results obtained in this work with those from other studies in order to refine existing correlations for finding news. Another point addressed in this work is the assessment of the suitability of the mudrocks studied for use as construction materials in infrastructure projects. Particular attention has been given to their performance as fills as evaluated on the basis of compaction characteristics and slopes as indicated by their breakdown performance. Finally, a further aim of this study is to provide a systematic approach to identifying potentially problematic mudrock materials by means of a classification based on the results of simple index tests suitable for use at the reconnaissance phase of site exploration.

The road network improvements currently at the design and construction phase in Portugal involve construction in large areas occupied by mudrock formations or formations containing mudrocks. Thus, there are a great number of cases in which these materials will be cut through in man-made slopes and used in the construction of road embankments. Given the small number of studies carried out in Portugal on the engineering behaviour of mudrocks, this work aims at making a contribution to improving knowledge of the engineering properties of these materials, particularly in connection with the two types of engineering works mentioned above.

The characterization of mudrocks was carried out on samples collected from formations of the western cenozoic border of Portugal and were obtained from boreholes and blocks collected from cut slopes. The samples collected were selected to provide a range of materials (cemented and compacted, shaly and massive) and were subjected to an extensive laboratory programme, which enabled them to be characterized from a mineralogical, geochemical, microtextural and geotechnical point of view. A field and laboratory classification of mudrocks is presented within the ambit of the research performed. The main geological controls, which influence the behaviour of these materials, were identified on the basis of the laboratory characterization carried out. The durability of these materials was evaluated in terms of a durability index devised for this

purpose. This index was based on the results obtained from the slake durability tests, and methylene blue adsorption and dry density values.

In the light of the above, this thesis goes beyond this introduction, in which reasons for the study are explained, to define its fundamental objectives, sampling, laboratory work and data analysis. It does this in nine chapters.

In the second and third Chapters, the question of the nomenclature of the terminology used to classify fine-grained sedimentary rocks is covered and the main geological and geotechnical characteristics of mudrocks are described, together with a succinct description of the laboratory techniques necessary to determine them. The geological and geotechnical classifications of mudrocks are reviewed in the third Chapter, which also presents the classification scheme developed to describe the sampled materials.

The laboratory study carried out on the mudrocks collected in the north Lisbon area is presented in the, fourth, fifth, sixth and seventh Chapters. The first of these chapters concerns the regional geological setting of the sites from which the samples were taken, describes the materials collected on the basis of the classification proposed and the procedures carried out to prepare the samples for the various tests performed.

The fifth Chapter describes the laboratory techniques used in the mineralogical characterization of the sampled rocks. The mineralogical composition of the various samples collected is determined on the basis of the results obtained from XRD, XRF and wet chemical analyses. This chapter also presents the studies of the microtextural characterization of the samples by optical- and scanning electron- microscopy. A classification scheme is proposed to describe the various microtextural aspects of mudrocks.

The sixth Chapter describes the tests carried out to characterize the materials from a geotechnical point of view. The properties determined include the density, plasticity, strength, swelling, durability and compaction characteristics of the sampled rocks. Finally, the results are analysed and discussed to see which index tests are most suited to the characterization of mudrocks.

The seventh Chapter evaluates the durability of some of the mudrocks studied upon the basis of natural exposure and simulated ageing tests. The methodology used to monitor the materials in order to investigate the mineralogical, geochemical and mechanical modifications of these rocks after these tests is also presented.

The eighth Chapter discusses with reference to the behaviour and geological character of other mudrock formations the geological controls that influence the engineering behaviour of mudrocks, on the basis of the laboratory testing carried out and identifies the most suitable parameters and index tests to be used in the classification of these materials. An index for the evaluation of mudrock durability is proposed and some comments are made on the behaviour of these rocks in natural- and cut-slopes and in embankments as construction material.

The ninth and final Chapter critically reviews the work as a whole, identifying the objectives attained and some future lines of study.

2 - DESCRIPTION AND LABORATORY INVESTIGATION OF MUDROCKS

2.1 - Introduction

Mudrocks constitute more than 60% of all sedimentary rocks (Potter *et al.*, 1980), but have, however, been studied less than other types of sedimentary rocks, such as sandstones or limestones (Picard, 1971). According to Picard (1971), Taylor & Spears (1981) and Tucker (1994) this is above all because mudrocks occur in superficially weathered outcrops and have fine grain size and complex composition which require detailed laboratory analyses if they are to be studied.

As a result of their wide distribution mudrocks are often encountered in engineering projects, either as construction materials, *e.g.* embankments, or in their natural undisturbed state, *e.g.* foundations, cut slopes, and underground excavations. However mudrocks are considered as problematic materials mainly due to their high clay content and poor induration state which can lead to great susceptibility to rapid degradation. This has resulted in many cases in which mudrocks have been associated with syn- and post-constructional failure in such engineering situations. Thus, the assessment of the geological and geotechnical properties which control mudrock behaviour is an essential task in engineering construction involving this type of rock.

The purpose of this chapter is therefore to characterize mudrock as a geological material, describe difficulties and features specific to these rocks, and methods of

investigation.

In this chapter the terminology used to classify fine-grained sedimentary rocks is reviewed and the main geological and the geotechnical characteristics of mudrocks and the laboratory tests necessary to determine them are also described. Geological characterization includes the mineralogical, textural and structural composition and colour, observed in mudrock. Various geotechnical properties can be used to characterize these materials, of which the most relevant are plasticity, strength/deformability, swelling and durability/slaking behaviour.

2.2 - Geological characterization of mudrocks

2.2.1 - Terminology and definitions

The classification and definition of the terms related to fine-grained sedimentary rocks have always given rise to confusion in the technical literature (Potter *et al.*, 1980). As explained in Chapter 3, the geological and geotechnical classifications used for the fine-grained sedimentary rocks are complicated by the use of differing definitions used for the same terms by soil scientists, geologists, engineering and other specialists. In addition different practices are followed in the USA, the UK and others countries. However, as the geological characteristics of mudrock are described in this chapter, it is appropriate to include this section which sets out the terminology used for these rocks in this work. This is summarised in Table 2.1 which shows a set of terms which it is argued below allows the materials studied to be described clearly and unambiguously.

Tourtlot (1960) concluded on an historical basis that the term *shale* is the general class name for fine-grained sedimentary rocks. However, because *shale* can also designate a laminated rock there is some misuse of this term. The double significance of this term and the confusion that arises from it, led to the proposal by Ingram (1954) that *mudrock* be used as an alternative term to designate that class of fine-grained rocks. This was adopted by Dunbar & Rogers (1957) and Blatt *et al.* (1980), who attributed to it a significance similar to the term sandstone and limestone.

In his review of the terminology of fine-grained sedimentary rocks Stow (1981) defines mudrocks as a rock in which more than 50% of the grains are siliciclastic composition and smaller than 63 μm (silt and/or clay). The term siliciclastic means formed out of silicate minerals and clastic granular material, and is applied to detrital grains that are mainly constituted of clay minerals and quartz.

Weaver (1989) concluded that the use of the term clay in both its textural and mineralogical meanings, was the main problem affecting the then current classifications of fine-grained sedimentary rocks. In order to overcome this problem, he proposed a new term, *physil* (Weaver, 1980) that includes all the phyllosilicates but has no dimensional significance. Accordingly, the term clay should be used only to describe particles finer than 2 μm and the term claystone should be used with the same textural significance, as that is, for example, attributed to the term sandstone.

Table 2.1 - The terminology adopted to describe fine-grained detrital sedimentary rocks.

Term	Significance
Sand	Material between 0.06 and 2 mm in diameter.
Mud	Material smaller than 0.06 mm (silt and clay mixture).
Silt	Material between 0.002 and 0.06 mm in diameter.
Clay	Material finer than 0.002 mm.
Mudrock	A general term for the class of fine-grained sedimentary rock that contains at least 50% of siliciclastic grains finer than 0.06 mm.
Siltstone	Indurated rock comprised of more than $\frac{2}{3}$ of silt-sized particles.
Mudstone	Indurated rock containing between $\frac{2}{3}$ to $\frac{1}{2}$ of silt-sized particles.
Claystone	Indurated rock comprised of more than $\frac{1}{2}$ of clay-sized particles.
Argillite	Weakly metamorphosed rock, firmly indurated without slaty cleavage.
Slate	Fine-grained metamorphic rock with slaty cleavage.
-Stone	Suffix applied when rock has a layering greater than 1 cm (siltstone, mudstone and claystone).
-Shale	Suffix applied when rock has a layering less than 1 cm (siltshale, mudshale and clayshale).
Sandy	Applies when rock is formed by more than 10% of sand sized particles.
Calcareous	Applies when rock contains between 10 and 50% of carbonate.
Fissility	Property of splitting or dividing into thin fragments along closely spaced (< 1 cm) planes parallel to the bedding or lamination.

2.2.2 - Mineralogical composition of mudrocks

The average mineral composition of mudrocks has been determined by several researchers in past decades in order to establish an *ideal* composition representative of all types of mudrocks. Table 2.2 presents some commonly quoted average compositions for mudrocks.

Table 2.2 -Average mineral composition of mudrocks.

	Yaalon (1962)	Shaw & Weaver (1965)	Pettijohn (1975)	Taylor & Smith (1986) UK*	USA*	Taylor (1988)*
Clay minerals	59	60.9	58	73	60	77
Quartz	20	30.8	28	20	32	19.5
Feldspar	8	4.5	6	1	3	0.5
Carbonates	7	3.6	5	4	3	1
Iron oxides	3	<0.5	2	-	-	1
Organic matter	-	1	-	1	1	2.3
Other minerals	3	<2.0	-	2	0	0.5

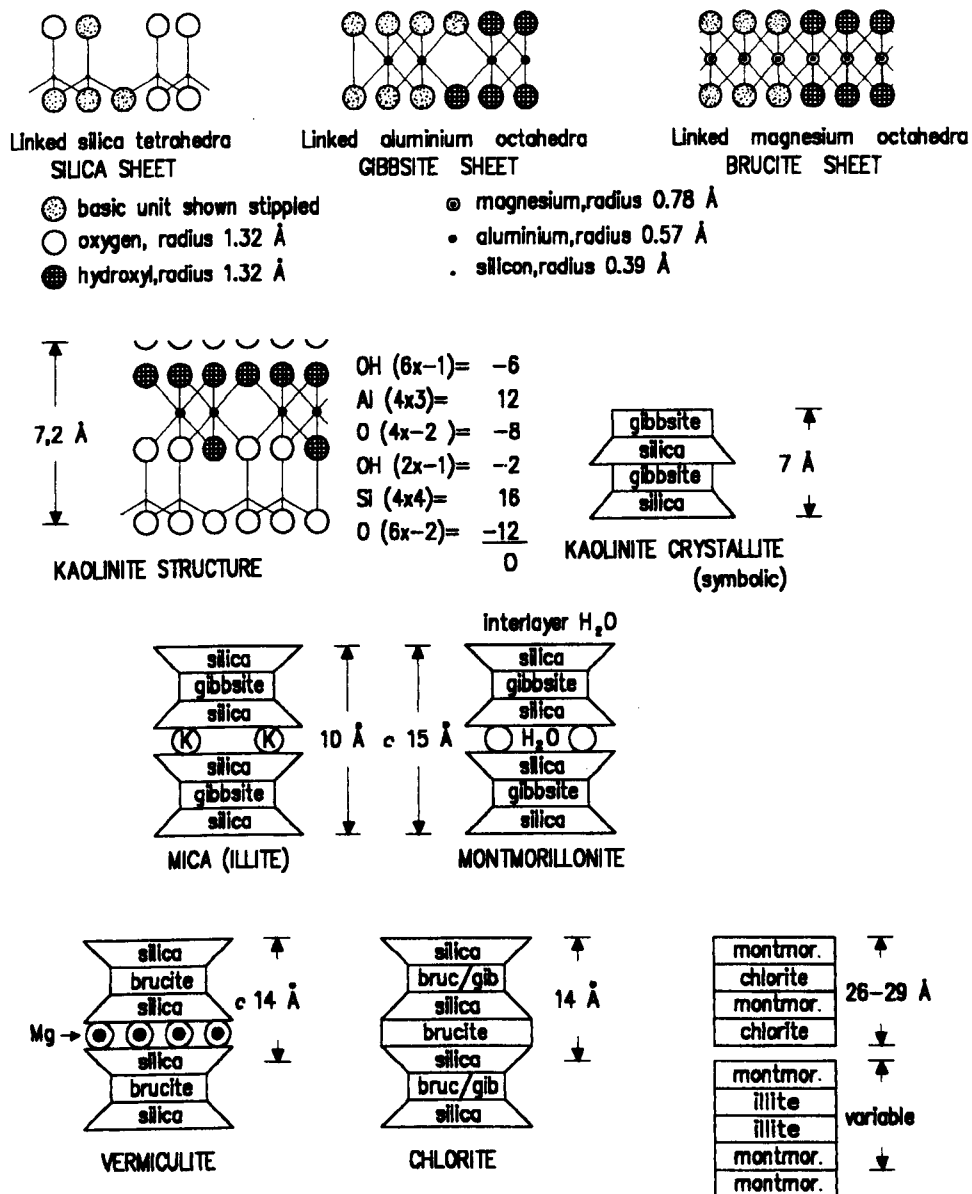
* UK Carboniferous mudrocks; * Cretaceous to Tertiary mudrocks.

It can be seen from Table 2.2 mudrocks are composed of more than 50% clastic debris that includes clay minerals, quartz and feldspar they also contain non-detrital minerals, such as carbonates, iron oxides and organic matter. The main constituents of mudrock are briefly described hereunder.

Clay Minerals

Clay minerals are the most abundant constituents of most mudrocks. These minerals belong to the phyllosilicate family and are hydrated aluminium and/or iron and magnesium silicates, which can also contain alkaline or alkaline-earth metals as essential components. Clay minerals, with exception of the group of sepiolite-palygorskite minerals, whose structure is in a ribbon form, are organised in sheets and layers. As Fig. 2.1 shows structurally clay minerals are composed by alternate silica tetrahedral layers and alumina octahedral layers that form 1:1 sheet type, *e.g.* kaolinite group, and 2:1 sheet type layers, *e.g.* groups of illite-smectite and chlorites. Mixed-

-layered clay minerals correspond to the regular or irregular overlaying of two or more different types of layers e.g. illite-smectite, chlorite-smectite, etc. Clay minerals have an extensive and complex mineralogy that is a result of the combination of the number and arrangement of sheets, ionic substitution in both tetrahedral and octahedral layers and the type and nature of the interlayered materials.



Top: INTERLAYERED
MONTMORILLONITE AND CHLORITE

Bottom: MIXED LAYER
MONTMORILLONITE/ILLITE

Fig. 2.1 – Schematic representation of the structure and composition of the main clay minerals (after Taylor & Cripps, 1984).

Clay minerals generally found in mudrocks are kaolinite, illite, smectite, chlorite and mixed-layered clays. These minerals are derived mainly by the weathering of rocks and soils forming the landmass and they usually form the largest fraction of the siliciclastic grains that compose mudrocks. Clays minerals undergo minor structural changes during weathering and deposition, although flocculation and the formation of fecal pellets can lead to the formation of silt sized aggregations of clay minerals. Structural modifications of clay minerals can occur during diagenesis. Such modifications are ruled by temperature, pore water chemistry and duration of exposure to particular environmental conditions and they lead to the conversion of smectites into illites via intermediate mixed-layer clays (smectite-illite). The progressive transformation of smectite to illite, *i.e.* illitisation, results in the disappearance of expandable layers within the structure of the minerals, thereby increase in the mechanical stability of the rocks concerned (Taylor & Spears, 1981).

Quartz

Quartz is the main detrital constituent of mudrock which can form 20-30% of the whole rock (Potter *et al.*, 1980). The quartz found in these rocks is predominantly angular single silt-sized particles (Blatt *et al.*, 1980). The origin of this quartz is usually either due to the abrasion and collisions suffered by the coarse quartz grains during the transport process, or from the release of silt-size grains from fine-grained crystalline clay rocks (*id.*). Quartz may be also occur as a diagenetic constituent in mudrock, formed as a *by-product* of the process of illitisation of mixed-layer illite-smectite clays (Blatt, 1982). Spears (1980) and Blatt (1982) showed that there is a correlation between the percentage of quartz in mudrock and the mean size of the quartz grains. According to these authors a decrease in the amount of quartz in a rock is accompanied by decrease in grain size.

Feldspars

Feldspars, together with quartz, constitute almost the entire residue, or primary mineral remaining after weathering, fraction of mudrocks (Taylor & Spears, 1981). In most cases other constituents such as rock fragments may be present in this fraction but they are of negligible importance. Feldspar generally occurs in lesser amounts than quartz (Potter *et al.*, 1980). Some secondary feldspar may also be present.

Carbonates

Calcite, dolomite and siderite are the common carbonate minerals in mudrocks. They can occur, either as cement, or as discrete particles. The relative importance of the different carbonated phases present is not well established in the literature, but as in sandstones and limestones calcite is usually dominant (Blatt *et al.*, 1980). The origin of calcite in mudrock is varied as it may occur as particulate material in the form of skeletal debris, as inorganic precipitated microcrystals spread through the rock, or concentrated in nodules or concretions formed by diagenetic processes (Tucker, 1994).

Other constituents

Other constituents present in many mudrocks are iron oxides and hydroxides, pyrite and organic matter. Iron oxides and hydroxides are important in mudrock as pigmentation agents and occur chiefly as coatings on clay minerals (Potter *et al.*, 1980). Hematite is the main iron oxide found in mudrock, however goethite and limonite (hydrated forms) can be abundant in weathered examples.

Pyrite is a common authigenic mineral which occurs in a finely disseminated form or as cubes, framboids (globular clusters) and nodules, especially in dark coloured organic-rich mudrocks (Tucker, 1994). Where occurring in the finely disseminated form, pyrite can be subject to more rapid oxidation (Taylor & Spears, 1981). Organic matter is also common in dark coloured mudrocks. The presence of both pyrite, and organic matter in mudrocks usually indicates that reducing conditions prevailed during the deposition

and/or early diagenetic environments. Thus sulphate reducing bacteria are active in reducing sulphate ions in sea water to sulphide which precipitates as pyrite.

2.2.3 - Textural and structural characterization of mudrocks

The study of texture in mudrock is made difficult by their extremely small grain size. The proportions of clay size, silt size and sand size fractions present are not easy to determine in such fine-grained sedimentary rocks. Particle size analysis often fails to provide realistic data because the results tend to be highly dependent on the method of disaggregation rather than the grain sizes in the original sediment. Moreover, clay minerals are often not deposited as single particles but as floccules and, due to the digestive processes of bottom-dwelling organisms, as aggregations or pellets of mud. However, some simple identification features are available by which siltstone, mudstones/mudshales and claystones/clayshales can be quite easily distinguished in the field (ISRM, 1994). Siltstones are recognized by the harshness to touch and by the fact that silt-sized quartz grains can be identified with a hand lens. Mudstones/mudshales are loamy to the touch and can be identified since they become gritty when chewed, however such a test should be applied only if there is no possibility of samples being contaminated with some poisonous substance. Claystones/clayshales are smooth to the touch and produce no abrasion when chewed.

The geometric arrangement of the particles, that is the fabric, in mudrocks is closely related both to the deposition environment and the geological stress history after sedimentation. In this respect Fig. 2.2 provides a schematic representation of the evolution with the depth of the main two types of association. In most sediments deposited under marine conditions flocculation produces a fabric of randomly orientated particles formed mainly by edge-to-face (EF) interparticle contacts. On the other hand, clays deposited in fresh water conditions tend not to be flocculated and the particles settle face-to-face (FF) producing a parallel orientated fabric.

Compaction produces a general increase in particle orientation with depth. At low overburden pressure (shallow depth) the sediments with EF interparticle contacts are

reorganized into small FF randomly orientated domains (Bennett *et al.*, 1981). With increasing depth these small domains tend to coalesce to form larger domains, but they do however retain a randomly orientated structure. Sediments with interparticle contacts of the FF type are subject to layering as the depth increases, producing a structure that is oriented in the direction of the stratification. Notwithstanding these differences other factors such as the bioturbation (Byres, 1974), the presence of silt and sand size particles, carbonates and organic matter (Odum, 1967) are also important in the initial formation of the fabric and they may influence post-depositional changes in fabric that occur during compaction. The diagenetic processes involving mineralogical transformations and neof ormation and recrystallization, may produce crystalline growth and changes in the morphology of the particles which, in turn, alter the microfabric of the sediment (Dunoyer De Segonzac, 1970).

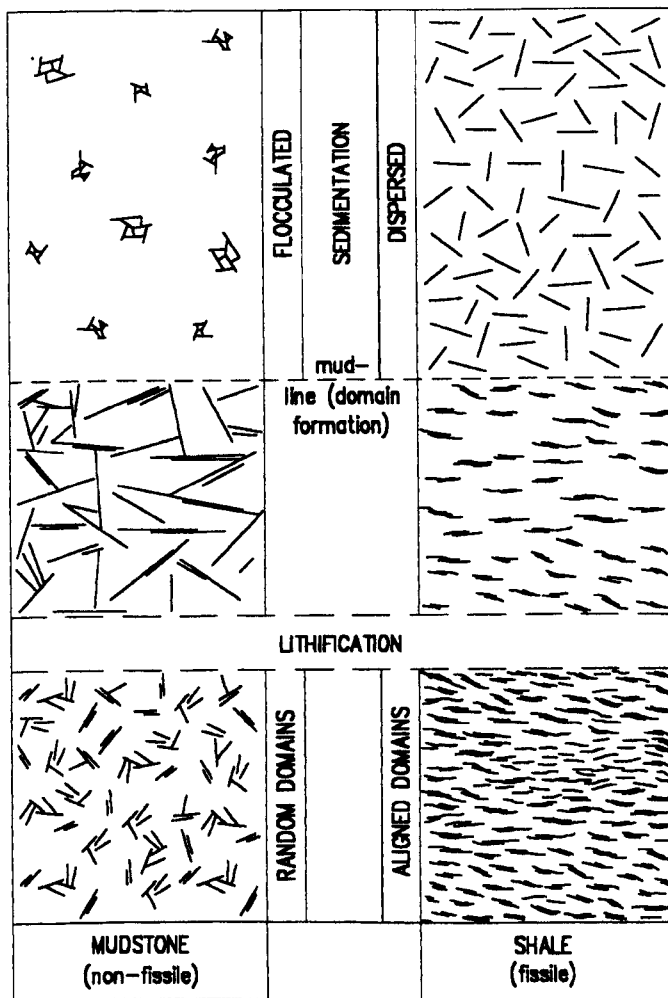


Fig. 2.2 - Schematic representation of the evolution of the fabric of respectively originally flocculated and dispersed textured mudrocks with the depth of burial (after Moon & Hurst, 1983).

Fissility and *stratification* are common features in mudrocks. The former is the tendency of the rock to split along lamination or bedding planes while stratification (bedding and lamination) is the result of vertical variations in composition, texture and/or fabric. Fissility tends to form in response to weathering action in which laminar weaknesses present in the rock are exploited so that it splits into a series of thin sheets. In Fig. 2.3 are presented the thickness classes proposed by various authors for stratification and fissility currently used in sedimentological texts to describe mudrocks. The classifications proposed by Ingram (1954) and Potter *et al.* (1980) establish an arbitrary distinction at 10 mm between beds and laminae, there being therefore no overlap of thickness classes in relation to the two terms. According to Campbell (1967) lamina is the lesser megascopic unit identified in a sedimentary sequence, and can reach a thickness of 200 mm or more. According to this classification the thicker classes of laminae overlap the finer thickness classes proposed for beds.

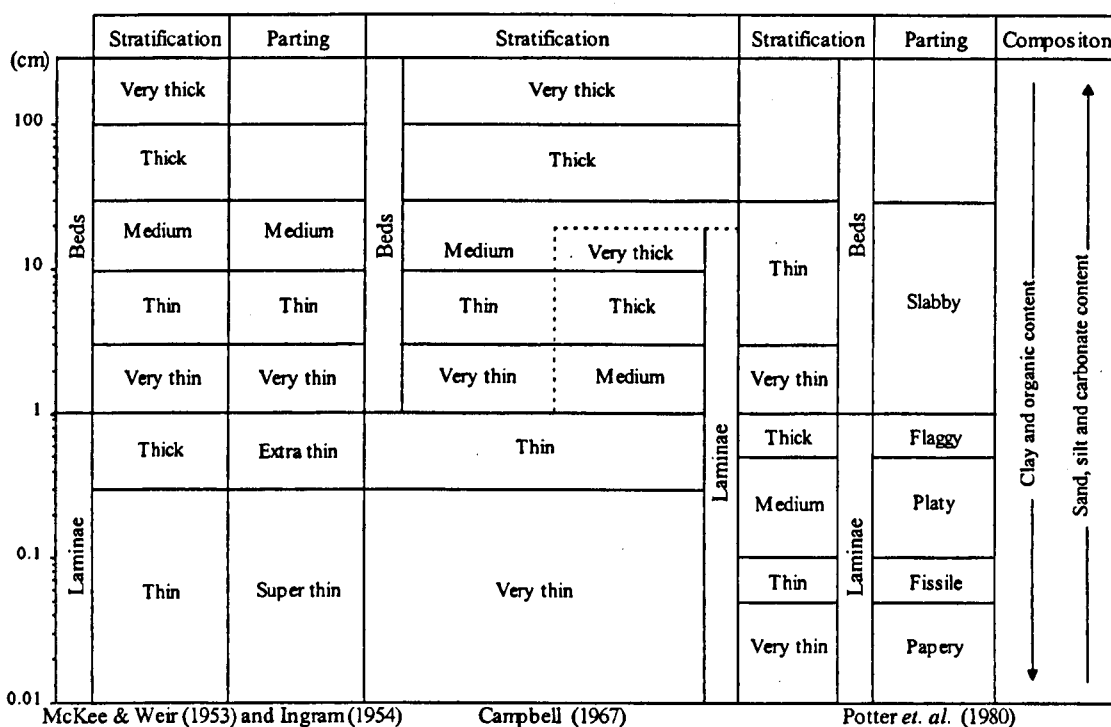


Fig. 2.3 - Thickness classes of stratification and fissility (adapted from McKee & Weir, 1953; Ingram, 1954; Campbell, 1967; Potter *et al.*, 1980).

Fissility is related to several factors, the most important of which are, the presence of laminae, the parallel orientation of lamellar minerals, for example clays or micas and the

concentration of organic matter on bedding planes (Ingram, 1953; Odom, 1967; O'Brein, 1970; Pettijohn, 1975; Spears, 1976; Blatt *et al.*, 1980). Spears (1976) observed from the study of Coal Measures mudrocks, that fissility was only found in surface samples collected from outcrops and was absent in laminated samples collected at depth from boreholes cores. Spears (1980) found that the size of the fragments resulted from the fissility in surface samples was of the same order of magnitude of laminae thickness in the boreholes cores and concluded that fissility is a surface expression of laminae that occur in mudrocks at depth.

From Fig. 2.3 it can be concluded that the separation between the fissility planes generally decrease as the degree of orientation of clay minerals and the content of organic matter increases. On the other hand, the presence of carbonates and of silt-sized and sand-sized quartz grains in the rock correspond to a thicker parting. However, in addition to the pre-disposition of the sediment to parting, the structure displayed is mostly the result of the stress relief and weathering due to exhumation. As noted by Weaver (1989), under overburden pressures, fine-grained sedimentary rocks with oriented lamellar minerals are massive, hence, exfoliation and sub-parallel parting occur only after unloading and weathering.

According to the classifications presented in Fig. 2.3 stratification is subdivided into two main classes, beds and laminae. This work adopts the classification scheme that considers laminae as layers thinner than 10 mm. Different types of lamination in terms of variations in fabric, grain size and colour can be distinguished in mudrocks (Lundegard & Samuels, 1980). These are represented schematically in Fig. 2.4.

Fabric lamination is the most common type. It is produced by the parallel orientation of sheet phyllosilicate mineral grains a few microns in size. Grain size lamination is due to the differences in settling rates of different components which usually produces alternating layers of clay mineral and silt-size quartz grain material. Colour laminations are produced by alternated layers of different colours. These may be due to compositional differences between the laminae, particularly variation in the amount of organic matter present and the grain size. Depending on the sedimentary conditions mudrocks may show only one lamination type or combinations with either or both of the others.

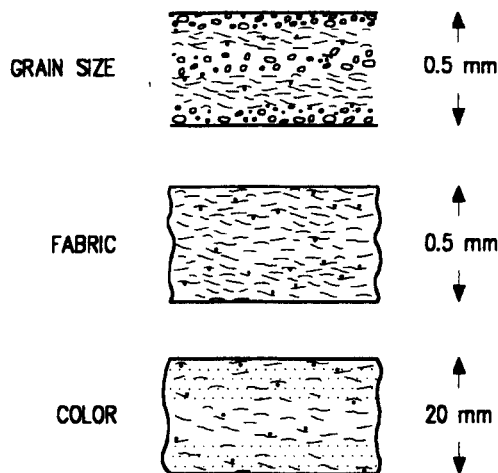


Fig. 2.4 - Different types of lamination in mudrock (after Lundegard & Samuels, 1980).

2.2.4 - Colour

Colour is the most obvious feature of mudrocks and for this reason, it is always recorded in descriptions. However the description of colour can be very subjective and it is therefore recommended that colour charts are used. The colour also varies with the moisture content of rocks and accordingly the saturation state (wet or dry) of the material should always be recorded. In general, colour should be determined in samples at their natural water content. The content of organic matter and oxidation state of iron are the main factors which control the colour of mudrocks. The former affects the shades between grey and black, while the latter produces shades of red, purple, brown, yellow and green.

Grey to black colours reflect the presence of organic matter in mudrock, in particular the amount and its distribution, size and type (Spears, 1980). The presence of finely disseminated iron sulphides, namely pyrite, also produces a dark colour in mudrock (Blatt *et al.*, 1980, Tucker, 1995).

Red and purple colours are caused by the presence of finely divided ferric oxide (hematite). A green colour reflects the absence of organic matter, pyrite and ferric oxide and is due of the ferrous iron present in the structure of clay minerals. A green colour

can also be a result of the reduction of Fe^{3+} (hematite), generally by the action of organic acids, to Fe^{2+} in mudrock that was originally red.

A yellow and brown colour can reflect the presence of limonite and goethite. Yellow and green colours can also be the result of the mixing of various pigmentation components. Colour mottling with subtle variations in grey, green, brown, yellow and red/pink colours may also be observed in mudrocks. Such features in the case of the different shades of grey may be due to bioturbation, while in the case of yellow/red/brown shades due either to root growth or to weathering action in which the movement of groundwater through the rock can lead to an irregular distribution of oxides, hydroxides and carbonates.

2.2.5 - Laboratory Techniques

Observations and descriptions in the field and of hand specimens can be complemented by laboratory studies that provide additional information on textural, mineralogical and chemical features of mudrocks. These studies should be carefully planned since many of the laboratory techniques require the use of sophisticated instruments, which are expensive and time consuming to operate. Given the objectives of a specific study the cost *versus* information obtained as a result of the use of the various laboratory techniques available, should always be pondered. The section hereunder presents the more valuable laboratory techniques for the study of mudrocks.

X-ray diffraction

X-ray diffraction is the best technique to determine the mineral constituents of mudrocks. In fact the small size of the grains generally prevents identification by other techniques. This technique can provide both the qualitative and quantitative determinations of the mineral species present. Depending on the objectives of the study samples for analysis can be subjected to various pre-treatments and different forms of sample preparation. For general characterization of a mudrock a whole rock randomly

orientated sample on material treated to remove organic matter is preferred. Detailed studies of the clay minerals usually require work on a fine fraction separation, prepared in an orientated fashion with scans run in the original state, after glycolation and after heating. The latter procedures are required for study of swelling clay minerals and also so that kaolinite may be distinguished from chlorite. Since various engineering properties of mudrocks are affected by the amount and type of expandable clay minerals present, these analyses are important aspects of this study. Further details are given in Chapter 5.

Polarizing microscopy

The polarizing microscope may be useful in the study of the mineralogy of mudrock constituents in the sand-sized and silt-sized fractions. However, particles in clay-sized range are irresolvable with this technique. In addition to which, since the grains are smaller than the standard thickness of slides (30 μm) the grains cannot be resolved. Nevertheless, polarizing microscope can be useful in the study of small scale features including cross bedding, particle orientations, micro-laminations and other micro-structures.

Scanning electron microscopy

Scanning electron microscopy (SEM) is used to study both mineralogical and textural aspects of mudrocks. A magnification range of between 20 x and 100,000 x and a great depth of focus make this technique of great value in the examination of rock surfaces (Trewin, 1988). Individual grains are within the resolution range and photomicrographs are very useful, especially for the study of textural aspects such as fabric, shape and size of the grains and pore space geometry. In this respect the method provides data that are superior to those available using other techniques whereas, although mineralogy may be determined, other suitable methods are available. However, using backscattered electron (BSE) images, which provide atomic number contrast, the various mineral phases can be distinguished. Furthermore, analytical facilities such as an energy dispersive X-ray analysis system (EDS) can be used jointly with SEM enabling the determination the

composition of grains. Such data enable the role of particular mineral phases, and association between mineral phases, within the mudrock fabric to be studied.

X-radiography of rock slabs

This technique uses rock slabs about 5 mm thick (Potter *et al.*, 1980). It is most useful for examining features of the fabric which are not discernible by direct observation. Internal features such as bedding, concretions, root tubules, fossils, organic matter, burrows, laminations and hairline fractures which are not visible to the naked eye can be readily seen by radiography.

Chemical analyses

Chemical techniques are commonly used in the study of mudrocks. Bulk chemical analysis for both major and trace elements can be obtained using wet chemical, Inductively Coupled Plasma Atomic Absorption Spectrometry (ICP-AAS), Atomic Absorption (AA) or X-ray Fluorescence (XRF) methods. X-ray fluorescence in particular, is a rapid procedure that enables analysis of most mudrock components. This enables validation of mineralogical determinations but is not suitable alone where volatile or sulphur rich components are present. In terms of assessing weathering effects chemical data have limited value because although mineralogical changes may occur, weathering may result in only small changes in chemical composition.

Wet chemical analysis techniques are commonly used to determine cationic exchange capacity, the amounts of organic matter, carbonates and the presence of sulphur minerals as well as to distinguish Fe^{2+} from Fe^{3+} in compounds. Sodium bisulfate fusion is a chemical technique described by Blatt *et al.* (1982) that is used to isolate quartz and feldspar grains from the other constituents of mudrocks. With this technique the resistate fraction of mudrocks can be determined.

2.3 - Compaction and weathering of mudrock

The geotechnical properties of mudrocks are deeply influenced by their composition, geological loading history and degree of weathering (Fleming *et al.*, 1970; Cripps & Taylor, 1981). The composition of mudrock is related to the geology and weathering environment of the source area, transportation mode, and to some extent, to the nature of the depositional and post-depositional environments.

The geological loading history of an over-consolidated clay or mudrock can be investigated using laboratory consolidation tests as was described by Fleming *et al.* (1970). Such tests are based on the works of Skempton (1964) and Bjerrum (1967) that show that the reduction in porosity with a steadily increasing overburden is directly related to the logarithm of the overburden pressure. Immediately after sedimentation mud has a porosity of between 70 to 90% which corresponds to 50-80% water by weight (Weaver, 1989) as represented schematically in Fig. 2.5(A) point *a*. The accumulation of more sediments causes an increase of the overburden pressure and a decrease in water content. The line *a-b-c* in Fig. 2.5(A) represent 'normally consolidated' clays where point *b* indicates a load equal to the present overburden pressure. The shear strength of 'normally consolidated' clay is proportional to the existing overburden pressure and, therefore is represented in Fig. 2.5(B) by a straight line passing through the points *a-b-c*.

Unloading the sediment by erosion to the present overburden pressure (point *e*) brings the sediment to an 'over-consolidated' condition. Although there is some increase in porosity, the void ratio does not increase to the value corresponding to point *b* on the chart. Thus, although the sediment is under the same overburden as at point *b* the water content (and porosity) is much less in the over-consolidated state. As well as this, due to the rearrangement of particles and denser state of the sediment, the shear strength is higher.

According to Bjerrum (1967) if the sediment represented by point *c* remains under the same effective pressure over a long time period a further reduction in water content occurs as a consequence of secondary consolidation. During this period the sediment

may be subject to diagenetic changes including recrystallization of particles, adhesion between particles and precipitation of cements. The bonds formed between particles through these processes are termed diagenetic bonds and because of them the sediment becomes stronger, less permeable and more brittle.

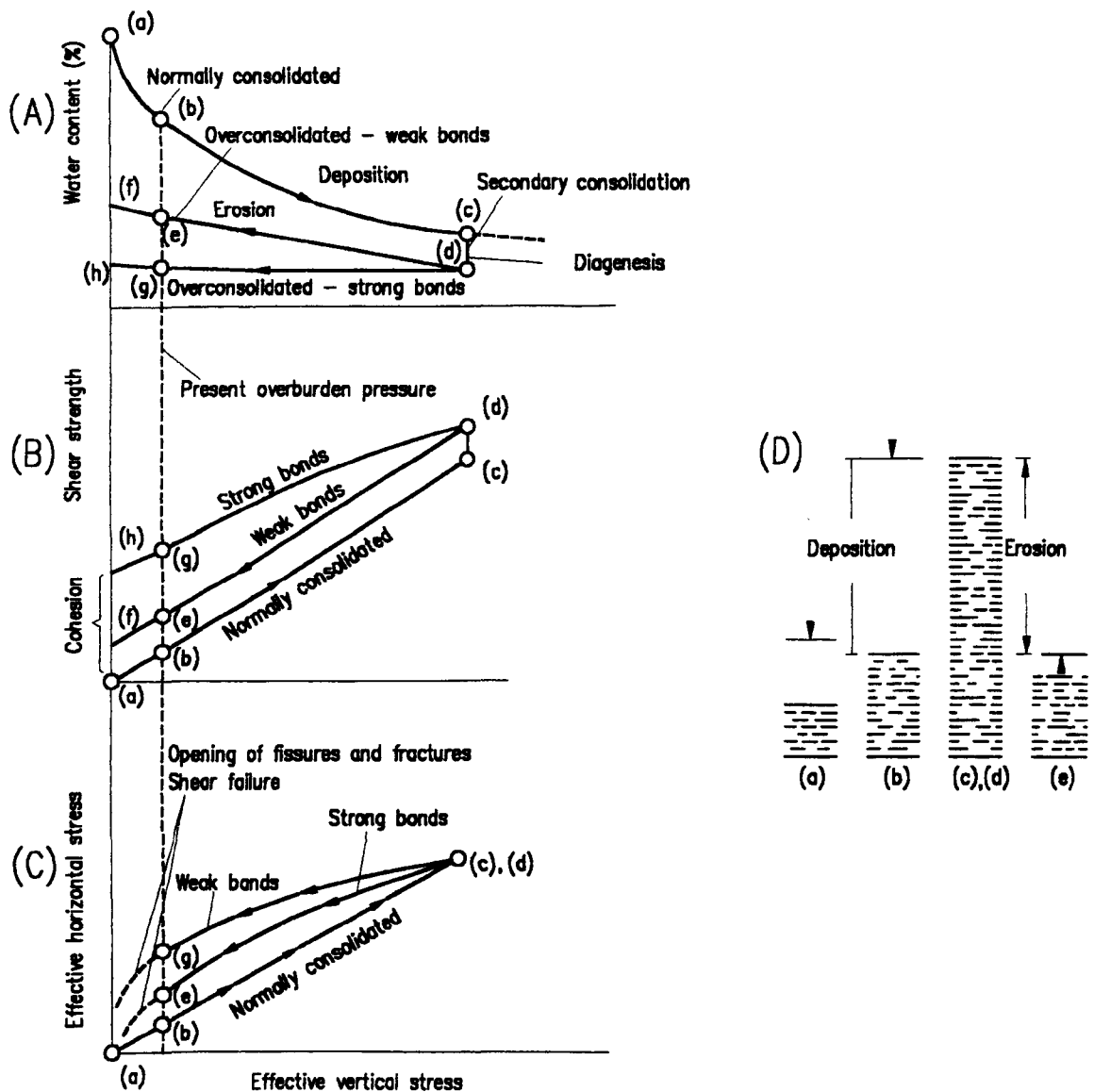


Fig. 2.5 - Schematic geological history of an overconsolidated clay or mudrock: (A) compaction and unloading; (B) effect of compaction and unloading on shear strength; (C) variation of horizontal and vertical stresses due to compaction and unloading (after Cripps & Taylor, 1981).

On unloading, because over-consolidated clays and mudrocks possess recoverable strain energy stored in compressed flexible flake-shaped clay particles, the materials swell and

the water content increases. The extent and timing of this expansion depends on the strength of the diagenetic bonds between particles as is shown by lines *d-e-f* and *d-g-h* in Fig. 2.5(A). The latter rebound curve as compared with the former shows that expansion of clays and mudrocks with strong diagenetic bonds will be restricted. However, as the breakdown of strong bonds is time-dependant, the strain energy will be released progressively thus leading, in the long-term, to softening of over-consolidated clays and mudrocks.

The importance of diagenetic interparticle bonding in the structure of the material is demonstrated well when the horizontal to vertical stress ratio is modelled as schematically illustrated in Fig. 2.5(C). On unloading the changes in vertical stress are larger than those in horizontal stress because the vertical expansion is greater than the horizontal expansion. For strongly bonded types the horizontal expansion is more restricted because the bonding prevents the expansion. As a result the effective horizontal stress is lower than that developed for weakly bonded types.

The weathering processes promote the disintegration of interparticle bonds and lead to the release of latent strain energy in the sediment. The resulting expansion, is accompanied by an increase in water content and compressibility, and a decrease in shear strength. The disintegration of the bonds is consequently related to the degree of weathering and thus, an indurated mudrock can eventually achieve the status of a remoulded 'normally consolidated' clay in the more weathered stages.

2.4 - Geotechnical characterization of mudrocks

2.4.1 - Geotechnical properties

By reputation mudrocks are regarded as poor engineering materials in the construction and mining industries. In comparison with other rock types they are more prone to failure in slopes, embankments and surface mining highwalls. The particular geotechnical features that characterize mudrocks are described in the following section.

Plasticity

It is related to the strength of interparticle bonds and also to the type, fabric and amount of the clay minerals (Heley & Maclver, 1970). Clay mineral interlayer cation type and concentration and the amount and composition of water, particularly in terms of changes in the ordered molecular layers of water associated with the clay mineral surfaces, also affect plasticity (Gillott, 1987). The assessment of plasticity in more indurated mudrocks types can be problematic since the materials are difficult to disaggregate without affecting the size distribution of the particles present.

Strength/Deformability

The strength and deformability are related to the degree of aggregation, type and arrangement of the minerals which build up the mudrock, but are mainly controlled by the degree of weathering (Heley & Maclver, 1971). These properties are also influenced by the presence of cements between particles, as well as mass features such as fissures. Mudrocks, especially, the stress-relieved laminated types, possess anisotropy so that measurements parallel and perpendicular to the main structure (bedding, lamination, parting, etc.) are recommended to obtain minimum and maximum values.

The formation of a rupture surface due to movement in shear leads to the re-orientation of platy clay particles. The fabric of the rock and the strength of interparticle bonds together with the angle between any plane structure in the rock (stratification, lamination etc.) and the shearing direction are the main controls over this reorientation. For undisturbed samples, the measured peak shear strength parallel to any lamination or clay mineral preferred orientation will be less than that for a random or flocculated fabric (Gillott, 1987).

According to Skempton (1964), residual shear strength is usually regarded as being a property which depends only on the composition of the material. It is thus independent of the normal stress value, type of sample and rate of strain. However, clay minerals are often aggregated in clusters and for this reason an increase in the normal stress can produce disaggregation of the material and thus reduce the residual shear strength. Thus

variation in residual shear with normal stress value has been noted by Cripps & Taylor (1981) for a number of UK overconsolidated clays (see Chandler *et al.*, 1973).

Mesri & Cepeda-Diaz (1986) have shown that the residual shear strength is mainly determined by the platyness of particles, although it might also be related to the mineralogical composition. These authors performed tests on pure clay minerals and with sodium montmorillonite samples they obtained the smallest values of residual shear strength. This they attributed to the predominant arrangement of the particles in face-to-face domains such that low interparticle contact pressures are developed. However, tests performed with the same samples after treatment with carbon tetrachloride which caused aggregation of the platy clay minerals particles into clusters, gave higher results similar to the ones obtained with silt-quartz samples, which demonstrated that residual shear strength is more influenced by the lamellar character of particles than by mineralogy *per se*.

Swelling

Swelling is a characteristic property of mudrocks which is a result of (a) stress-relief of the geological materials and (b) physico-chemical reactions with water. The latter include hydration of clay minerals and chemical alteration of non-swelling minerals into swelling minerals (ISRM, 1983).

Mechanical swelling occurs in response to elastic and time-dependent stress unloading which may be caused by man in digging excavations or by nature in tectonic uplift and erosion (Taylor & Smith, 1986). Since mudrocks are low permeability materials, the balance of moisture in the rocks during swelling can be inhibited due to deficient water percolation within the pore space. Thus, unloading can give rise to the development of negative pore water pressures (suction) in materials that will correspond to an increase in the effective stress acting on the rock. Mechanical swelling and the reabsorption of water causes softening and weakening of the rock and high stresses developed during this process may produce failure of the fabric of the rock, *i.e.* fissuring.

The physico-chemical swelling mechanisms related to the hydration of clay minerals can be intercrystalline or osmotic and intracrystalline. Fig. 2.6 shows the intercrystalline

and intracrystalline water absorption mechanisms schematically. The term intercrystalline swelling is used to characterize the water absorption phenomena that occur on the external surfaces of clay crystals and in the voids between crystals. According to Gillott (1987) intracrystalline expansion is a result of the forces of attraction that link structural sheets being weaker than the attractive forces responsible for the moisture uptake. The water absorbed by this mechanism forms successive monolayers on the surfaces of clay minerals that keep them apart.

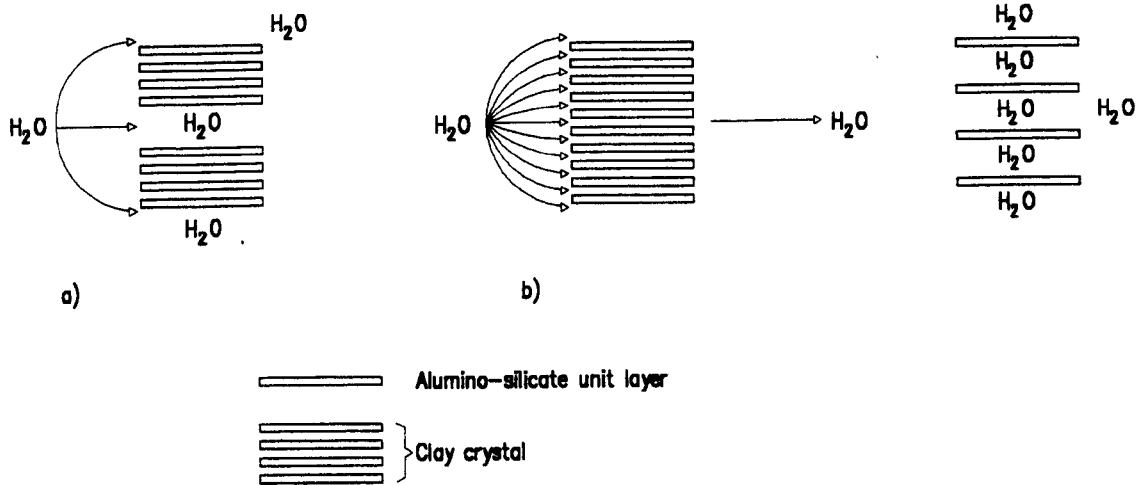


Fig. 2.6 - Moisture uptake by clay minerals: (a) intercrystalline absorption of water in a non-expanding lattice; (b) intracrystalline absorption of water in an expanding lattice (after Gillott, 1987).

The absorption of water by the internal surfaces of clay minerals is influenced by the nature of the interlayer cations. The smectite group together with vermiculite, swelling chlorites and some mixed-layered minerals are the main clay minerals that exhibit intracrystalline swelling.

Swelling by the osmotic mechanism results from the interaction between the diffuse double water layers possessed by clay minerals particles. This interaction is related to the thickness of the double layer, which is controlled by the dielectric constant, type and concentration of cations and temperature of the pore fluid (Taylor & Smith, 1986, Hongxi, 1993; Bell *et al.*, 1993).

According to the model proposed by Taylor & Smith (1986), if the space between the clay platelets is less than 15\AA , the atoms in the clay minerals develop attractive forces of the van der Waals type. In these conditions the cations are uniformly distributed between any two clay platelets, and do not form separate diffuse double layers. If the space between the clay particles is greater than 15\AA then electrostatic repulsion forces dominate and separate double-layers are formed, thereby increasing the distance between the clay platelets (Fig. 2.7). In the first case, when double layers overlap, there is an excess cation concentration between the clay particles. Equilibrium is restored by free water being drawn into the system from adjacent pores and capillaries. In practical terms, monovalent cations in weak concentrations give rise to more extensive diffuse double layers, while an increase of valence and/or concentration will reduce swelling.

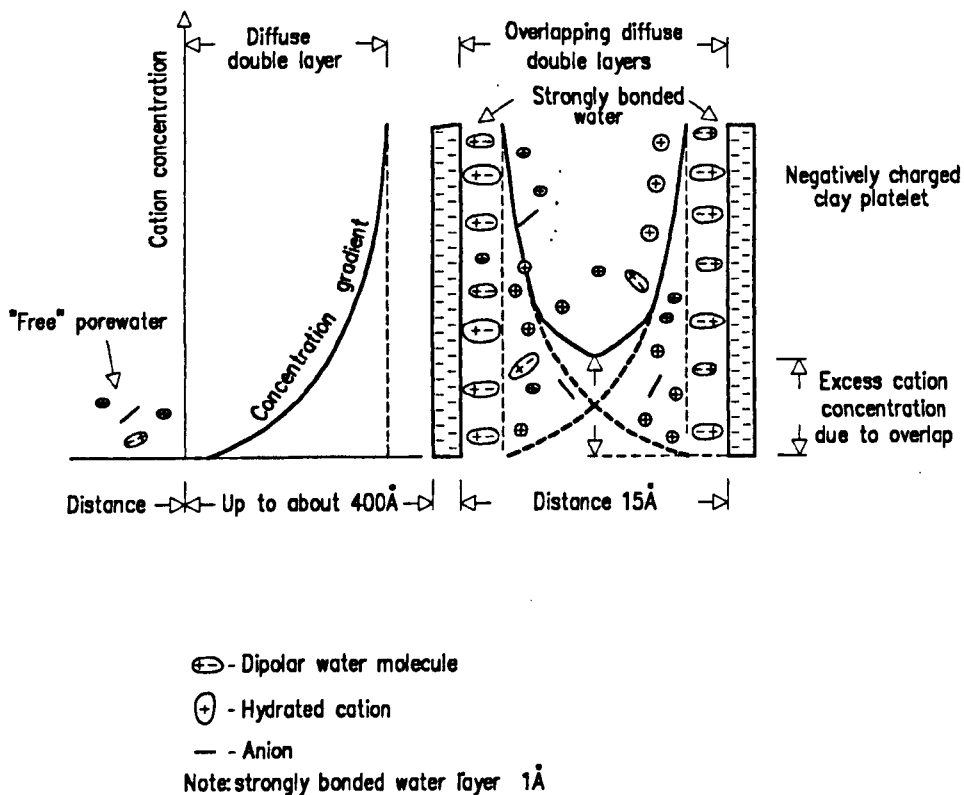


Fig. 2.7 - Model proposed to explain osmotic swelling mechanism between two clay platelets (after Taylor & Smith, 1986).

The swelling of mudrocks can also be a result of the chemical alteration of non-expansive minerals in expansive minerals. The hydration of anhydrite leads to the

formation of gypsum with a maximum increase of volume of about 60% (ISRM, 1983). The oxidation of pyrite, frequently by complex biochemical processes, produces sulphuric acid and hydrated iron sulphates that cause an increase in volume (Penner *et al.*, 1973). Precipitation of gypsum, as a result of a reaction with calcium, derived from the dissolution of the carbonates can occur, which also leads to an increase in volume (*op. cit.*).

The magnitude of swelling in mudrocks is controlled by mineralogical factors such as nature and relative amount of expandable and non-expandable clay minerals, the extension of cementation, and by textural factors such as compaction, microfissuration and lamination (Ordaz & Argandoña, 1981; Kojima *et al.*, 1981). The presence of abundant expandable clay minerals is the main control of mudrock swelling. As noted by Ordaz & Argandoña (*op. cit.*), Sarma & Shakoor (1990) and Sarma *et al.* (1994) in mudrocks without expandable clay minerals and in some very massive (non-laminated) mudrocks, texture seems to play the principal role in controlling swelling behaviour. In such mudrocks swelling depends on porosity defined by the geometry and distribution of the pore-crack system which controls the water suction by capillary action. Furthermore, Ordaz & Argandoña (*op. cit.*) claimed that swelling strain rate and swelling anisotropy are also mainly influenced by textural factors such as porosity. The swelling anisotropy of mudrocks may also be due to mineral particle preferred orientation, other features of the fabric and grain size, lamination, parting and the arrangement of voids.

Durability/Slaking

In the context of engineering geology, the term durability may be defined as the resistance to weathering breakdown of the rocks with time after exposure to surface and/or underground environmental conditions (Gamble, 1971; Franklin & Chandra, 1972). The weathering agents responsible for rock breakdown are variable and may include, in order of importance, wetting and drying, frost action and salt crystallization, leaching, mechanical abrasion, solution and chemical alteration (Franklin & Chandra, 1972). In the context of engineering geology *time* should be related to the 'life' duration

of the engineering structures. The evaluation of mudrock durability is extremely important, as breakdown may occur on engineering time-scales. Due to rapid degradation the initial properties used in design may be entirely inapplicable to the behaviour of the material during the life of a structure, or even during the construction period. Problems can also arise due to changes in behaviour and disintegration that occurs during sampling operations.

The durability of rock materials is controlled by intrinsic factors inherent to their characteristics and by extrinsic factors that reflect environmental conditions to which rocks are exposed or to which they will be subjected. Climate, topography, hydrological conditions are all important factors which assume a different significance on a case by case basis, according to the circumstances of the specific application. The analysis of the influence of these latter factors on the durability of mudrock is beyond the scope of this study. Accordingly, studies and methods that seek to evaluate the durability component of mudrock based on the intrinsic characteristics of these materials, in relation to the most probable weathering mechanisms in the most common applications of these rocks, are preferred.

Research has shown (Russel, 1982; Shakoor & Brock, 1987; Taylor, 1988; Dick & Shakoor, 1992; Dick *et al.*, 1994) that mudrock durability is controlled by lithological, mineralogical and structural characteristics, such as, clay content, proportion of expandable clay minerals, cementing agents, rock fabric and presence or absence of microstructures like laminae, slickensides and microfissures. As such it is closely related to swelling capacity.

Mudrock durability is usually evaluated as the resistance to slaking in term of a *slake durability* parameter. Slaking has been defined as the disintegration of rocks when exposed to air or moisture or to alternate drying and wetting. A more elaborate definition of slaking that focuses on the underlying mechanisms and the rate of breakdown has been proposed by Andrews *et al.* (1980) and quoted by Perry & Andrews (1982):

'Slaking is the short-term physical disintegration of a geologic material following the removal of confining stresses. Breakage may result either from the establishment or

occurrence of sufficient stresses within the material or from the decrease in structural strength. The significance of disintegration rate is dependent on the specific engineering considerations; for definition, *short-term* may be taken to mean less than several years.'

The mode, rate and degree of slaking depends on several factors which include particle size, mineralogy, rock fabric and bedding characteristics (Perry & Andrews, 1982). Two modes of slaking of mudrock are referred to by Perry & Andrews (*op. cit.*). In the first one 'chip slaking', fragments that range in thickness from 0.6 to 2.0 mm and in length and width from 2.5 to 15.0 cm, are produced which exhibit resistance to further degradation. In the second mode 'slaking', disintegration into inherent fine-grained particles leads to the complete destruction of the original structure of the rock.

According to Taylor & Cripps (1987) the main mechanisms that influence slaking are as follows: (a) incidence of sedimentary structures and discontinuities, (b) pore air compression (c) swelling of expansive clay minerals. The important discontinuities in disintegration are the bedding surfaces of depositional or diagenetic origin and structural discontinuities, such as, joints, fissures and fractures, and shearing surfaces.

The pore air mechanism is a function of the capillary and suction characteristics of the materials as described by Taylor & Spears (1970). These authors found that the breakdown of Coal Measures mudrocks, as a result of simple static slaking tests, was less when the tests were conducted in a vacuum, than when conducted in air. According to Taylor & Spears (*op. cit.*), the breakdown mechanism operates in the following manner, during dry periods evaporation from the surfaces promotes suction, which in turn increases shearing resistance of rock fragments. In the case of extreme desiccation the voids remain filled with air. In these conditions, if the material is rapidly immersed in water, the air in the pores is compressed by the development of capillary pressures in the outer pores, which can cause failure of the rock fabric along the weakest planes.

The mechanisms associated with the swelling of clay minerals were described above under the heading of swelling.

2.4.2 - Laboratory tests

The laboratory tests mainly characterize the geotechnical properties of intact rock material. It is then necessary to determine the influence of bedding, joints, fissures, faults and other significant discontinuities, geological structure and groundwater conditions in order to assess rock mass behaviour. However, in this work only those aspects related to the laboratory description of rock material will be covered. The laboratory tests used in the study of mudrock were reviewed in detail by Taylor & Spears (1981). The tests and methods commonly used in the characterization of mudrock properties are outlined in the following sections.

2.4.2.1 - Identification tests

Under this designation the fundamental properties, such as, natural water content, grain specific gravity, density, and porosity, and the tests used for soil classification, *i.e.* particle size analysis and Atterberg limits are included.

The determination of the fundamental properties of mudrock that have a predominantly soil-character can be effected according to standards NP-84 (1965), NP-83 (1965), BS 1377: Part 2 (1990), ASTM D2216 (1998), ASTM D854 (1992) and ASTM D4254 (1996). In the case of more indurated mudrock (rock-character) these properties can be obtained by the methods proposed in ISRM (1979*b*).

The determination of natural water content is very easy to perform and gives valuable information. High natural water contents may indicate the presence of mudrocks with greater amounts of clay minerals, in particular expandable clay minerals. In addition to natural water content, water absorption resulting from the immersion of rock fragments and water adsorption due to exposure of specimens to specific moisture conditions are frequently determined. Several methods are given in ISRM (1979*b*) for determining density and total and effective porosity. Effective porosity or volume of interconnected pores, indicates the percentage of the pore space that can be reached by water, whilst the comparison between total and effective porosity indicates the extent of cementation.

The methods used for determination of pore volume, that is those used to determine effective porosity, commonly requires vacuum saturation by water immersion. However, this is impossible to perform in mudrocks that slake in water. An alternative method is to measure the pore volume by gas or mercury intrusion porosimetry. The latter method was used in this work (Chapter 7).

The methods for determination of particle size analysis and Atterberg limits are given in the following standards E-196 (LNEC, 1967a), E-239 (LNEC, 1971), NP-143 (1969), BS 1377: Part 2 (1990), ASTM D422 (1998) and ASTM D4318 (1998). They require the prior disaggregation of the material. The interparticle bonding characteristics of the mudrocks may not permit disaggregation of the material into individual particles which remain in aggregated or clustered of group of particles. This affects the determination of grain size and measured plasticity. Therefore, the values obtained for properties depend on the method and effort used to process (disaggregate) the material. The methods of disaggregation and their effect have been investigated in detail by Heley & MacIver (1971) which recommended that the material should be processed (a) from undried material, (b) after a single cycle of air-drying and slaking, and (c) after disaggregation by a high speed food blender. Oakland & Lovell (1982) suggested the use of ultrasonic devices to promote the degradation of the material and Sarman *et al.* (1994) recommend the use of alternate cycles of wetting and drying to disaggregate mudrocks.

Particle size distributions are usually based on wet or dry sieving followed by hydrometer analysis of the <75 μm fraction. The latter determination is used to determine the amount of silt-size (material with a size between 60 μm and 2 μm) and clay-size (material with size less than 2 μm) material present. The liquid limit is commonly determined by the Casagrande apparatus or cone penetrometer methods on samples passing 425 μm . Liquid and plastic limits are important quantitative indexes in the characterization of the behaviour of mudrock that are used in several engineering classifications (see Chapter 3). Again the results can be affected by the method used for the disaggregation of specimens. The plasticity index is defined by the difference between the liquid limit and the plastic limit. Table 2.3 shows the classification of plasticity in terms of the liquid limit and the plasticity index.

Table 2.3 - Classification of plasticity in terms of liquid limit and plasticity index (adapted from IAEG, 1981).

Term	Range of liquid limit (%)	Term	Range of plasticity index (%)
Low plasticity	< 35	Non-plastic	< 1
Intermediate plasticity	35 - 50	Slightly plastic	1 - 7
High plasticity	50 - 70	Moderately plastic	7 - 17
Very high plasticity	70 - 90	Highly plastic	17 - 35
Extremely high plasticity	> 90	Extremely plastic	> 35

The liquidity index correlates the Atterberg limits of the material to its natural water content and is defined by:

$$LI = \frac{w - PL}{PI} \quad (2.1)$$

where,

LI - liquidity index

w - natural water content

PL - plastic limit

PI - plasticity index

Values for LI greater than 1, mean that the water content *in situ* is greater than the liquid limit, and thus the material is extremely soft in its natural state. Values of LI between 0 and 1 mean that the natural water content is equal to or less than the liquid limit. Values for LI less than 0, *i.e.* negative, mean that the water content *in situ* is less than the plastic limit, and thus the material behaves like a brittle solid.

Although activity* may be influenced by other factors in addition to mineralogy. These include the composition and concentration of the pore water solutions and the presence of organic constituents. It is generally found that values below 0.75 are related to the occurrence of non-expansive clay minerals of the kaolinite type, values close to 1 with clay minerals of the illite type and values clearly greater than 1 with expansive clay minerals of the smectite type. The classification of fine materials (silt and clay) can be based on the plasticity chart (Fig. 2.8). In this diagram the silt materials are projected in the area under A-line and the clay materials in the area above this line. The U-line shown in Fig. 2.8 has been empirically determined to be the approximate 'upper limit' for natural soils.

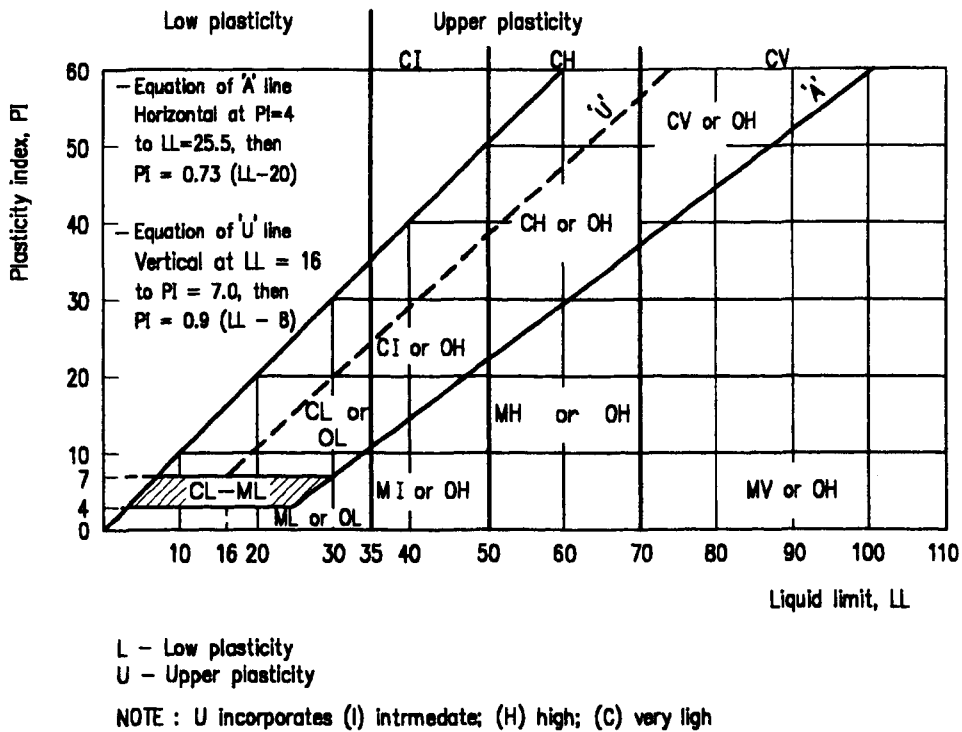


Fig. 2.8 - Plasticity chart.

2.4.2.2 - Strength tests

A number of different strength tests are available for engineering design and material characterization through index tests. The strength of mudrocks may be measured

* Activity is the plasticity index of a soil, divided by the percentage, by weight, of soil particles within it that are less than 2 μ m in size.

directly using triaxial, uniaxial compressive, tensile or shear strength tests, or it may be estimated using indirect tests such as the point load test, Schmidt hammer (rebound hardness test), NCB cone indenter and Shore scleroscope.

The uniaxial compressive strength tests were extensively investigated by Hawkes & Mellor (1970) and by ISRM (1979a) which specify appropriate testing procedures. The requirements for the sample preparation of samples into regular shapes constitute the main drawback of this test for mudrocks. Difficulties arise in forming specimens having suitable dimensions for testing (commonly the core diameter is NX or greater and the height should be at least twice the core diameter) especially in laminated mudrocks. It is also necessary to maintain samples at their natural water content as the compressive strength of the mudrocks is significantly affected by water content. Hence, rocks are often tested dry, at natural water content and saturated conditions in order to evaluate the loss of strength with increase in water content.

Uniaxial compressive tests can be used for the assessment of strength anisotropy in mudrocks. Once more, coring suitably orientated specimens parallel and perpendicular to the plane of weakness could be the main difficulty.

The suggested methods for laboratory testing of tensile strength are described in ISRM (1978b). The application of direct tension to specimens involves laboratory testing difficulties and often diametral compression (Brazilian) tests are used. However, the latter compression tests give an 'indirect' tensile strength because the stress conditions at failure are different from those of direct tensile tests. Diametral testing pre-determines the failure surface to specimens and consequently gives results in general higher than the values determined in direct tensile tests (Rocha, 1981). Tensile strength is always lower than compressive strength. Taylor & Spears (1981) have reported that the former may be up to about 17 times lower than the latter in anisotropic mudrocks.

The point load test has been investigated in detail in the last decades by several workers including Franklin *et al.* (1971), Broch & Franklin (1972), Bieniawski (1975) Brook (1980) and Guifu & Hong (1986) and suggested methods for testing have been reviewed by ISRM (1972; 1985). The point load test is extensively used in indurated rock types but it is not suitable for weak or weathered materials. The main advantages of the point

load test are: (a) no sample preparation is required and so irregular lumps specimens may be used, (b) ease and speed of testing which allows the execution of many tests, (c) the apparatus is portable and so the test can be carried out in the field and (d) samples are tested at their natural water content. On the other hand, the main disadvantage of this test is that typically the results show significant scatter. This problem can be overcome to some extent by running a large number of tests and standardising the specimen size and shape.

In order to take account of variations due to size and shape effects, correction charts have been developed which adjust the index to the 50 mm standard-sized specimen (I_{S50}) (Franklin, 1981; ISRM, 1985). Guifu & Hong (1986) has proposed that the area of the failure surface should be measured arguing that this is a more realistic method of computing the failure stress than using the area computed from the distance between the platens.

Investigations on the effects of size and shape variations of irregular samples have shown inaccuracies that increase that where the axial distance (diameter) becomes less than 25 mm and/or 1.0-1.4 times than the average width (ISRM, 1985). Such criteria are difficult to follow in mudrocks because the lumps produced by these rocks are usually flat with the smallest dimension normal to the bedding or parting which is usually also the loading direction in tests. Therefore, in terms of the standardization of the procedures in mudrock testing, Oakland & Lovell (1982) have recommended the use of as close as possible equant samples with the loading direction normal to the bedding or parting planes. The index values are related to the uniaxial compressive strength and a number of correlations have been proposed to estimate the latter (Franklin *et al.*, 1971; Bieniawski, 1975). For mudrocks, however, it is advised to determine a correlation factor for each individual formation.

Testing methods for the Schmidt rebound test-hammer are provided by ISRM (1978a). The Schmidt hammer is mainly used for *in situ* testing (quarries, surface slopes, etc.) but it can also be used in laboratory tests on large diameter core samples which need to be securely clamped. Aufmuth (1974) has found good correlation between rebound number and uniaxial compressive strength and modulus of elasticity for different types of rocks. The use of the type N19 Schmidt hammer for mudrocks has been investigated by Carter

& Mills (1976) and Carter & Sneddon (1977) who proposed correlation curves to convert the rebound number to uniaxial compressive strength values. Another type of rebound test available for the characterization of mudrocks is the Shore scleroscope but relatively poor results were obtained by Lutton (1977) on tests on mudrocks.

The National Coal Board (NCB) cone indenter was developed by Mining Research Development Establishment (MRDE) and was first described in 1969 (Anon., 1969). The test methods include modifications for weak and hard rocks and are given by National Coal Board (1977). The cone indenter is a portable instrument (Fig. 6.10) which tests the strength of very small specimens not bigger than 12x12x6 (mm). The test is suitable for testing small chips of fractured or thinly parted mudrocks and does not require elaborate specimen preparation.

The uniaxial compressive strength of intact rock can be estimated from the cone indenter number and some correlations have been attempted (National Coal Board, 1977; Stimpson & Acott, 1983). However, these correlation factors can not be used universally and a site-specific correlation should be determined before the cone indenter values are used to predict compressive strength (Stimpson & Acott, 1983).

The determination of shear strength parameters is particularly important in stability analysis and design of natural and man-made slopes in mudrocks.

The different behaviour shown by weak mudrocks (or overconsolidated clays) and harder mudrocks, results in different approaches in the assessment of shear strength parameters. In the first case, these parameters depend on the characteristics of the materials and are achieved by carrying out tests habitually used for the determination of the shear strength in soils. In the case of harder mudrocks, the shear strength of rock mass is conditioned by the occurrence of discontinuities, and thus the tests used in Rock Mechanics are applied to determine this property.

The peak, remoulded and residual shear strength parameters of weak mudrock can be determined using triaxial, shear-box and ring-shear apparatus.

Shear-box tests on both undisturbed and remoulded specimens can be used to determine peak, fully softened and residual shear strength parameters in mudrocks. Diagrammatic

shear stress versus displacement curves for these cases are shown in Fig. 2.9. Residual shear strength can be determined using a reversing shear-box apparatus with or without pre-split specimens. However, reorientation of the particles on each reversal, change of the area of the shear surface during the test and finite displacement are disadvantages of this test. The ring shear apparatus such as that described by Bromhead (1979) overcomes these difficulties, but the sample is of limited size.

ISRM (1974) has suggested a laboratory test using the small-box apparatus suitable for the measuring of peak, remoulded and residual shear strength of discontinuities and joint infillings found in harder mudrocks. The use of a large 0.3x0.3 (m) box is proposed by Taylor & Spears (1981) for the assessment of shear strength parameters of major discontinuities and of mudrock aggregates. The orientation of the bedding and the laminations impart an anisotropy to mudrocks which has an important effect on the determination of shear strength parameters. Shear-box tests are customarily used to access this behaviour, being the tests conducted with the structures normal and parallel to the shear plane. Shear-box tests performed on Oxford Clay have shown that tests performed with the laminations normal to the shear plane had slightly higher values of peak and residual effective angle of friction compared with tests in which the laminations were parallel to the shear plane (Jackson & Fookes, 1974).

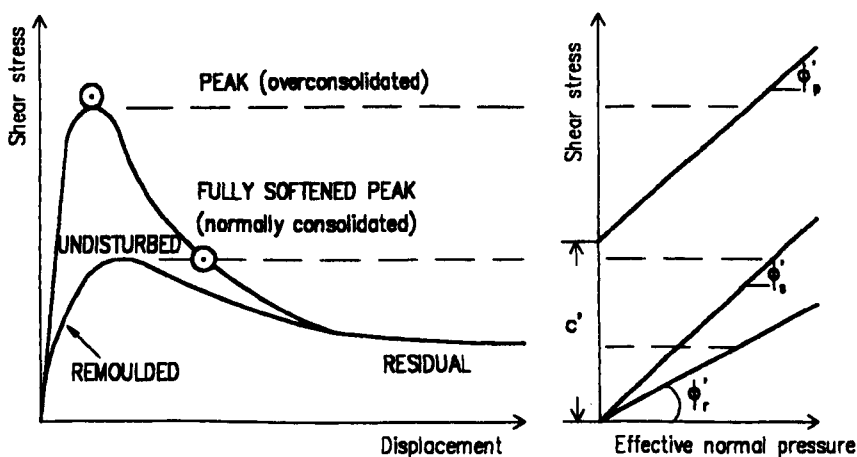


Fig. 2.9 - Relationship between peak, fully softened and residual shear strength of an overconsolidated fissured clay (after Taylor & Spears, 1981).

2.4.2.3 - Swelling tests

Several swelling tests have been developed in the last decades (LNEC, 1967*d*; Nascimento *et al.*, 1968; Duncan, *et al.*, 1968; Volger, 1985; ISRM, 1979*b* and 1989). The parameters determined vary according to the type of test and sample used (undisturbed or powdered).

In ISRM (1979*b*) two methods are given for determining swelling strain. In the former test the axial strain developed in a radially confined specimen against a constant surcharge of 3 kPa is measured. The second method (used in this work) measures the unconfined specimen swelling strain simultaneously on three orthogonal axes. In general the specimen is prepared in such a way that one of the axis is normal to the bedding or parting and therefore any swelling anisotropy can be readily detected.

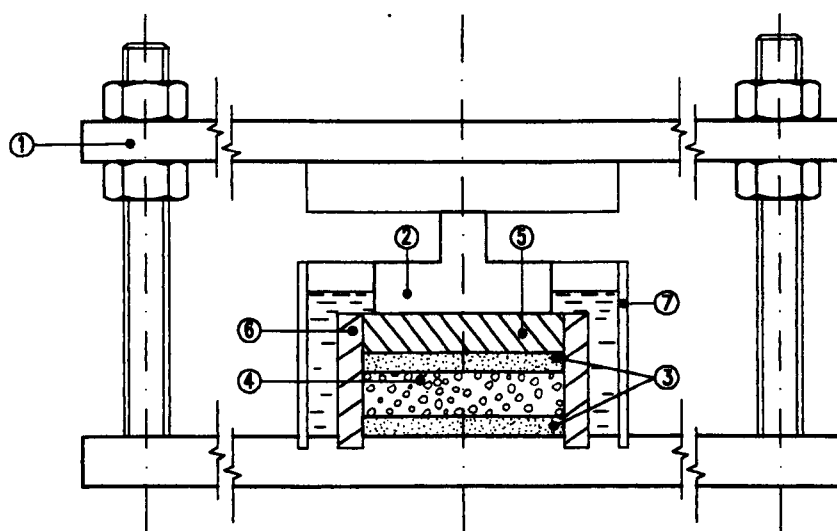
The suggested test method proposed by ISRM (1989) is especially designed for use with argillaceous rocks. According to this method both axial and radial free swelling strains are measured on an unconfined disc shaped specimen (irregular specimens can also be tested). The radial strain is measured with flexible stainless steel band calibrated at 0.1 mm intervals which is attached to the specimen. The main drawback of this method is that the radial swelling strain cannot be monitored during the test. It can only be determined at the end of the test.

From earlier considerations described in Section 2.4.1 swelling may depend on textural features of the rock. Powder swelling tests are a useful method of separating mineralogical and textural influences from each other. For this, the free swell of a powdered sample is measured on immersion in water. The test consists of the measurement in a graduated glass cylinder of the difference between the volumes of the dry powdered sample and after the addition of distilled water. Another method used at LNEC and described in E-200 (LNEC, 1967*d*) uses a deflectometer to determine the swelling of a sample compacted with a plunger which applies a pressure of 0.5 MPa (Fig. 6.12). This method was performed in this work and is described in detail in Section 6.4.1.

When the swelling is constrained the rock develops swelling stress which can be measured using a variety of swelling stress tests: ISRM (1979b and 1989), Franklin (1984), Volger (1985) and Jeremias (1993). Oedometer tests may be used to determine the swelling parameters (swell pressure and free swell) in less indurated mudrocks (BS 1377: Part 5, 1990).

In tests suggested by ISRM (1979b and 1989) a loading device capable of continuous adjustment to keep the volume of the specimen constant is required. Jeremias (1993) has been reasonably successful using an electrical load cell to measure the swelling stress parameters of Cretaceous mudrocks (Fig. 2.10).

For the design and analysis of structures in swelling mudrocks, ISRM (1989) has suggested a special method for determining the axial swelling stress as function of the axial swelling strain. Using this it is possible to estimate the swelling strain necessary to reduce the swelling stress to a value required for the particular application.



- ① - Rigid frame ② - Load measuring device ③ - Porous metal plates ④ - Specimen
⑤ - Stainless steel loading plate ⑥ - Stainless steel ring ⑦ - Cell

Fig. 2.10 - Equipment used to measure axial swelling stress of an undisturbed radially confined rock specimen (after Jeremias, 1993).

2.4.2.4 - Durability tests

From earlier considerations (Section 2.4.1), mudrock durability assessment must be related to a specific agent of weathering. The assessment of mudrock durability in terms of different weathering mechanisms can be obtained by carrying out several ageing tests that simulate the conditions that operate in those mechanisms (in Chapter 7 simulated ageing tests performed to assess mudrock breakdown are described). Simulated ageing tests are, however, very time-consuming and therefore they are mainly used in research studies.

Gamble (1971) and Deo *et al.* (1974) have used modified soundness tests to characterize the durability of mudrocks. Mugrider & Young (1983) have investigated the influence in mudrock breakdown of frost action and cyclic wetting and drying. These researchers have concluded that cycling wetting, freezing, thawing and drying caused more rapid disintegration to the material than only alternate cycles of wetting and drying. However, as pointed out by Franklin & Chandra (1972), climatic slaking is the most effective weathering agent and therefore it is the one that has been included in tests to assess mudrock durability.

Susceptibility to slaking can be evaluated by several test methods described in the literature (Badger *et al.*, 1956; Taylor & Spears, 1970; Franklin *et al.*, 1971; Gamble, 1971; Franklin & Chandra, 1972; Morgenstern & Eigenbrod, 1974; Deo *et al.*, 1974; Wood & Deo, 1975; Chapman *et al.*, 1976; Lutton, 1977; ISRM, 1979b; Venter, 1980; Okamoto *et al.*, 1981; Surendra *et al.*, 1981; Oakland & Lovell, 1982; Dusseault *et al.*, 1983; Hopkins & Deen, 1984). However, the slake durability test developed by Franklin & Chandra (1972), recommended by ISRM (1979b) and standardized by ASTM D 4644 (1992) is by far the most commonly used method. The slake durability index is defined as the percentage of the material retained in a 2 mm mesh drum after two standard cycles of drying and wetting. In each cycle 10 lumps of sample each weighing 40-60 g are rotated 200 revolutions in the slaking fluid in a mesh drum for 10 minutes and then they are oven-dried at 105°C. The effects of several modifications to the standard procedure have been investigated, as set out in Table 2.4.

According to Taylor & Spears (1981), the main drawback of the slake durability test is that reproducibility tends to be poor for weak and very weak mudrocks and it does not distinguish sufficiently between harder and more durable samples. However, it is a very helpful test to assess the potential breakdown features of mudrocks from slaking effects and the two cycle slaking durability (I_{d2}) is used in several classifications of mudrock durability (see Chapter 3).

Table 2.4 - Variables investigated in slake-durability testing procedures.

Variables	Gamble (1971)	Franklin & Chandra (1972)	Venter (1980)	Hopkins & Deen (1984)
Mesh size		X	X	
Weight and number of lumps	X	X		
Initial moisture content of the sample		X		X
Temperature of drying			X	
Drying time		X		
Slaking time	X	X		X
Number of cycles	X		X	X
Nature and temperature of the slaking fluid		X		

The slaking of mudrocks can also be monitored by other types of test such as the static slake test. In its standard form as proposed by Morgenstern & Eigenbrod (1974), this test is very time-consuming but modified test procedures have been developed using one and five wet-dry cycles. The one-cycle slaking test consists of placing in water an oven-dried rock fragment and observing its behaviour over a 24 hours period. A qualitative index provided by Lutton (1977), Dusseault *et al.* (1983), Hopkins & Deen (1984) and Czerewko (1997) allows classification of the slaking behaviour. The five-cycle slaking test consists of an extension of the 1-cycle test that involves 5 wet-dry cycles in which the material is washed over a 2 mm sieve after each cycle (Chapman *et al.*, 1976; Surendra *et al.*, 1981; Oakland & Lovell, 1982). This test provides a quantitative index defined as the percentage of material retained on a 2 mm sieve (#10 ASTM) at the end of 5 cycles, which can be related to the index of slake durability test.

2.4.2.5 - Compaction tests

Compaction tests are intended to determine the dry density - moisture content relationship (compaction curve) of fill materials at one or more compactive efforts. Laboratory compaction curves are derived from tests in which the material under test is compacted at different moisture contents using standardised compactive energy and determining the dry density of the compacted material. The compactive effort is designed to simulate field compaction. The values of maximum dry density (γ_{dmax}) and the corresponding optimum moisture content (w_{opt}) are used as an end-result specification in the construction and control of compacted mudrock embankment and other earthwork structures (Monahan, 1986).

The standard Proctor test [light compaction ASTM D698 (1998)] and modified Proctor test [heavy compaction ASTM D1557 (1998)] are the laboratory procedures customarily used to perform compaction tests. The energy of the latter is about 4.5 times that of the former. All manual compaction tests are performed in a similar way but with differences in the compaction energy (weight of rammer and number of layers and of blows per layer) used and in the size of the mould and sample. The E-197 (LNEC, 1967*b*), the BS 1377: Part 4 (1991) and the ASTM standards referred to above describe the test procedures for the various types of compaction tests.

In weak mudrocks that absorb added water the compaction tests are carried out as for soils using the water content as variable, so that for a specific material and compaction effort an optimum moisture content and maximum density occur (Oakland & Lovell, 1982). On the contrary, in harder mudrocks, due to poorer water absorption characteristics it is difficult to produce a homogeneous moisture content throughout the sample when water is added so a different test procedure is recommended. For this, compaction is carried out at a constant water content such as the natural water content and compaction effort is varied to determine the minimum compaction effort required to produce the selected density value.

The original grading of the material and the change of grading due to compaction in mudrock materials are two variables to consider in both laboratory and field compaction. In practice field compaction may include a high percentage of large

particles affecting the extrapolation of the results of compaction tests determined on less coarse fractions [the percentage retained in the #3/4" ASTM (19 mm) sieve has to be less than 30% (ASTM and BS standards) and/or less than 10% in the #1½" ASTM (37.5 mm) sieve (BS standards)]. However, generally speaking coarser particles are the most susceptible to breakdown and thus cause a large change in the size distribution of the aggregate. This can lead to deterioration of the material in the structure. In order to overcome these difficulties, two main practical methods are used to account for the rock fraction in compaction testing (Houston & Walsh, 1993):

- a) the scalp-and-replace method in which the fraction greater than 19 mm (#3/4" ASTM sieve) is replaced by an equal amount in weight of material in the range of 4.76 mm (#4 ASTM sieve) to 19 mm;
- b) the rock correction equation method in which allowance is made for the coarse fraction in the values of maximum dry density (γ_{dmax}) and optimum moisture content (W_{opt}) determined for the material finer than 4.76 mm (#4 ASTM sieve) as using procedures such as ASTM D4718 (1994) or AASHTO T224 (1982).

Both methods are suited to providing compaction specifications, although it must be recognized that the values of maximum dry density obtained from the former method are customarily lower than those estimated from rock correction equations (Houston & Walsh, 1993). This needs to be taken into account in assessing field compaction performance.

The change of grading between uncompacted and compacted material has been defined as a measure of the degradability of the mudrock occurring during compaction due to breakdown of individual fragments (Hale *et al.*, 1981). These authors reported a compaction-degradation test designed to evaluate the degradability of mudrocks. In this test the index of crushing is determined. This is the initial grading (before compaction)

of the sample fitted to the cumulative distribution given by the following expression (*op. cit.*):

$$P = 100 (d / D)^n \quad (2.2)$$

where,

P - percentage by weight finer than size d,

d - sieve mesh size,

D - maximum aggregate diameter,

n - 1

A CBR mould is used to compact the sample and therefore the maximum aggregate size recommended is 3.8 cm. The compaction is performed in three layers using a modified Proctor hammer with 30 blows per layer. The final grading is measured by dry-sieving and the index of crushing (IC) determined by the difference of the sum of the weighted fractions of size classes between the initial and final gradings and expressed as a percentage of the value of the initial grading.

Tests carried out on Midwestern (USA) mudrocks by Hale *et al.* (*op. cit.*) have demonstrated that the larger sizes of aggregates, mainly, 38-19 mm had the greatest loss of weight due to breakdown of large fragments which increased the amount of smaller sizes classes in the compacted sample. An example of the aggregate size distributions for initial and final gradations at a specific compactive effort is shown in Fig. 2.11 and from the comparison of the two distributions it is also clear that the degradation process produces an aggregate with a smaller mean size.

The moisture condition test is also intended to evaluate the compaction characteristics of compacted materials including mudrocks. It is described in BS 1377: Part 4 (1990). The test uses a specific apparatus, represented schematically in Fig. 2.12, in which the relationship between change of penetration and number of blows is determined for a sample passing a 20 mm sieve. The Moisture Condition Value (MCV) is derived from the steepest straight line that fits the experimental curve (Fig. 2.13) that passes through

the 5 mm change in penetration and is computed as ten times the logarithm of the number of blows at which the changes in penetration equals 5 mm.

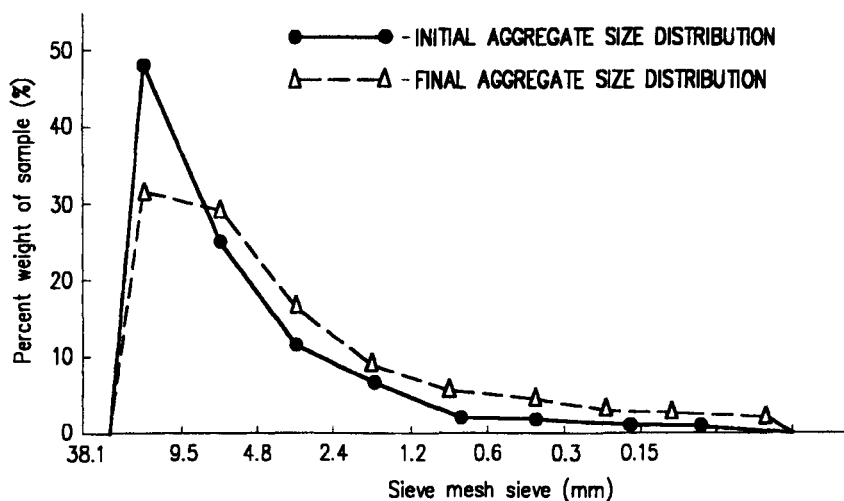


Fig. 2.11 - Initial and final aggregate size distributions for New Providence shale (after Hale et al., 1981).

The apparatus for the moisture condition test (MCV) can be used to determine the Chalk Crushing Value [CCV (BS 1377: Part 4, 1990)] or a similar one to obtain the Aggregate Impact Value [AIV (BS 812: Part 112, 1990)]. Both tests can be used to give a measure of the degradability or crushing of a mudrock aggregate. The former uses a sample in the size range of 20 to 10 mm and the latter of 10 to 14 mm. The CCV is derived from the relation of penetration versus logarithm of number of blows and is computed as one tenth of the slope of the straight line which fits this relationship. The determination of AIV is only suitable for harder mudrocks and is designed as the amount of material finer than 2.36 mm calculated as a percentage of the initial sample weight (Collis & Fox, 1985).

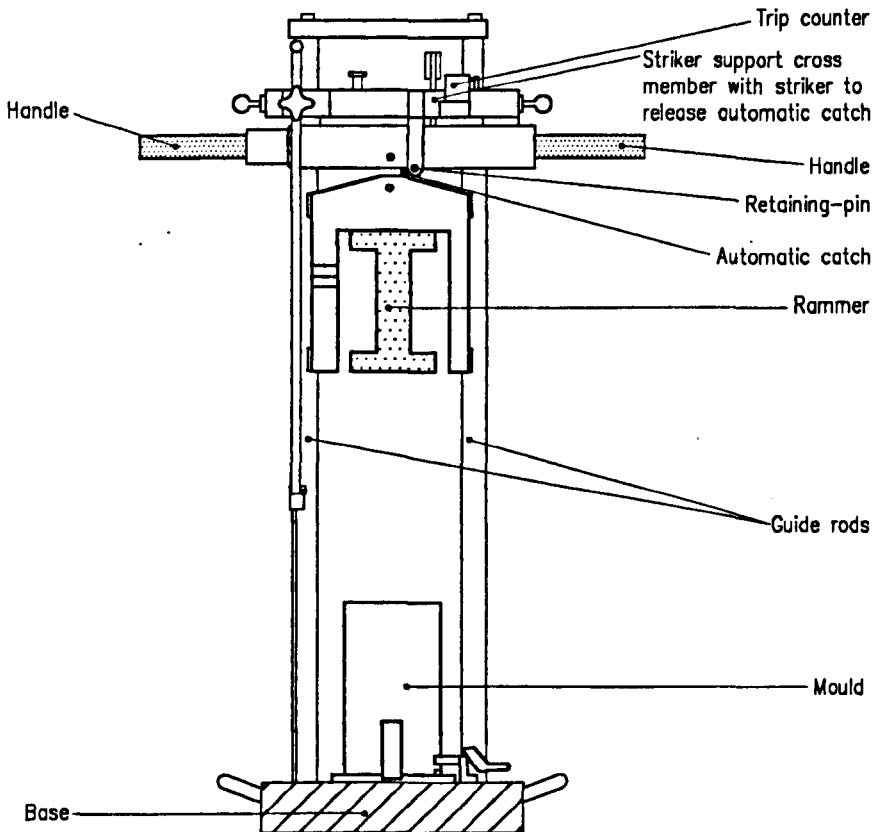


Fig. 2.12 - Moisture condition apparatus (after BS 1377: Part 4, 1990).

The assessment of the behaviour of compacted mudrock samples by means of an empirical strength criterion is provided by California Bearing Ratio Value (CBR). CBR tests [E-198 (LNEC, 1967c); ASTM D1883, (1994)] are widely used for pavement design and construction. For this the force required to cause a cylindrical plunger to penetrate the material sample at a given rate is determined. The CBR value is determined for the force measured at 2.5 and 5.0 mm penetrations which are calculated as a percentage of the standard forces at these penetrations. The CBR test can be performed for various compaction efforts and different water contents. Thus, the evolution of CBR according to the compaction efforts can be determined in relation to a given water content, or for a specific compaction effort, in relation to variation of water content.

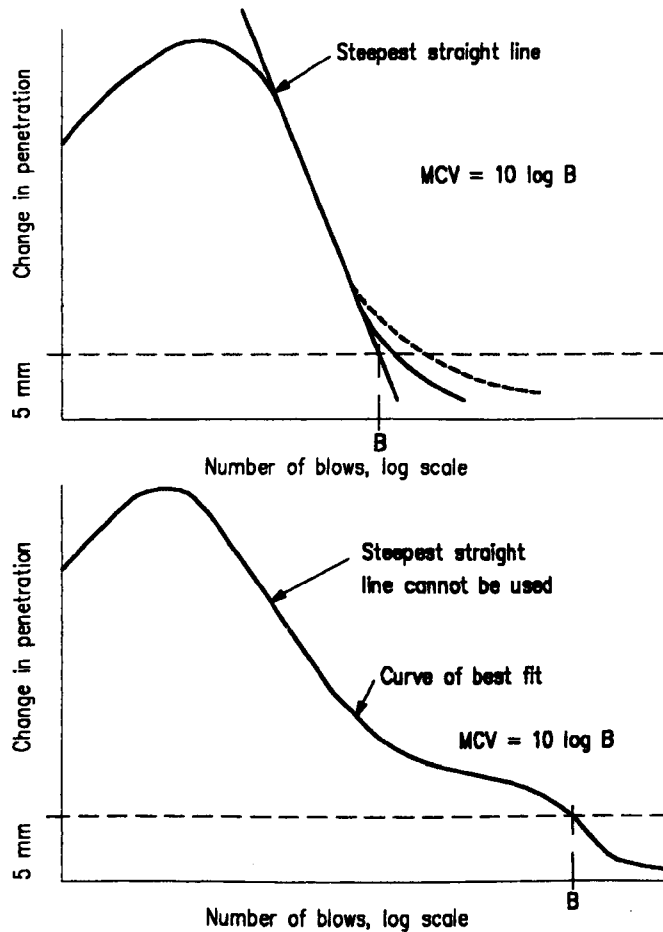


Fig. 2.13 - Relation between change in penetration and number of blows (after BS 1377: Part 4, 1990).

2.5 - Summary

Mudrocks are fine-grained sedimentary rocks which contain more than 50% of siliciclastic grains smaller than 63 μm in size. The siliciclastic grains include, mainly, clay minerals, quartz and feldspar which together customarily make up more than 90% of the total. Clay minerals usually control mudrock behaviour and can reach about 60% of the total. Carbonates occur as a cementing agent and other non-detrital minerals customarily found in mudrocks include pyrite and organic matter together with iron-

-bearing compounds that are important as pigmenting agents. Grey and dark mudrocks usually signify the presence of free carbon and/or pyrite, whilst red and green colours usually relate to the oxidized state of the iron present. The fabric of mudrocks is controlled by depositional environment and the geological stress history. A common texture is one in which the clay flakes are parallel to bedding. Certain mudrocks are prone to splitting or parting along bedding and lamination planes, or discontinuities related to the presence of compaction-induced alignment of clay minerals. The process of splitting is often greatly enhanced by the effects of weathering action. Lamination reflects the vertical variations in composition and texture for layers defined as thinner than 10 mm. The mineralogical composition of mudrocks are readily determined by XRD analyses and the chemical composition by wet chemistry and/or X-ray fluorescence techniques. SEM is the most helpful tool to study their textural features.

The engineering properties of mudrocks are the result of many genetic factors such as composition, degree of over-consolidation and diagenetic changes. Consequently, the increase of depth of burial and the enhancement of diagenetic bonding produces a stronger, more brittle and more durable sediment. However, during weathering, which is initiated by erosion and uplift or by man-made excavation, the material releases its strain energy and the acquired interparticle bonds deteriorate, eventually returning the material to a normally consolidated condition. The degree of weathering together with the composition of the clay size fraction exert a strong control over the geotechnical properties of mudrocks. Weathering in mudrocks, mainly those with a high amount of clay minerals, especially expandable types, leads to reductions in strength and increase in deformability, plasticity and a tendency to undergo swelling and slaking behaviour. These properties can be determined by several laboratory tests selected according to whether the material is 'rock-like' or 'soil-like' in character. However, it can be difficult to determine realistic design parameters for mudrocks since sampling and preparation procedures can cause disturbance to specimens. In particular when values of geotechnical properties are very sensitive to the water content and it can be difficult to maintain samples at their natural water content. As a result of these factors often it is only the stronger more stable types that are tested and thus there can be a tendency to over-estimate the geotechnical performance of the materials.

3 - MUDROCK CLASSIFICATIONS

3.1 - Introduction

The classification of mudrocks is problematic when compared to other sedimentary rock types because of the difficulties in the characterization and description of the properties of these rocks. This fact probably explains why there is no generally accepted geological classification for these rocks. The geological and geotechnical features of mudrocks were analysed in the previous chapter, being some of these properties used as classification parameters in the schemes presented in the following sections.

The classification proposed by the IAEG (1979) for the detrital sedimentary rocks (Fig. 3.1) included mudrocks and can be used as a reference classification of these rocks for engineering purposes. However, this classification does not define the compositional and grain size limits of some of the lithotypes proposed.

Since geotechnical properties vary between the various lithotypes that constitute mudrocks, rigour in the terminology adopted in the classification of these rocks is needed. This objective is pursued in this chapter, in which a terminology defined on the basis of geological criteria for the classification of mudrocks also extended to the area of Engineering Geology, is presented.

DETRITAL SEDIMENTARY ROCKS						
Composition		Grains of rock, quartz, feldspar and clay minerals				> 50% of carbonate grains
Grain size (mm)	60	Very coarse-grained	Rudaceous	Cobbles		Calcarudite
		Coarse-grained		Gravel		
	2	Medium-grained	Arenaceous	Sand	Sandstone: grains are mainly mineral fragments Quartz sandstone: 95% quartz, voids empty or cemented Greywacke: 75% quartz, 15% fine detrital material; rock and feldspar fragments Arkose: 75% qz, up to 25% feldspar: voids empty or cemented	Calcarenite
	0.06	Fine-grained	Argillaceous or lutaceous	Silt	Siltstone: 50% fine-grained particles	Calcisiltite Chalk
	0.002	Very fine-grained		Clay	Claystone: 50% very fine grained particles	Calclutite

Fig. 3.1 - Classification of detrital sedimentary rocks (adapted from IAEG, 1979).

The organization of this chapter is based on three main points: (i) the geological classifications, (ii) the geotechnical classifications, and (iii) the classification scheme adopted for the rocks studied in this work. Thus, in relation to the former, both the geological criteria used as classification parameters and the schemes proposed by the different authors are described. A review and description of some of the geotechnical classifications used to characterize the rock materials applicable to mudrock is also presented. Finally, this chapter presents the classification scheme to describe the mudrocks occurring in the north Lisbon area based on the following parameters: strength, colour, stratification thickness, rock name, discontinuity spacing, other characteristics (when applicable) and weathering state.

Although rock mass features are used in the scheme to describe the materials studied, this chapter does not cover classifications developed for rock mass. The objective of these classification systems, namely, those proposed by Wickham *et al.* (1972), Bieniawski (1973) and Barton *et al.* (1974) is to obtain rock mass parameters that can be used in the design of structures, especially, for tunnelling. Despite the relevance of the application of these rock mass classification systems to the rocks studied in this work, this was not possible due to the difficulties in determining some of the parameters

required by these classifications such as the groundwater conditions. Thus, the revision and analysis of the geotechnical classifications presented in this chapter only cover those that characterize the rock material.

3.2 - Geological classifications

3.2.1 - Geological criteria used for classification of mudrocks

Several criteria have been used by different authors for classification of fine-grained sedimentary rocks. Picard (1971) has reviewed those used in North American literature which include texture (particle size), parting (fissility), mineral composition, colour, chemical composition, degree of metamorphism and tectonic association or depositional environment. Nevertheless, *texture* and *structure* (fissility and stratification) are the properties customarily used in mudrock classification.

Texture is characterized by the particle size of the components of mudrocks, *i.e.* mainly by the relative amounts of clay size and silt size fractions present on these rocks. However, the boundary between silt and clay can be taken as $4\ \mu\text{m}$ ($1/256\ \text{mm}$) using the Wentworth's scale or as $2\ \mu\text{m}$ like it is defined in geotechnical engineering. The higher silt limit (silt-sand boundary) can also have different values as it is shown in Fig. 3.2.

Most of geological classifications of mudrocks consider a less than $4\ \mu\text{m}$ clay fraction, which include clay minerals and clay size components such as carbonate and silica. Nevertheless, Pettijohn (1975) advocated for consolidated sediments the use of $1/100\ \text{mm}$ limit to distinguish between siltstone and mudstone/shale because rocks coarser than this limit have the field features of sandstones and those that are finer have the characteristics of mudstone/shales.

Grain size determination is a difficult task in mudrocks. Field criteria such as appearance (hand lens observation) and sense of touch (grittiness, smoothness and plasticity) are used to estimate roughly the relative amounts of silt-sized and clay-sized particles present in mudrocks. In laboratory particle size distributions can be determined

by size analysis (sieving and sedimentation) and petrographic and SEM techniques. Size analysis carried out in mudrocks may reflect more the effectiveness of the disaggregation and dispersing techniques applied rather than the original particle assemblage of the sediment. (Spears, 1980; Blatt *et al.*, 1980; Hawkins & Pinches, 1992). Size measurements using petrographic thin-sections are limited to the coarse silt and sand fractions. SEM studies provide very valuable data but are not practical for routine analysis. Furthermore, clay minerals may flocculate during sedimentation and deposition as silt size aggregates rather than single particles. As well as diagenetic processes may form new clay minerals modifying also the initial size distribution. Therefore, description schemes relying only on grain size determination can be of reduced significance and imprecise for classification purposes of mudrocks.

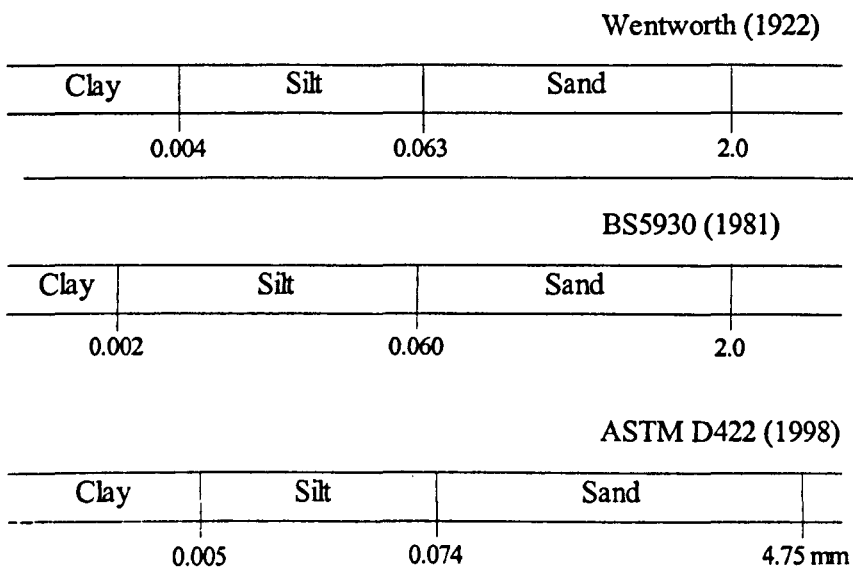


Fig. 3.2 - Comparison of the grain size limits defined by the *Wentworth (1922)*, *BS 5930 (1981)* and *ASTM D422 (1998)* scales.

Structure is characterized by stratification and fissility which were described in Section 2.2.3. On mudrocks fissility can be related either with the preferred alignment of clay particles or with compositional laminae which produces weakness surfaces parallel to the stratification. In spite of fabric alignment may account to produce anisotropy of properties (such as strength) of fresh mudrocks, the development of fissility is very enhanced by superficial weathering processes, being absent in rocks collected at depth.

Consequently, as classification factor the utility of fissility is limited to the surface samples (Lundegard & Samuels, 1981).

Stratification may be characterized by variations in colour, composition and/or fabric and is subdivided in laminae and beds at the 10 mm boundary. The classes of thickness for each one are given at Table 3.2. When beds are presented the suffix *-stone* is attached accordingly to the grain size class (silt, mud or clay) whilst if laminae occur, the suffix *-shale* is used. Thus, *shale* means a laminated mudrock.

In summary, grain size and stratification seem to be the most helpful properties for describing and classifying mudrocks. Descriptive modifiers such as colour, mineralogy, fossil content, type of fracture and state of induration are commonly attached to the root names proposed in classifications in order to define better the mudrock.

3.2.2 - Classifications

Several schemes to describe and classify mudrocks have been proposed in the last decades, however, there is no classification for these fine-grained sedimentary rocks widely accepted amongst geologists (Pettijohn, 1975; Potter *et al.*, 1980; Lundegard & Samuels, 1980; Grainger, 1984). Consequently, the lack of a standard terminology for fine-grained rocks leads that often confusion arise when, for example, geologists and engineers are describing and classifying these rocks.

The genetic classifications based on tectonic associations and environments of deposition have failed to prove to distinguish amongst the various types of mudrocks. Therefore, descriptive schemes based on features (see Section 3.2.1) with some genetic significance have been the way chosen to classify these rocks. The mudrock geological classifications most widely accepted are reviewed next.

Classifications based on texture

Wentworth (1922) proposed the size limits used for both sediments and clastic rocks and class terms according to certain percentages for the mixtures of clay, silt and sand: silty sand (sand > silt >10%, others <10%); sandy silt (silt > sand >10%, others <10%); silt (silt >80%); clayey silt (silt > clay >10%, others <10%); silty clay (clay > silt >10%, others <10%); and clay (clay >80%). Lithified equivalents can be derived from these classes such as silty sandstone, sandy siltstone, siltstone, clayey siltstone, silty claystone and claystone.

The field classification proposed by Picard (1971) is based on the proportions of clay, silt and sand, and on sorting. The sediments and fine-grained rocks are classified using a triangular diagram whose endpoints are clay, silt and sand (Fig. 3.3). This author used the 50% percent limit to define four main divisions: claystone, siltstone, sandstone and mudstone. Three classes for sorting were also proposed based on the amount of silt or clay: good (>90% of silt or clay), fair (75 to 90% of silt or clay) and poor (<75% of silt or clay). Others features of the rocks such as splitting characteristics, colour, type of cement, fossil content and sedimentary structures are also recommended to be included in the field descriptions.

Classifications based on texture and fissility

Ingram (1953) suggested a classification based on the grain size and on the splitting (fissility) characteristics of fine-grained sedimentary rocks that contain more than 50% of silt and/or clay (Table 3.1). This author proposed the terms massive, flaky-fissile and flaggy-fissile to describe the fragments that result from the breaking of the sedimentary rocks. Folk (1968) used the Ingram's classification scheme but proposed limits for the amount of silt and/or clay of each class (Table 3.1). This author suggested that mudstone is defined by subequal silt and clay fraction.

Blatt *et al.* (1980) proposed a similar classification but defined an ideal size distribution between $\frac{1}{3}$ and $\frac{2}{3}$ of silt for mudstone/mudshale (Table 3.1). Stow (1981) suggested a

mudrock terminology including textural and compositional descriptors that follow the previous classifications (Table 3.1).

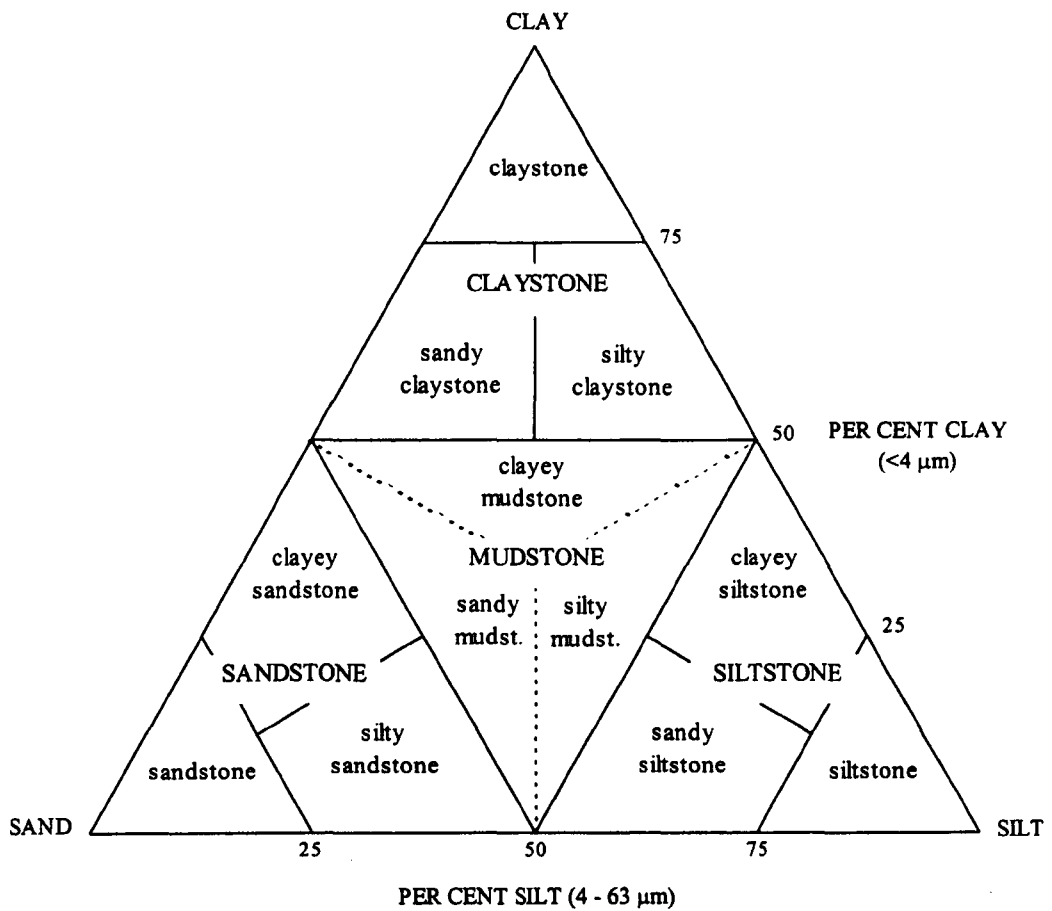


Fig. 3.3 - Textural classification of sedimentary rocks of sand-silt-clay grain sizes (after Picard, 1971).

Classifications based on texture and stratification

Potter *et al.* (1980) proposed a classification for mudrocks that is based on the state of induration, the relative amounts of clay-size and silt-size constituents, and bedding and laminae thickness (Fig. 3.4). This classification does not use fissility as classification factor, but the presence or absence of lamination to distinguish between massive and ‘shale’ (laminated) mudrocks. The terms bedded and laminated siltstone are suggested in place of siltstone and siltshale. These authors also suggested common modifiers to be used in mudrock descriptions..

Table 3.1 - Classifications of fine-grained sedimentary rocks containing more than 50% grains less than 63 μm (silt and/or clay) suggested by Ingram (1953), Folk (1968) Blatt et al. (1980) and Stow (1981).

Ingram terminology			
	No connotation as to breaking characteristics	Massive	Fissile
No connotation as to relative amounts of silt and clay	Mudrock	Mudstone	Mudshale
Silt predominant over clay	Siltrock	Siltstone	Siltshale
Clay predominant over silt	Clayrock	Claystone	Clayshale
Folk terminology			
Grain size of mud fraction		Non-fissile	Fissile
> $\frac{2}{3}$ Silt		Siltstone	Siltshale
Subequal silt and clay		Mudstone	Mudshale
> $\frac{2}{3}$ Clay		Claystone	Clayshale
Blatt, Middleton & Murray terminology			
Ideal size definition	Field criteria	Non-fissile	Fissile
> $\frac{2}{3}$ Silt	Abundant silt visible with hand lens	Siltstone	Siltshale
> $\frac{1}{3}$ < $\frac{2}{3}$ Silt	Feels gritty when chewed	Mudstone	Mudshale
> $\frac{2}{3}$ Clay	Feels smooth when chewed	Claystone	Clayshale
Stow terminology			
Mudrock (> 50% siliciclastic, > 50% less than 63 μm)			
Basic terms unlithified	Approximated proportions/grain size	Lithified/non-fissil	Lithified/Fissile
Silt	> $\frac{2}{3}$ Silt sized (4 - 63 μm)	Siltstone	Siltshale
Mud	Silt and clay mixture (< 63 μm)	Mudstone	Mudshale
Clay	> $\frac{2}{3}$ Clay sized (< 4 μm)	Claystone	Clayshale
<u>Metamorphic terms</u>			
Argillite	Slit and clay mixture	Slightly metamorphosed/non-fissile	
Slate	Silt and clay mixture	Metamorphosed/fissile	
<u>Textural descriptors</u>		<u>Approximated proportions</u>	
Silty	> 10% Silt size		
Muddy	> 10% Silt size or clay size (applied to non-mudrock sediments)		
Clayey	> 10% Clay size		
Sandy, pebbly, etc	> 10% Sand size, pebble size, etc		
<u>Compositional descriptors</u>		<u>Approximated proportions</u>	
Calcareous	> 10% CaCO_3 (foraminiferal, nannofossil, etc)		
Siliceous	> 10% SiO_2 (diatomaceous, radiolarian, etc)		
Carbonaceous	> 1% Organic carbon		
Pyritiferous	Commonly used for contents greater than about 1- 5 %		
Ferruginous			
Micaceous			
Others			

Percentage clay-size constituents		0 - 32	33 - 65	66 - 100	
Field Adjective		Gritty	Loamy	Fat or Slick	
NONINDURATED	Beds	Greater than 10 mm	BEDDED SILT	BEDDED MUD	BEDDED CLAYMUD
	Laminae	Less than 10 mm	LAMINATED SILT	LAMINATED MUD	LAMINATED CLAYMUD
INDURATED	Beds	Greater than 10 mm	BEDDED SILTSTONE	MUDSTONE	CLAYSTONE
	Laminae	Less than 10 mm	LAMINATED SILTSTONE	MUDSHALE	CLAYSHALE
METAMORPHOSED	Degree of metamorphism	LOW ↓ HIGH	QUARTZ ARGILLITE	ARGILLITE	
			QUARTZ SLATE	SLATE	
			PHYLLITE AND/OR MICA SCHIST		

Fig. 3.4 - Classification of mudrocks proposed by Potter et al. (1980).

Lundegrad & Samuels (1980) suggested a classification very similar to the previous one which uses grain size (silt content) and stratification (presence or absence of lamination) for subdivision of classes. These authors suggested that 10% of laminae is a generally acceptable limit to consider mudrock as a 'shale' in rocks with less than $\frac{2}{3}$ of silt and recommend the use of the term siltstone for all rocks with a percentage of silt greater than $\frac{2}{3}$.

A modified form of Potter *et al.*'s classification has been used by Dick & Shakoor (1992) and Dick *et al.* (1994). These authors suggested the placement of the textural division between mudstones and claystones at 50% of clay because this boundary reflects a change in the durability behaviour of mudrocks.

Classifications based on mineral composition

Using the textural terminology of his field classification Picard (1971) proposed a laboratory classification of fine-grained clastic rocks based on the mineral composition. Thin-section petrographic studies and XRD analyses were used to determine the mineral composition of silt-size and clay-size fractions. This author suggested that the fine-grained rocks should be classed according to the sandstone nomenclature and the dominant clay mineral present.

The laboratory classification of very fine-grained rocks presented by Lewan (1978) is also based on textural and compositional features. According to this classification the silt content is evaluated using thin-sections and the mineralogy is determined by XRD analyses.

Spears (1980) has proposed a mudrock classification based on quartz percentage (Table 3.2). This author noted that the decrease in grain size in mudrocks is followed by a decrease in the quartz percentage. Thus, the silt and clay fractions in mudrocks can be estimated from the proportions of quartz and clay minerals present in the rock. The quartz content can be determined by chemical dissolution methods (Trostel & Wynne, 1940; Chapman *et al.*, 1969) or by a X-ray diffraction method (Till & Spears, 1969).

Table 3.2 - Mudrock classification based on quartz percentage (after Spears, 1980).

	Mudrocks	
	Fissile	Non-fissile
> 40% Quartz	Flaggy* siltstone	Massive* siltstone
30 - 40% Quartz	Very coarse shale	Very coarse mudstone
20 - 30% Quartz	Coarse shale	Coarse mudstone
10 - 20% Quartz	Fine shale	Fine mudstone
< 10% Quartz	Very fine shale	Very fine mudstone

* Following McKee & Weir, 1953.

From the study of Coal Measures Spears (*op. cit.*) found that a quartz content larger than 40% corresponds to rocks which are identified in the field as siltstones with median grain sizes greater than $1/_{100}$. The subdivisions shown in Table 3.2 were developed to Coal Measures which contain negligible feldspar and non-detrital minerals in less than

10% by weight. An excess of the content of these components should be taken into account when this classification is used.

Weaver (1989) advocated the need of a new term *physil* which include all sheet silicate minerals and has no size mean (see Section 2.2.1). This author suggested a classification of fine-grained rocks (Table 3.3) for both non-indurated and indurated types based on texture and on the physil content. Therefore, the terms physil and physilitic can be used if the physil content is greater than 50% (physil clay, calcareous physil claystone, etc.) or less than 50% (calcareous physilitic clay, physilitic silt, etc.).

Table 3.3 - Classification of fine-grained rocks based on proportion of phyllosilicates (after Weaver, 1980; 1989).

Texture	Composition			
	Non-indurated		Indurated	
	>50% Physils	<50% Physils	>50% Physils	<50% Physils
>50% Silt ($1/256 - 1/16$ mm)	Physil silt	Physilitic silt	Physil siltstone	Physilitic siltstone
>50% Clay ($<1/256$ mm)	Physil clay	Physilitic clay	Physil claystone	Physilitic claystone

3.3 - Classifications of mudrocks for engineering proposes

3.3.1 - Engineering definition of mudrock

A continuous geotechnical spectrum of materials from loose sands and soft clays to hard rocks exists, however, a main concern in geotechnical practice dealing with mudrocks has been the placement of a soil/rock boundary (Hencher, 1993). From a geological point of view as noted by Cripps & Taylor (1981), there is no distinction between mudrocks and overconsolidated clays and the differentiation between ‘soil-like’ and ‘rock-like’ properties are markedly influenced by factors such as the state of induration (bonding and cementation), rebound history and degree of weathering. One of the first approaches to this problem was the distinction between ‘compacted shales’ and ‘cement shales’ proposed by Mead (1936) and followed by Underwood’s (1967) classification

which recognizes the importance of the 'soil-like' and 'rock-like' character in geotechnical properties of mudrocks. In the first group the materials are the result of consolidation due to the weight of overlying sediments, they have no inter-granular cement and are subdivided, according to their grain size characteristics. In the second group the rocks have inter-granular cement which may be calcareous, siliceous, ferrous, gypsiferous, phosphatic, etc. The various lithotypes in this group are classified according to their chemical composition.

Further attempts for a definition of a soil/rock boundary rely commonly on the results of laboratorial tests. Morgenstern & Eigenbrod's (1974) criteria used the undrained shear strength value of 1.8 MPa*, *i.e.* an uniaxial compressive strength (UCS) of 3.6 MPa ($S_u = C_u = 1/2 \sigma_c$), to differentiate between mudstones and clays. From tests conducted on a variety of materials which included both soil and rock samples (sands and clays; mudstones, limestones, schists, etc.) Rocha (1977) concluded that cohesion and uniaxial compressive strength are the best parameters to distinguish between soils and rocks. Based on the results obtained Rocha (*op. cit.*) proposed that materials with a cohesion greater than 0.3 MPa and a uniaxial compressive strength larger than 2 MPa are classified as rocks. The latter value was used by ISRM (1981) in BGD (Basical Geotechnical Classification) for the lower limit of rock strength. Rocks were assigned to very weak (UCS 0.6-1.25 MPa) and weak (UCS 1.25-5 MPa) following BS5930 (1981) and IAEG (1981) recommended a UCS value of 1.25 MPa as the lower limit of strength of rocks. According to the method of Morgenstern & Eigenbrod (1974) a compressive strength value of 0.6 MPa (undrained shear strength of 0.3 MPa) was suggested by Grainger (1984) for the lower value of soil-like mudrocks.

In Fig. 3.5 some of the limits suggested for different institutions for the soil/rock boundary are presented and as it is shown no standardization exists for definition of weak rock. Thus, mudrocks with low UCS values are classified as rocks according to some classifications and as soils by others. This can have serious geotechnical and contractual implications in engineering works where these rocks occur. Another problem as noted by Oliveira (1993) is the proper term of weak rock which is also a

* $S_u = 1/2 \sigma_c$ which is equivalent to a uniaxial compression strength (UCS) of 3.6 MPa.

relative concept in engineering because any material may be considered weak if it fails under loads imposed by the construction of structures.

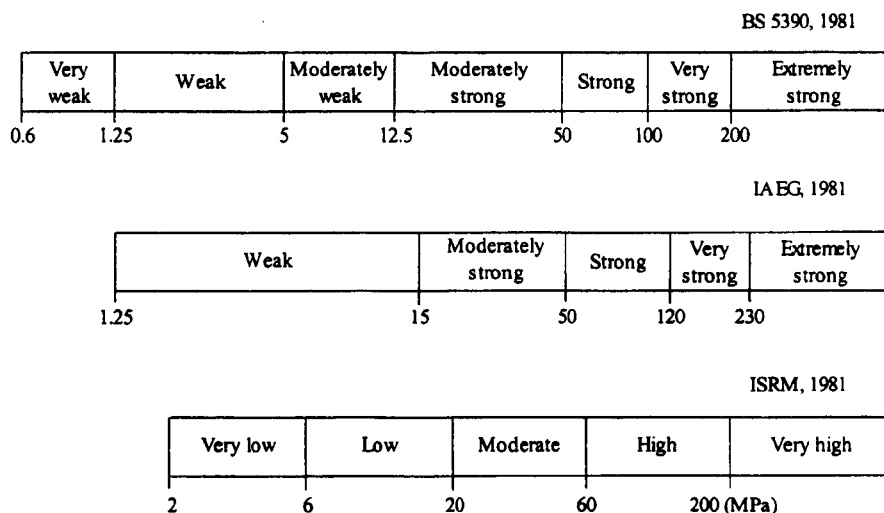


Fig. 3.5 - Definitions of weak rock according to various standards (adapted de ISRM, 1981; IAEG, 1981 e BS 5930, 1981).

3.3.2 - Classifications

Difficulties arise with the classifications of mudrocks. Those based on geological features noted by Deen (1981) do not provide suitable information for engineering purposes. On the other hand soil engineering classification based on grain size distribution and Atterberg limits is of limited application to mudrocks because it can only be used for less indurated types.

Clark & Walker (1977) propose a classification scheme for the engineering description of a range of sedimentary materials between the extremes of total carbonate and total non-carbonate. According to their scheme the separation of the materials is based on grain size, carbonate content, degree of induration and strength. They provided an approximation of the unconfined compressive strength for each material type and suggest, for the assessment of strength in the field, the use of a pocket penetrometer, hand vane or point load tester.

A detail engineering geological classification scheme presented by Hawkins & Pinches (1992) for the field identification and description of mudrocks is based on colour,

bedding and discontinuities characteristics, degree of weathering and strength. They considered that siltstone and claystone are markedly different in both geological features and engineering behaviour due to their composition. They therefore redefined the boundary between these rocks based on percentage of clay fraction (claystone >40% clay fraction; siltstone <25% clay fraction). This classification also suggested placing the rock/soil boundary at 20% soil and provided criteria for the assessment of field strength for both soils and rocks.

In the last decades, mainly due to the increase of engineering construction involving mudrocks, several workers have proposed various classification schemes of rock material based on mechanical and engineering properties (Deen, 1981). Thus, the classification of mudrocks on the basis of these schemes provides criteria on selection of the materials, which can be applied in site selection, design, construction and maintenance of major structures. Table 3.4 presents the soil and rock characteristics used in some of the classifications found in the literature.

Table 3.4 - Soil and rock characteristics used in engineering geological classifications of mudrocks.

Soil and rock characteristics	Classifications											
	Deere & Miller (1966)	Gamble (1971)	Deo <i>et al.</i> (1974)	Morg. & Eigen. (1974)	Lutton (1977)	Olivier (1976)	Franklin (1981)	Grainger (1984)	Rodrigues (1986)	Felix (1987)	Taylor (1988)	Dick <i>et al.</i> (1994)
Mineralogy (form XRD analysis)								X			X	
Anisotropy (flakiness ratio)								X				
Microfracture frequency index												X
Porosity									X			
Grain size								X				
Absorption water												X
Atterberg limits		X		X			X	X				
Uniaxial compressive strength	X					X		X		X	X	
Undrained shear strength				X				X				
Young's modulus (E_1 or E_2)	X											
Point load strength						X	X	X			X	
Cone Indenter number								X				
Free swelling strain						X			X	X		
Slake durability (evaluated from Jar slake)			X	X								
Slake durability (evaluated from slake durability test)		X	X		X		X	X			X	X
Rate of slaking				X								
Durability (evaluated from cyclic wet-dry tests*)			X									

*Tests carried out using a sodium sulphate solution.

The data presented in Table 3.4 show that several classifications use the slake durability test to predict the behaviour of mudrocks. Plasticity obtained from the Atterberg limits is adopted mainly to classify the less indurated types. Strength parameters determined from uniaxial and triaxial compressive tests, or from point load tests are customarily used to distinguish between durable and non-durable mudrocks and to subdivide the harder types.

Deere & Miller (1966) have proposed a general classification chart for intact rock materials based on uniaxial compressive strength and Young's modulus, which differentiated between specific rock types, including mudrocks (Fig. 3.6).

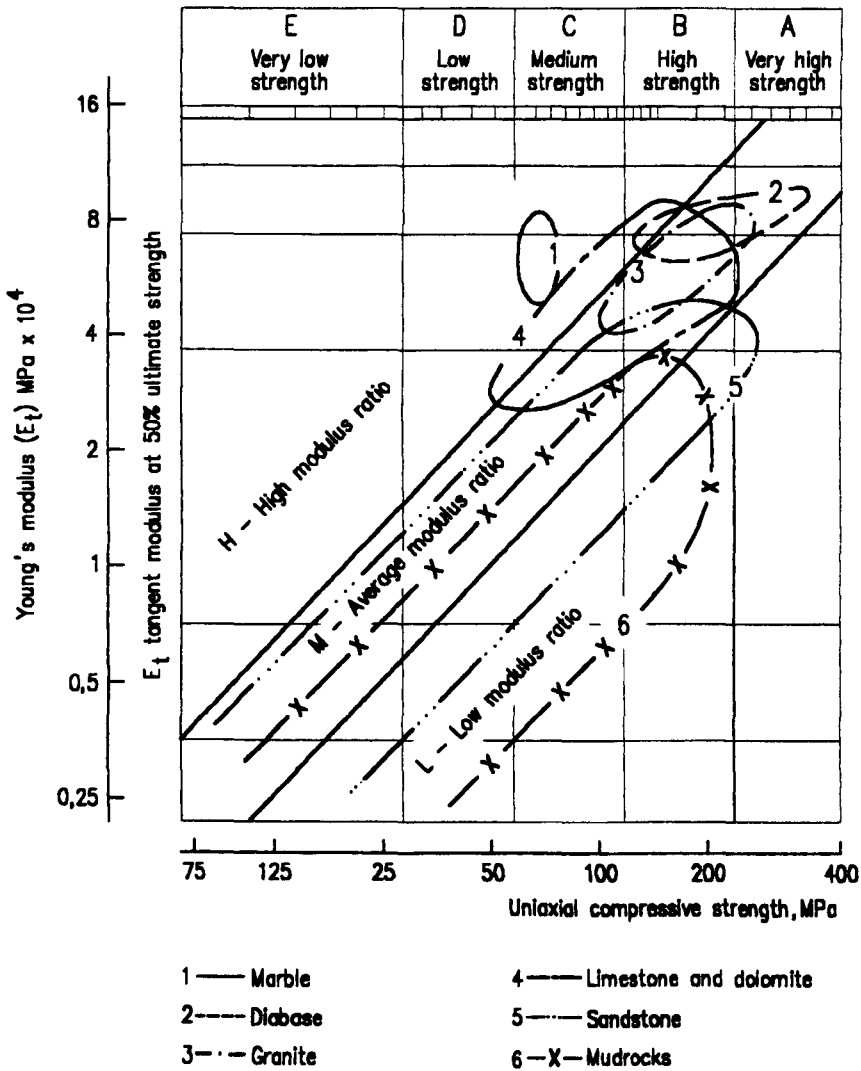


Fig. 3.6 - Engineering classification of intact rock showing fields for igneous, sedimentary and metamorphic rocks (after Deere & Miller, 1966).

They noted that the envelope for mudrocks extends into the zone of low modulus ratio (modulus/uniaxial compressive strength) which they concluded to be a result of anisotropy ascribable to presence of bedding and lamination. However, the application of this classification to the Karoo mudrocks by Olivier (1976) revealed its inability to differentiate between rocks of high and low durability. This he attributed to the lack of consideration in the classification of swelling properties of the rocks studied.

Gamble's (1971) durability-plasticity classification of mudrocks recognizes six classes of durability based on plasticity index and two-cycle slake durability. The durability classes are defined in the graph presented in Fig. 3.7. The application of this classification by Olivier (1976) to the Karoo mudrocks in South Africa showed that it is not sensitive to the important distinction between durable and non-durable mudrocks. This is mainly because the rock material disintegrates into fragments that are retained on the 2 mm mesh of the slake durability apparatus and thus over-estimated the durability of the rocks. As noted by Franklin (1981) another problem concerned with the application of this classification to hard mudrocks, is related to disaggregatibility of such rocks in order to determine the Atterberg limits.

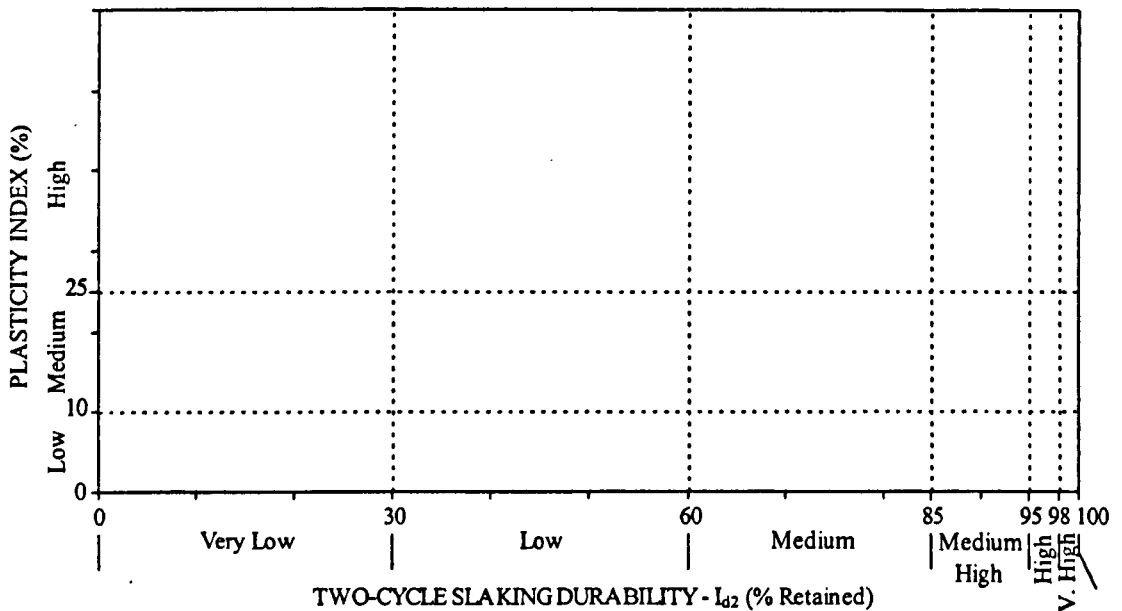


Fig. 3.7 -Durability-plasticity chart of Gamble (1971).

Morgenstern & Eigenbrod (1974) proposed an engineering classification for argillaceous materials based on a strength softening test, slaking test, rate of slaking and liquid limit. From the results of the former test they suggested a major differentiation between clays and mudstones on the basis of an undrained shear strength of 1.8 MPa. They suggested also that the liquid limit can be used to predict the amount of slaking and together with the rate of swelling classed the materials in terms of slaking characteristics. Unfortunately the complete scheme proposed by Morgenstern & Eigenbrod (*id.*) is too time-consuming to use in most practical situations, tests to determine strength softening being particularly laborious. Accordingly only that part of the scheme relating to the assessment of slaking characteristics on the basis of liquidity limit and slaking rate is usually adopted (Chapman *et al.*, 1976).

Wood and Deo (1975) proposed a classification for assessment of mudrock durability for use in highway embankments. This is based on a slake test, slake durability test performed on dry and soaked samples, and a modified sodium sulphate soundness test. According to the flow chart in Fig. 3.8 the rocks were classified in different embankment-use categories from soil-like shales (non-durable) to rock-like shales (durable).

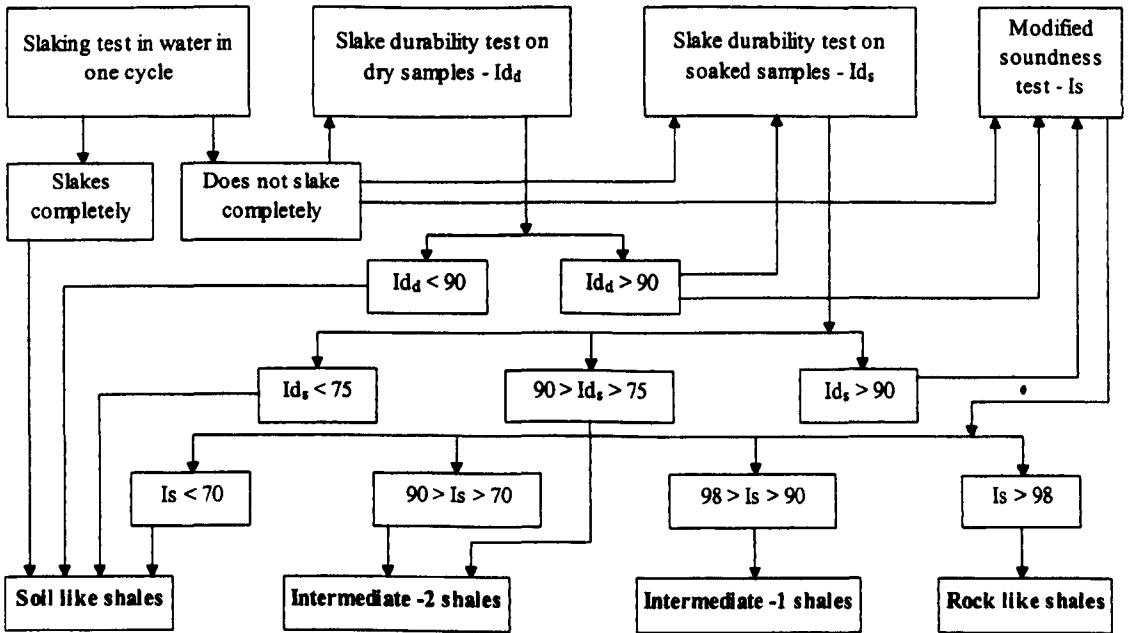


Fig. 3.8 - Classification of mudrocks for embankment construction (after Deo *et al.*, 1974).

A *Geodurability* classification was developed by Olivier (1976; 1979) for the siltstones, sandstones and mudstones of Karoo Supergroup in South Africa and is based on uniaxial compressive strength or point load strength, and 'Duncan' free swelling coefficient (Fig. 3.9). He proposed six classes to rank the rock materials from very poor to excellent and considered that one of the limitations of his classification is the variation of the index properties selected within rock units or lithological horizons. To overcome this problem he recommended that large number of samples be tested in order to provide representative values. However, the need for a great number of swelling tests or uniaxial compressive tests in mudrocks remains a problem.

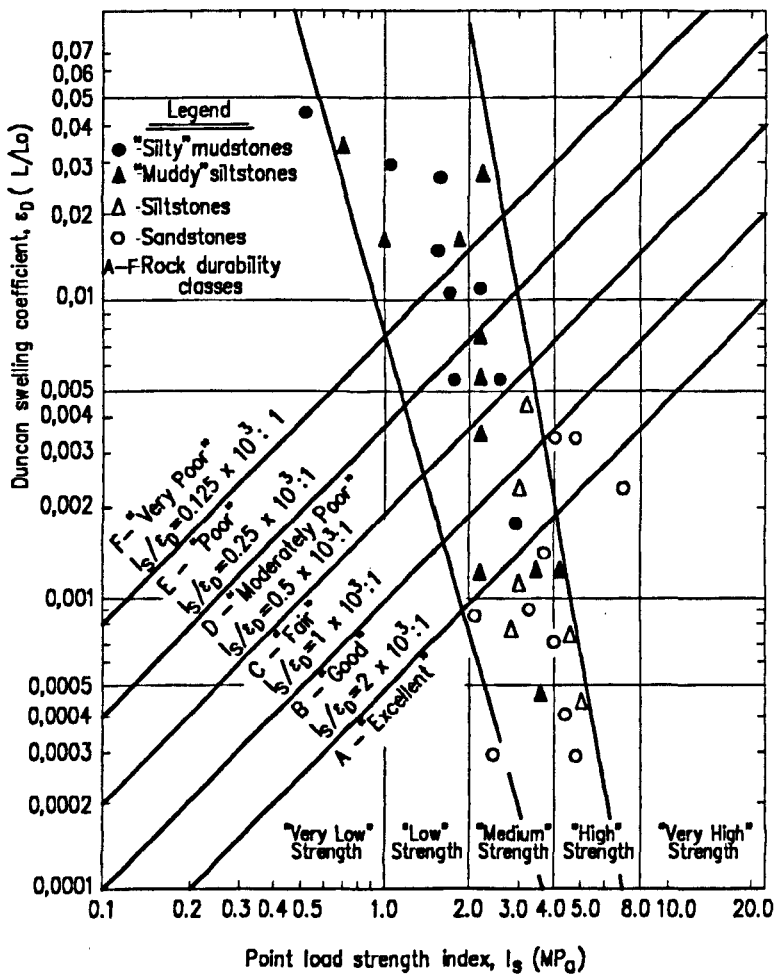


Fig. 3.9 - Olivier's geodurability classification developed for strong mudrocks and arenaceous types of the Karoo Supergroup (after Olivier, 1976).

Lutton (1977) carried out an extensive study relating slake-durability, construction lift thickness and embankment performance on mudrocks placed in highway fills in USA. On the basis of this research he proposed the graph presented in Fig. 3.10 where the results of slake durability test can be used to evaluate and predict the behaviour of existing embankments, as well as to define the lift thickness to be used on construction of new embankments. Following this work Strohm *et al.* (1978) suggested technical guidelines for highway embankment design based on durability characteristics of mudrocks.

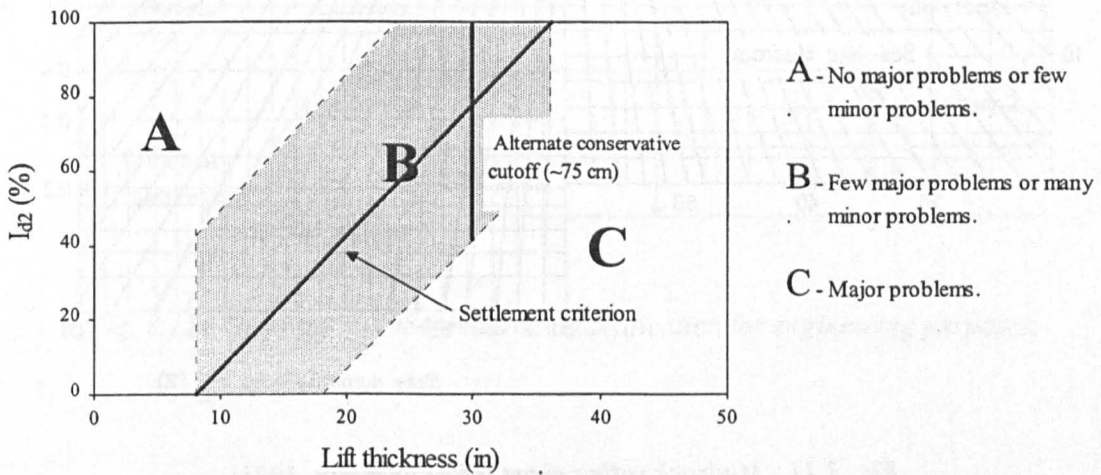


Fig. 3.10 - Criterion for evaluating embankment construction on the basis of slaking behaviour of materials (after Lutton, 1977).

Franklin (1981) proposed a mudrock rating system based on slake durability, point load strength and plasticity index. The shale rating chart shown in Fig. 3.11, provides a continuous and quantitative classification of mudrocks. A rating number is assigned according to: (a) its slake durability and plasticity if the mudrock is soil-like and has slake durability index less than 80%, (b) its slake durability and strength (point load strength) if the mudrock is rock-like and has slake durability index (I_{d2}) greater than 80%. Franklin (*id.*) attempted correlations linking the rating number to aspects of engineering performance of mudrocks observed in construction projects such as foundations, embankments and cut slopes, however, as noted by Franklin (1981) care should be taken in using these correlations (*e.g.* in design) because they are based on limited data.

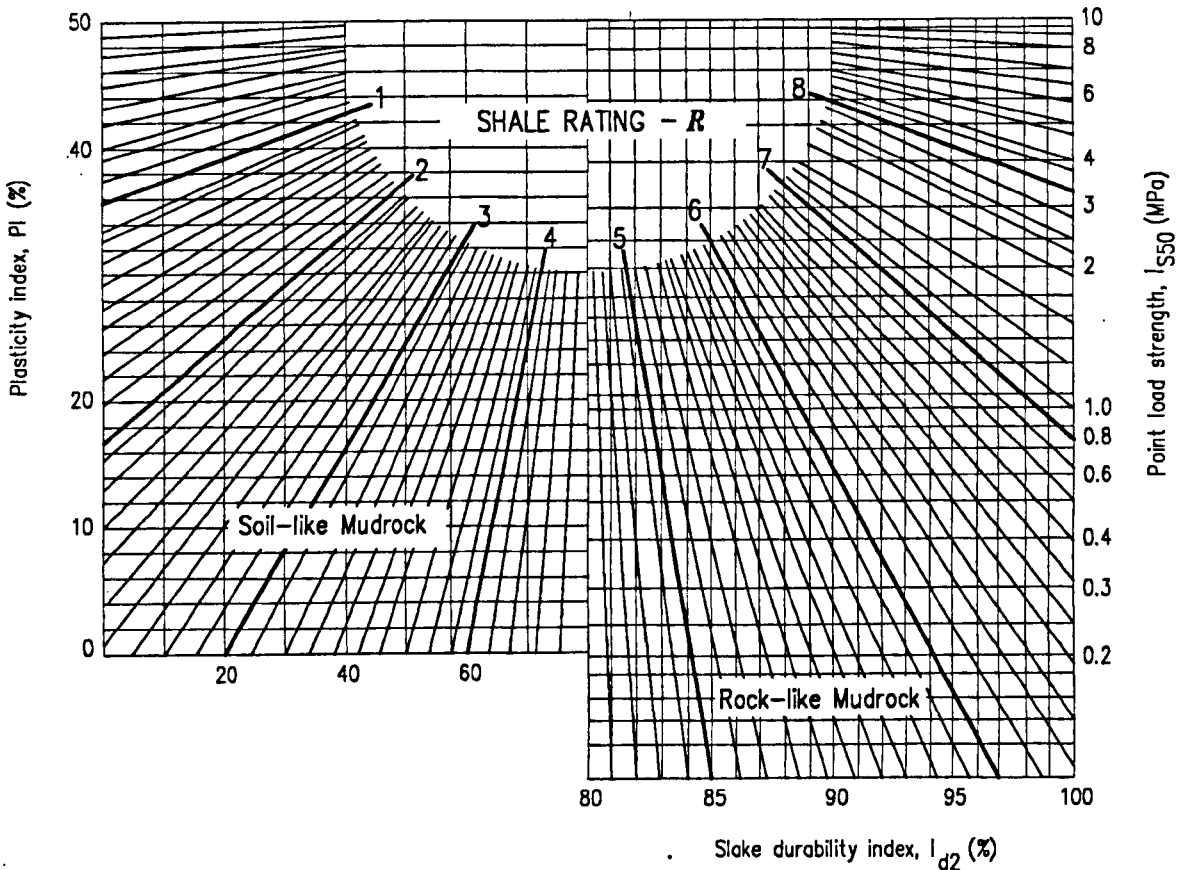


Fig. 3.11 - Mudrock rating chart (after Franklin, 1981).

Grainger (1984) proposed an engineering classification of mudrocks (Fig. 3.12) based on composition, slake durability, compressive strength and an anisotropy criterion. As noted by Taylor (1988) Grainger's scheme unifies some previous classification suggestions. He used the quartz content method proposed by Spears (1980) to subdivide the more indurated mudrocks and Morgenstern & Eigenbrod's (1974) criterion in conjunction with a slake durability (I_{d2}) of 90% to distinguish between durable and non-durable mudrocks. He also suggested that the 'shale' lithotypes are distinguished on the basis of the assessment of strength anisotropy. As strength anisotropy is not practical to measure in non-durable mudrocks, Grainger (1984) suggested that a criterion of flakiness ratio (shortest dimension divided by intermediate dimension) of particles produced by natural or artificial fracture should be used to assess the anisotropy character of materials, whilst for durable mudrocks strength anisotropy is determined by point load or cone indenter testing in orthogonal directions.

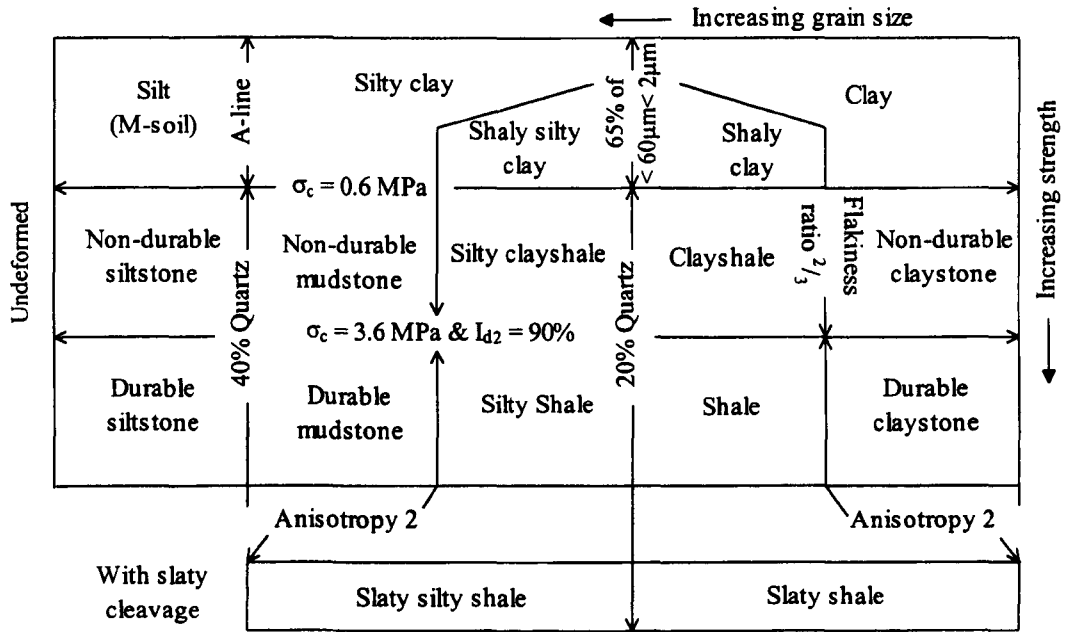
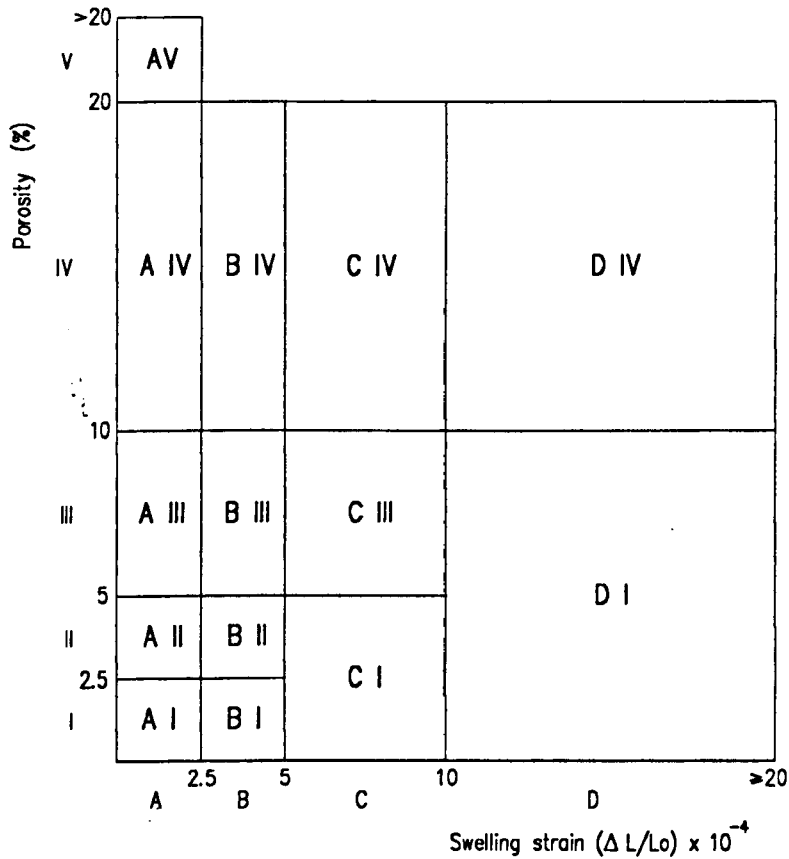


Fig. 3.12 - Grainger's (1984) mudrock classification for engineering purposes.

Using a wide variety of Portuguese and Algerian carbonate rocks ranging from pure limestones to argillaceous rich carbonate rocks, Rodrigues (1986) proposed a classification based on free swelling strain and effective porosity. The latter parameter was determined by vacuum saturation and buoyancy techniques. Rodrigues (*id.*) justified the selection of these classification parameters because they evaluate two different main properties of rock materials, respectively, the content of clay minerals and the amount of pore space. Fig. 3.13 shows the classification scheme. As noted by Rodrigues (*ibid.*), although the limits of the different fields are arbitrary, reflect differences in the behaviour of the rocks in ageing tests and construction works. The use of this type classification is not practical in mudrocks as effective porosity requires mercury intrusion porosimetry which is not suitable for routine classification.



Proposed porosity classes

- I - Very low porosity rocks
- II - Low porosity rocks
- III - Medium porosity rocks
- IV - High porosity rocks
- V - Very high porosity rocks

Proposed swelling strain classes

- A - Very low swelling rocks
- B - Low swelling rocks
- C - Medium swelling rocks
- D - High swelling rocks

Fig. 3.13 - Proposed abacus for the geotechnical classification of carbonates rocks (after Rodrigues, 1988).

Felix (1987) proposed a classification for sandstones which recognized nine classes of durability based on free swelling strain and the ratio between saturated and dry uniaxial compressive strength. The use of these classification parameters as criteria was questioned by Rodrigues & Jeremias (1989) as both parameters are liable to clay minerals in the behaviour of the rocks. Furthermore, with mudrocks it is difficult to obtain specimens suitable for compression testing and to prevent slaking during saturated compression tests. This is especially the case in the softer, less durable materials.

Taylor (1988) developed a classification for British Coal Measures based on composition, uniaxial compressive strength and slake durability. Using the Spears's (1980) method of quartz content to evaluate the grain size of mudrocks, Taylor (1988) suggested the boundary between siltstones and mudstones of 40% quartz [like Spears (1980)] and the boundary between siltstones and sandstones of 60% quartz. Following the Morgenstern & Eigenbrod's (1974) criterion he suggested that durable Coal Measures mudrocks should be distinguished on the basis of a compressive strength of more than 3.6 MPa and a slake durability index achieved on a third cycle (200 rotations per cycle) greater than 60%.

Finally, Dick *et al.* (1994) proposed a mudrock durability classification based on lithologic characteristics of a large variety of mudrocks (Fig. 3.14). These researchers considered that durability behaviour of mudrocks varies accordingly to lithotype and suggested a geological differentiation of mudrocks into claystones, mudstones, siltstones, shales and argillites based on the amount of clay-size material, the presence or absence of laminae, and the state of induration. They also suggested that the assessment of durability of different mudrock types can be achieved from quantitative relationships between slake durability index (I_{d2}) and specific lithological characteristics. According to the results obtained, as indicated in Fig. 3.14, they concluded that claystones correlate best with the quantity of expandable clay minerals, mudstones with the frequency of microfractures and both siltstones and shales with water absorption value.

Durability	Claystone	Mudstone		Shale	Combined Siltstone-Siltshale	Argillite
		<i>Slickensided</i>	I_{mf} (microfractures/cm)	Absorption (%)	Absorption (%)	
High: $I_{d2} > 85\%$	NA	NA	< 0,4	< 5,5	< 5	All
Medium: $50 < I_{d2} < 85\%$	NA	NA	0,8 - 0,4	10 - 5,5	9,5 - 5	NA
Low: $I_{d2} < 50\%$	All	All	> 0,8	> 10	> 9,5	NA

Note: NA - not applicable.

Fig. 3.14 - Mudrock durability classification system based on lithological characteristics (after, Dick et al., 1994).

3.4 - Engineering geological mudrock description scheme adopted in the study

Fundamental geological aspects and features of engineering relevance need to be described which is the objective of the engineering geological mudrock description scheme presented. Following Anon. (1995) the classification descriptor of weathering state appears with the geological formation name instead of being part of the description.

The practice recommended and presented in Anon. (1995) has been used, in which the following word order was applied for the rock descriptions:

1. strength;
2. colour;
3. stratification thickness;
4. ROCK NAME;
5. discontinuity spacing;
6. other characteristics (when applicable);
7. weathering state.

3.4.1 - Strength

The strength of the samples was based on the values of uniaxial compression strength (UCS) obtained in laboratory testing. However, for a few samples it was not possible to obtain suitable specimens for compression tests, so the strength estimated qualitatively according to the field criteria presented in Table 3.5 was applied. Several scales of uniaxial compressive strength have been provided by the Engineering Group Working Party Anon. (1970) and Anon.(1977), IAEG (1979), ISRM (1981), BS5930 (1981) and Hawkins & Pinches (1992) which differ both in terms of the number of classes considered and in the values selected to define the limits of these classes. In Table 3.5

the classification of uniaxial compressive strength adopted is presented. The strength intervals proposed by Anon (1970) and BS5930 (1981) were selected because they provided four classes in the range of weak rocks (UCS less than 50 MPa) which allows a better discrimination of the mudrocks studied.

Table 3.5 - Classification adopted to evaluate rock strength based on UCS values and/or on field criteria.

Interval (MPa) ¹	Description	Field Criteria ²
> 200	Extremely strong	Unscratchable. Chipped on floor.
100 - 200	Very strong	Unscratchable. Difficult to break.
50 - 100	Strong	Scratchable. Chipped in hand.
12.5 - 50	Moderately strong	Scratchable. Broken by hammer blows.
5 - 12.5	Moderately weak	Groovable. Easily broken by hammer.
1.25 - 5	Weak	Cutable. Broken by hand.
< 1.25	Very weak	Crumbles in hand.

¹(Adapted from BS 5930, 1981); ²(Adapted from Hawkins & Pinches, 1992)

3.4.2 - Colour

Colour of mudrocks was described using a rock-colour chart (Geological Society of America, 1995) based on the Munsell Colour System. Colours of the mudrocks were determined on dry fresh surfaces.

3.4.3 - Stratification thickness

Stratification is subdivided into beds and laminae at 10 mm thickness boundary (McKee & Weir, 1953; Ingram, 1954; Spears, 1980; Potter *et al.*, 1980) being this limit considered, following Lundegard & Samuels (1980) and Potter *et al.* (*op. cit.*), to subdivide mudrocks into non-laminated and laminated as shown in the classification presented in Table 3.7. Therefore, the latter term is used for mudrocks displaying a parallel arrangement of layers lesser than 10 mm thick (lamination). Table 3.6 shows the

classification of layer thickness adopted. The class limits for bed thickness are those proposed by IAEG (1979), ISRM (1981) and BS5930 (1981). However, as these classifications have different limits to distinguish beds from laminae, an interval of between 60 and 10 mm was adopted for the 'very thinly bedded' class. It was sought, in this way, to conjugate the terminology used in Engineering Geology to designate the thickness classes of sedimentary rocks with the geological criterion that separates beds from laminae. In Table 3.6, two classes for laminae thickness, according to the terminology suggested by Ingram (1954) and Tucker (1996), are also considered.

Table 3.6 - Classification adopted to bedding and lamination thickness.

Spacing (mm)	Term
> 2000	Very thickly bedded
600 - 2000	Thickly bedded
200 - 600	Medium bedded
60 - 200	Thinly bedded
10 - 60	Very thinly bedded
3 - 10	Thickly laminated
< 3	Thinly laminated

(Adapted from Ingram, 1954; IAEG, 1979; ISRM, 1981; BS 5930, 1981 and Tucker, 1996)

3.4.4 - Rock Name

Silt-clay proportions of mudrocks were found by Spears (1980) to be closely related to the quartz content and, therefore, he proposed a classification based on quartz percentage to subdivide indurated mudrocks. However, the silt-size fraction of the present mudrocks consists of quartz and feldspar (see Chapter 5) which together are assumed to provide a measure of the resistate fraction. The quartz content was determined by the chemical dissolution method proposed by Chapman *et al.*, 1969 and described in detail in Section 5.2.3.1. The feldspar content was determined from the whole rock X-ray diffraction pattern using the method devised by Hooton & Giorgetta (1977) and described in detail in Section 5.2.1.5. The boundaries between claystone and mudstone at 20% quartz+feldspar, mudstone and siltstone at 40% quartz+feldspar and

siltstone and sandstone at 60% quartz+feldspar suggested by Spears (1980), Grainger (1984) and Taylor (1988) for quartz alone were followed. A correction for the dilution effect was considered, as recommended by Spears (1980), to mudrocks samples with a carbonate content greater than 5%. Table 3.7 shows the classification adopted to describe the fine-grained sedimentary rocks studied in this work. In the case of extremely weathered rocks, the methodology proposed by Hawkins & Pinches (1992) that classifies these materials as soils and not as rocks, was used, with the adoption of the following terminology, based on the boundaries defined in Table 3.7, silt, mud and clay.

Table 3.7 - Classification adopted to the fine-grained rocks of the north Lisbon area.

Quartz+feldspar content ¹	Field criteria	Non-indurated ²	Indurated	
			Massive	Laminated
> 60%	Grains recognised to naked eye or with hand lens	Sand	Sandstone	NA
40 - 60%	Abundant silt visible with hand lens	Silt	Siltstone	Siltshale
20 - 40%	Feels gritty when chewed*	Mud	Mudstone	Mudshale
< 20%	Feels smooth when chewed*	Clay	Claystone	Clayshale

¹Adapted from Spears (1980), Grainger (1984) and Taylor (1988); ²Rocks with more than 10% of carbonates have the term calcareous before the root name; NA - Not applicable; *Not recommended in routine investigation.

3.4.5 - Discontinuity spacing

The discontinuities present in rock masses can be of different types, but two main types may be recognised: those that occur in sets, for example, bedding planes (beds and laminae), joints, cleavages and those that occur singly, for example individual faults. Only discontinuities of the first type are concerned in the classification adopted in this study. It should be noted that bedding planes should only be considered to be discontinuities when the tensile strength of these surfaces is significantly less than that of the rock material. Discontinuities can be described on the basis of various features, such as: orientation, spacing, persistence, roughness, shear strength, opening (aperture) and nature of infillings. However, in order to simplify the classification adopted in this

study, the description of the discontinuities was based solely on spacing. The intervals of classes of spacing are common to most of the classifications found in the literature. The classification in Table 3.8 for the discontinuity spacing is that recommended by BS 5930 (1981) which provides one class 'extremely closely' for spacing less than 20 mm.

Table 3.8 - Classification adopted to describe discontinuity spacing.

Spacing (mm)	Term
> 2000	Very widely
600 - 2000	Widely
200 - 600	Medium
60 - 200	Closely
20 - 60	Very closely
< 20	Extremely closely

(Adapted from BS 5930, 1981)

3.4.6 - Other characteristics

Other characteristics of the mudrocks studied, such as, fissility, grain size, mineralogy, fossil content, quantity of organic matter and type of fracture, were, when applicable, included in the descriptions in order to complement the classification of these rocks.

Fissility was described on the basis of spacing between planes (Table 3.9), following the earlier schemes of McKee & Weir (1953) and Ingram (1954). Textural descriptors such as sandy and pebbly are proposed accordingly when mudrocks contain more than 10% of sand or pebbles (Stow, 1981). The use of compositional descriptors such as micaceous or ferruginous, was adopted when the proportions of mica and iron oxides identified macroscopically were greater than 5% (Stow, 1981). The fossil content should be described on the basis of the following aspects, type, distribution, state of conservation and orientation. However, in the rocks studied only rather quite broken fragments of shells, which could not be identified, were found. The presence of organic matter in rocks was described in terms of the distribution and size of the fragments. Fracture was described using the following terms: conchoidal, irregular and planar.

Table 3.9 - Classification adopted to describe fissility.

Thickness (mm)	Term
> 10	Massive
3 - 10	Fissile
< 3	Very fissile

(adapted from McKee & Weir, 1953 and Ingram, 1954)

3.4.7 - Weathering state

The description of rock mass weathering and rock material weathering for engineering purposes can be done according to several classifications proposed in the literature (Chandler, 1969; Anon., 1970; Anon., 1977; ISRM, 1981; IAEG, 1979, 1981; BS 5930, 1981; Anon., 1995). The description and classification of rock mass weathering is based on the characterization of the different stages developed in weathering profiles of previously sound rock. Thus, rock mass weathering classifications describe the various stages on the basis of percentages of matrix (soil) and rock material present, characteristics of rock fragments and features of discontinuities. The description and classification of rock material weathering is based on the variation of discoloration, decomposition or disintegration that weathered materials suffer in relation to sound rock. The classifications proposed by Chandler (1969), Anon. (1970), Anon. (1977), ISRM (1981) only characterize rock mass weathering, while that suggested by IAEG (1979) only describes rock material weathering. The remaining classifications contain descriptive schemes, for both rock mass and rock material weathering.

In the case of mudrocks, both material and mass features need to be taken into consideration in the description of weathering state of these rocks. The classification recommended by IAEG (1981) proposes a scale of percentages of weathering for rock material, however it does not provide descriptions that help to apply this scheme. The classification suggested by BS 5930 (1981) provides descriptions for the characterization of weathering state as both material (small) and at mass (large) scale, however the schemes proposed are generic and do not take the specific features of weak

rocks into account. Additionally, the classifications used to describe weathering state of rock material were developed for stronger rock types (e.g. granites) that show a clear gradation of their geotechnical properties during weathering process. Anon. (1995) recommends varying the approach according to the rock type and proposes descriptions of the weathering state at material and mass scales. In relation to the description of the weathering state of weak rocks Anon. (1995) recommends that mass and material features cannot be separated readily nor usefully and they are accordingly included in the same classification scheme. The classification proposed by Anon. (1995) for weak rocks reproduced in Table 3.10 was adopted to describe the weathering state of the mudrocks studied.

Table 3.10 - Classification adopted to describe weathering state.

Class	Descriptor	Typical characteristics
A	Unweathered	Original strength, colour, fracture spacing.
B	Partially weathered	Slightly reduced strength, slightly closer fracture spacing, weathering penetrating in from fractures, brown oxidation.
C	Distinctly weathered	Further weakened, much closer fracture spacing, grey reduction.
D	Destructured	Greatly weakened, mottled, lithorelicts in matrix becoming weakened and disordered, bedding disturbed.
E	Residual or reworked	Matrix with occasional altered random or 'apparent' lithorelicts, bedding destroyed. Classed as reworked when foreign inclusions are present as a result of transportation.

(Adapted from Anon, 1995)

The characterization of the weathering state of the mudrocks studied was based on the observation of the following features: colour changes, reduction in strength, changes in fracture state, as well as presence, character and extent of weathering products. Colour changes give rise to local or widespread discolorations, sometimes only observed close to discontinuities. Changes in fracture state and in strength should be reported using the defined terminology described under the strength and discontinuity spacing headings.

The presence of compounds resulting from weathering was reported in order to define their character and extent.

3.5 - Summary

The geological classifications of mudrocks are mainly based on the following characteristics: grain size, fissility, stratification and mineralogical composition. Difficulties on determination of grain size in mudrocks, justify the adoption of the scheme proposed by Spears (1980) which evaluated the silt size fraction based on quartz content. In the rocks studied, the sum of the percentages of quartz and feldspar was used. The combination of this scheme with the presence or absence of lamination provides a coherent geological classification for mudrocks, that was adopted in this study.

The geotechnical classifications developed or applicable to mudrocks are mostly based on the results of slake durability, uniaxial or point load strength, Atterberg limits and swelling. According to the various classifications described, it is suggested that Gamble's (1971) classification should be adopted for less indurated mudrocks, since their disaggregation allows the determination of plasticity. For harder mudrocks the classifications of Olivier (1976), in the version where point load strength is used, and that of Franklin (1981) seem to be most appropriate.

The classification adopted to describe mudrocks of the north Lisbon area is based on the following features: strength, colour, stratification thickness, rock name, discontinuity spacing, other characteristics (when applicable) and weathering state. As almost all of the samples were collected from boreholes, thus providing a reconnaissance of the rock mass, it seemed advantageous to include some mass features (weathering state and discontinuity spacing) in this classification, in addition to descriptive parameters referring to rock material.

4 - GEOLOGICAL SETTING AND SAMPLING

4.1 - Introduction

This chapter introduces the geological materials used in the experimental study and aims at providing the geological setting of the formations from which the samples were collected and to classify and describe the rocks in order that this information can be correlated with the results of laboratory characterization presented in following chapters.

The samples were collected from mudrock formations of the north Lisbon area (Fig. 4.1) using the sampling recovered from the boreholes carried out for the Preliminary Study of the A10 motorway between Bucelas and Carregado. Another two samples were collected from the cut slopes of the IC1- Loures - Caldas da Rainha motorway.

To summarise, this chapter gives a brief description of the geological aspects of the lithostratigraphic units from which the samples were collected and the techniques used in sampling and preparation of the rocks. Finally, the classification proposed in Chapter 3 is applied to describe these materials.

4.2 - Geological setting

4.2.1 - Geological description of the Arruda dos Vinhos area

The study area of the A10 motorway is located on sedimentary formations included in the Arruda dos Vinhos Basin. Geological mapping of the Arruda dos Vinhos area at 1:50,000 scale (sheets 34B-Loures and 30B-Alenquer) is presented in Fig. 4.1. It can be seen that all sampling points are located on the Abadia Formation which ranges from lower to middle Kimmeridgian in age.

The stratigraphic sequence of upper Jurassic sediments of the Arruda dos Vinhos area which include the Abadia Formation is presented in Fig. 4.2. The *Abadia Beds* are mainly composed by grey or greenish grey micaceous calcareous siltstones and mudstones, with abundant plant fragments, ripple marks and cross bedding. Occasionally, this formation contains calcareous, sandy and pebbly layers interbedded in the mudrock beds reaching in total a thickness of 800 m (Zbyszewski & Assunção, 1965). A calcareous facies which may either be rich in bivalves - *Lima pseudoalternicosta Beds* or corals - *Amaral Coral Limestone* (Wilson, 1979) overlies the *Abadia Beds*. In the eastern border of the Arruda basin, at Vila Franca de Xira and Castanheira areas the *Abadia Beds* developed another facies comprising arkosic sandstones and conglomerates aggregated by calcareous cement, which were not included in the present work.

Locally, the geological structure of the Arruda dos Vinhos area consists of an anticline in which the accumulated Jurassic sediments reach a thickness of about 2.5 km. The relatively small lateral dimensions of the Arruda Basin (about 20 km) and the very thick fill of Kimmeridgian sediments, coupled with the rapid facies change from breccias and conglomerates in the southeast of the basin to finer grained detrital facies in the northwest, denote a strong influence of local tectonic structures on sedimentation and is characteristic of basins controlled by wrench tectonics (Wilson, 1979).

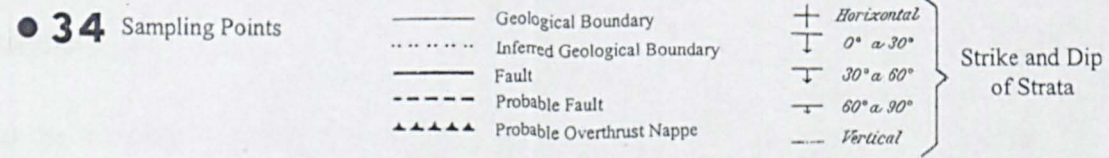
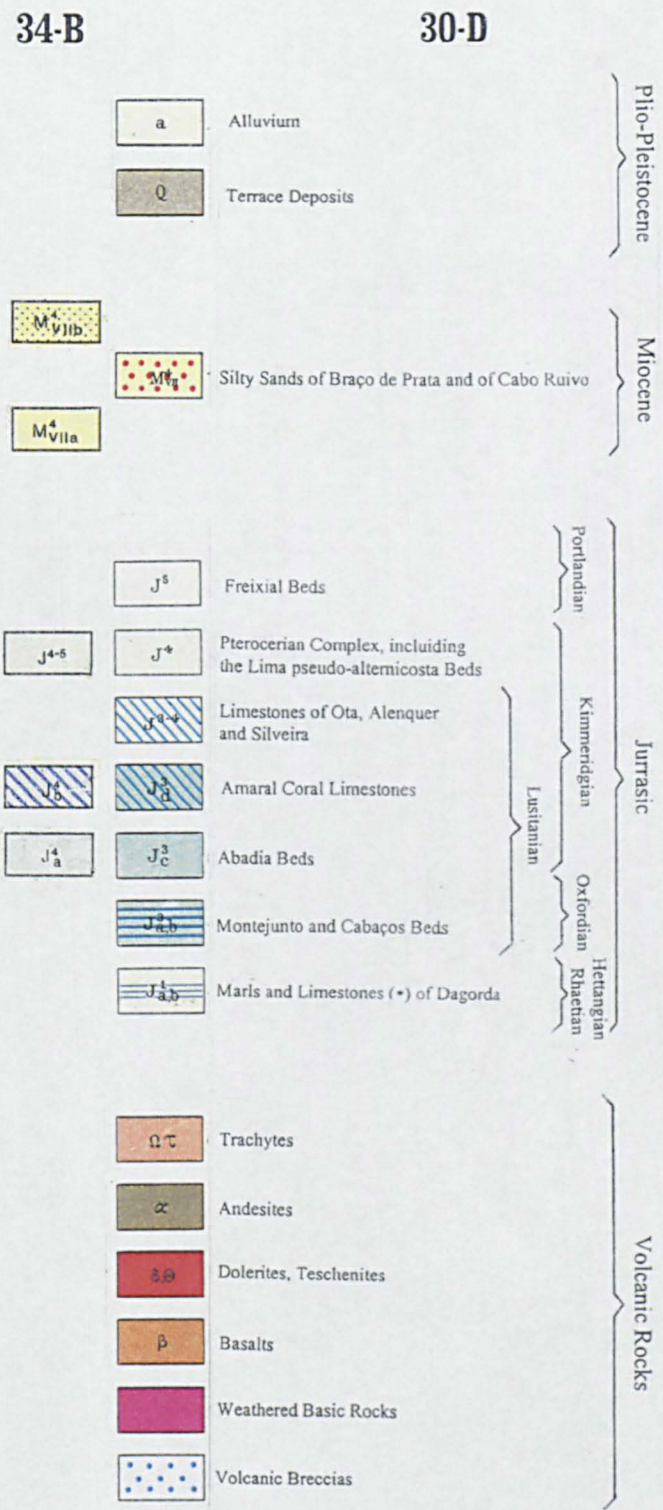
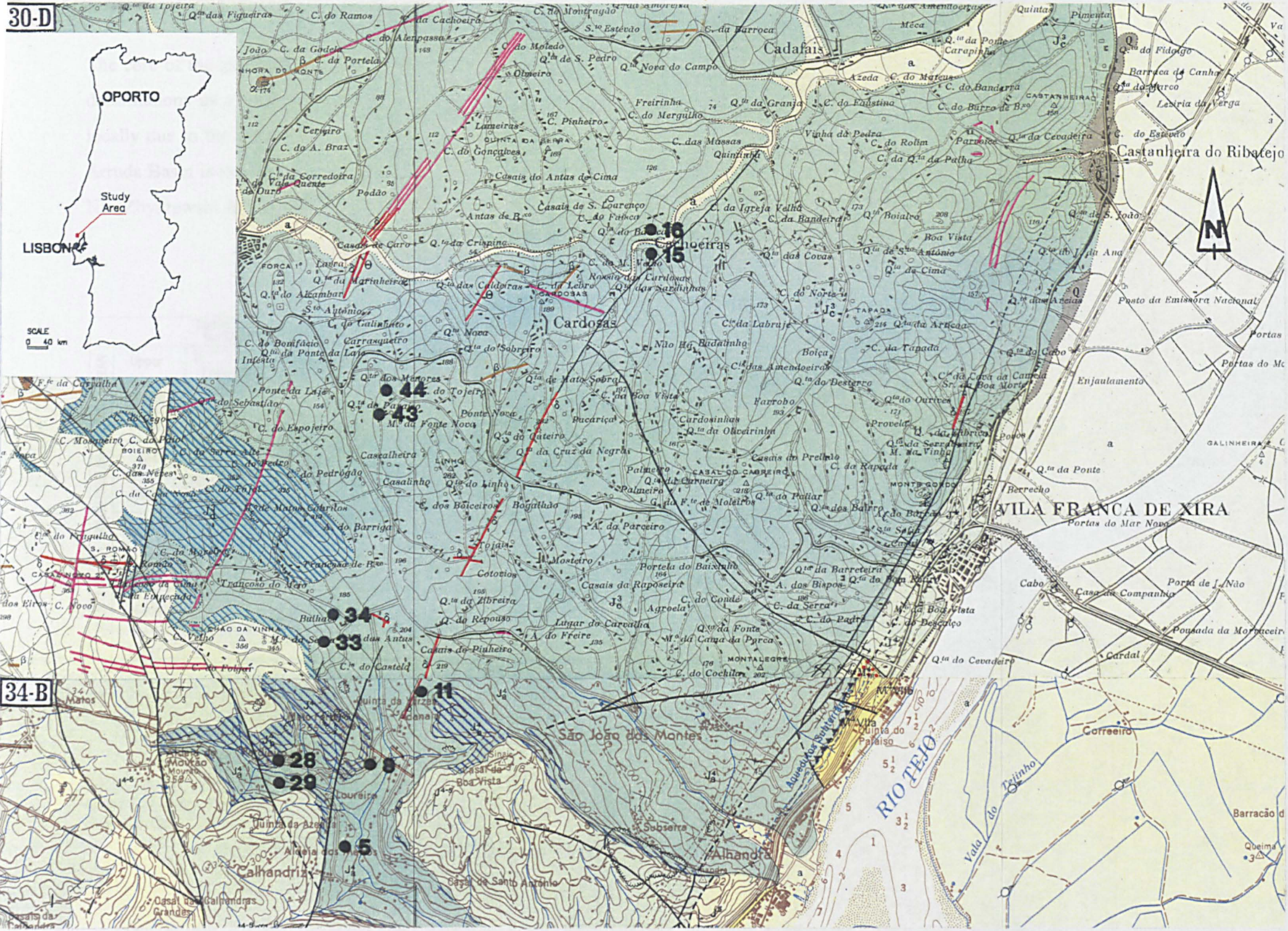


Fig. 4.1 - Geological Map at 1/50,000 scale of Arruda dos Vinhos area (based on the sheets 30D - Alenquer and 34B - Loures) with the location of the sampling points.

The core of the anticlinal structure is occupied by the *Abadia Beds*, which show large deformations as a result of faulting. Although the regional trend of dip may change locally due to the effects of fault movements, the dip of strata in the south area of the Arruda Basin is predominantly towards SE, but northwards the dip of strata changes to NE (Zbyszewski & Assunção, 1965).

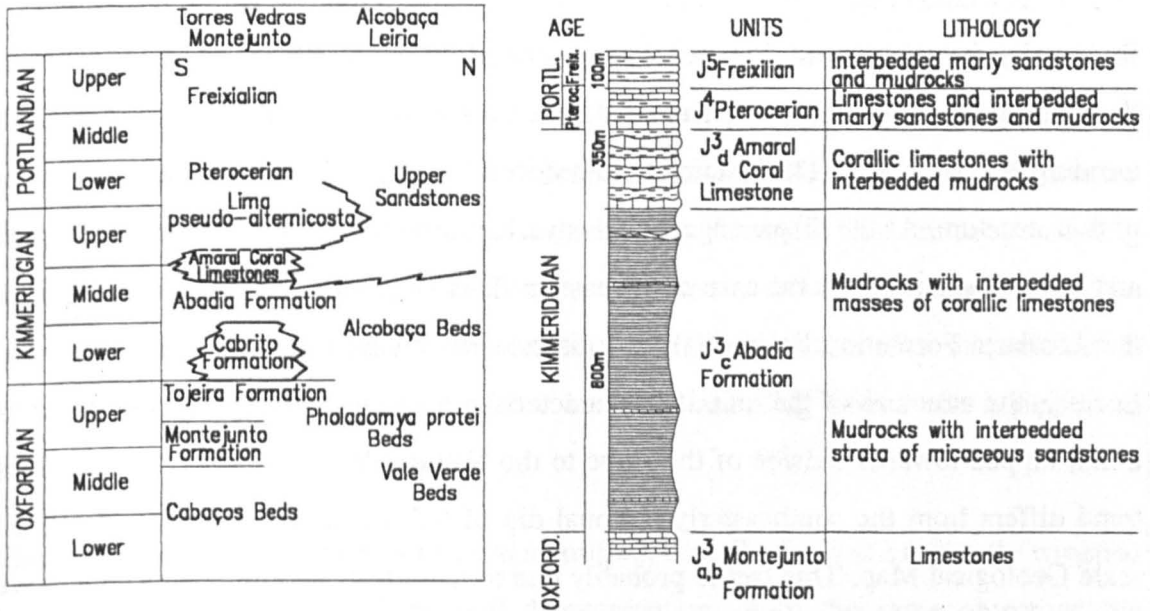


Fig. 4.2 - (A) Upper Jurassic stratigraphy of the Lusitanian Basin in the Arruda and Alcobaça areas (adapted from Fürsich, 1987); (B) Stratigraphic column for the Arruda Area (adapted from Coelho, 1979).

4.2.2 - Geological setting of the man-made slopes in IC1 motorway

The second location at which samples were collected (cut slopes in IC1 Loures - Caldas da Rainha motorway) is situated on the eastern flank of the anticlinal structure of the Caldas da Rainha diapir.

According to the Geological Map of Portugal at scale of 1/50,000 [sheet 26D - Caldas da Rainha (Zbyszewski & Moitinho de Almeida, 1960)] the samples were collected

from the *Alcobaça Beds* ranging from lower to middle Kimmeridgian in age. This formation is the lateral equivalent to the north of the *Abadia Beds*. The *Alcobaça Beds* are constituted by grey and/or brown-yellow, when weathered, calcareous mudstones and siltstones, occasionally with an important sandy fraction and with calcarenite and limestone intercalations. The thickness of this unit is significantly less than that of the *Abadia Beds* reaching a maximum of about 200 to 300 m (Wilson, 1979). At the top of this formation lies the *Upper sandstones with plant and dinosaur fossils* unit constituted mainly by coarse clastic sediments which range from Pterocerian to Freixialian in age.

Regionally the structure of this area was controlled by salt tectonics, which gave rise to the installation of the Caldas da Rainha diapir. This structure is formed in a NNE-SSW trending anticlinal fold. The Hetangian formations ('Dagorda Marl') outcrop in the core of this structure. At the diapir edges this is overlain discordantly by the Jurassic Dogger and Malm formations. In the case of the eastern flank where the samples were collected, the Alcobaça Formation lies directly but disconcordantly on the Hetangian formations. Locally, the structure of the massif is characterised by layers oriented along a NE-SW trend, dipped towards outside of the slope to the NW quadrant at about 5° to 15°. This trend differs from the southeasterly regional dip of the formations shown on 1:50,000 scale Geological Map. This fact is probably due to the effects of salt tectonics that give rise to a complex geological structure characterised by intense fracturing and faulting with important local deformations. It has been noted that at some points the layers dip towards SE.

4.3 - Sampling

4.3.1 - Methods

It is stated in the Introduction (Section 4.1) that the samples used in this work were collected at two distinct locations, the Arruda dos Vinhos area and the man-made slopes of the IC1 motorway close to Óbidos. The sampling techniques used were different in each location, as described hereunder. The samples collected in Arruda area were

obtained from boreholes carried out for the Feasibility Study of the A10 Bucelas-Carregado motorway. The boreholes were put down by the rotary coring technique, using double tube core barrel with an external diameter of 86 mm. Water was used as drilling fluid in order to lift the drill cuttings out of the borehole and to cool the bit. This fact negatively affected the determination of the natural water content of the rocks because the use of water during drilling changed significantly the moisture content of the samples.

After drilling, all the rock cores from a total of 44 boreholes were inspected and 11 were selected for study (numbers 5, 8, 11, 15, 16, 28, 19, 33, 34, 43 and 44) on the basis of their spatial distribution and sample quality. The criteria adopted in the selection of cores were as follows: (a) sampling at different locations within the Abadia Formation in order to investigate the variation of materials that comprise this unit, (b) sampling rocks with different weathering grades because due to the fact that the weathered rocks can occur at significant depths, these are the materials which are often encountered in engineering works. The locations of the borehole sampling points are indicated in Fig. 4.1.

The samples selected in each bore were identified, described and subsequently wrapped with plastic film in order to prevent disaggregation. With the same objective, the samples were transported to Sheffield in cardboard boxes. The space between the cores and the walls of the boxes was filled with styrene foam.

In July of 1994 during the construction of the IC1 motorway a landslide occurred in the man-made slopes located on the eastern flank of the Caldas da Rainha diapir near Óbidos. As LNEC was requested to carry out the slope stability studies and because the failures affected formations equivalent to those of Arruda, two samples that characterized the mudrock formations occurring on site were collected.

Taking into account the facilities present on site, two blocks with an approximate size of 60x60x30 (cm) were identified, photographed and subsequently wrapped with plastic film and then with aluminium foil and were finally covered with paraffin wax. In order to prevent the disaggregation of the blocks they were transported to LNEC in wooden boxes. Before coring the specimens for laboratory testing, the blocks were kept in a

humidified chamber. The samples selected for laboratory testing carried out in Sheffield were transported in cardboard boxes. The space between the samples and the walls of the boxes was filled with styrene foam.

4.3.2 - Sample descriptions

In this section the sample descriptions using the classification described in Chapter 3 are presented. As mentioned the classification was based on the following parameters: strength, colour, stratification thickness, Rock Name, discontinuity spacing, other characteristics (when applicable) and weathering state.

The examination and classification of the rock cores made it possible to identify not only mudrocks but also other rock types such as sandstones, calcarenites and limestones. Calcarenite and limestone layers interbedded with mudrocks are shown in Fig. 4.3 in respect of borehole 34. Fig. 4.4 shows the laminated character of the mudrocks present in the study area.

It could be seen from a visual examination that some of the fractures in samples were caused by the drilling operations. In addition the core recovery and the quality of the samples from the finest and less indurated layers were poor with the cores from such zones being generally very fractured.

Figs. 4.5 to 4.15 show the borehole logs from which samples were collected. Only the samples selected for laboratory work were classified in detail. They are described in the logs (Figs. 4.5 to 4.15) at the depths at which they were collected. The classification of the samples collected is synthesised in Table 4.1. From a total of 57 samples collected from the 11 boreholes mentioned above (Section 4.3.1), 29 were selected for laboratory characterization. The samples were selected on the basis of their spatial and stratigraphic distribution, core fracturing and size of the sample in the light of the requirements of the tests to be performed.



Fig. 4.3 - Borehole 34 sampling between 8.00 and 16.40 m depth.

Given the volume of material required to carry out the laboratory tests, a core about 0.8 m long was as a rule taken for the various samples at the depths shown in the logs presented in Figs. 4.5 to 4.15.

The samples were identified using three figures, the first two indicate the borehole number and the last indicates the order, from top to bottom of the bore, of the samples collected from each borehole. In the case of boreholes 5 and 8 the samples are designated by only two figures. Thus, for example, the sample 156 means that it was

collected from borehole 15 and that from top to bottom it was the sixth sample to be collected.

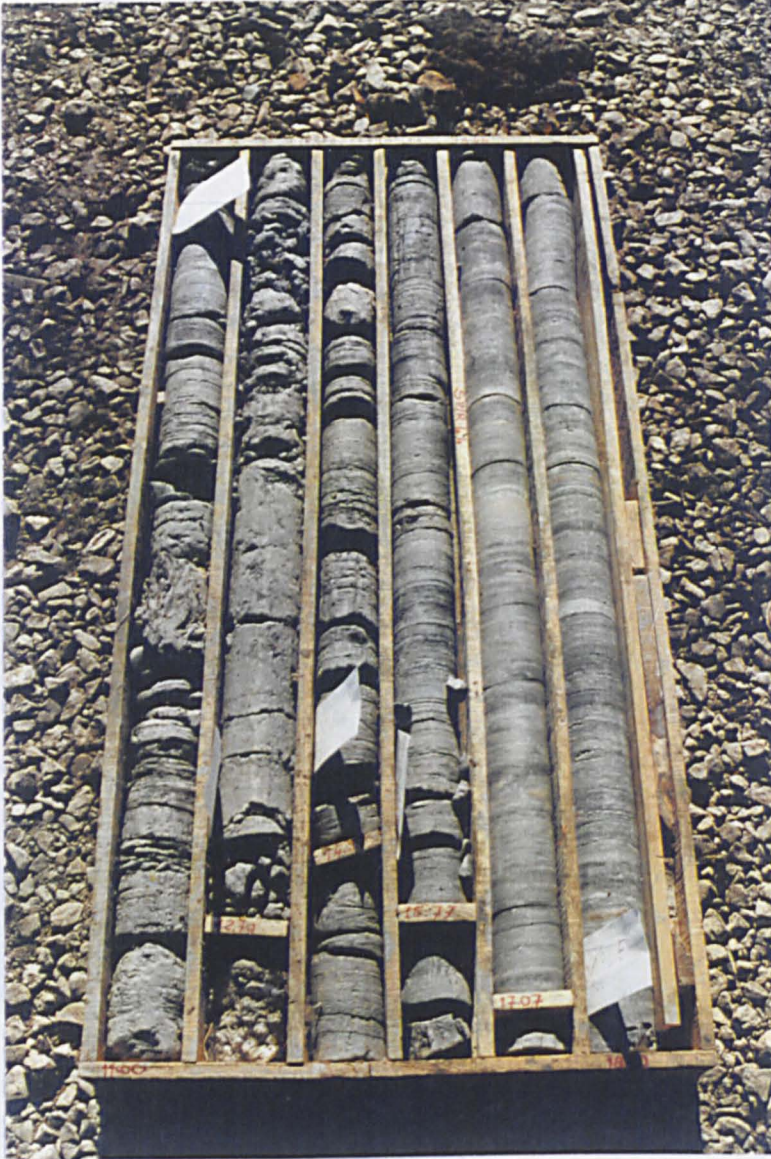


Fig. 4.4 - Borehole 44 sampling between 8.50 and 18.30 m depth.

Although the objective of this work is to investigate the engineering properties of mudrocks, the inclusion of the samples 83 (calcareous sandstone) and 345 (oolitic limestone) is justified by the fact that they represent marginal rock types frequently associated with mudrocks. In addition to this, as they are harder rocks, the characteristics determined for them can be used as a reference in the study of the properties of mudrocks.

Table 4.1 - Classification and sampling depth.

Sample	Classification	Depth (m)	Sample	Classification	Depth (m)
51	Carbonate clay	2.0	286	Calcareous mudstone	9.5
52	Calcareous mudshale	10.5	294	Calcareous claystone	7.5
81	Mudstone	6.5	296	Mudstone	10.5
83	Calcareous sandstone	10.5	332	Calcareous silt	2.0
111	Silt	2.0	333	Mudstone	3.5
112	Calcareous siltstone	5.0	334	Calcareous siltshale	7.0
114	Calcareous siltstone	9.5	336	Mudstone	9.5
151	Calcareous clay	1.0	342	Calcareous siltshale	8.5
152	Calcareous clayshale	3.0	345	Oolitic limestone	13.0
153	Calcareous mudshale	4.5	431	Calcareous siltshale	9.0
154	Calcareous mudshale	7.0	436	Calcareous mudstone	17.0
156	Mudshale	10.5	441	Calcareous mudshale	8.5
162	Calcareous mudstone	3.4	445	Mudshale	18.0
163	Calcareous siltstone	4.1	OB1	Calcareous siltstone	Outcrop
283	Calcareous mudstone	4.5	OB2	Calcareous siltstone	Outcrop
285	Calcareous mudstone	6.0			

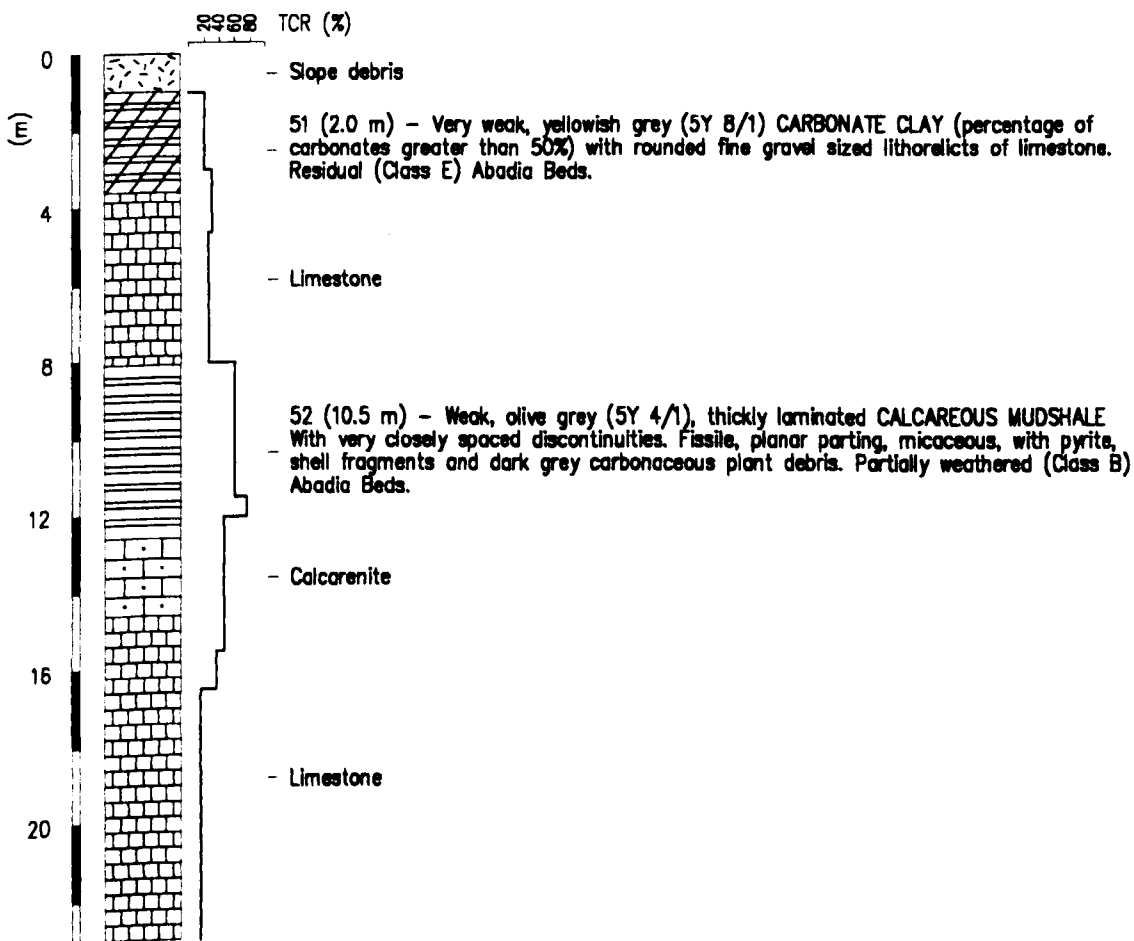


Fig. 4.5 - Log of borehole 5 with the description of samples 51 and 52.

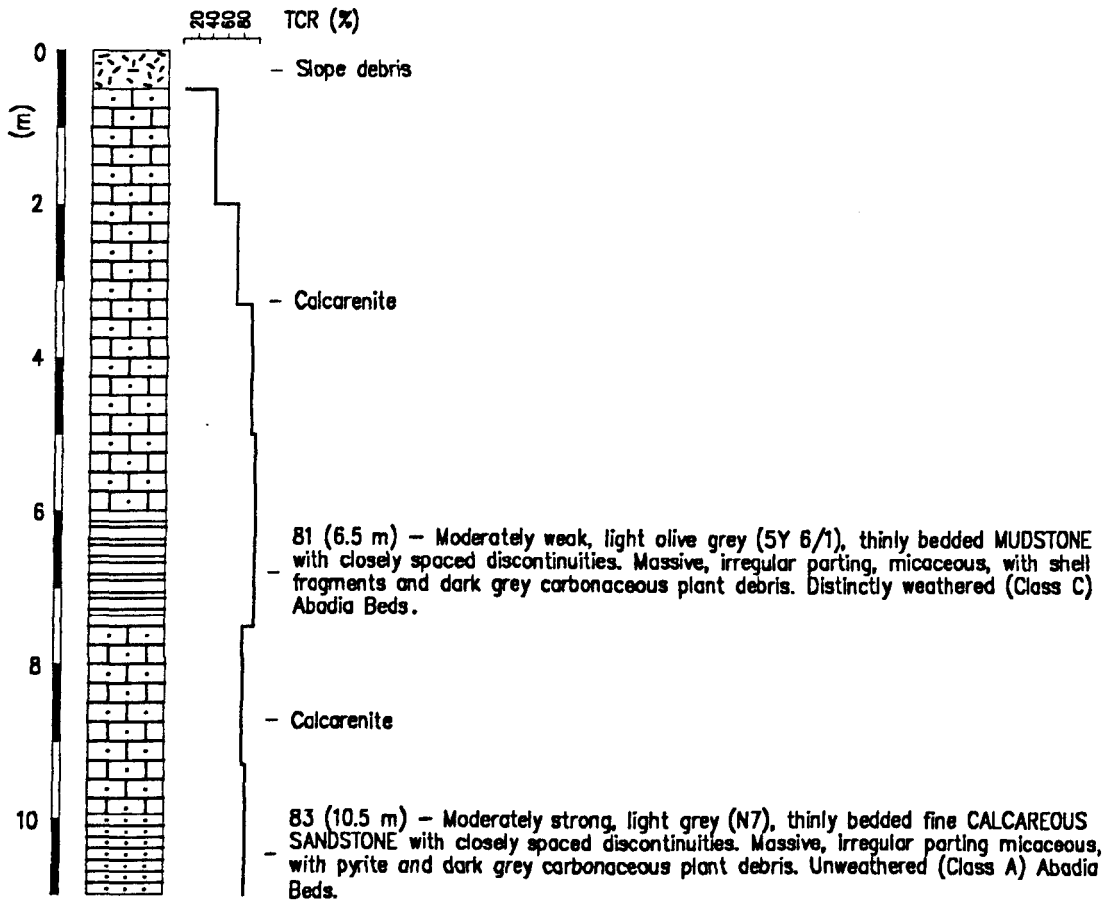


Fig. 4.6 - Log of borehole 8 with the description of samples 81 and 83.

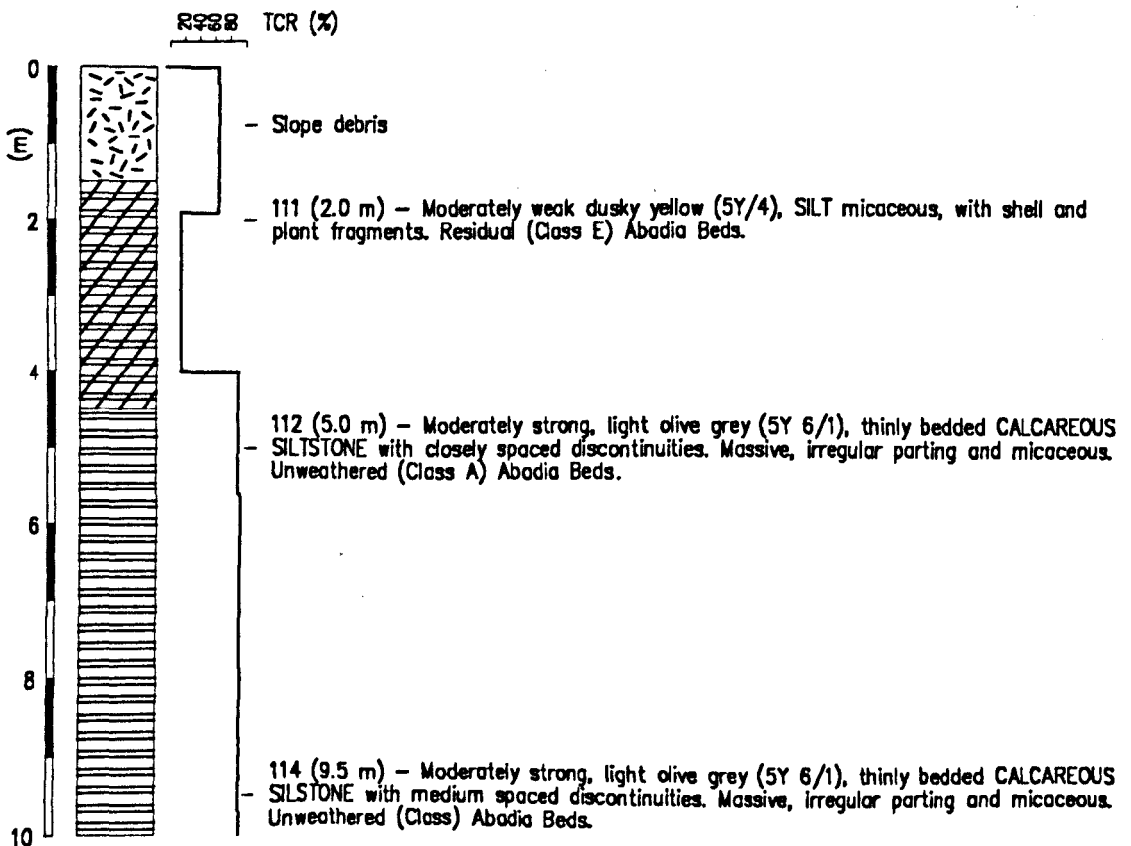


Fig. 4.7 - Log of borehole 11 with the description of samples 111, 112 and 114.

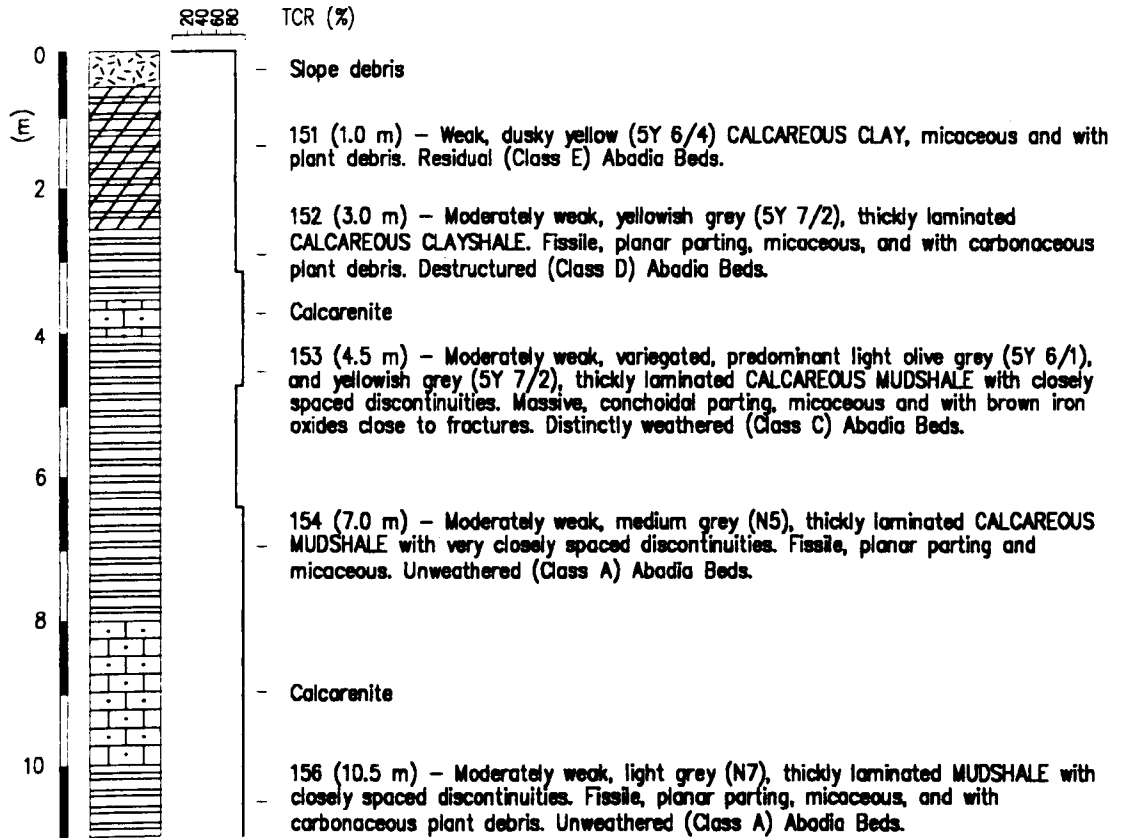


Fig. 4.8 - Log of borehole 15 with the description of samples 151, 152, 153, 154 and 156.

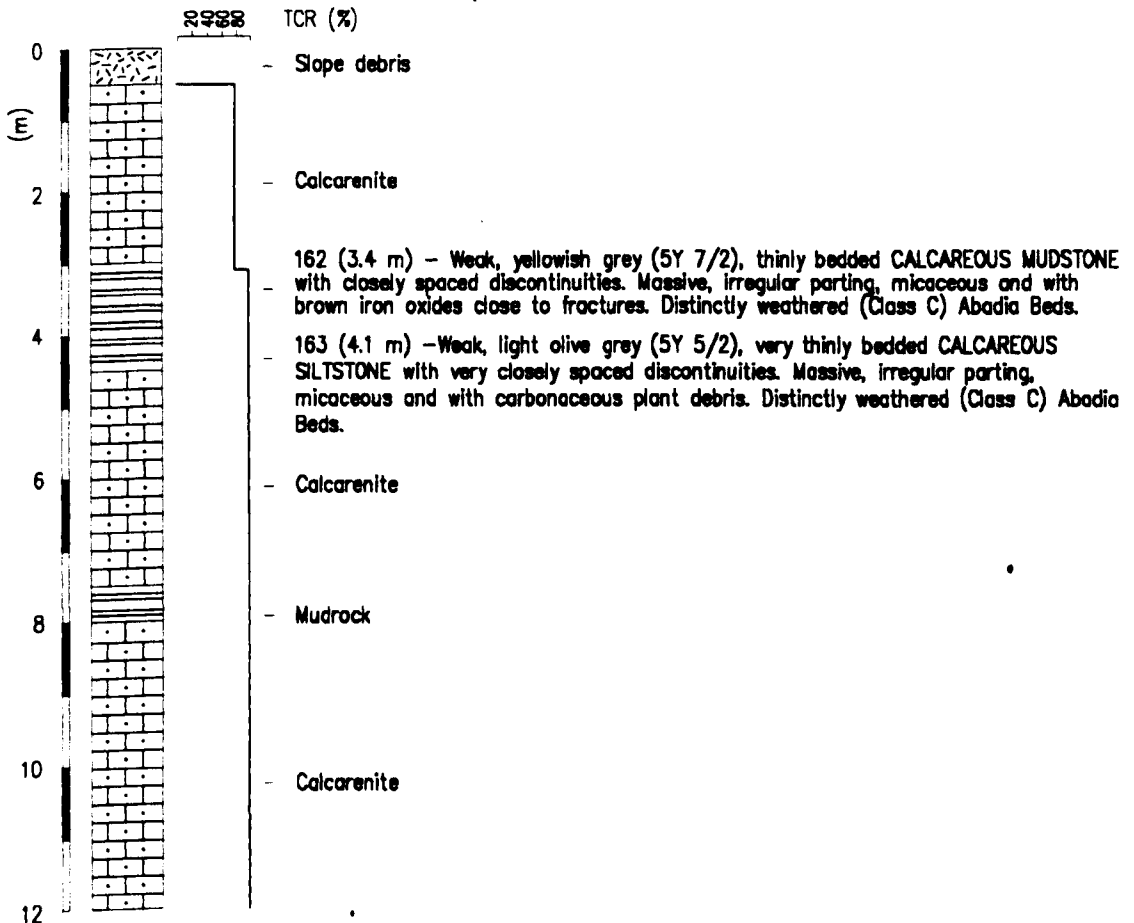


Fig. 4.9 - log of borehole 16 with the description of samples 162 and 163.

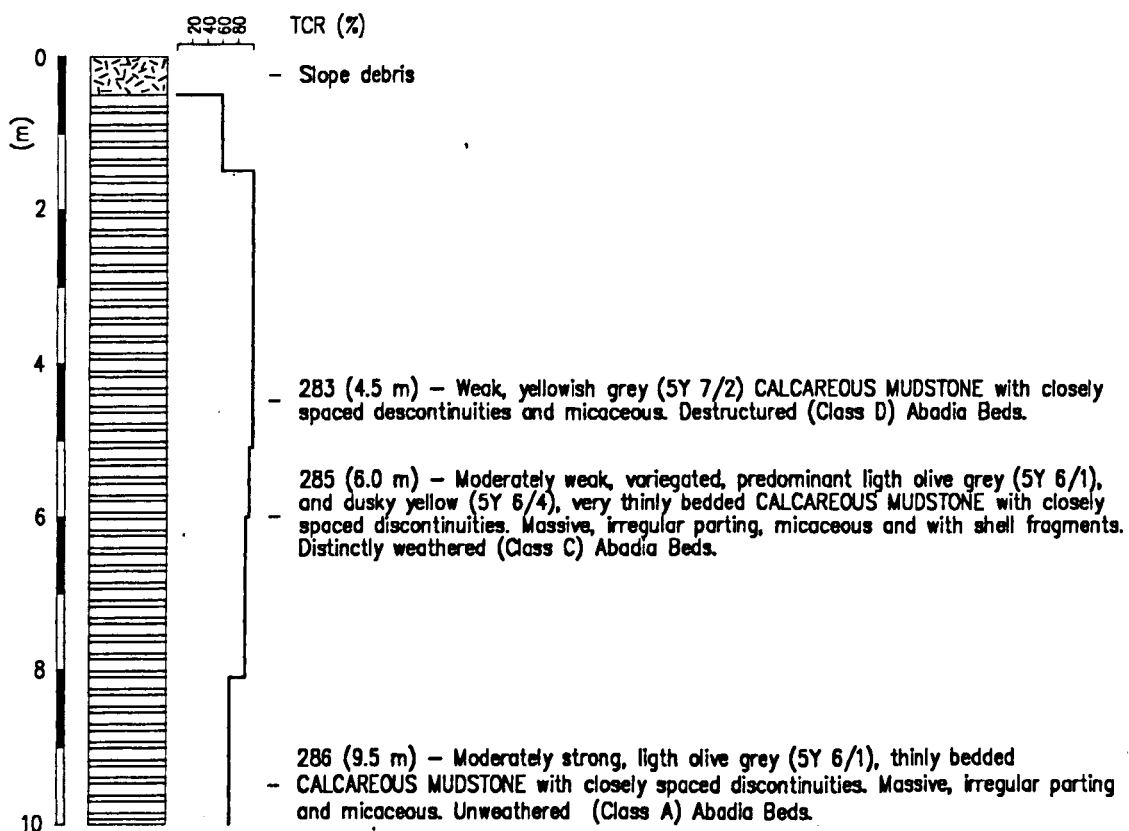


Fig. 4.10 - Log of borehole 28 with the description of samples 283, 285 and 286.

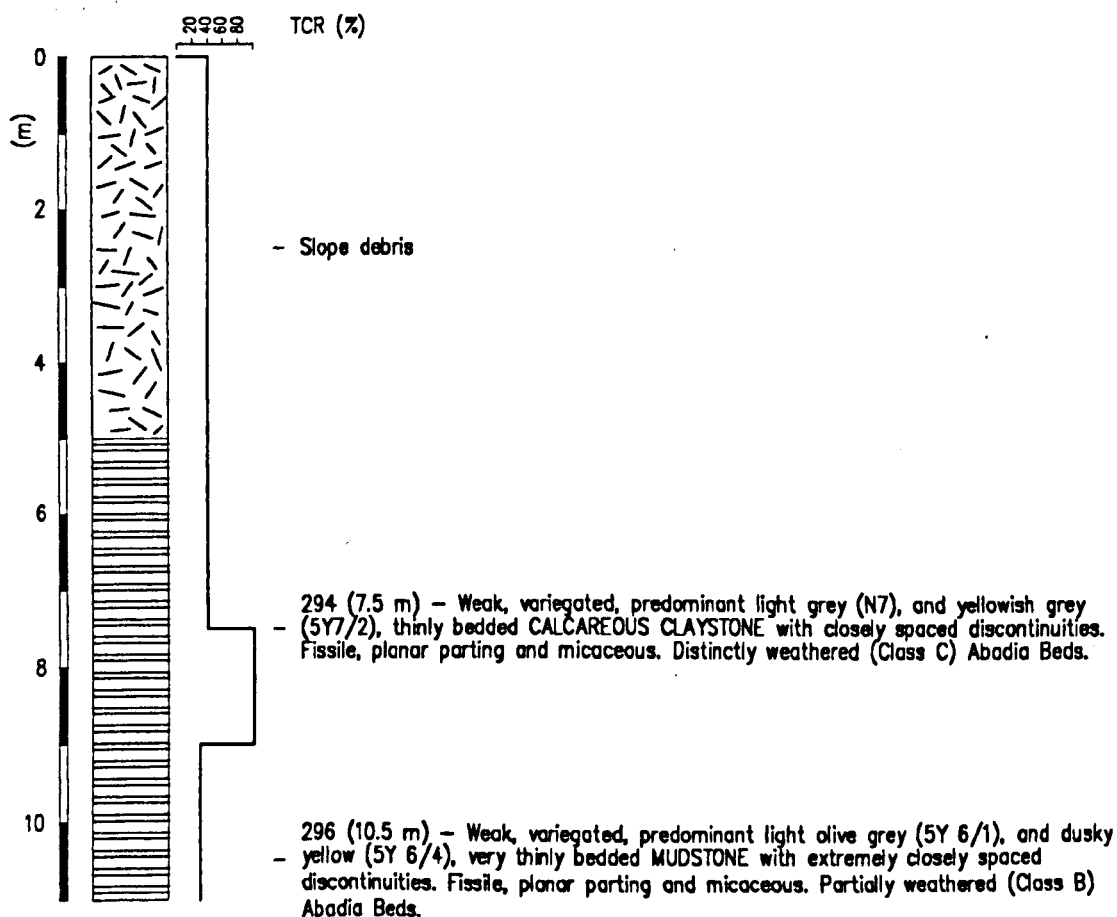


Fig. 4.11 - Log of borehole 29 with the description of samples 294 and 296.

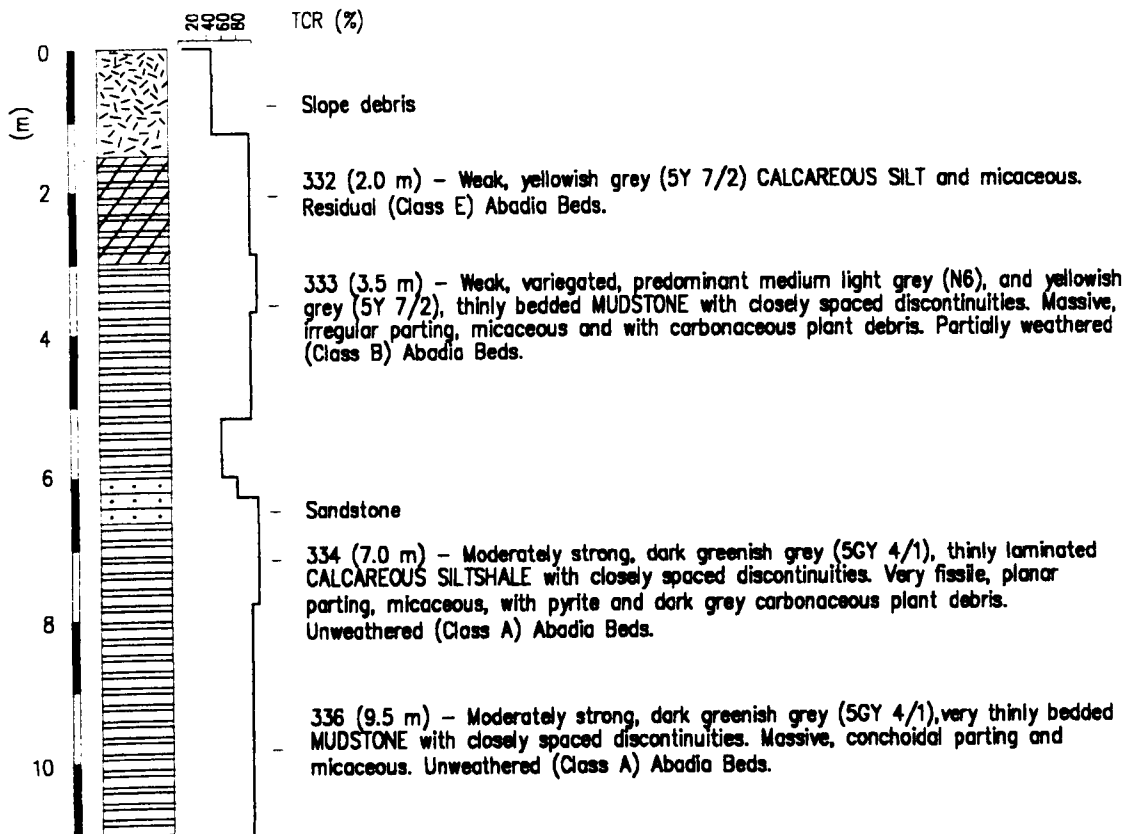


Fig. 4.12 - Log of borehole 33 with the description of samples 332, 333, 334 and 336.

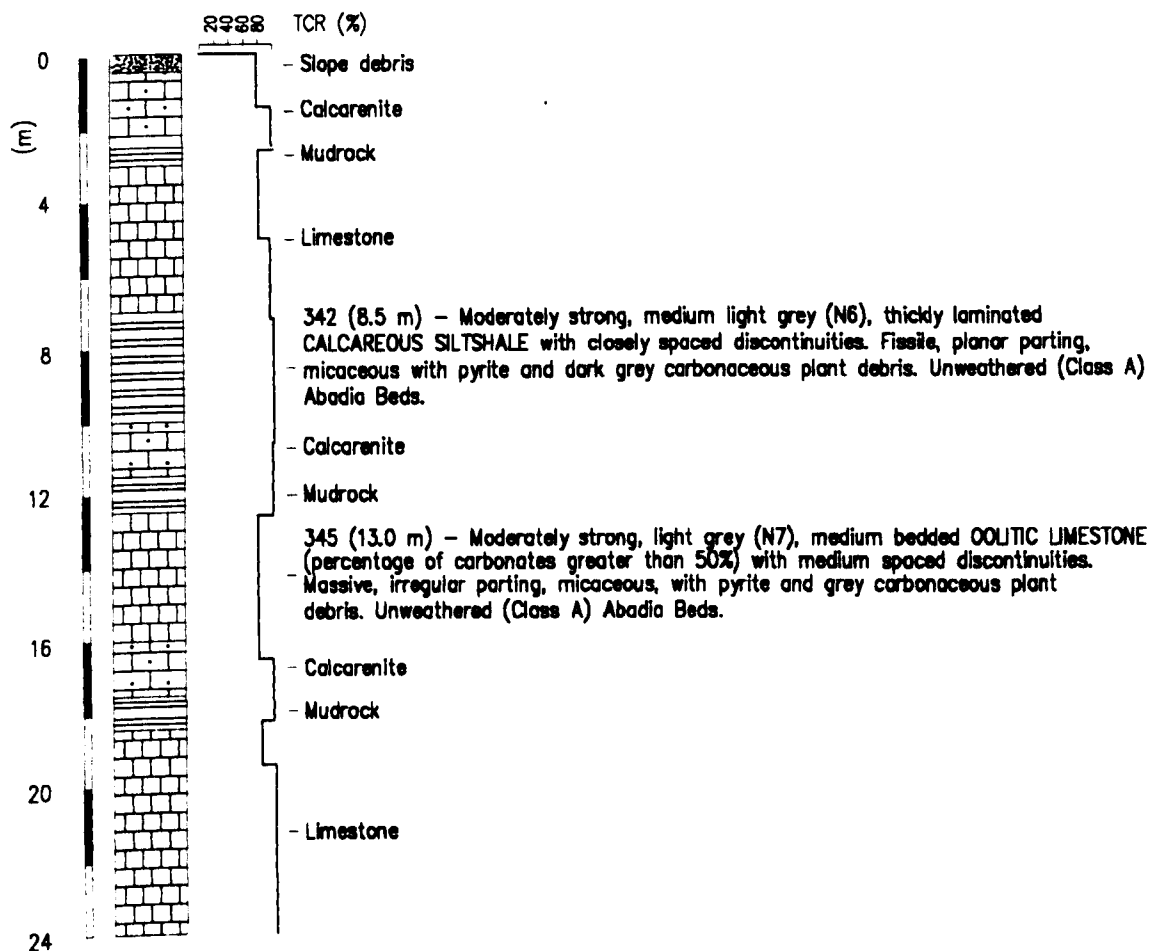


Fig. 4.13 - Log of borehole 34 with the description of samples 342 and 345.

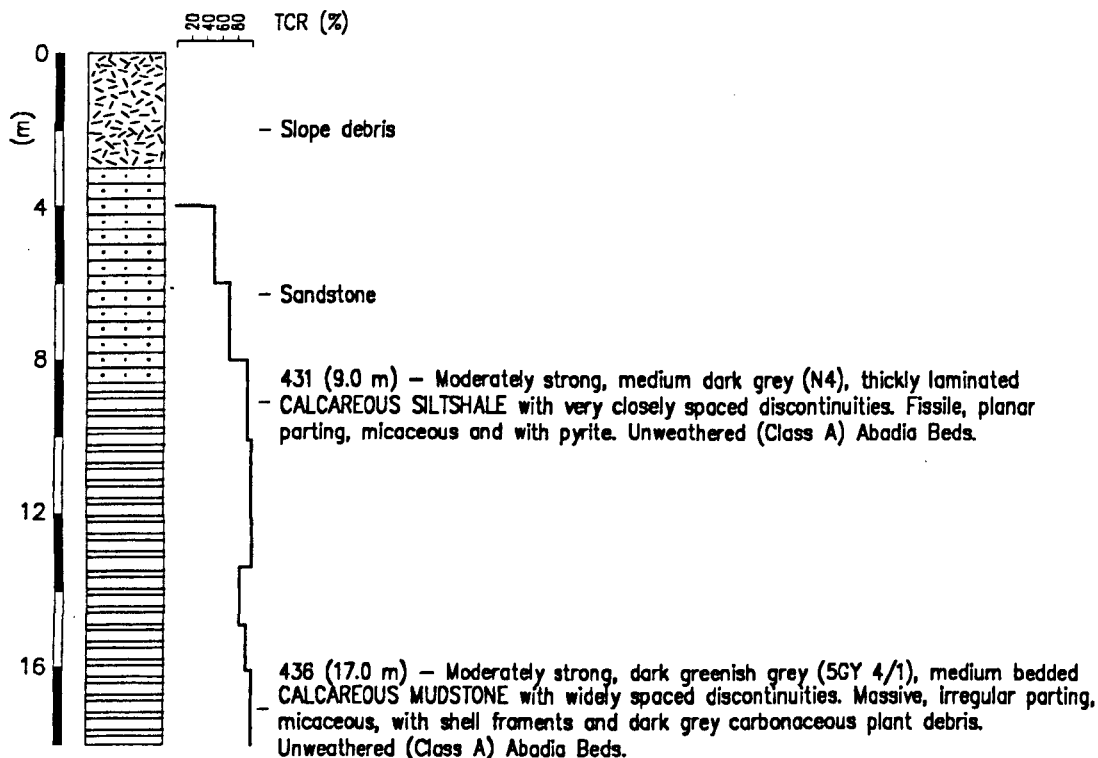


Fig. 4.14 - Log of borehole 43 with the description of samples 431 and 436.

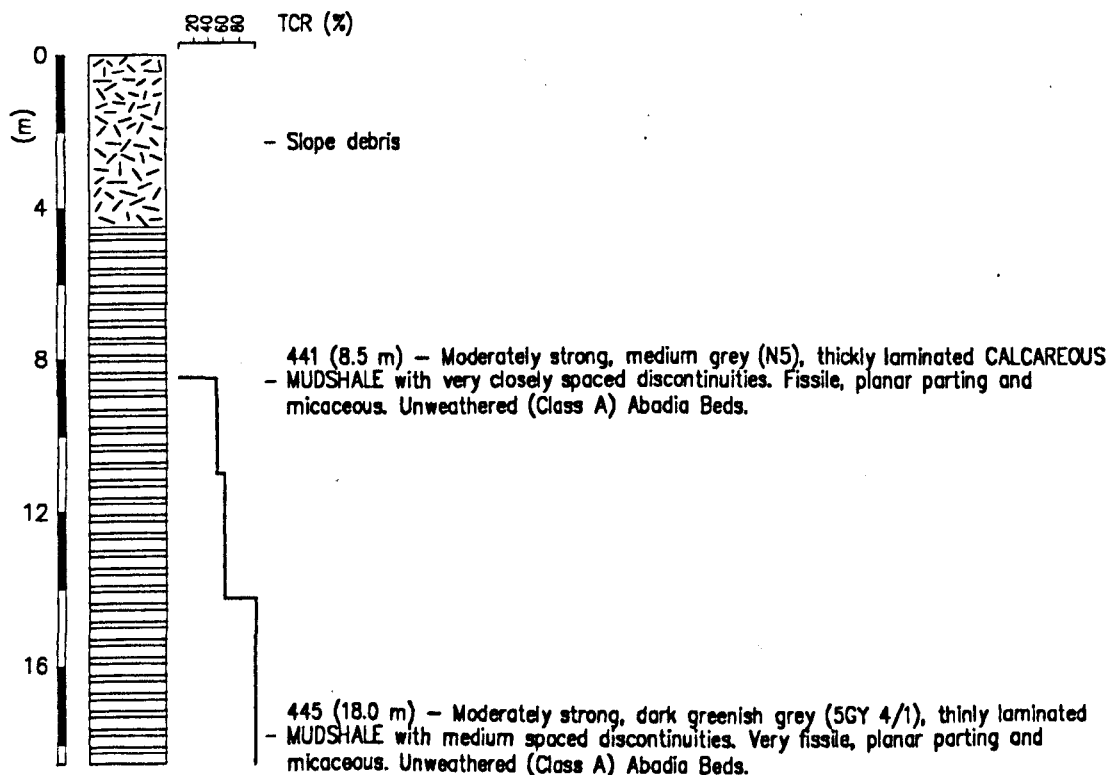


Fig. 4.15 - Geological profile of borehole 44 with the description of samples 441 and 445.

The samples from the Alcobaça Formation collected from the cut slopes of the IC1 motorway, consisted of two blocks taken at the same horizon and identified as OB1 and OB2, as described hereunder:

OB1 - Moderately strong, greenish grey (5GY 6/1), thickly bedded CALCAREOUS SILTSTONE with medium spaced discontinuities. Massive, irregular parting, micaceous and with dark grey carbonaceous plant debris. Unweathered (Class A) Alcobaça Beds.

OB2 - Moderately strong, greenish grey (5GY 6/1), thickly bedded CALCAREOUS SILTSTONE with medium spaced discontinuities. Massive, irregular parting, micaceous and with dark grey carbonaceous plant debris. Unweathered (Class A) Alcobaça Beds.

To summarise, the sampling included various rock types detailed in Table 4.2. It can be seen from this table that the formations from which samples were taken are mainly constituted by siltstones, mudstones and mudshales in which non-laminated types predominate.

Table 4.2 - Distribution of the samples collected according to the rock types identified.

Rock types	Total
Non-indurated materials	4
Oolitic limestone	1
Sandstone	1
Siltstone	5
Siltshale	3
Mudstone	9
Mudshale	6
Claystone	1
Clayshale	1

4.3.3 - Preparation of the samples

The samples collected in the Arruda area were taken, as it is stated in Section 4.3.2, from cores with an approximate length of 0.8 m. All samples, except the ones for uniaxial compression and triaxial swelling tests, were homogenised in order to reduce any lithological differences occurring within those stratigraphic intervals. The technique applied involved breaking the rock cores for each sample with several hammer blows and then mixing manually for several minutes the resulting fragments in a large aluminium tray. This procedure was not used for blocks OB1 and OB2 because they come from a specific horizon which does not have significant lithological variations.

A portion of approximately 200 g of material was taken from each sample for mineralogical and geochemical testing. These subsamples were first broken up with a hammer and then crushed to $<212 \mu\text{m}$ using a tungsten carbide disc mill ('tema' crusher) for 30 seconds. A representative subsample weighing approximately 100g was then taken by using a sample splitter apparatus.

The preparation of the specimens for uniaxial compression tests from rock cores only required the diametrical cut of the edges according to the height recommended for the tests. In the cases of blocks OB1 and OB2 cored samples were taken, using a sampler with approximately 62.5 mm nominal internal diameter. Afterwards, coring specimens were cut diametrically according to the height required for those tests. The specimens used in triaxial swelling tests were identical to those used in compression tests, but were dry cut into regular 30 mm cubes.

Atterberg limits, grain specific gravity, methylene blue adsorption value, swelling (except triaxial) and direct shear tests required the previous disaggregation of the material. In the selection of the process to be used to disaggregate the samples, it was sought to select a method that simulated the weathering mechanisms that most commonly affect these rocks in natural environments. The samples were accordingly subjected to cycles of drying and wetting, using the slake durability test equipment to accelerate the disaggregation of the samples during the wetting periods. The scheme applied to disaggregate the samples consisted of cycles of drying and wetting during which the materials were immersed and subjected to about 1200 rotations in the slake

durability apparatus following oven drying at 65°C. The residue deposited in the tanks of the slake durability test equipment was dried in an oven at 65°C and then was carefully disaggregated using a rubber rammer and stored in plastic bags.

The number of cycles required to disaggregate the samples varied according to the amount of the material required for the tests, as well as to the induration and weathering state of the rocks. After these operations, when the amount of the disaggregated material was sufficient to carry out the tests above quoted, representative subsamples were taken using a splitter apparatus. The subsamples to be used in the determination of grain specific gravity and Atterberg limits as well as in swelling and direct shear tests were passed through a #40 ASTM (425 µm) sieve, while those used to determine methylene blue adsorption value were passed through a #200 ASTM (75 µm) sieve. In both cases the material retained in the sieves was rejected. The samples used for modified Proctor tests were crushed in a jaw crusher in order that the particles used in the preparation of the mixtures were not larger than 4.76 mm (#4 ASTM sieve).

The fragments used in the slake durability tests were shaped by hand using a sharp knife. The specimens used to determine porosity and dry density as well as jar slake tests and natural exposure and simulated ageing tests were dry cut using a thin diamond disk mounted on an electric saw. The specimens dimensions varied according to the requirements of the various tests.

5 - MINERALOGICAL AND TEXTURAL CHARACTERIZATION

5.1 - Introduction

This chapter presents the mineralogical and textural characterization of mudrocks collected in the Arruda and Óbidos areas. The methods used were briefly introduced, in Section 2.2.5, but the techniques applied in the laboratory work are described in detail in this chapter.

Since the mineralogical composition of mudrocks strongly controls the geotechnical properties of these materials, the qualitative and quantitative determination of the mineral phases present is a fundamental task in the study of these rocks. Furthermore, the size, arrangement and links between the various constituents also determine the behaviour of these materials. Thus, this chapter describes the experimental work intended to determine the mineralogical composition of the samples and to investigate their relevant textural aspects. The influence of these mineralogical and textural factors on the geotechnical properties of mudrocks will be discussed in Chapter 8.

Firstly the various experimental techniques used in the mineralogical characterization including X-ray diffraction (XRD) which was applied (i) to the whole rock fraction to identify the mineral phases present in the rocks and in the determination of the

percentages of feldspar, and (ii) to the less than 2 μm fraction in order to determine the relative abundances of clay mineral species, are described.

In addition to this X-ray fluorescence (XRF) was used to determine the elemental abundances within the samples. The data from this technique also enabled the determination of the percentages of apatite and rutile present in the rocks. Wet geochemical techniques were used to determine the proportions of quartz, carbonates (calcite and dolomite), pyrite and organic matter present in the rocks. The mineralogical composition of the samples was recalculated from the data obtained using the laboratory techniques referred to. Furthermore, the distribution of the different mineral phases as a function of the depth in the borehole profiles were also analysed.

The textural description of the samples was carried out on the basis of the observation of thin sections under the optical microscope and scanning electron microscope (SEM). The SEM studies undertaken included backscattered electron (BSE) images and qualitative analyses performed using an energy dispersive X-ray analysis system (EDS).

The observations of all the samples were organised on the basis of a descriptive scheme used to characterize the microtextural aspects of mudrocks. Finally, the most relevant microtextural aspects of the various rock types identified in the sample collection are described.

5.2 - Mineralogical characterization

5.2.1 - X-ray diffraction: mineral identification and clay mineral and feldspar abundances

Due to small crystal size the use of routine optical petrographic techniques in the study of the mudrock mineralogy for the identification of clay minerals is impracticable. However, because clay minerals have a regular crystalline structure, it is easy to identify them by X-ray diffraction. Thus, the use of this technique enables the distinction of the

different clay mineral species present in a mixture and the calculation of their relative percentage to an acceptable degree of accuracy.

5.2.1.1 - X-ray diffraction theory

The theoretical basis of X-ray diffraction is described in detail in Klug & Alexander (1974) and Moore & Reynolds (1989) it being beyond the scope of this thesis to cover these aspects in depth.

In a laboratory diffractometer, X-rays are produced by the bombardment of a metal target, the anode, with a beam of high energy electrons emitted by the cathode (filament), where a voltage difference of 20 - 60 kV is applied.

Fig. 5.1 schematically displays the geometry of a modern diffractometer. The X-rays produced in the anode pass through a collimator system to produce a sub-parallel beam. The divergence of this beam is controlled by the divergence slit, the aperture of which depends on the work interval selected for the diffraction angles at which the analysis will be performed (Hardy & Tucker, 1988). The divergent beam is then directed at the specimen, which is mounted in the sample holder, which is motor driven to rotate at a regular speed. The rotation movement allows the mineral planes in the sample to attain an appropriate angle at which they will diffract the X-rays according to Bragg's law. The X-ray diffracted beam also passes through an optical system (receiving and scatter slits) and then to the detector (Hardy & Tucker, 1988).

The phenomenon of the X-ray diffraction by a crystalline structure is represented schematically in Fig. 5.2, and only occurs when the geometrical condition expressed by

Bragg's law is satisfied:

$$n\lambda = 2d \sin\theta \quad (5.1)$$

where,

n (integer = 0, 1, 2, 3,....) - integer of wavelengths;

λ - wavelength of the X-rays;

d - lattice spacing;

θ - angle of diffraction.

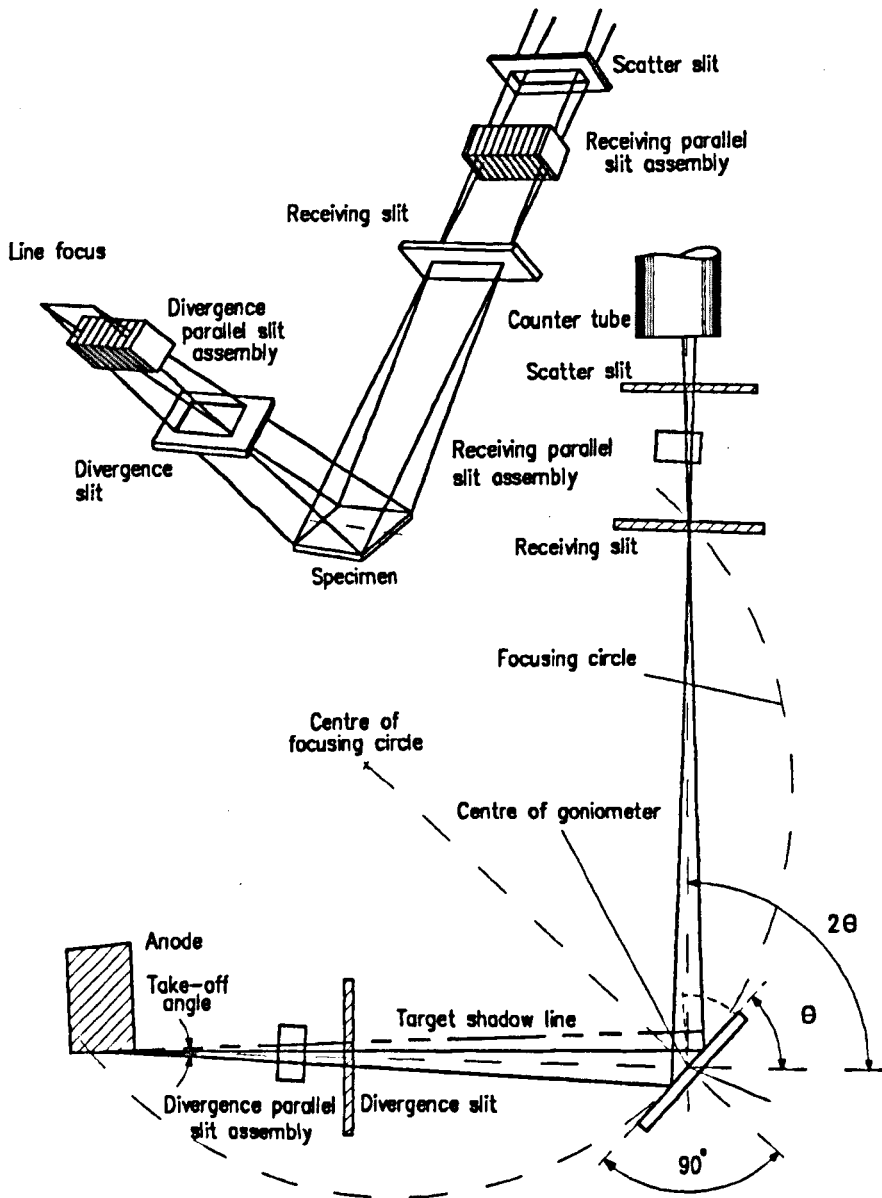


Fig. 5.1 - Schematic representation of the geometry of a typical diffractometer (adapted from Hardy & Tucker, 1988).

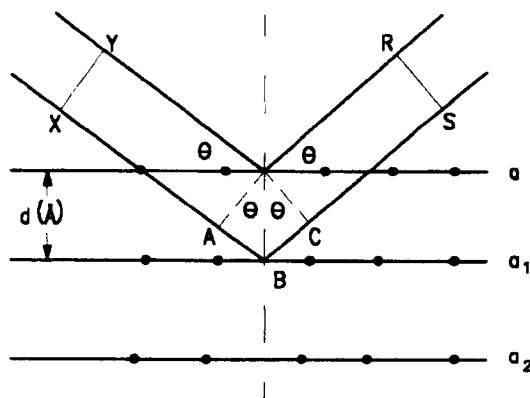


Fig. 5.2 - Geometry of the X-ray diffraction by more than one row of atoms illustrating Bragg's law.

According to the scheme represented in Fig. 5.2 when a wavefront (x - y) is incident on atomic planes a - a₁, it is found that the reflection path of the rays reflected in plane a₁ is increased by AB+ BC which corresponds to $2d\sin\theta$. In this way, for a specific λ , d, and n, there is only one angle θ to which the rays reflected by a set of atomic planes are in phase, *i.e.* the difference in paths of wavefronts must be equal to a whole number of wavelengths ($n\lambda$). For any other angular positions of these planes there is destructive interference and the diffraction phenomenon does not occur.

In the apparatus used the diffractometric method consists briefly on the rotation of the sample around a focused beam of X-rays and in the measurement of the radiation diffracted by a detector (counter tube) assembled on the mobile arm of a goniometer. In order to preserve the so-called parafocusing arrangement of the goniometer, it is necessary that the detector has an angular speed, twice that of the sample holder, *i.e.* if the latter rotates through θ degrees, the goniometer executes a rotation of 2θ degrees (Wilson, 1987). Consequently, the angle at which the radiation is received by the detector is measured in 2θ . The diffraction pattern directly reflects the intensities (peaks) corresponding to the radiation diffracted by the crystalline structures of the various minerals present, as a function of the diffraction angle 2θ .

In the case of pure minerals, the respective diffraction pattern is characterised by a series of peaks of different intensities at various angles 2θ corresponding to the reflection of

the X rays by the various atomic planes that constitute the crystalline structure of a given mineral. Thus, minerals have distinct diffraction patterns which are listed in tables both in angular values 2θ and in lattice spacing values d for the most intense peaks of standard diffraction pattern of the various minerals. These tables are used to identify the various mineral phases present in a mixture.

Rock samples can be seen as mixtures of minerals and they produce diffraction patterns with various sets of peaks which are characteristic of the different mineral phases present in the rock. In practice, however, only the most intense reflections for each mineral are detected, so that the mineral phases in the mixture can be identified on the basis of the position of angle 2θ and their relative abundances may be determined from the intensities of the peaks present in the diffraction pattern. Since the intensity or relative size, of the peaks increase in proportion to the amount of mineral present, it is also possible to estimate quantities of the minerals. Unfortunately as minerals vary in their reflectivity, to achieve quantification of the minerals present in a mixed assemblage requires careful calibration of the system. The means by which a quantitative mineral analysis may be obtained is discussed in Sections 5.2.1.4 and 5.2.1.5.

5.2.1.2 - Preparation of the samples

a) Whole rock

X-ray diffraction analysis of whole rock samples aims at giving a general mineralogical characterization of rocks. The manner in which mounts are prepared affects the results. Basically, the samples can be prepared either so that the platy minerals such as clays are arranged in a similar direction (smear mount), or in such a way that all the constituents are randomly oriented (powder mount). The latter are used where mixtures of platy and equant minerals are being studied.

In the preparation of oriented mounts, lamellar particles, *e.g.* the clay minerals, tend to be aligned with their long axes parallel to the glass slide. In clay minerals the basal spacing planes [planes (001)] are parallel to their long axes so that the preparation of oriented samples maximizes the intensity of the reflections generated by these minerals.

This type of preparation increases the sensitivity of the diffraction technique to the occurrence of small quantities of clay minerals, but can, however, reduce the intensities for non-clay constituents.

This is not the case for random mounts where a large number of different lattice planes are presented to the X-rays beam, allowing the study of both clay and non-clay mineral species.

Whole rock smear mounts were used in the experimental work carried out because the preparation technique is extremely easy and because the relative proportions of non-clay species, except for feldspars, were not determined by quantitative diffraction analysis (Biscaye, 1965). However, according to Moore & Reynolds (1989), the preparation technique used has some disadvantages such as: (a) the orientation obtained is only fair, and (b) the aggregate is usually particle-size segregated with the finest material deposited at the top of the mount, *i.e.* on the face exposed to the X-ray beam.

The preparation of smear mounts consisted of grinding a small amount of dried sample to a fine powder in an agate pestle and mortar. Thereafter, a little distilled water was added, and the mixture was homogenised. The suspension formed was deposited on the surface of a glass slide using the pestle. The aggregate in suspension was concentrated by evaporation of water at room temperature, the excess of material deposited on the glass slide was removed with a sharp knife. The film obtained by sedimentation was placed on the diffractometer sample holder and analysed.

The slides were scanned using Cu K α radiation ($\lambda = 1.541838 \text{ \AA}$) produced at 35 kV and 20 mA using a Philips PW 2253/20 Cu tube. The whole rock smear mounts were scanned between 4° and 44° 2 θ at a rate of 2° per minute. The operating system was computer controlled and data were processed using specific Sietronics Diffractometer Automation v.2.2 software.

b) Less than 2 μm fraction

It was necessary, in order to determine the relative percentages of clay species present in the rocks, to prepare samples on less than 2 μm fraction. Whole rock diffraction

patterns are not suitable for the quantitative analysis of clay minerals because peaks related to these minerals generally have weak intensities. This can be explained by:

- high level of background radiation;
- the dilution of crystalline minerals by material invisible to X-ray, e.g. organic matter and amorphous oxides;
- lack of mineral orientation.

Among the reasons presented, the poor orientation of the minerals is, probably, the main factor that determines the weak intensity of the peaks of clay mineral species. Insufficient disaggregation of whole rock samples can give rise to large clay aggregates that prevent the individual platelets from being deposited with planes 001 parallel to the slide. The difficulties that arise from the disaggregation of samples can be a consequence of the degree of cementation and inter-granular bonds developed during the compaction and diagenesis processes. In addition to this, the presence of high proportions of cements can also result in the dilution of clay minerals, which also results in a reduction of the intensity of the peaks of those minerals.

The method adopted - *The Milipore® filter transfer method* - in less than 2 μm fraction preparations is described in detail in Moore & Reynolds (1989). The preparation technique consisted of making a suspension with about 10g of sample and 70 to 80 ml of distilled water, and then disaggregating it in an ultra-sonic bath for 15 minutes. The less than 2 μm fraction was separated from the remaining material by centrifugation. As a rule, for a temperature of 20°C (ordinary laboratory temperature) the samples were centrifuged at 900 r.p.m. for 2.5 minutes. The final suspension was decanted and the coarsest material discarded.

As the diffraction patterns of the clay minerals, mainly of the expandable clays (smectites and some mixed-layer clay minerals), vary with the number and kind of exchangeable cations, the samples are generally saturated with a specific cation by treating it with an excess of the solution of the chosen cation (Brown & Brindley, 1980). In this study the procedure adopted for the flocculation of the samples used CaCl_2 , making the suspension to 0.1M concentrate.

The clay films for analysis by X-ray diffraction were prepared from the suspensions, using a filtration equipment developed by *Milipore® Corporation*. This equipment consists of a side-necked vacuum flask and a funnel reservoir clamped to a flat porous glass base on which the filter (Whatmans 0.45 μm pore size, 47 mm diameter) is placed (Fig. 5.3).

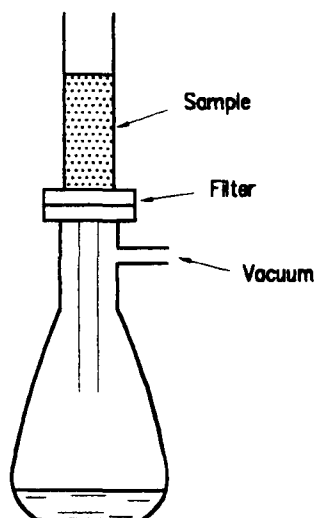


Fig. 5.3 - Filtration apparatus (after Moore & Reynolds, 1989).

The procedure used to prepare the clay films consisted of adding the clay suspension to the funnel, stirring it gently, in order to keep the suspension homogeneous. A filtration period of up to 3 minutes was used because it was sufficient to obtain a thick film for analysis by X-ray diffraction and short to prevent any sample segregation from occurring. The clay film collected on the filter was carefully removed from the porous glass base and dried in a oven set at 50°C for some minutes (generally 3 to 4 minutes). After partial drying of the filter (it is convenient that the surface of the filter is still relatively wet), it was inverted and the clay film was placed on the glass slide as illustrated in Fig. 5.4.

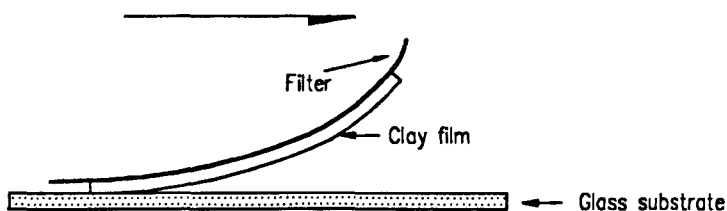


Fig. 5.4 - Application of a wet clay film onto a glass substrate (after Moore & Reynolds, 1989).

The main advantage of this technique in the preparation of less than 2 μm oriented samples in relation to others, is that there is no significant particle size segregation within the clay film because the vertical movement of the suspension due to filtration is faster than the settling rate of the coarsest particles. This also explains why it is necessary to invert the filter, presenting the most particle-size-representative portion of the sample to the X-ray beam, while the other face that is enriched in the finest sizes, becomes in contact with the glass slide.

5.2.1.3 - Mineral identification

a) Whole rock fraction

The following non-clay mineral phases were identified in some or all of the samples present using the data compiled by JCPDS (1974).

Quartz - identified by the sharp peaks at 3.34 \AA ($26.67^\circ 2\theta$) and 4.26 \AA ($20.85^\circ 2\theta$).

Calcite - identified by the sharp peak at 3.03 \AA ($29.43^\circ 2\theta$) and by two smaller peaks at 2.29 \AA ($39.43^\circ 2\theta$) and 2.09 \AA ($43.18^\circ 2\theta$).

Dolomite - identified by the peak at 2.89 \AA ($30.99^\circ 2\theta$).

Feldspars - identified by the smaller peaks at 3.24 \AA ($27.50^\circ 2\theta$) (K-feldspar) and at 3.19 \AA ($27.95^\circ 2\theta$) (plagioclase).

Pyrite - identified by the small peak at 2.71 Å (33.07° 2θ).

The following clay minerals were noted in the whole rock scans: kaolinite, illite, chlorite as well as expandable clay minerals of smectite and/or mixed-layer illite/smectite. The scans of whole rock fractions are presented in Appendix I.1.

b) Less than 2 μm fraction

The procedure used in identification of the clay minerals in the less than 2 μm fraction consisted on analysing the samples in their natural state (air-dried), after glycolation by treatment with ethylene-glycol vapour at 60°C in a desiccator for 12 h and finally after heating at 550°C for at least 1 h in an oven.

The absorption of the ethylene-glycol vapour by the lattices of swelling clay minerals leads to an increase in interlattice spacing of these minerals altering, consequently, the position (2θ) of their diffraction peak in a distinctive manner. Inversely, heating causes the collapse of the structure of swelling clay minerals, reducing the interlattice spacing to a minimum. The heating of the samples to 550°C also causes the collapse of kaolinite.

Fig. 5.5 schematically displays the methodology used in the identification of clay minerals.

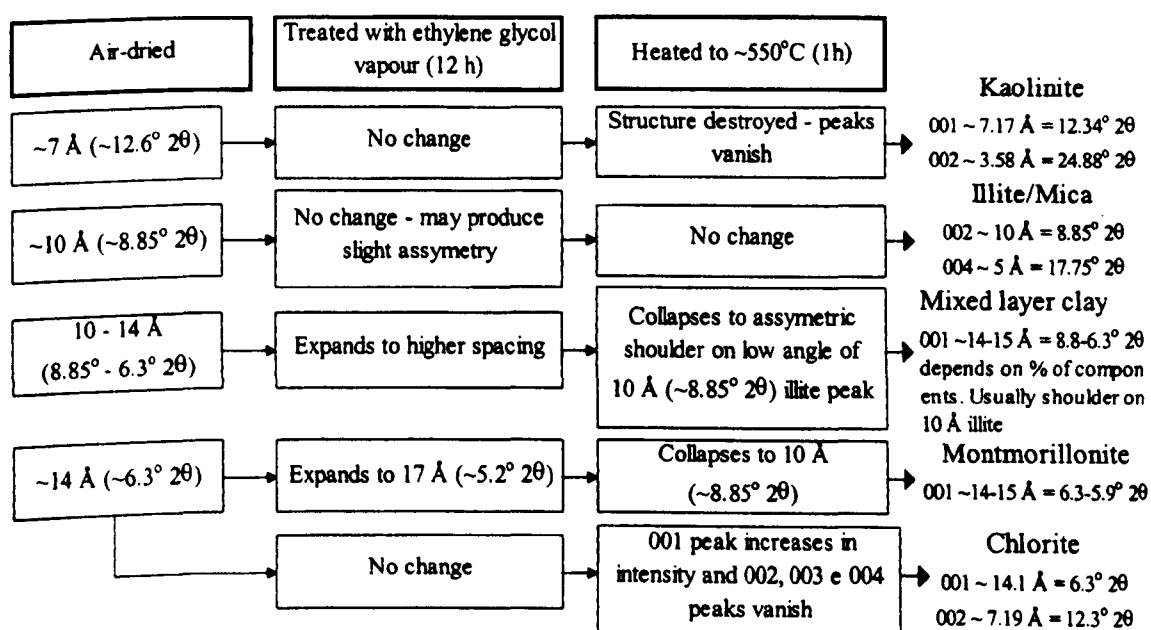


Fig. 5.5 - Flow chart used for clay mineral identification (adapted from Starkey et al., 1984).

The scans of the samples in the air-dried and glycolated states were run between 4-44 °2θ at a scan rate of 2 °2θ/minute. While the scans of the samples in heated state were run only to 30 °2θ because the main diffraction peaks of the clay minerals present, that are of interest for identification, occur in this range. The scans of less than 2 μm fraction of all samples run under the conditions referred to above are presented in Appendix I.1.

According to the flow chart presented in Fig. 5.5 the clay minerals identified in the samples were as follows:

Kaolinite - identified by the strong peak at 7.17 Å (12.34° 2θ) destroyed on heating to 550°C;

Illite - identified by the strong peak at 10 Å (8.85° 2θ) which after glycolation may become asymmetrical. Heating to 550°C generally caused an increase in intensity due to the collapse of the structures of the swelling clay minerals to 10 Å.

Smectite - identified by the peak at 14 Å (~6.3° 2θ) expanding to 17 Å (~5.2° 2θ) after glycolation and collapsing to 10 Å (8.85° 2θ) after heating to 550°C, increasing the intensity of the existing 10 Å illite peak.

Chlorite - identified by the peak at 14 Å (~6.3° 2θ) which is not affected by glycolation and increases its intensity after heating to 550°C; some samples show partial resolution of the 004 chlorite peak at 3.55 Å (~25.1° 2θ) from the kaolinite peak at 3.58 Å (~24.9° 2θ) which allows the identification of both minerals; with exception of reflection 001 which increases its intensity, the remaining 002, 003 and 004 chlorite reflections are much weakened after heating to 550°C (Moore & Reynolds, 1989).

Mixed-layer illite-smectite - identified according to Starkey *et al.* (1984) on the basis of the following characteristics: in the air-dried state the illite peak at 10 Å possesses a shoulder on the side with highest d spacing which spread to 14 Å; after treatment with ethylene-glycol the position of this asymmetry moves to a 2θ value characteristic of a larger d spacing, forming a wide ragged peak rather than a discrete peak; after heating, this ragged peak collapses to 10 Å increasing the intensity of the illite peak (10 Å).

5.2.1.4 - Determination of the relative percentage of clay minerals

The relative proportions of the minerals identified in mudrocks can be determined by XRD. This method consists of the comparison of the areas of selected peaks of the mineral being analysed with the peak produced by an internal standard, usually boehmite, which is added in a known percentage during the preparation of the sample.

The application of this method involves the calibration by X-ray diffraction of various synthetic mixtures prepared for different proportions of pure minerals (standards) and of internal standard mineral. In this way, by measuring the areas of the peaks relative to pure minerals and the internal standard, it is possible to construct calibration curves used in the quantification of the mineral species (identical to pure minerals) occurring in the samples to be analysed.

This methodology used in quantitative analysis is mainly applicable to chemically simple species such as quartz (Till & Spears, 1969) and feldspars (Fellows & Spears, 1978). However, it is impracticable to extend this methodology to the quantification of clay minerals occurring in natural samples because these minerals are chemically heterogeneous and exhibit variable composition and crystallinity. It follows from this, that the diffraction traces associated with reference clay minerals (standards) used in the calibrations are different from those of naturally occurring clay minerals (Biscaye, 1965).

The determination of the proportions of clay minerals in natural samples can alternatively be based on semi-quantitative methods such as those proposed by Schultz (1964), Biscaye (1965) and Weir *et al.* (1975). The first method has been adopted by several authors (Burnett, 1974; Russell, 1982; Dick & Shakoor, 1992 and Dick *et al.*, 1994) in the quantification of the clay minerals present in mudrocks, being followed in this study too. The Schultz (1964) semi-quantitative method uses the 7Å and 10Å peak areas (*i.e.* intensity) and the 7Å, 10Å, 14Å and 17Å peak heights achieved on oriented samples in an air-dried state, after treated with ethylene-glycol (glycolated) and after

heating to 550°C, to calculate the proportions of kaolinite, illite, chlorite, smectite and mixed-layer illite-smectite.

According to this method the area of the diffraction peaks is directly related to the concentration of the mineral that produces these peaks, *i.e.*, identical concentrations of different clay minerals in a sample produce diffraction peaks with similar areas. This fact was found experimentally by Schultz (1960) for clay minerals of the illite and smectite types, while in the case of mixtures with similar concentrations of kaolinite and illite, the 7 Å peak area when compared to the 10 Å peak is a function of the degree of kaolinite crystallinity (defined as area to peak height ratio). In order to make the area of 7 Å and 10 Å peaks directly comparable, Schultz (*id.*) multiplied the area of 7 Å peak by an experimentally derived correction factor which is a function of the degree of kaolinite crystallinity.

The Schultz (1964) method assumes that the concentration of illite is directly proportional to the 10 Å peak area after treatment with ethylene-glycol. Heating to 550°C, the interstratified expansive minerals of the illite/smectite type collapse to 10 Å, representing the area of this peak the sum of the concentrations of these minerals and of illite. The proportion of mixed-layered clay minerals can, therefore, be calculated by subtraction of the glycolated peak area from the heat treated peak area.

In the case of chlorite the area of the 7 Å peak corresponds with the sum of the kaolinite and chlorite basal reflections at 7.17 Å (12.34° 2θ) and 7.19 Å (12.3° 2θ). In order to determine the contribution of chlorite to the area of 7 Å peak, Schultz (*id.*) found experimentally that the ratio between the heights of chlorite 14 Å (after heating to 550°C) and 7 Å peaks were approximately 1.5. According to this method the percentage of chlorite is calculated by multiplying the corrected 7 Å peak area by the 14 Å to 7 Å peak height ratio.

According to Schultz (*ibid.*) the differentiation between smectite and mixed-layer illite-smectite can be considered to be unrealistic. According to this author, it can be understood that all material that produces a reflection at 17 Å is only constituted by

expansive interstratified minerals, rather than by a combination of smectite and mixed-layer clay.

In this work the methodology proposed by Schultz has been adopted and smectite was only considered when the reflection at 17 Å (in the glycolated sample) was strong and the shift of the position of angle 2θ for the smectite peak between the dry and glycolated was clear. Schultz (1964) found experimentally that the ratio between smectite and mixed-layer clay, calculated by the ratio between the heights of 17 Å and 10 Å peaks (the latter achieved on heat treated samples) varied between 4 and 5, using an average value of 4.5. Therefore the percentage of smectite is calculated by multiplying the sum of the minerals that collapse to 10 Å at 550°C by the 17 Å to 10 Å peak height ratio.

The application of the method proposed by Schultz (1964) involves the measurement of the areas and of the height of the peaks referred to above, which were determined in the scans of the fraction smaller than 2 µm using the Philips PW 1877/92 (automatic powder diffraction) computer program. In order to correct the area of the kaolinite peak (7 Å) on the basis of factors (7Å/10Å) determined experimentally by Schultz (1960), it was necessary to measure the kaolinite crystallinity taken as the ratio between the area and the height of the 7 Å peak.

According to the method proposed by Schultz, the areas of the peaks are obtained by the sum of five measurements of the height, in counts per second, above the baseline. One measurement is at the peak position and the other four on each side at $1/2^\circ$ and $1^\circ 2\theta$ from the peak position. As the areas of the peaks obtained by the computer program are not comparable with the measurements obtained by the method described above, the area of peak 7 Å was calculated according to the procedure proposed by Schultz. The correction factors 7Å/10Å were derived from the experimental calibration curve deduced by Schultz (1960) on the basis of the values calculated for the degree of kaolinite crystallinity (Fig. 5.6).

The equations used to calculate the relative percentages of the various clay minerals are as follows:

$$\text{Corrected } 7\text{\AA} \text{ peak area} = \frac{7\text{\AA} \text{ peak area}}{7\text{\AA}/10\text{\AA} \text{ intensity ratio}} \quad (5.2)$$

$$\text{Kaolinite + Chlorite (\%)} = \frac{\text{Corrected } 7\text{\AA} \text{ peak area}}{\text{Corrected } 7\text{\AA} \text{ peak area} + 10\text{\AA } 550^\circ\text{C} \text{ peak area}} \times 100 \quad (5.3)$$

$$\text{Chlorite (\%)} = (\text{Kaolinite + Chlorite}) \times \frac{14\text{\AA } 550^\circ\text{C} \text{ peak height}}{1.5 \times 7\text{\AA} \text{ peak height}} \quad (5.4)$$

$$\text{Kaolinite (\%)} = (\text{Kaolinite + Chlorite}) - \text{Chlorite} \quad (5.5)$$

$$\text{Illite (\%)} = \frac{10\text{\AA} \text{ glycolated peak area}}{\text{Corrected } 7\text{\AA} \text{ peak area} + 10\text{\AA } 550^\circ\text{C} \text{ peak area}} \times 100 \quad (5.6)$$

$$\text{Smectite (\%)} = \frac{17\text{\AA} \text{ glycolated peak height}}{4.5 \times 10\text{\AA } 550^\circ\text{C} \text{ peak height}} \times (100 - \text{Kaolinite} - \text{Chlorite}) \quad (5.7)$$

$$\text{Mixed-layer clay (\%)} = 100 - (\text{Kaolinite} + \text{Chlorite} + \text{Illite} + \text{Smectite}) \quad (5.8)$$

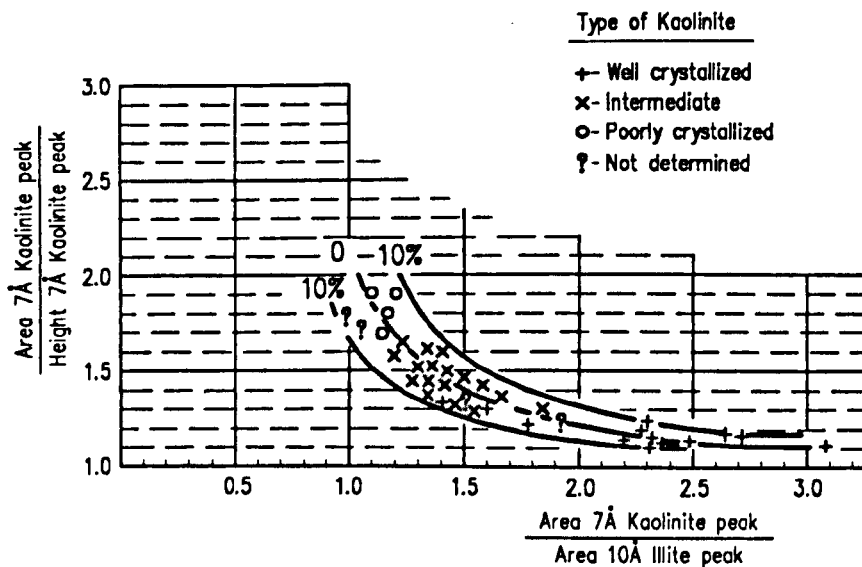


Fig. 5.6. - Experimental curve deduced by Schultz (1960) for mixtures of various types of kaolinite with equal amounts of the same illite sample in which the degree of kaolinite crystallinity is related to the ratio of the 7 Å/10 Å peak areas.

Table 5.1 presents the correction factors 7Å/10Å used and the values determined for the degree of kaolinite crystallinity and for the corrected 7 Å peak area, as well as the

relative percentages calculated to 100% of the clay minerals occurring in the samples studied.

Table 5.1 - Relative proportions of clay minerals identified in the samples and the factors used to recalculate them.

Sample	DKC	FC 7Å/10Å	Área 7Å _{corr.}	Área 7Å _{total}	Chlorite	Kaolinite	Illite	Smectite	MLC	Total
51	1.60	1.20	119.2	22.7	0	23	42	15	20	100
52	1.35	1.55	561.3	25.7	4	21	21	7	47	100
81	1.35	1.55	425.8	15.6	0	16	26	7	51	100
83	1.15	2.30	587.4	25.8	2	24	27	9	38	100
111	1.30	1.70	466.5	20.0	2	18	23	0	57	100
112	1.25	1.85	382.2	17.4	2	15	30	0	53	100
114	1.25	1.85	650.3	22.0	4	18	35	0	43	100
151	1.45	1.40	405.0	19.0	2	17	21	0	60	100
152	1.30	1.70	603.5	20.4	2	19	32	0	47	100
153	1.30	1.70	531.8	18.5	1	17	33	0	49	100
154	1.35	1.55	981.9	35.0	5	30	35	0	30	100
156	1.20	2.10	658.1	25.6	1	24	34	0	41	100
162	1.20	2.10	421.0	31.9	1	31	55	0	13	100
163	1.15	2.30	375.2	24.5	1	24	44	0	31	100
283	1.40	1.50	412.0	20.0	2	18	31	0	49	100
285	1.40	1.50	370.0	20.2	1	19	26	0	54	100
286	1.40	1.50	449.3	23.6	5	19	28	0	48	100
294	1.45	1.40	427.1	19.8	2	18	33	0	47	100
296	1.40	1.50	472.7	20.1	3	17	30	0	50	100
332	1.25	1.85	494.1	21.9	1	21	27	11	40	100
333	1.25	1.85	528.1	21.1	1	20	25	8	46	100
334	1.15	2.30	684.3	28.3	3	25	31	7	34	100
336	1.30	1.70	628.2	19.6	4	15	30	10	41	100
342	1.35	1.55	456.1	16.4	4	13	26	12	45	100
345	1.35	1.55	96.1	56.5	0	57	26	0	17	100
431	1.20	2.10	898.1	28.2	3	25	42	0	30	100
436	1.35	1.55	681.3	28.9	5	24	46	0	25	100
441	1.35	1.55	1155.5	34.5	6	29	33	0	32	100
445	1.30	1.70	1155.3	36.9	4	33	29	0	34	100
OB1	1.25	1.85	398.9	22.2	3	19	38	0	40	100
OB2	1.20	2.10	325.2	19.8	3	17	43	0	37	100

DKC - Degree of kaolinite crystallinity; FC 7Å/10Å - 7Å/10Å intensity ratio; 7Å_{corr.} - Corrected 7Å peak area; 7Å_{total} - Total 7Åclay (kaolinite + chlorite); MLC - Mixed-layer clay.

5.2.1.5 - Feldspar determination

The quantification of the feldspars in mudrocks can be achieved by wet chemical analysis and by XRD.

The technique proposed by Blatt *et al.* (1982), referred to in Section 2.2.5, consists of the fusion of a rock mixture with sodium bisulphate. This technique allows the isolation

of quartz and feldspar, being the proportions of the various types of feldspars present evaluated by spectrophotometric determination of potassium, sodium and calcium after the fusion. This technique was based on the work of Kiely & Jackson (1965) regarding the determination by fusion with sodium bisulphate of percentages of quartz, feldspar and micas in soils. The results obtained in the studies by Kiely & Jackson (*op. cit.*) demonstrated that although with this technique, the dissolution of feldspars was reduced, the percentage dissolved could not be ignored and was a function of the mineralogy and grain size. In order to eliminate the errors introduced by the dissolution of feldspars, these authors proposed a series of correction factors derived from standard samples of feldspars. However, as the correction factors vary as a function of composition and grain size of the feldspars, difficulties arise in applying the appropriate correction factor to unknown mudrocks (Fellows & Spears, 1978).

Fellows & Spears (1978) proposed a method based on X-ray diffraction analysis, which involves the pre-ignition of the sample at 950°C, and the use of boehmite as an internal standard. According to this method, the X-ray diffraction analysis is carried out on mixtures in a proportion of 9 of rock to 1 of boehmite. The percentages of the feldspars present in the samples are calculated on the basis of the measurement of the areas of the boehmite, microcline and albite peaks, according to the equations proposed by Fellows & Spears (*id.*). This method was applied to calculate the percentages of feldspars in Coal Measures mudrocks for which they advocated this procedure. However, the main disadvantage of this method resides in the fact that the albite reacts with the potassium released from the structures of the clay minerals during the fusion of the samples to 950°C, giving rise to the formation of potassium feldspars which consequently alters the proportions of sodium and potassium feldspars present in the samples.

The quantification of the feldspars in the samples studied in this work was based on the method developed by Hooton and Giorgetta (1977). This method allows the calculation of the concentrations of the various components of a mixture on the basis of the measurement of the intensities of the chosen peaks of the components on a diffraction pattern. In order to apply this method it is necessary to know the reference intensities (RI) of the respective component and to use a mineral present in the rock as an internal standard. The concentration of the component is calculated in relation to the mineral

chosen as internal standard. Since quartz is present in all samples, it was used as internal standard. Its concentration was determined by wet chemical analysis (see Section 5.2.3.1). The reference intensities used for quartz and feldspars were taken from Baylis (1986). The RI values generally refer to the most intense peaks for the minerals, however, in the case of quartz, as its main reflection suffers interference from illite, the RI corresponding to peak $20.85^\circ 2\theta$ (100 peak) was used. The reference intensities used for quartz and feldspars were as follows:

Quartz ($20.85^\circ 2\theta$)	RI = 1
K-Feldspar ($27.50^\circ 2\theta$)	RI = 2.4
Plagioclase ($27.95^\circ 2\theta$)	RI = 1.7

To summarise, the application of this method consisted of the measurement of the peak intensities referred to above in the whole rock scans, and since the concentration of quartz (see Section 5.2.3.1) was determined by chemical analysis, the percentages of feldspars were calculated on the basis of the following equation proposed by Hooton & Giorgetta (1977):

$$\frac{\% \text{ Mineral}}{\% \text{ Quartz}} = \frac{\text{RIR mineral}}{\text{RIR quartz}} \times \frac{I \text{ mineral}}{I \text{ quartz}} \quad (5.9)$$

where,

RIR - reference intensity ratio

I - intensity of mineral peak

The results for the K-feldspar and plagioclase are presented in Table 5.8.

5.2.2 - X-ray fluorescence analysis

5.2.2.1 - X-ray fluorescence theory

The chemical composition of mudrocks and other materials is determined simply and accurately using the X-ray fluorescence technique, described in detail by Norrish & Hutton (1969), Norrish & Chappell (1977), Potts (1987) and Bennett & Oliver (1992) being outside the scope of this study to discuss these aspects in detail.

Very briefly, the principle of this technique is that when a beam of primary X-rays hits a sample, secondary fluorescent X-ray radiation is emitted with the wavelengths and intensities dependent on the elements present. The wavelengths are resolved by diffraction by a crystal analyser with a known d spacing, the radiation then passes to a counter system that measures the intensities of the spectral lines in impulses per second. The concentrations of the elements in the samples are determined by comparison of the intensities produced by these elements with the measurements in standards with known concentrations (in these elements).

Measurements made in spectrometers are processed using sophisticated computer programs that enable to correct spectral line interference, absorption and matrix effects. Experimental errors are in turn minimized by the careful preparation of the samples and by rigorous control of the X-ray spectrometer operating conditions. The reproducibility of this technique is increased by the use of previously homogenized samples prepared, either in the form of pressed pellets, or in the form of fused disks. The preparation of samples according to this latter technique is considered to be better for determination of the major elements (Fairchild *et al.*, 1988) where as the former method is more appropriate where minor elements are being analysed.

5.2.2.2 - Preparation of fused disks

X-ray fluorescence analysis aims at determining the bulk geochemical composition of the major elements present in rocks. For this reason, the analyses were carried out using

samples prepared in the form of fused disks. The technique used in the preparation of the fused disks is described hereunder.

Before fusion, samples were first pre-ignited to 900°C in order to destroy some components such as organic matter, carbonates and pyrites. The presence of these components may cause problems during the fusion of the samples. For example, pyrite attacks the platinum and gold alloy crucibles used in the preparation of fusions.

The procedure used in the determination of loss on ignition (LOI) of the samples consisted in placing approximately 2 g of material in a silica crucible that was first heated in an oven to 105°C for 24 h and then ignited in an electric furnace at 900°C for about 8 h. The weights of the samples were recorded before and after being heated to 105°C and 900°C in order to determine the water content and the loss on ignition (weight of the dry sample less the weight of the sample after ignited to 900°C) in percent. Finally, the samples were reground to a fine powder using an agate pestle and mortar.

Using the standard Department of Earth Sciences procedure the fusions were prepared mixing exactly 0.75 g of the ignited sample with 7.5 g of lithium tetraborate (Johnson Matthey spectroflux 100) in a platinum and gold alloy crucible. The mixtures were fused by heating to 1100°C for 20 minutes in an electric muffle furnace, stirring twice during this period. The dissolved samples were then poured carefully into a platinum and gold alloy mould pre-heated to 1100°C. The disks were allowed to cool in air for about 30 minutes before analysis. The X-ray fluorescence analyses were carried out on a spectrometer Philips PW 140 with a DEC PDP 11/23 computer running Philips X14D analytical software.

5.2.2.3 - Determination of bulk rock geochemistry

The results of the X-ray fluorescence analysis were recalculated, in order to be used to determine the bulk rock geochemistry.

The totals of the percentages of the major elements (raw XRF data) obtained from the analyses were greater than 98.5 % with the exception of samples 81 and 345 for which the total of elemental percentages exceeded 94 %. These values reflect a level of precision acceptable for X-ray fluorescence analysis, being the variation in totals due to random counting errors and slight oscillations of the operating conditions of the spectrometer (Norrish & Hutton, 1969). The difference between the totals of the samples 81 and 345 and the average totals obtained for the remaining samples could be due to small weighing errors of the former during the preparation of the fused disks (Pike, 1989).

The concentrations of the major elements obtained from the X-ray fluorescence analysis were first recalculated to sum to 100%. The XRF results as determined express the concentrations of the elements within the pre-ignited samples rather than in whole rock because volatile components were destroyed during the ignition process. The values obtained for the loss on ignition correspond to the sum of the components lost during the preparation of the samples for XRF analysis and principally included carbonates, pyrite, organic matter and water from the structural layers of the clay minerals. Therefore, in order to determine the bulk geochemical composition of the rocks, the XRF results have to be recalculated to sum to (100-LOI)% for each sample.

The raw XRF data of all samples are presented in Appendix I.2 and the bulk geochemical composition and LOI values of each rock are given in Table 5.2.

5.2.2.4 - Determination of apatite and rutile

Apatite and rutile were not identified in the whole rock XRD scans because they occurred in mudrocks in quantities too small to be detected by that technique. The percentages of these two accessory minerals can be determined directly from the XRF data (presented in Table 5.2). In this way, the concentrations of apatite and rutile were accordingly calculated on the basis of the percentages of P_2O_5 and TiO_2 . To recalculate apatite, the phosphate (P_2O_5) percentage is multiplied by 1.5 to give the percentage $P_3O_{15/2}$ which was then multiplied by 2.37 (molecular weight apatite/molecular weight

P₃O_{15/2}) (Campbell,1993). The percentage of rutile was assumed to equate directly with the XRF determined percentage of TiO₂ (Campbell, 1993). The results for apatite and rutile are presented in Table 5.8.

Table 5.2 - Recalculated geochemical composition of the mudrocks studied.

Sample	SiO ₂	TiO ₂	Al ₂ O ₃	Fe ₂ O ₃	MnO	MgO	CaO	Na ₂ O	K ₂ O	P ₂ O ₅	SO ₃	Total	Loss on ignition (%)
51	11.67	0.20	4.99	2.36	0.03	1.17	43.26	0.06	0.03	0.13	0.25	64.15	35.85
52	44.93	0.88	17.43	6.97	0.06	3.24	8.30	0.40	3.19	0.10	0.07	85.57	14.43
81	51.54	0.83	18.66	4.96	0.03	2.55	5.73	0.17	3.61	0.09	0.15	88.32	11.68
83	56.03	0.72	12.59	3.71	0.04	2.88	7.43	0.97	2.80	0.09	0.27	87.53	12.47
111	59.19	1.02	16.12	6.27	0.11	1.69	3.20	1.58	2.86	0.06	0.07	92.17	7.83
112	49.08	0.75	14.83	6.23	0.07	2.61	9.31	0.78	2.86	0.16	0.07	86.75	13.25
114	49.03	0.76	14.81	4.98	0.06	2.65	9.77	0.77	2.90	0.12	0.12	85.97	14.03
151	41.19	0.72	16.49	6.55	0.06	1.67	13.57	0.51	3.01	0.10	0.15	84.02	15.98
152	45.35	0.81	17.45	5.33	0.06	2.33	10.00	0.60	3.39	0.09	0.05	85.46	14.54
153	46.67	0.83	17.98	6.18	0.05	2.62	8.21	0.72	3.50	0.12	0.05	86.93	13.07
154	47.26	0.83	17.40	5.39	0.05	2.84	8.41	0.94	3.38	0.13	0.23	86.86	13.14
156	52.99	0.97	18.59	5.40	0.05	2.51	4.31	0.71	3.48	0.09	0.08	89.18	10.82
162	46.45	0.80	18.55	5.04	0.04	2.26	8.68	0.79	3.93	0.07	0.05	86.66	13.34
163	49.57	0.71	14.92	4.99	0.04	2.32	9.75	0.89	3.22	0.12	0.14	86.67	13.33
283	42.60	0.68	13.00	4.59	0.08	2.26	15.89	0.68	2.57	0.11	0.22	82.68	17.32
285	44.89	0.74	15.38	5.51	0.06	2.81	11.36	0.61	3.06	0.09	0.17	84.68	15.32
286	43.06	0.64	13.22	5.06	0.08	2.48	14.82	0.78	2.65	0.12	0.21	83.12	16.88
294	45.04	0.76	17.12	6.78	0.07	2.71	9.62	0.27	3.30	0.14	0.40	86.21	13.79
296	43.81	0.72	15.83	5.54	0.08	2.77	11.76	0.69	3.08	0.10	0.25	84.63	15.37
332	54.40	0.93	14.63	3.78	0.04	2.10	8.88	0.83	3.10	0.08	0.12	88.89	11.11
333	53.86	0.83	17.11	4.93	0.03	2.32	5.92	0.70	3.55	0.11	0.22	89.58	10.42
334	50.36	0.77	15.34	5.77	0.04	2.65	4.60	0.94	3.23	0.10	0.53	84.33	15.67
336	50.17	0.85	19.18	5.17	0.04	3.22	5.64	0.24	3.68	0.09	0.05	88.33	11.67
342	53.86	0.82	14.01	4.36	0.04	2.51	8.40	0.79	3.02	0.09	0.53	88.43	11.57
345	23.94	0.25	5.04	1.53	0.06	2.60	33.44	1.62	1.13	0.08	0.41	70.10	29.90
431	51.31	0.95	18.72	4.96	0.03	2.58	5.09	0.94	3.38	0.10	0.19	88.25	11.75
436	42.82	0.73	16.96	5.53	0.06	2.80	11.59	0.53	3.43	0.09	0.14	84.68	15.32
441	47.61	0.84	19.01	5.84	0.07	3.24	6.07	0.79	3.39	0.07	0.04	86.97	13.03
445	51.15	0.98	20.20	5.95	0.05	2.67	4.36	0.96	3.42	0.09	0.09	89.92	10.08
OB1	45.04	0.63	13.56	4.35	0.05	2.86	13.27	0.14	3.28	0.11	0.43	83.72	16.28
OB2	44.95	0.63	13.88	4.11	0.05	1.69	14.57	0.36	3.34	0.12	0.40	84.10	15.90

5.2.3 - Mineralogical determinations by wet chemical analysis techniques

The percentages of the non-clay minerals occurring in the mudrocks investigated were calculated using wet chemical analysis techniques except for feldspars, apatite and rutile that were determined, respectively, by XRD and XRF. The determination by wet chemical analysis techniques of the non-clay minerals occurring in rocks is justified, in the case of the quantification of the quartz and carbonates because the techniques adopted are rigorous and have a high level of reproducibility, while in the case of the determination of pyrite and organic matter, XRD and XRF are neither very rigorous nor applied.

5.2.3.1 - Quartz determination

The percentage of quartz in the mudrocks can be determined by XRD techniques using the method proposed by Till & Spears (1969). According to this method, the samples are first pre-ignited to 950°C and then mixed with boehmite in the weight proportion of 9 (sample) to 1 (boehmite). The percentage of quartz is calculated on the basis of the ratio between the areas of the quartz peaks at 4.26 Å (20.8° 2θ) and of the boehmite at 6.18 Å (14.5° 2θ). The determination of the percentage of quartz according to this method implies the prior establishment of the calibration curve between the ratio quartz peak area/boehmite peak area and the concentrations of quartz. Calibration curves can be obtained from the literature (Till & Spears, 1969; Campbell, 1993; Czerewko, 1997) or experimentally either by using standard compounds, having first produced a series of mixtures with various proportions of quartz and boehmite, or via determination by chemical analysis of the percentages of quartz in the various samples used to produce the calibration curve. In the first case, the calibration curve parameters adopted may not be appropriate because they have been determined with equipment (diffractometer) and in operating conditions that differ from those used for a particular analysis. In the second case, the additional experimental work is significant, mainly when it is not possible to use standard compounds. In research studies it is preferable to produce an

individual calibration curve which implies an increase in the experimental work involved in this method. This fact, together with the good reproducibility of wet chemical analysis techniques justified the decision to determine the concentration of quartz in the rocks studied by chemical analysis.

Several methods for quantitative determination of quartz by chemical analysis are found in the literature such as that proposed by Trostel & Wynne (1940) Kiely & Jackson (1965) and Chapman *et al.* (1969). The first method involves the fusion of the sample with potassium bisulphate. The use of this compound for fusion is not recommended as it can lead to the formation of impurities that are removed neither during the hydrochloric and distilled water washing process, nor during treatment with sulphuric and hexafluorosilicic acid, and thus alters the results obtained for quartz concentrations (Campbell, 1993).

In the samples studied, the method proposed by Chapman *et al.* (1965) based on the original method developed by Kiely & Jackson (1965), was adopted in the quantitative determination of quartz, which involves fusion of the samples with sodium bisulphate. The use of this compound in fusions does not involve the problems encountered with potassium bisulphate.

The followed method involves fusion of approximately 200 mg of powdered sample with 12 g of sodium bisulphate ($\text{Na}_2\text{S}_2\text{O}_7$) in a silica crucible. After fusion the residue was first boiled in 3*N* hydrochloric acid (HCl) and then washed three times with hydrochloric acid and once with distilled water. During each wash the residue was centrifuged and the supernatant solution removed. Thereafter, the residue was boiled in a solution of 0.5*N* sodium hydroxide (NaOH) for 2.5 minutes, and then washed three times with 3*N* hydrochloric acid and once with distilled water. Finally, the residue was transferred to polyethylene tubes and treated with 5 ml of a 30% solution of hexafluorosilicic acid (H_2SiF_6). The solutions in the tubes were stirred twice daily. The samples treated with hydrofluosilicic acid were kept at a temperature of between 15° and 20°C for three days in order to prevent the formation of free hydrofluoric acid (HF) which dissolves quartz. This period is, generally, sufficient for all the constituents, with exception of the quartz, to be dissolved by the hexafluorosilicic acid. The efficiency of this treatment can be confirmed by analysis of the final residue by X-ray diffraction.

After the period of treatment, the solutions containing hexafluorosilicic acid were washed with distilled water, and the residue was centrifuged. The percentage of quartz was calculated by gravimetric determination using pre-calibrated platinum crucibles.

Fig. 5.7 schematically represents the laboratory procedure used in the quantitative determination of the quartz in the mudrocks investigated. The determination of the percentages of quartz was performed on two subsamples. Table 5.3 shows the results determined for the two subsamples as well as the average values calculated for each one.

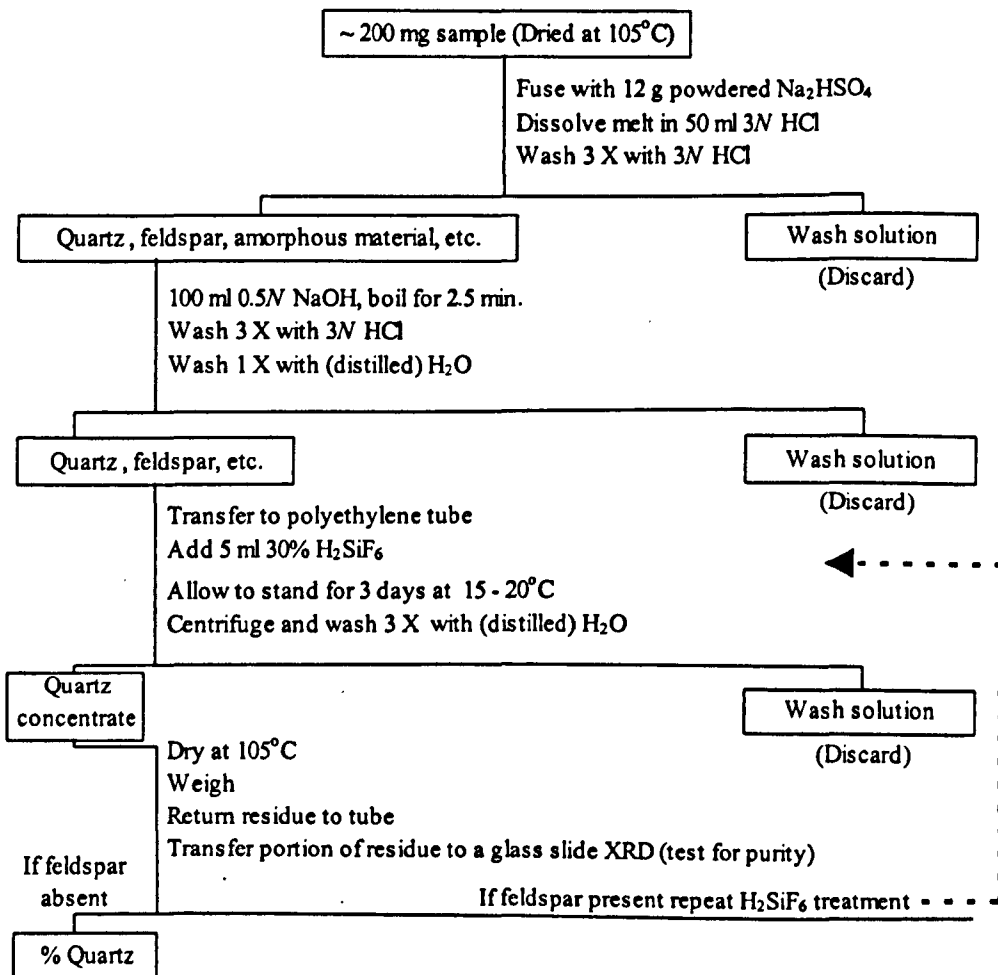


Fig. 5.7 - Flow sheet for the quantitative determination of quartz (after Chapman et al., 1969).

Table 5.3 - Quartz percentages of the mudrock samples determined by the method proposed by Chapman et al. (1965).

Sample	Test 1 (%)	Test 2 (%)	Mean (%)	Sample	Test 1 (%)	Test 2 (%)	Mean (%)
51	0.32	0.29	0.3	286	11.80	11.48	11.6
52	10.48	10.84	10.7	294	6.12	5.89	6.0
81	14.95	14.57	14.8	296	7.52	7.65	7.6
83	26.96	27.03	27.0	332	21.41	20.65	21.0
111	20.17	20.84	20.5	333	21.48	22.02	21.8
112	18.88	18.52	18.7	334	23.32	23.84	23.6
114	16.03	16.13	16.1	336	14.91	13.88	14.4
151	5.10	5.58	5.3	342	23.65	23.40	23.5
152	7.32	7.16	7.2	345	12.50	13.05	12.8
153	10.22	9.19	9.7	431	16.56	16.15	16.4
154	9.06	9.33	9.2	436	12.01	11.17	11.6
156	13.18	12.17	12.7	441	11.67	11.29	11.5
162	6.92	7.22	7.1	445	14.86	14.26	14.6
163	15.76	16.03	15.9	OB1	17.75	17.70	17.7
283	11.40	11.86	11.6	OB2	18.55	18.85	18.7
285	9.08	8.81	8.9				

5.2.3.2 - Determination of carbonates - calcite and dolomite

The concentrations of carbonates in mudrocks can be determined by XRD using the methodology followed for the calculation of the feldspars described in Section 5.2.1.5. However, the percentage of carbonates can be quantified easily and accurately on the basis of the determination of the volume of carbon dioxide (CO₂) released during the reaction of these minerals with an acid. The principle behind this procedure consists of measuring the volume of CO₂ released when the carbonate minerals within a mudrock react with the phosphoric acid using a non-aqueous titration technique.

In this work this procedure was followed in order to determine the CO₂. This consisted of adding about 25 ml of phosphoric acid (H₃PO₄) to a small amount (generally between 200 and 500 mg of sample). The CO₂ produced was first dried by bubbling through chromic acid and then absorbed into a 3.3% solution of ethanolamine in dimethyl formamide containing thymolphthalein indicator. The quantity of CO₂ absorbed was determined by titrating the absorbent with 0.1 tetra-n-butyl ammonium hydroxide in

toluene/methanol. The percentage of CO₂ released during the digestion of the samples was calculated by the volume of titration solution used, according to the following expression:

$$\text{CO}_2 (\%) = \frac{\text{Volume of titrant used (ml)} \times 4.4}{\text{Weight of sample (g)} \times 10} \quad (5.10)$$

Based on whole rock XRD scans, it was recognised that the carbonates consist of calcite (CaCO₃) and dolomite (CaMg(CO₃)₂) with the exception of samples 111 and 151, in which only the presence of calcite was identified. Thus, when calcite and dolomite are present, the quantity of CO₂ produced reflects the total percentage of carbonates, but does not indicate the relative concentrations of each phase. In order to quantify calcite and dolomite it is, therefore, necessary to calculate the relative proportions in which these two minerals occur in the various samples. Schultz (1964) found that the sum of the heights of the peaks of calcite (3.04Å-29.43° 2θ) and dolomite (2.89Å-30.99° 2θ) was proportional to the quantity of carbonates soluble in acid. In this way, the total percentage of carbonates may be apportioned between calcite and dolomite, according to the proportions obtained by the ratio between the heights of the peaks in respect of dolomite and calcite. The concentrations of these minerals are determined by the following expression:

$$\text{Calcite (\%)} = \text{CO}_2 (\%) \times \left(1 - \frac{\text{dol}}{\text{calc}}\right) \times 2.27 \quad (5.11)$$

$$\text{Dolomite (\%)} = \text{CO}_2 (\%) \times \left(\frac{\text{dol}}{\text{calc}}\right) \times 2.10 \quad (5.12)$$

where,

CO₂ (%) - percentage of CO₂ determined from expression 5.10;

dol/calc - dolomite to calcite peak heights ratio;

2.27 - molecular weight of calcite/molecular weight carbon dioxide;

2.10 - molecular weight of dolomite/molecular weight carbon dioxide.

The percentage of CO₂ in the rocks was determined on two subsamples taken from each rock. Table 5.4 shows the results of each test and the average values used to calculate the proportions of calcite and dolomite. Table 5.4 also presents the dolomite to calcite peak heights ratio measured on whole rock scans for each sample, and the percentages of calcite and dolomite calculated accordingly with expressions 5.11 and 5.12.

Table 5.4 - Percentages of CO₂, calcite and dolomite present in the rocks studied.

Sample	Test 1 (%)	Test 2 (%)	Mean (%)	Ratio ¹ dol/calc	Calcite (%)	Dolomite (%)	Total of carbonates (%)
51	33.12	33.15	33.13	0.03	72.9	2.1	75.0
52	7.12	7.05	7.08	0.46	8.7	6.9	15.6
81	4.23	4.05	4.14	0.36	6.0	3.1	9.1
83	8.65	8.43	8.54	0.60	7.7	10.7	18.4
111	2.03	2.05	2.04	-	4.5	-	4.5
112	8.16	8.10	8.13	0.28	13.2	4.8	18.0
114	8.60	8.66	8.63	0.32	13.3	5.8	19.1
151	10.17	10.23	10.20	-	23.2	-	23.2
152	8.37	8.19	8.28	0.21	14.9	3.7	18.5
153	7.40	7.14	7.27	0.44	9.3	6.7	16.0
154	7.89	8.20	8.04	0.36	11.6	6.0	17.7
156	4.40	4.52	4.46	0.34	6.7	3.2	10.0
162	8.03	7.97	8.00	0.29	12.9	4.9	17.8
163	8.90	8.78	8.84	0.24	15.2	4.4	19.6
283	13.78	13.51	13.64	0.10	27.8	2.9	30.6
285	9.40	10.05	9.73	0.17	18.3	3.5	21.7
286	14.46	14.54	14.50	0.09	30.0	2.7	32.7
294	7.95	7.62	7.79	0.23	13.6	3.8	17.4
296	10.04	10.20	10.12	0.15	19.5	3.2	22.7
332	7.44	7.12	7.28	0.19	13.4	2.9	16.3
333	4.67	4.82	4.74	0.44	6.0	4.3	10.3
334	4.71	4.81	4.76	0.81	2.1	8.2	10.2
336	4.54	4.42	4.48	0.49	5.2	4.6	9.8
342	7.35	7.63	7.49	0.20	13.6	3.2	16.8
345	30.16	30.68	30.42	0.19	55.9	12.1	68.0
431	5.53	5.40	5.47	0.49	6.4	5.7	12.0
436	12.41	11.88	12.15	0.14	23.6	3.6	27.2
441	6.24	6.23	6.23	0.56	6.2	7.3	13.5
445	4.00	4.23	4.11	0.42	5.4	3.6	9.0
OB1	11.90	11.48	11.69	0.21	21.0	5.2	26.1
OB2	12.09	11.30	11.70	0.04	25.5	1.0	26.5

¹Dolomite 2.89 Å (30.99° 2θ) to calcite 3.04 Å (29.43° 2θ) peak heights ratio.

5.2.3.3 - Determination of pyrite

Pyrite is a common accessory mineral present in most mudrocks. However, due to its atmospheric instability it is an important factor in mudrock breakdown, which justifies its determination even when it is presented in small amounts.

The concentrations of pyrite can be determined by XRD techniques or by wet geochemical analysis. The quantification of pyrite by XRD is in general difficult to perform either due to dilution by other minerals or to settling within the smear mount because of its high specific gravity.

The quantification of pyrite by wet geochemical analysis can be achieved by determination either of total iron and acid soluble iron with the difference being assigned to pyrite, or of sulphide-sulphur (pyrite). This latter approach (Maxwell, 1981) was adopted in this work as sulphates* (e.g. gypsum) were not detected in the samples. Therefore, it was assumed that all the sulphur present in the rocks was combined in the form of sulphides (pyrite).

The technique used to determine total sulphur involves the dissolution of a powdered mudrock with *aqua regia* (HNO₃/HCl mix) in order to decompose the pyrite and to release the sulphur in the form of sulphate (SO₄²⁻). Thereafter, the iron (Fe) was reduced and removed by filtration. Then, the sulphate was precipitated in the form of barium sulphate (BaSO₄) using a solution of barium chloride (BaCl₂). Finally, the solution of barium sulphate was filtered and the paper filter burned in a furnace at 550°C. The percentage of pyrite was calculated on the basis of the total residue measured gravimetrically.

Fig. 5.8 represents the flow sheet for the quantitative determination of pyrite. The percentages of pyrite were calculated on the basis of two determinations. The results of each test and the average content for all samples are given in Table 5.5.

* The occurrence of sulphates in rocks can be detected with the following test: about 1 g of sample is boiled with diluted hydrochloric acid (1:4) being the solution then filtered; the presence of sulphates is confirmed if a white precipitate appears when a few drops of a 5% solution of barium chloride are added to the filtered solution.

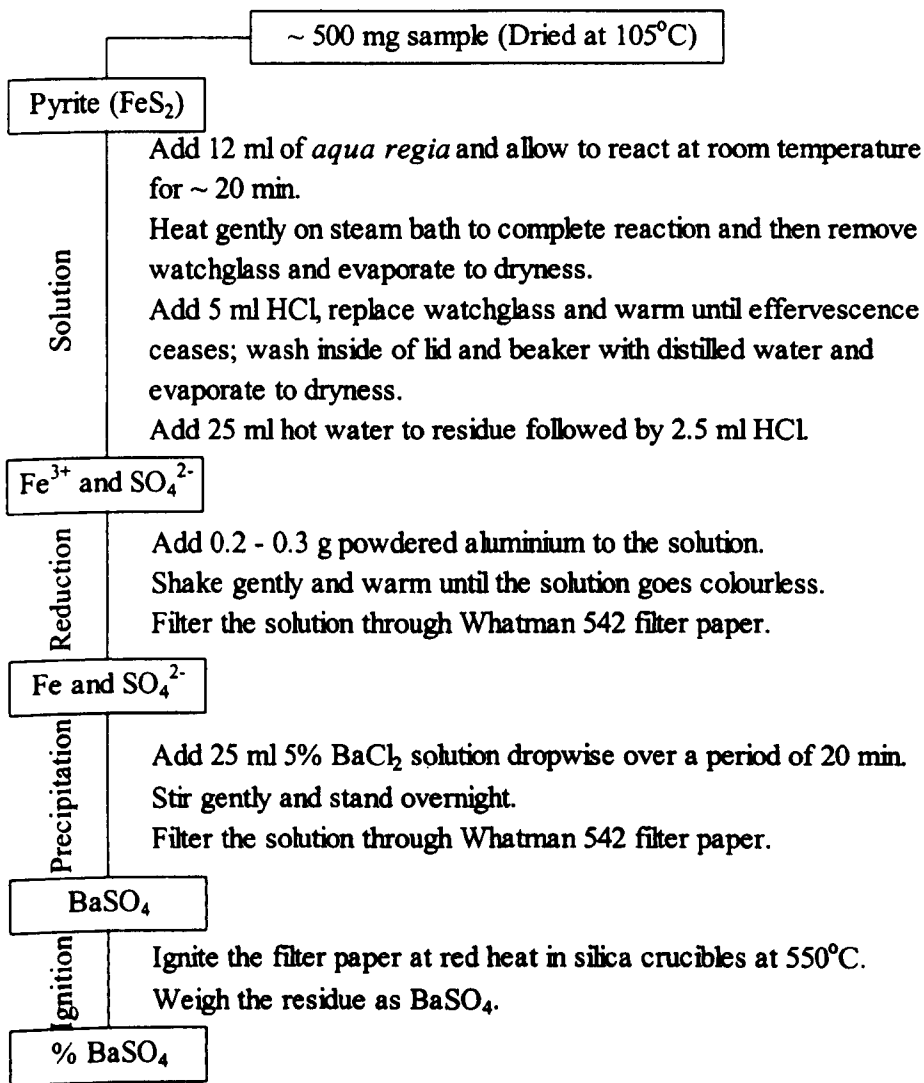


Fig. 5.8 - Flow sheet used for the quantification of pyrite.

Table 5.5 -Results of pyrite determinations.

Sample	test 1 (%)	Test 2 (%)	Mean (%)	Sample	Test 1 (%)	Test 2 (%)	Mean (%)
51	0.28	0.29	0.3	286	1.12	1.32	1.2
52	1.03	0.65	0.8	294	1.22	1.39	1.3
81	0.96	0.90	0.9	296	0.27	0.32	0.3
83	2.63	2.48	2.6	332	0.15	0.14	0.1
111	0.34	0.16	0.3	333	0.11	0.11	0.1
112	0.34	0.53	0.4	334	6.49	6.38	6.4
114	1.03	0.83	0.9	336	1.20	1.40	1.3
151	0.28	0.53	0.4	342	3.61	3.98	3.8
152	0.16	0.19	0.2	345	2.02	2.08	2.1
153	0.17	0.13	0.2	431	2.06	1.73	1.9
154	0.58	0.40	0.5	436	0.92	1.05	1.0
156	0.39	0.30	0.3	441	0.89	0.94	0.9
162	0.13	0.16	0.1	445	0.72	0.43	0.6
163	0.15	0.19	0.2	OB1	1.21	1.18	1.2
283	0.49	0.40	0.4	OB2	1.15	1.23	1.2
285	0.13	0.17	0.2				

5.2.3.4 - Determination of organic matter

The organic matter content of the mudrocks was determined by wet chemical analysis according to standard E-201 (LNEC, 1967e).

The laboratory procedure is based on determination by titration of the volume of potassium dichromate solution spent in the wet oxidation of the organic matter present in a given sample. The test technique involves the dissolution of 2 to 5 g of powdered sample with potassium dichromate and sulphuric acid. Thereafter, distilled water, orthophosphoric acid and an indicator (sodium diphenylaminesulphonate solution) were added to the solution. Then, volumes of 0.5 cm³ (V₁ volume) of ferrous sulphate solution were added until the colour changed from blue to green. A further volume of 0.5 cm³ of potassium dichromate solution was added, changing the colour to blue again. Finally, a new titration was carried out with the ferrous sulphate solution drop by drop until the colour of the solution changed from blue to green after the addition of a single drop. The volume of ferrous sulphate solution used was recorded (volume V₂).

To determine the organic matter content in mudrocks it was first necessary to measure the volume of potassium dichromate solution spent in the oxidation of the organic matter, which is given by the following expression

$$V_t = 10.5 \left(1 - \frac{V_2}{V_1} \right) \quad (5.13)$$

where,

V_t - total volume of potassium dichromate used in wet oxidation of the organic matter present in the sample (cm³);

V_1 - total volume of ferrous sulphate solution used in the titration (cm³);

V_2 - total volume of ferrous sulphate solution used in the determination (cm³).

The organic matter content is calculated from the volume V_t and dry mass of sample using the following expression:

$$\text{MO (\%)} = \frac{0.67 V_t}{m} \quad (5.14)$$

where,

MO (%) - organic matter content;

m - dry mass of sample used in the test (g).

The calculation of the organic matter content using equation 5.14 was developed for determinations on soils for which it is assumed that the average organic carbon in soil organic matter is 58%. The method employed oxidizes approximately 77% of the carbon in the organic matter, being these factors included in the parameter adopted in the equation 5.14. In the absence of data on the percentage of carbon present in the organic matter occurring in the mudrocks studied, the factors used for soil were applied to these rocks.

The organic matter content of the rocks investigated was determined on duplicate specimens. The results of each test and the average values are presented in Table 5.6.

Table 5.6 - Results of organic matter content determinations.

Sample	Test 1 (%)	Test 2 (%)	Mean (%)	Sample	Test 1 (%)	Test 2 (%)	Mean (%)
51	0.16	0.16	0.2	286	1.28	1.28	1.3
52	2.11	2.10	2.1	294	1.26	1.32	1.3
81	1.42	1.47	1.4	296	1.96	1.95	2.0
83	1.39	1.41	1.4	332	0.45	0.49	0.5
111	0.81	0.82	0.8	333	1.21	1.17	1.2
112	1.21	1.25	1.2	334	6.60	6.54	6.6
114	2.15	2.00	2.1	336	1.76	1.81	1.8
151	0.51	0.55	0.5	342	1.35	1.37	1.4
152	1.38	1.34	1.4	345	0.63	0.75	0.7
153	1.03	1.03	1.0	431	3.83	3.59	3.7
154	2.43	2.50	2.5	436	2.06	2.09	2.1
156	2.41	2.42	2.4	441	3.29	3.53	3.4
162	1.38	1.37	1.4	445	2.08	2.08	2.1
163	1.09	1.06	1.1	OB1	2.27	2.29	2.3
283	0.53	0.58	0.6	OB2	1.85	1.87	1.9
285	1.18	1.16	1.2				

5.2.4 - Discussion of the results determined in mineralogical characterization

5.2.4.1 - Errors introduced in the determination of the mineralogical composition of the rocks

The mineralogical and geochemical determinations carried out according to the techniques described in previous sections can be affected by:

- machine error in XRD and XRF;
- weighing, measurement and homogenization errors;
- operator errors in the preparation of samples and reproducibility of wet geochemistry.

Errors introduced in the results by the use of XRD and XRF equipment are small when compared with errors introduced during the sampling and preparation phases.

The reproducibility of the results obtained from XRD analysis was studied by Gibbs (1965), who suggests that a value of $\pm 10\%$ may be an acceptable error in the quantification of clay minerals. Errors of the same order of magnitude (between 7 and 10%) were obtained by Burnett (1974) in the determination of the percentages of clay minerals, occurring in high concentrations (20-50%), while in the case of clay minerals present in small proportions ($< 2\%$) the introduced error increased to around 30%. In the determination of the percentages of clay minerals using the semi-quantitative method described in Section 5.2.1.4 the errors introduced mainly have their origin in the background radiation levels considered. Therefore, the final results suggest a precision of $\pm 10\%$ for clay minerals which is similar to that report by Gibbs (1965).

Determinations performed on standard minerals demonstrate the high reproducibility of XRF technique, in which anomalous results are associated with errors in the weighing and homogenization of samples (Pike, 1989).

The subsamples used in the mineralogical and geochemical analyses (see Section 4.3.3) were obtained using a sample splitter, seeking in this way to reduce the errors introduced by the inhomogeneity of the samples. The weight measurements were performed with a balance accurate to 0.0001g, being assumed that instrument errors are probably negligible.

Operator errors performed during the laboratory procedures are the main source of error that affects the results obtained in the mineralogical and geochemical determinations. Among these, the procedures used in sample preparation for XRD and XRF and the wet geochemical techniques used to quantify non-clay minerals are some of the most important. The magnitude of the errors introduced in the results due to the reproducibility of wet geochemical techniques can be evaluated by the coefficient of variation, calculated for the results obtained from the various determinations performed in each sample. However, it must be pointed out that the value of the coefficient of variation, although reflecting the variability of the experimental procedures to be examined, may also reflect errors due to inhomogeneity of the samples. In the absence

of tests carried out on standard samples of known composition, the results presented should be considered to be only indicative, in relation to the reproducibility of the wet geochemical techniques used. Table 5.7 shows the coefficients of variation calculated for the quartz, carbonate, pyrite and organic matter determinations.

It can be seen from the results presented in Table 5.7 that the average values of the coefficient of variation for quartz, carbonates and organic matter determinations are of the same order of magnitude; it is therefore considered that the reproducibility of the associated techniques is high. In the case of pyrite the average value of the coefficient of variation obtained is greater than that calculated for the previous techniques, which indicates a poorer reproducibility of the experimental procedure associated with the determination of this mineral. The reasons for this fact could probably be found in losses during the filtration stage and in the non-homogenization of the samples. As pyrite occurs in rocks in very small percentages and it is determined using a small amount of sample (0.5 g) the results may reflect the occurrence of slight compositional variations between the subsamples of the same sample. This fact is most evident in rocks with lower concentrations of pyrite.

The average value of the coefficient of variation calculated for pyrite determination is much greater than that obtained for organic matter, despite the fact that these two constituents sometimes occur in the rocks studied in similar concentrations. This difference is probably related to the fact that the amount of sample (between 2 and 5 g) used to determine the organic matter is significantly greater than that used for pyrite, which, therefore, compensates slight compositional variations that occur in the subsamples tested.

The source of errors analysed above combine to affect the results calculated for the mineralogical composition of the samples. The methodology used to quantify the constituents of the rocks is described in the following section.

Table 5.7 - Coefficients of variation calculated for the results of wet geochemical determinations.

Sample	Quartz	CO ₂	Pyrite	Organic Matter
51	6.42	0.07	2.44	0.00
52	2.40	0.70	32.24	0.34
81	1.79	3.15	4.36	2.45
83	0.19	1.81	4.20	1.01
111	2.32	0.51	51.12	0.87
112	1.37	0.46	30.26	2.30
114	0.41	0.49	14.72	5.11
151	6.42	0.40	43.56	5.34
152	1.54	1.52	11.69	2.08
153	7.49	2.52	19.11	0.00
154	2.07	2.81	25.90	2.01
156	5.60	1.90	18.04	0.29
162	2.94	0.50	14.68	0.51
163	1.23	0.92	16.22	1.97
283	2.77	1.38	13.11	6.37
285	2.16	4.68	18.13	1.21
286	1.95	0.39	11.89	0.00
294	2.65	2.94	9.21	3.29
296	1.28	1.11	12.35	0.36
332	2.53	3.09	5.71	6.02
333	1.76	2.16	0.01	2.38
334	1.56	1.59	1.17	0.65
336	5.05	1.77	10.83	1.98
342	0.77	2.66	6.92	1.04
345	3.03	1.21	2.12	12.30
431	1.78	1.62	12.38	4.57
436	5.10	3.12	9.12	1.02
441	2.38	0.20	3.73	4.98
445	2.96	3.88	35.86	0.00
OB1	0.20	2.54	1.78	0.62
OB2	1.12	4.78	4.75	0.76
	Mean = 2.62	Mean = 1.83	Mean = 14.44	Mean = 2.32

5.2.4.2 - Calculation of the mineralogical composition of the mudrocks studied

The mineralogical composition of the mudrocks was calculated from the determinations of the various constituents identified in the samples.

Thus, as far as non-clay constituents are concerned, their concentrations were obtained by:

- XRD techniques, in the case of feldspars;
- XRF techniques, in the case of apatite and rutile;
- wet geochemical techniques, in the case of quartz, carbonates (calcite and dolomite), pyrite and organic matter.

The techniques used to determine the non-clay constituents provided directly the concentrations in which they occur in rocks. In this way, the total of non-clay constituents is directly obtained by the sum of the percentages corresponding to each non-clay mineral component.

The relative proportions of clay minerals in the samples were determined in the less than 2 μm fraction using the semi-quantitative method described in detail in Section 5.2.1.4, due to difficulties that arose with using whole rock preparations in the quantification of clay minerals (see Section 5.2.1.2).

The extrapolation of the percentages of clay minerals determined in the less than 2 μm fraction to the concentrations at which these minerals occur in the original samples, is criticised by Towe (1974) who claimed that the distribution of clay minerals within the various grain size fractions is influenced by the disaggregation and preparation methods used. Thus, according to this author grain size segregation can occur in relation to some clay types, and the percentages obtained in the less than 2 μm fraction do not reflect the real concentrations present in the whole rock. However, the preparation technique used for the less than 2 μm fraction significantly minimizes the grain size segregation of the particles (see Section 5.2.1.2). Therefore, the concentrations obtained in the less than

2 μm fraction are considered to represent more realistically the true percentages at which clay minerals occur in rocks than those obtained from whole rock determinations. Moreover, the method used to determine clay minerals is difficult to apply to whole rock scans due to dilution by quartz and calcite especially when they occur in high percentages.

In summary, it was assumed that the total percentage of clay minerals (TCM) present in the various samples corresponds to the difference between 100% and the sum of non-clay constituents (TNCC). The proportions of different clay phases in the various samples were recalculated using the relative percentages (which sum to 100%) obtained from the less than 2 μm fraction (Table 5.1) for the total clay minerals (TCM) corresponding to each sample.

The mineralogical compositions calculated to 100% of the mudrocks studied are presented in Table 5.8. The distribution of quartz, feldspar, carbonates and clay minerals (kaolinite, illite and MLC) along the profiles of bores 11, 15, 28, 33 and 44 are presented in Figs. 5.9 to 5.13. As chlorite occurs in minute concentrations, its distribution is not detailed in the profiles presented in Figs. 5.9 to 5.13. Nevertheless, its concentration is included in the total percentage of clay minerals (TCM).

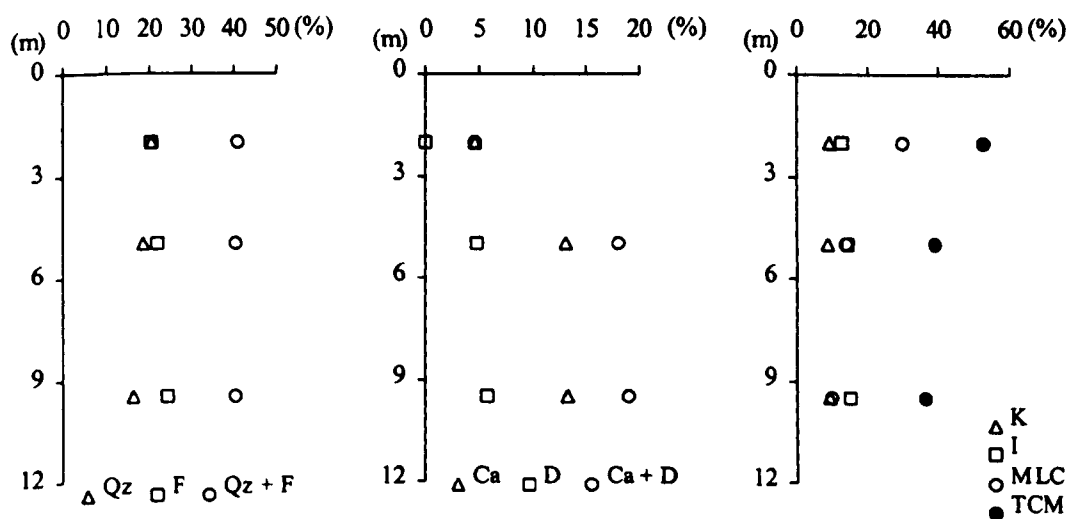


Fig. 5.9 - Mineralogical distribution along borehole 11.

Table 5.8 - Mineralogical composition of the mudrocks studied.

Sample	Quartz	K-Felds.	Plag.	Calcite	Dolomite	Pyrite	Apatite	Rutile	OM	TNCC	Chlorite	Kaolinite	Illite	Smectite	MLC	TCM	Total
51	0.3	0.0	0.0	72.9	2.1	0.3	0.5	0.2	0.2	76.5	0.0	5.4	9.9	3.5	4.7	23.5	100.0
52	10.7	6.0	2.4	8.7	6.9	0.8	0.4	0.9	2.1	38.9	2.4	12.8	12.8	4.3	28.8	61.1	100.0
81	14.8	8.4	3.5	6.0	3.1	0.9	0.3	0.8	1.4	39.2	0.0	9.7	15.8	4.3	31.0	60.8	100.0
83	27.0	19.6	20.5	7.7	10.7	2.6	0.3	0.7	1.4	90.5	0.2	2.3	2.6	0.9	3.5	9.5	100.0
111	20.5	6.6	13.7	4.5	0.0	0.3	0.2	1.0	0.8	47.6	1.0	9.4	12.1	0.0	29.9	52.4	100.0
112	18.7	9.0	12.7	13.2	4.8	0.4	0.6	0.8	1.2	61.4	0.8	5.8	11.6	0.0	20.4	38.6	100.0
114	16.1	14.6	9.9	13.3	5.8	0.9	0.4	0.8	2.1	63.9	1.4	6.5	12.6	0.0	15.6	36.1	100.0
151	5.3	3.1	3.6	23.2	0.0	0.4	0.4	0.7	0.5	37.2	1.3	10.7	13.2	0.0	37.6	62.8	100.0
152	7.2	3.5	4.2	14.9	3.7	0.2	0.3	0.8	1.4	36.2	1.3	12.1	20.4	0.0	30.0	63.8	100.0
153	9.7	4.4	6.3	9.3	6.7	0.2	0.4	0.8	1.0	38.8	0.6	10.4	20.2	0.0	30.0	61.2	100.0
154	9.2	4.9	10.1	11.6	6.0	0.5	0.5	0.8	2.5	46.1	2.7	16.2	18.9	0.0	16.1	53.9	100.0
156	12.7	5.8	17.5	6.7	3.2	0.3	0.3	1.0	2.4	49.9	0.5	12.0	17.0	0.0	20.6	50.1	100.0
162	7.1	7.0	6.8	12.9	4.9	0.1	0.2	0.8	1.4	41.2	0.6	18.2	32.3	0.0	7.7	58.8	100.0
163	15.9	12.7	14.8	15.2	4.4	0.2	0.4	0.7	1.1	65.4	0.3	8.3	15.2	0.0	10.8	34.6	100.0
283	11.6	2.6	10.5	27.8	2.9	0.4	0.4	0.7	0.6	57.5	0.9	7.7	13.2	0.0	20.7	42.5	100.0
285	8.9	4.0	8.4	18.3	3.5	0.2	0.3	0.7	1.2	45.5	0.5	10.4	14.2	0.0	29.4	54.5	100.0
286	11.6	3.6	7.9	30.0	2.7	1.2	0.4	0.6	1.3	59.3	2.0	7.7	11.4	0.0	19.6	40.7	100.0
294	6.0	2.7	4.0	13.6	3.8	1.3	0.5	0.8	1.3	34.0	1.3	11.9	21.8	0.0	31.0	66.0	100.0
296	7.6	4.4	4.8	19.5	3.2	0.3	0.4	0.7	2.0	42.9	1.7	9.7	17.1	0.0	28.6	57.1	100.0
332	21.0	12.2	12.8	13.4	2.9	0.1	0.3	0.9	0.5	64.1	0.4	7.5	9.7	3.9	14.4	35.9	100.0
333	21.8	5.5	9.7	6.0	4.3	0.1	0.4	0.8	1.2	49.8	0.5	10.0	12.6	4.0	23.1	50.2	100.0
334	23.6	7.2	10.2	2.1	8.2	6.4	0.4	0.8	6.6	65.5	1.0	8.6	10.7	2.4	11.8	34.5	100.0
336	14.4	6.6	6.6	5.2	4.6	1.3	0.3	0.9	1.8	41.7	2.3	8.7	17.5	5.8	24.0	58.3	100.0
342	23.5	10.3	13.3	13.6	3.2	3.8	0.3	0.8	1.4	70.2	1.2	3.9	7.7	3.6	13.4	29.8	100.0
345	12.8	2.2	7.8	55.9	12.1	2.1	0.3	0.3	0.7	94.2	0.0	3.3	1.5	0.0	1.0	5.8	100.0
431	16.4	5.9	15.8	6.4	5.7	1.9	0.3	1.0	3.7	57.1	1.3	10.7	18.0	0.0	12.9	42.9	100.0
436	11.6	5.3	6.9	23.6	3.6	1.0	0.3	0.7	2.1	55.1	2.2	10.8	20.7	0.0	11.2	44.9	100.0
441	11.5	4.2	7.9	6.2	7.3	0.9	0.2	0.8	3.4	42.4	3.5	16.7	19.0	0.0	18.4	57.6	100.0
445	14.6	10.0	14.2	5.4	3.6	0.6	0.3	1.0	2.1	51.8	1.9	15.9	14.0	0.0	16.4	48.2	100.0
OB1	17.7	10.6	5.5	21.0	5.2	1.2	0.4	0.6	2.3	64.5	1.1	6.7	13.5	0.0	14.2	35.5	100.0
OB2	18.7	11.0	3.9	25.5	1.0	1.2	0.4	0.6	1.9	64.2	1.1	6.1	15.4	0.0	13.2	35.8	100.0

K-Felds. - K-Feldspar; Plag. - Plagioclase; OM - Organic matter; TNCC - Total of non-clay constituents; MLC - Mixed layer clays; TCM - Total of clay minerals.

From Figs 5.9 to 5.13 it can be concluded that the percentage of resistate fraction (quartz plus feldspar) is similar or increases slightly with depth, except for the samples from bores 33 and 43 (not presented) where the concentrations of these minerals are higher in samples collected closer to surface.

As far as carbonates are concerned, the sum of calcite plus dolomite percentages neither vary significantly nor increase with depth, except in the case of bore 15, where the carbonate content decreased along the bore.

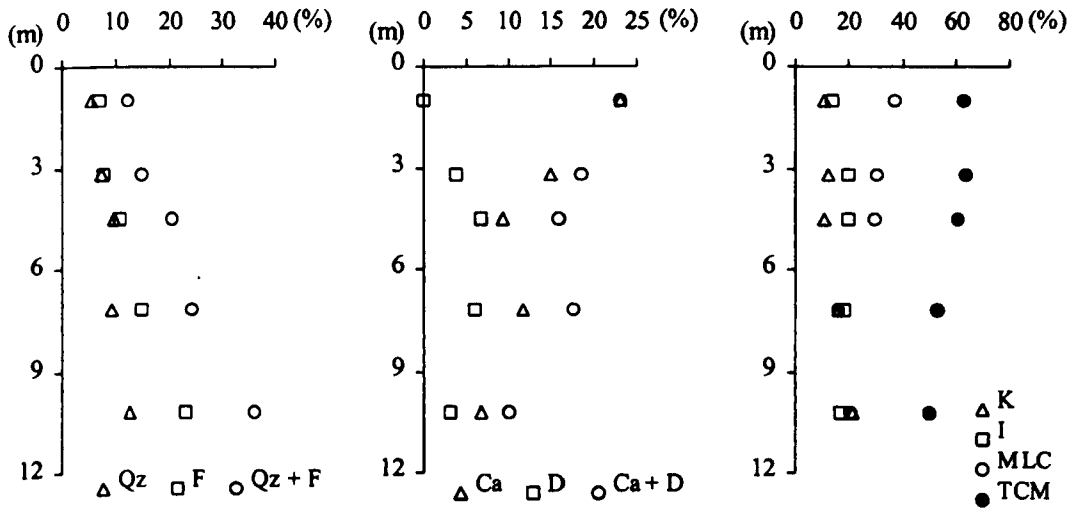


Fig. 5.10 - Mineralogical distribution along borehole 15.

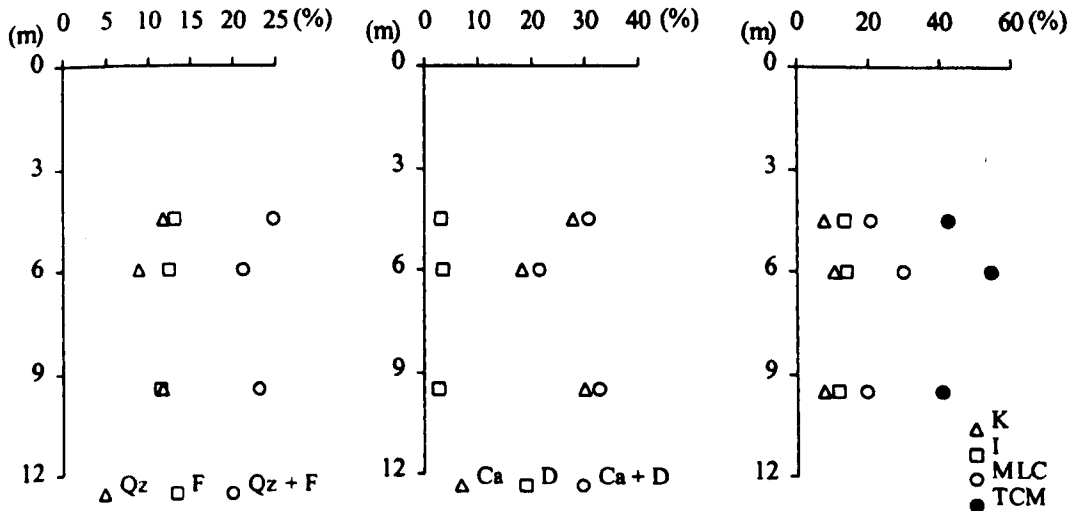


Fig. 5.11 - Mineralogical distribution along borehole 28.

Finally, in relation to clay minerals, it can be seen that the percentage of expandable mixed-layer clay (MLC), which in the case of bore 33 also includes smectite content, is generally greater in the most weathered samples, *i.e.* it increases towards the surface. In this way, the concentrations of kaolinite and illite tend not to vary substantially throughout the profiles, while the total percentage of clay minerals decreases with depth, due to the fact that MLC occur in higher proportions in samples nearest to the surface. Further discussion of the variation in composition is presented in Section 5.3.3.

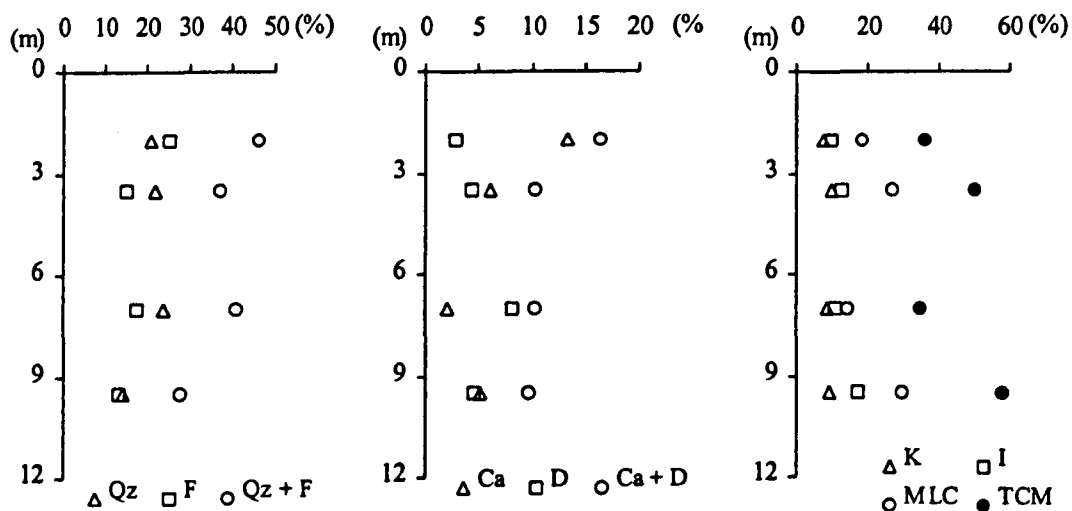


Fig. 5.12 - Mineralogical distribution along borehole 33.

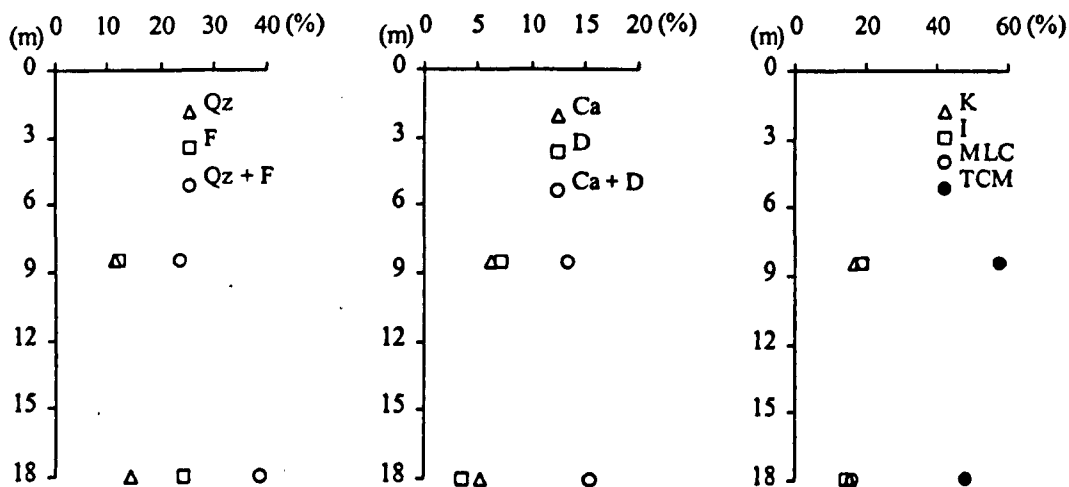


Fig. 5.13 - Mineralogical distribution along borehole 44.

5.3 - Textural characterization

The main objective of the use of optical microscopy and scanning electron microscopy (SEM) techniques in the study of mudrocks was to characterize the microtextural aspects of these rocks. However, the application of these techniques, mainly SEM and energy dispersive X-ray microanalysis system (EDS) also complemented qualitative mineralogical information obtained by the techniques described in Section 5.2. Thus, the characterization of rocks on the basis of the said techniques included both textural and mineralogical aspects, when appropriate. As the relation between these aspects is close, it was decided to describe them together and not to include the mineralogical aspects covered here, in Section 5.2.

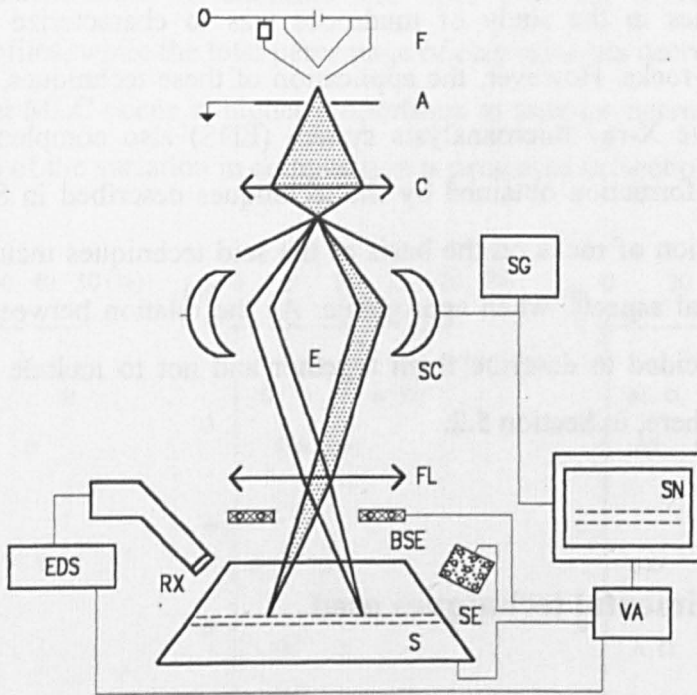
5.3.1 - Experimental techniques used

The studies were carried out on thin sections produced from rock slices cut perpendicularly to stratification. As the rocks analysed are very sensitive to water, the rock slices were cut dry with a diamond saw, using during trimming oil as a lubricant. Finally, the rock slices were polished using a 1 μm diamond paste. SEM studies required the prior application of a conductive coating, generally of carbon or gold, to the samples, which meant that the optical microscope examinations had to be carried out first. In order to improve the quality of SEM observations, the thin sections were polished again with 1 μm diamond before being coated. Freshly-fractured surfaces of all samples were also examined under the SEM.

The textural characterization of the samples was done with a petrographic microscope (Zeiss Axioplan Pol) and a scanning electron microscope (Jeol - JMS 6400). In relation to the first, samples were examined in plane-polarized light (PPL) and with crossed polars (XPL) using magnifications of x50 and x100.

The principle of SEM consists of the scanning of the surface of the sample with a finely focused electron beam, modulating the brightness at each point of the image obtained on a screen, according to the intensity of the radiation emitted by the sample (Sá, 1993).

The image built up depends on the type of radiation generated and the detector used. Fig. 5.14 schematically represents the basic functional features of a scanning electron microscope.



EDS - Energy dispersive spectrometer; SE, BSE and RX - Detectors of secondary and backscattered electrons and X-rays; E - Electron beam; S - Sample; SG - Scan generator; SC - Scan coils; VA - Video amplifier; SN - Screen; F - Filament; A - Anode; FL - Final lens; C - Condenser.

Fig. 5.14 - Schematic diagram of the elements of a SEM. (Sá, 1993).

It is usual in the application of SEM to the study of rocks to examine the specimens in secondary electron (SE) and backscattered electron (BSE) modes. These two operation modes of the SEM arise from the detection of reflected (BSE) and emitted (SE) electrons from the sample when bombarded with the primary electron beam (Fig. 5.15).

Secondary electrons are emitted by the area of the surface of the specimen near the point of impact of the beam, and are characterized by having low energy (<50 eV). They are a result of interactive processes between primary and backscattered electrons with lower energy bonding electrons within the analysed material.

The backscattered electrons due to their high energy (>50 eV), which is close to the energy of the primary incident electrons, are produced from layers relatively deep within

the sample. This characteristic of backscattered electrons means that image resolution is a function of the energy of the incident beam and of the average local atomic number of the material. Backscattered electron images therefore depend on the chemical composition of the analysed sample. When associated with X-ray microanalysis, the application of this observation mode to the study of rocks permits the recognition of the various mineral phases present in the sample, as well as their mineralogical composition (White et al., 1984). However, when the average atomic number of the various mineral phases is similar due to having similar chemical compositions, the contrast between the various phases is weak, and identification less evident. Backscattered electron images are also characterized by having a lesser resolution than secondary electron images and to achieve acceptable image quality the surface must be completely flat.

The recognition of several different phases in backscattered electron images requires initial calibration, during which a correspondence is established between the grey tones in the image and the different mineral phases present, which are identified on the basis of qualitative or quantitative analyses carried out by the X-ray microanalysis system (EDS or WDS) attached to SEM.

X-ray microanalysis systems are based on the fact that when a high energy electron beam interacts with a sample, X-rays are emitted with energy and wavelengths characteristic of the elementary composition of the material under analysis. The detection and measurement of this characteristic radiation either by the discrimination of its energy spectrum, or its wavelength spectrum, enables the evaluation of the chemical composition of microvolumes of the sample. Thus, X-ray microanalysis systems can include energy dispersive systems (EDS) suitable for identification and qualitative analysis of the constituents present in the sample, and wavelength dispersive systems (WDS), which are mainly used in applications that require quantitative chemical analysis of the minerals (*e.g.* microprobe). The simultaneous association of two systems (EDS and WDS) takes advantage of their complementary characteristics. The first type is more usually used and allows the identification of the various mineral phases, provided that the volume of the sample analysed is sufficiently small (commonly the limit is a spot of about 1 μm diameter) to refer to only one mineral type.

In this study polished sections (thin sections) and freshly-fractured surfaces of all samples were examined on secondary electron mode. Backscattered electron mode was only used on thin sections, because of the poorer resolution of BSE images on freshly-fractured surfaces. The magnifications used in SEM studies varied according to the grain size of the rocks and the resolution obtained for each sample, which depended partly on the degree to which the surfaces examined were polished. Semi-quantitative chemical composition of the minerals present in rocks was determined by a Tracor Series 2 energy-dispersive X-ray analyzer (EDS) attached to the scanning electron microscope.

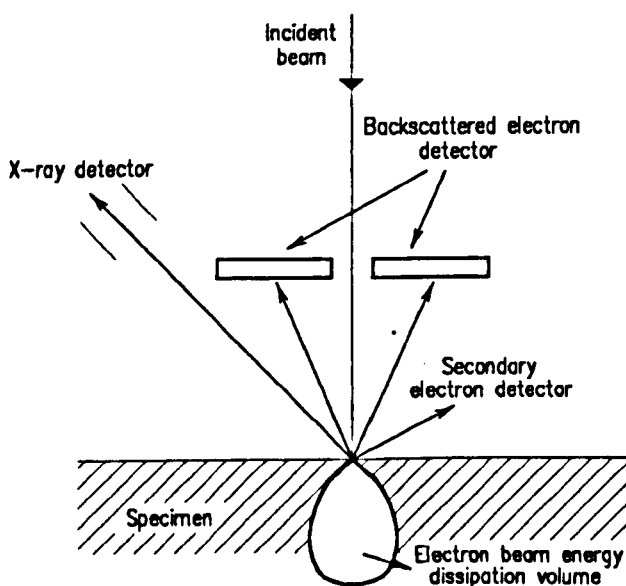


Fig. 5.15 - Schematic diagram of the different types of radiation emitted by the specimen and of the position of the detectors (White et al., 1984).

5.3.2 - Study method

The textural characterization carried out on mudrocks was based on the previous works of Collins & McGown (1974), Krinsley et al. (1983), Pye & Krinsley (1986), Bennett & O'Brien (1991), Reynolds & Gorsline (1992), Macquaker & Gawthorpe (1993), Krinsley et al. (1993), Tsige et al. (1994) and Macquaker (1994).

The optical and scanning electron microscope observations of the samples were systematized on the basis of the descriptive parameters presented in Table 5.9, referring to the following microtextural features.

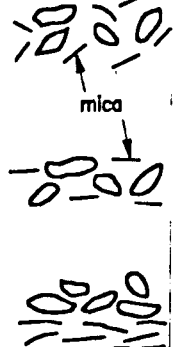
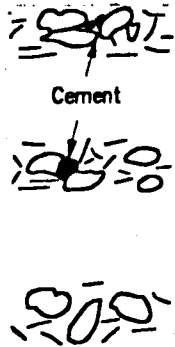
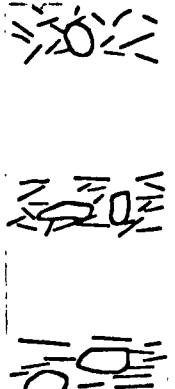
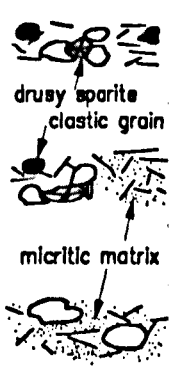
A - Particle orientation. In the description of this microtextural feature, three modes were defined to describe the rock types: massive (in which the rock constituents are randomly distributed), weakly laminated or non-laminated (in which some constituents, such as micas and flakes of organic matter show some preferred orientation) and laminated or microlaminated (in which the rock shows well-developed lamination and a high degree of parallelism of micas and clay minerals).

B - Grain-to-grain relations. Two distinct modes were defined in the description of silt size and/or sand size grain-to-grain relations (mainly quartz and feldspars). In the former, the grains have long or point contacts and/or developed cementation bonds; while in the latter the grains are dispersed in the 'clay matrix' - floating grains. In relation to this microtextural feature, the samples were also distinguished on the basis of the proportions in which both of the said modes can occur in the rock.

C - Clay fabric. This microtextural feature was described on the basis of the clay particle association mode, three modes were defined to describe the rock types. In the former, the clay particles are arranged in predominantly edge-to-edge (EE) and edge-to-face (EF) orientations, which give rise to an open and loose structure (high porosity and low density). Other types of arrangement results from the association of the clay particles in EF and FF contacts in similar percentages and/or in low angle EF contacts, which correspond to a denser and less porous structure than the former. In the latter type the arrangement of the clay particles is essentially of the face-to-face type (FF) which gives rise to a very dense structure with small amount of voids (low porosity).

D - Carbonate occurrence mode. Two modes of occurrence were defined to characterize the distribution of carbonates (calcite and dolomite) in the samples. In the former, carbonate minerals occur in the form of individual grains greater than 5 μm in diameter (e.g. skeletal grains) or as sparry cement; in the latter they occur in the form of a finely disseminated microcrystalline aggregate (micrite). In relation to this microtextural feature, the samples were also distinguished on the basis of the proportions in which both of the modes described occur in the rock.

Table 5.9 - Description of the microtextural features observed in the rocks studied.

FEATURE	VISUAL DESCRIPTION	
<i>A - Particle orientation</i>	<p>1 - Microlamination absent, the rock constituents have a random orientation.</p> <p>2 - Microlamination absent, but the platy minerals e.g. micas show some preferred orientation.</p> <p>3 - Well-developed lamination or microlamination.</p>	 <p>Diagram 1: Random orientation of mica grains. An arrow points to a grain labeled 'mica'.</p> <p>Diagram 2: Preferred orientation of mica grains.</p> <p>Diagram 3: Well-developed lamination of mica grains.</p>
<i>B - Grain-to-grain relations</i>	<p>1 - Predominantly grain-to-grain relations by long or point contacts, and/or by the development of cementation bonds.</p> <p>2 - Occurrence, both of grain-to-grain contacts (1), and of floating grains (3).</p> <p>3 - Predominantly floating grains.</p>	 <p>Diagram 1: Grain-to-grain contacts with cementation bonds. Labeled 'Cement'.</p> <p>Diagram 2: Occurrence of both grain-to-grain contacts and floating grains.</p> <p>Diagram 3: Predominantly floating grains.</p>
<i>C - Clay fabric</i>	<p>1 - Mostly clay particle arrangements of EE and EF types, loose structure, high porosity.</p> <p>2 - Clay particle arrangements of EF, FF and low-angle EF types, denser and less porous structure than the former (1).</p> <p>3 - Predominantly clay particle arrangement of the FF type, very dense structure, low porosity.</p>	 <p>Diagram 1: Loose structure, high porosity (EE and EF types).</p> <p>Diagram 2: Denser structure (EF, FF and low-angle EF types).</p> <p>Diagram 3: Very dense structure, low porosity (FF type).</p>
<i>D - Carbonate occurrence mode</i>	<p>1 - Carbonate minerals occur mainly as individual grains greater than 5 μm in diameter, or as sparry cement.</p> <p>2 - Carbonate minerals occur in both modes described in (1) and (3).</p> <p>3 - Carbonate minerals essentially occur as a fine-grained micrite matrix.</p>	 <p>Diagram 1: Individual grains or sparry cement. Labeled 'drusy sparite clastic grain'.</p> <p>Diagram 2: Both modes from (1) and (3).</p> <p>Diagram 3: Fine-grained micrite matrix. Labeled 'micritic matrix'.</p>

The study method used in the textural characterisation of rocks consists of describing the various microtextural features analysed - A, B, C and D - on the basis of the parameter proposed - 1, 2 and 3 - which best apply to each sample. The descriptions produced in this way simplify the comparison of the textural aspects of the various samples and their correlation with other rock characteristics. The following section presents the description of the samples.

5.3.3 - Sample descriptions

The results of the microtextural characterization of all samples, performed according to the microtextural parameters defined in Table 5.9, are presented in Table 5.10.

Table 5.10 - Microtextural characteristics of the rocks studied.

Sample	Description	Sample	Description
51	A ₁ B ₃ C ₁ D ₃	286	A ₂ B ₂ C ₂ D ₃
52	A ₃ B ₂ C ₁ D ₂	294	A ₂ B ₃ C ₁ D ₂
81	A ₂ B ₃ C ₁ D ₃	296	A ₂ B ₃ C ₁ D ₃
83	A ₁ B ₁ C ₂ D ₂	332	A ₁ B ₃ C ₁ D ₂
111	A ₁ B ₃ C ₁ D ₃	333	A ₂ B ₃ C ₁ D ₃
112	A ₂ B ₂ C ₂ D ₂	334	A ₃ B ₂ C ₂ D ₂
114	A ₂ B ₂ C ₂ D ₂	336	A ₁ B ₂ C ₂ D ₃
151	A ₁ B ₃ C ₁ D ₂	342	A ₃ B ₂ C ₂ D ₂
152	A ₃ B ₃ C ₁ D ₂	345	A ₁ B ₁ C*D ₁
153	A ₃ B ₃ C ₁ D ₂	431	A ₃ B ₂ C ₃ D ₂
154	A ₃ B ₂ C ₂ D ₂	436	A ₁ B ₂ C ₂ D ₃
156	A ₃ B ₂ C ₂ D ₂	441	A ₃ B ₂ C ₃ D ₂
162	A ₁ B ₃ C ₁ D ₂	445	A ₃ B ₂ C ₃ D ₂
163	A ₁ B ₂ C ₂ D ₂	OB1	A ₂ B ₂ C ₂ D ₂
283	A ₁ B ₃ C ₁ D ₂	OB2	A ₂ B ₂ C ₂ D ₂
285	A ₁ B ₃ C ₁ D ₂	* Not applicable	

According to the classification proposed in Section 3.4 various rock types were recognized. The microtextural characteristics are described hereunder in general terms and illustrated by photographs taken with the optical and scanning electron microscopes.

a) Non-indurated materials

Non-indurated materials (silts and clays) are constituted of coarse grains of quartz and feldspar, which are generally sub-angular, fine-sand to medium-silt in size (200 - 10 μm) and by finer clay particles (mainly mixed-layer illite-smectite) smaller than 4 μm in size (Fig. 5.16A, C and D). The percentage of coarse grains is high in the case of silts (samples 111 and 332), while in the case of clay samples 51 and 151 the occurrence thereof is less. The colour of the non-indurated materials in plane-polarized light (PPL) is yellowish, sometimes with darker brownish areas that correspond to zones rich in organic matter (Fig. 5.16A).

The samples are neither laminated nor do their constituents exhibit some preferred orientation (Fig. 5.16A, C and D). These materials have a loose structure, indicating high amount of voids (pores and fissures) (Fig. 5.16B).

The backscattered electron images in Fig. 5.16C and D show the following issue:

- a) the coarse grains are disseminated in the clay matrix;
- b) the carbonate minerals (mainly calcite) are disseminated in the rock, in the case of sample 111, while in sample 151 they occur in small grains and as micrite matrix;
- c) the organic matter is distributed irregularly in the rock either in layers around the coarsest grains, or in small concentrations with diffuse limits.

Fig. 5.16C refers to sample 151 showing the presence of pyrite framboids (very bright appearance).

b) Sandstone

Sample 83 classified as fine calcareous sandstone is composed mainly by quartz, feldspar and calcite grains, predominantly, of fine-sand and coarse-silt size (200 - 20 μm). Between these grains others of smaller size (< 20 μm) and a matrix composed of a mixture of clay minerals and micrite and/or dolomicrite occur.

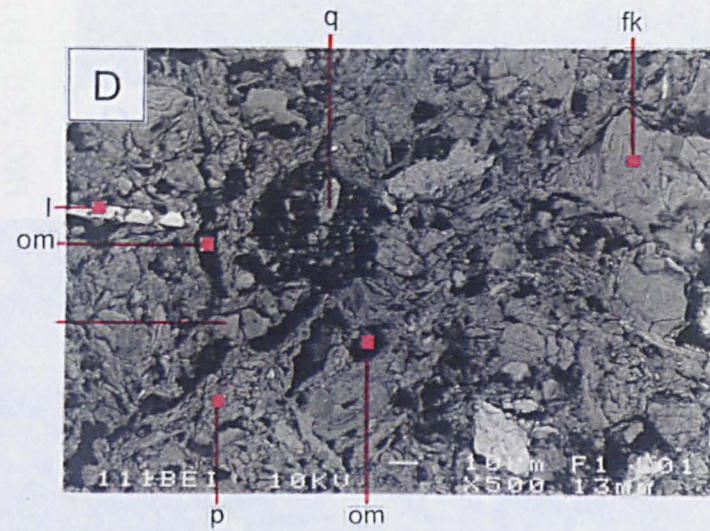
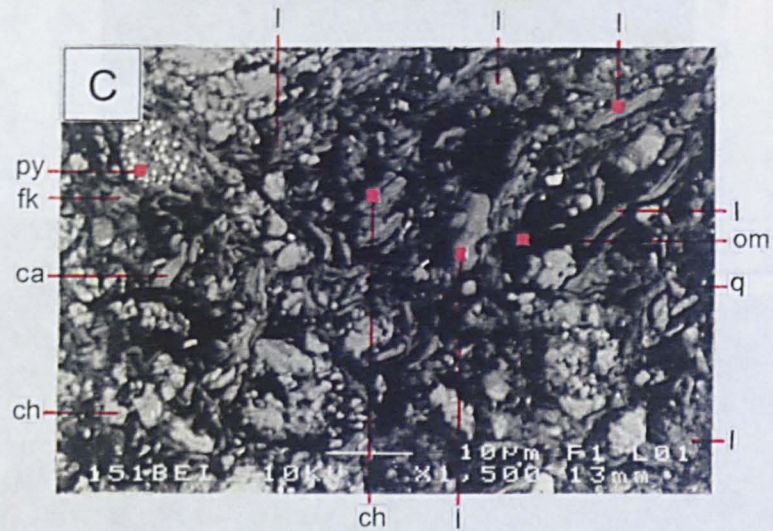
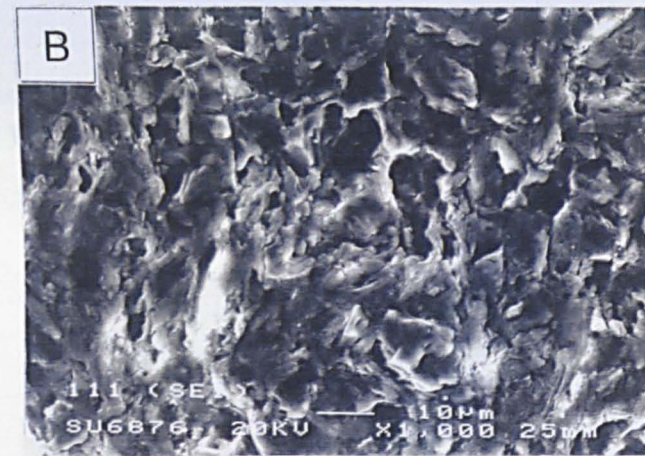
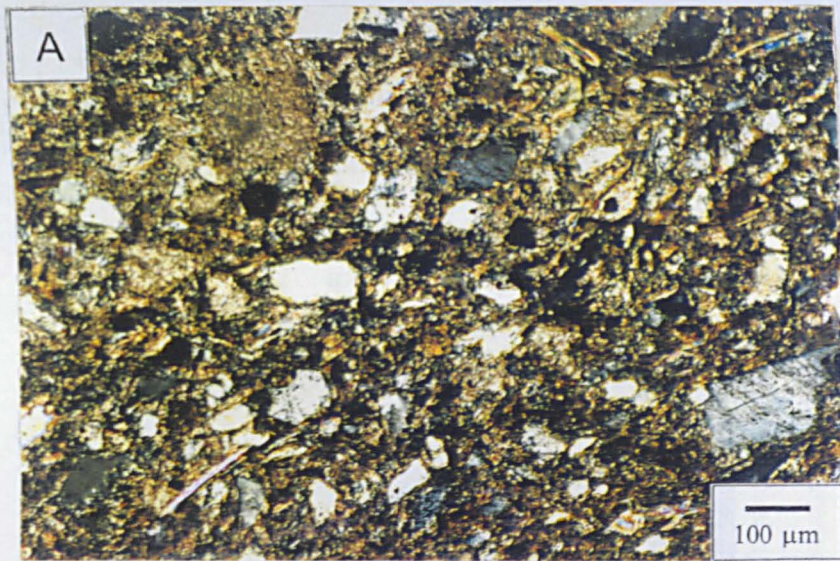


Fig. 5.16 - Non-indurated materials: (A) Photomicrograph of sample 332, XPL; (B) Secondary electron image (SEI) of sample 111 (thin section); (C) Backscattered electron image (BEI) of sample 151, (q) quartz, (fk) K-feldspar, (ca) calcite, (ch) chlorite, (I) illite/mica, (om) organic matter, (py) pyrite; (D) Backscattered electron image (BEI) of sample 111, (q) quartz, (fk) K-feldspar, (p) plagioclase, (I) illite/mica, (om) organic matter.

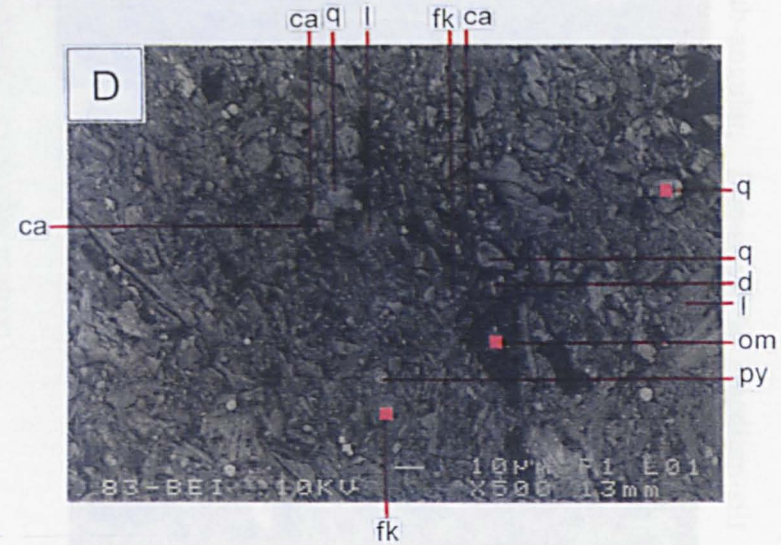
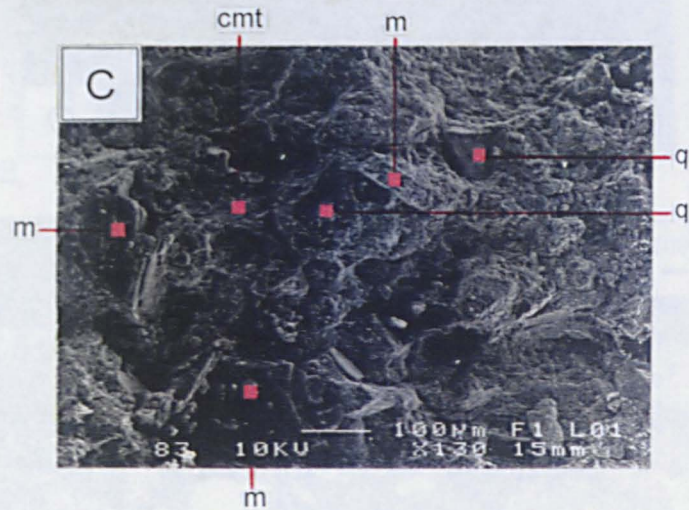
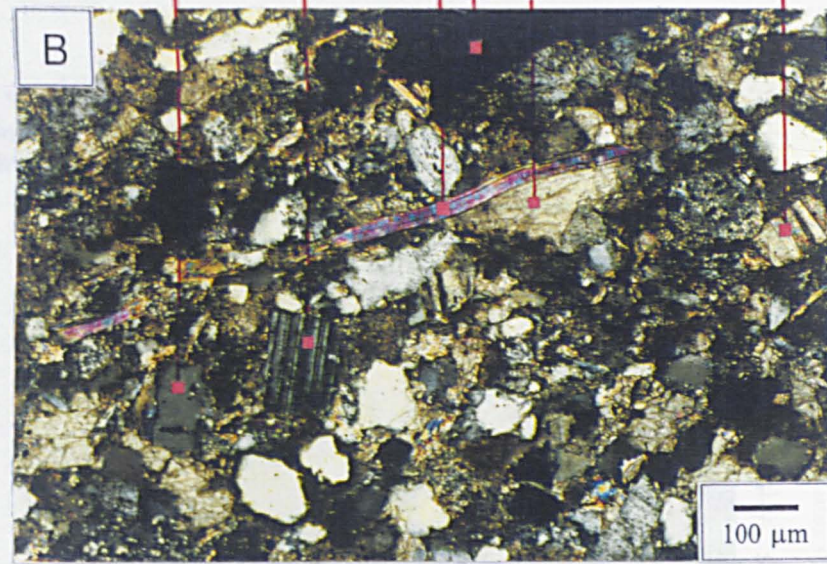


Fig. 5.17 - Sandstone (sample 83); (A) Photomicrograph, PPL; (B) Photomicrograph, XPL, (q) quartz, (p) plagioclase, (m) muscovite, (ca) calcite, (om) organic matter; (C) Secondary electron image (SEI) of a freshly-fractured surface, (q) quartz, (m) muscovite, (cmt) presence of calcite on matrix; (D) Backscattered electron image (BEI), (q) quartz, (fk) K-feldspar, (ca) calcite, (d) dolomite, (l) illite/mica, (om) organic matter, (py) pyrite.

The colour in plane-polarized light (PPL) is greyish yellow. The rock forming constituents do not show some preferred orientation (Fig. 5.17A). The rock has a moderate densely packed structure occasionally with the pore filled with carbonate cement (Fig. 5.17C).

Occasionally, feldspar grains are altered to sericite and calcite, while muscovite and quartz particles appear sound (Fig. 5.17B). The quartz and feldspar grains are sub-angular and predominantly point or long contacts and/or cementation bonds of sparite were observed (Fig. 5.17D). However, in some areas of the rock the detrital grains seem to be cemented with micrite.

Organic matter occurs in very fine layers and in large pockets, while pyrite is present as framboids (Fig. 5.17D).

c) Siltstones and siltshales

Siltstones include samples 112, 114, 163, OB1 and OB2, while siltshales comprise samples 334, 342 and 431. The former are composed of sub-angular randomly oriented quartz and feldspar grains predominantly 10 to 50 μm in diameter (Fig. 5.18A and B). Grain-to-grain contacts or floating grains in the micrite- and clay-rich matrix may occur. The colour of the rocks in plane-polarized light (PPL) is yellowish with darker layers of organic matter which show some preferred orientation (Fig. 5.18A).

The constituents of siltshales have a preferred orientation parallel to the laminae, which are generally less than 0.5 mm thick (Fig. 5.18C and D). The laminae can be distinguished on the basis of their mineralogical composition. The darker layers are mainly composed of a clay-, organic- and micrite-rich matrix and the lighter layers by quartz and feldspar grains (Fig. 5.18C). Laminae can also be subdivided on the basis of the grain size of their constituents. The coarse-grained laminae are formed by coarse-silt to fine-sand sized quartz, feldspar and carbonate grains, and the fine-grained laminae (grains < 10 μm) are composed mainly by clay minerals, organic matter and micrite (Fig. 5.18D). However, in the case of sample 334 it was recognised that the grain size of quartz particles present in the two types of laminae do not differ significantly (Fig. 5.18C).

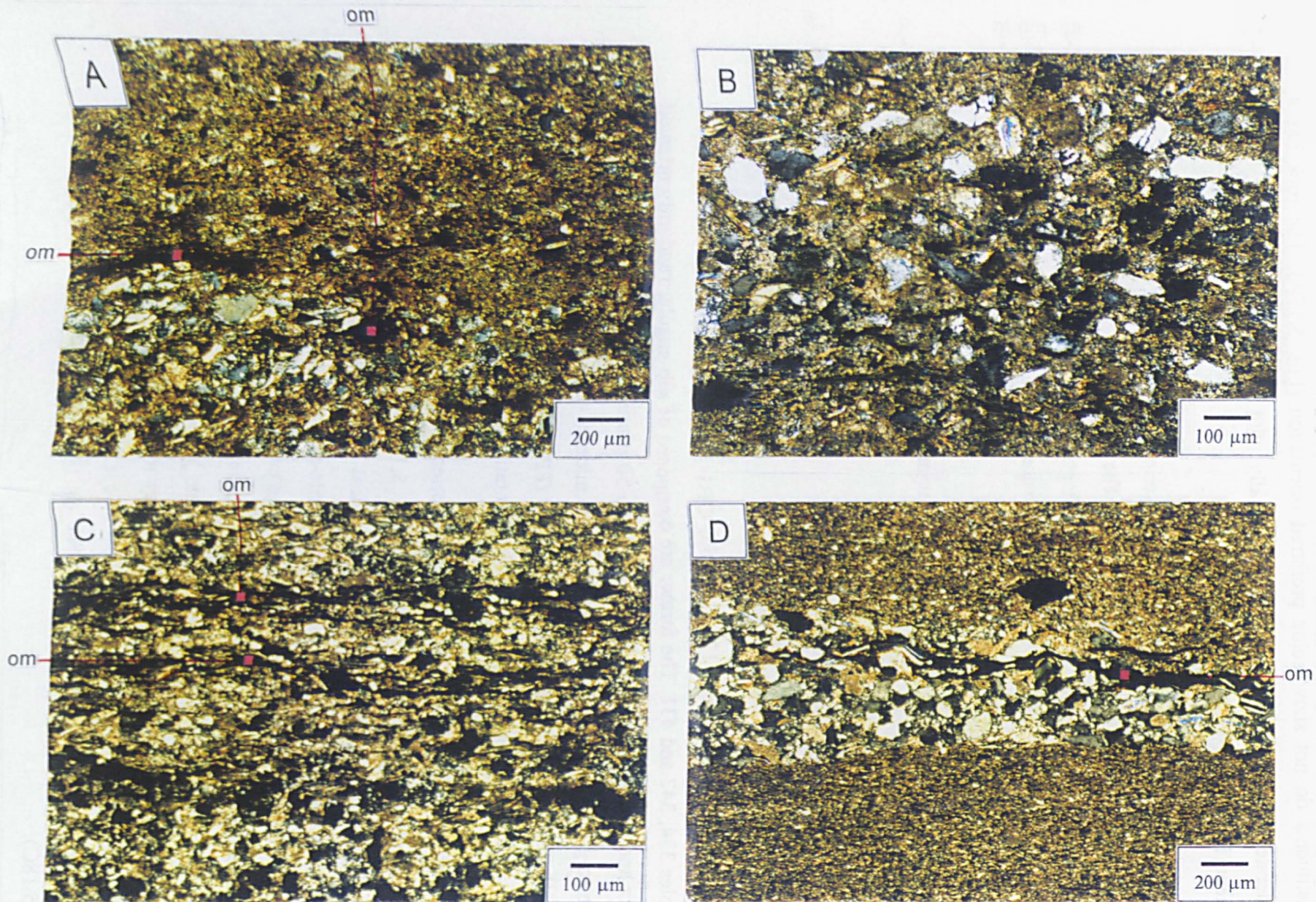


Fig. 5.18 - Siltstones and siltshales: (A) Photomicrograph of sample 163 (siltstone), XPL, (om) organic matter; (B) Photomicrograph of sample OB2 (siltstone), XPL; (C) Photomicrograph of sample 334 (siltshale), XPL, (om) organic matter; (D) Photomicrograph of sample 431 (siltshale), XPL, (om) organic matter.

The examination of backscattered electron images also shows that the grains in siltstones and siltshales can occur randomly spread throughout the rock (Fig. 5.19B), or with a preferred orientation parallel to the lamination or bedding (Fig. 5.19A, C and D). They may be linked by grain-to-grain contacts or cementation bonds, and/or can occur dispersed in the matrix (floating grains). Although sample 114 is not laminated, its constituents, particularly platy minerals (micas) and layers of organic matter, have a preferred orientation (Fig. 5.19A).

The association of clay particles in siltstones and siltshales seems to be essentially of the FF and low angle EF types, which gives a densely compacted structure with low amount of void. In particular, sample 431 which is characterized by a very fine-grained and densely packed texture (Fig. 5.19D) corresponds to the lowest porosity value, as determined by the mercury intrusion method (see Section 6.2.3).

Carbonate minerals, in general calcite, are present as grains (Fig. 5.19B and C), sparite cement (Fig. 5.19B) and micrite matrix (Fig. 5.19D). Dolomite is the main carbonate of sample 334. The SEM examination shows that it occurs in the same way as calcite (Fig. 5.19C).

The matrix of siltstones and siltshales is mainly composed of clay minerals, although the small size in which they occur prevented the accurate determination of the mineralogical composition of the matrix. Energy dispersive X-ray analysis (EDS) carried out on the matrix led to the conclusion that the darker zones in the BEI images have a chemical composition similar to kaolinite, while the lighter zones have a chemical composition similar to illite and/or smectite. Clay minerals can also occur in larger packets. Flakes of chlorite (Fig. 5.19C), illite (Fig. 5.19B, C and D) and kaolinite (Fig. 5.19B and C) have been identified.

Organic matter is found randomly distributed throughout the rock or in layers parallel to lamination and/or bedding. Pyrite occasionally occurs associated with organic matter covering wide zones of this constituent (Fig. 5.19B).

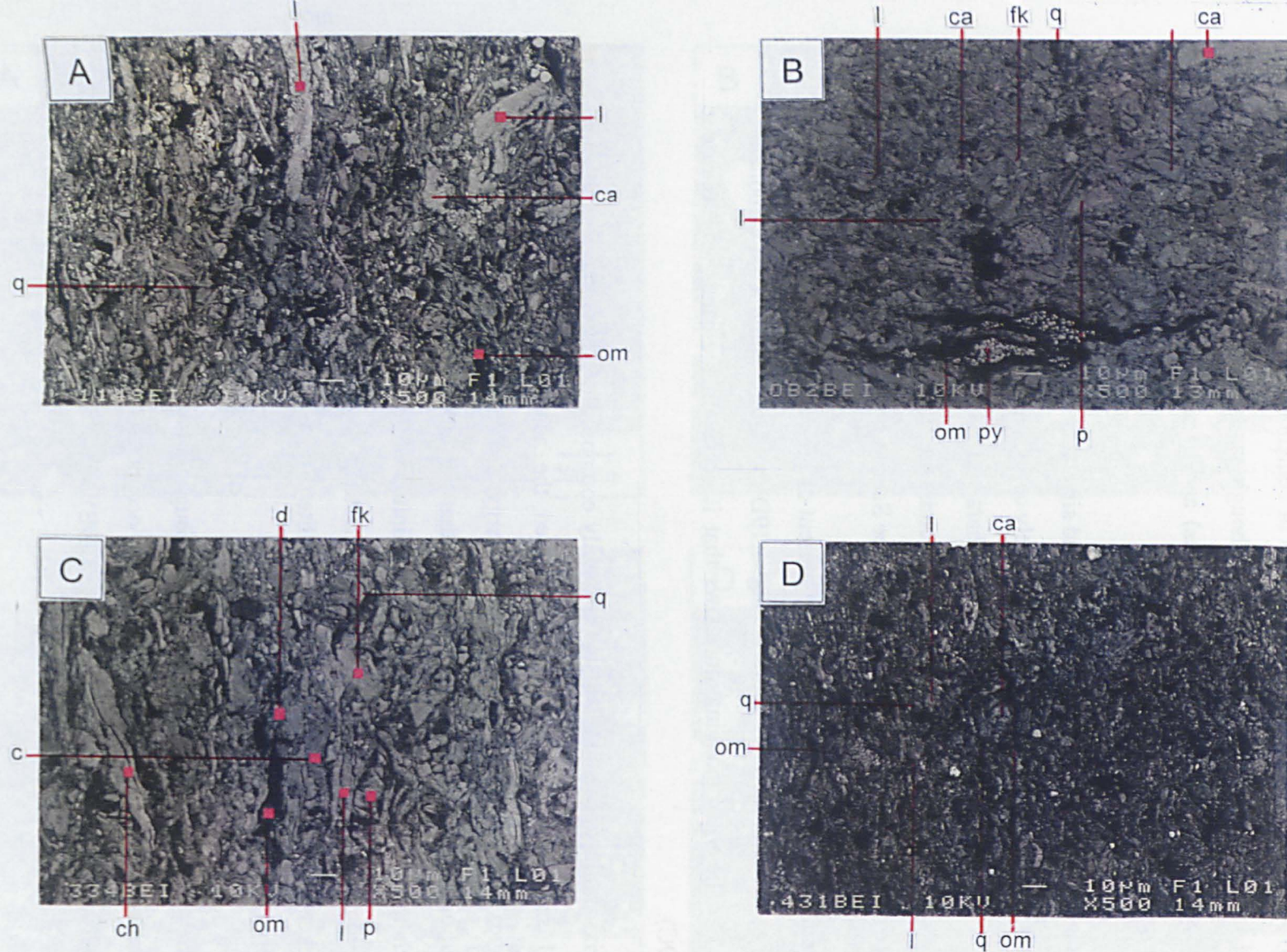


Fig. 5.19 - Siltstones and siltshales (cont.); (A) Backscattered electron image (BEI) of sample 114 (siltstone), (q) quartz, (ca) calcite, (I) illite/mica, (om) organic matter; (B) Backscattered electron image (BEI) of sample OB2 (siltstone), (q) quartz, (fk) K-feldspar, (p) plagioclase, (ca) calcite, (I) illite/mica, (om) organic matter, (py) pyrite; (C) Backscattered electron image (BEI) of sample 334 (siltshale), (q) quartz, (fk) K-feldspar, (p) plagioclase, (d) dolomite, (I) illite/mica, (k) kaolinite, (ch) chlorite, (om) organic matter; (D) Backscattered electron image (BEI) of sample 431 (siltshale), (q) quartz, (ca) calcite, (I) illite/mica, (om) organic matter.

c) Mudstones and mudshales

Mudstones include samples 81, 162, 283, 285, 286, 296, 333, 336 and 436, while mudshales comprise samples 52, 153, 154, 156, 441, and 445. Mudstones are constituted of sub-angular grains of quartz and feldspar predominantly finer than 30 μm which occur spread in the matrix. Weathered samples (81, 162, 283, 285, 296 and 333) are in general more poorly-graded than unweathered samples and the former can contain fine-sand size quartz and feldspar grains (*e.g.* samples 162 and 333).

Mudstones show some diversity in texture and composition. Thus, some samples have a micrite-rich matrix which gives to the rocks a browner hue (Fig. 5.20A), while others are mainly clay-rich matrix imparting to the samples a yellowish colour (Fig. 5.20B). Moreover, some of the constituents of the mudstones, such as organic layers, can occur with a preferred orientation (Fig. 5.20A) or spread throughout the rock (Fig. 5.20B).

Mudshales are characterised by the occurrence of laminae with a thickness, in general, varying between 250-500 μm . The laminae are distinguished in terms of variations in grain size and composition. In this way, it is found that the coarse-grained light coloured laminae consist of sub-angular medium- to coarse-silt size (Fig. 5.20C) or coarse-silt to fine-sand size (Fig. 5.20D) quartz and feldspar grains and by very fine-grained dark coloured laminae (grains < 4 μm) composed mainly of clay minerals, carbonates (micrite) and organic matter. The fine-grained (dark) laminae may also contain quartz, feldspar and carbonate grains smaller than 15 μm in diameter. Occasionally, organic matter occurs in the coarse-grained (light) lamina in discontinuous layers parallel to the lamination (Fig. 5.20C).

The examination of backscattered electron images also shows that the particles (*e.g.* micas) in mudstones may occur randomly orientated (Fig. 5.21A and B), or with a preferred orientation parallel to lamination (Fig. 5.21C and D). In mudstones, the grains are predominantly disseminated in the matrix (floating grains) although some grains (basically quartz and feldspar) show point and/or long grain-to-grain contacts, and cementation bonds. In mudshales the grains that form the coarse-grained (light) laminae have predominantly grain-to-grain contacts and cementation bonds (almost all drusy sparite), while in fine-grained (dark) laminae the grains are mostly disseminated in the matrix (floating grains).

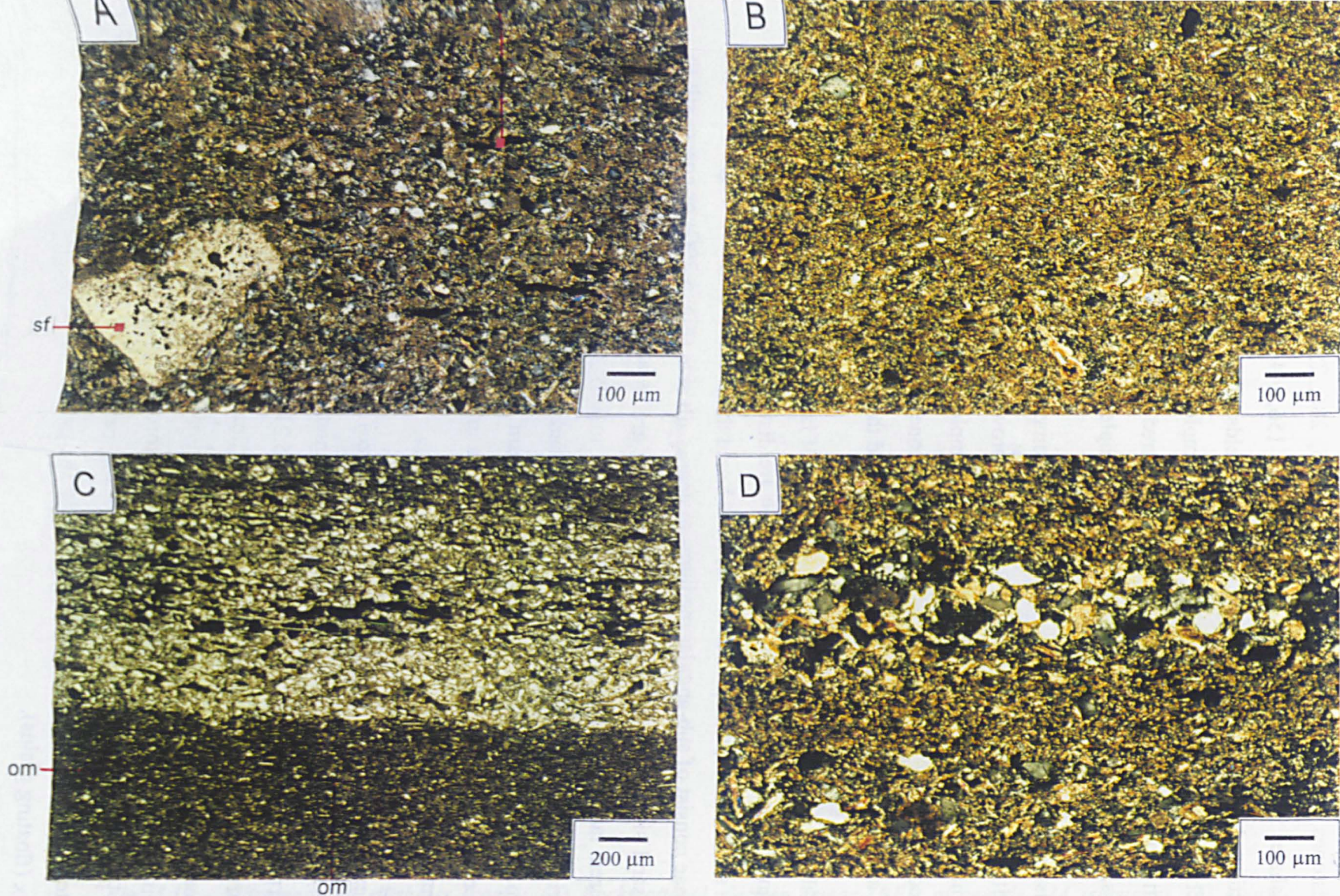


Fig. 5.20 - Mudstones and mudshales; (A) Photomicrograph of sample 286 (mudstone), XPL, (sf) shell fragment, (om) organic matter; (B) Photomicrograph of sample 336 (mudstone), XPL; (C) Photomicrograph of sample 154 (mudshale), PPL, (om) organic matter; (D) Photomicrograph of sample 445 (mudshale), XPL.

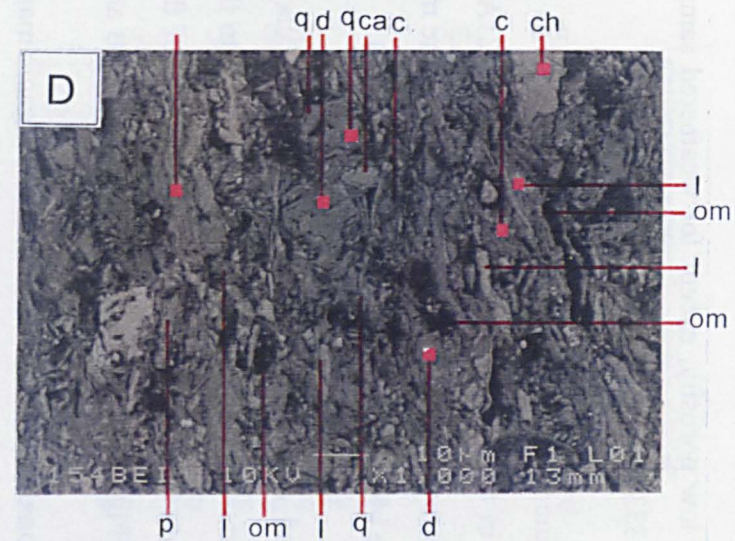
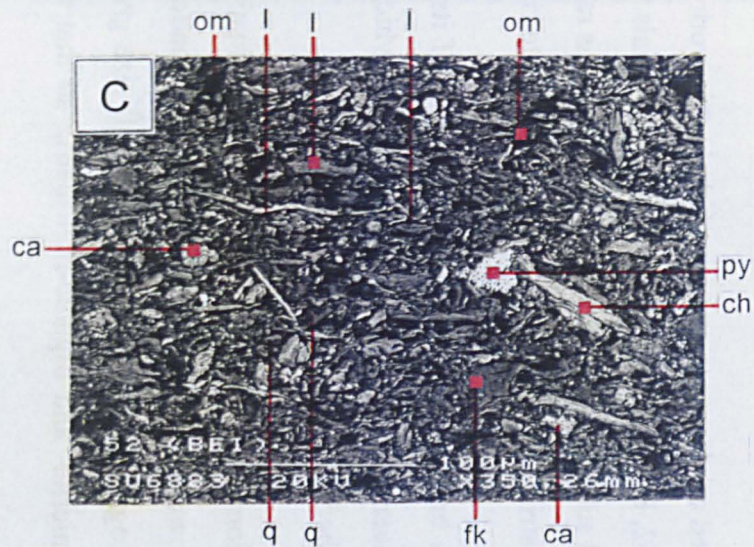
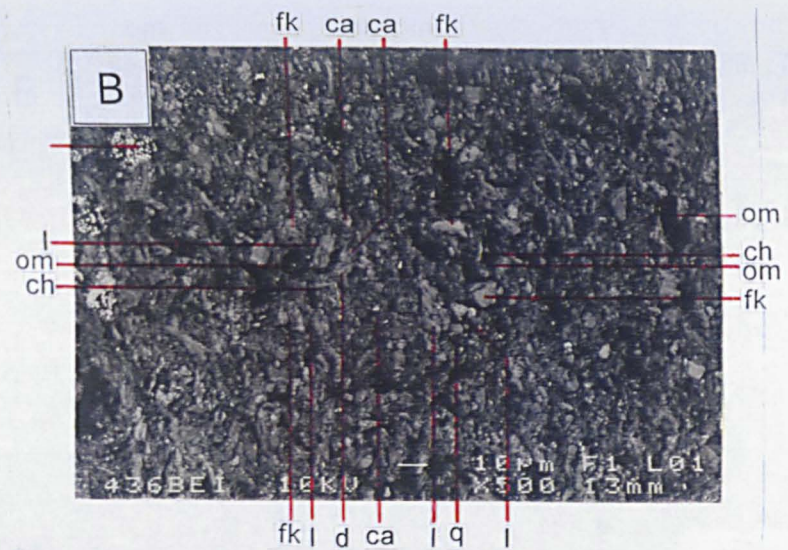
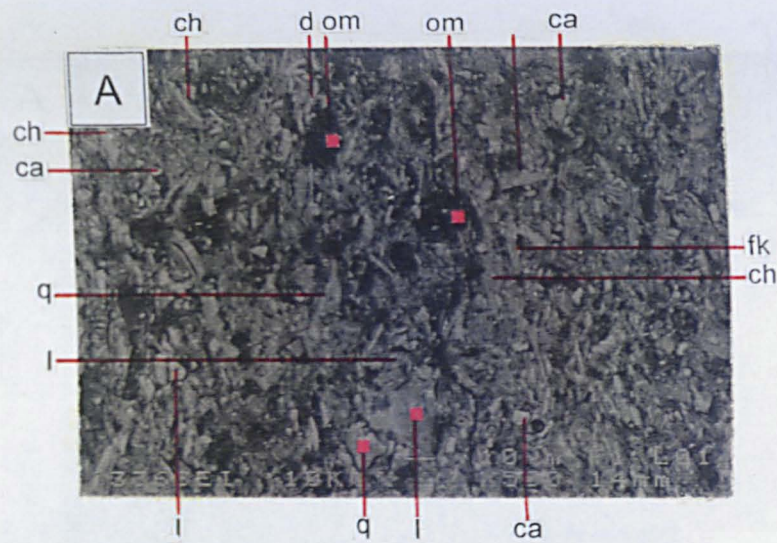


Fig. 5.21 - Mudstones and mudshales (cont.); (A) Backscattered electron image (BEI) of sample 336 (mudstone), (q) quartz, (fk) K-feldspar, (ca) calcite, (d) dolomite, (l) illite/mica, (ch) chlorite, (om) organic matter; (B) Backscattered electron image (BEI) of sample 436 (mudstone), (q) quartz, (fk) K-feldspar, (ca) calcite, (d) dolomite, (l) illite/mica, (ch) chlorite, (om) organic matter; (C) Backscattered electron image (BEI) of sample 52 (mudshale), (q) quartz, (fk) K-feldspar, (ca) calcite, (l) illite/mica, (py) pyrite; (D) Backscattered electron image (BEI) of sample 154 (mudshale), (q) quartz, (fk) K-feldspar, (p) plagioclase, (ca) calcite, (d) dolomite, (l) illite/mica, (ch) chlorite, (k) kaolinite, (om) organic matter.

The features described in relation to the structure of siltstones and siltshales are generally applicable to mudstones and mudshales which show a densely compacted structure and low porosity, except for weathered samples (e.g. 52, 81, 153, 162, 283, 285, 296 and 333).

Carbonate minerals usually occur in these rocks as grains (Fig. 5.21C and D) and disseminated in the rock as micrite matrix (Fig. 5.21A and B). The presence of sparite was only detected in coarse-grained laminae in some mudshales, such as 156. Grains of dolomite were identified in sample 154 (Fig. 5.21D).

Mudstones and mudshales have predominantly a clay-rich matrix showing the EDS analysis undertaken that its composition is similar to that described for siltstones. Clay minerals also occur in larger packets, in the form of flakes of illite (Fig. 5.21A, B and D), kaolinite (Fig. 5.21D) and chlorite (Fig. 5.21A, B and D).

Pyrite, occasionally, occurs associated with organic matter (Fig. 5.21B and C).

e) Claystone and clayshale

Rocks classified as claystone and clayshale in this work include accordingly sample 294 and sample 152, both of which are weathered materials. These rock types consist mostly of angular and sub-angular quartz and feldspar grains ranging between 10 and 40 μm in size, evenly distributed throughout a clay- and micrite-rich matrix.

Sample 294 is brown in colour displaying some of its constituents, such as flakes of mica and stringers of black/brown organic matter which follow a preferred orientation parallel to the bedding (Fig. 5.22A).

The examination of sample 152 shows that lamination was partially destroyed by weathering. However, and despite the fact that lamination has poorly defined limits, it is possible to recognize yellow layers rich in silt size grains of quartz alternated with a brown clay-, micrite- and organic-rich matrix so that to create discontinuous laminae (Fig. 5.22B).

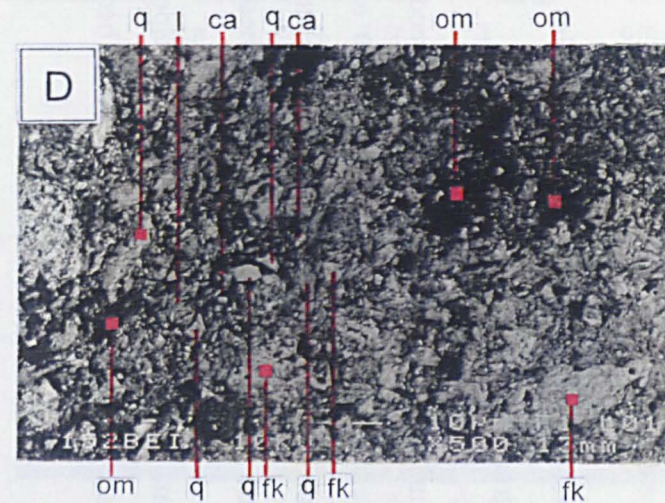
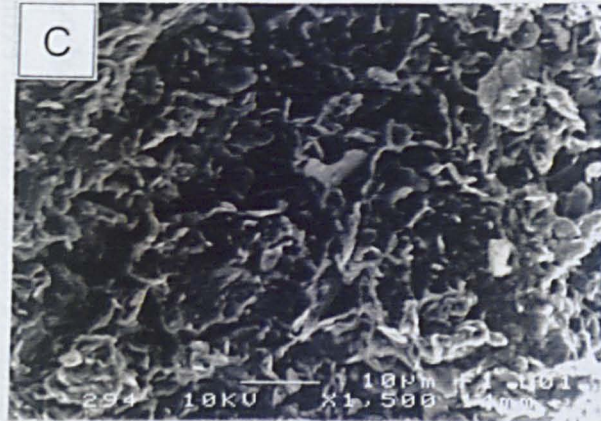
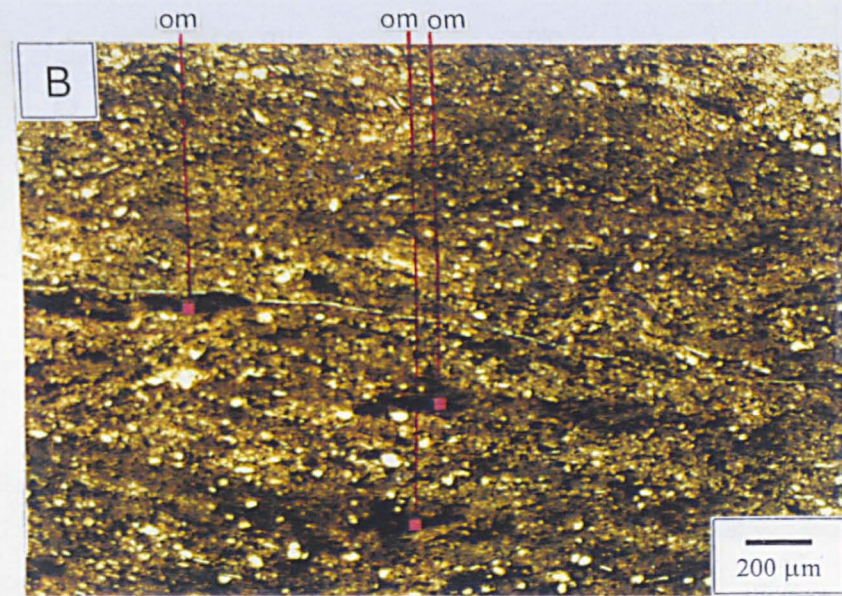
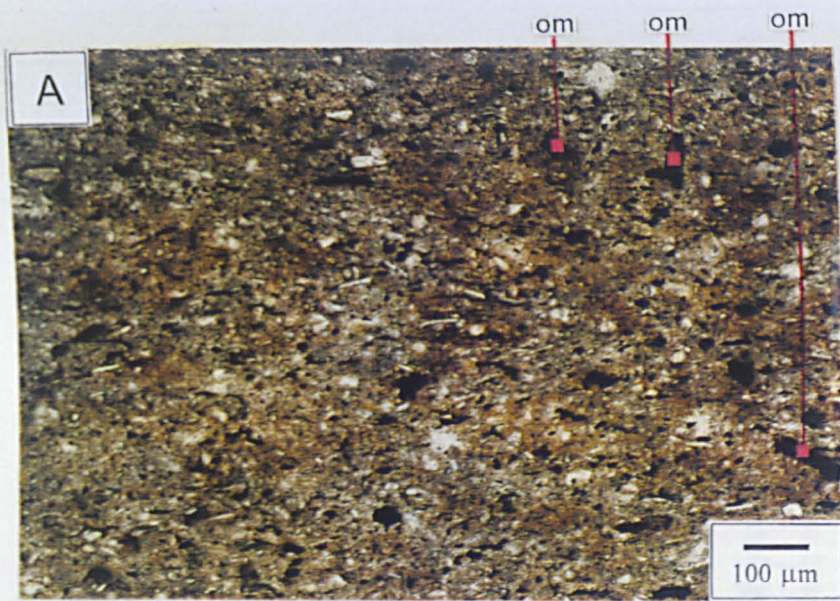


Fig. 5.22 - Claystone and clayshale; (A) Photomicrograph of sample 294 (claystone), PPL, (om) organic matter; (B) Photomicrograph of sample 152 (clayshale), PPL, (om) organic matter; (C) Secondary electron image (SEI) of a freshly-fractured surface (sample 294); (D) Backscattered electron image (BEI) of sample 152, (q) quartz, (fk) K-feldspar, (ca) calcite, (l) illite/mica, (om) organic matter.

These samples show a loosely compact structure characterized by a large amount of void space (high porosity). The clay particles arrangements are predominantly of EE and EF types (Fig. 5.22C). However, the clay fabric displayed may also have been produced by weathering.

Carbonate minerals occur mostly in these samples as micrite matrix and on a lesser proportion as grains (Fig. 5.22D).

EDS analysis undertaken on matrix enabled to recognize that the darker zones in the BSE images have a chemical composition similar to kaolinite, while the lighter zones have a chemical composition close to illite and/or smectite. Flakes of illite (Fig. 5.22D) and chlorite (sample 294) were also identified in these samples.

The organic matter is present as randomly dispersed pockets (Fig. 5.22D) or as discontinuous stringers with a moderate degree of bedding-parallelism (Fig. 5.22B).

f) Oolitic limestone

Sample 345, classified as oolitic limestone, is composed mainly of dark brown ooids smaller than 1 mm in diameter and angular and sub-angular fine-sand to coarse-silt size quartz grains, both cemented by sparite. The rock forming constituents do not show a preferred orientation (Fig. 5.23A). The rock has a densely compacted structure characterized by small amount of void space (low porosity) (Fig. 5.23C).

The ooids consist of regular concentric lamellae developed around a nucleus formed by quartz, feldspar and carbonate grains. The latter comprise micrite and sparite aggregates and skeletal fragments (Fig. 5.23B). The examination of the rock showed that most of the ooids have a concentric laminae structure, although some with a radial structure were also found (Fig. 5.23A).

The examination of the sample with crossed polars (XPL) showed that some of the quartz is polycrystalline exhibiting undulose extinction (Fig. 5.23B). Plagioclase grains are often weathered showing a dusty appearance caused by replacement by sericite and calcite.

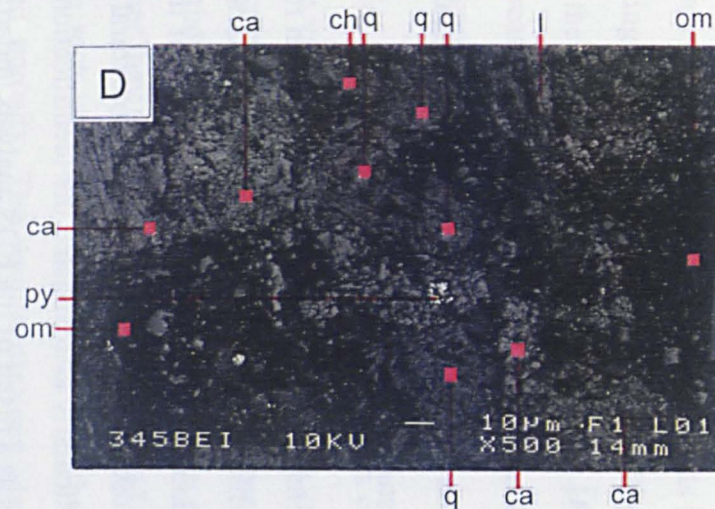
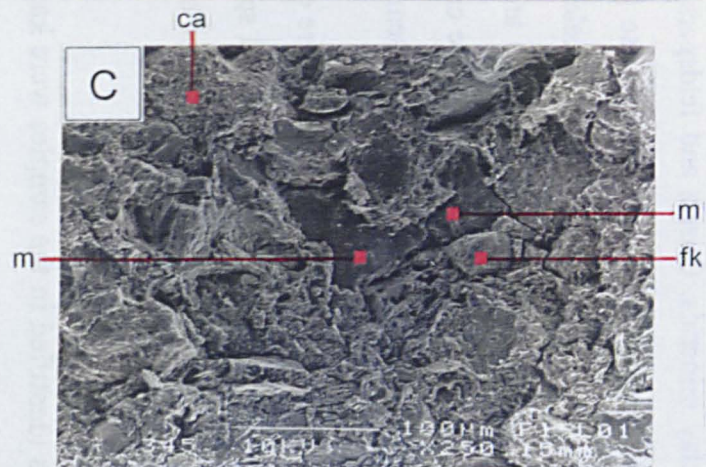
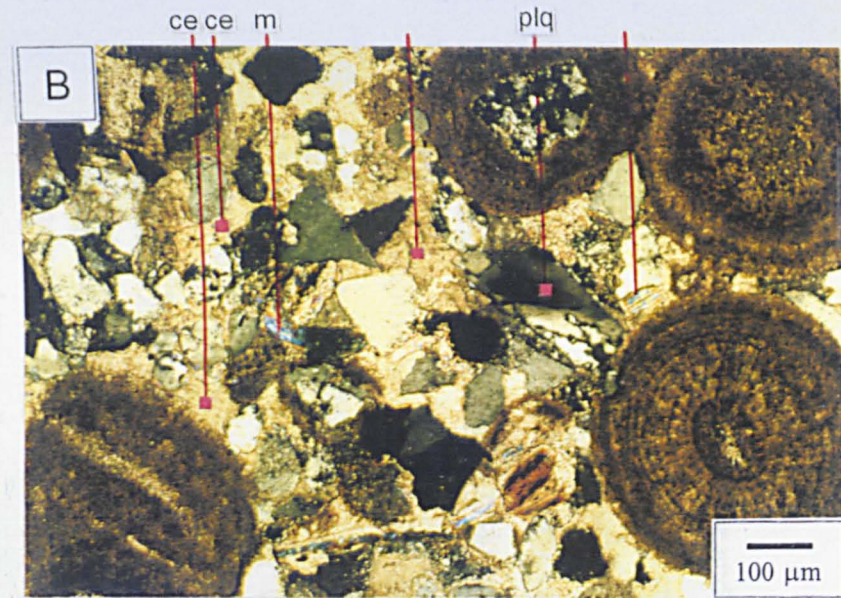
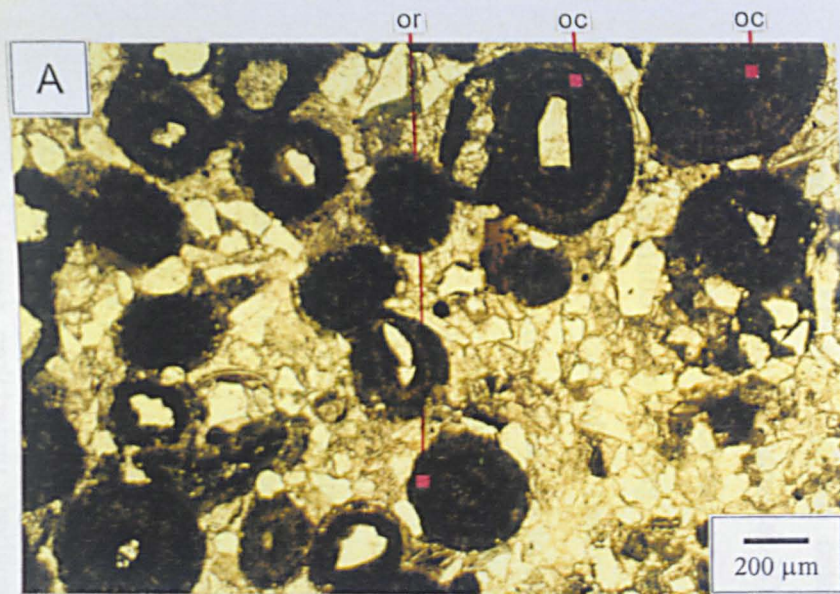


Fig. 5.23 - Oolitic limestone (sample 345); (A) Photomicrograph, PPL, (oc) ooid with concentric structure, (or) ooid with radial structure; (B) Photomicrograph, XPL, (plq) polycrystalline quartz with undulose extinction, (m) muscovite, (scc) sparry calcite cement; (C) Secondary electron image (SEI) of a freshly-fractured surface, (fk) K-feldspar, (m) muscovite, (ca) calcite; (D) Backscattered electron image (BEI), (q) quartz, (ca) calcite, (l) illite/mica, (ch) chlorite, (py) pyrite, (om) organic matter.

The organic matter occurs in the ooids located chiefly between lamellae (Fig. 5.23B) and in randomly pockets spread throughout the rock which occasionally also contain the presence of pyrite framboids (Fig. 5.23D).

5.4 - Final comments

This chapter covers the topics related to the mineralogical and textural characterization of mudrocks studied.

The proportions of various components present in rocks were determined using various techniques which include X-ray diffraction, X-ray fluorescence and wet chemical analysis. Although the aim of the examination of the samples by optical and scanning electron microscopes was mainly the microtextural description of the rocks, the latter technique particularly also assisted the identification of the various constituents present in the samples as a result of the EDS analysis undertaken.

The mineralogical composition of the rocks consisted chiefly of quartz, feldspars, carbonates and clay minerals. Quartz and feldspars (K-feldspar and plagioclase) form the coarser detrital fraction of these rocks. These grains can occur as floating grains spread in the matrix or constitute a granular skeleton by grain-to-grain contacts and cementation bonds. The grain to grain relations are related to the rock type studied. Thus, grain-to-grain contacts predominated in the case of siltstones, while at the other extreme, in claystones, the grains are, mostly, disseminated in the matrix.

The carbonate minerals identified in the rocks were calcite and dolomite which occur in the rock either as micrite matrix or as grains and sparry cement. From examination of the samples it was concluded that both modes of occurrence are generally present in most of the rocks analysed.

The clay minerals identified in the samples were kaolinite, illite, chlorite, smectite and mixed-layer illite-smectite. Clay minerals are the main constituent of the matrix (particles of a size finer than 4 μm). The EDS analysis undertaken revealed the

occurrence of zones in the matrix with a kaolinitic composition and others with a chemical composition similar to illite and/or smectite. Chlorite and illite also occur as flakes.

Pyrite, organic matter, anatase and apatite occur as accessory components in these rocks. The organic matter can occur as stringers with a preferred orientation (Fig. 5.20A) or as random pockets spread throughout the rock. Pyrite occurs as framboids often associated and apparently covering large areas of organics. Apatite and anatase are minor constituents present in the rocks as small crystals.

The descriptive scheme proposed for the microtextural characterization of the samples enabled the individualization of the various rock types studied. The rocks described as A₃ correspond to laminated rock types according to the classification presented in 3.4, while the classification of rocks without lamination was subdivided into classes A₂ and A₁, according respectively as whether they did or did not show preferred orientation of the rock forming constituents. The rock structure was described on the basis of the arrangements of clay particles and porosity. The results obtained showed a good correlation between the parameters (1, 2 and 3) of clay fabric determined and the degree of weathering of the samples.

6 - GEOTECHNICAL CHARACTERIZATION

6.1 - Introduction

Laboratory testing plays a fundamental role in the geotechnical characterization of mudrocks since the properties of rock material represent to a large extent the behaviour of rock mass (Oliveira, 1993). Physical and mechanical properties must be determined on the basis of a set of tests, which must be suitable for a proper characterization but also simple and rapid to perform and sufficiently attractive in terms of costs in order to enable its applicability to a wide extent.

This chapter describes part of the experimental work carried out on the mudrocks. Its objective is to set out procedures used to determine the geotechnical properties of a set of samples and to investigate which index tests are most appropriate to characterize them. The results are evaluated and discussed in terms of their relative importance as controls of mudrock breakdown.

This chapter is organised in accordance with the properties of the materials as determined in the tests. Accordingly, the tests used to evaluate the fundamental properties of the rocks, namely grain specific gravity, dry density, porosity and water adsorption, are described first. The determination of the natural water content, which is usually included in this set of tests, was not carried out, because of the sampling technique used to collect almost all of the rocks tested (see Section 4.3.1). In addition to

these tests methylene blue adsorption and Atterberg limits, which enable the characterization of the clay fraction present in the rocks, are also described.

The strength of the rocks was determined directly using uniaxial compression and estimated indirectly by carrying out tests with the NCB cone indenter. In a few samples the deformation modulus was determined.

Swelling strain was measured on remoulded specimens and in intact rock samples in three orthogonal directions. These two types of tests allowed the evaluation of the influence of mineralogy and texture on this property.

Although the slake durability and jar slake tests were developed to evaluate the durability of soft rocks and are therefore described in Section 2.4.2.4, the importance of slaking in the geotechnical characterization of mudrocks as well as its correlation with other physical and mechanical properties, justifies its inclusion in the present chapter. The slake durability tests were carried out using the standard procedure and also it was modified by increasing the slaking time in order to achieve greater breakdown of the rocks and therefore have a better discrimination of the behaviour of the various samples.

The compaction characteristics of the mudrocks collected were determined for mixtures comprising different samples selected according to their composition and the results of the slake durability test (I_{d2}). Despite the fact that this methodology is not the most appropriate, it is justified given the small amount of material collected for each sample in relation to the requirements of the compaction tests. The evaluation of the strength of compacted mixtures was determined using penetration tests with a CBR plunger.

Lastly, the results of the various tests are analysed and discussed in order to evaluate the importance of the properties determined in the behaviour of mudrocks.

6.2 - Identification tests

This includes the tests used to determine physical properties such as porosity, dry density, grain specific gravity and water adsorption, as well as the tests used for geotechnical characterization *i.e.* methylene blue adsorption and Atterberg limits.

6.2.1 - Grain specific gravity

The grain specific gravity values determined represent an average density resulting from the assortment of minerals which comprise the rock and on the relative proportions of each mineral present. In the case of the mudrocks, grain specific gravity depends mostly on the relative percentages in which quartz (specific gravity 2.65), feldspars (specific gravity varies according to the mineralogical species: K-feldspars 2.54 - 2.57; plagioclases 2.62 - 2.76), calcite (specific gravity 2.71) and clay minerals (specific gravity varies according to the mineralogical species: kaolinite 2.6; illite 2.6 - 2.9; smectites 2 - 3) are present (Hurlbut & Klein, 1985).

To determine grain specific gravity, the samples were first powdered and the tests carried out on the fraction passing the #40 ASTM (425 μm) sieve. Grain specific gravity was determined according to the procedure described in NP - 83 (1965) using subsamples of about 25 g, which had been dried previously in an oven at 105°C. Grain specific gravity (G_s) at test temperature t_x , in relation to distilled water at 20°C is calculated as follows:

$$G_s = \frac{m_1}{m_2 - (m_3 - m_1)} \times k \quad (6.1)$$

where,

m_1 - mass of the dry powder (g);

m_2 - mass of density bottle full of distilled water at test temperature t_x (g);

m_3 - mass of density bottle, powder and distilled water at test temperature t_x (g);

k - density of water at test temperature t_x to density of water at 20°C ratio.

Usually the mass of the density bottle full of distilled water (m_2) was determined earlier, therefore, it was necessary to correct its value to the water temperature t_x used during the test stage. The weights were carried out using a balance readable to 0.01g. The grain specific gravity was determined for at least two subsamples from each sample, the average values are presented in Table 6.1 and in Fig. 6.1.

Table 6.1 - Results (average values) of the identification tests and soil classification of the samples studied.

Sample	G_s	ρ_d (Mg.m ⁻³)	N (%)	APD (μ m)	w_{95} (%)	MBA (g/100g fines)	LL (%)	PL (%)	PI (%)	USCS
51	2.71	1.86	33.9	0.09	2.12	3.6	48.0	24.4	23.6	CL (lean clay)
52	2.70	1.93	22.7	0.06	6.09	6.0	54.2	25.0	29.2	CH (fat clay)
81	2.71	2.19	19.8	0.55	3.70	4.1	43.7	23.1	20.6	CL (lean clay)
83	2.71	2.41	16.3	0.30	1.29	2.3	34.8	18.8	16.0	CL (lean clay)
111	2.67	1.98	24.8	0.30	5.49	4.5	44.0	21.8	22.2	CL (lean clay)
112	2.69	2.25	17.3	0.07	3.09	3.3	40.4	21.6	18.8	CL (lean clay)
114	2.71	2.33	14.9	0.07	2.79	2.6	26.8	17.2	9.6	CL (lean clay)
151	2.75	2.08	19.9	0.07	5.08	4.4	47.3	23.9	23.4	CL (lean clay)
152	2.73	2.17	22.9	0.15	3.89	3.5	40.8	22.6	18.2	CL (lean clay)
153	2.72	2.13	22.0	0.07	3.46	3.1	39.0	21.6	17.4	CL (lean clay)
154	2.71	2.25	16.7	0.18	3.40	2.9	34.2	19.8	14.4	CL (lean clay)
156	2.73	2.38	12.7	0.15	2.54	3.1	35.7	20.2	15.5	CL (lean clay)
162	2.71	2.10	19.7	0.04	4.05	4.3	48.4	24.0	24.4	CL (lean clay)
163	2.70	2.18	17.9	0.05	3.92	4.0	44.3	22.5	21.8	CL (lean clay)
283	2.70	2.11	20.2	0.15	3.98	4.6	43.9	22.3	21.6	CL (lean clay)
285	2.69	2.22	20.7	0.14	4.14	4.1	44.2	23.2	21.0	CL (lean clay)
286	2.67	2.39	15.8	0.08	3.46	4.0	41.8	23.1	18.7	CL (lean clay)
294	2.80	2.13	23.6	0.09	5.44	5.7	51.7	24.0	27.7	CH (fat clay)
296	2.77	2.03	21.6	0.08	4.11	5.2	49.4	24.6	24.8	CL (lean clay)
332	2.69	2.10	22.7	0.22	4.33	4.9	45.8	22.1	23.7	CL (lean clay)
333	2.68	2.10	22.3	0.25	4.34	4.9	49.3	25.0	24.3	CL (lean clay)
334	2.70	2.28	16.0	0.04	4.97	4.6	46.5	24.0	22.5	CL (lean clay)
336	2.68	2.30	15.3	0.05	4.35	5.8	54.2	26.8	27.4	CH (fat clay)
342	2.67	2.31	15.8	0.02	1.96	4.2	33.2	17.9	15.3	CL (lean clay)
345	2.71	2.49	12.9	0.02	1.17	2.1	33.8	18.6	15.2	CL (lean clay)
431	2.71	2.37	11.7	0.01	2.65	3.3	37.2	22.0	15.2	CL (lean clay)
436	2.72	2.38	12.4	0.01	3.36	3.5	35.8	20.4	15.4	CL (lean clay)
441	2.71	2.40	12.3	0.03	3.79	3.3	35.3	19.6	15.7	CL (lean clay)
445	2.70	2.45	12.5	0.02	2.30	3.2	32.4	19.5	12.9	CL (lean clay)
OB1	2.78	2.16	18.2	0.09	3.86	4.1	41.8	23.0	18.8	CL (lean clay)
OB2	2.77	2.17	20.6	0.10	3.64	4.6	38.5	20.6	17.9	CL (lean clay)

G_s - Grain specific gravity; ρ_d - Dry density; N - Effective porosity; APD - Average pore diameter; w_{95} - Water adsorption at 95%RH;

MBA - Methylene blue adsorption value; LL - Liquid limit; PL - Plastic limit; PI - Plasticity Index; USCS - Unified soil classification system.

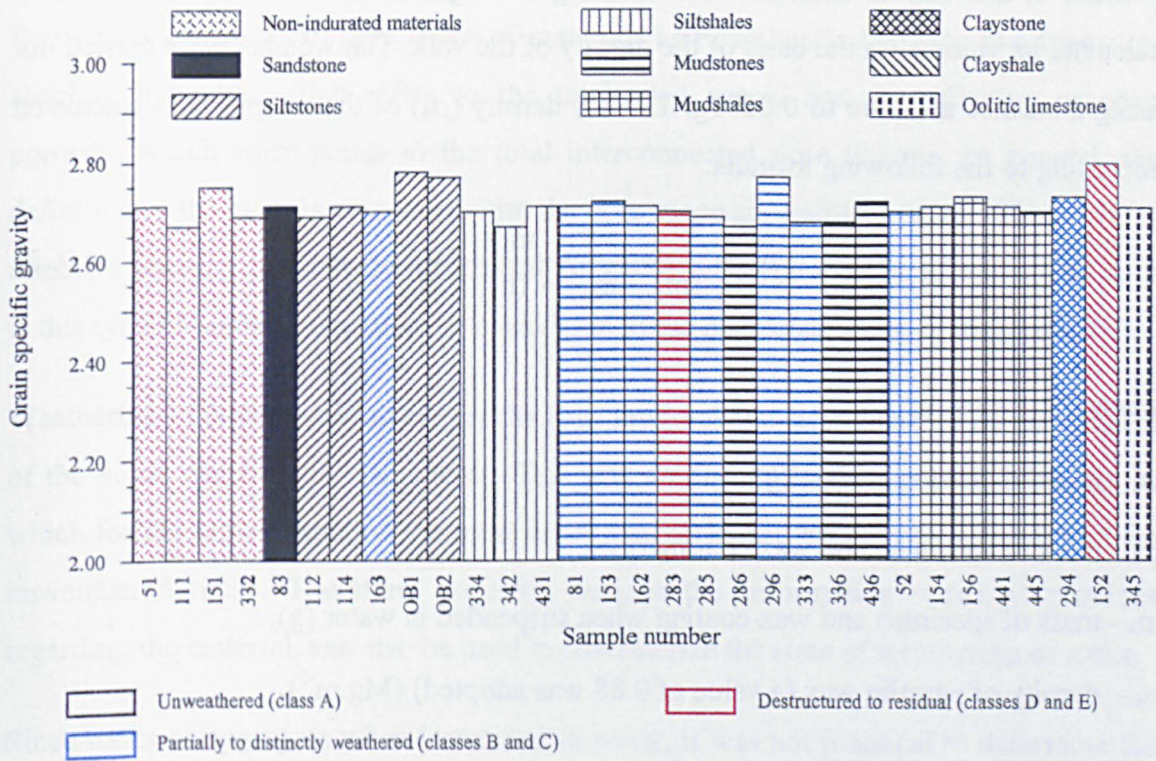


Fig. 6.1 - A comparison of average grain specific gravities of the various samples studied.

6.2.2 - Dry density

Dry density is mainly influenced by mineralogical composition and by the amount of void space. Since mudrocks generally comprise a suite of identical minerals, this property mostly reflects the degree of consolidation and state of weathering of the materials tested (Hudec, 1982, Dick *et al.*, 1992, Bell, 1992).

Small rock specimens of a regular geometry, with volumes between 8 and 20 cm³ were used to determine dry density. Density and porosity of rock materials are most often determined using vacuum saturation and buoyancy techniques.

However, in the case of the samples collected for this work, the rocks disaggregate when immersed in water, a process that accelerated if vacuum saturation was used. No standard procedure to determine dry density exists, therefore a water immersion method based on Archimedes principle was used. This method involves the coating of the

samples with paraffin wax having first been oven dried at 105°C and cooled. It was possible in this way to determine the submerged weight of the waxed specimen and to calculate its volume on the basis of the density of the wax. The weights were carried out using a balance accurate to 0.0001g. The dry density (ρ_d) of the samples was calculated according to the following formula:

$$\rho_d = \frac{m_1}{(m_2 - m_3) - (m_2 - m_1) / \rho_p} \quad (6.2)$$

where,

m_1 - mass of dried specimen (g);

m_2 - mass of specimen and wax coating (g);

m_3 - mass of specimen and wax coating when suspended in water (g);

ρ_p - density of paraffin wax (a value of 0.88 was adopted) (Mg.m^{-3}).

The dry density was determined for at least three specimens per sample, the average values are presented in Table 6.1 and in Fig. 6.2.

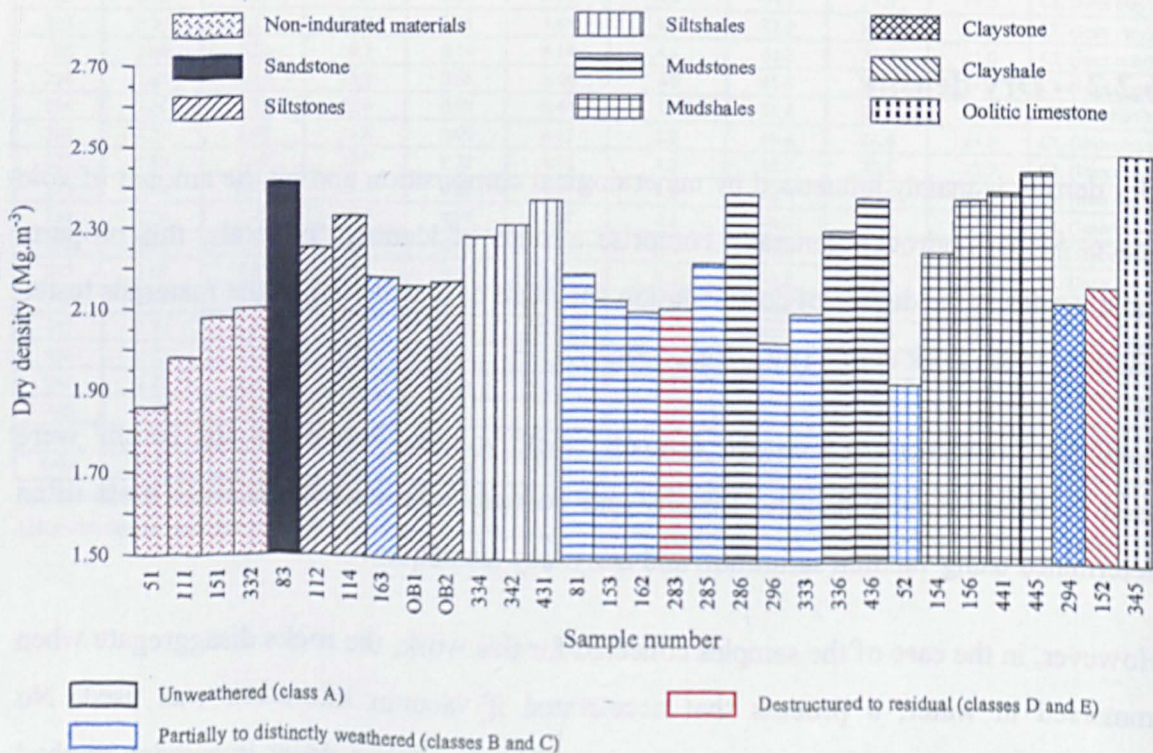


Fig. 6.2 - A comparison of average dry densities of the various samples studied.

6.2.3 - Porosity

Porosity is a measure of pore space of materials and can be divided into two types: (a) absolute porosity, which refers to the total void space, and (b) effective or open porosity, which corresponds to the total interconnected pore volume. In general, the definition of the latter is associated with the pore space accessible to water. Therefore, is effective porosity that mostly influenced the geotechnical properties of rocks, and so it is this type of porosity that must be considered in the characterization of materials.

Weathering of porous sedimentary rocks (*e.g.* mudrocks) is accompanied by an increase of the voids which water can access. This was confirmed in the samples collected, in which for the same formation the most weathered rocks had higher porosity values than unweathered rocks. Therefore, porosity, besides the information which it provides regarding the material, can also be used to characterize the state of weathering of rocks.

Since rocks disaggregate when immersed in water, it was not practical to determine the effective porosity using vacuum saturation and buoyancy techniques. Therefore, porosity was determined using a mercury porosimeter. The theoretical basis of mercury porosimetry are described in detail in Lowell & Shields (1991) and the experimental technique, in test method LERO-PE15 (LNEC, 1996) and in standard ASTM D4404-84. Briefly, the method involves the evacuation of air from the sample, the filling under vacuum of the cell with mercury and its pressurization in order to force mercury to intrude into the voids of the sample and lastly, in the monitoring both the applied pressure and the intruded volume. The latter corresponds accordingly to a measurement of the interconnected pore space of the rock, being considered to be a good reflection to the pore space accessible to water (Shakoor & Scholer, 1985). Thus, effective porosity is given by the ratio between intruded volume of mercury and sample volume. The latter parameter is obtained from the mass of mercury displaced when the sample is immersed in this liquid.

According to Shakoor & Scholer (1985) the determination of porosity using a mercury porosimeter has some limitations as follows:

- a) in the calculations it is assumed a model of cylindrical pore geometry, which is not correct for most rocks;
- b) if a void has an entrance smaller than its body the whole void volume will be recorded as being the size of the entrance, therefore the pore size distribution is biased toward smaller pore sizes;
- c) the results may be also affected due to the compressibility of the test specimen and the incomplete evacuation of air from the sample prior to mercury intrusion.

Taking into account the previous limitations focused to this technique and after evaluating the mercury porosimetry data as well as examination of the pore distribution using SEM it was decided only to present the results of porosity and average pore diameter.

The tests were carried out using a porosimeter (Autoscan 60) with capability to apply pressures of up to 414 MPa, which corresponds of measuring pore sizes down to a size of 18 Å. The equipment and data acquisition (pressure applied and volume of intruded mercury) were controlled by computer using a specific software.

The tests were performed in accordance with the test method LERO-PE15 (LNEC, 1996). A penetrometer cell with a large capacity (approximately 17 cm³) was used which enabled rock samples with volumes between 3 and 9 cm³ to be tested. The samples were oven dried at 105°C for 48 hours prior to testing. The samples were not touched by hand to avoid greasing the surfaces which would affect the evacuation of air. Depending on the pore size distribution of the sample it was found that adequate air evacuation took between 6 to 18 hours. The weights were carried out using a balance readable to 0.0001g.

At least two test specimens per sample were tested. The results of the effective porosity are presented in Table 6.1 and in Fig. 6.3. The results of average pore diameter are also presented in Table 6.1.

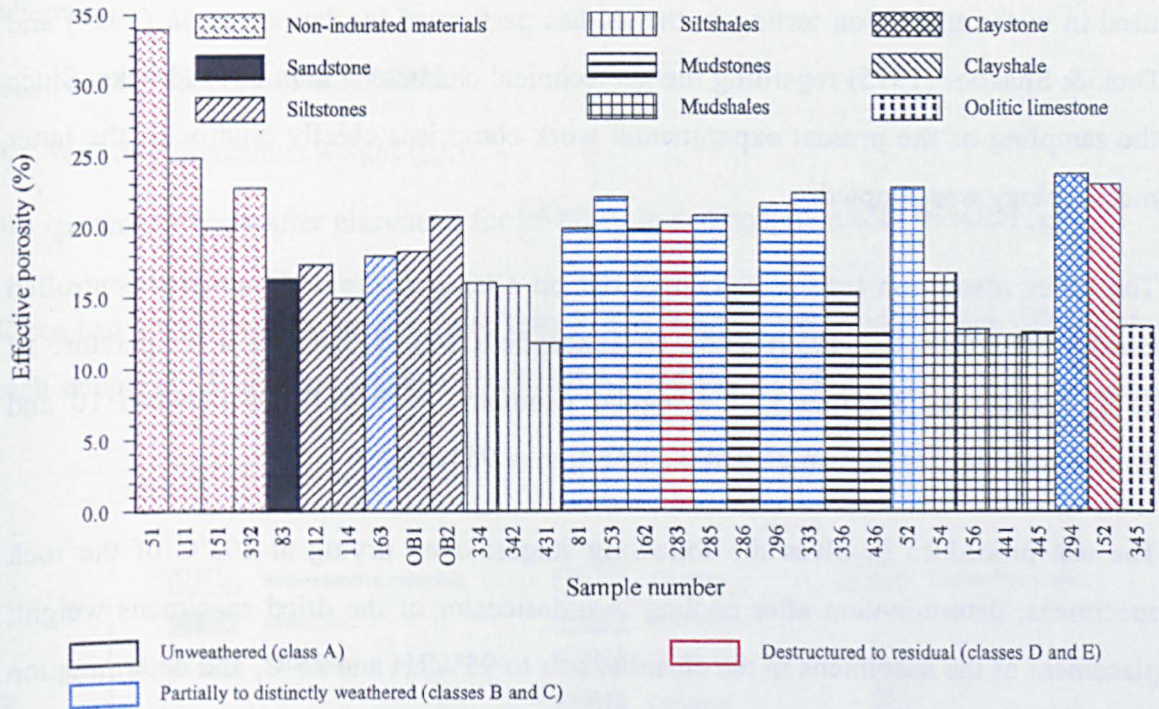


Fig. 6.3 - A comparison of average effective porosities of the various samples studied.

6.2.4 - Water Adsorption in a controlled-humidity atmosphere

The capacity to adsorb water vapour is one characteristic property of clay minerals. The clay structure formed of layers of silica tetrahedra bound to others layers by cations allows water molecules to occupy positions between sheets and in the voids within the crystal lattices.

In previous studies Rodrigues (1986) carried out water adsorption tests on powdered samples of various rock types using a controlled-humidity atmosphere of 75%RH (relative humidity). Powdering the rock results in the destruction of inter-granular porous structure that gives rises to capillary adsorption, which is a characteristic of all

fine grained materials even if clay minerals are absent. In the test conditions referred to, the equilibrium water content is sensitive to the percentage of clay minerals present in the rock (*id.*) as well as their propensity for intra crystalline water adsorption.

Water adsorption tests may also be performed on rock samples to evaluate their water adsorption capacity due to both mineralogy and texture. This methodology has been used in water adsorption testing in the studies performed by Sarman *et al.* (1994) and Dick & Shakoor (1995) regarding the geotechnical characterization of mudrocks. Since the sampling of the present experimental work comprises chiefly mudrocks, the latter methodology was adopted.

The water adsorption tests were carried out on a temperature and humidity controlled chamber (Heraeus HC 4030) using an atmosphere with 95%RH at a temperature of 25°C. Small rock specimens of a regular geometry, with volumes between 10 and 40 cm³ were used to determine water adsorption at 95%RH.

The test procedure involves the following stages: oven drying at 105°C of the rock specimens; determination after cooling in a desiccator of the dried specimens weight; placement of the specimens in the chamber sets to 95%RH and 25°C; and determination of the weight of the specimens after 96 hours of testing. Since no significant change in weight of the specimens were recorded when they were exposed for longer periods than 96 hours in a 95%RH atmosphere at 25°C, it was concluded that the equilibrium water content was reached in that time. Therefore, 96 hours was adopted as a suitable test time.

The masses were determined using a balance accurate to 0.0001g. It was found that the exchanges of moisture between the specimens and room atmosphere took place rapidly. Therefore special care had to be taken during weighing operations in order to eliminate or reduce this source of error.

Since the test result is a water content, it is expressed as a percentage of the dried specimen weight, in accordance with the following formula:

$$W_{ad95} = \frac{P_f - P_i}{P_i} \times 100 \quad (6.3)$$

where,

W_{ad95} - water adsorption at 95%RH;

P_i - oven dried specimen weight (g);

P_f - specimen weight after placement for 96 hours in a atmosphere with 95%RH (g).

Three test specimens per sample were tested. The average water adsorption values for each sample at 95%RH are presented in Table 6.1 and in Fig. 6.4.

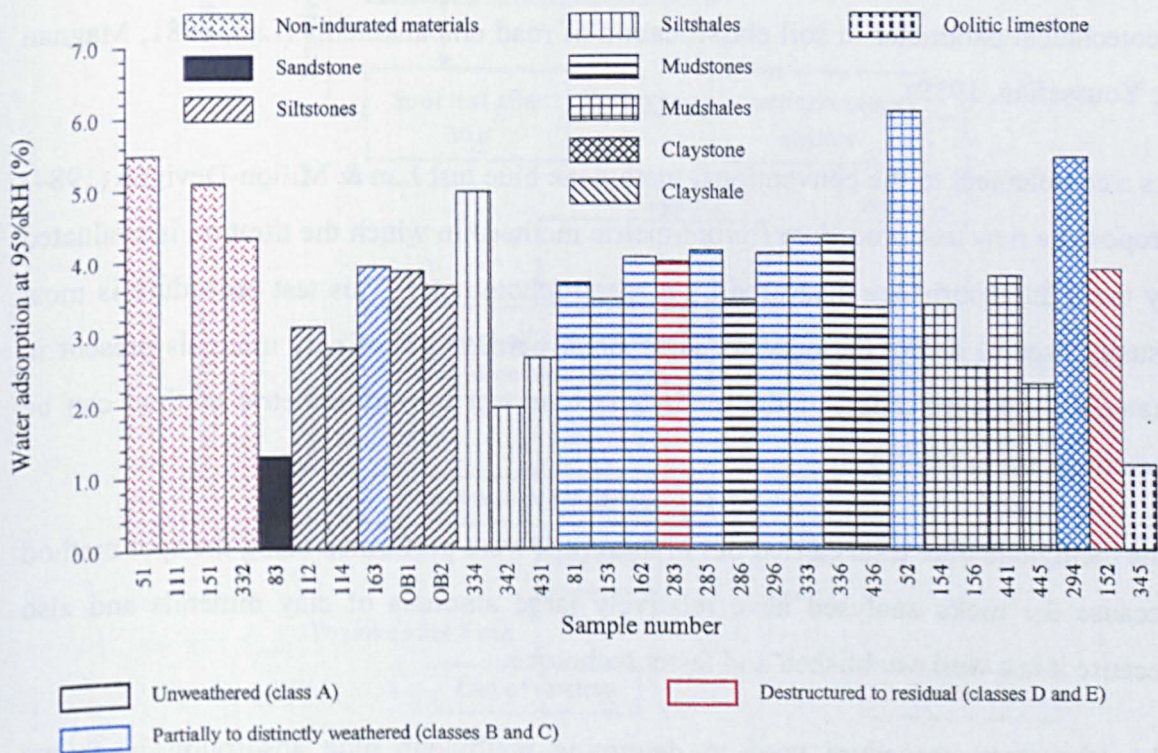


Fig. 6.4 - A comparison of average water adsorptions of the various samples studied

6.2.5 - Methylene blue adsorption determined by the spot method

The degradation of the geotechnical properties of rock materials, especially when associated with the presence of water, is in general related to the presence and species of clay minerals present (Denis *et al.*, 1980). The adsorption of methylene blue by clay minerals makes it possible to measure their hydrophilic surface characteristics and thus evaluates the capacity of these minerals to retain water (*id.*). Furthermore, the fact that methylene blue is not adsorbed by inert minerals (quartz, feldspars, calcite, etc.) makes it possible to characterize the clay fraction of rocks without having to isolate it from the rest of the material (*ibid.*).

The application of the methylene blue test to geotechnical work has merited particular attention, particularly in studies undertaken by the researchers of the Laboratoire des Ponts et Chaussées, who proposed that it be used as a soil classification test in place of the Atterberg limits, in the evaluation of the clay fraction present in rock aggregates, soils, sands, bituminous materials, aggregates for concrete and rocks, as well as a geotechnical parameter in soil classification of road embankments (Lan, 1981; Magnan & Youssefian, 1989).

As a complement to the conventional methylene blue test Lan & Millon-Devigne (1984) proposed a new test procedure (turbidimetric method) in which the titration is evaluated by the light absorbance measured by a spectrophotometer. This test procedure is most usually used to detect the occurrence of small percentages of clay minerals present in materials. An application of the methylene blue test by turbidimetric method can be seen in Jeremias (1991).

The methylene blue tests carried out in this work were performed using the spot method because the rocks analysed have relatively large amounts of clay minerals and also because it is a well established and faster technique.

The laboratory procedure used to determine methylene blue adsorption is shown schematically in Fig. 6.5. About 10 g of sample passed through a #200 ASTM (75 μm) sieve is mixed with 100 ml of distilled water. Once the slurry is homogeneous volumes of 5 cm^3 of methylene blue at a concentration of 10 g/l are added to the soil suspension from a burette. Thirty seconds later after each addition of methylene blue to the soil

suspension a glass rod is used to apply a drop of the slurry to a filter paper for visual examination. The resulting spot comprises a central area with a strong blue colour surrounded by a wet area. The spot test is considered positive when there is a light blue halo around the central area and is negative if this halo is clear. Once the first positive result is obtained the spot test is carried out every minute. The titration ends if the spot test is positive after 5 minutes. In the opposite case, that is if the halo disappears before the fifth spot test, volumes of 2 cm³ of the methylene blue solution are added and the spot test is repeated thereafter every minute. The titration continues until the spot test is positive after five minutes.

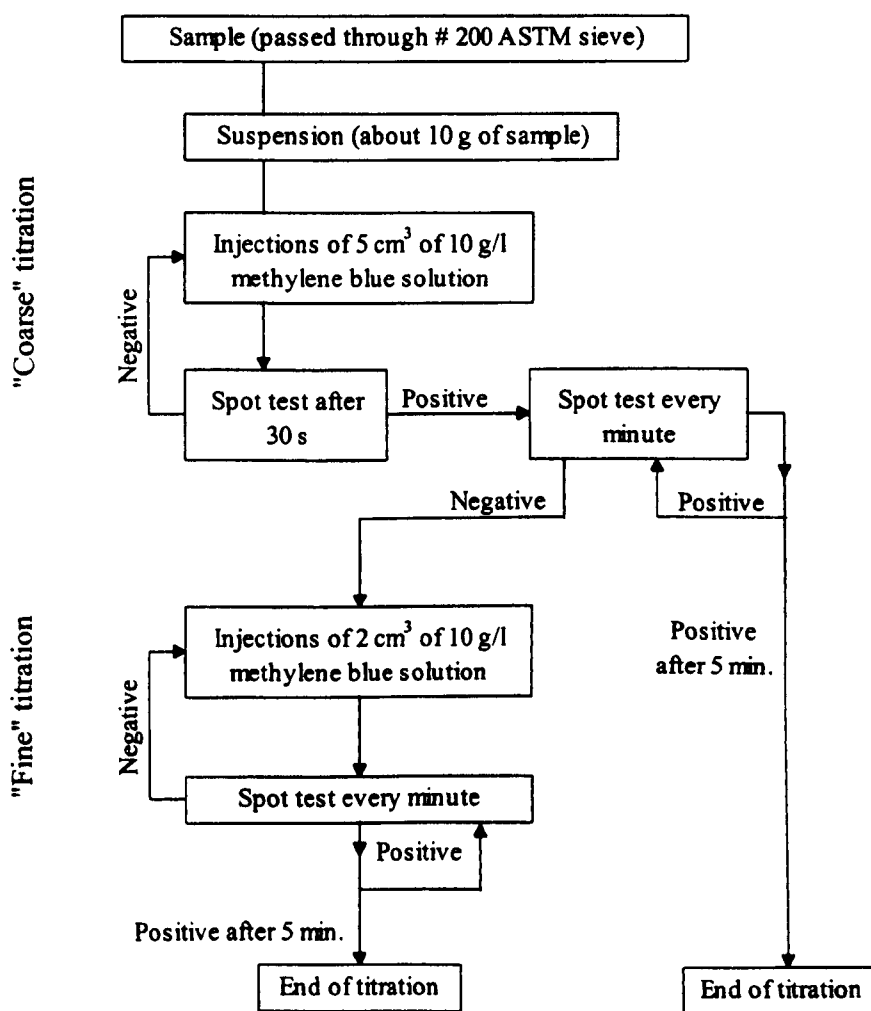


Fig. 6.5 - Flow sheet used in the determination of the methylene blue adsorption.

The methylene blue test by the spot method is easy and fast to perform (depending on the nature and proportion of the clay minerals present it takes 10 to 40 minutes) and

requires no special equipment. The main draw-back of this test is the subjectivity with which the end of the titration is evaluated. This, may introduce operator error quantified as one injection more or less of methylene blue.

The samples were powdered with the fraction retained on the #200 ASTM (75 μm) sieve rejected. The use for testing of the fraction finer than 75 μm is justified by the fact that the clay minerals (evaluated by this test) present in the samples mainly occur within that fraction.

The methylene blue adsorption value (MBA) expressed in grams of methylene blue per 100 g of sample, is calculated according to the following formula:

$$\text{MBA} = \frac{V_t}{10} \quad (6.4)$$

where,

V_t - total volume of methylene blue solution at 10 g/l used in the determination (ml).

Two subsamples from each sample were tested. The average methylene blue adsorption values for each sample are presented in Table 6.1 and in Fig. 6.6.

6.2.6 - Atterberg limits

The fine-grained fraction of the sediments (silt and clay) is adequately characterized by the determination of Atterberg limits being the various types of fine-grained soils classified according to the position of the plasticity index versus liquid limit plot on the Casagrande's plasticity chart. The extension of this methodology, which has a widespread use in classification of soils for engineering purposes, to the characterization of the fine fraction of mudrocks has some limitations due to the difficulties arising from disaggregation of these rocks (see Section 2.4.2.1). However, for soft mudrocks the determination of Atterberg limits is justified because it characterizes the plasticity characteristics and provides a classification of the materials tested in relation to the mineralogy.

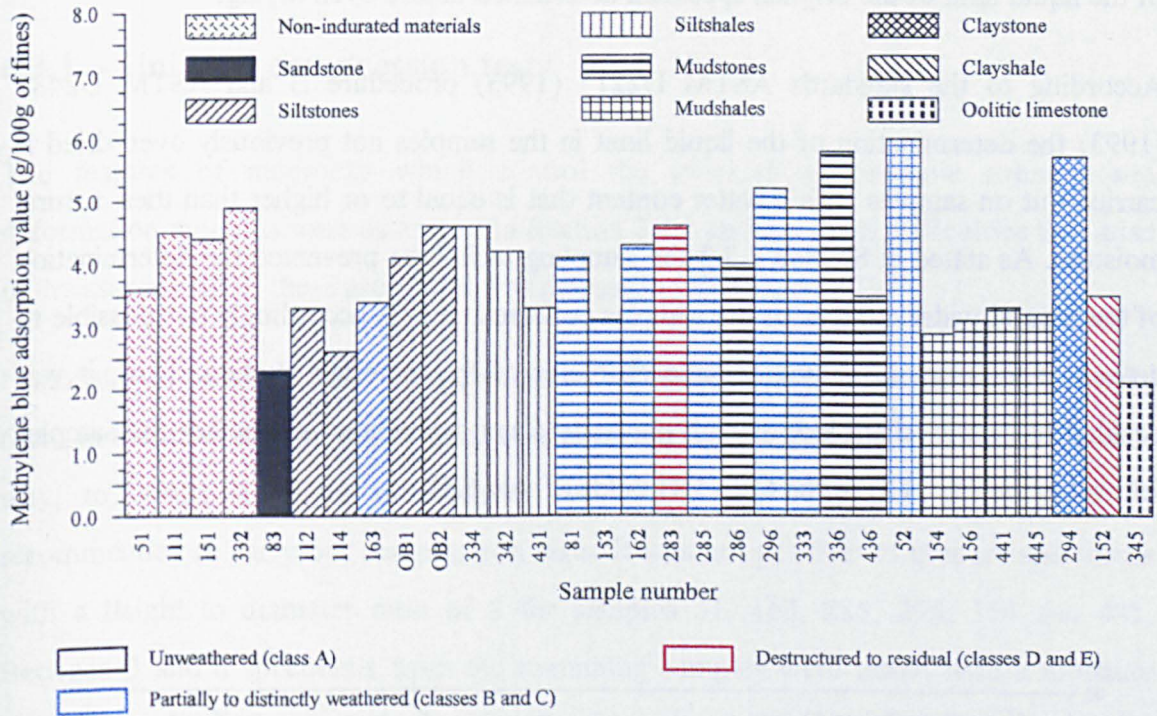


Fig. 6.6 - A comparison of average methylene blue adsorption values of the various samples studied.

The determination of Atterberg limits requires the prior disaggregation of the samples as the tests are carried out on the fraction passing the #40 ASTM (425 μm) sieve in accordance with NP - 143 (1969) standard. The Casagrande liquid limit apparatus was used to determine the liquid limit of samples. As the shrinkage limit is not used in soil classification and is of less interest as a quantitative index in the characterization of the behaviour of mudrocks, it was not determined.

The results obtained for liquid and plastic limits and for the plasticity index are presented in Table 6.1. A plot of Atterberg limits on Casagrande's plasticity chart is shown in Fig. 6.7. Samples 83 (calcareous sandstone), 152 (clayshale), 294 (claystone) and 345 (oolitic limestone) were identified in order to simplify the plot of the various rock types in the plasticity chart.

It was founded from the analysis of Fig. 6.7 that the samples tested fall within groups CL - OL and CH - OH. The group symbols OL and OH are applicable when soils are

organic. A soil is considered organic if the liquid limit after oven drying is less than 75% of the liquid limit of the original specimen determined before oven drying.

According to the standards ASTM D2217 (1993) procedure B and ASTM D2487 (1993) the determination of the liquid limit in the samples not previously oven dried is carried out on samples with a water content that is equal to or higher than their natural moisture. As stated in Section 4.3.3 the sampling technique prevented the determination of the natural water content of the samples collected. It was accordingly not possible to determine the organic or non-organic character of the materials studied. Thus, it was decided to classify them low or high plasticity clays depending on whether the samples fell within the CL - OL or the CH - OH fields (Table 6.1).

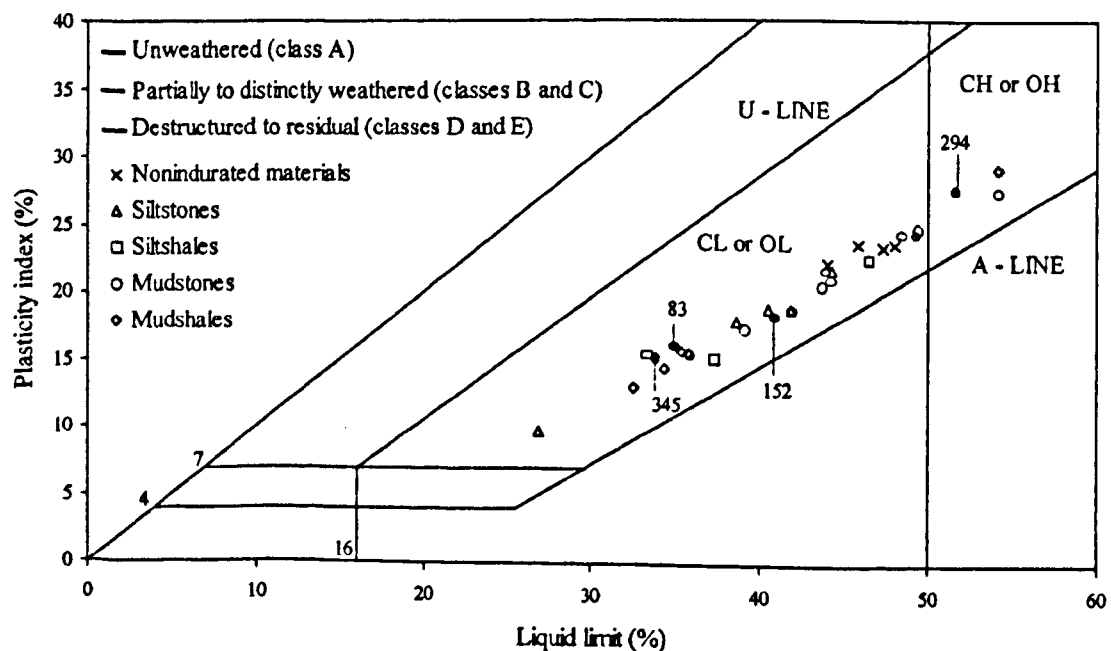


Fig. 6.7 - Casagrande's plasticity chart showing composition of the rocks studied with respect to the soil type.

6.3 - Strength and deformability

6.3.1 - Uniaxial compression tests

The features of mudrocks which control the uniaxial compressive strength and deformation modulus were described in Section 2.4.1 and the main difficulties that arise in the assessment of these properties was discussed in Section 2.4.2.2.

Uniaxial compressive tests were performed on cylindrical specimens approximately 6 cm in diameter and 12 cm in height taken from the rock cores. It was sought, in this way, to ensure a height to diameter ratio of 2, the minimum value generally recommended to carry out compression tests. It was not possible to prepare specimens with a height to diameter ratio of 2 for samples 51, 163, 285, 296, 154 and 441. Between 3 and 6 specimens from the remaining samples were tested with a moisture content resulting from air-drying (in the laboratory). The specimens were loaded practically normal to the bedding/lamination planes which minimized the influence of this feature on the results obtained.

The uniaxial compressive strength results usually show some dispersion. Therefore, it is necessary to repeat the tests on a number of specimens (5 determinations is the minimum recommended by the ISRM, 1979a) in order to provide a more representative result. Difficulties due to the lack of the amount of sample available prevented the testing of a larger number of specimens. The heterogeneity due to weathering and the presence of fractures also contributed to a scatter of the results and biased them towards lower values in some samples, mainly in those collected at shallow depths.

The results obtained for ultimate compressive stress permit classification of the rocks according to their strength. In this study the classes proposed by BS 5930 (1981) presented in Table 3.8 were adopted in the descriptions of the samples (see Fig 3.5 to 3.15). The average uniaxial compressive strength values for the various samples are presented in Fig. 6.8 and in Table 6.2.

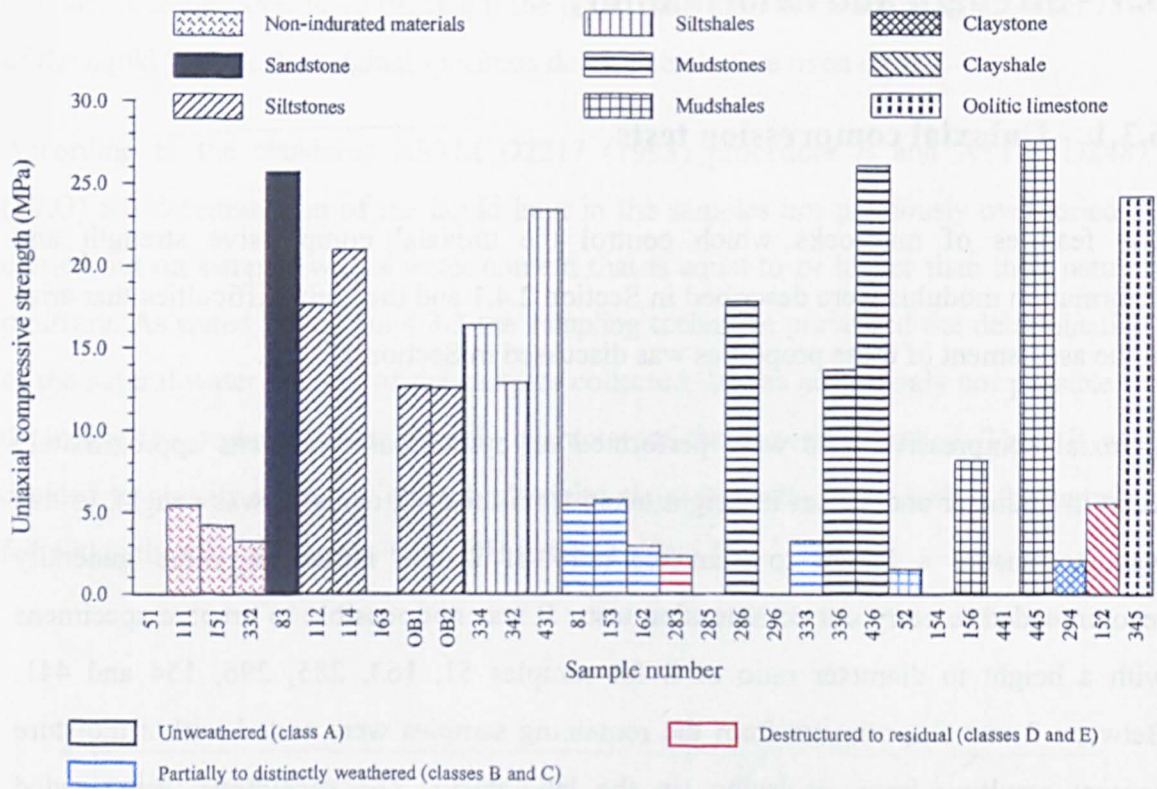


Fig. 6.8 - A comparison of average uniaxial compressive strengths of the various samples studied.

The deformation modulus was determined on a few samples in relation to which it was possible to prepare specimens with dimensions suitable for the measurement of axial strain using the mechanical measuring device represented in Fig. 6.9. The strain measurements between the brass plates previously cemented to the specimen were determined with a micrometer dial gauge reading to 0.001 mm (Fig. 6.9). The brass plates (gauge points) were placed approximately $\frac{1}{2}$ diameter from the top and bottom of the specimen. The distance between the gauge points in the tests varied in the range of 9 to 10 cm.

For each test three cycles of loading and unloading were performed. Axial strains were recorded for stress intervals defined according to the state of weathering of the samples. Accordingly, in the case of the most weathered samples (81, 283 and 332) the axial strains were recorded for a range of 0.1 MPa up to 0.5 MPa. So far as the sound samples were concerned (83, 286, 345 and 431) the axial strains were recorded over the range of 1 MPa up to 5 MPa. The deformation modulus was expressed using the secant

modulus (E_{sec}) calculated from the following equation:

$$E_{sec} = \frac{\Delta\sigma_a}{\Delta\varepsilon_a} \quad (6.5)$$

where,

$\Delta\sigma_a$ - interval between zero stress and maximum axial stress applied (MPa);

$\Delta\varepsilon_a$ - interval between origin or in the case of the 2nd and 3rd loading cycles from non-recoverable strain value measured and axial strain taken at maximum axial stress applied.

Table 6.2 - Strength parameters and secant modulus of the samples studied.

Sample	σ_c (MPa)	E_{sec} (GPa)	$CI_{(0.23)}$	$CI_{(0.635)}$
51	-	-	-	-
52	1.5	-	0.89	0.81
81	5.4	0.59	0.66	0.65
83	25.7	7.69	3.34	3.03
111	5.4	-	0.55	0.59
112	17.6	-	1.64	1.25
114	21.0	-	1.88	1.51
151	4.2	-	0.67	0.51
152	5.5	-	0.81	0.70
153	5.7	-	1.00	0.98
154	-	-	0.80	0.78
156	8.1	-	1.36	1.21
162	2.9	-	0.57	0.58
163	-	-	1.01	0.77
283	2.3	0.09	1.05	0.85
285	-	-	0.88	0.83
286	17.8	1.41	1.48	1.17
294	2.0	-	0.78	0.70
296	-	-	0.63	0.51
332	3.2	0.24	0.60	0.52
333	3.2	-	0.82	0.68
334	16.4	-	1.22	1.03
336	13.6	-	1.06	0.84
342	12.9	-	1.81	1.74
345	24.1	5.98	2.17	2.12
431	23.4	1.17	1.85	1.37
436	26.0	-	2.30	1.51
441	-	-	1.67	1.33
445	27.6	-	2.09	1.63
OB1	12.7	-	1.16	0.93
OB2	12.6	-	1.07	0.89

σ_c - Ultimate compressive stress; E_{sec} - Secant modulus; $CI_{(0.23)}$ and $CI_{(0.635)}$ - Cone indenter numbers measured for steel blade deflections, respectively, of 0.23 and 0.635 mm.



Fig. 6.9 - Apparatus used to measure axial strains (right hand specimen showing brass gauge points and left hand specimen monitoring frame and gauge).

The secant modulus calculated for the first loading cycle differs significantly from those obtained for the second and third loading cycles due to the fact that non-recoverable strains occurred after the first cycle. For this reason the values of the secant modulus presented in Table 6.2 refer to the mean of the modulus calculated for the second and third loading cycles. The secant modulus values of all samples were obtained from a non-significant number of specimens, therefore the results presented are merely indicative. The axial stress - axial strain curves of the various specimens tested are presented in Appendix II.1.

6.3.2 - NCB Cone Indenter tests

The assessment of strength of rock materials through the uniaxial compressive test requires the preparation of specimens. In the case of mudrocks difficulties may arise during this operation. Consequently it is normal to estimate the strength of materials through indirect tests of which the most extensively used is the point load test. However, it was not possible to perform this test on the samples collected because most of them are very weak to moderately weak. Therefore, the strength of rock materials was estimated using the NCB Cone Indenter (see Section 2.4.2.2). The main advantages of this test are the same as the point load test, which are:

- a) irregular samples can be used;
- b) ease and speed of testing which allow running a large number of tests;
- c) the device is portable and so the tests can be performed in the field;
- d) the results can be used to estimate uniaxial compressive strength.

An additional advantage is that very small specimens of rock can be tested. The NCB cone indenter is illustrated diagrammatically in Fig. 6.10. It consists of a steel frame in the centre of which is a steel beam clamped at both ends of the frame. On one side of the frame is a micrometer which has at the end a tungsten carbide indenter whose conical tip has a 40° cone angle. The micrometer is free to rotate on its mounting. On the opposite side of the frame is a dial gauge (readable to 0.01 mm), which measures the deflection of the steel blade.

A rock chip not larger than 12x12x6 mm is placed between the indenter and the steel blade and the micrometer is screwed up until the fragment is just held. Thereafter, the dial gauge is reset to zero and the initial reading of the micrometer is recorded. Then the micrometer is screwed slowly until the spring deflection, as indicated by the dial gauge, is approximately 0.635 mm. Lastly, the final dial gauge reading and the corresponding (final) position of the micrometer are recorded.

Cone indenter tests can be carried out for various steel blade deflection values, which correspond to the application of different forces to the specimen. The standard cone indenter procedure is carried out for a deflection value of 0.635 mm, which corresponds to a force of 40 N. In addition to this standard version, the National Coal Board (1977) also developed a version for soft rocks which uses a deflection of 0.23 mm (12 N) and a version for hard rocks which uses a deflection value of 1.27 mm (110N).

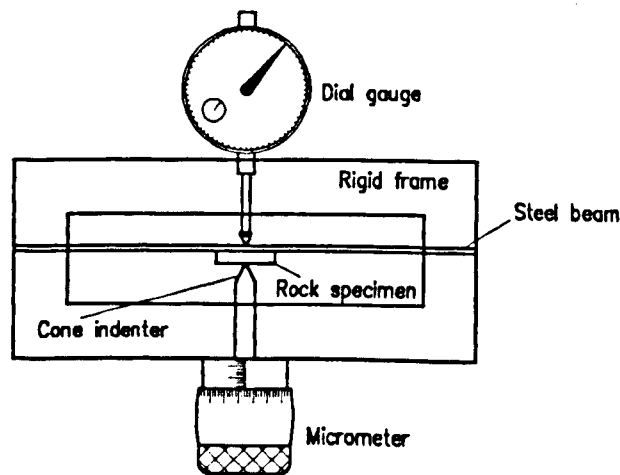


Fig. 6.10 - Diagrammatic illustration of NCB cone indenter (after Stacey et al., 1988).

The cone indenter number - CI - is non-dimensional and expresses a rock hardness which is calculated by:

$$CI = \frac{VD}{(M_f - M_i) - D} \quad (6.6)$$

where,

VD - the steel blade deflection value for which the test is performed, according to the version chosen VD may be equal to 0.23, 0.635 or 1.27 mm;

M_i - initial micrometer reading (mm);

M_f - final micrometer reading (mm);

D - final dial gauge reading (mm).

In this work the cone indenter number was obtained using the standard procedure and the modified procedure for weak rock accordingly with values of VD of 0.635 and 0.23 mm. The use of the latter procedure was justified because the most weathered samples often fractured with standard testing.

The specimens were prepared from rock fragments a few centimetres long using a hammer and chisel in order to obtain rock chips with the required dimensions (12x12x6 mm) for the test. At least 10 specimens of each sample were tested with a moisture content resulting from air-drying (in the laboratory). The 'mean' value of CI was obtained by deleting the highest and lowest values and calculating the mean of the remaining values.

The standard and weak rock CI values are presented in Table 6.2. The results of the former are also shown in Fig. 6.11.

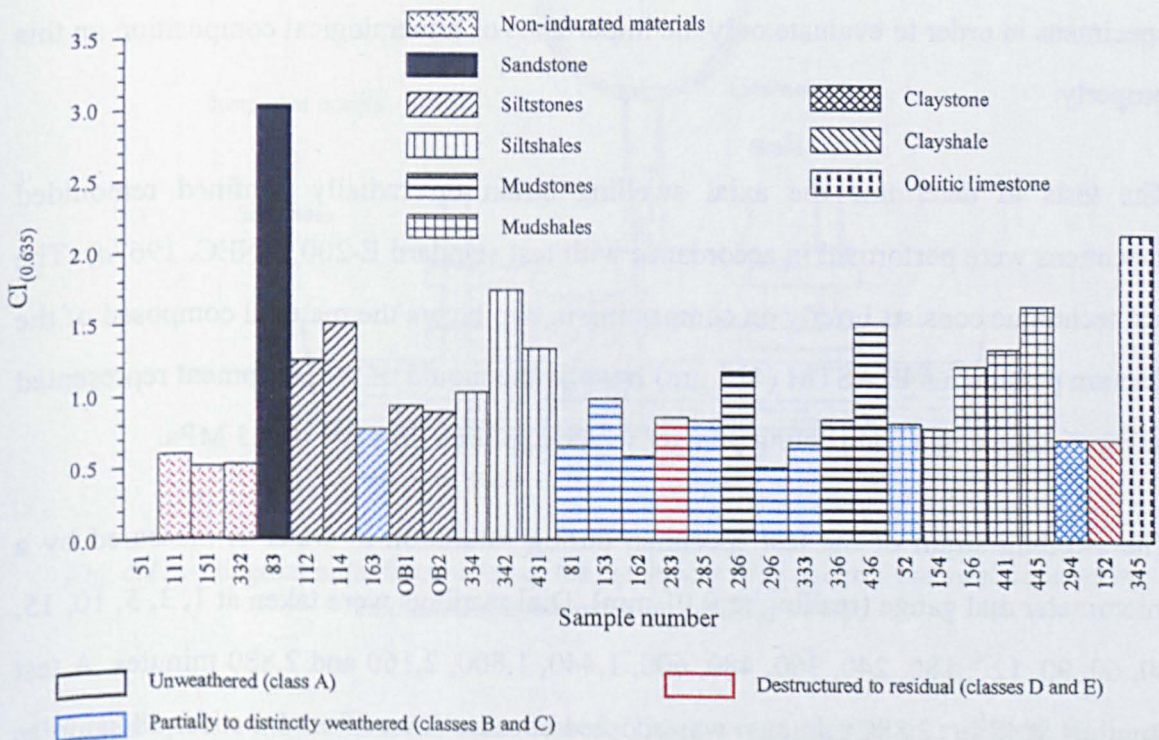


Fig. 6.11 - Relative strength of the rocks studied in terms of cone indenter number (standard procedure).

6.4 - Swelling

6.4.1 - Swelling test performed on a radially confined remoulded specimens

The swelling of mudrocks is caused mainly by the hydration of the clay minerals present in these materials. The swelling mechanisms related to this process were discussed in Section 2.4.1. The tests usually performed to determine swelling are described in Section 2.4.2.3. The swelling of mudrocks can be due, in addition to the mineralogical aspects related to the amount and type of clay minerals present, to textural and structural features such as the occurrence of lamination, degree of cementation, microfissuration, etc. Since the swelling of mudrocks can depend on textural and structural aspects of these rocks it was decided to carry out swelling tests on remoulded specimens in order to evaluate only the importance of mineralogical composition on this property.

The tests to determine the axial swelling strain on radially confined remoulded specimens were performed in accordance with test standard E-200 (LNEC, 1967*d*). The test technique consists briefly on compacting in two layers the material composed of the fraction passing a #40 ASTM (425 μm) sieve in the mould of the equipment represented in Fig. 6.12, using a compacting plunger which applies a pressure of 0.5 MPa.

The swelling strain of the test specimen during saturation in water is measured by a micrometer dial gauge (reading to 0.01 mm). Dial readings were taken at 1, 3, 5, 10, 15, 30, 60, 90, 120, 180, 240, 360, 480, 600, 1,440, 1,800, 2,160 and 2,880 minutes. A test duration of 48 h. (2,880 minutes) was adopted because it was found that for all samples the maximum swelling strain was reached during this period. The swelling strain of the

remoulded specimen (ϵ_s) is given as a percentage by the following formula:

$$\epsilon_s = \frac{\Delta L}{L_0} \times 100 \quad (6.7)$$

where,

ΔL - change in length after swelling (mm);

L_0 - initial length (height of the specimen), which due to the mould used is 15 mm.

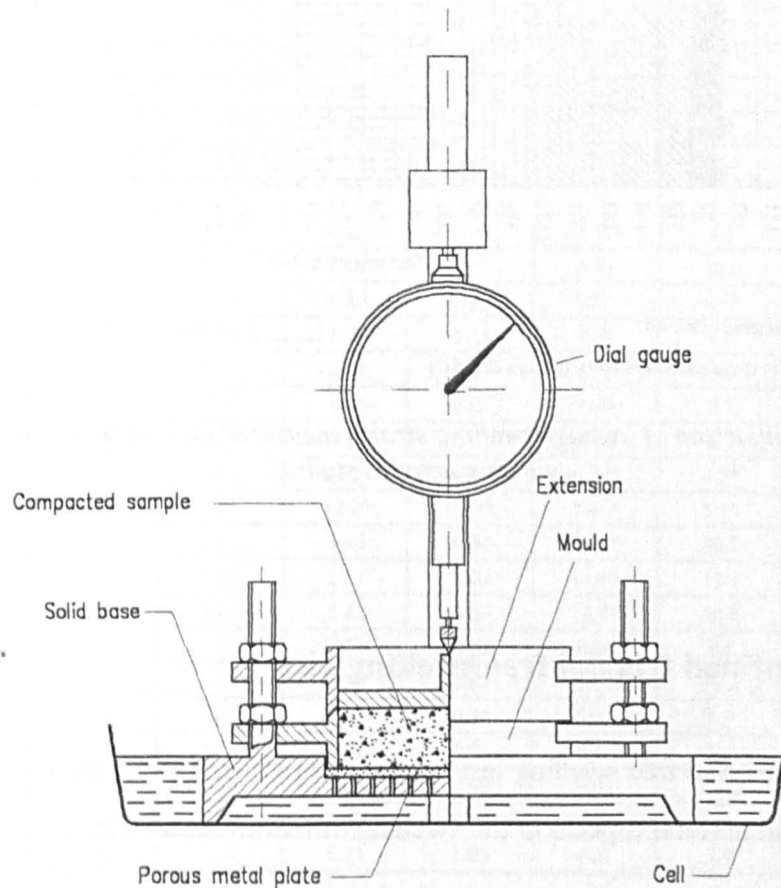


Fig. 6.12 - Diagrammatic illustration of the equipment used to carry out swelling tests on remoulded specimens (after LNEC, 1967d).

Two test specimens per sample were tested. The average results of swelling strain are presented in Fig. 6.13 and in Table 6.3. The plots for swelling strain-time for all samples are present in Appendix II.2.

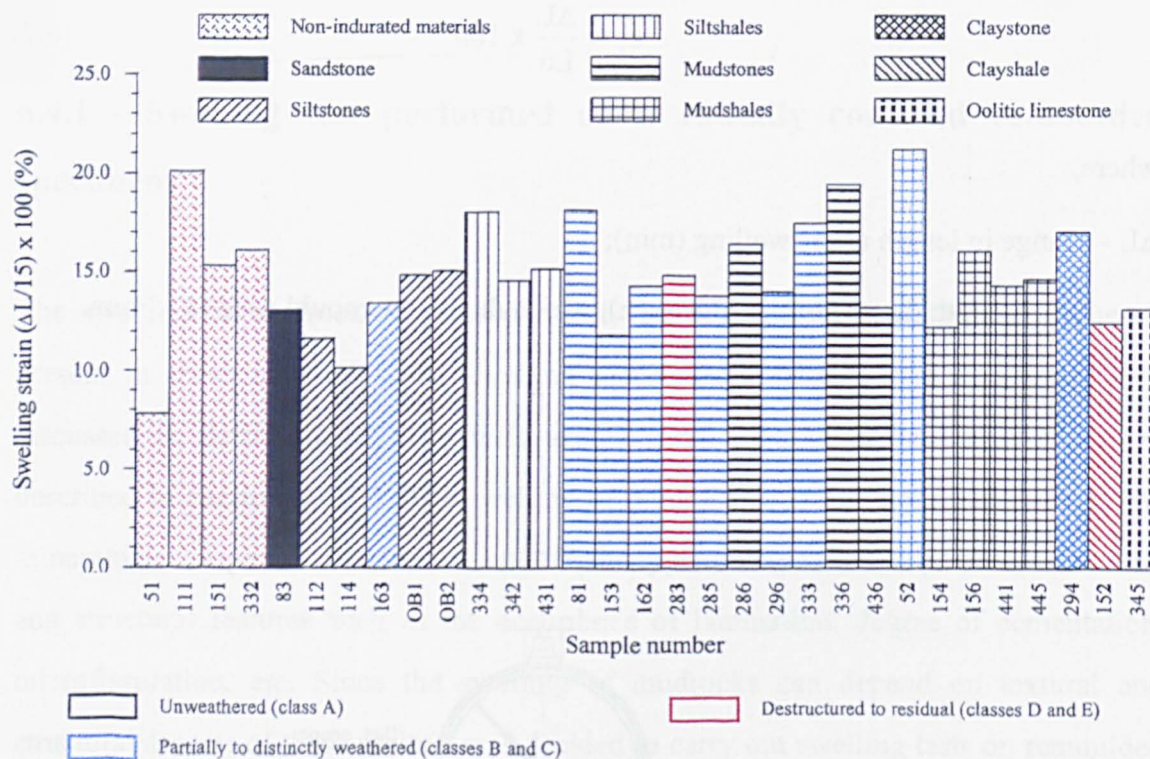


Fig. 6.13 - A comparison of average swelling strains measured on remoulded specimens of the various samples studied.

6.4.2 - Unconfined triaxial free swelling test

The unconfined triaxial free swelling test is intended to characterize the influence of both mineralogical and textural aspects in the swelling of mudrocks studied.

The tests were carried out using an equipment similar to that described by ISRM (1979b) which is illustrated schematically in Fig. 6.14. This equipment allows measurement of the swelling strain of an undisturbed rock specimen along three orthogonal axes. Furthermore, with only a single test it can be evaluated whether the rock behaves in an anisotropic behaviour. The apparatus consists essentially of a cell capable of being filled with water to a level above the top of the specimen, in which three micrometer dial gauge (reading to 0.001 mm) are mounted against the centre of each of the three faces of the test specimen.

Table 6.3 - Swelling tests results.

Sample	ϵ_z (%)	ϵ_x (%)	ϵ_y (%)	ϵ_z (%)	ΔV (%)
51	7.8	.*	.*	.*	.*
52	21.2	1.51	0.99	9.45	12.2
81	18.1	3.42	0.02	7.28	11.0
83	13.0	0.15	0.00	1.57	1.7
111	20.1	0.25	0.09	3.21	3.6
112	11.6	1.28	0.69	1.72	3.7
114	10.1	1.22	0.89	1.97	4.1
151	15.3	2.07*	0.22*	6.34*	8.8*
152	12.4	0.03*	0.00*	8.40*	8.4*
153	11.8	0.59	0.11	4.34	5.1
154	12.2	0.89	0.61	5.99	7.6
156	16.0	0.61	0.03	2.01	2.7
162	14.3	0.28	0.01	7.90	8.2
163	13.4	1.00	0.71	8.71	10.6
283	14.8	0.00*	0.00*	0.71*	0.7*
285	13.8	1.48	1.06	2.07	4.7
286	16.4	0.41	0.19	2.83	3.5
294	17.0	1.44	0.06	1.98	3.5
296	14.0	0.24	0.17	4.31	4.7
332	16.1	0.12*	0.00*	4.22*	4.3*
333	17.5	1.52*	0.15*	3.41*	5.1*
334	18.0	5.95	4.96	16.66	29.7
336	19.4	0.51	0.09	11.61	12.3
342	14.5	4.42	3.69	11.59	20.8
345	13.1	0.21	0.12	0.26	0.6
431	15.1	1.29	0.07	9.16	11.3
436	13.2	1.03	0.54	5.63	7.3
441	14.3	1.51	0.03	5.48	7.1
445	14.6	1.25	0.90	9.92	12.3
OB1	14.8	1.00	0.77	4.59	6.5
OB2	15.0	1.94	1.03	4.81	7.9

ϵ_z - Swelling strain measured on remoulded specimens; ϵ_x and ϵ_y - swelling strain measured on intact specimens parallel to bedding/lamination; ϵ_z - Swelling strain measured on intact specimens perpendicular to bedding/lamination; ΔV - Volumetric strain; * Breakdown of the undisturbed rock specimen during testing.

The mudrock samples were pre-cut cubes of approximately 30 mm side lengths, two faces were parallel to the bedding. The use of regular shaped test specimens allowed the determination of the corresponding volumetric strain after testing. The samples were oven dried at 105°C for 24 h prior to testing and then cooled in a desiccator before being tested.

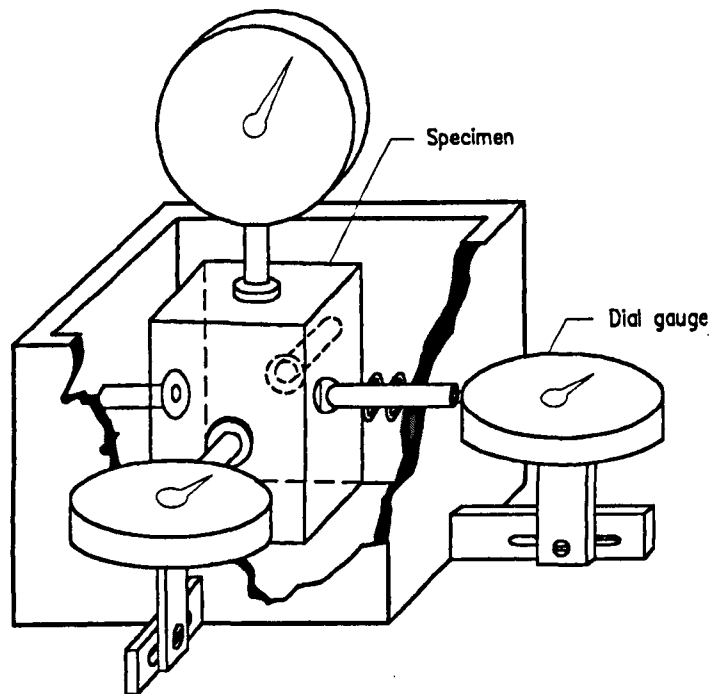


Fig. 6.14 - Diagrammatic illustration of the equipment used to measure swelling strain in three directions (after ISRM, 1979b).

After the cell have been flooded with water dial readings were taken at 1, 2, 3, 4, 5, 10, 15, 20, 30, 45, 60, 90, 120, 150, 180, 240, 360, 480, 600 1,440, 1,800, 2,160 and 2,880 minutes. For the samples in which the expansion was not terminated during 2,880 minutes the tests continued with dial readings taken at an interval of 12 h, until a constant value was reached. Flattening of the swelling strain/time curve indicates when swelling is substantially complete.

The swelling strain along the three axes (ϵ_x , ϵ_y and ϵ_z) was determined as a percentage according to the following formula:

$$\epsilon_{x, y \text{ and } z} = \frac{\Delta L_{(x, y \text{ and } z)}}{L_{0(x, y \text{ and } z)}} \times 100 \quad (6.8)$$

where,

$\Delta L_{(x, y \text{ and } z)}$ - change in length along axes x, y and z after swelling (mm);

$L_{0(x, y \text{ and } z)}$ - initial length of the test specimen along axes x, y and z (mm).

The results obtained for swelling strain along axes x, y and z and for volumetric strain are presented in Table 6.3. The swelling strain values determined perpendicular to bedding and/or lamination for the samples tested are shown in Fig. 6.15. The plots for swelling strain/time along axes x, y and z are presented in Appendix II.2.

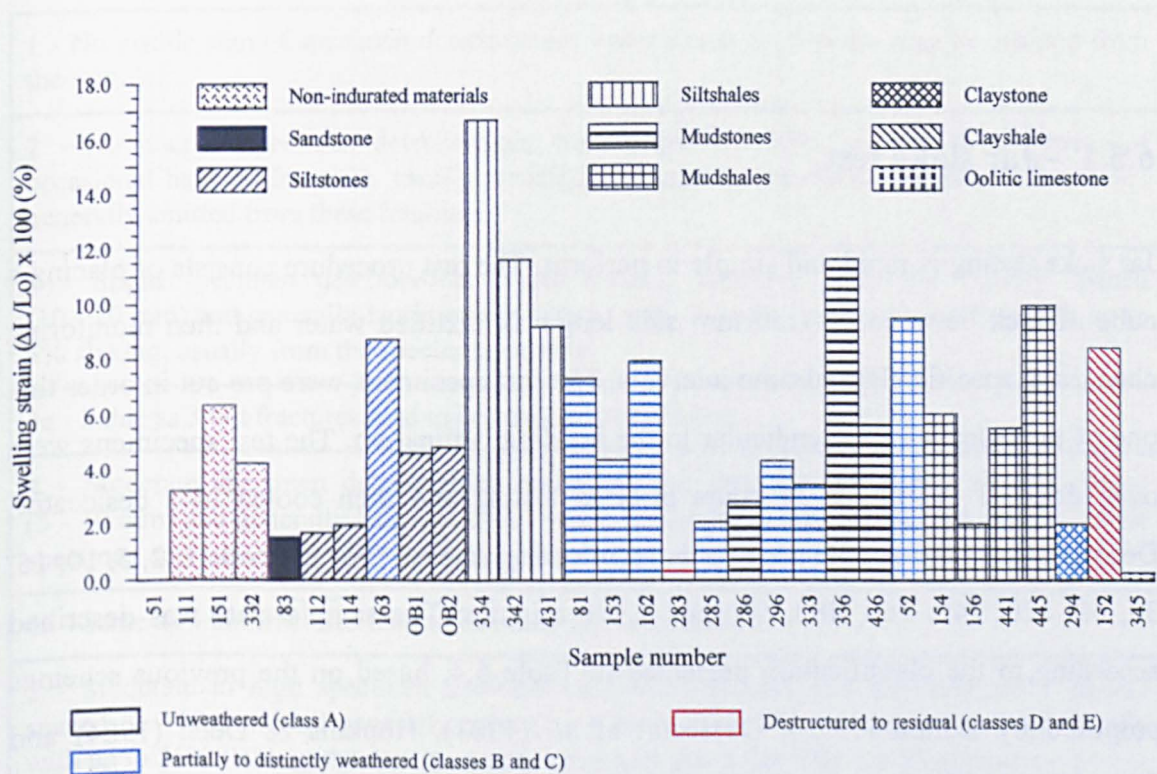


Fig. 6.15 - A comparison of the results obtained for swelling strain as measured in rock specimens perpendicular to bedding/lamination of the various samples studied.

6.5 - Slaking

The assessment of rock durability with respect to the various weathering mechanisms present in nature can be evaluated by ageing tests which seek to simulate in the laboratory the conditions that operate in those mechanisms. This methodology was adopted in this work by carrying out the tests described in Chapter 7. However, as climatic slaking is the main weathering mechanism in mudrocks, this process is usually adopted to evaluate mudrock durability. The main mechanisms that influence slaking were reviewed in Section 2.4.1 and the tests usually performed to evaluate it, in

Section 2.4.2.4. In this study the durability of the mudrocks studied was evaluated by static and dynamic slaking tests. The information obtained from the former - *jar slake test* - is qualitative based on monitoring the breakdown of a fragment of mudrock in water during a specific slaking time while the latter - *slake durability test* - provides a quantitative index.

6.5.1 - Jar slake test

Jar slake testing is rapid and simple to perform. The test procedure consists of placing a cube of rock between 40 - 50 mm side length in distilled water and then monitoring changes at specific elapsed time intervals. The test specimens were pre-cut in order that one of the sides was perpendicular to the bedding/lamination. The test specimens were oven dried at 105°C for 24 hours prior to testing and then cooled in a desiccator. Descriptions of the sample were made at following elapsed time intervals 1, 2, 5, 10, 15, 30, 60, 120, 240, 360, 480, 600 and 1,440 minutes. The sample state was described according to the classification presented in Table 6.4, based on the previous schemes proposed by Lutton (1977), Dusseault *et al.* (1983), Hopkins & Deen (1984) and Czerewko (1997). The classification adopted to describe the sample state has 8 classes, each of which is designated by an index (Ij1 to Ij8). The scheme was designed to evaluate the development of discontinuities over time and the extent of slaking (amount of material separated from the test specimen). The discontinuities were described according to their length, orientation, spacing and aperture.

A test duration of 24 hours (1,440 min.) was adopted because it was found that there were no significant modifications in the sample state after this time. It was also found that in some samples disintegration was rapid within an hour, while in other samples the process was slower with the test specimens showing progressive changes throughout the duration of the test (24 hours). Therefore, the test result given by the index Ij corresponding to the sample state after 24 hours was also designated as fast or slow according to the rate at which slaking proceeded. The results for the jar slake test are presented in Table 6.5, including the overall value and rate.

Table 6.4 - Jar slake classification.

1 - No visible sign of specimen deterioration; water clean; air bubbles may be emitted from the sample.
2 - No notable specimen deterioration; water clean or slight muddy; development of occasional hairline fractures, usually bedding fractures or parallel to bedding; air bubbles generally emitted from these fractures.
3 - Slight specimen deterioration; water muddy; fractures extremely closely spaced (10 - 20 mm) and generally hairline to (≤ 1 mm) open, usually parallel to bedding with up to 5% slaking, usually from the specimen corners.
3a - Same as 3 but fractures tend to be randomly orientated.
4 - Moderate specimen deterioration; water muddy; fractures extremely closely spaced (5 - 10 mm) and generally hairline to (≤ 2 mm) open, usually with up to 10% slaking of the specimen consisting of gravel sized fragments and shards.
4a - Same as 4 but fractures tend to be randomly orientated.
5 - Moderate to high specimen deterioration; water muddy; fractures extremely closely spaced (2 - 10 mm) and generally open (1 - 4 mm), generally parallel to bedding, usually with up to 25% slaking; the specimen may have split into a few free-standing blocks.
5a - Same as 5 but fractures tend to be randomly orientated.
6 - High degree of specimen deterioration, water muddy; fractures extremely closely spaced (2 - 6 mm) and generally open (> 2 mm), usually parallel to bedding with occasional crossed fractures; only a partial specimen shape retained, usually the specimen have split into a few free-standing blocks, with up to 50% of slaking.
7 - Partial to total specimen disintegration; water muddy to quite muddy; the slaked debris generally consists of a pile of angular gravel sized shards or blocky fragments, and occasionally with free-standing fragments of the original specimen block.
8 - Total specimen disintegration; water muddy to quite muddy; disintegration into a pile of soil like debris <i>i.e.</i> high proportion of sub-gravel sized debris and some fine to medium gravel sized fragments

Table 6.5 - Jar slake test results.

Sample	1 min	2 min	5 min	10 min	15 min	30 min	1 h	2 h	4 h	6 h	8 h	24 h	SR
51	Ij6	Ij6	Ij8	Ij8	Ij8	Ij8	Ij8	Ij8	Ij8	Ij8	-	Ij8	Fast
52	Ij2	Ij3	Ij5	Ij6	Ij7	Ij7	Ij7	Ij7	Ij7	Ij7	-	Ij7	Fast
81	Ij3a	Ij3/4a	Ij4/5a	Ij6	Ij8	Ij8	Ij8	Ij8	Ij8	Ij8	Ij8	Ij8	Fast
83	Ij2	Ij2	Ij2	Ij2	Ij2	Ij2	Ij3a	Ij3a	Ij3a	Ij3a	Ij3a	Ij3a	Slow
111	Ij3a	Ij3a	Ij4a	Ij6	Ij8	Ij8	Ij8	Ij8	Ij8	Ij8	Ij8	Ij8	Fast
112	Ij1	Ij1	Ij2	Ij2	Ij2	Ij3a	Ij4a	Ij4a	Ij4/5a	Ij4/5a	Ij4/5a	Ij4/5a	Slow
114	Ij1	Ij1	Ij2	Ij2	Ij2	Ij3a	Ij3a	Ij3a	Ij3a	-	Ij3a	Ij3a	Slow
151	Ij3	Ij3	Ij4	Ij4	Ij5/6	Ij7/8	Ij8	Ij8	Ij8	Ij8	-	Ij8	Fast
152	Ij2	Ij3	Ij3	Ij4	Ij6	Ij7	Ij7	Ij7	Ij7	Ij7	-	Ij7	Fast
153	Ij2	Ij3	Ij3	Ij4/5	Ij4/5	Ij6	Ij6	Ij6	Ij6	Ij6	-	Ij6	Fast
154	Ij2	Ij2	Ij3	Ij3	Ij3	Ij3/4	Ij4	Ij4	Ij4/5	Ij4/5	-	Ij4/5	Slow
156	Ij1	Ij1	Ij1	Ij2	Ij2	Ij2	Ij3	Ij3	Ij3	Ij4	Ij4	Ij4	Slow
162	Ij2	Ij3	Ij3	Ij3	Ij3/4	Ij4/5	Ij7	Ij7/8	Ij7/8	Ij7/8	-	Ij7/8	Fast
163	Ij1	Ij2	Ij3	Ij3/4	Ij4	Ij4/5	Ij5	Ij5	Ij6	Ij6	-	Ij6	Fast
283	Ij3	Ij3	Ij3	Ij3/4	Ij4	Ij5	Ij5/6	Ij6	Ij6	-	-	Ij6	Fast
285	Ij2	Ij3	Ij3	Ij3/4	Ij5	Ij6	Ij6	Ij6	Ij6	-	-	Ij6	Fast
286	Ij1	Ij2	Ij3a	Ij3a	Ij3a	Ij3a	Ij3a	Ij3a	Ij3a	Ij3a	-	Ij3a	Slow
294	Ij3	Ij3	Ij4	Ij5	Ij6	Ij8	Ij8	Ij8	Ij8	Ij8	-	Ij8	Fast
296	Ij3	Ij3	Ij4	Ij6	Ij7	Ij8	Ij8	Ij8	Ij8	Ij8	-	Ij8	Fast
332	Ij3	Ij4	Ij5/6	Ij8	Ij8	Ij8	Ij8	Ij8	Ij8	Ij8	-	Ij8	Fast
333	Ij3	Ij4	Ij5/6	Ij8	Ij8	Ij8	Ij8	Ij8	Ij8	Ij8	-	Ij8	Fast
334	Ij2	Ij2	Ij3	Ij3	Ij3/4	Ij4	Ij6	Ij6	Ij6	Ij6	-	Ij6	Slow
336	Ij2/3	Ij2/3	Ij3	Ij4/5	Ij4/5	Ij5/6	Ij7	Ij7	Ij7	Ij7	Ij7	Ij7	Fast
342	Ij1	Ij1	Ij1	Ij1	Ij1	Ij1	Ij1	Ij1	Ij1	Ij1	Ij1	Ij1	Slow
345	Ij1	Ij1	Ij1	Ij1	Ij1	Ij2	Ij3	Ij3	Ij3	Ij3	Ij3	Ij3	Slow
431	Ij2	Ij2	Ij3	Ij3	Ij3	Ij3/4	Ij4	Ij4	Ij4/5	-	Ij4/5 (7h)	Ij4/5	Slow
436	Ij1	Ij1	Ij2	Ij2	Ij3	Ij3	Ij4	Ij4/5	Ij4/5	-	Ij4/5 (7h)	Ij4/5	Slow
441	Ij1	Ij2	Ij2	Ij2	Ij2	Ij3	Ij3	Ij3/4	Ij4	Ij4	Ij4/5	Ij4/5	Slow
445	Ij1	Ij1	Ij1	Ij1	Ij1	Ij1	Ij1	Ij2	Ij2	Ij2	-	Ij3	Slow
OB1	Ij1	Ij2	Ij3	Ij3	Ij3	Ij3/4	Ij4	Ij4/5	Ij5	Ij5	-	Ij5	Slow
OB2	Ij1	Ij3	Ij3	Ij3	Ij3	Ij4/5	Ij5	Ij5	Ij5	Ij5	-	Ij5	Slow

SR - Slaking rate. Ij1 Ij3 Ij4 Ij4/5 Ij5 Ij6 Ij7 Ij7/8 Ij8

6.5.2 - Slake durability test

The slake durability tests were performed using an apparatus similar to that described in ISRM (1979b). It was found that the standard test procedure was too insensitive for the mudrocks studied and therefore the procedure was modified. This involved in addition to the two cycles performed in standard conditions (200 + 200 rotations of the apparatus with samples immersed), the execution of a third cycle of wetting and drying in which the slaking time was increased (600 rotations of the apparatus with samples immersed). The slaking time was increased mainly with the purpose of improving the differentiation between medium to low durability materials. Low results were obtained for some samples after the three cycles, which previously had relatively high percentages of

material retained in the test drum at the end of the second cycle.

The samples were prepared in order to have ten rock lumps, each with a mass of 40-60 g, preferably equi-dimensional shaped and with the corners rounded. In relation to the preparation of thinly bedding or laminated samples difficulties arose because the lumps fractured along these planes. Therefore, it was often impossible to obtain equi-dimensional shaped fragments with the mass required for testing (40 to 60 g) but rather an approximately elongated shaped lump.

A further modification to the standard procedure was introduced in order to evaluate the extent of breakdown of the material. The fraction retained in the drum mesh (larger than 2 mm) at the end of the three cycles was described in accordance with the scheme presented in Table 6.6 and the fraction smaller than 2 mm was characterized by grain-size analyses (sieving and sedimentation). According to this scheme, sample debris are described in terms of the amount of breakdown of the material after testing as well as in terms of their final shape.

Table 6.6 - Descriptive scheme of the material retained in drum mesh during the slake durability test.

A - Description of breakdown of retained fraction after testing (I _{d5} - 1000 rotations)	A.1 - <u>Minor breakdown</u> - Less than 25% of the fragments have been reduced in size by half of their initial size (approximately between 30 to 40 mm)
	A.2 - <u>Moderate breakdown</u> - Approximately 25% to 50% of the fragments are reduced to up to half their initial size.
	A.3 - <u>High breakdown</u> - More than half of the fragments have been reduced by more than 50% of their initial size.
	A.4 - <u>Extremely high breakdown</u> - At least 75% of the fragments, either undergone total disintegration or the initial size of the lumps have been reduced to a clast size of between 5 to 15 mm.
B - Description of fragment shapes after testing (I _{d5} - 1000 rotations)	B.1 - <u>Rounded</u> - The fragments retained a relatively equant shape.
	B.2 - <u>Almond shaped</u> - The fragments usually have a flattened surface.
	B.3 - <u>Platy</u> - The fragments may have angular or rounded edges.

The slake durability index is calculated by dividing the weight of the sample retained by the 2 mm mesh by its original weight and expressing the result as a percentage. The slake durability index (I_{d2}) in the standard procedure is given for the second cycle. This is because the first cycle slake durability index (I_{d1}) is more influenced by the initial form of the fragments, so the results show significant scatter.

The I_{d1} (200 rotations), I_{d2} (400 rotations) and I_{d5} (1,000 rotations) slake durability indexes, the description of the material retained in the drum at the end of the test (after 1,000 rotations) and the durability classification according to the classes proposed by Dick *et al.* (1994) are presented in Table 6.7.

Table 6.7 - Results of slake durability test and mudrock durability classification.

Sample	I_{d1} (%)	I_{d2} (%)	I_{d5} (%)	Description ¹	Durability ²
51	21.4	11.3	0.0	*	Low
52	43.9	14.7	0.1	A4, B3	Low
81	50.5	8.3	0.7	A4, B3	Low
83	98.2	96.3	91.9	A1, B1	High
111	64.3	38.3	8.7	A4, B2/B3	Low
112	92.7	85.6	66.9	A2, B2/B3	High
114	94.9	90.6	77.6	A1, B1	High
151	55.6	17.1	1.9	A4, B2/B3	Low
152	65.7	18.5	1.2	A4, B2/B3	Low
153	67.1	42.8	7.9	A4, B2/B3	Low
154	88.6	74.5	28.9	A3, B2/B3	Medium
156	92.6	84.0	60.8	A2, B2/B3	Medium
162	73.5	49.5	17.3	A3, B2	Low
163	86.4	68.7	43.7	A3, B2	Medium
283	69.2	48.5	17.0	A3, B2	Low
285	79.3	59.2	25.3	A3, B1/B2	Medium
286	95.7	92.3	82.4	A1, B1	High
294	67.3	2.5	0.2	*	Low
296	74.5	49.1	27.6	A3, B2	Low
332	39.4	23.8	2.9	A4, B2/B3	Low
333	34.7	4.1	0.0	*	Low
334	81.4	44.2	4.0	A4, B3	Low
336	76.9	42.3	12.5	A4, B2	Low
342	62.8	34.3	26.5	A3, B2	Low
345	89.1	74.5	62.4	A2, B1	Medium
431	93.8	84.2	66.0	A2, B3	Medium
436	97.0	90.7	74.5	A2, B3	High
441	90.3	79.7	54.4	A2, B2/B3	Medium
445	96.5	92.7	82.8	A2, B2/B3	High
OB1	89.7	81.3	58.1	A2, B1	Medium
OB2	91.0	83.1	62.4	A2, B1	Medium

I_{d1} , I_{d2} e I_{d5} - Percentages of retained material, respectively, after 200, 400 and 1,000 rotations; * - Without retained material in the mesh drum at the end of test; ¹Description of retained material in the mesh drum according to the classification presented in Table 6.6; ²Assessment of mudrock durability according to the classification proposed by Dick *et al.* (1994); Highlight samples for differences between I_{d2} and I_{d5} greater than 20%.

According to this classification the durability of materials may be low, medium or high, depending on whether the values for the I_{d2} index are lower than 50%, between 50 and 85%, or greater than 85% (see Section 3.3.2). Although the designation I_{d5} should be only applied to 5 separate cycles of drying and wetting of 200 rotations each, it was adopted to designate the percentage in weight of the material retained during the third cycle performed in accordance with the procedure adopted in this study, because for these test conditions the samples were also subjected to a total of 1,000 rotations.

The results of I_{d2} and I_{d5} indexes for the various samples are presented accordingly in Fig. 6.16 and Fig. 6.17. The particle size distribution plots for the fraction smaller than 2 mm and the photographic record of the fragments retained in the drum at the end of the test for all samples are presented in Appendix II.3.

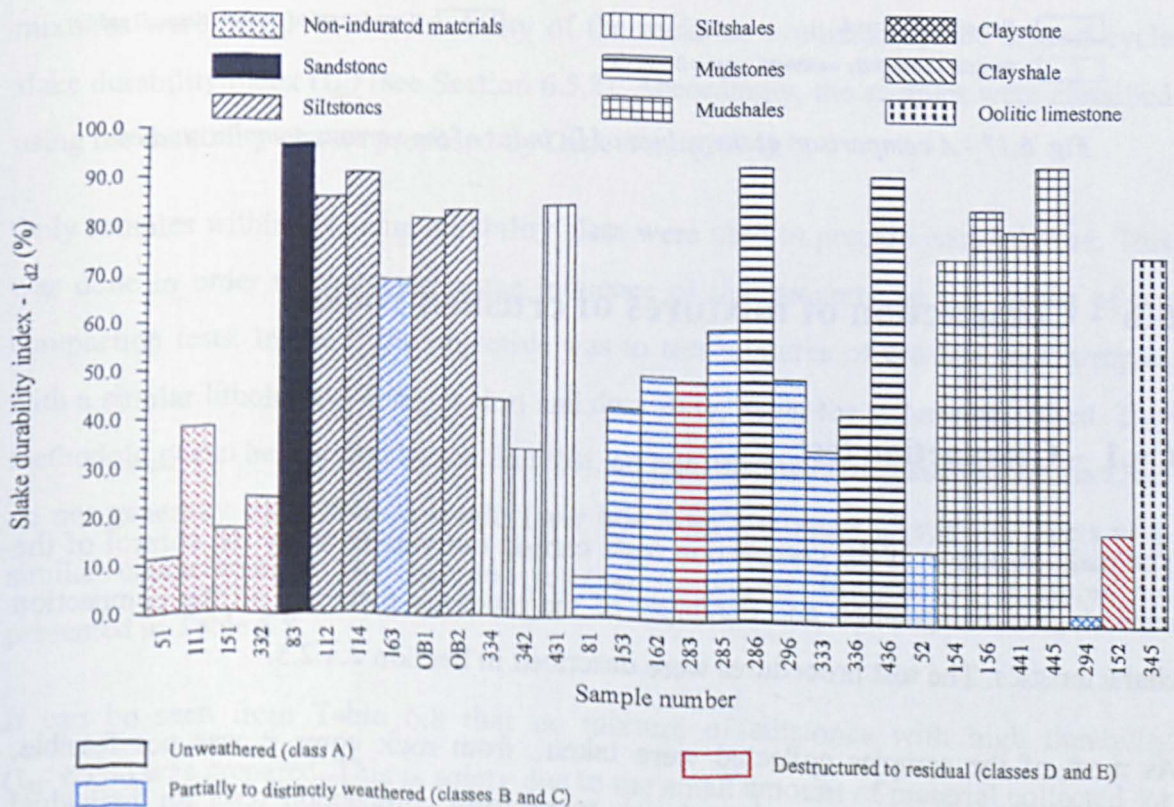


Fig. 6.16 - A comparison of the values of I_{d2} index of the various samples studied.

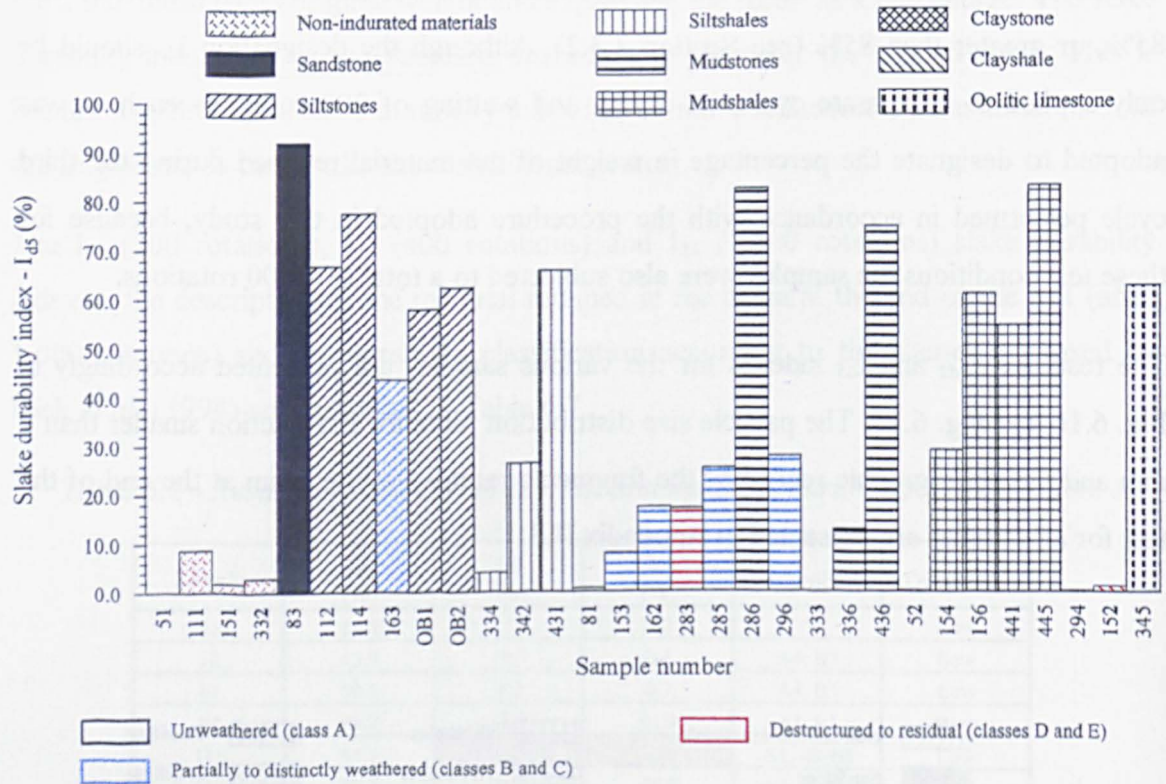


Fig. 6.17 - A comparison of the values of I_{d5} index of the various samples studied.

6.6 - Compaction of mixtures of crushed rocks

6.6.1 - Compaction test

The main objective of the compaction tests carried out was to study the control of the mineralogical composition and durability of the mudrock materials on the compaction characteristics. The test procedures were described in Section 2.4.2.5.

As most of the samples collected were taken from rock cores it was not feasible, because there were not enough material, to perform compaction tests for individual samples. The solution adopted to overcome this difficulty was to carry out some tests on composite samples consisting of mixtures of different samples. Sample OB2 (designated as S2 in the compaction tests) was collected from a block providing enough amount of

material to carry out an individual compaction test. Therefore, it was decided not to mix it with other samples.

The selection of the components of the various mixtures was on the basis of the similarity in composition and durability of the materials. The mixtures were prepared, in general, using siltstones or mudstones because these are the predominant rock types in sampling. Sample 83 (designated as A1 in the compaction tests) is the only sample that had a sandy composition, which justifies its compaction characteristics being determined and that it be tested without being mixed with other samples, despite the fact that the amount of this material was only enough to prepare two test specimens. Although the testing of mixtures of claystones/clayshales would have been of great interest, the small amount available (samples 152 and 294) precluded compaction tests being performed on these materials.

The other criteria adopted in the selection of the samples for the preparation of the mixtures were based on the durability of the rocks as evaluated by the second cycle slake durability index (I_{d2}) (see Section 6.5.2). Accordingly, the samples were classified using the durability classes proposed by Dick *et al.* (1994).

Only samples within the same durability class were used to prepare each mixture. This was done in order to characterize the influence of this property on the results of the compaction tests. In short, the objective was to test mixtures of crushed rock samples with a similar lithological composition and durability, using the criteria described. This methodology can be justified by the fact that, on site, the materials used to construct fills do not generally come from a single layer but from a mixture of various layers with similar characteristics. The samples selected to prepare the various mixtures are presented in Table 6.8.

It can be seen from Table 6.8 that no mixture of siltstones with high durability ($I_{d2} > 85\%$) was prepared. This is solely due to the small amount of material collected for samples 112 and 114, which prevented to undertake compaction tests. Mixture SA2 of samples 154, 156 and 441 only provided enough material to test two test specimens.

The rock samples selected were crushed prior to testing. The tests were carried out on the fraction passing #4 ASTM (4,76 mm) sieve. Thereafter, the mixtures were

homogenised and split into four fractions, each one with enough material to prepare a test specimen.

Table 6.8 - Samples used to make the mixtures tested.

Mixture tested	Samples	Lithological composition	I _{d2} Value
S1	334 and 342	Siltshale	< 50%
SA1	153, 162, and 283	Mudstone and mudshale	<50%
S2	OB2	Siltstone	50 - 85%
SA2	154, 156 and 441	Mudshale	50 - 85%
A1	83	Sandstone	> 85%
SA3	286, 436 and 445	Mudstone and mudshale	> 85%

The compaction tests were carried out in accordance with test standard E-197 (LNEC, 1967b). The method using 4.54 kg rammer (modified Proctor) and small mould was adopted. The small mould was selected because of the limitations on the quantity of material available, while modified Proctor compaction effort was chosen for these tests because it is the one that best simulates the compaction conditions generally present on earthworks.

The use of the small mould in the compaction tests meant that the percentage of material retained on #4 ASTM (4.76 mm) sieve should be less than 20%. Since the samples tested were prepared by crushing rock material, the percentage of material larger than 4.76 mm would be arbitrary and would not reflect the size range in the natural soil. Therefore, the fraction retained on the #4 ASTM (4.76 mm) sieve was crushed so that all the particles used in the preparation of the mixtures were smaller than 4.76 mm.

The test procedure for the compaction effort and mould selected consists of making test specimens comprised five layers, each of which was compacted by 25 blows with a 4.54 kg rammer free-falling 457 mm. The mass of the test specimen was determined in order to calculate dry density using a balance readable to 1 g. The water content of compacted material was obtained using a balance accurate to 0.01g. In addition to the compaction tests, grain size analyses by sieving and sedimentation of the materials which composed the mixtures (before testing) were undertaken.

The results for the compaction tests are presented in Table 6.9. The compaction curves and particle size distribution plots are presented in Appendix II.4.

Table 6.9 - Results of the compaction tests and of CBR plunger penetration tests.

Mixture	γ_{dmax} (kN.m ⁻³)	w_{opt} (%)	Evaluation with a CBR plunger of the forces corresponding to penetrations on samples of 10 and 25 mm				
			Deviation from w_{opt} before soaking (%)	Deviation from w_{opt} after soaking (%)	Δw_{96h} (%)	$F_{CBR(10\text{ mm})}$ (kN)	$F_{CBR(25\text{ mm})}$ (kN)
S1	19.5	12.1	-4.4	4.4	8.8	0.8	2.2
			-1.3	3.3	4.4	1.4	4.6
			+1.1	2.7	1.6	2.3	5.6
			+3.1	4.1	1.0	2.3	4.4
SA1	19.1	12.4	-2.6	2.7	5.2	0.7	2.2
			-0.4	5.3	5.7	1.1	2.7
			+1.9	4.1	2.2	1.9	4.4
			+4.9	5.5	0.6	1.8	3.4
S2	19.9	11.5	+6.6	7.5	0.9	1.1	1.9
			-3.0	3.2	6.2	2.6	6.7
			-1.0	2.0	3.0	3.6	9.8
			+1.0	2.0	1.0	4.1	10.5
SA2	19.8	11.2	+2.9	3.4	0.5	3.2	6.0
			-0.6	2.4	3.0	2.6	7.5
			+2.4	3.4	1.0	3.1	6.7
			-0.3	0.6	0.9	-	-
A1	21.2	8.8	+2.3	5.0	2.7	6.5	-
			-4.0	3.2	7.2	1.4	4.9
SA3	20.4	11.1	-1.6	2.1	3.7	2.5	7.9
			+0.7	3.7	1.4	3.6	8.9
			+3.1	+3.1	0.6	2.9	5.7
			-4.0	3.2	7.2	1.4	4.9

γ_{dmax} - Maximum dry density; w_{opt} - Optimum moisture content; Δw_{96h} - Water content increment after soaking during 96 h;
 $F_{CBR(10\text{ mm})}$ - Force corresponding to a penetration of 10 mm; $F_{CBR(25\text{ mm})}$ - Force corresponding to a penetration of 25 mm.

6.6.2 - Evaluation of the strength of compacted mixtures of crushed rocks to penetration of a 'CBR plunger'

CBR plunger penetration tests were carried out in order to evaluate the behaviour of the various compacted mixtures of crushed rocks on the basis of a strength criterion. The test procedure adopted is basically a modified version of the CBR standard test [standard E-198 (LNEC, 1967c)]. However, this designation is not used because the tests were carried out on test specimens with different dimensions than those required by the CBR standard test. The test specimens used in the CBR standard test are

compacted in a large mould, which, due to the lack of material, could not be adopted in the compaction tests carried out (see Section 6.6.1).

The test procedure used consisted of soaking the mixtures resulting from the compaction tests for 96 h and, thereafter, the determination of the forces required for a cylindrical plunger of a standard cross-sectional area (CBR plunger) to penetrate the test specimens to a specific depth at a given rate. In the CBR standard test, surcharge discs are fitted to the test specimens during the soaking with the objective of simulating the pressure caused by the weight of the road pavement. As the tests carried out in this work were not intended to have a specific application, surcharge discs of approximately 5 kg, the minimum recommended in the standard, were applied during soaking to all test specimens.

According to the penetration test procedure (*id.*), the test specimens were tested using a load frame capable of applying a rate of penetration of the plunger of 1 mm/min. The total penetration value (12.5 mm) usually adopted in CBR standard procedure was increased so that the behaviour of the various test specimens of each sample could be identified more clearly. The tests were accordingly carried out to a maximum penetration of 25 mm. Readings of the forces were recorded at the following penetrations 0.5, 1.0, 1.5, 2.0, 2.5, 3.0, 4.0, 5.0, 6.0, 7.5, 10.0, 12.5, 15.0, 17.5, 20.0 22.5 and 25.0 mm. The water content of the test specimens was determined after each test using a balance readable to 0.01g. The equipment used during this phase of the tests is shown in Fig. 6.18.

The forces recorded for penetrations of 10.0 and 25.0 mm and the water content values before and after soaking are presented in Table 6.9. The force-penetration plots for all test specimens are presented in Appendix II.4.

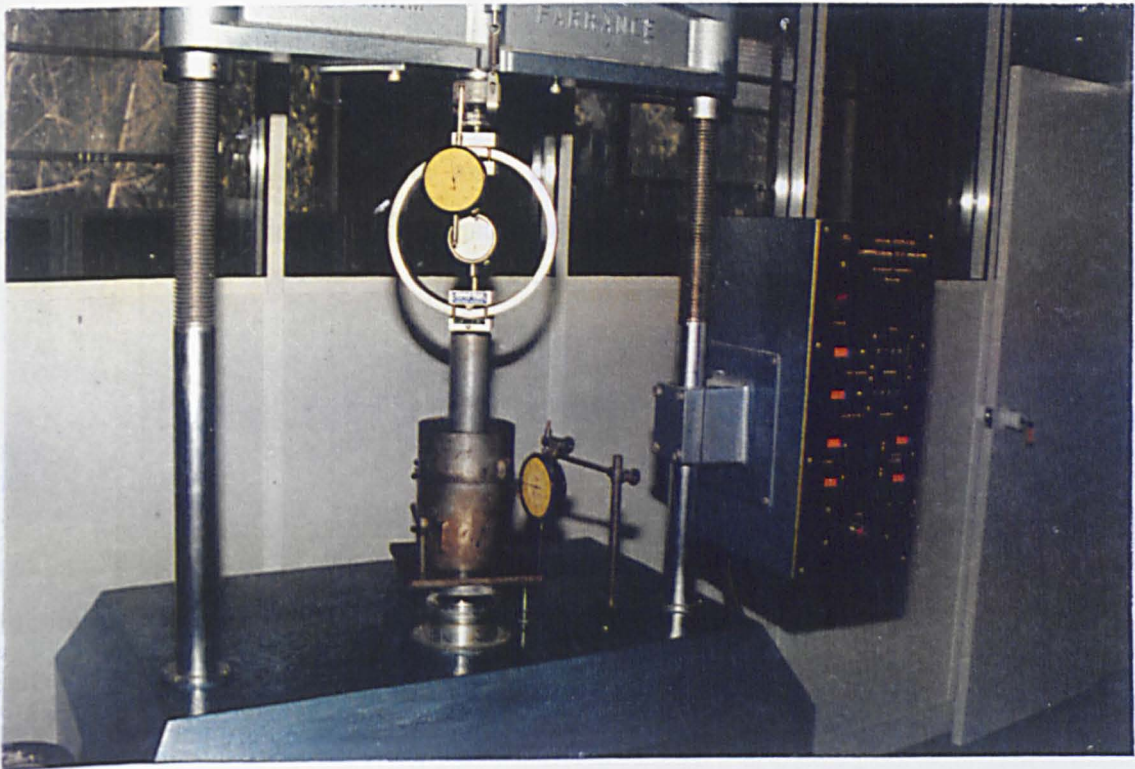


Fig. 6.18 - Apparatus used during the stage of penetration of a 'CBR plunger'.

6.7 - Discussion of results

The correlation of the geotechnical properties of the mudrocks studied with their mineralogical and textural characteristics will be discussed, in detail, in Chapter 8. In this section an integrated analysis of the results obtained in the various tests carried out, in order to obtain additional information regarding these materials and to investigate which parameters are most suited to characterize them is presented.

The tests carried out led to a large amount of data. However, it is important to emphasize that given the limited amount of sample material available, it was not possible to use the recommended number of samples for some tests. This was particularly the case in the uniaxial compression and compaction tests, the latter being carried out using mixtures of samples. In addition, the results obtained were also affected by the heterogeneity of some samples, due to fracturing, textural and mineralogical variations as well as weathering zonation. It is considered, however, that

although this reduced the statistical significance of the results obtained, the main conclusions are not significantly affected.

In research studies concerning rock materials, the determination of relationships between the various parameters obtained in tests is extremely important for the assessment of their behaviour. The most significant relationships determined in this study are presented in the following paragraphs.

a) Correlations with porosity

The samples studied have an effective porosity of between 11.7 and 33.9%. This extremely wide range is a reflection of the presence in sampling of non-indurated materials and rocks with different states of weathering. It can be seen from Fig. 6.3 that the highest porosity values correspond to non-indurated materials (samples 51, 111, 151 and 332) and to partially weathered or destructured rocks (samples 52, 81, 152, 153, 162, 163, 283, 285, 294, 296, 333).

Fig. 6.19 presents the relation between porosity and uniaxial compressive strength (UCS) in which there is a band that reflects a direct relationship between the two parameters which include most of the samples tested. Samples 83, 111, 152 and OB2 had UCS values higher than would have been expected on the basis of their porosity. Sample 83 is a sandstone and therefore does not fit in to the relationship established for the mudrocks studied. Sample OB2 was collected from a different formation in which the materials are significantly more porous than those collected in the Arruda area. Samples 111 and 152 have rather high UCS values. As these are weathered materials and there are only a limited number of tests, the high UCS values may be a consequence of variations in the composition and/or weathering state of the specimens tested. The UCS results of sample 156 (laminated) were affected by the presence of some fractures in the test specimens, which explains the low values obtained.

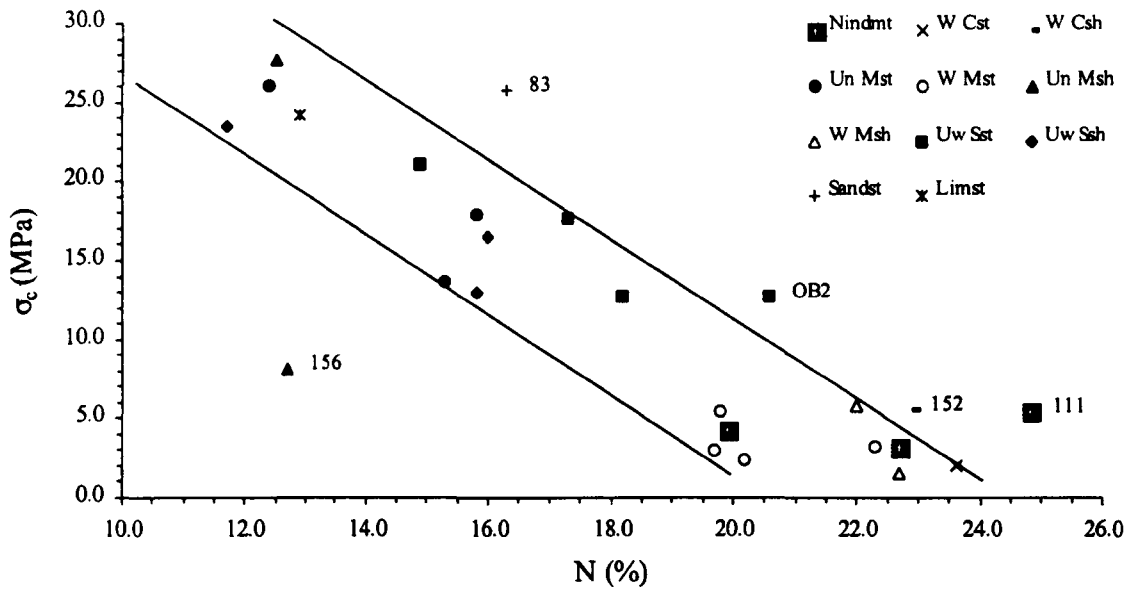


Fig. 6.19 - Relationship between uniaxial compressive strength (σ_c) and porosity (N).

b) Correlations with the methylene blue adsorption value

The importance and nature of the clay fraction present in the materials studied were characterized on the basis of the results of methylene blue adsorption value (MBA), plasticity index (PI), swelling strain determined on radially confined remoulded specimens (ϵ_s) and partially on water adsorption at 95%RH (w_{ad95}). Figs. 5.22 to 5.24 presents the relations obtained between the methylene blue adsorption and the other parameters. These figures also contain bands, which seek to show the relationships between the parameters.

Although the water absorption at 95%RH is mainly controlled by the clay mineralogy of the materials, the results of the tests undertaken may also reflect the textural and structural aspects of the samples, because rock lumps were used. The methylene blue adsorption, swelling and Atterberg limits were carried out on powdered samples and thus they reflect only the mineralogical characteristics of the materials, *i.e.* the proportion and type of clay minerals present.

Fig. 6.20 shows the relationship determined for most samples between the methylene blue adsorption and water adsorption at 95%RH. The plot of samples 154, 296, 336 and 342 outside of the band may be explained on the basis of the aspects referred to before. The relatively high w_{ad95} value of sample 154 is a consequence of its laminated structure comprising layers of clay minerals and of organic matter. In the case of samples 296 and 336, the high percentage of mixed-layer clay explains the relative high methylene blue adsorption results obtained for these materials. Sample 342 is a siltshale and thus does not have a high clay mineral content. However, expansive clay minerals (including smectite) constitute more than 50% of the clay fraction total, which explains the result obtained.

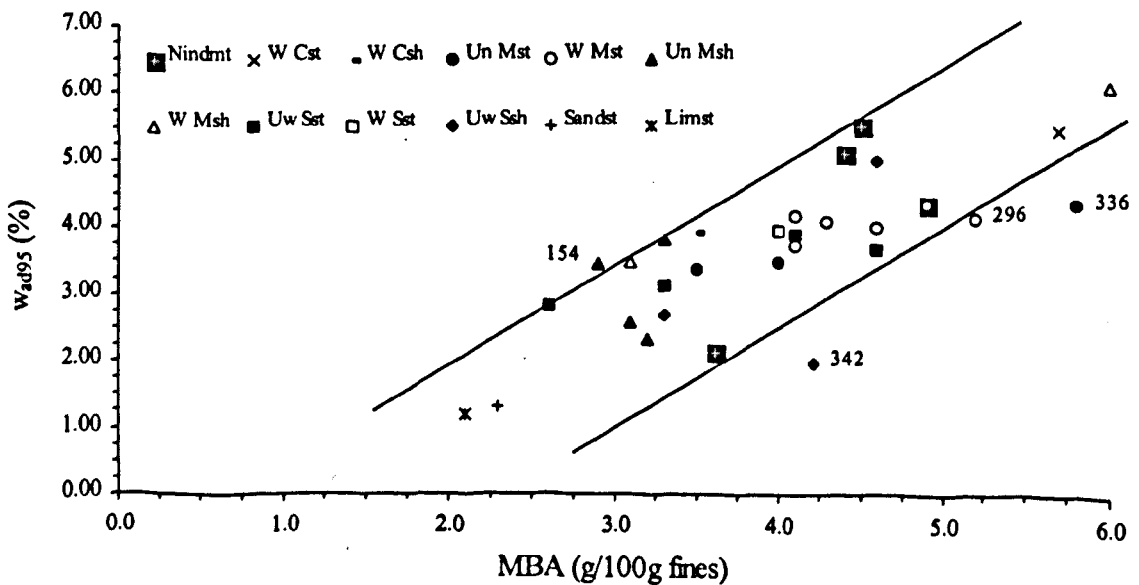


Fig. 6.20 - Relationship between methylene blue adsorption (MBA) and water adsorption at 95%RH (w_{ad95}).

Figs. 6.21 and 6.22 show that samples 154 and 336 conform with these general relationships. As these parameters were determined on powdered materials, in the case of sample 154, this confirms control only by mineralogy and not structure. It should however be noted, that samples 296 (Fig. 6.21) and 342 (Fig. 6.22) still have methylene blue adsorption values higher than expected.

The low PI value of sample OB2 (Fig. 6.22) appears to be anomalous in the context of the present discussion and it is probably due to a feature of the material tested. Fig. 6.22

shows also that the relationship between the two parameters appears to be stronger when the values of PI and MBA are higher, *i.e.* for the samples richer in clay minerals, namely those of expansive nature.

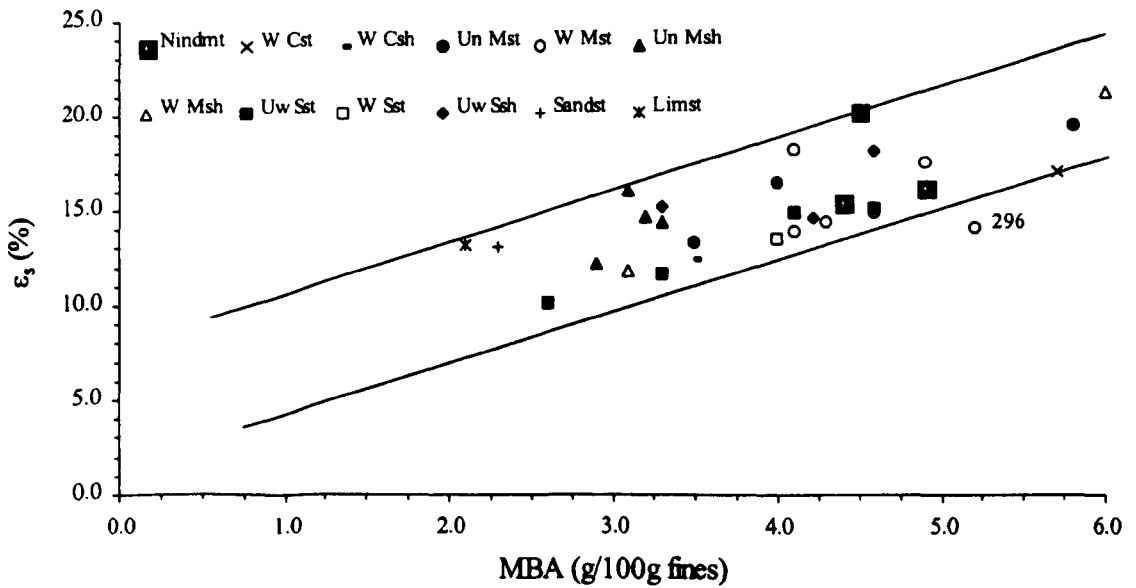


Fig. 6.21 - Relationship between methylene blue adsorption (MBA) and swelling strain measured on remoulded specimens (ϵ_s).

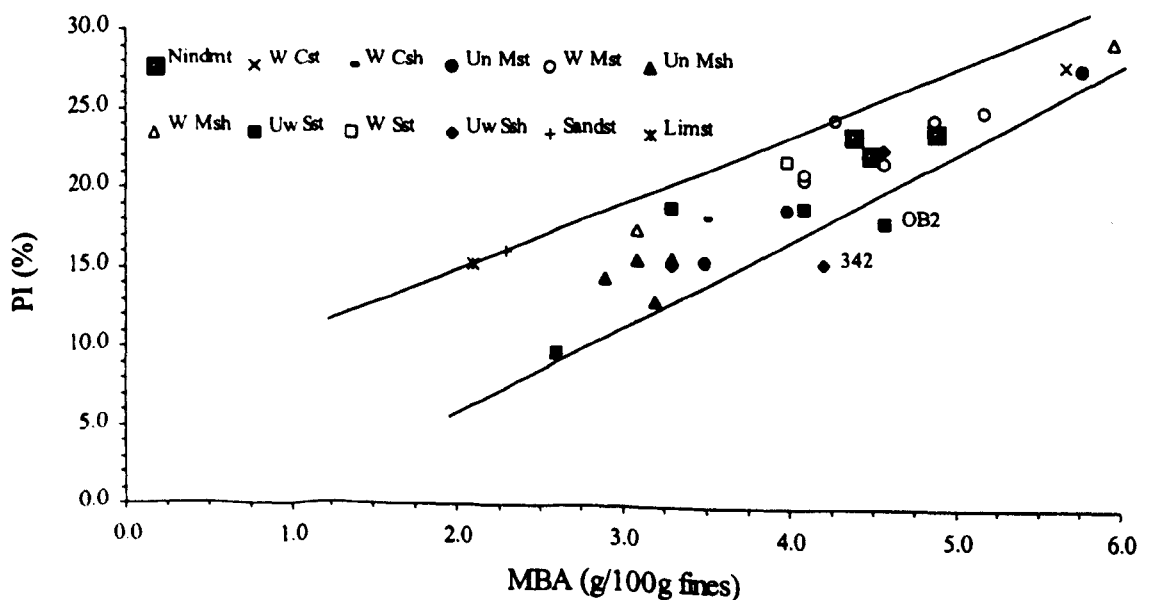


Fig. 6.22 - Relationship between methylene blue adsorption (MBA) and plasticity index (PI).

c) Correlations with the strength parameters

The cone indenter tests were performed for two steel blade deflection values, being the correlation between the results obtained from the two test versions were characterized by a very good fit ($R^2 = 0.94$). Therefore, when the test specimens fracture before reaching a deflection value of 0.635 mm the equation in Fig. 6.23 can be used to estimate the standard cone indenter values ($CI_{(0.635)}$), from the results obtained from the version used for soft rocks ($CI_{(0.23)}$).

Cone indenter results are habitually used to estimate the uniaxial compressive strength of materials, as these parameters usually show a good reciprocal correlation. However, it was found, in the case of the materials studied, that the R^2 values calculated for all samples were relatively low ($R^2 = 0.77$ for $\sigma_c/CI_{(0.23)}$ and $R^2 = 0.62$ for $\sigma_c/CI_{(0.635)}$). This fact is mainly due to the heterogeneities present in the test specimens used to determine the uniaxial compressive strength, since the lack of material available prevents the testing of a greater number of test specimens in order to compensate the anomalous results. Examination of the test specimens from samples 153, 156, 283, 294, 333 and 342 revealed the presence of fractures which explained the excessively low values determined for uniaxial compressive strength. It is accordingly considered, because these samples had uniaxial compressive strength values lower than normal, that they should be excluded from the correlation between this parameter and the cone indenter data.

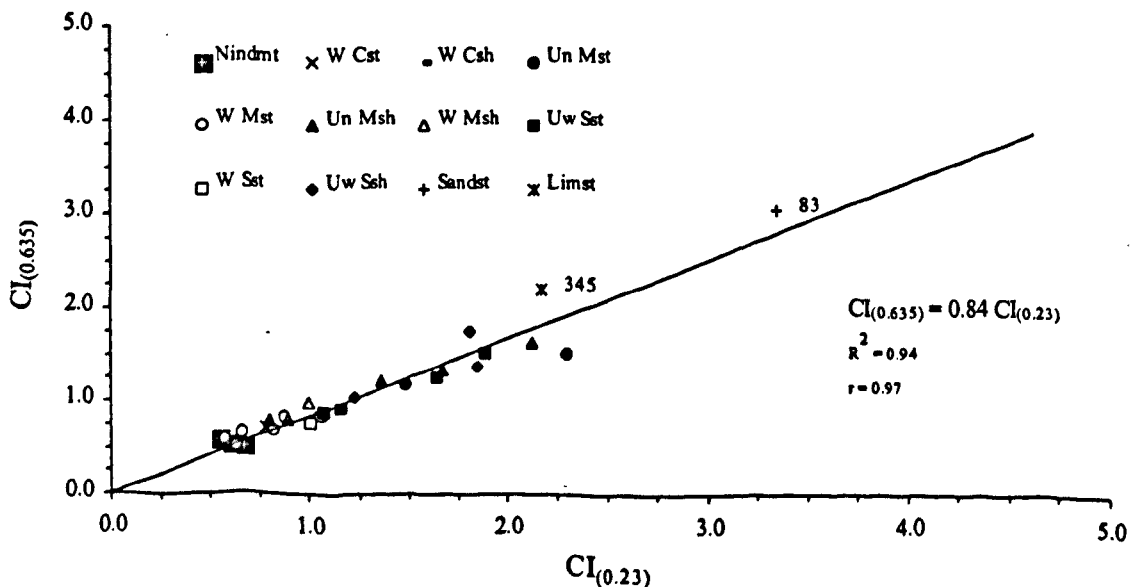


Fig. 6.23 - Correlation between the cone indenter numbers measured according to the standard ($CI_{(0.635)}$) and soft rock ($CI_{(0.23)}$) versions.

Examination of the test specimens from sample 83 used in uniaxial compression testing did not reveal the presence of fractures or fissures. It is accordingly considered that the position of sample 83 in the relationships is due to the fact that it is a sandstone and thus has a mechanical behaviour different from that of mudrock. The R^2 values calculated without the data of the samples 83, 153, 156, 283, 294, 333 and 342, which are now significantly higher ($R^2 = 0.96$ for $\sigma_c/CI_{(0.23)}$ and $R^2 = 0.86$ for $\sigma_c/CI_{(0.635)}$), and the equations determined by the least-squares method with intercept equal a zero which adjust better to both parameters are presented in Figs. 6.24 and 6.25.

The importance of composition, namely the amount and type of clay minerals, in the strength of the materials studied is clear from the relation presented in Fig. 6.26 between ϵ_s and the $CI_{(0.23)}$ values.

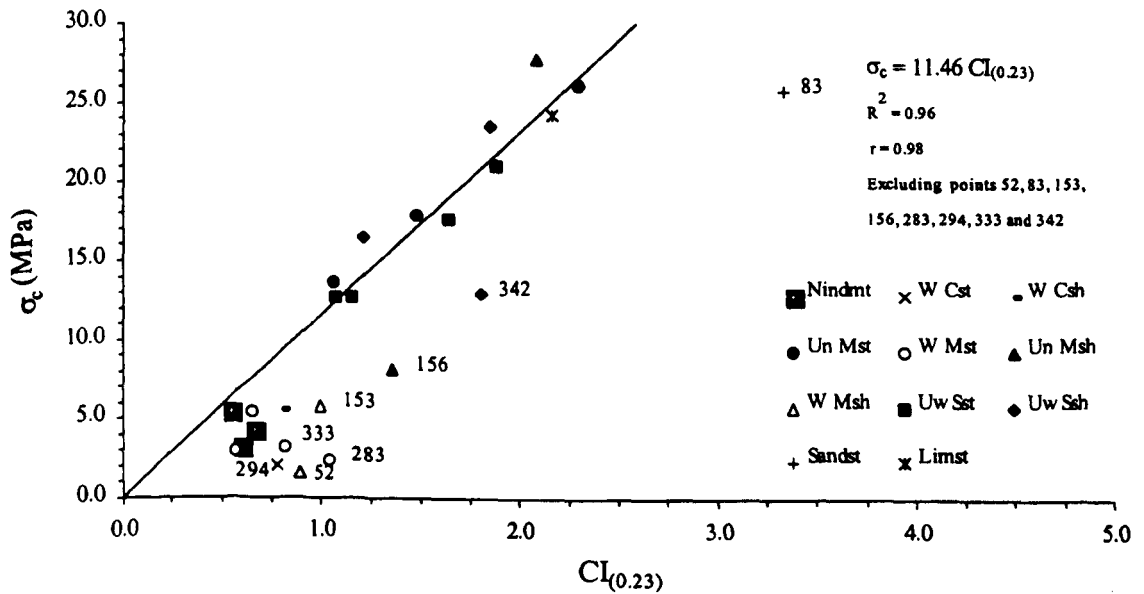


Fig. 6.24 - Correlation between uniaxial compressive strength and cone indenter number measured according to the soft rock version ($CI_{(0.23)}$).

From the analysis of this figure it can be seen that there is a negative relationship between these two parameters, that is a tendency for lower strength samples to undergo more swelling. From Fig. 6.26 it is also evident that the samples are distributed along two different alignments. The first, which is plotted as line A, includes most of the unweathered samples (156, 286, 334, 336, 342, 431, 436, 441, 445) while the second (line B) mainly includes the partially to very weathered rocks (81, 111, 151, 152, 153,

162, 163, 283, 285, 294, 296, 332 and 333). Unweathered samples 154, OB1 and OB2 have anomalous strength values because they are too low and form part of the alignment defined for weathered materials. Samples 112 and 114 do not fit into any of the alignments defined, while sample 83 once again has a singular behaviour, which is probably due to its different lithological nature.

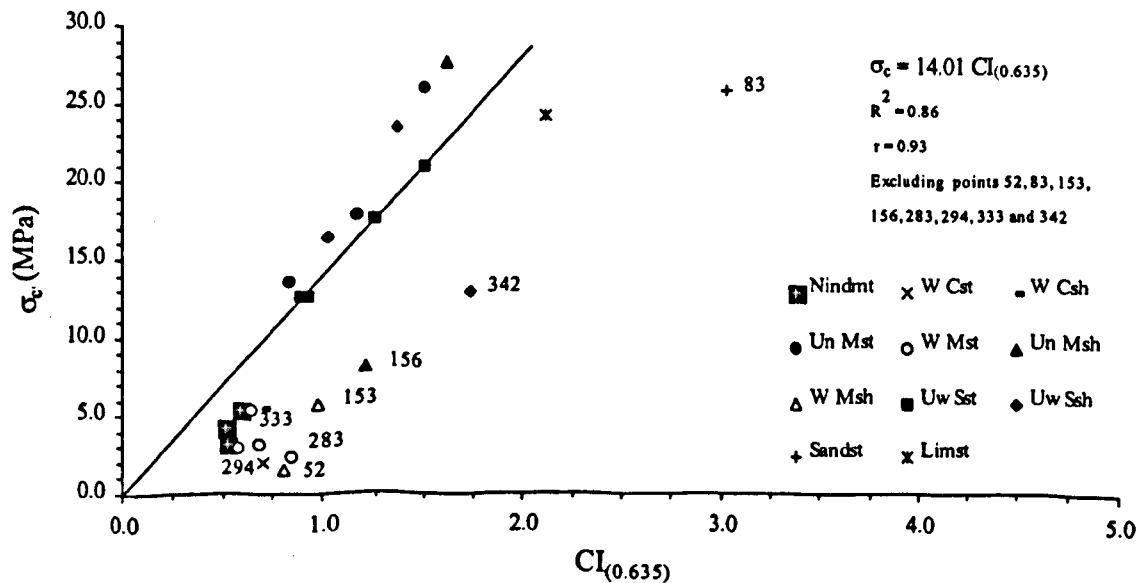


Fig. 6.25 - Correlation between uniaxial compressive strength and cone indenter number measured according to the standard version ($CI_{(0.635)}$).

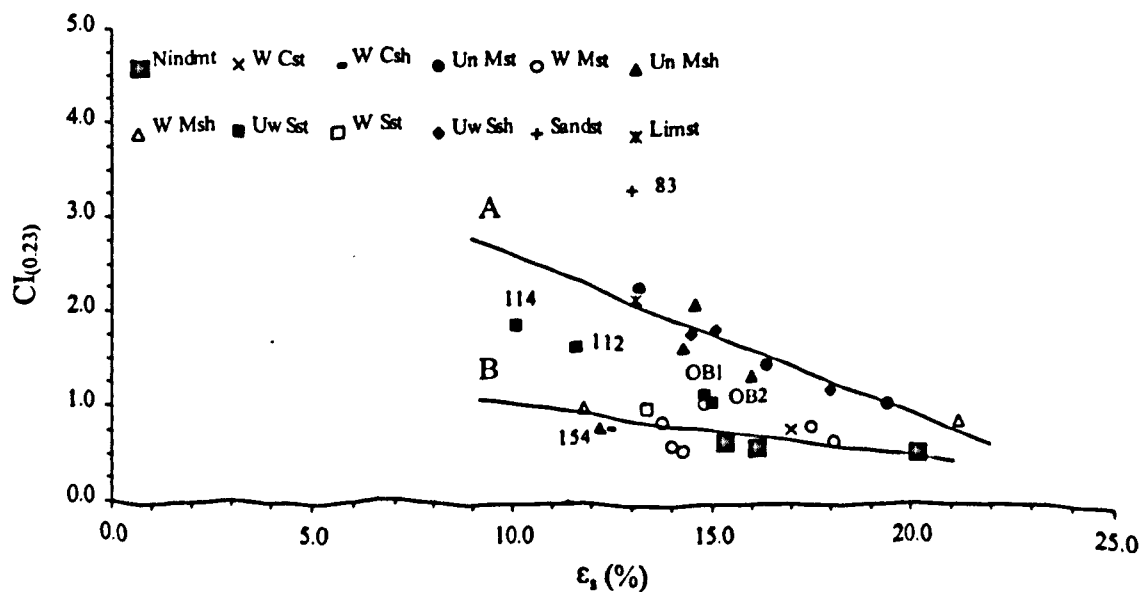


Fig. 6.26 - Relationship between swelling strain measured on remoulded specimens and cone indenter number measured according to the soft rock version ($CI_{(0.23)}$).

d) Correlations with swelling strain

The swelling of the materials studied was characterized on the basis of testing of remoulded specimens and intact specimens. It was sought in this way to obtain information regarding the importance of the mineralogical, textural and structural characteristics in the determination of this property. The swelling determined in the first type of test is solely a function of mineralogical composition, *i.e.* of the percentage and type of clay minerals present and for this reason had already been introduced to characterize the clay fraction.

The swelling determined on intact specimens evaluates not only mineralogical aspects but also the textural and structural aspects of the materials. Difficulties arise in the interpretation of the results due to the slaking of more weathered rock specimens during testing. This fact, consequently, leads to swelling strain values probably lower than those that would be expected if the specimens did not disaggregate.

It can be seen from the swelling strain versus time curves presented in Appendix II.2 that the major swelling direction in all samples is perpendicular to bedding. This anisotropic behaviour reflects the influence of textural and structural effects, such as the occurrence of lamination and the preferential orientation of clay minerals on property.

Fig. 6.27 shows the relationship between the swelling strain values determined in remoulded specimens (ϵ_r) and in intact specimens perpendicular to bedding/lamination (ϵ_i). Besides the scatter of the results it can be seen from the figure that there is a slight positive correlation between the two parameters *i.e.* a higher clay mineral content gives rise to higher swelling strain values in both tests.

However, the great scatter of the results reflects the textural and structural effects of the rocks on the determination of ϵ_r . Samples 334, 342, 431 and 445 are laminated and have the highest ϵ_r values. This does not apply in the cases of samples 52 and 336 for which mineralogical composition apparently accounts high ϵ_r values. The swelling obtained for

sample 52 appears above all to reflect its mineralogical composition, because both the ϵ_z and ϵ_s values are high, despite the fact that it is laminated. The ϵ_z value of non-laminated sample 336 also reflects its mineralogical composition, *i.e.* its high clay mineral content, since its components do not have a preferential orientation (see Figs. 5.20B and 5.21A).

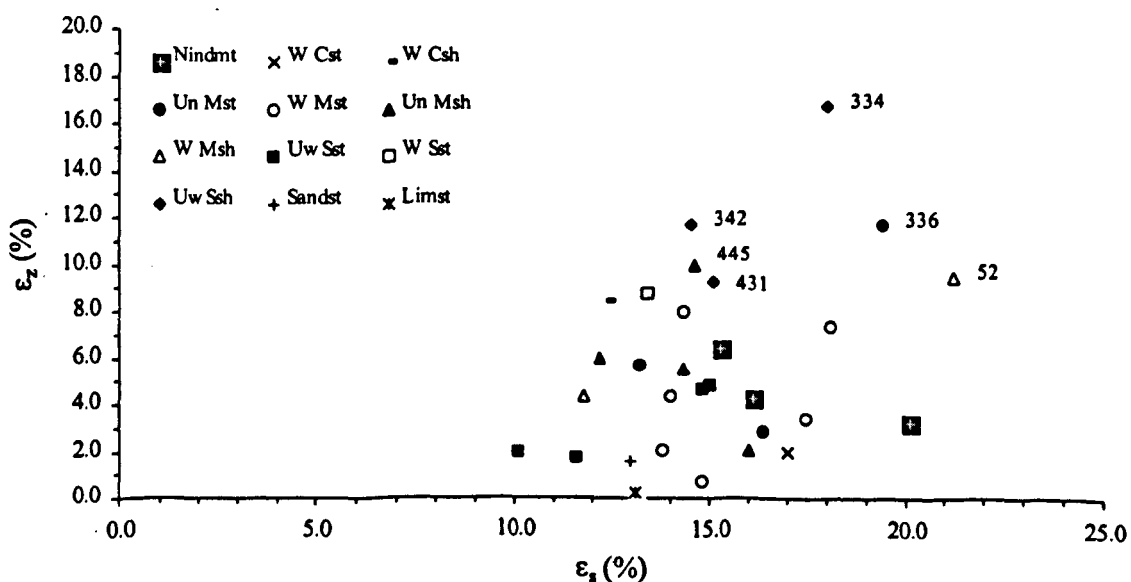


Fig. 6.27 - Relationship between swelling strain measured on remoulded specimens (ϵ_z) and on intact specimens perpendicular to bedding/lamination (ϵ_s).

The relationship presented in Fig. 6.28 between porosity and swelling strain determined perpendicular to bedding on intact specimens confirms the results obtained in previous studies by Rodrigues (1986) and Rodrigues & Jeremias (1989) which concluded that these parameters are relatively independent of each other. This is the case since it is clay minerals that swell in contact with water rather than the pore space. It can however be seen from Fig. 6.28 that there is a slight trend for a positive correlation between these two parameters which is understandable given that increased porosity affords easier access of water to the inner space of the materials, namely into clay minerals.

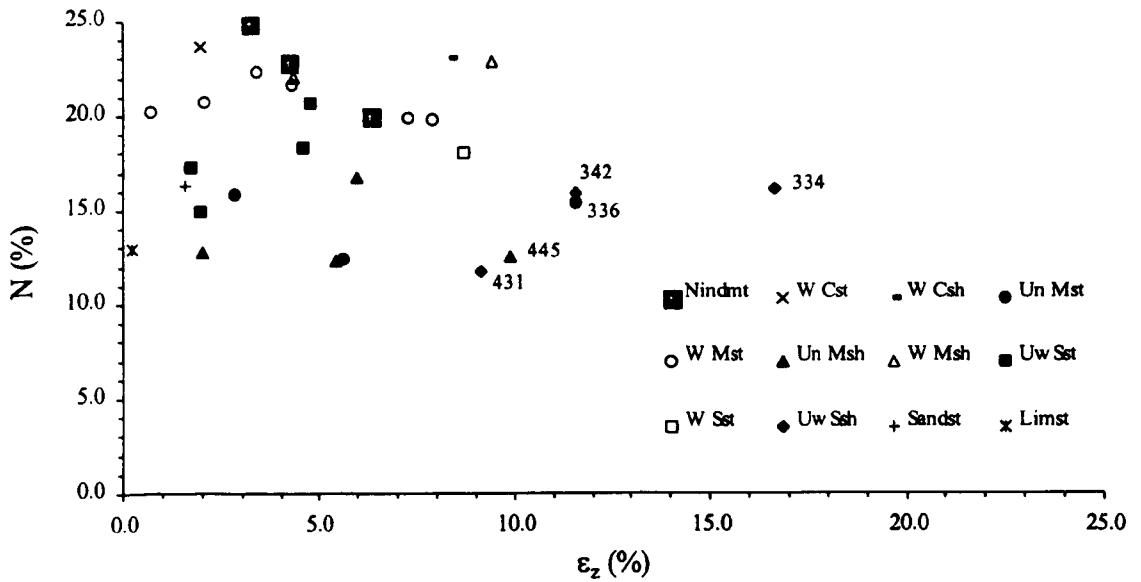


Fig. 6.28 - Relationship between porosity (N) and swelling strain measured on intact specimens perpendicular to bedding/lamination (ϵ_z).

e) Correlations with the jar slake and slake durability test results

The slaking of the rocks studied was characterized on the basis of jar slake and slake durability tests. Fig. 6.29 shows the relationship between the results of the jar slake test and of the swelling strain measured in rock samples perpendicular to bedding. Despite the great scatter of the plot there is a slight trend for a positive correlation between these parameters, *i.e.* the samples with a higher swelling strain are also those that are most likely to slake. However, the high swelling of laminated samples 342 and 445 is not apparently reflected by a greater susceptibility to slaking. Inversely, some of the materials (samples 111, 294, 296, 332 and 333) described with an I_j of 8 appear to have exaggeratedly low swelling strain values. As these samples are non-indurated and weathered materials, the determination of their swelling was affected by the fact that they disintegrated to a greater or lesser extent during testing. The results obtained are accordingly probably lower than would have been obtained if the test samples had not disintegrated.

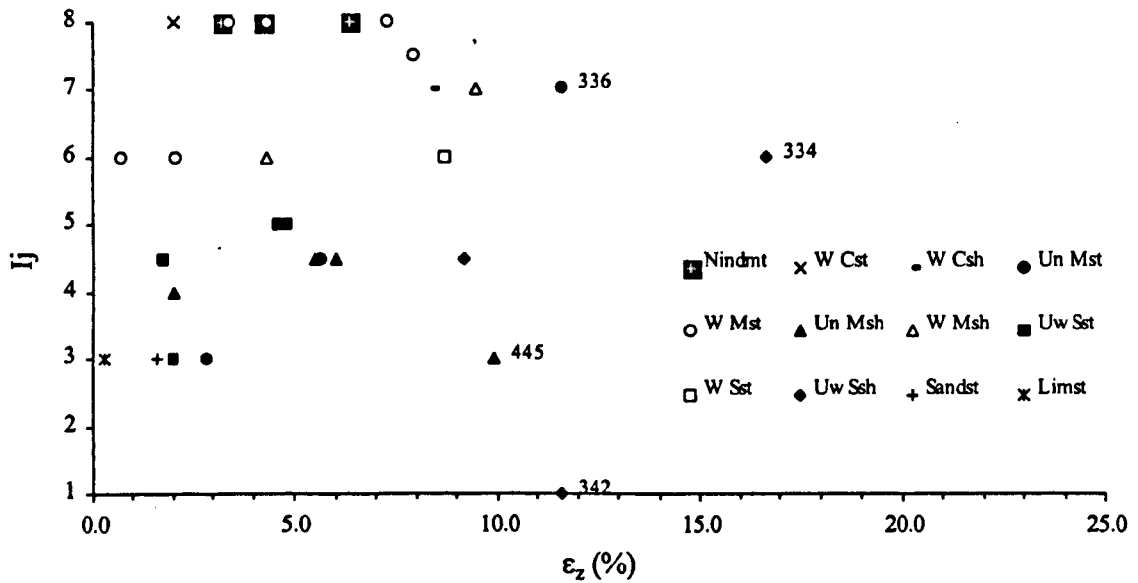


Fig. 6.29 - Relationship between I_j index results and swelling strain measured on intact specimens perpendicular to bedding/lamination (ϵ_z).

Fig. 6.30 shows the relationship between the results obtained in the jar slake test and porosity. It can be seen that there is a slight trend for a positive correlation between the two parameters which is understood as increased porosity allows a greater access of water to the inner space of the materials, which in turn leads to physical disintegration.

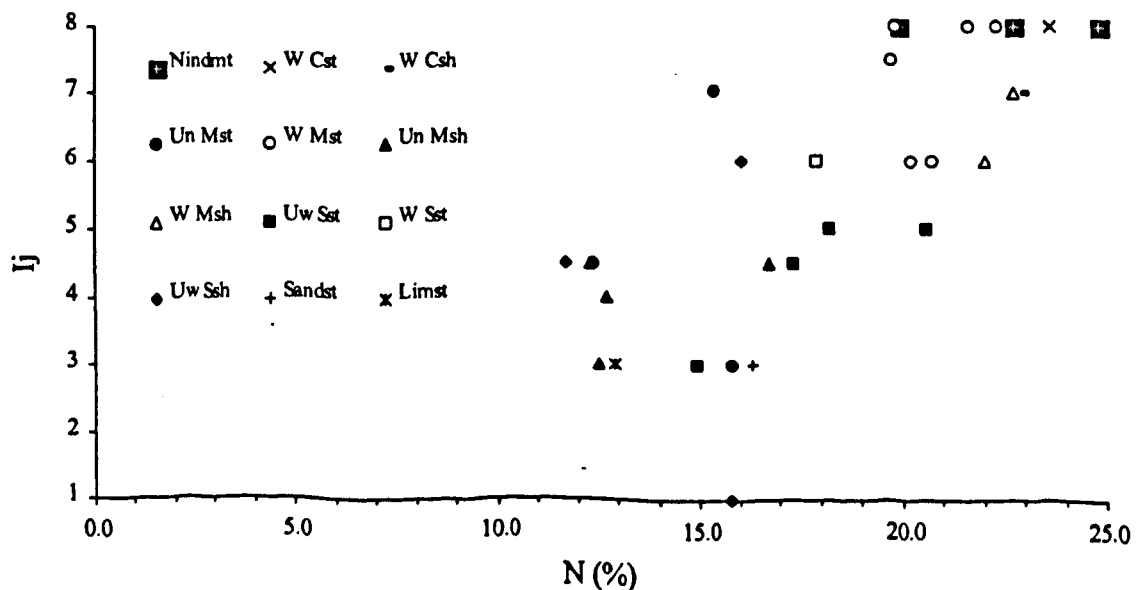


Fig. 6.30 - Relationship between I_j index results and porosity (N).

The slaking of mudrocks is also related to their strength. Fig. 6.31 shows the relationship between the I_j values and the results of the standard version of the NCB cone indenter test. It can be seen from the figure that there is a negative correlation between these two parameters which indicates that stronger materials are less prone to slaking. Samples 83 and 345 do not conform to the correlation established by the other materials, showing a higher strength. Since, they comprise distinct lithological types (calcareous sandstone and oolitic limestone), different mechanical behaviour from the mudrock materials is to be expected.

Slake durability tests involved three cycles (200+200+600 rotations) so that samples were subjected to a total of 1,000 rotations of the apparatus were performed. The performance of a third cycle in which the slaking time was increased, mainly affected non-indurated and weathered materials (samples 51, 52, 81, 111, 151, 152, 153, 162, 163, 283, 285, 294, 296, 332 and 333). These samples show percentages in weight of material retained equal to zero (no fragments in the drum) or very low (< 30%) (Fig. 6.16 and 6.19). The influence of the state of weathering of samples on their durability was therefore perfectly demonstrated by increasing test time. The relationship between the percentages in weight of the material retained after 400 rotations (I_{42}) and 1,000 rotations (I_{45}) presented in Fig. 6.32, also show this.

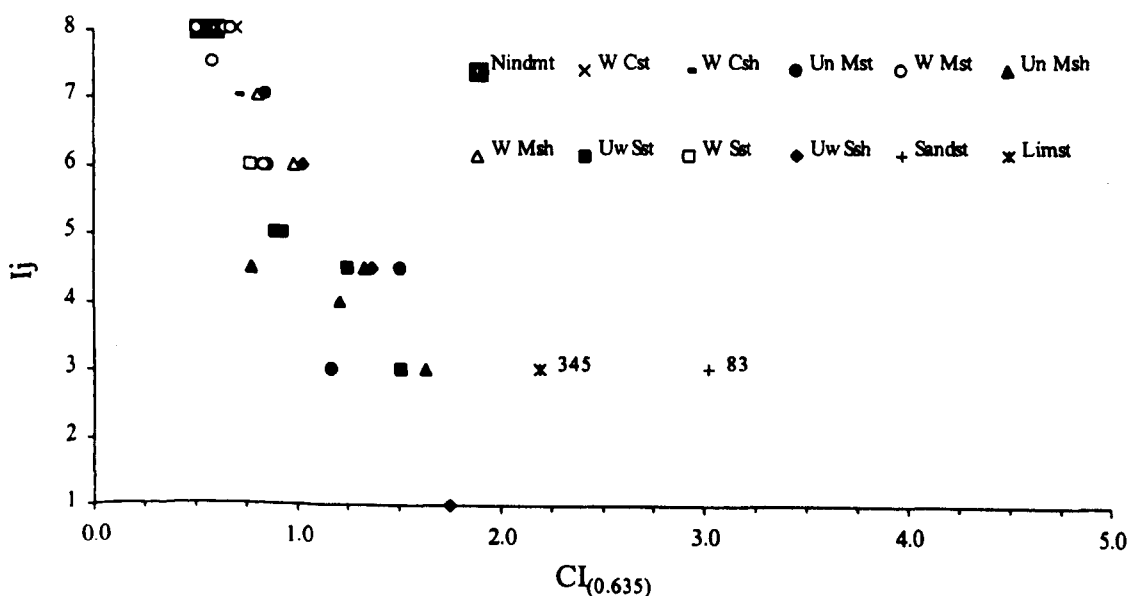


Fig. 6.31 - Relationship between I_j index results and cone indenter number measured according to the standard version ($CI_{(0.635)}$).

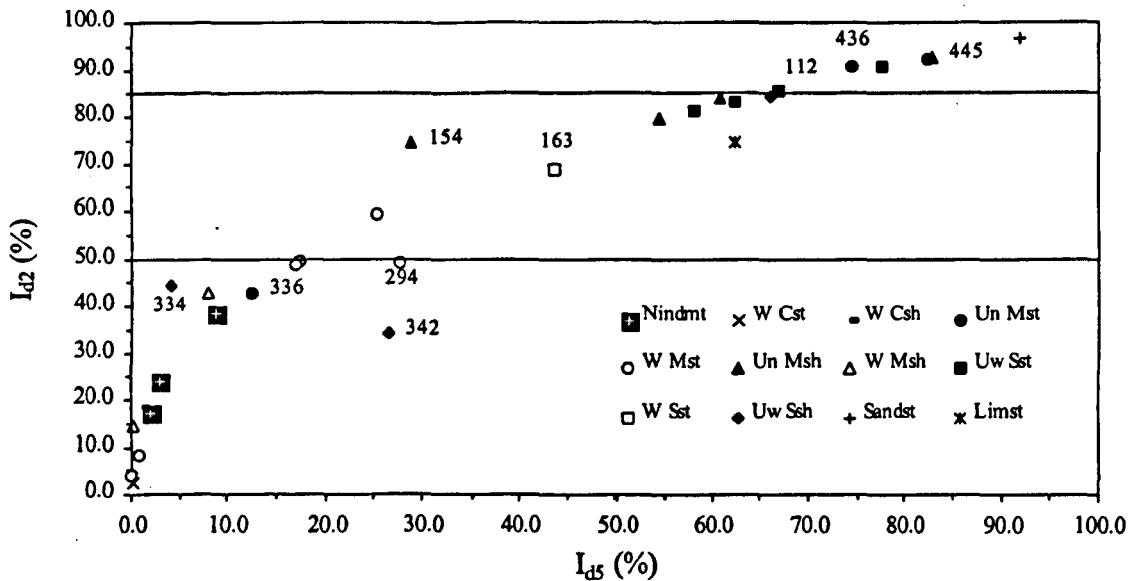


Fig. 6.32 - Relationship between the results of I_{d2} and I_{d5} indexes.

It can be seen from this figure that the difference between the values of I_{d2} and I_{d5} indexes is extremely high in less indurated mudrocks. This suggests that less durable materials tend to be more loosely held by diagenetic bonds such as cementation therefore producing greater breakdown of the samples down to a smaller aggregate size within the sand and silt size range. In the case of stronger materials the difference between the values of I_{d2} and I_{d5} indexes is attenuated, therefore the increase of test time does not lead to a significantly greater breakdown of the samples down to the size of mesh drum.

Samples 334 and 336, despite the fact that they are sound materials, have very low percentages of retained material. These results are compatible with the behaviour recorded for both samples in the jar slake test.

Sample 342 is an exception to the trend established by the other materials which shows that increased test time did not result in the breakdown predictable by the I_{d2} value. It can be concluded from the examination of the material retained in the drum (see Appendix II.3) and from the behaviour shown by this sample in the jar slake test that it is a heterogeneous sample with some layers stronger than others. The sample used in the slake durability test accordingly comprised weak lumps which mainly broke up during

the first 400 rotations and stronger lumps which had sustained hardly any breakdown after the three cycles (1,000 rotations). Inversely, sample 154 had a lesser percentage of retained material at the end of the test than would have been expected on the basis of the I_{d2} value determined. The semi-rounded and lamellar shape of the lumps of this sample after testing (see Appendix II.3) showed the influence of lamination on the results obtained. The subdivision of the lumps along the lamination planes accordingly gives rise to smaller tabular fragments which are subject to more significant breakdown with an increase of test time than would probably be obtained if the test samples retained their initial equant shape.

Samples 112 and 436 have I_{d2} values greater than 85% and are therefore considered durable according to the classification proposed by Dick *et al.* (1994). However, it can be noted from the examination of the lumps retained in the drum (see Appendix II.3) that they subdivided during testing. Therefore the I_{d2} and I_{d5} values determined do not reflect the disaggregation of these samples because the fragments produced are larger than the drum mesh size which is 2 mm. Given this limitation of the slake durability test the results obtained overestimated the durability of these samples (112 and 436).

The particle size distribution plots concerning the fraction smaller than 2 mm show that the materials resulting from the disaggregation of the mudrocks during slake durability tests have similar particle size distributions in which predominate the silt-sized particles (0.06 - 0.002 mm). Moreover, the fraction finer than 2 μm do not represent on average more than 25% of all disaggregated material.

Fig. 6.33 shows the relationship between I_{d2} and $CI_{(0.23)}$ values. It can be seen from the figure that the discrimination between less durable materials is slight corresponding to the same range of $CI_{(0.23)}$ values materials with durability quite different ($0\% < I_{d2} < 80\%$). So far as more durable materials are concerned ($I_{d2} > 80\%$) there is a positive correlation, despite the scatter of the results. The durability of sample 342 is anomalous for the reasons stated above. Samples 83 (calcareous sandstone) and 345 (oolitic limestone) differ from the others probably because they correspond to different lithological types.

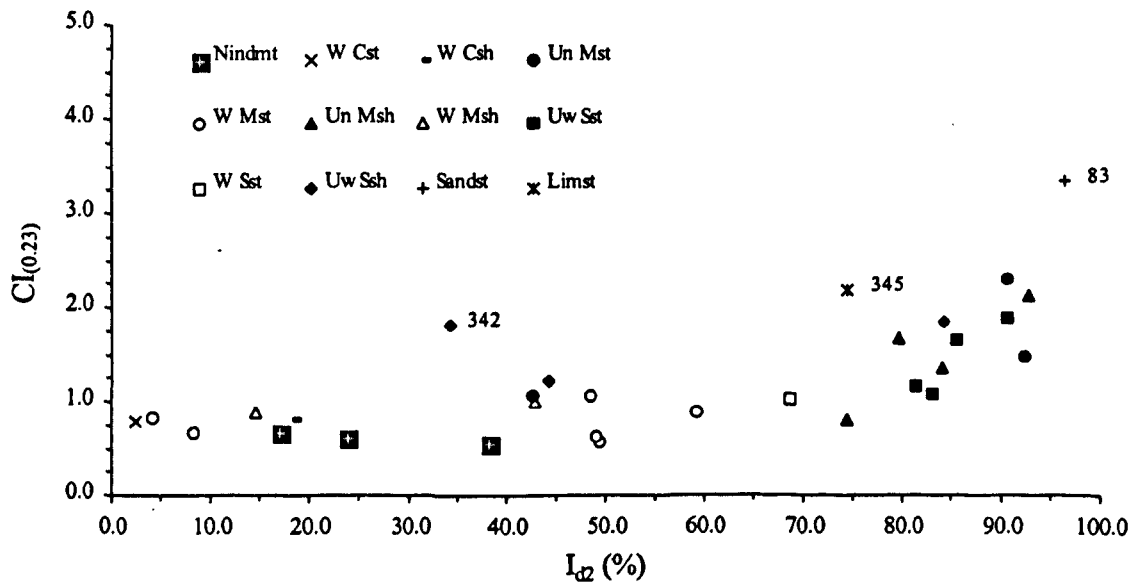


Fig. 6.33 - Relationship between the I_{d2} index and cone indenter number measured according to the soft rock version ($CI_{(0.23)}$).

Fig. 6.34 shows the relationship between the I_j and the I_{d2} values. The results display a slight negative correlation between the two parameters. The samples described with I_j values of 6 and 8 showing a more intense disaggregation are also those which exhibit greatest breakdown with values of $I_{d2} < 50\%$. The materials described with I_j values of 4 and 5 (moderate to high state of disintegration) correspond to samples which have I_{d2} values between 50 and 85%. While those materials that showing slight or no deterioration in the jar slake test described with I_j values between 1 and 3, correspond to samples with I_{d2} values greater than 85%. It was sought, on the basis of this analysis to establish durability classes (low, medium and high) for the I_j index derived from the classes proposed by Dick *et al.* (1994) for the I_{d2} index.

Fig. 6.34 shows the classes adopted for the two parameters. With the exception of some samples, a good agreement was found in the classification of the durability of the mudrocks, both on the basis of the I_j index and the I_{d2} index. The position of sample 342 is once again anomalous for the reasons already stated.

Sample 345 (oolitic limestone) showed slight deterioration in the jar slake test. Therefore, the I_{d2} value obtained is considered unexpectedly low. Examination of the

lumps, after the first cycle showed that some of them had fractures which probably accelerated their breakdown and affected the test result. The remaining lumps did not exhibit significant breakdown (see Appendix II.3) and their behaviour was in line with that observed in the jar slake test.

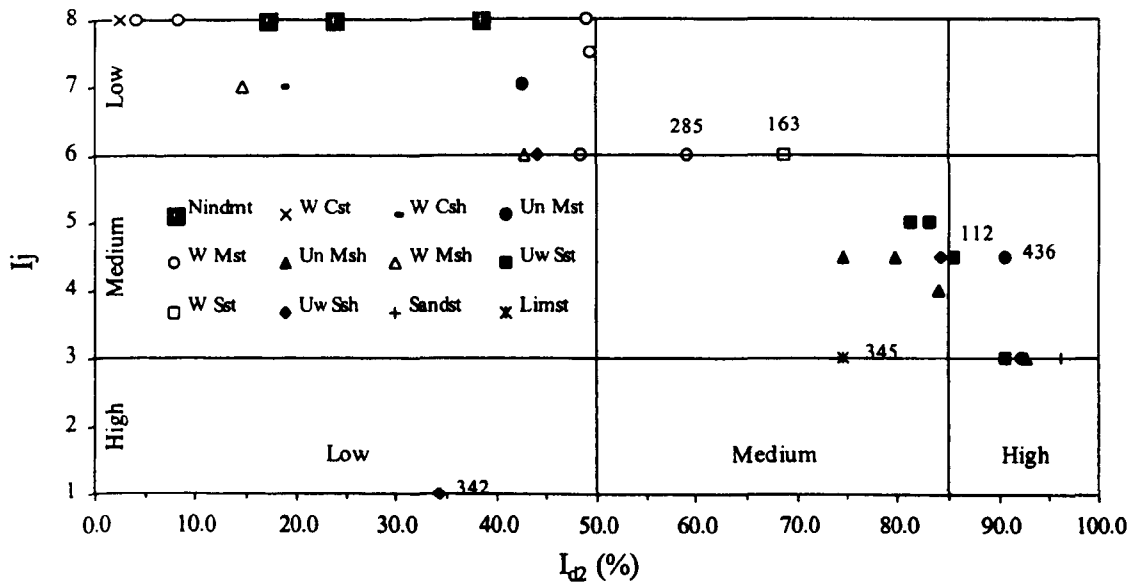


Fig. 6.34 - Relationship between Ij and Id2 indexes.

The Ij value of 4 or 5 achieved for samples 112 and 436 resulted from the fact that the specimens of these samples at the end of the jar slake test showed many fractures and considerable amounts of slake debris. Samples 163 and 285 also showed high degree of deterioration in the jar slake test. The behaviour of these samples in the jar slake test confirms the susceptibility to breakdown of these mudrocks, which is not properly reflected by the Id2 values, for the reasons already stated.

f) Correlations with the parameters derived from the compaction tests

The compaction tests were conducted on mixtures of crushed rocks coming from various samples, with the exception of mixtures S2 and A1 produced accordingly from samples OB2 and 83. It should be noted that the amount of material for the samples, which comprise mixtures SA3 and A1, were sufficient only for the preparation and

testing of two test samples and therefore the results obtained accordingly do not have the same representativeness as the results obtained for other mixtures.

It can be seen from the plots in Appendix II.4 that the mixtures derived from siltstones and siltshales (S1 and S2) as well as from mudstones and mudshales (SA1) consist of relatively undifferentiated grain sizes. Silt-sized particles predominate, at percentages of between 52 and 56%. Mixtures S1 and SA1 compose materials with relatively low durability and higher clay size fraction than the mixtures of materials with a higher durability (S2). The grain sizes curves for mixtures SA2 and SA3 are distinguished from the latter mixtures because, although they also have a predominantly silt size composition (with silt percentages of 51 and 47% respectively) fine gravel sized particles are also present. The composition of mixture A1 derived from sandstone (sample 83) is very obvious from the grain size distribution of this mixture in which sand sized particles predominate.

It can be seen from the analysis of the results of compaction tests that, for materials with an identical lithological composition the values of maximum dry density (γ_{dmax}) are higher for mixtures of higher durability samples. It was also found that, for materials included in the same durability class, the mixtures deriving from siltstones and siltshale samples have higher γ_{dmax} values. Mixture A1, which has a sandy composition, differed from the others because it has a distinctly higher γ_{dmax} value. However, it should be noted that this analysis only deals with γ_{dmax} values and the extrapolation to strength and deformability parameters used in the design of embankments requires consideration of others parameters.

Penetration tests using a CBR plunger were conducted to determine the behaviour of compacted materials on the basis of a strength criterion. It can be seen from the force/penetration plots presented in Appendix II.4 and the results in Table 6.9, that the highest strength values were obtained for test samples compacted in the Proctor test, with water contents nearest to the optimum moisture content value (w_{opt}). It can also be noted that the test samples compacted with a water content lower than the w_{opt} value (dry side of the compaction curve) showed substantially higher increases in water content after 96 hours of soaking (Δw_{96h}) than those recorded for test samples compacted

with a water content higher than the w_{opt} value (wet side of the compaction curve). This greater increase in water content found in test samples compacted on the dry side can probably explain their lower strength, considering that materials compacted on the dry side show in general higher strength characteristics.

The results of the CBR plunger strength penetration tests reveal that for the same durability class, mixtures composed of siltstones and siltshales have higher strength values than those deriving from mudstones and mudshales. It was also found that the strength values are greater in mixtures consisting of materials with a higher durability. As in the Proctor tests, mixture A1 (with a sandy composition) differed from the others in that it showed significantly higher strength values.

g) General conclusions

In conclusion the integrated analysis of the results of all geotechnical tests undertaken led to several relationships between the various parameters, which help to explain the behaviour of the mudrocks studied. The most important features are as follows:

- the increases of porosity, swelling and plasticity in these materials correspond to lower strength characteristics;
- the susceptibility to breakdown is greater in mudrocks which have higher swelling strain and porosity values;
- given the limitations of the slake durability test, the mudrock durability should be evaluated on the basis of jar slake and slake durability test results;
- the compaction and strength characteristics obtained for the mixtures tested reflect the durability and lithological composition of the materials used to make them;
- mixtures deriving from materials with a coarser lithological composition (siltstone, siltshale) and with higher durability accordingly have higher γ_{dmax} and 'CBR' strength values.

7 - EVALUATION OF DURABILITY: NATURAL EXPOSURE AND SIMULATED AGEING TESTS

7.1 - Introduction

Besides the determination of mineralogical, geochemical, textural and geotechnical characteristics of the mudrocks, this study also assesses the long-term behaviour of these materials with an evaluation of their durability.

The results of jar slake and slake durability tests are presented in the preceding chapter together with the tests for geotechnical characterization. These provide extremely valuable information regarding the behaviour of mudrocks. Furthermore, the results of these tests are used in various classifications to evaluate the durability of these materials (see Section 3.3.2).

Another approach adopted here is to evaluate durability by the use of both natural exposure and simulated ageing tests. These tests are described in this chapter in which the aim is (i) to study the rate of disintegration of the mudrocks in relation to frequently occurring weathering mechanisms; (ii) to study controls on these processes, including mineralogical, chemical and textural factors; and (iii) to investigate ways of predicting this behaviour by the use of index tests. The tests carried out involve short-term natural exposure of the samples, two types of drying and wetting tests and a salt crystallization

test. The monitoring of the samples involved the periodic recording of the changes, XRD and XRF analyses and NCB cone indenter strength tests at the end of the weathering experiments. It was sought, in this way, to investigate whether significant mineralogical, geochemical and mechanical changes in the materials occurred.

To summarise, this chapter describes the natural exposure and simulated ageing tests as well as the methodology used to perform and monitor them, lastly the results obtained are analysed.

7.2 - Methodology and description of the weathering experiments

7.2.1 - Outline of the test methodology

Given the large number of samples collected, it was not feasible to carry out natural exposure and simulated ageing tests for all materials. Thus, 10 samples were selected for the weathering experiments including both laminated and non-laminated rock types with varying degrees of weathering. Table 7.1 summarises the geological characteristics of the tested samples.

Table 7.1 - Geological characteristics of the samples used in the weathering experiments.

Sample	Lithological Type	Weathering State
83	Calcareous sandstone	Unweathered (A)
114	Calcareous siltstone	Unweathered(A)
OB2	Calcareous siltstone	Unweathered (A)
342	Calcareous siltshale	Unweathered (A)
431	Calcareous siltshale	Unweathered (A)
333	Mudstone	Partially weathered (B)
336	Mudstone	Unweathered (A)
283	Calcareous mudstone	Destructured (D)
286	Calcareous mudstone	Unweathered (A)
441	Calcareous mudshale	Unweathered (A)

Although sample 83 (calcareous sandstone) does not correspond to a predominant lithological type among the rocks collected, it was selected for these tests because, in terms of grain size and strength, it represents an extreme of the materials studied and, as such, its results are of particular interest in order to place the other results in context.

The breakdown of mudrocks is mainly a consequence of climatic slaking resulting from the exposure of these rocks to air or moisture or to alternate drying and wetting. The durability of these materials was accordingly evaluated in relation to the action of the effects of drying and wetting arising from natural exposure and via the execution of the following types of simulated ageing tests:

- in an environmental chamber with temperature and relative humidity control (cycles of RH/T);
- exposure to atmospheric conditions and periodic treatment of the test samples with a 5% solution of sulphuric acid (H_2SO_4).

In addition to these tests, the durability of rocks was also evaluated in relation to the salt weathering through tests undertaken in a salt spray chamber. The natural exposure and simulated ageing tests were carried out between July 1996 and April 1997, with the exception of the salt crystallization tests. This testing period was considered enough to discriminate between the various materials being studied. This period was also chosen because, in the case of the tests performed outdoors, it included the winter season during which the atmospheric conditions are generally harshest.

The evolution of the materials studied was monitored by periodic visual examination and photographing of the samples as well as by XRD and XRF analyses and NCB cone indenter tests, at the end of the weathering experiments. So far as the XRD analyses are concerned, the objective was to investigate whether significant mineralogical changes had occurred in the samples, upon the basis of their original composition. The purpose of the XRF analyses was to study whether important geochemical changes occur in relation to the original composition, namely as a result of the dissolution of specific mineral constituents. NCB cone indenter tests were performed in order to have a strength criterion which could be used to evaluate the evolution of this property in the samples subjected to natural exposure and simulated ageing tests.

7.2.2 - Description of the weathering experiments

The weathering experiments carried out were as follows:

- exposure to the atmospheric conditions (tests designated N);
- exposure to the atmospheric conditions with a periodic treatment (every 15 days) with a 5% solution of H_2SO_4 (tests designated HS);
- in environmental chamber varying temperature and relative humidity (tests designated HT);
- in salt spray chamber varying temperature and with periods of saline spray (tests designated SC)

The tests conducted outdoors were carried out on the roof of LNEC's Geotechnical Department Building. The samples used in the weathering experiments were dry cut with a diamond saw (see Section 4.3.3) so that small geometrically shaped test samples (weighing between 40-60g) were obtained. Any breakdown was in this way made visible and recorded. However, this procedure was not feasible for some samples for which there was not enough material available. In these cases fragments with an irregular shape were used. The test samples were placed on 2 mm stainless steel mesh, in test cells covered with 10 μ m nylon mesh which allowed exposure of the samples to sunlight, allowed rain water access but restricted access of wind blown material such as leaves and dust as well as prevented the removal of rock fragments by wind. A schematic illustration of the sample test cell used in tests carried out outdoors is presented in Fig. 7.1.

The use of 2 mm stainless steel mesh was used to evaluate the breakdown of the test samples on the basis of the loss (in percentage weight) of material finer than that dimension, in order to compare the data obtained with the results of the slake durability test. However, particularly in the case of the test samples tested in the salt spray chamber and subject to treatment with H_2SO_4 , the formation of crusts and weathering products, as a result of the reaction of the acid with carbonates, was noted. It was also found that the removal by scraping of the superficial layer gave rise to losses of material from test

samples greater than that caused solely by the slaking due to the natural exposure and simulated ageing tests. Therefore, it was not possible to evaluate the breakdown of the samples simply on the basis of periodic weighing of the test samples. The arrangement of the test frame used in the tests carried out outdoors is presented in Fig. 7.2.

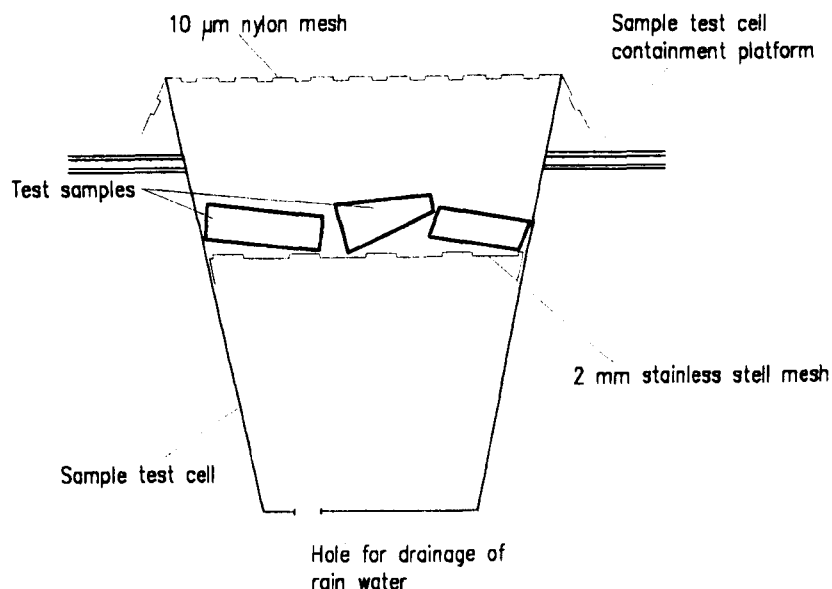


Fig. 7.1 - Schematic representation of the weathering sample test cell design used in the outdoor weathering experiments.

The laboratory simulated ageing tests were performed in an environmental chamber with temperature and relative humidity control (Heraeus, HC 4030 model) and in a salt spray chamber (MPC, PBS model).

The simulated ageing tests carried out in the environmental chamber (HT) sought to simulate the drying and wetting weathering mechanism, although in these test conditions the rocks were neither immersed nor sprayed with water but merely subjected to a change in the moisture content. The cycles were conducted in accordance with the test conditions illustrated schematically in Fig. 7.3, with the temperature being varied between 25° and 65°C and the relative humidity varying between 0 and 95%. The cycle adopted was adjusted in order to have a duration of one day and the samples were subjected to a total of 300 cycles.

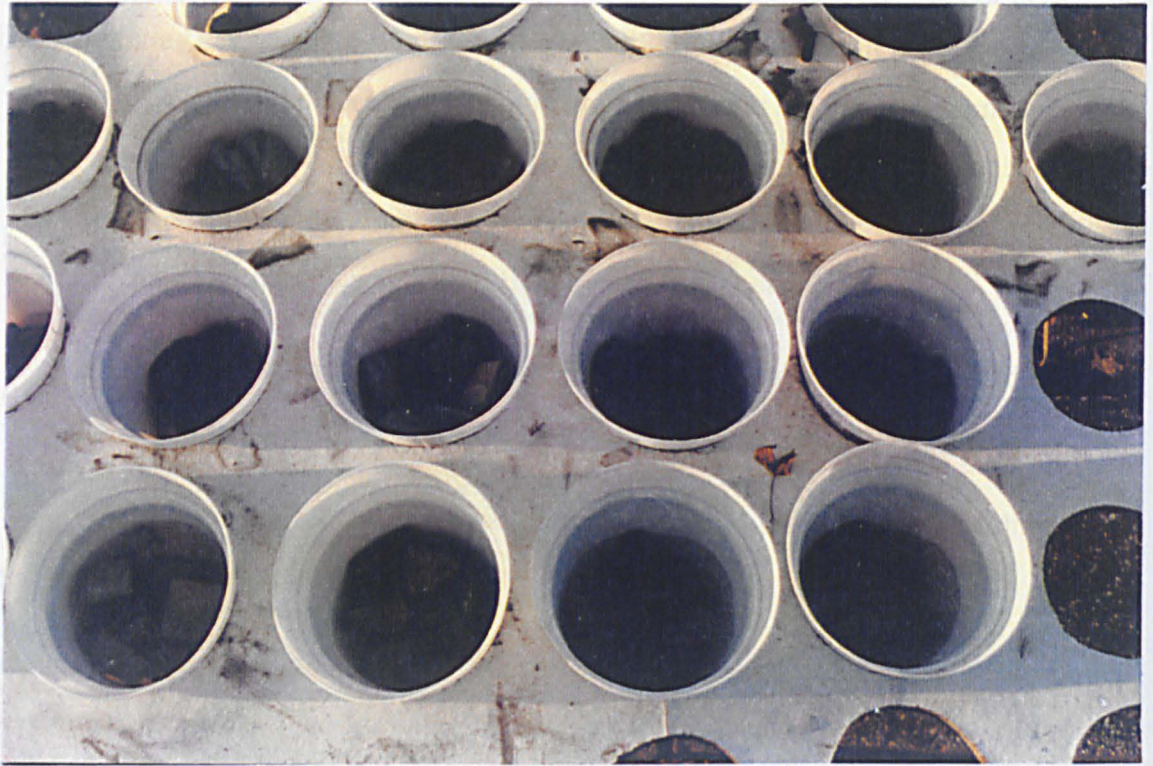


Fig. 7.2 -View of the weathering experiments performed outdoors.

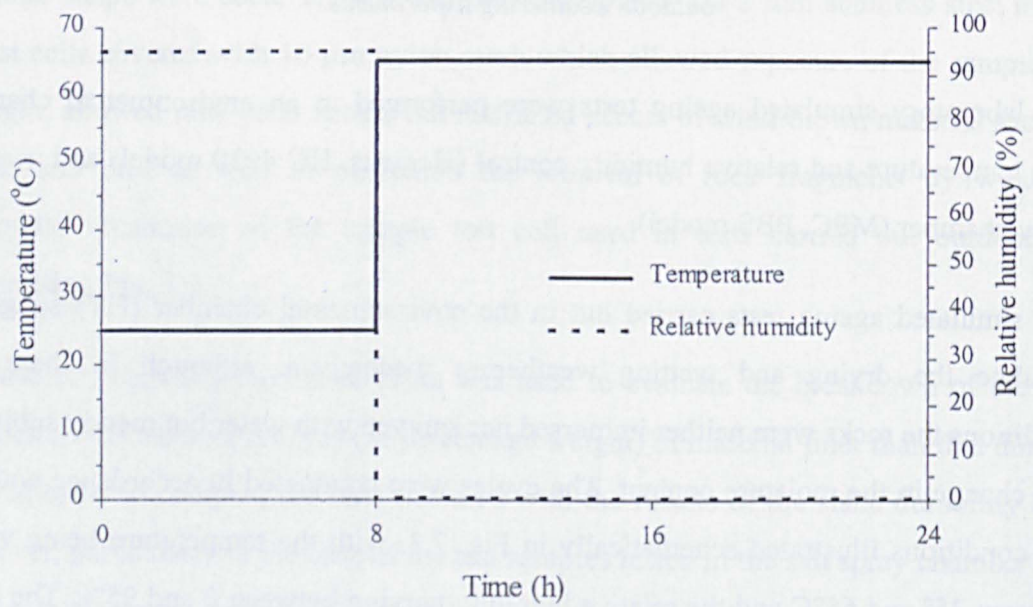


Fig. 7.3 - Cycle used in the RH/T ageing process.

The aim of the simulated ageing tests undertaken in the salt spray chamber (SC) was to study the behaviour of the samples in relation to an expansive mineral weathering process. A 10% solution of sodium chloride was used for these tests. The cycle adopted, which is illustrated schematically in Fig. 7.4, included approximately three 30 minute periods of saline spray at ambient temperature (approximately 25°C), during the first three hours, followed by a consecutive drying and crystallization period of approximately 9h, at 50°C. The simulated ageing tests performed in the salt spray chamber, like the HT tests, comprised 300 cycles which were carried out at the rate of 2 cycles per day (12h + 12h) between July and November 1996.

The photographic record concerning the state of the test samples studied before and after the weathering experiments described above is presented in Appendix III.

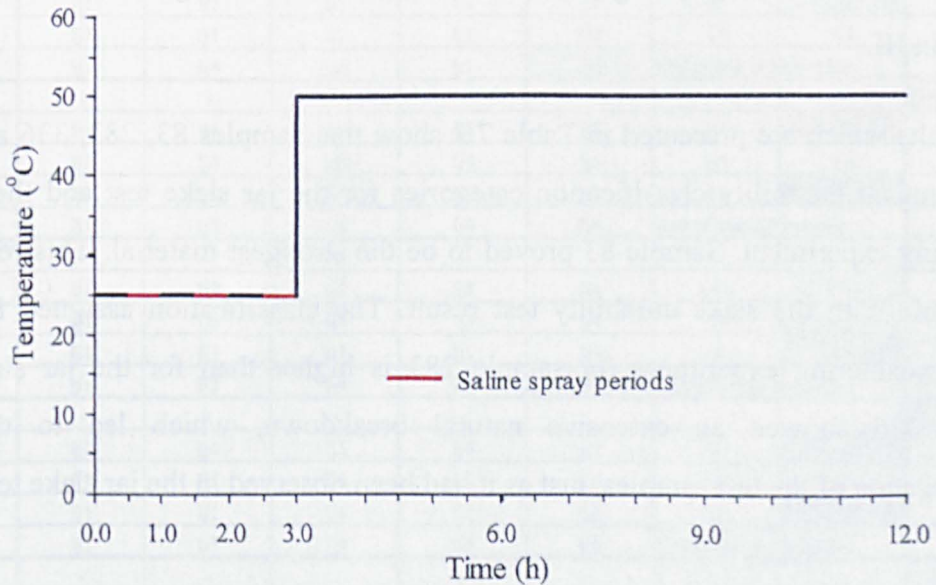


Fig. 7.4 - Cycle used in the ageing tests conducted in the salt spray chamber.

7.3 - Visual, mineralogical, geochemical and mechanical monitoring of the rock materials subjected to the weathering experiments

7.3.1 - Visual description of the extent of sample slaking

The samples were monitored periodically throughout the ten months during which the tests were carried out and were described on the basis of the classification proposed for the jar slake tests presented in Table 6.4. The descriptions made, presented in Table 7.2, show that many of the studied samples performed differently according to the type of test to which they were subjected.

The natural weathering experiments (designated N) reflect the breakdown of the materials according to the climatic conditions of Lisbon (close to the airport). The photographic record with regard to the state of breakdown of the various samples before and after the natural weathering experiments is presented in Figs. AIII.1 to AIII.5 in Appendix III.

The results which are presented in Table 7.2 show that samples 83, 283, 336 and OB2 have identical durability classification categories for the jar slake test and the natural weathering experiment. Sample 83 proved to be the strongest material. This result was compatible with the slake durability test result. The classification assigned from the natural weathering experiment for sample 283 is higher than for the jar slake test. Sample 336 showed an extensive natural breakdown, which led to the total disaggregation of the test samples, just as it had been observed in the jar slake tests

Sample OB2 was included in class Ij5 because it was still possible to identify the original shape of the test samples after the natural weathering experiment. However, due to the extensive fissuration developed in the test samples, these fragments split easily into many smaller fragments when handled. (Fig. AIII.5D).

Table 7.2 - Weathering sample descriptions using the jar slake classification scheme.

Sample	(Jul 96)	(Aug 96)	(Sep 96)	(Oct 96)	(Dec 96)	(Feb 97)	(Apr 97)	Ij
83	-	-	-	-	-	-	-	Ij3a
83N	Ij1	Ij3a	Ij3a	Ij3a	Ij3a	Ij3a	Ij3a	-
83HS	Ij1	Ij3a	Ij3a	Ij3a	Ij3a	Ij3/4a	Ij4a	-
83HT	Ij1	Ij1	Ij1	Ij1	Ij1	Ij2/3	Ij2/3	-
83SC	Ij1	Ij3a	Ij4a	Ij5a	Ij5a	End of test in November.		-
114	-	-	-	-	-	-	-	Ij4a
114N	Ij1	Ij3a	Ij3a	Ij3a	Ij3/4a	Ij5/6	Ij5/6	-
114HS	Ij1	Ij3a	Ij4a	Ij4a	Ij4a	Ij5a	Ij5a	-
114HT	Ij1	Ij1	Ij1	Ij1	Ij2-3	Ij2-3	Ij2-3	-
114SC	Ij1	Ij3a	Ij3a	Ij5a	Ij6	End of test in November.		-
283	-	-	-	-	-	-	-	Ij6
283N	Ij1	Ij4	Ij4	Ij4	Ij4	Ij6	Ij6	-
283HS	Ij1	Ij3	Ij3	Ij3	Ij3	Ij4	Ij5	-
283HT	Ij1	Ij1	Ij1	Ij1	Ij1	Ij2	Ij3	-
283SC	Ij1	Ij4	Ij4	Ij5	Ij6	End of test in November.		-
286	-	-	-	-	-	-	-	Ij4a
286N	Ij1	Ij2	Ij3a	Ij3a	Ij3/4a	Ij5/6	Ij5/6	-
286HS	Ij1	Ij4a	Ij5a	Ij5a	Ij5a	Ij6	Ij6	-
286HT	Ij1	Ij1	Ij1	Ij1	Ij3a	Ij3a	Ij3a	-
286SC	Ij1	Ij4a	Ij5a	Ij6	Ij6	End of test in November.		-
333	-	-	-	-	-	-	-	Ij8
333N	Ij1	Ij3	Ij5	Ij6	Ij6	Ij6	Ij6	-
333HS	Ij1	Ij3	Ij5	Ij5	Ij5	Ij5	Ij5	-
333HT	Ij1	Ij1	Ij1	Ij1	Ij2	Ij2	Ij2	-
333SC	Ij1	Ij4	Ij5	Ij5	Ij5	End of test in November.		-
336	-	-	-	-	-	-	-	Ij7
336N	Ij1	Ij5	Ij6	Ij6	Ij7	Ij7	Ij7	-
336HS	Ij1	Ij4	Ij6	Ij6	Ij6	Ij6	Ij6	-
336HT	Ij1	Ij1	Ij1	Ij1	Ij3	Ij3	Ij3	-
336SC	Ij1	Ij5	Ij6	Ij6	Ij6	End of test in November.		-
342	-	-	-	-	-	-	-	Ij1
342N	Ij1	Ij2	Ij3	Ij3	Ij4	Ij4/5	Ij4/5	-
342HS	Ij1	Ij3	Ij3	Ij3	Ij4	Ij4	Ij4/5	-
342HT	Ij1	Ij1	Ij1	Ij1	Ij1	Ij2/3	Ij2/3	-
342SC	Ij1	Ij3	Ij4	Ij5	Ij5	End of test in November.		-
431	-	-	-	-	-	-	-	Ij4/5
431N	Ij1	Ij4	Ij5	Ij6	Ij7	Ij7	Ij7	-
431HS	Ij1	Ij5	Ij6	Ij6	Ij6	Ij6	Ij6	-
431HT	Ij1	Ij1	Ij1	Ij1	Ij3	Ij3	Ij3	-
431SC	Ij1	Ij3	Ij4	Ij6	Ij6	End of test in November.		-
441	-	-	-	-	-	-	-	Ij4/5
441N	Ij1	Ij3	Ij4	Ij4	Ij4	Ij6	Ij6/7	-
441HS	Ij1	Ij3	Ij3	Ij4	Ij4	Ij4/5	Ij4/5	-
441HT	Ij1	Ij1	Ij1	Ij1	Ij2	Ij3	Ij3	-
441SC	Ij1	Ij2/3	Ij3	Ij4	Ij6	End of test in November.		-
OB2	-	-	-	-	-	-	-	Ij5
OB2N	Ij1	Ij3	Ij3	Ij4	Ij4	Ij5	Ij5	-
OB2HS	Ij1	Ij3	Ij3	Ij4	Ij4	Ij5	Ij5	-
OB2HT	Ij1	Ij1	Ij1	Ij1	Ij1	Ij1	Ij2	-
OB2SC	Ij1	Ij3	Ij3/4	Ij5	Ij5	End of test in November.		-

Ij - Jar slake test result.

Ij1 - Ij2	Ij2/3 - Ij3	Ij4	Ij4/5	Ij5	Ij5/6 - Ij6	Ij6/7 - Ij7	Ij7/8	Ij8
-----------	-------------	-----	-------	-----	-------------	-------------	-------	-----

The breakdown of the rock fragments of samples 114, 286, 431 and 441, at the end of the natural weathering experiment, was greater than that obtained in the jar slake test. However, it should be noted that the behaviour of these materials during the first 4 to 6 months of testing was similar in both tests and as such they were described using the same I_j values. The increase of the extent of breakdown of these samples in the natural weathering experiment, after the mentioned period, was due to the progressive dissolution of the carbonate cements. The jar slake test accordingly overestimated the durability of these samples, as the 24 h period adopted for this test was insufficient to allow the dissolution of the carbonate cements. It was noted, on the basis of the observations carried out, that the rock fragments of samples 114, 286, 431 and 441 subjected to jar slake still remained intact after 24 h of testing, despite the fact that they contained fractures, while after the natural weathering experiment the test specimens split into many fragments.

Sample 342 is a heterogeneous calcareous siltshale containing strong and weak layers. It was accordingly found that the breakdown of some of the test samples subjected to the natural weathering experiment was more severe than in others. This fact explains the discrepancy found between the results of the natural weathering experiment and the jar slake. The lower I_j value was adopted to describe this material. However, it should be noted that the behaviour of the stronger fragments in the natural weathering experiment was similar to that observed in the jar slake test.

Sample 333 showed a moderately rapid rate of breakdown. However, the state of breakdown noted in the jar slake was not attained. Heterogeneities in materials, which were not identified during the selection of the materials for the tests, may probably account for the differences found in the results.

The photographic record with regard to the state of breakdown of the various samples before and after the HS experiment is presented in Figs. AIII.6 to AIII.10 in Appendix III.

The visual description of the samples subjected to the HS experiment proved not to be a very effective way of classifying the durability of the rocks. At the end of these tests the evolution of the various samples exhibited a certain homogeneity with almost all the materials described having I_j values of 5 or 6. Furthermore, the materials apparently showed a better behaviour in the HS experiment than in the natural weathering experiment. Therefore, all samples, except for sample 83, were described with I_j values equal to or lower than those used to classify the samples merely exposed to atmospheric conditions (Table 7.2). The explanation of this behaviour can probably be found in the coating of the test samples with a layer composed of the products of the reaction of the acid solution with the carbonate minerals, which had masked the real weathering state of the samples*. As a consequence, the visual descriptions overestimated the durability of the materials subjected to the HS experiment.

As in the case of the natural weathering experiment, sample 83 had the best behaviour under testing and it was clearly the most durable material. However, it should be noted that it was found from the examination of the rock fragments from this sample, that treatment with acid had accelerated their degradation. Samples 114, 286 and 431 showed a greater state of breakdown due to the progressive dissolution of carbonate cements. It was particularly noteworthy, in the case of sample 431 (probably because it has a lower carbonate content) that the addition of the acid solution accelerated the process so that the maximum state of breakdown of the test samples was reached after 2 months of testing. After this period no notable specimen deterioration was recorded.

The I_j value used to describe sample 283 at the end of the HS experiment was marginal to those adopted in the natural weathering experiment and jar slake test, which reflects the fact that this material attained a comparable state of breakdown in the three tests. The durability classification assigned to samples 333 and 342 at the end of the HS experiment is similar to that assigned to the natural weathering experiment and clearly different from that obtained in the jar slake test. This may be, as it has already been

* Indeed, the treatment with H_2SO_4 accelerated the degradation of the materials this being proved by the lower strength values determined for the HS samples in the cone indenter strength tests.

stated, due to the fact that these materials are heterogeneous and sample fragments with different characteristics may have been used for the various types of tests carried out.

Sample 336, as expected, showed a very rapid rate of breakdown. However, it did not reach the state of breakdown observed in the subsamples subjected to the natural weathering experiment and the jar slake test. The state of breakdown showed by sample 441 at the end of HS experiment was comparable to that recorded for the jar slake test. However, in both tests the state of fragmentation reached was not as great as that recorded for the sample subjected to the natural weathering experiment. Sample OB2 showed in the HS experiment, a breakdown performance similar to that noted in the natural weathering experiment and the jar slake test.

According to the data of Table 7.2 and the photographic record presented in Figs. AIII.11 to AIII.15 in Appendix III, the simulated ageing tests carried out in the environmental chamber with temperature and relative humidity control did not lead to significant deterioration of the materials after 300 cycles. This weathering experiment was accordingly not very useful to differentiate the durability of the rocks studied.

The weathering experiments performed in the salt spray chamber (about 300 cycles) proved to be effective in the acceleration of the deterioration of some samples. This method was accordingly useful to distinguish the breakdown behaviour of those materials. The crystallization of the salt during the drying phase promoted the breakdown of the rocks. The photographic record with regard to the state of breakdown of the various samples before and after the SC experiment is presented in Figs. AIII.16 to AIII.20 in Appendix III.

During the SC weathering experiment the test samples became covered by a superficial layer composed of slaking material and NaCl, which was periodically removed. Sample 83 which did not show notable deterioration in the jar slake and in natural weathering experiment, exhibited at the end of the SC experiment relevant breakdown. Accordingly, the rock fragments of this sample at the end of SC experiment were very fractured and partially disaggregated. It can be concluded that this material is less

sensitive to the effect of drying and wetting cycles than to the deterioration caused by salt weathering. In this way, the breakdown of this sample is more effectively controlled by porosity than by the presence of expandable clay minerals (present in a percentage of less than 5%), which increase sensitivity to water content changes. Despite the differences which may have occurred in sample selection, as already mentioned with respect to the rock fragments of sample 342, it can be concluded that a higher state of breakdown occurred in the SC test than in the other weathering experiments.

Samples 114, 336, 431 and 441 are assigned a lower durability classification from the SC experiment than from the natural weathering experiment. However, it was found that this apparently more satisfactory behaviour was not real, because despite the fact that the test samples kept their original shape, they were deeply weathered and fractured, splitting easily into many fragments. Finally, the state of breakdown of samples 283, 286, 333 and OB2 at the end of the SC experiment was not substantially different from that observed in the other tests carried out (N, HS, and jar slake).

7.3.2 - Mineralogical analysis by XRD of the weathered samples

The mineralogical characterization by XRD was aimed at qualitative determination of the mineral species present in the samples at the end of the weathering experiments, in order to investigate if any notable mineralogical changes had occurred.

XRD analyses were undertaken on all samples subjected to the weathering experiments. As the aim was to obtain a general mineralogical characterization of rocks at the end of the weathering experiments, the analyses were carried out on whole rock samples obtained from representative fractions of each of the materials. The procedures used in the preparation of the whole rock samples and in carrying out the XRD analyses are described in Chapter 5.

The traces for naturally weathered (N), ageing weathered (HS, HT and SC) and unweathered whole rock (WR) analysis for each sample are presented in the same figure

for comparative purposes (Figs. 7.5 to 7.14). The highest peak heights were cut and identified with a vertical arrow, with their real intensity values (cps) as shown, in order to avoid the overlapping of such peaks on the overlying trace. In these cases, the intensity (cps) of a non-cut peak was also plotted in order to help the interpretation of the results. Since the sodium chloride peak ($31.72^\circ 2\theta$) is only present in the traces of SC experiment, its intensity is not important. Thus, the real intensity of sodium chloride peak was not plotted when the peak was cut.

Comparison between the whole rock (WR) diffraction patterns for the weathering materials (N, HS, HT and SC) generally shows that the intensities of the peaks of the latter tend to be weaker, probably due to degradation of the mineral species due to weathering resulting in less coherent mineral reflectors. Furthermore, in the SC traces the high percentage of NaCl present in the material attenuates the peaks of other minerals, being only possible to identify those with higher intensities. Accordingly, the most important peaks of the mineral phases identified in the figures were essentially referenced in the whole rock traces (WR) according to the legend presented in Fig. 7.5.

Sodium chloride peaks (27.37° and $31.72^\circ 2\theta$) identified in the diffraction traces of SC experiment result from saturation of samples with a solution containing this reagent. Therefore, the presence of this compound does not reflect any mineralogical change occurred on the materials during testing.

It was found from the analysis of the data of all samples that the natural exposure and simulated ageing tests did not significantly change the mineralogical composition of the materials. The most notable mineralogical change occurred in the materials subjected to the HS experiment, showing the diffraction traces the presence of gypsum formed due to the reaction between H_2SO_4 and carbonates. A qualitative evaluation, for all samples, of the changes recorded in mineralogical composition, between unweathered samples and the materials subjected to the various weathering experiments is presented in the following paragraphs. As gypsum occurs in all tested samples no further reference is made to its occurrence in the materials subjected to the HS experiment.

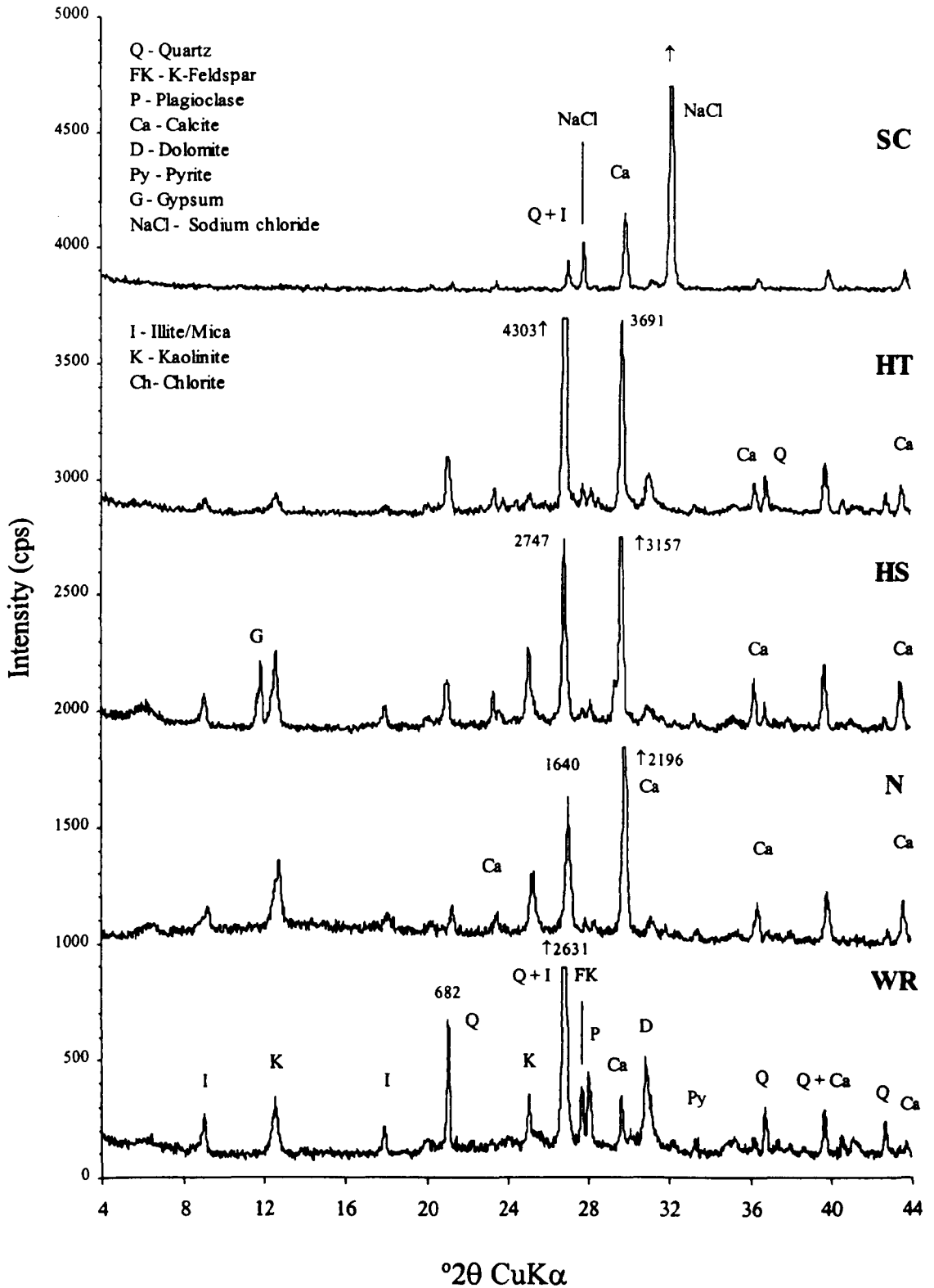


Fig. 7.5 - XRD traces of sample 83 referring to whole rock (WR) and to the materials subjected to natural exposure (N) and simulated ageing tests (HS, HT and SC).

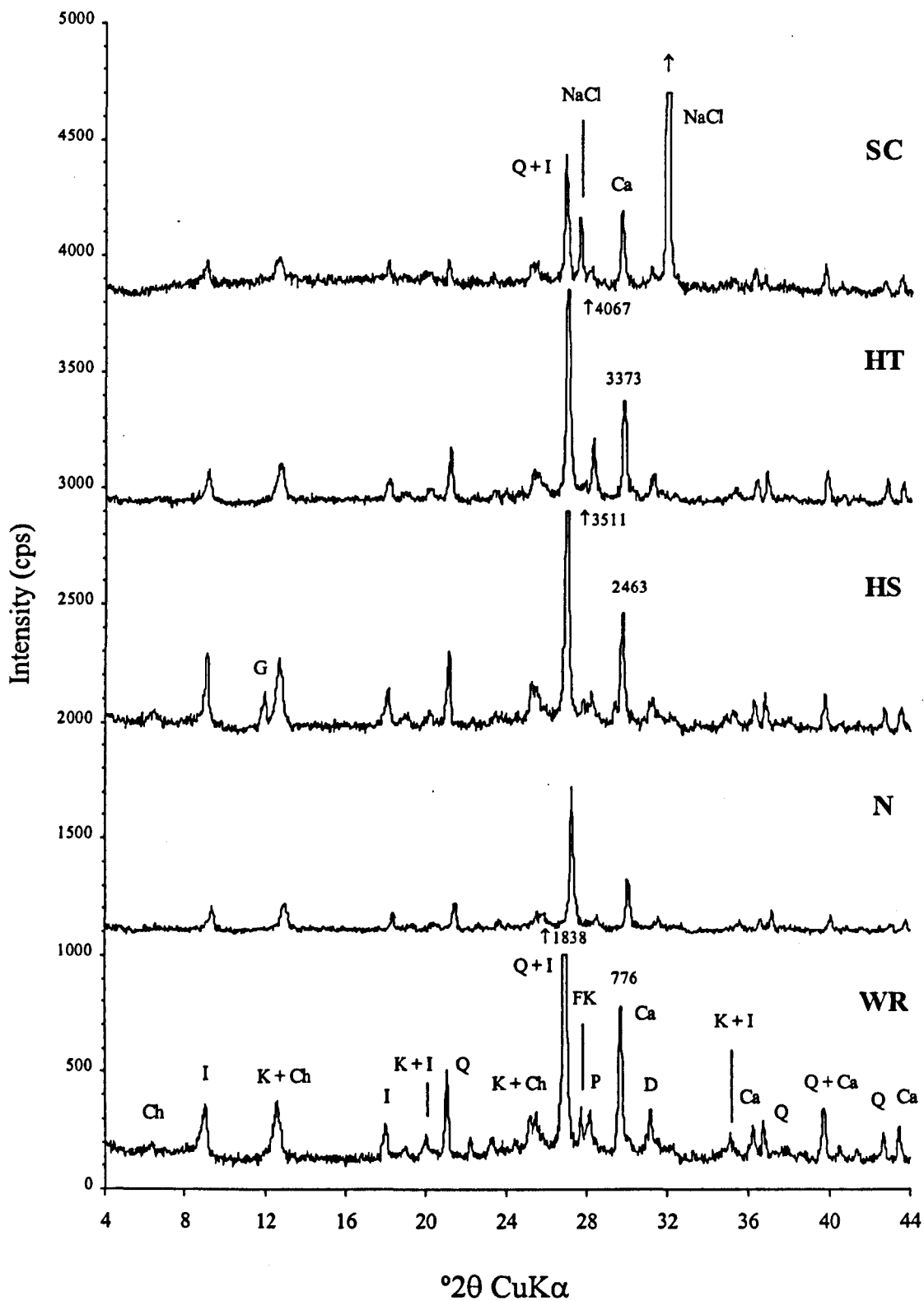


Fig. 7.6 - XRD traces of sample 114 referring to whole rock (WR) and to the materials subjected to natural exposure (N) and simulated ageing tests (HS, HT and SC).

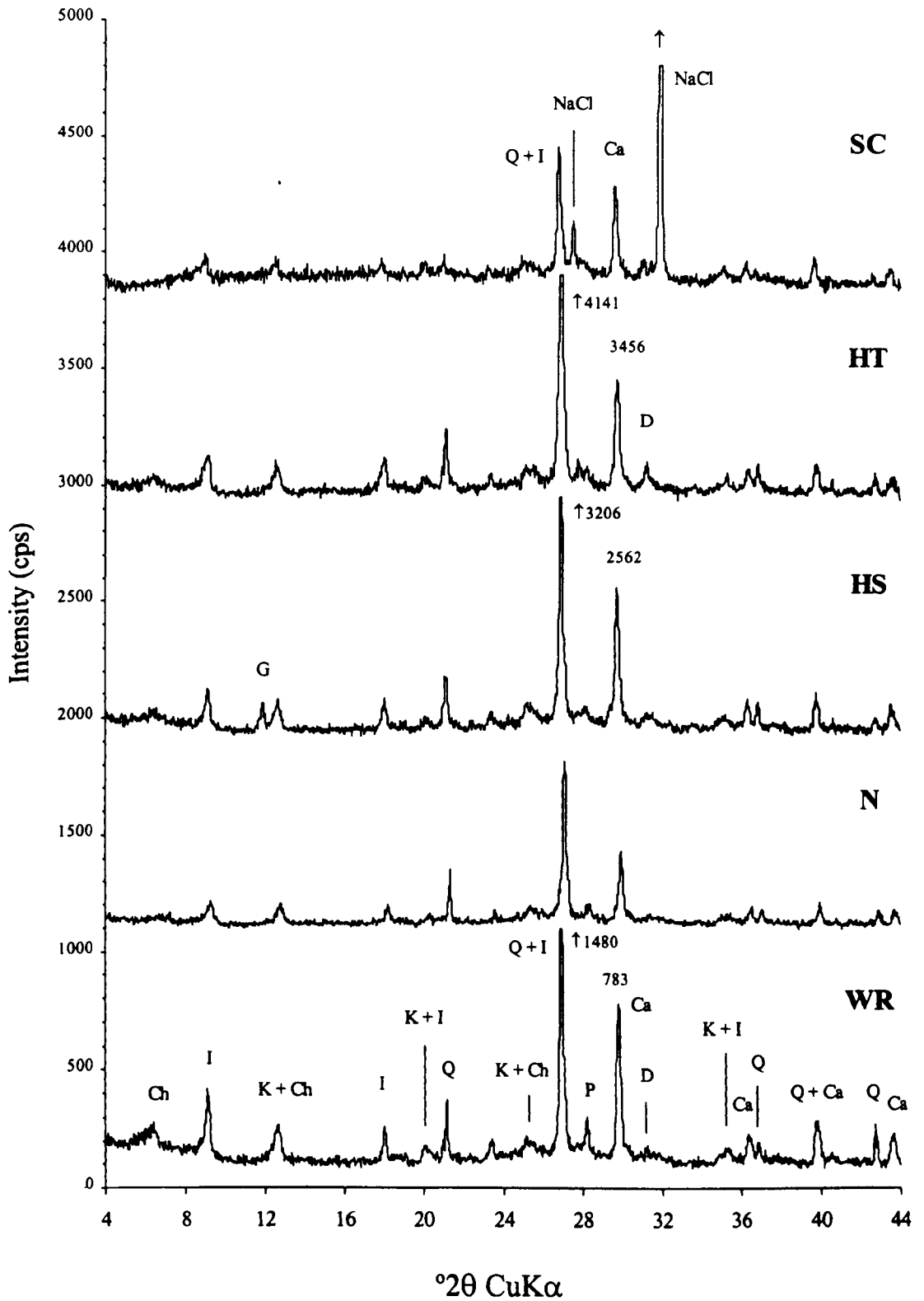


Fig. 7.7 - XRD traces of sample 283 referring to whole rock (WR) and to the materials subjected to natural exposure (N) and simulated ageing tests (HS, HT and SC).

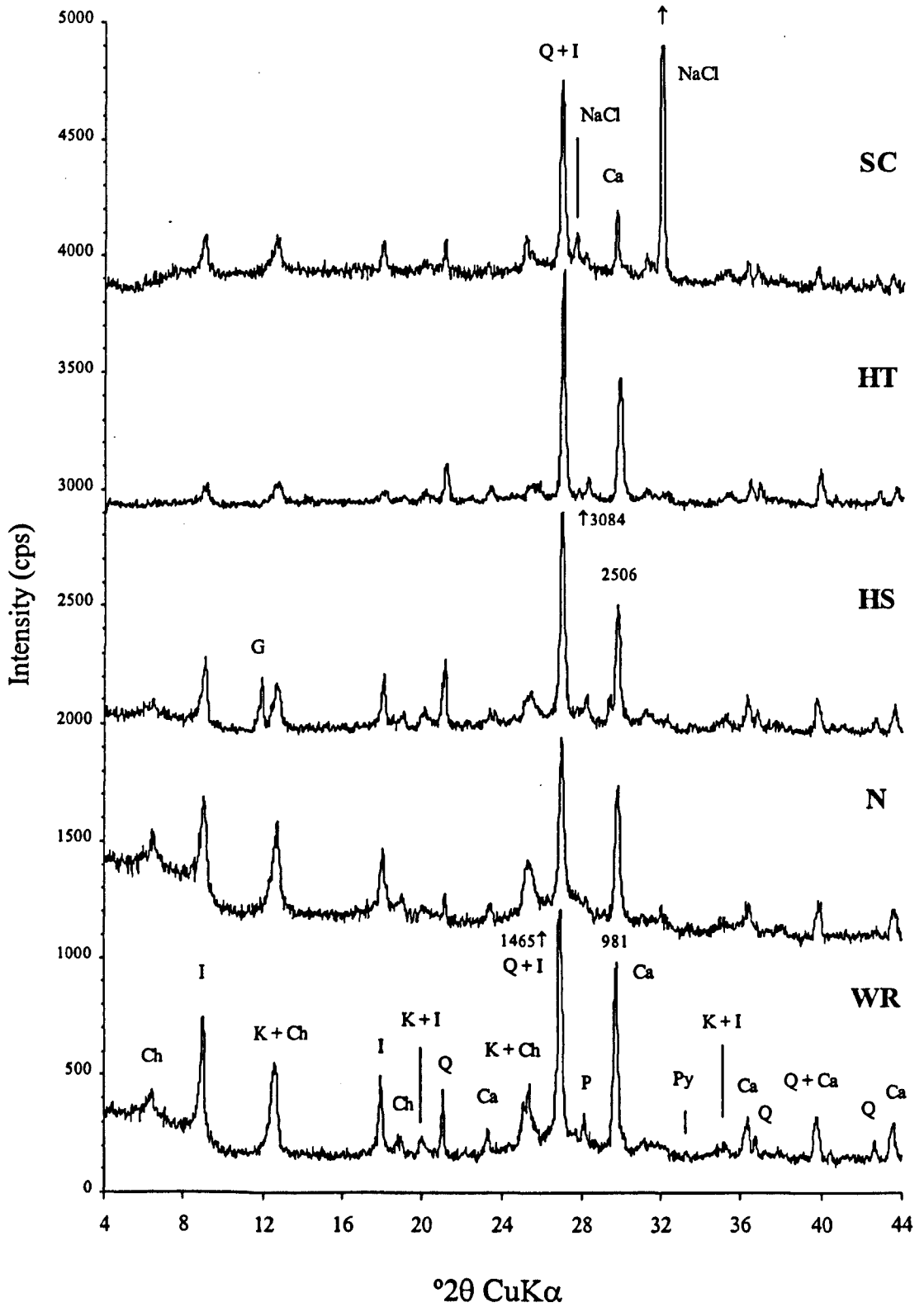


Fig. 7.8 - XRD traces of sample 286 referring to whole rock (WR) and to the materials subjected to natural exposure (N) and simulated ageing tests (HS, HT and SC).

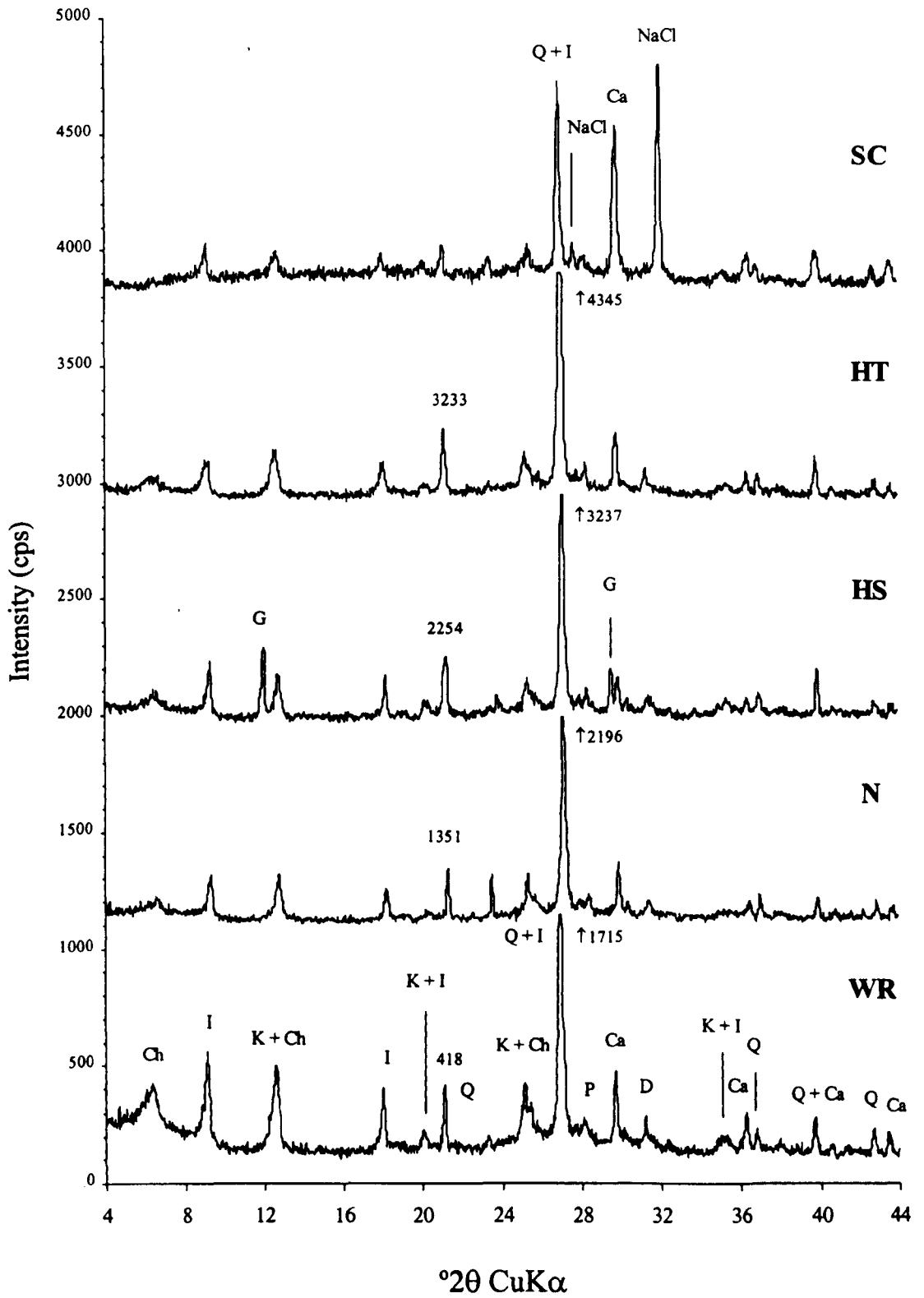


Fig. 7.9 - XRD traces of sample 333 referring to whole rock (WR) and to the materials subjected to natural exposure (N) and simulated ageing tests (HS, HT and SC).

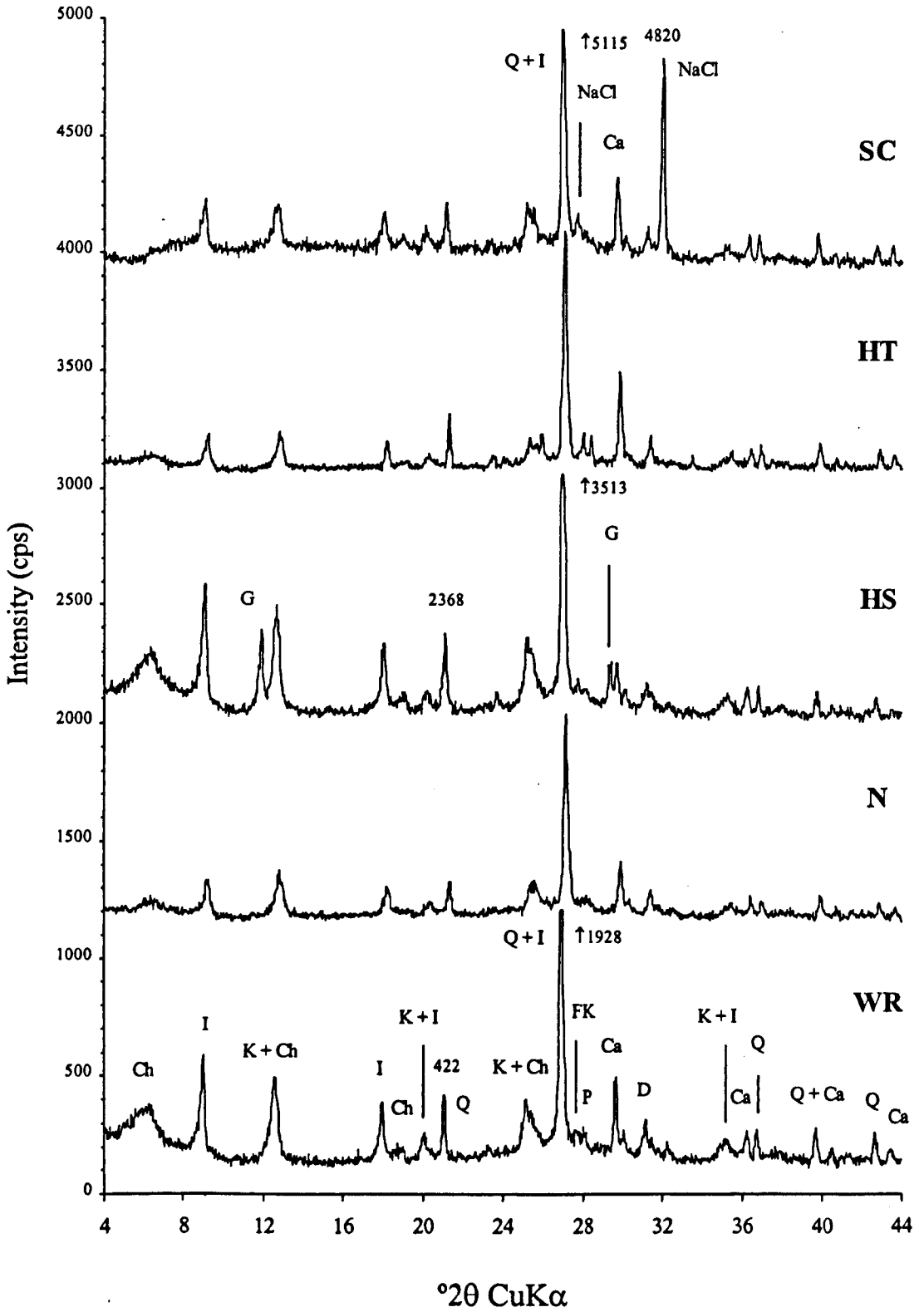


Fig. 7.10 - XRD traces of sample 336 referring to whole rock (WR) and to the materials subjected to natural exposure (N) and simulated ageing tests (HS, HT and SC).

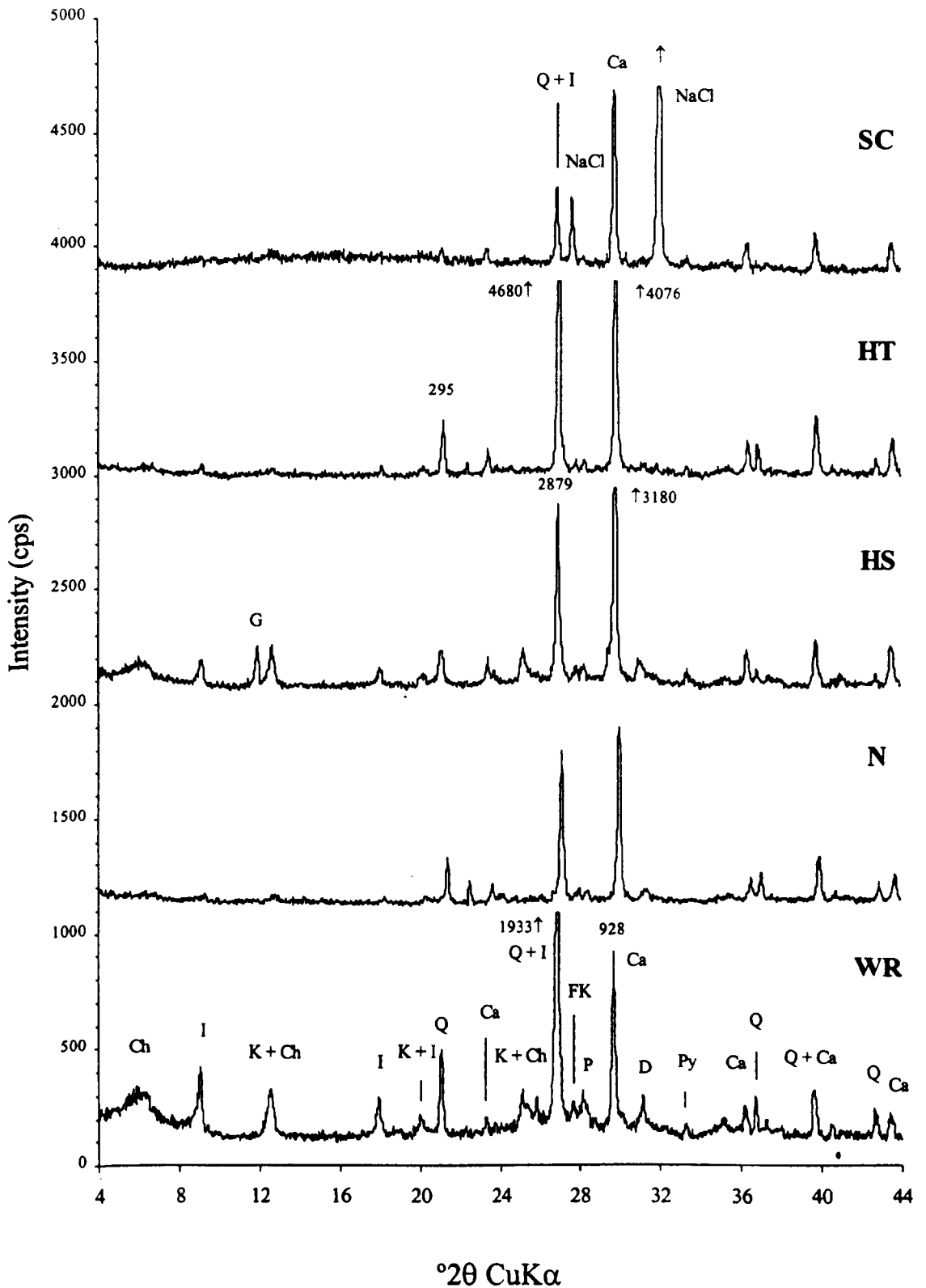


Fig. 7.11 - XRD traces of sample 342 referring to whole rock (WR) and to the materials subjected to natural exposure (N) and simulated ageing tests (HS, HT and SC).

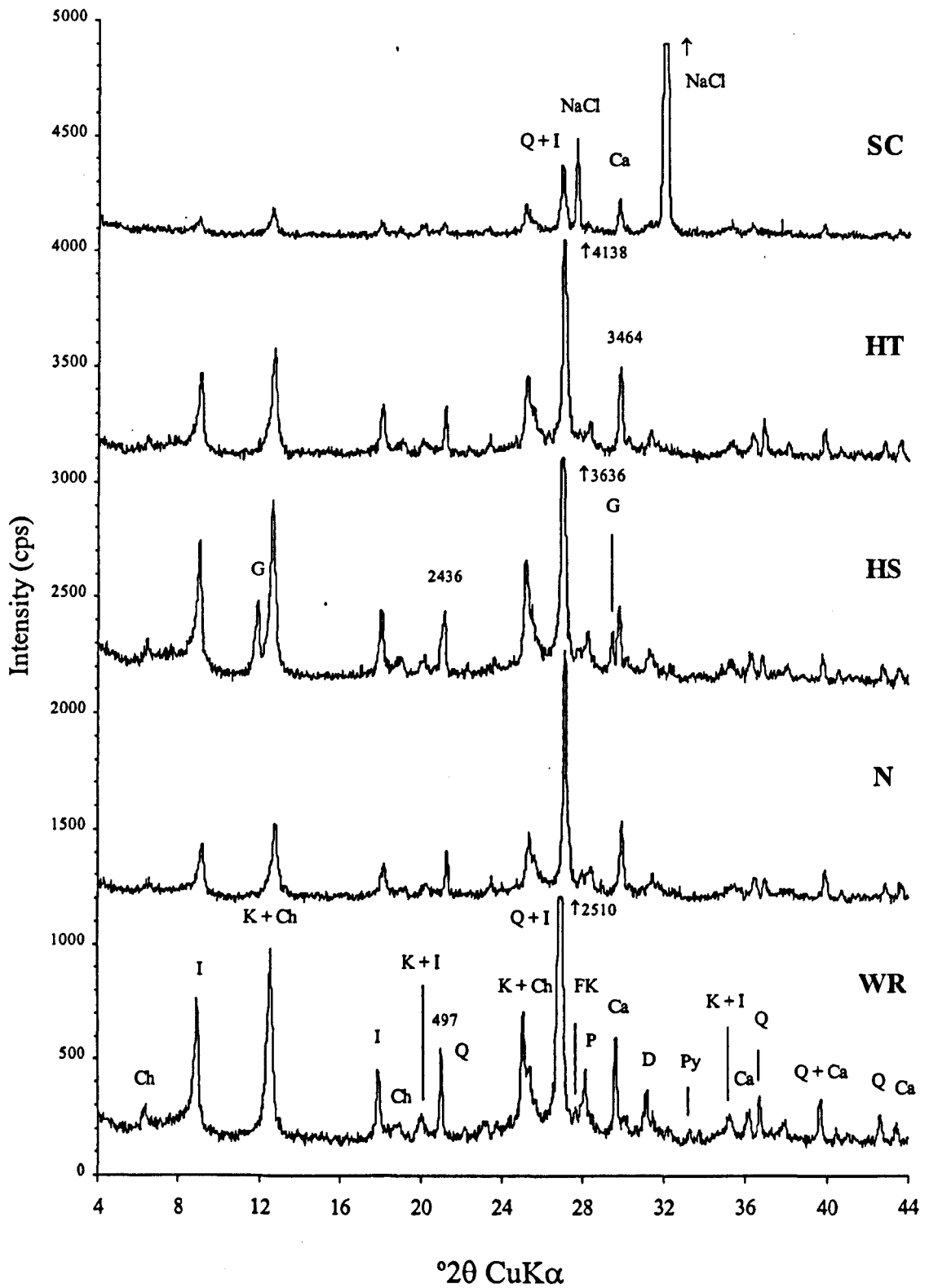


Fig. 7.12 - XRD traces of sample 431 referring to whole rock (WR) and to the materials subjected to natural exposure (N) and simulated ageing tests (HS, HT and SC).

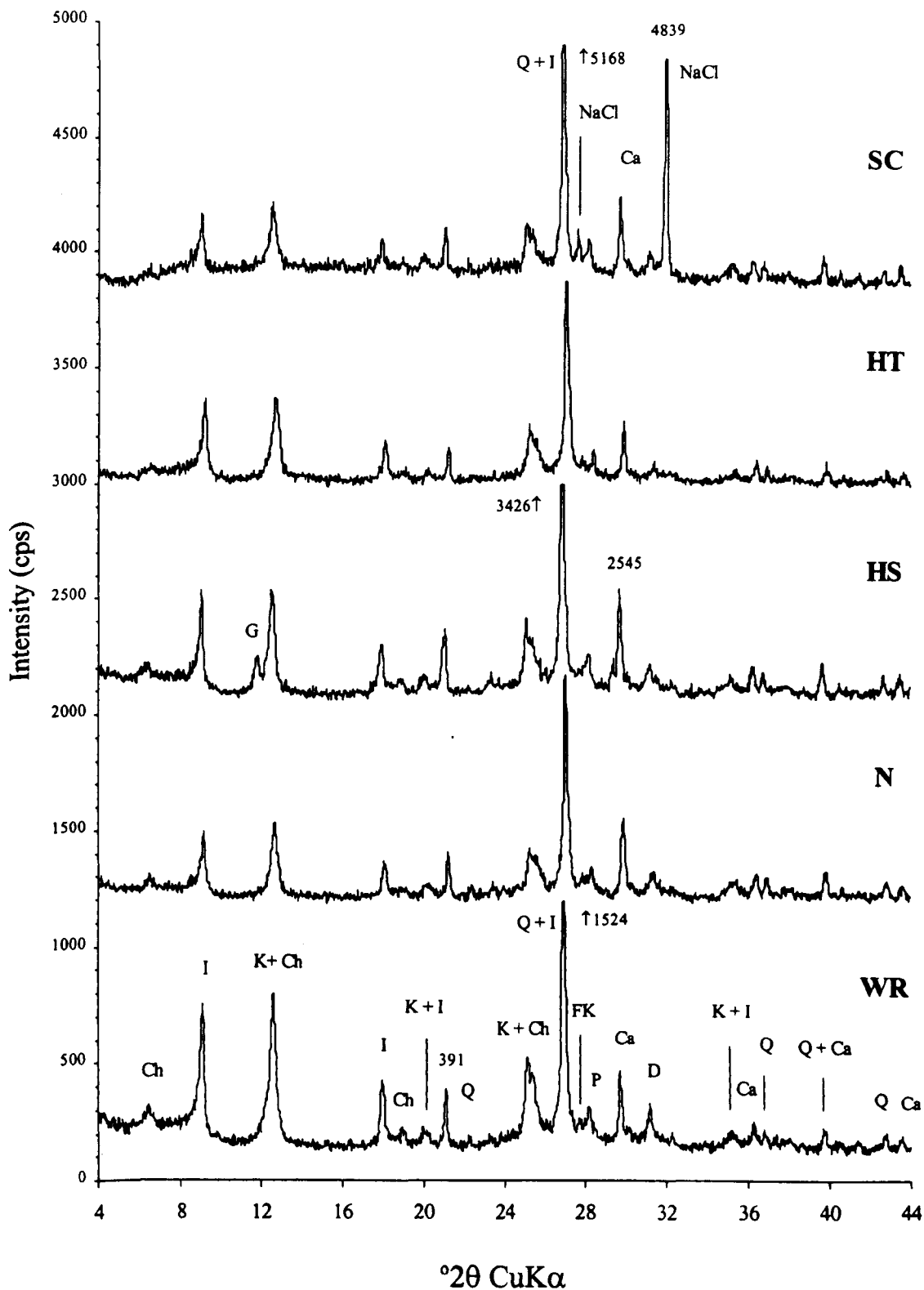


Fig. 7.13 - XRD traces of sample 441 referring to whole rock (WR) and to the materials subjected to natural exposure (N) and simulated ageing tests (HS, HT and SC).

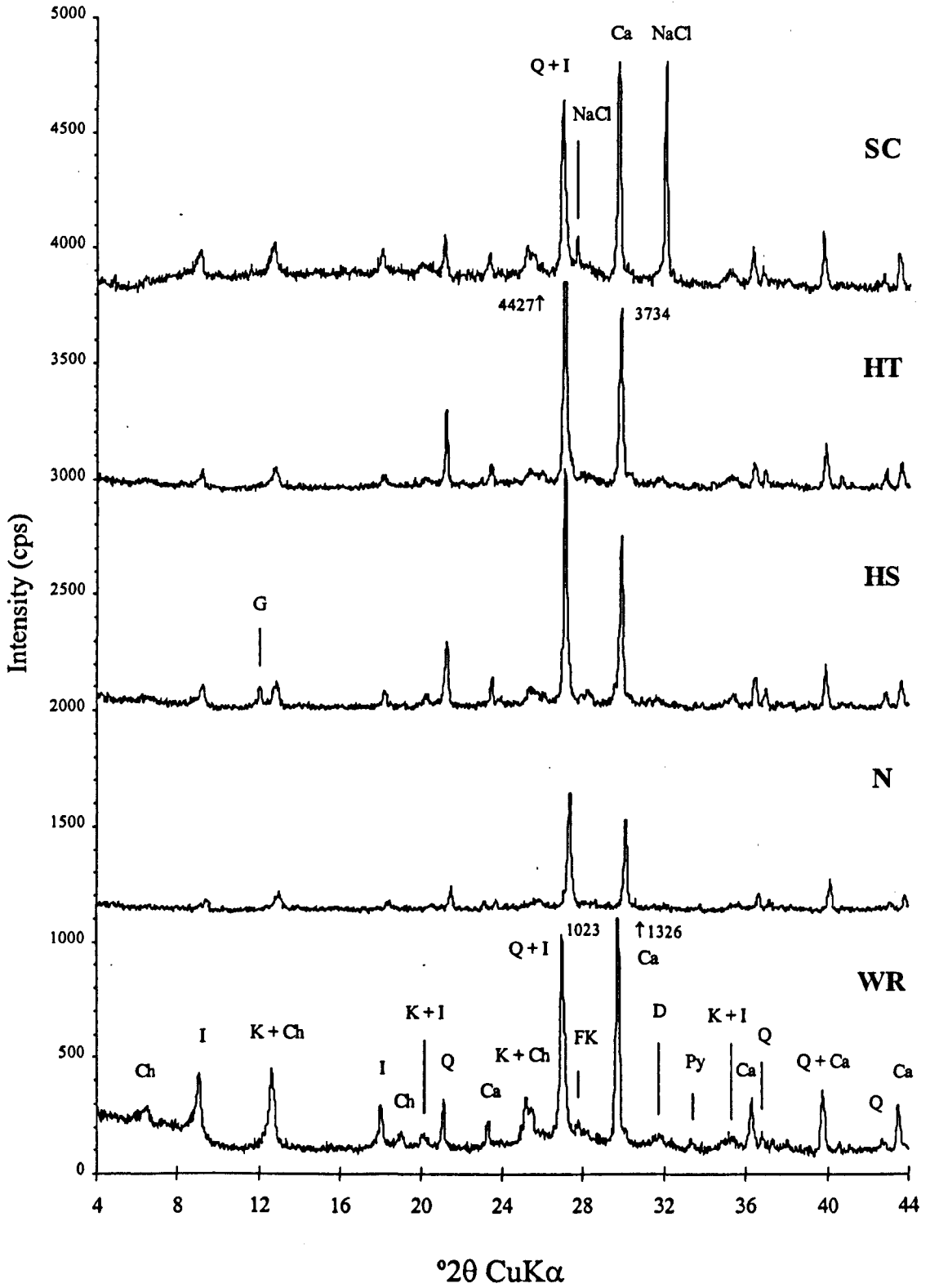


Fig. 7.14 - XRD traces of sample OB2 referring to whole rock (WR) and to the materials subjected to natural exposure (N) and simulated ageing tests (HS, HT and SC).

From the traces for sample 83 presented in Fig. 7.5 it can be seen that the whole rock sample and the weathered materials are composed chiefly of quartz, feldspars (K-feldspar and plagioclase), calcite, dolomite, pyrite, illite and kaolinite. The higher heights of the calcite peaks in the traces of the weathered materials may reflect a slight compositional variation that was not detected during the sample selection for weathering experiments.

The diffraction patterns for sample 114 presented in Fig. 7.6 show that the whole rock sample and the weathered materials are constituted mainly of quartz, feldspars (K-feldspar and plagioclase), calcite, dolomite, kaolinite, illite and chlorite. The evanescence of the K-feldspar peak ($27,50^\circ 2\theta$) in the HT trace is probably due to a compositional variation that was not identified during the sample selection of the fragments used for this experiment.

From the diffraction traces for sample 283 presented in Fig. 7.7 it can be seen that the whole rock sample and the weathered materials are composed essentially of quartz, plagioclase, calcite, dolomite, illite, kaolinite and chlorite. Slight compositional variations in the test samples selected for the HT experiment probably explains the higher intensity of the dolomite peak ($30,99^\circ 2\theta$) in the HT trace.

The diffraction traces for sample 286 presented in Fig. 7.8 show that the whole rock sample and the weathered materials are formed chiefly of quartz, plagioclase, calcite, pyrite, illite, kaolinite and chlorite.

From the diffraction patterns for sample 333 presented in Fig. 7.9 it can be seen that the whole rock sample and the weathered materials are composed mainly of quartz, plagioclase, calcite, dolomite, kaolinite, illite and chlorite. In the HS trace the reduction of calcite and dolomite peak intensities reflects the dissolution of these minerals caused by the H_2SO_4 treatment.

The traces for sample 336 presented in Fig. 7.10 show that the whole rock sample and the weathered materials are composed chiefly of quartz, feldspars (K-feldspar and plagioclase), calcite, dolomite, illite, kaolinite and chlorite. The intensities of the calcite

and dolomite peaks are also reduced in the HS trace which reflects the dissolution of these minerals due to the H₂SO₄ treatment.

The diffraction traces for sample 342 presented in Fig. 7.11 show that the whole rock sample and the weathered materials are constituted mainly of quartz, feldspars (K-feldspar and plagioclase), calcite, dolomite, pyrite, illite, kaolinite and chlorite. In the naturally weathered sample the intensities of the illite, kaolinite and chlorite peaks have been reduced and the pyrite peak has been eliminated.

The diffraction patterns for sample 431 presented in Fig. 7.12 show that the whole rock sample and the weathered materials are composed chiefly of quartz, feldspars (K-feldspar and plagioclase), calcite, dolomite, pyrite, illite, kaolinite and chlorite.

The traces for sample 441 presented in Fig. 7.13 show that the whole rock sample and the weathered materials are formed mainly of quartz, feldspars (K-feldspar and plagioclase), calcite, dolomite, pyrite, illite, kaolinite and chlorite.

The diffraction patterns for sample OB2 presented in Fig. 7.14 show that the whole rock sample and the weathered materials are composed chiefly of quartz, K-feldspar, calcite, dolomite, pyrite, illite, kaolinite and chlorite. The N, HS and SC traces show a reduction in clay minerals (illite, kaolinite and chlorite) peak intensities.

7.3.3 - Geochemical analysis of the weathered samples by XRF

Geochemical analyses by X-ray fluorescence were carried out on all samples subjected to the weathering experiments. The purpose of these analyses was to evaluate possible changes in major elements during the weathering experiments. The geochemical composition (major elements) and the loss of ignition values for whole rock samples (WR) and for weathered materials (N, HS, HT and SC) are presented in Table 7.3. The percentages of the major elements presented in Table 7.3 were recalculated in accordance with the methodology described in 5.2.2.3. These results are also presented graphically in Figs. 7.15 to 7.24 which more clearly shows the oxide phase changes which have occurred during the course of the weathering experiments.

It was found that, except for Na_2O , in general the percentages of the main oxides are lower in the materials subjected to the SC experiment than those determined in the whole rock samples (WR) and in the other weathered materials (N, HS and HT). The high percentages of Na_2O and Cl^* found are evidence of the contamination with sodium chloride of the rocks subjected to the SC experiment. Furthermore, they prove that sodium chloride was not completely destroyed and removed during the phases of preparation of the samples and fusion of the disks. Moreover, the higher loss of ignition values determined for SC samples were also a consequence of the presence of NaCl which gave rise to a relative decrease in the proportions of the other oxides. Therefore, compositional differences determined for the materials subject to the SC experiment result mainly from the contamination of the samples with the NaCl solution used during testing rather than changes caused by the chemical alteration of the mineral species present.

The analysis of the geochemical composition of the samples subjected to the HS experiment shows higher SO_3 percentages caused probably by the partial decomposition of the gypsum (formed due to the H_2SO_4 treatment) during the phases of sample preparation and fusion of the disks.

In the following paragraphs, a qualitative evaluation of the changes in the geochemical compositions of whole rock samples (WR) for samples subjected to the various weathering experiments is presented. As the geochemical aspects already referred to regarding the HS and SC experiments are common to almost all tested samples, they were not dealt with again. Therefore, only the features related to other compositional changes are discussed.

* The Cl percentage in the WR samples and in the weathered materials subjected to the other weathering experiments is negligible.

Table 7.3 - Recalculated geochemical composition of whole rock samples (WR) and of weathered materials (N, HS, HT and SC).

Sample	SiO ₂	TiO ₂	Al ₂ O ₃	Fe ₂ O ₃	MnO	MgO	CaO	Na ₂ O	K ₂ O	P ₂ O ₅	SO ₃	Cl	Total	Loss on ignition (%)
83	56.03	0.72	12.59	3.71	0.04	2.88	7.43	0.97	2.80	0.09	0.27		87.53	12.47
83N	47.43	0.38	9.45	1.99	0.04	1.72	17.22	1.14	1.88	0.10	1.02		82.37	17.63
83HS	47.82	0.35	9.07	1.98	0.00	1.39	15.87	1.26	2.12	0.08	4.59		84.53	15.47
83HT	47.46	0.45	9.49	2.11	0.05	2.90	15.66	1.06	2.00	0.11	1.51		82.80	17.20
83SC	20.26	0.29	4.41	1.51	0.05	1.16	22.13	4.43	1.05	0.11	2.10	8.28	65.78	34.22
114	49.03	0.76	14.81	4.98	0.06	2.65	9.77	0.77	2.90	0.12	0.12		85.97	14.03
114N	47.34	0.66	16.37	4.86	0.06	3.47	8.95	1.42	2.83	0.08	0.45		86.49	13.51
114HS	48.56	0.68	15.05	4.89	0.06	2.74	8.90	1.10	2.74	0.10	2.51		87.33	12.67
114HT	47.54	0.70	15.69	4.84	0.06	3.10	9.37	1.29	2.91	0.09	1.15		86.74	13.26
114SC	35.89	0.56	11.23	4.37	0.05	2.01	7.53	5.95	2.20	0.12	1.13	6.30	77.34	22.66
283	42.60	0.68	13.00	4.59	0.08	2.26	15.89	0.68	2.57	0.11	0.22		82.68	17.32
283N	45.70	0.67	16.20	5.08	0.05	3.16	10.44	0.80	2.87	0.11	0.01		85.09	14.91
283HS	41.58	0.58	14.42	5.00	0.07	2.37	13.83	0.89	2.57	0.10	2.14		83.55	16.45
283HT	45.03	0.68	15.60	6.12	0.07	2.74	10.85	1.67	2.86	0.10	0.01		85.73	14.27
283SC	29.85	0.51	10.15	4.11	0.05	1.55	7.08	7.06	2.06	0.13	0.41	10.42	73.38	26.62
286	43.06	0.64	13.22	5.06	0.08	2.48	14.82	0.78	2.65	0.12	0.21		83.12	16.88
286N	42.30	0.58	13.88	5.12	0.07	3.16	13.88	0.95	2.21	0.12	0.50		82.77	17.23
286HS	42.85	0.61	14.96	4.85	0.06	2.82	11.80	0.84	2.65	0.12	3.45		85.01	14.99
286HT	43.97	0.60	13.51	4.97	0.08	2.75	13.25	1.20	2.42	0.11	1.11		83.97	16.03
286SC	30.36	0.45	8.84	4.56	0.08	1.91	12.58	5.60	1.79	0.10	1.15	6.12	73.54	26.46
333	53.86	0.83	17.11	4.93	0.03	2.32	5.92	0.70	3.55	0.11	0.22		89.58	10.42
333N	52.43	0.85	17.65	4.89	0.04	2.54	6.27	0.81	3.52	0.10	0.01		89.11	10.89
333HS	51.36	0.78	17.40	4.78	0.05	2.53	5.32	0.66	3.18	0.08	4.21		90.35	9.65
333HT	51.91	0.79	17.90	4.61	0.04	2.76	6.65	0.65	3.39	0.11	0.01		88.82	11.18
333SC	37.36	0.62	12.17	3.68	0.03	1.71	4.12	8.21	2.46	0.11	0.01	7.03	77.51	22.49
336	50.17	0.85	19.18	5.17	0.04	3.22	5.64	0.24	3.68	0.09	0.05		88.33	11.67
336N	49.69	0.68	19.77	4.56	0.04	3.44	5.55	0.59	3.51	0.09	0.10		88.02	11.98
336HS	49.36	0.69	20.38	4.54	0.04	3.80	4.70	0.93	3.47	0.07	1.04		89.02	10.98
336HT	48.55	0.67	17.15	4.82	0.04	2.93	8.73	0.42	3.17	0.10	1.29		87.87	12.13
336SC	38.18	0.59	13.18	3.62	0.03	2.03	5.18	6.49	2.62	0.10	2.06	6.93	81.01	18.99
342	53.86	0.82	14.01	4.36	0.04	2.51	8.40	0.79	3.02	0.09	0.53		88.43	11.57
342N	41.50	0.35	8.56	2.56	0.05	1.57	19.86	0.77	1.77	0.09	2.69		79.77	20.23
342HS	42.49	0.31	8.05	2.46	0.05	1.63	18.85	1.40	1.90	0.11	4.86		82.11	17.89
342HT	38.70	0.41	8.34	2.88	0.05	1.61	20.88	0.86	1.75	0.09	3.78		79.35	20.65
342SC	27.51	0.35	5.53	3.17	0.04	0.85	16.77	5.45	1.41	0.12	6.56	7.23	74.99	25.01
431	51.31	0.95	18.72	4.96	0.03	2.58	5.09	0.94	3.38	0.10	0.19		88.25	11.75
431N	46.92	0.77	19.67	5.04	0.05	3.56	6.74	1.16	3.19	0.10	0.01		87.21	12.79
431HS	48.07	0.89	18.55	5.03	0.04	2.52	5.94	0.84	3.32	0.10	3.23		88.53	11.47
431HT	46.04	0.75	19.98	4.89	0.04	2.96	7.07	1.09	3.45	0.10	0.25		86.62	13.38
431SC	35.50	0.68	14.76	4.45	0.04	1.87	5.79	6.60	2.68	0.11	1.00	5.93	79.41	20.59
441	47.61	0.84	19.01	5.84	0.07	3.24	6.07	0.79	3.39	0.07	0.04		86.97	13.03
441N	47.32	0.83	18.09	5.71	0.07	2.93	7.73	0.53	3.27	0.10	0.38		86.96	13.04
441HS	46.01	0.78	18.36	5.19	0.06	3.17	7.69	1.11	3.20	0.09	1.57		87.23	12.77
441HT	47.57	0.78	18.02	6.12	0.07	3.19	6.92	1.00	3.09	0.08	0.01		86.85	13.15
441SC	39.54	0.72	14.47	4.47	0.05	2.23	5.90	5.57	2.68	0.12	0.51	5.67	81.93	18.07
OB2	44.95	0.63	13.88	4.11	0.05	1.69	14.57	0.36	3.34	0.12	0.40		84.10	15.90
OB2N	45.62	0.54	13.25	3.90	0.05	1.77	13.34	0.72	2.86	0.10	2.62		84.77	15.23
OB2HS	46.39	0.51	13.07	3.29	0.05	1.88	13.48	0.95	2.96	0.10	2.71		85.39	14.61
OB2HT	47.45	0.53	12.72	3.34	0.05	1.56	13.71	0.42	2.91	0.08	2.26		85.03	14.97
OB2SC	35.41	0.48	10.23	2.94	0.04	1.24	11.42	4.94	2.60	0.12	1.30	6.25	76.97	23.03

Sample 83 (Fig. 7.15) shows slight reductions in SiO_2 , Al_2O_3 and Fe_2O_3 percentages for the test samples subjected to N, HS and HT experiments and, together with the rock fragments, subjected to SC experiment, an increase in CaO content in relation to the composition of the whole rock sample (WR). The loss of ignition values obtained for samples 83N, 83HS and 83HT are slightly higher than the value determined for the WR sample.

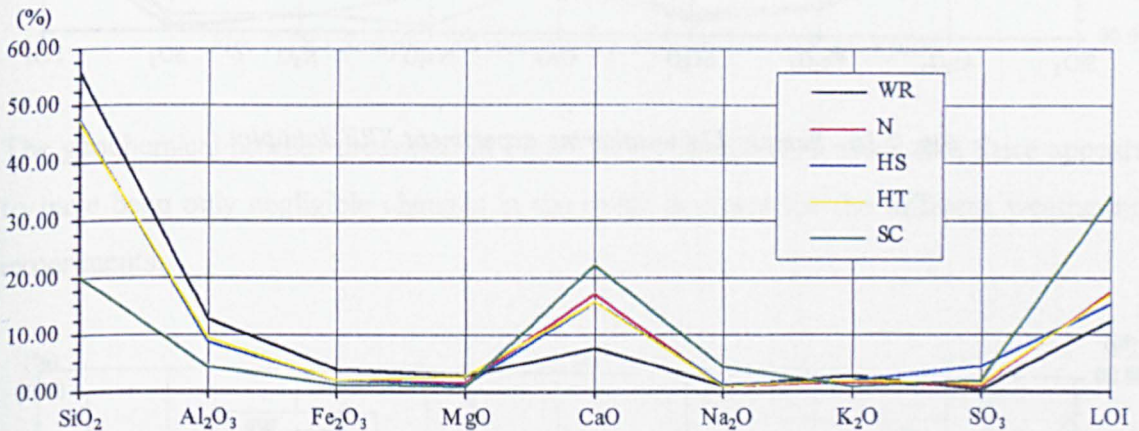


Fig. 7.15 - Sample 83 weathering experiment XRF data plot.

Sample 114 (Fig. 7.16) shows that there are only negligible changes in the oxide contents between the whole rock sample (WR) and the materials subjected to N, HS and HT experiments.

Sample 283 (Fig. 7.17) shows a slight increase in SiO_2 , Al_2O_3 and Fe_2O_3 contents for the test samples subjected to N and HT experiments and a slight reduction in CaO percentage. The evolution of the composition of the materials in the HS experiment is similar to that described already, except for SiO_2 content which is practically the same as in the whole rock sample (WR). The loss of ignition values determined for materials 283N, 283HS and 283HT are slightly lower than the value obtained for whole rock sample (WR). This fact plus the reduction in the CaO content already referred to probably reflects the dissolution of the calcite originally present in this sample.

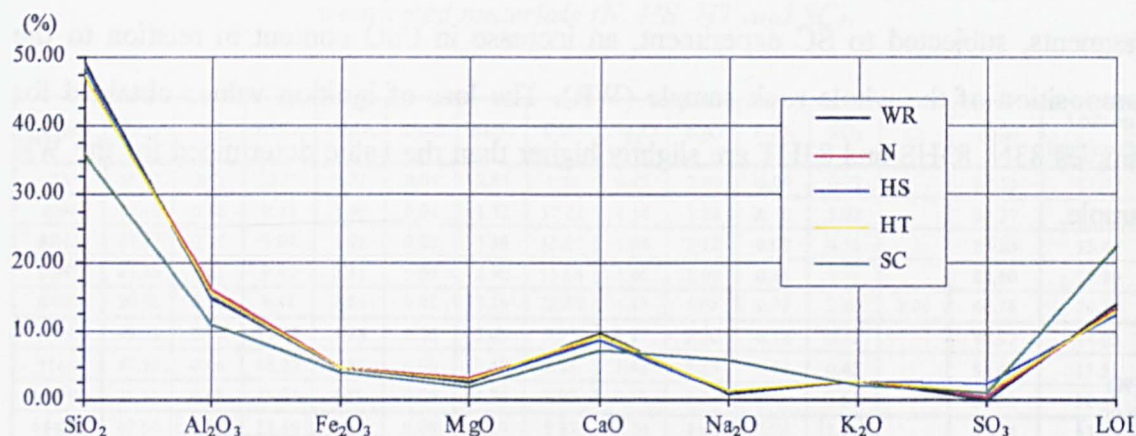


Fig. 7.16 - Sample 114 weathering experiment XRF data plot.

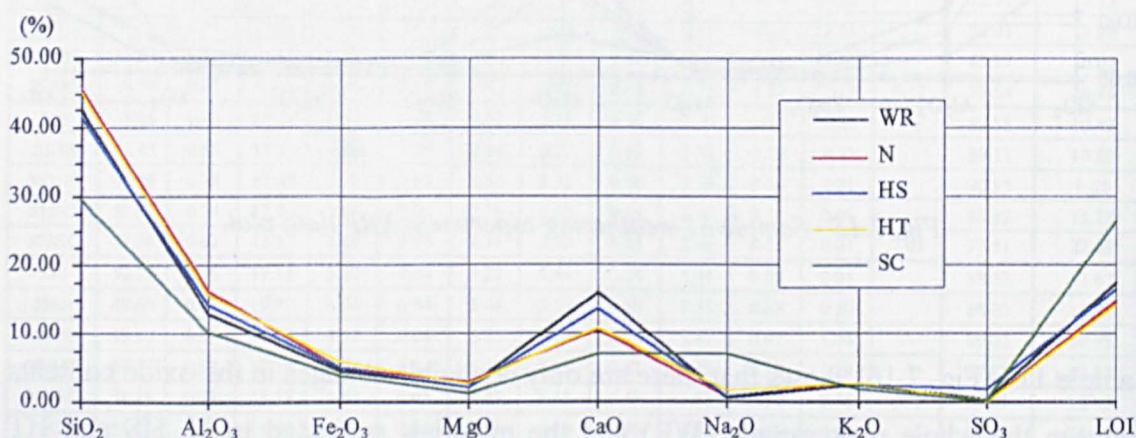


Fig. 7.17 - Sample 283 weathering experiment XRF data plot.

Sample 286 (Fig. 7.18) shows that the test samples subjected to the N, HS and HT experiments have in general lower CaO contents and loss of ignition values than in the whole rock sample (WR), which probably reflects, as in the case of the sample 283*, the dissolution of the calcite.

* Samples 283 and 286 have the highest carbonate contents of all the samples selected for the weathering experiments.

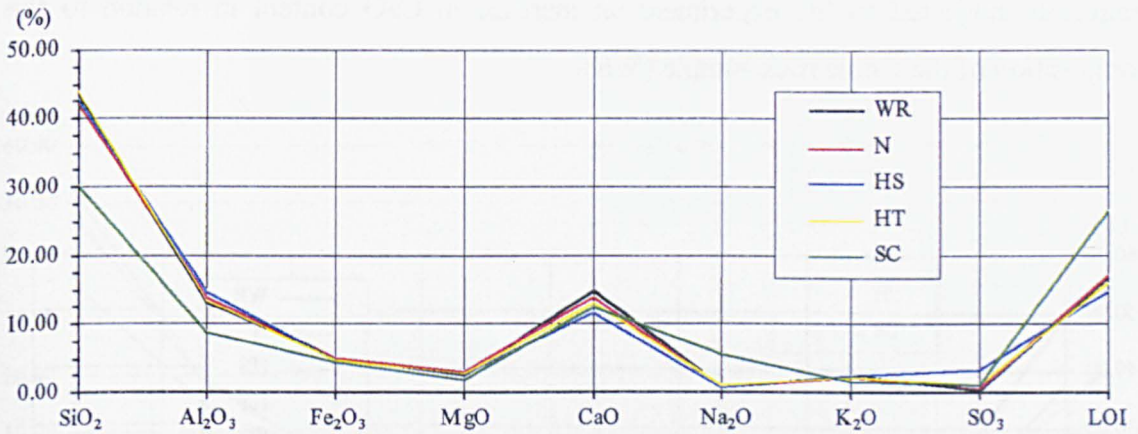


Fig. 7.18 - Sample 286 weathering experiment XRF data plot.

The geochemical profiles presented in Fig. 7.19 for sample 333 show that there appears to have been only negligible changes in the oxide contents for the different weathering experiments.

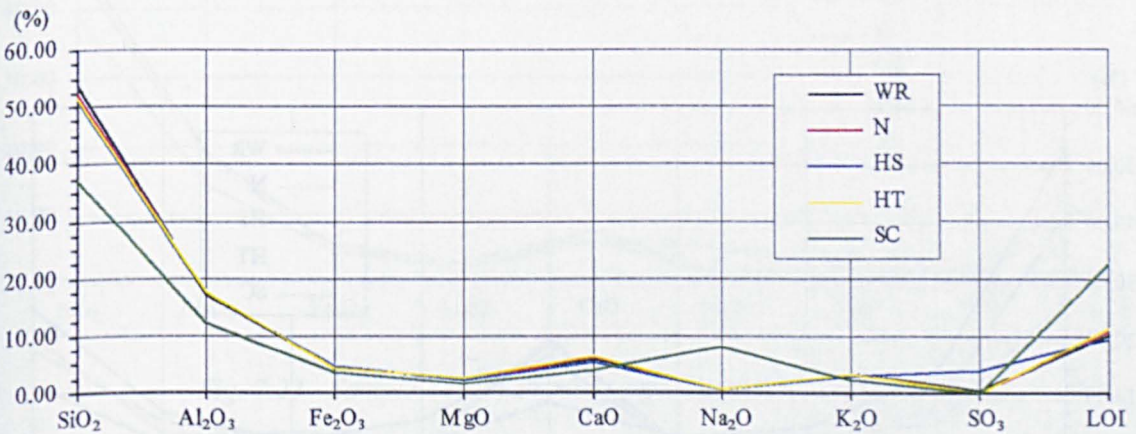


Fig. 7.19 - Sample 333 weathering experiment XRF data plot.

Sample 336 (Fig. 7.20) shows that there are only negligible changes in the oxide contents between the whole rock sample (WR) and naturally weathered materials (N). The geochemical profile corresponding to the HT experiment shows a higher CaO content than that determined in the whole rock sample (WR), which is probably due to a compositional variation that was not identified during the sample selection of the fragments used for this experiment (HT).

Sample 342 (Fig. 7.21) shows reductions in SiO₂, Al₂O₃ and Fe₂O₃ percentages for the test samples subjected to N, HS and HT experiments and together with the rock

fragments subjected to SC experiment an increase in CaO content in relation to the composition of the whole rock sample (WR).

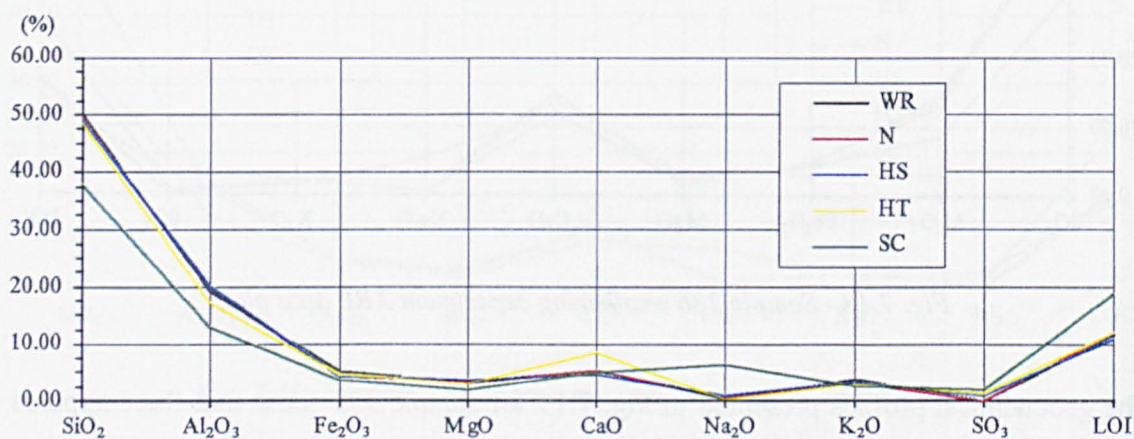


Fig. 7.20 - Sample 336 weathering experiment XRF data plot.

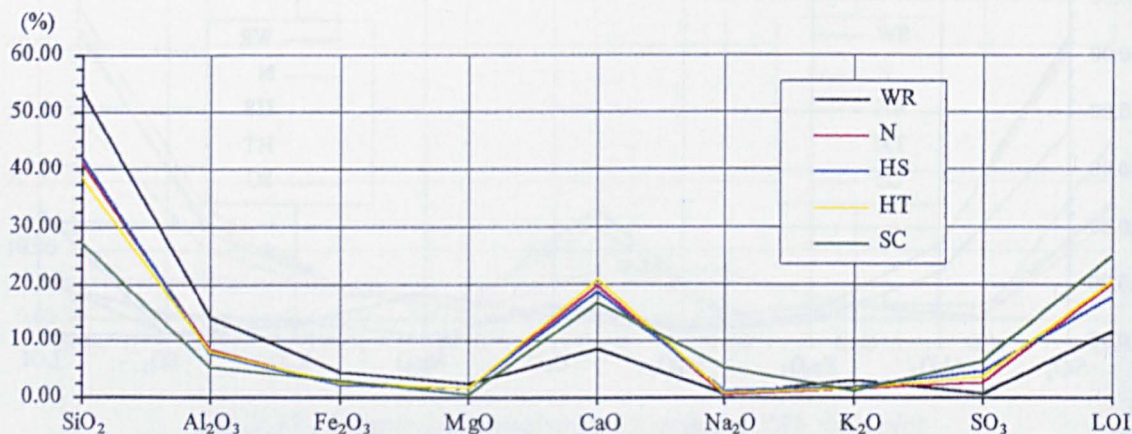


Fig. 7.21 - Sample 342 weathering experiment XRF data plot.

Sample 431 (Fig. 7.22) shows despite slight reductions in SiO₂ content that there appears to have been only negligible changes in the oxide contents for the weathered materials in the N, HS and HT experiments.

The geochemical profiles presented in Figs. 7.23 and 7.24 for samples 441 and OB2 show that there are only negligible changes in the oxide contents between the whole rock sample (WR) and the weathered materials subject to the N, HS and HT experiments.

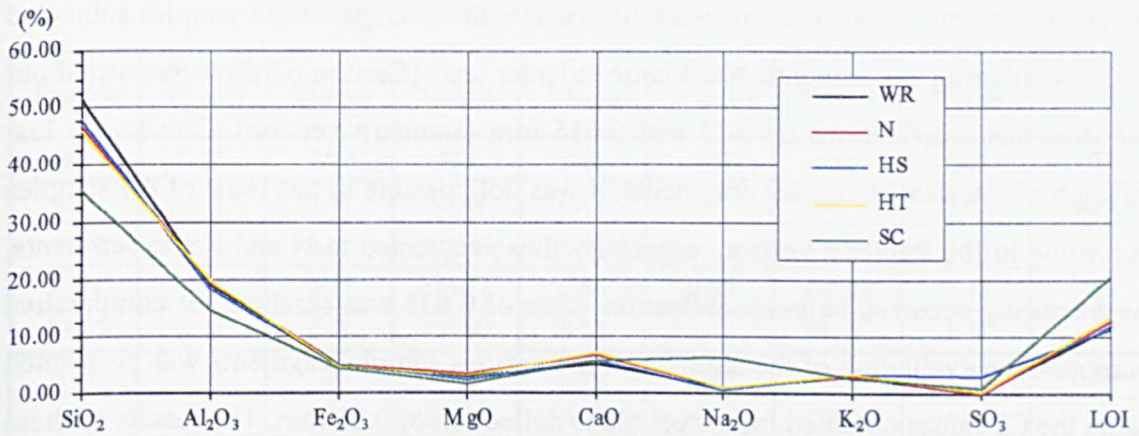


Fig. 7.22 - Sample 431 weathering experiment XRF data plot.

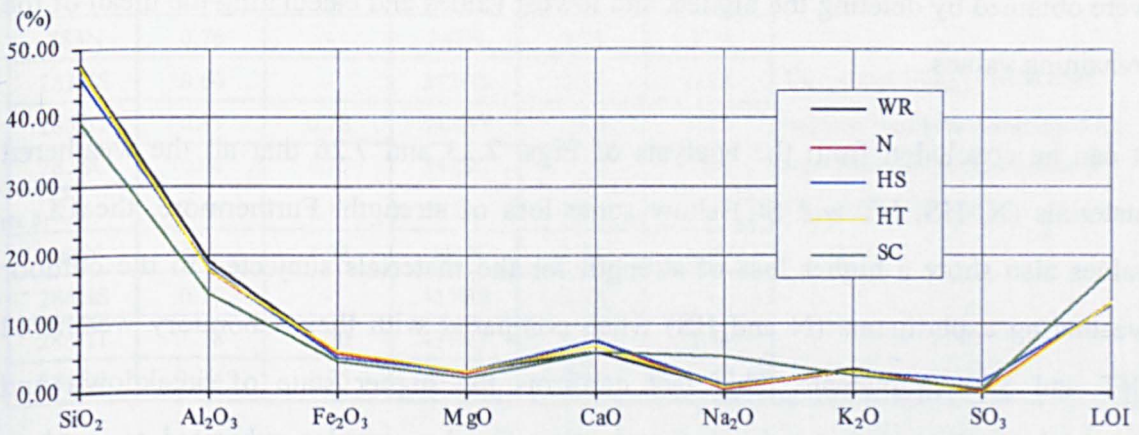


Fig. 7.23 - Sample 441 weathering experiment XRF data plot.

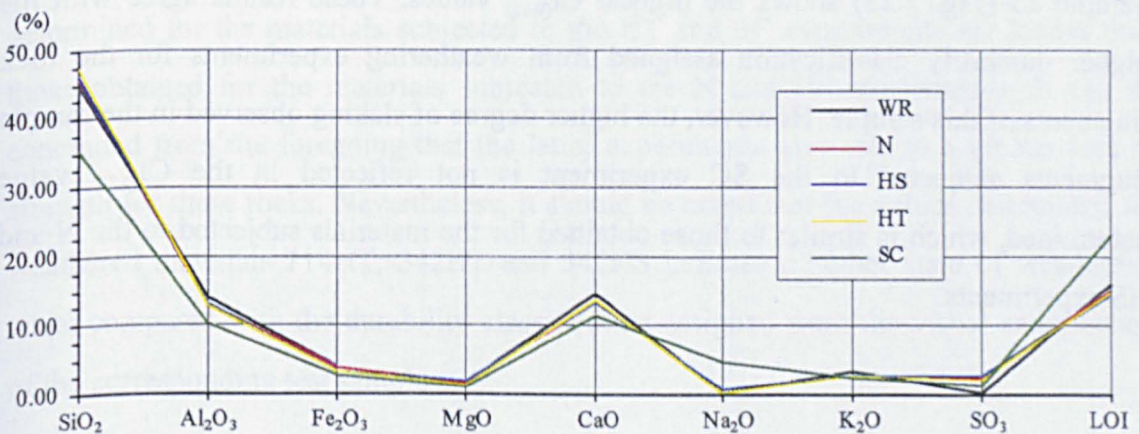


Fig. 7.24 - Sample OB2 weathering experiment XRF data plot.

7.3.4 - NCB cone indenter tests

NCB cone indenter tests were intended to evaluate the strength of the samples subjected to the weathering experiments. NCB cone indenter tests (Section 6.3.2) were carried out for steel blade deflections of 0.23 and 0.635 mm (standard version). Due to the low strength of the weathered rock fragments, it was not possible to test most of the samples according to the standard version, especially those subjected to N and HS experiments. As fracturing occurred before a deflection value of 0.635 was reached, for comparative purposes, the evaluation of the strength of the various sample fragments was performed using the CI values obtained for a steel blade deflection of 0.23 mm. The results of these tests are presented in Table 7.4 and in Figs 7.25 and 7.26. For each type of weathering experiment at least 10 specimens per sample were tested. The 'mean' values of $CI_{(0.23)}$ were obtained by deleting the highest and lowest values and calculating the mean of the remaining values.

It can be concluded from the analysis of Figs. 7.25 and 7.26 that all the weathered materials (N, HS, HT and SC) show some loss of strength. Furthermore, the $CI_{(0.23)}$ values also show a higher loss of strength for the materials subjected to the outdoor weathering experiments (N and HS) when compared with their laboratory weathered (HT and SC) equivalents. This fact confirms the higher state of breakdown and weathering assigned from visual examination for the samples subjected to outdoor weathering experiments.

Sample 83 (Fig. 7.25) shows the highest $CI_{(0.23)}$ values. These results agree with the higher durability classification assigned from weathering experiments for the rock fragments of this sample. However, the higher degree of slaking observed in the sample fragments subjected to the SC experiment is not reflected in the $CI_{(0.23)}$ value determined, which is similar to those obtained for the materials subjected to the N and HS experiments.

Table 7.4 - Cone indenter test results for the 'original' rock and for the tested materials (N; HS; HT and SC).

Sample	CI _(0.23)	CI _(0.635)	Sample	CI _(0.23)	CI _(0.635)	Sample	CI _(0.23)	CI _(0.635)
83	3.34	3.03	333	0.82	0.68	441	1.67	1.33
83N	1.37	1.44	333N	0.47	-	441N	1.05	0.98
83HS	1.44	1.31	333HS	0.49	-	441HS	1.03	-
83HT	2.52	2.27	333HT	0.56	0.60	441HT	1.36	1.38
83SC	1.51	1.51	333SC	0.53	-	441SC	1.37	1.08
114	1.88	1.51	336	1.06	0.84	OB2	1.07	0.89
114N	1.12	0.98	336N	0.92	-	OB2N	0.49	-
114HS	0.99	0.71	336HS	0.58	-	OB2HS	0.66	0.53
114HT	1.28	1.12	336HT	1.00	0.91	OB2HT	0.98	1.06
114SC	1.54	1.12	336SC	0.78	0.75	OB2SC	0.93	0.85
283	1.05	0.85	342	1.81	1.74	CI _(0.23) and CI _(0.65) - NCB cone indenter numbers determined for steel blade deflection values of 0.23 and 0.635 mm.		
283N	0.76	-	342N	0.86	0.79			
283HS	0.60	-	342HS	0.50	0.72			
283HT	0.81	0.78	342HT	1.18	0.93			
283SC	0.94	0.75	342SC	1.32	1.34			
286	1.48	1.17	431	1.85	1.37			
286N	1.18	1.07	431N	1.11	1.00			
286HS	0.70	-	431HS	0.98	-			
286HT	1.28	1.20	431HT	1.77	1.34			
286SC	1.34	1.05	431SC	0.96	0.95			

The curves presented in Fig. 7.25 for samples 114 and 342 show that the CI_(0.23) values determined for the materials subjected to the HT and SC experiments are higher than those obtained for the materials subjected to the N and HS experiments. It can be concluded from the foregoing that the latter experiments give rise to a greater loss of strength for these rocks. Nevertheless, it should be noted that the values determined for weathered materials 114HT, 342HT and 342HS indicate a higher state of weathering when compared with the durability classification assigned from the visual examination of the corresponding test samples.

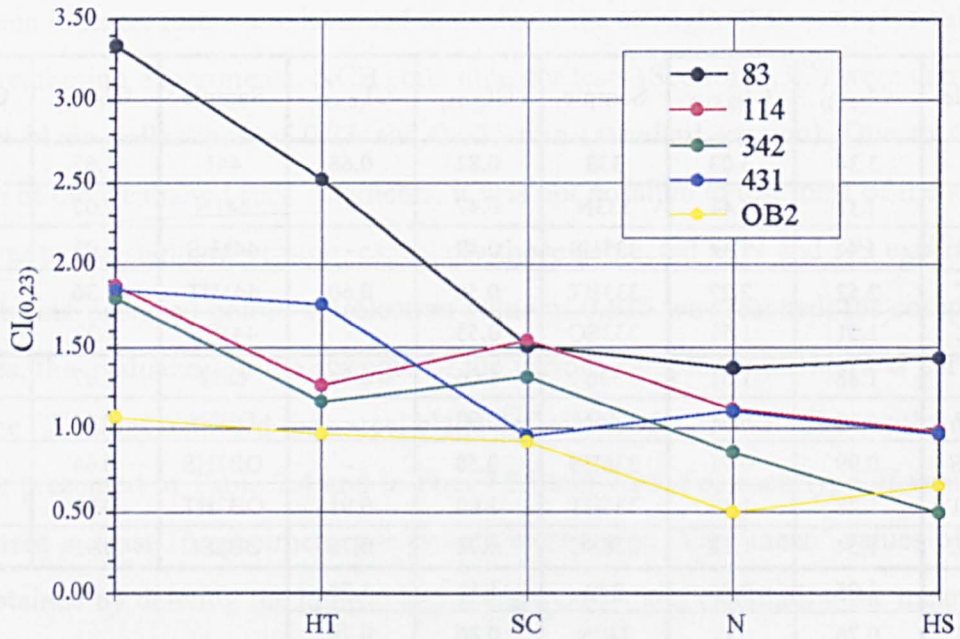


Fig. 7.25 - Comparison of the cone indenter test results determined for sandstone and siltstone samples.

The curve presented in Fig. 7.25 for sample 431 shows that $CI_{(0,23)}$ values determined for unweathered rock and for sample fragments subjected to the HT experiment are similar and significantly higher than those obtained in the other weathering experiments (N, HS and SC). These results conform with the greater state of breakdown and weathering assigned from visual examination for the samples subjected to N, HS and SC experiments.

The curve for sample OB2 presented in Fig. 7.25 shows that $CI_{(0,23)}$ values obtained for unweathered rock and for weathered materials subjected to HT and SC experiments are similar and significantly greater than those determined in the N and HS experiments. However, the high $CI_{(0,23)}$ value obtained for materials subjected to the SC experiment does not reflect the degree of breakdown exhibited by the corresponding sample fragments.

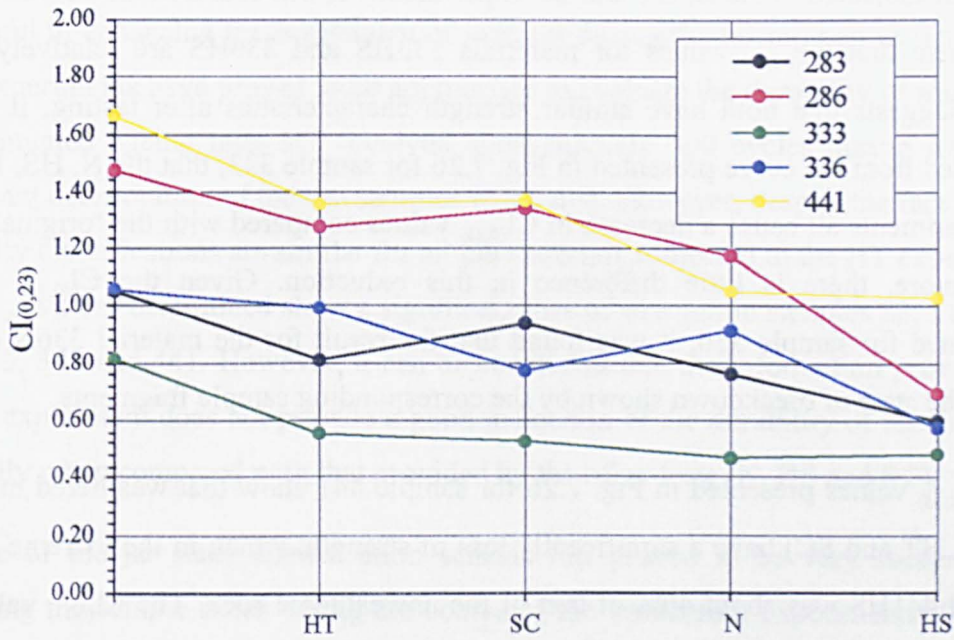


Fig. 7.26 - Comparison of the cone indenter test results determined for mudstone samples.

Samples 283 and 286 were collected from the same borehole. The former comprises a weathered material (class D), while the latter is a sound rock (class A). This explains why the $CI_{(0.23)}$ values determined in 'original' rock materials are so different, with sample 286 being significantly stronger. This fact is reflected in the results obtained for the rock fragments subjected to weathering experiments with the exception of sample 286HS, which has a $CI_{0.23}$ value similar to that of sample 283HS. It can be seen from the curves presented in Fig. 7.26 for these two samples, that the $CI_{(0.23)}$ values are higher in materials subjected to the HT and SC experiments. The distinction based on the $CI_{(0.23)}$ values between the materials subjected to the N and HS experiments does not have equivalence in the durability classification assigned for these rocks. This is especially the case of sample 286. In addition, $CI_{(0.23)}$ values for materials 283 HT and 283SC appear to indicate a greater state of weathering for the former, although this was not noted by the visual examination of the test samples.

Samples 333 and 336 also come from the same borehole. The former comprises a partially weathered material (class B) while the latter is a sound rock (class A). This fact explains the strength differences determined on 'original' rock materials and on the materials subjected to the N, HT and SC experiments. It was found in the case of the HS experiment that $CI_{(0.23)}$ values for materials 333HS and 336HS are relatively close, which suggests that both have similar strength characteristics after testing. It can be concluded from the curve presented in Fig. 7.26 for sample 333, that the N, HS, HT and SC experiments all cause a decrease in $CI_{(0.23)}$ values compared with the 'original' rock. Furthermore, there is little difference in this reduction. Given the $CI_{(0.23)}$ values determined for sample 336, it was found that the result for the material 336N did not reflect the state of breakdown shown by the corresponding sample fragments.

The $CI_{(0.23)}$ values presented in Fig. 7.26 for sample 441 show that weathered materials (N, HS, HT and SC) have a significantly loss of strength, which in the extreme case of material 441HS was about 40% of that of the unweathered rock. The $CI_{(0.23)}$ values for 441SC and 441HS do not agree with the durability classification assigned for these materials. On this basis the $CI_{(0.23)}$ value of sample 441SC is abnormally high. On the other hand, the result for material 441HS indicates a greater degree of weathering than those assigned from the visual examination of the corresponding test samples.

In conclusion, from the analysis of $CI_{(0.23)}$ values it can be stated that samples 114, 286, 431 and 441 have strength characteristics higher at the end of weathering experiments than samples 283, 333, 336, 342 and OB2. The results of the cone indenter tests do not always agree with the durability classification assigned from visual examination of the corresponding sample fragments. Therefore, the results obtained for materials 114HT, 283HT, 286HS, 342HT, 342HS and 441HS indicate a higher state of weathering than those assigned from the visual examination of the corresponding test samples, while, in the case of samples 83SC, 336N, 441SC and OB2SC, the results do not reflect the state of deterioration shown by the test samples.

7.4 - Discussion

The natural exposure (N) and simulated ageing (HS and SC) tests have proved to be successful in enhancing the breakdown of samples during the testing period. Therefore, these experiments have proved to be appropriate to evaluate the durability of mudrocks. The simulated ageing tests HT involved approximately 300 cycles during which no significant deterioration of the test samples was noted. However, despite the fact that the durability classifications are similar for all the materials subjected to the HT experiment, the $CI_{(0.23)}$ values determined show a significant loss of strength in samples 83, 114, 283, 286, 333, 342 and 441. However, it can be concluded that the information provided by the HT experiment does not provide a good indication of the durability of the materials especially when compared with that provided by the other tests (N, HS and SC).

The use of the jar slake classification scheme has proved to be very successful in describing the sample states during the course of the weathering experiments. Samples 83, 283, 336 and OB2 have achieved a level of breakdown at the end of natural weathering experiment similar to that observed in the jar slake test. Samples 83, 114, 286, 342, 431 and 441 have achieved a higher level of breakdown at the end of HS and SC experiments than that observed in the jar slake test. Previous works of several researchers (Badger *et al.*, 1956; Sasaki *et al.*, 1981; Seedsman, 1986; Taylor, 1988) have supported the idea that the main mechanisms involved in the disintegration of mudrocks are due to the effects of water. These mechanisms, which are briefly described in Chapter 2, are the physical disintegration of rocks caused by air breakage resulting from capillary suction of water into voids and breakdown caused by the effects of water on expansive clay species. Furthermore, the durability of mudrocks is also controlled by porosity, since the access of water to the interior of materials is controlled by the geometry and volume of the pore space (Sasaki *et al.*, 1981; Hongxi, 1993) and durability is also enhanced by the presence of carbonate cements (Lo *et al.*, 1978; Russel, 1982).

The data from X-ray diffraction and fluorescence analyses show that the mineralogical and geochemical changes in the samples have been minor and mainly related to the dissolution of carbonate cements. In the materials subjected to the HS experiment, the presence of gypsum also reflects this process since this compound is formed by the

dissolution of carbonate minerals due to acid (H_2SO_4) attack. The dissolution of carbonate cements also promotes the increase of porosity of materials allowing a greater water access into pores and discontinuities and to the sites of expansive clay mineral species which in turn leads to the physical disintegration of the rocks. Similarly, the removal of pyrite would have the effect of increasing porosity as well as generating acid which attacks carbonates. As far as samples 83, 342 and OB2 are concerned, the analysis of the X-ray diffraction traces and of SiO_2 , Al_2O_3 and Fe_2O_3 concentrations for the weathered materials subjected to N, HS and HT experiments also show the dissolution of chlorite (only in sample 342), iron oxides (samples 83 and 342) and to a lesser extent illitic phases.

It can be seen from the analysis of the data from cone indenter tests that this determination has proved to be successful as a strength criterion in the evaluation of the durability of the mudrocks. However, because this test is carried out on small rock fragments, the results obtained may not reflect the level of breakdown of the sample. The $CI_{(0.23)}$ values determined allowed the various samples as well as which types of weathering experiments that gave rise to a greater loss of strength characteristics of the materials to be distinguished.

Table 7.5 presents mineralogical and physical data which are considered to have a control on sample stability during the weathering experiments conducted.

Table 7.5 - Selected mineralogical and physical characteristics of the materials subjected to the weathering experiments.

Sample	N (%)	I_{ds} (%)	Carbonates (%)	TMLC (%)
83	16.3	91.9	18.4	4.5
114	14.9	77.6	19.1	15.7
283	20.2	17.0	30.6	20.8
286	15.8	82.4	32.7	19.6
333	22.3	0.0	10.3	27.0
336	15.3	12.5	9.8	29.7
342	15.8	26.5	16.8	17.1
431	11.7	66.0	12.0	12.8
441	12.3	54.4	13.5	18.8
OB2	20.6	62.4	26.5	13.4

TMLC - Total of mixed-layer clay minerals

With the exception of sample 83, the samples tested showed a great deal of breakdown at the end of the natural weathering (N) and in the HS and SC simulated ageing tests. The initial test samples were split into numerous fragments. However, it was possible to distinguish the samples according to the strength of the fragments formed and to relate the breakdown behaviour showed by the materials to their mineralogical and lithological characteristics. Accordingly, the samples tested can be subdivided into the following groups:

Calcareous Sandstone (sample 83) - Slight sample breakdown is shown by the rock fragments for this sample at the end of the weathering experiments and mainly consisted of the development of randomly orientated fractures. The principal control on breakdown is mechanical, presumably as a result of air breakage within pores and along micro-discontinuities. Furthermore, due to the low expansive clay mineral content of this sample, it is more sensitive to the effects of salt weathering than to changes in water content (wetting and drying cycles). Therefore, it can be concluded that porosity is the major control on the breakdown of this sample. The higher $CI_{(0.23)}$ values obtained for this sample also confirmed the more durable character of the rock fragments of this sample at the end of the weathering experiments. However, it should be noted that there was a loss of strength of over 50% between the unweathered rock and the materials subjected to the N, HS, and SC experiments.

Clayey mudrocks (samples 333 and 336) - These samples showed a high amount of breakdown over the initial 2 months of testing which reflected a rapid rate of breakdown. The principal control on breakdown was considered to be physico-chemical as a result of air breakage within pores and along micro-discontinuities and swelling of expansive clay minerals. The very high state of breakdown exhibited by these materials at the end of the experiments that simulated climatic slaking (alternated cycles of wetting and drying) is a reflection of the high percentage of expansive clay minerals present in these samples, as these minerals are particularly sensitive to changes in water content. Sample 336, although an unweathered mudrock, shows low strength characteristics which are similar to those of the rock materials initially weathered (sample 333). Furthermore, the larger amount of breakdown noted for the materials subjected to natural exposure experiment (N) cannot be deduced on the basis of the

$CI_{(0,23)}$ values determined. Therefore, it can be concluded that although the test samples exhibit a greater state of breakdown at the end of the said experiment, the resulting fragments do not exhibit greater loss of strength.

Calcareous mudrocks (samples 114, 283, 286, 342, 431, 441 and OB2) - The samples of calcareous siltstones (114, 342, 431 and OB2) and the samples of calcareous mudstones (283, 286 and 441) were included in the same group because it was found that they did not show a differentiated behaviour in the natural exposure and simulated ageing tests conducted. There is a moderately slow progressive rate of breakdown over the first 4 to 6 months of testing (except for sample 431 which showed that sample breakdown occurred mostly during the initial two months of testing). After this period of time the breakdown became more intense. The principal control on breakdown of these samples was apparently initially chemical with the progressive dissolution of carbonate cements (this process was most predominant in the N and HS outdoor experiments). This process allows water access into voids and discontinuities and to the sites of expansive clay mineral species, which promotes the secondary breakdown control which is physico-chemical resulting from the rock and causing slaking by clay mineral expansion and air breakage weakening. The $CI_{(0,23)}$ values determined confirmed that the materials that were initially stronger (114, 286, 431 and 441) were those whose fragments had the highest strength after the weathering experiments. However, the large loss of strength (in excess of 40%) found between unweathered rock fragments of these samples and mainly those subjected to N and HS experiments, should be noted. Sample 342 (unweathered rock) also shows a loss of strength of between 50 and 70%. These value are similar to those obtained for sample 283 which corresponds to a weathered mudrock. Samples 283 and OB2 comprise materials with initial low strength which is reflected in the $CI_{(0,23)}$ values determined on the rock fragments subjected to the various weathering experiments. However, as in the case of the previous samples, the loss of strength exhibited by these rocks after being subjected to N and HS experiments, is particularly evident.

In conclusion, the mineralogical characteristics of mudrocks control their durability allowing its knowledge to predict the rate and potential type of breakdown of these materials.

8 - GEOLOGICAL CONTROLS ON THE ENGINEERING PROPERTIES OF MUDROCKS

8.1 - Introduction

In the experimental study presented in Chapters 4, 5 and 6 of this work the mineralogical, textural, structural and geotechnical aspects of the mudrocks sampled were characterised. Based on the test data obtained from this laboratory study the present chapter is intended to determine the geological controls which govern mudrock durability.

With this objective, a linear correlation analysis between the determined mineralogical, physical and geotechnical properties for the main lithotypes present in the sampling (siltstones, mudstones and laminated mudstones) was carried out. By identifying the properties potentially of importance in controlling the behaviour of mudrocks it may be possible to design index tests that can be used to classify these materials. An attempt was accordingly made to evaluate mudrock durability via an index based on the percentage of material retained in the second cycle of the slake durability test, dry density and methylene blue adsorption value. The results obtained were compared with those determined by the application of the classification schemes currently used for assessment of mudrock durability.

Finally, the behaviour of the mudrocks in natural and cut slopes and in fills as a construction material were analysed on the basis of the information obtained from the experimental work carried out.

8.2 - Characterization of the various lithotypes studied

The studies undertaken in recent decades by numerous researchers Badger *et al.* (1956), Gamble (1971), Taylor & Spears (1981), Cripps & Taylor (1981), Hudec (1982), Russel (1982), Steward & Cripps (1983), Taylor & Smith (1986), Shakoor & Brock (1987), Taylor (1988), and Dick & Shakoor (1992) showed that the behaviour of mudrocks and their main geotechnical properties, *i.e.* durability (slaking), swelling and strength are controlled by mineralogical factors - percentage of clay minerals and particularly of expandable clay minerals, textural factors - rock fabric and porosity; structural factors - the presence or absence of lamination, microfractures and slickensides; and geological factors - lithology and degree of cementation as well as recrystallization due to diagenetic effects.

The analysis carried out in Section 6.7 concerning the whole data set showed many significant correlations between the determined geotechnical properties and some of the physical and mineralogical parameters referred to above. However, Dick & Shakoor (1992) have suggested that the correlation analysis between the various parameters must be performed separately for each lithotype included in the mudrock class. According to these researchers, this methodology makes it possible to identify the main physical and mineralogical parameters that control the geotechnical properties of separate lithological groups. This methodology was adopted in this work and the mudrocks were separated according to the lithological groups indicated by those researchers. These groups basically correspond to the lithotypes defined in the classification adopted for these rocks (see Table 3.5) and are as follows:

- argillite
- claystone

- mudstone
- mudshale (fissile/laminated mudstone)
- combined siltstone-siltshale

Since the samples collected for this work included mainly siltstones (including siltshales), mudstones and mudshales the correlation analysis performed take into account only the determined parameters for these lithotypes.

According to Dick (1992) and Swan & Sandilands (1995) linear correlation coefficients (r) greater than 0.8 reflect a strong relationship between two variables, positive values indicating direct trends and negative values inverse trends. Accordingly, the methodology adopted consisted, for each lithological group, of the selection of physical and mineralogical parameters of the samples which strongly correlate with geotechnical properties, as well as the index tests most suitable for the evaluation of those parameters. Although the source of error resulting from the small size of the sample may reduce the statistical value of the linear correlation analysis carried out, it is not considered that the main conclusions reached are significantly affected thereby.

In the construction of the linear correlation matrices only unweathered and partially weathered samples (classes A and B) were taken into consideration. Distinctly and highly weathered samples (classes C and D) were analysed separately. This methodology was adopted because it was concluded that the determined geotechnical properties for materials included in classes C and D are mostly controlled by their weathering grade. This fact prevented the inclusion of weathered sample data on the correlations between the mineralogical and physical parameters and geotechnical properties obtained for unweathered or partially weathered (classes A and B) materials with the same lithological composition. Non-indurated materials representing extremes of the lithotypes studied were also analysed separately for the same reasons. Since only single samples of calcareous sandstone (83) and oolitic limestone (345) were included, it was not possible to process their data statistically.

8.2.1 - Assessment of non-indurated materials durability

The non-indurated materials comprised samples 51, 111, 151 and 332. SEM examination of these materials revealed a loose structure (see Fig. 5.16), characterized by high porosity values. These materials have weak strength characteristics and high swelling potential. Since these samples disaggregate easily when soaked the swelling potential depends on mineralogy, particularly on expandable clay content. Non-indurated materials disaggregated very rapidly in jar slake tests with the test samples being reduced to silt and sand size debris. Slake durability test data also showed that these materials have very low durability, with percentages of retained material of less than 10% after 1000 rotations. The durability of these materials is extremely low and can be evaluated on the basis of the jar slake and slake durability tests.

8.2.2 - Assessment of weathered mudrocks durability

Weathered mudrocks include samples 81, 152, 153, 162, 163, 283, 285 and 294. All these materials show high susceptibility to swelling and slaking and have low strength characteristics. Since these rocks are very prone to slaking the major control on swelling potential is the mineralogy, principally the amount of expandable clay minerals present.

All the weathered mudrock samples subjected to the jar slake tests showed rapid and extremely extensive deterioration (I_j between 6 and 8) with a reduction of the test fragments to sand and/or fine gravel size debris in samples 81, 152 and 162. The results of slake durability tests mainly those obtained after 1000 rotations, also show the low durability of these rocks. It was found that expandable clay minerals content and void distribution (including micro-discontinuities) are the two major controls on durability of these materials and can be evaluated on the basis of the I_{d2} , I_{d5} and I_j indices.

8.2.3 - Assessment of mudstone durability

The mudstones analysed comprised samples 286, 296, 333, 336 and 436. The correlation coefficient matrix is presented in Table 8.1, and the most significant correlations are as follows:

- I_{d2} : Carb ($r = 0.89$), w_{ad95} ($r = -0.92$), I_j ($r = -0.88$);
- I_{d5} : Carb ($r = 0.94$), TECM ($r = -0.83$), w_{ad95} ($r = -0.98$), MBA ($r = -0.84$), PI ($r = -0.88$), $CI_{(0.635)}$ ($r = 0.81$), I_j ($r = -0.93$);
- I_j : Carb ($r = -0.80$), TCM ($r = 0.85$), ρ_d ($r = -0.87$), w_{ad95} ($r = 0.90$), PI ($r = 0.80$), $CI_{(0.635)}$ ($r = -0.84$), I_{d2} ($r = -0.88$), I_{d5} ($r = -0.93$);
- ϵ_s : σ_c ($r = -0.88$);
- σ_c : TECM ($r = -0.87$), ϵ_s ($r = -0.88$);
- $CI_{(0.23)}$: TECM ($r = -0.95$), ρ_d ($r = 0.82$), N ($r = -0.87$), w_{ad95} ($r = -0.84$), MBA ($r = -0.82$), PI ($r = -0.88$);
- $CI_{(0.635)}$: TECM ($r = -0.93$), ρ_d ($r = 0.89$), N ($r = -0.89$), w_{ad95} ($r = -0.86$), MBA ($r = -0.82$), PI ($r = -0.87$), I_{d2} ($r = 0.81$), I_j ($r = -0.84$).

Plots of selected correlations are presented in Fig. 8.1 to 8.16.

Additional strong correlations exist between the percentage of expansive clay minerals (TECM) and adsorbed water content at 95% HR ($r = 0.92$), methylene blue adsorption value ($r = 0.95$) and the plasticity index ($r = 0.98$). It is also seen that porosity affects the I_{d2} values ($r = -0.77$).

It must also be pointed out that a correlation exists between the carbonate content and the I_{d2} values. SEM examination of the samples included in this lithological group revealed, in fact, that the carbonates in these materials occur preferentially disseminated in the matrix in the form of cement (see Table 5.10), which explains the control of this mineralogical feature on the mudstone durability.

Table 8.1 - Correlation coefficient matrix between the main mineralogical, physical and geotechnical parameters determined for mudstones.

	Q+F	Carb	TCM	TECM	LOI	% Clay	G_s	ρ_d	N	w_{ad95}	MBA	PI	ϵ_s	ϵ_z	ΔV	σ_c	$CI_{(0.23)}$	$CI_{(0.635)}$	I_{20}	I_{40}	I_j
Q+F	1.00	-0.66	-0.05	0.18	-0.82	-0.59	-0.68	-0.05	0.22	0.43	0.15	0.22	0.60	0.05	0.17	-0.47	-0.12	-0.08	-0.65	-0.52	0.26
Carb		1.00	-0.72	-0.70	0.97	-0.03	0.21	0.46	-0.41	-0.91	-0.77	-0.79	-0.68	-0.54	-0.58	0.44	0.55	0.58	0.89	0.94	-0.80
TCM			1.00	0.79	-0.53	0.54	0.37	-0.62	0.41	0.83	0.90	0.87	0.32	0.61	0.56	-0.33	-0.67	-0.74	-0.61	-0.79	0.85
TECM				1.00	-0.56	-0.04	0.02	-0.67	0.70	0.92	0.95	0.98	0.63	0.30	0.22	-0.87	-0.95	-0.93	-0.76	-0.83	0.76
LOI					1.00	0.16	0.35	0.38	-0.38	-0.82	-0.61	-0.65	-0.67	-0.41	-0.49	0.42	0.44	0.45	0.88	0.88	-0.70
% Clay						1.00	0.59	0.02	-0.37	0.00	0.20	0.08	-0.32	0.62	0.58	0.59	0.17	0.07	0.25	0.02	0.18
G_s							1.00	-0.56	0.29	-0.02	0.03	0.00	-0.74	-0.19	-0.24	0.97	-0.17	-0.29	0.06	-0.01	0.37
ρ_d								1.00	-0.93	-0.69	-0.56	-0.62	0.05	0.22	0.25	0.67	0.82	0.89	0.75	0.72	-0.87
N									1.00	0.67	0.50	0.59	0.12	-0.40	-0.43	-0.68	-0.87	-0.89	-0.77	-0.68	0.74
w_{ad95}										1.00	0.93	0.96	0.63	0.39	0.37	-0.66	-0.84	-0.86	-0.92	-0.98	0.90
MBA											1.00	0.99	0.65	0.57	0.49	-0.70	-0.82	-0.82	-0.70	-0.84	0.77
PI												1.00	0.67	0.47	0.40	-0.76	-0.88	-0.87	-0.77	-0.88	0.80
ϵ_s													1.00	0.52	0.50	-0.88	-0.43	-0.34	-0.52	-0.55	0.23
ϵ_z														1.00	0.98	-0.03	0.00	-0.02	-0.11	-0.34	0.23
ΔV															1.00	0.05	0.08	0.06	-0.15	-0.35	0.23
σ_c																1.00	0.93	0.86	0.56	0.54	-0.51
$CI_{(0.23)}$																	1.00	0.99	0.76	0.77	-0.76
$CI_{(0.635)}$																		1.00	0.78	0.81	-0.84
I_{20}																			1.00	0.96	-0.88
I_{40}																				1.00	-0.93
I_j																					1.00

Q+F - Sum of percentages of quartz plus feldspar; Carb - Percentage of carbonates; TCM - Total clay minerals content (%); TECM - Expandable clay minerals content (%); LOI - Loss on ignition (%); % Clay - Percentage of material < 2 μ m determined in slake durability test residue; G_s - Grain specific gravity; ρ_d - Dry density (Mg.m⁻³); N - Porosity (%); w_{ad95} - Water adsorption at 95%RH (%); MBA - Methylene blue adsorption value (g/100g fines); PI - Plasticity index (%); ϵ_s - Swelling strain measured on remoulded specimens (%); ϵ_z - Swelling strain measured on intact specimens perpendicular to stratification (%); ΔV - Volumetric strain (%); σ_c - Ultimate compressive stress (MPa); $CI_{(0.23)}$ and $CI_{(0.635)}$ - Cone indenter numbers measured for steel blade deflections, respectively, of 0.23 and 0.635 mm; I_{20} and I_{40} - Percentages of retained material in slake durability test, respectively, after 200, 400 and 1,000 rotations (%); I_j - Jar slake index.

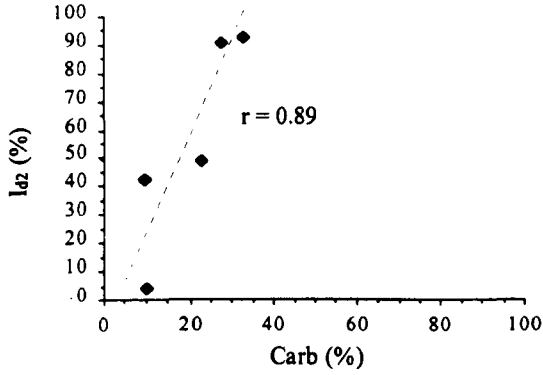


Fig. 8.1 - Plot of I_{d2} versus Carb (%).

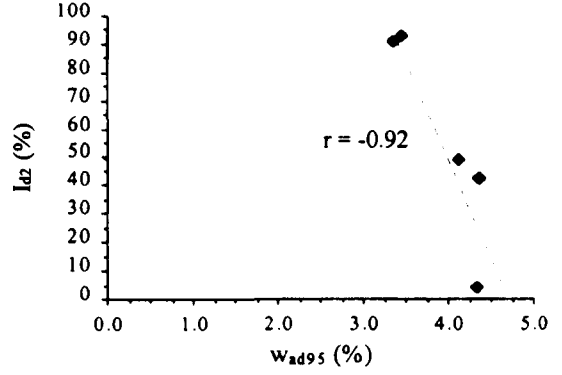


Fig. 8.2 - Plot of I_{d2} versus w_{ad95} .

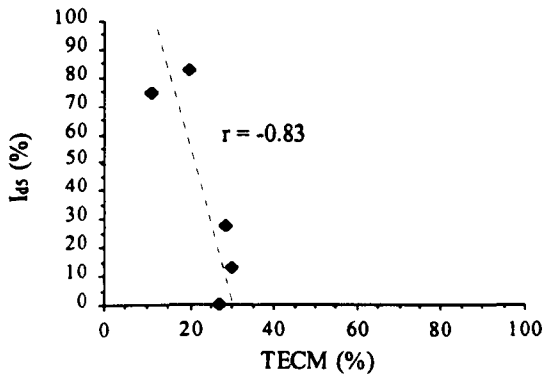


Fig. 8.3 - Plot of I_{d5} versus TECM (%).

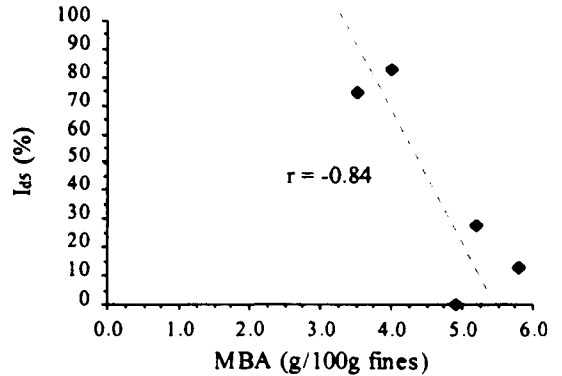


Fig. 8.4 - Plot of I_{d5} versus MBA.

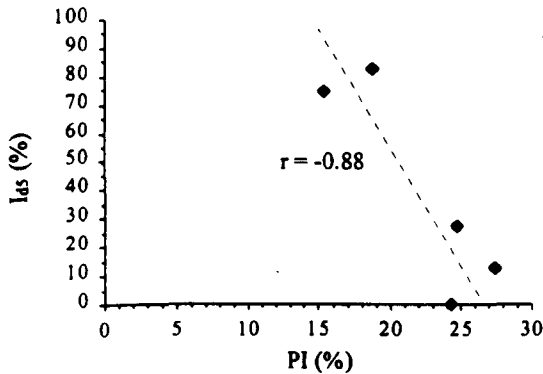


Fig. 8.5 - Plot of I_{d5} versus PI.

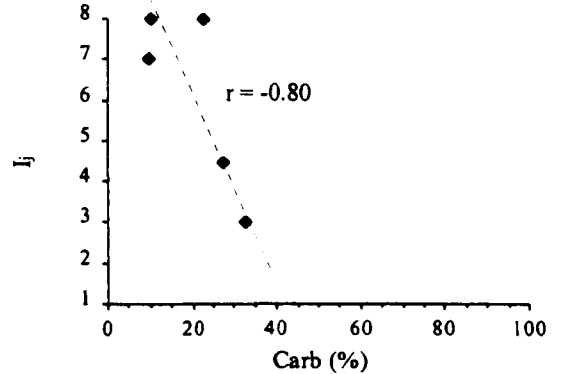


Fig. 8.6 - Plot of I_j versus Carb (%).

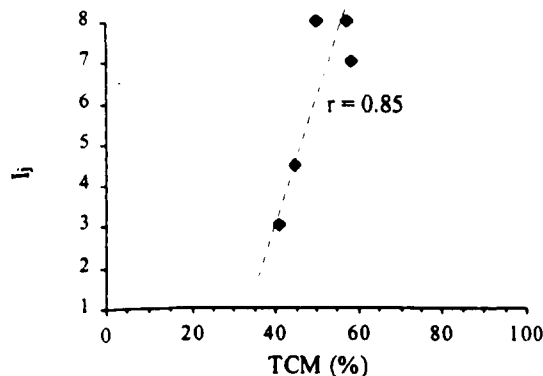


Fig. 8.7 - Plot of I_j versus TCM (%).

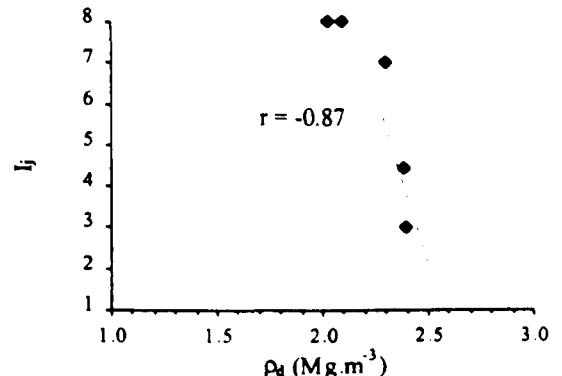


Fig. 8.8 - Plot of I_j versus ρ_d .

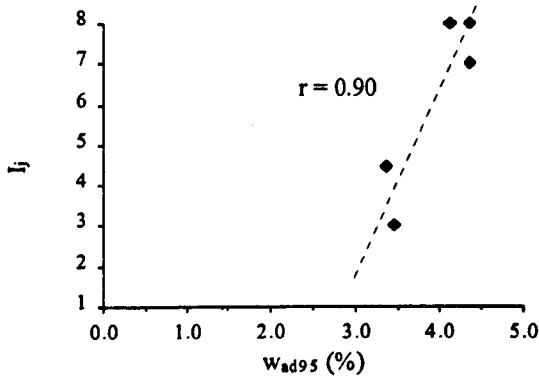


Fig. 8.9 - Plot of I_j versus w_{ad95} .

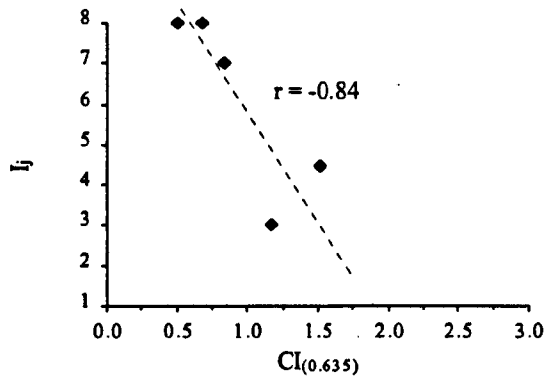


Fig. 8.10 - Plot of I_j versus $CI_{(0.635)}$.

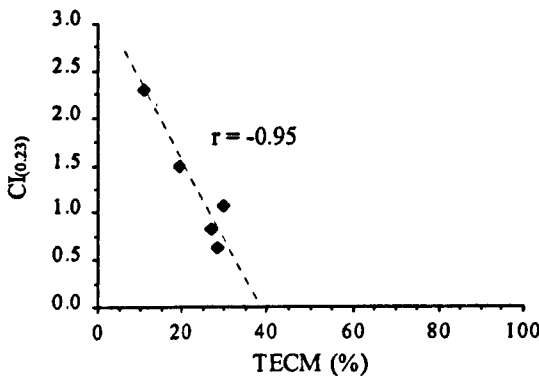


Fig. 8.11 - Plot of $CI_{(0.23)}$ versus TECM (%).

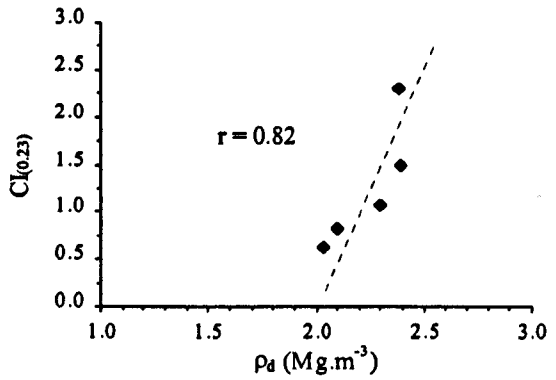


Fig. 8.12 - Plot of $CI_{(0.23)}$ versus ρ_d .

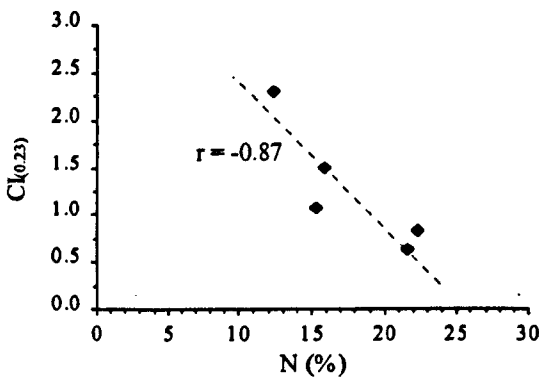


Fig. 8.13 - Plot of $CI_{(0.23)}$ versus N.

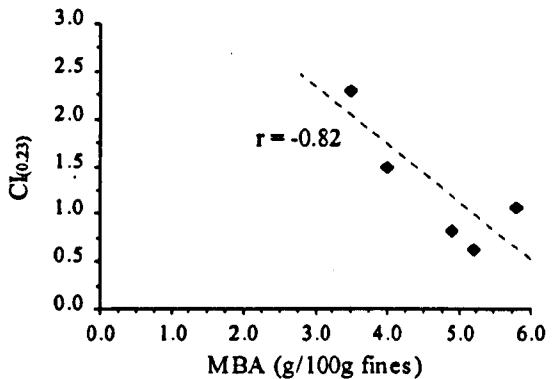


Fig. 8.14 - Plot of $CI_{(0.23)}$ versus MBA.

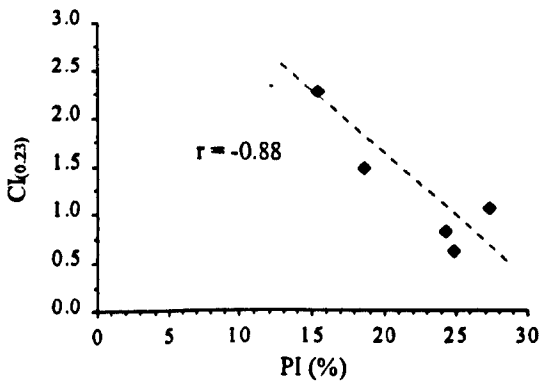


Fig. 8.15 - Plot of $CI_{(0.23)}$ versus PI.

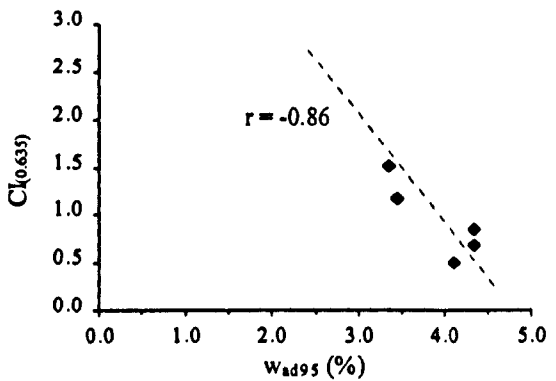


Fig. 8.16 - Plot of $CI_{(0.635)}$ versus w_{ad95} .

It can be concluded from the correlations identified, that the durability and strength of mudstones is controlled by the expansive clay minerals content and by porosity. Mudstone durability may also be controlled by the carbonate content.

The assessment of the potential durability of these rocks may be evaluated by the determination of the methylene blue adsorption value, dry density, adsorbed water at 95%RH and PI, I_{d2} and I_j indices.

8.2.4 - Assessment of mudshale durability

The mudshales studied consisted of samples 52, 154, 156, 441 and 445. The correlation coefficient matrix is presented in Table 8.2. There are a number of strong correlations:

- I_{d2} : TCM ($r = -0.83$), TECM ($r = -0.94$), ρ_d ($r = 0.98$), N ($r = -0.95$), w_{ad95} ($r = -0.96$), MBA ($r = -0.96$), PI ($r = -0.98$), ϵ_s ($r = -0.84$), I_j ($r = -0.97$);
- I_{d5} : Q+F ($r = 0.88$), TCM ($r = -0.82$), ρ_d ($r = 0.95$), N ($r = -0.93$), w_{ad95} ($r = -0.90$), PI ($r = -0.83$), σ_c ($r = 0.86$), $CI_{(0.23)}$ ($r = 0.88$), $CI_{(0.635)}$ ($r = 0.92$), I_j ($r = -0.94$);
- I_j : Q+F ($r = -0.84$), TCM ($r = 0.91$), TECM ($r = 0.90$), ρ_d ($r = -0.95$), N ($r = 0.91$), w_{ad95} ($r = 0.98$), MBA ($r = 0.89$), PI ($r = 0.95$), I_{d2} ($r = -0.97$), I_{d5} ($r = -0.94$);
- ϵ_s : TECM ($r = 0.97$), σ_c ($r = -0.83$), I_{d2} ($r = -0.84$);
- σ_c : TECM ($r = -0.84$), ϵ_s ($r = -0.83$), I_{d5} ($r = 0.86$);
- $CI_{(0.23)}$: I_{d5} ($r = 0.88$);
- $CI_{(0.635)}$: ρ_d ($r = 0.80$), N ($r = -0.80$), I_{d5} ($r = 0.92$).

Plots of selected correlations are presented in Fig. 8.17 to 8.32.

Table 8.2 - Correlation coefficient matrix between the main mineralogical, physical and geotechnical parameters determined for mudshales.

	Q+F	Carb	TCM	TECM	LOI	% Clay	G_s	ρ_d	N	w_{295}	MBA	PI	ϵ_x	ϵ_z	ΔV	σ_c	$CI_{(0.23)}$	$CI_{(0.635)}$	I_{22}	I_{45}	Ij
Q+F	1.00	-0.88	-0.93	-0.56	-1.00	-0.87	0.34	0.74	-0.71	-0.87	-0.58	-0.66	-0.34	-0.17	-0.21	0.78	0.69	0.75	0.74	0.88	-0.84
Carb		1.00	0.66	0.27	0.88	0.87	-0.27	-0.64	0.66	0.64	0.31	0.41	0.02	0.11	0.13	-0.78	-0.83	-0.87	-0.55	-0.83	0.65
TCM			1.00	0.76	0.93	0.74	-0.35	-0.76	0.71	0.94	0.76	0.81	0.59	0.2	0.27	-0.79	-0.52	-0.58	-0.83	-0.82	0.91
TECM				1.00	0.62	0.36	-0.25	-0.87	0.82	0.88	0.97	0.99	0.97	0.30	0.34	-0.84	-0.45	-0.48	-0.94	-0.74	0.90
LOI					1.00	0.86	-0.33	-0.80	0.77	0.90	0.64	0.72	0.40	0.18	0.22	-0.80	-0.74	-0.79	-0.80	-0.92	0.89
% Clay						1.00	-0.69	-0.65	0.69	0.74	0.49	0.50	0.16	0.54	0.56	-0.35	-0.54	-0.62	-0.62	-0.74	0.65
G_s							1.00	0.37	-0.45	-0.45	-0.47	-0.34	-0.23	-0.97	-0.97	-0.27	-0.10	-0.01	0.40	0.25	-0.28
ρ_d								1.00	-0.99	-0.92	-0.90	-0.94	-0.75	-0.37	-0.41	0.78	0.76	0.80	0.98	0.95	-0.95
N									1.00	0.89	0.86	0.89	0.70	0.45	0.48	-0.71	-0.75	-0.80	-0.95	-0.93	0.91
w_{295}										1.00	0.91	0.94	0.75	0.39	0.43	-0.74	-0.60	-0.66	-0.96	-0.90	0.98
MBA											1.00	0.98	0.94	0.51	0.55	-0.57	-0.40	-0.45	-0.96	-0.74	0.89
PI												1.00	0.92	0.36	0.40	-0.79	-0.54	-0.58	-0.98	-0.83	0.95
ϵ_x													1.00	0.33	0.36	-0.83	-0.26	-0.27	-0.84	-0.56	0.77
ϵ_z														1.00	1.00	0.32	0.15	0.08	-0.40	-0.18	0.23
ΔV															1.00	0.28	0.13	0.05	-0.44	-0.22	0.27
σ_c																1.00	0.99	0.97	0.77	0.86	-0.70
$CI_{(0.23)}$																	1.00	1.00	0.64	0.88	-0.71
$CI_{(0.635)}$																		1.00	0.68	0.92	-0.75
I_{22}																			1.00	0.90	-0.97
I_{45}																				1.00	-0.94

Q+F - Sum of percentages of quartz plus feldspar; Carb - Percentage of carbonates; TCM - Total clay minerals content (%); TECM - Expandable clay minerals content (%); LOI - Loss on ignition (%); % Clay - Percentage of material < 2 μ m determined in slake durability test residue; G_s - Grain specific gravity; ρ_d - Dry density ($Mg.m^{-3}$); N - Porosity (%); w_{295} - Water adsorption at 95%RH (%); MBA - Methylene blue adsorption value (g/100g fines); PI - Plasticity index (%); ϵ_x - Swelling strain measured on remoulded specimens (%); ϵ_z - Swelling strain measured on intact specimens perpendicular to stratification (%); ΔV - Volumetric strain (%); σ_c - Ultimate compressive stress (MPa); $CI_{(0.23)}$ and $CI_{(0.635)}$ - Cone indenter numbers measured for steel blade deflections, respectively, of 0.23 and 0.635 mm; I_{22} and I_{45} - Percentages of retained material in slake durability test, respectively, after 200, 400 and 1,000 rotations (%); Ij - Jar slake index.

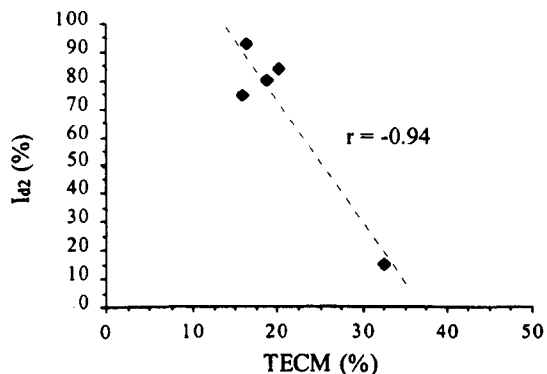


Fig. 8.17 - Plot of I_{d2} versus TECM (%).

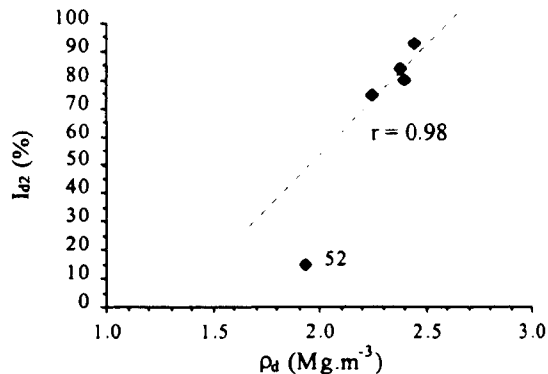


Fig. 8.18 - Plot of I_{d2} versus ρ_d .

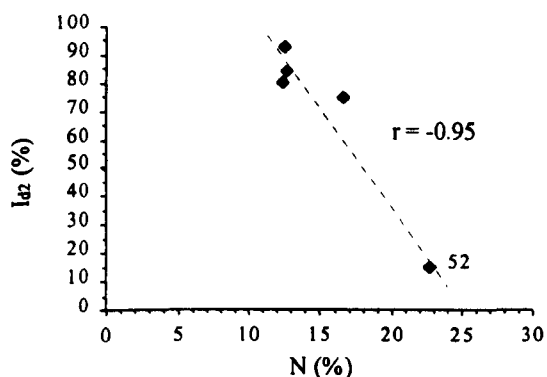


Fig. 8.19 - Plot of I_{d2} versus N.

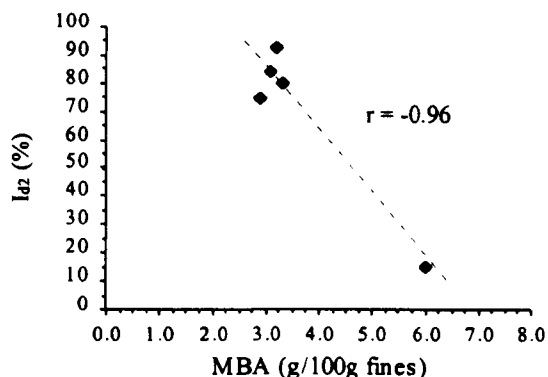


Fig. 8.20 - Plot of I_{d2} versus MBA.

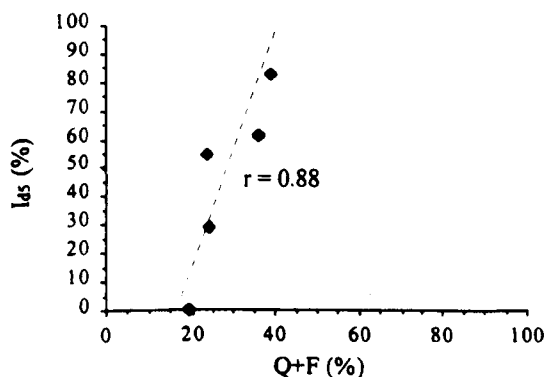


Fig. 8.21 - Plot of I_{d5} versus Q+F (%).

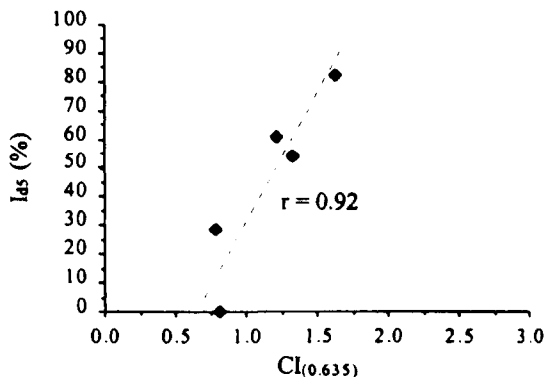


Fig. 8.22 - Plot of I_{d5} versus $CI_{(0.635)}$.

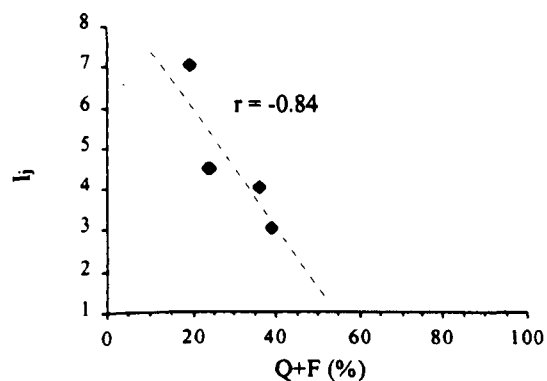


Fig. 8.23 - Plot of I_j versus Q+F (%).

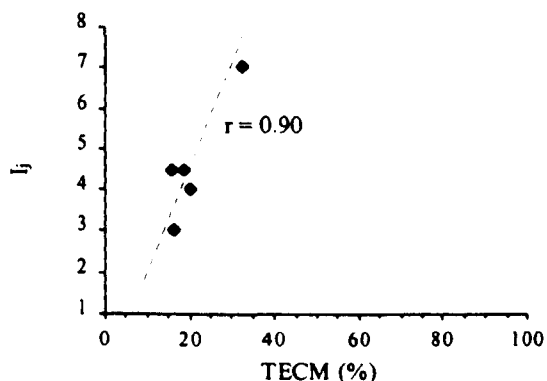


Fig. 8.24 - Plot of I_j versus TECM (%).

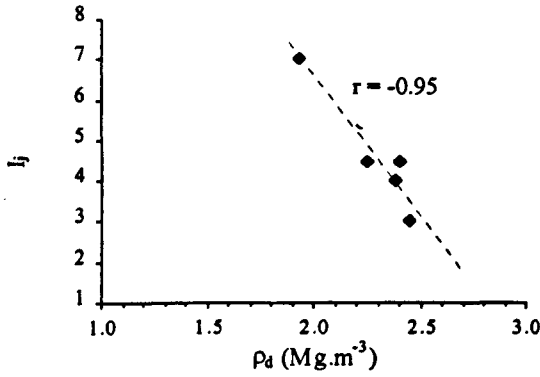


Fig. 8.25 - Plot of I_j versus ρ_d .

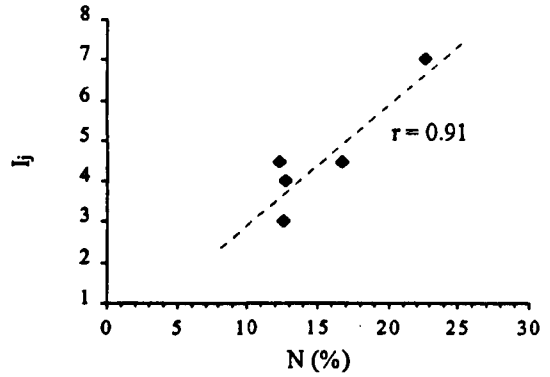


Fig. 8.26 - Plot of I_j versus N .

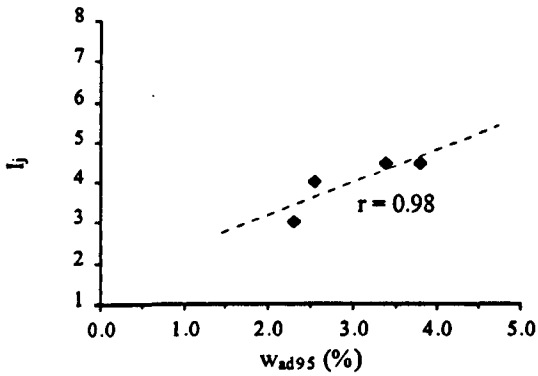


Fig. 8.27 - Plot of I_j versus w_{ad95} .

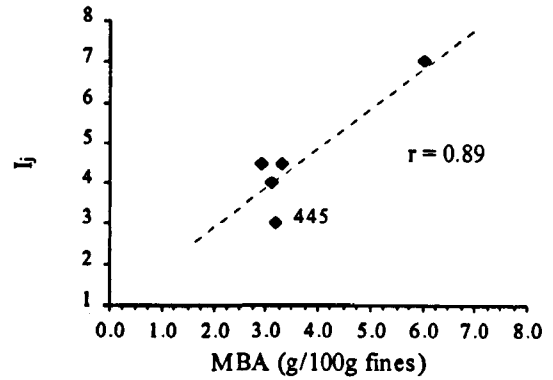


Fig. 8.28 - Plot of I_j versus MBA.

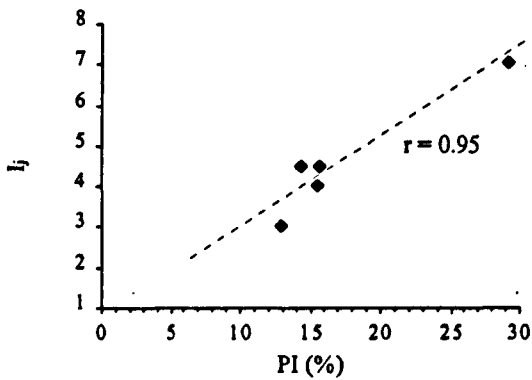


Fig. 8.29 - Plot of I_j versus PI.

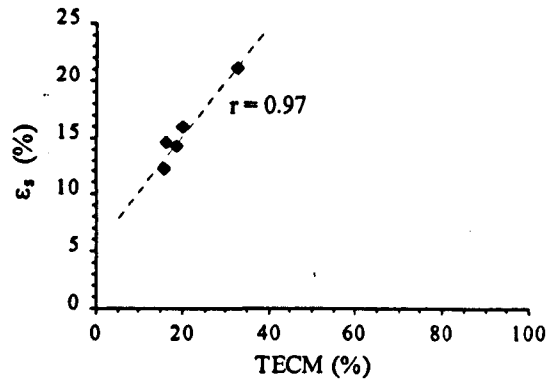


Fig. 8.30 - Plot of ϵ_s versus TECM (%).

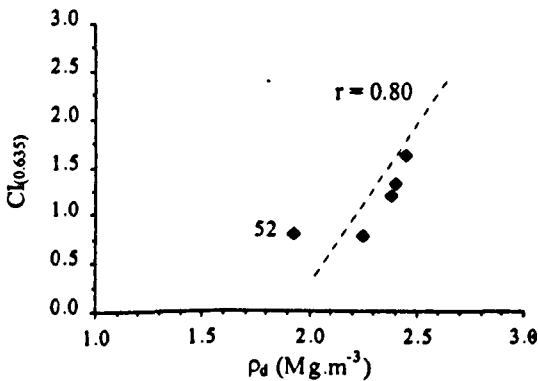


Fig. 8.31 - Plot of $CI_{(0.635)}$ versus ρ_d .

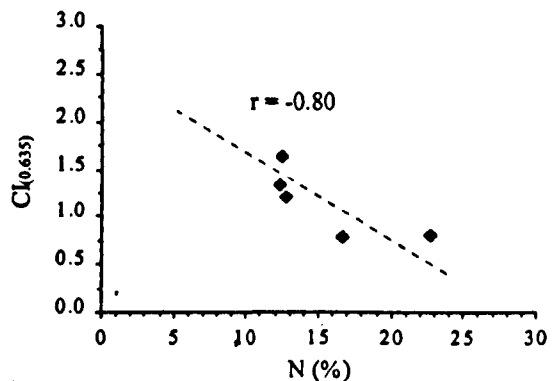


Fig. 8.32 - Plot of $CI_{(0.635)}$ versus N .

In addition important correlations also exist between percentage of expansive clay minerals, water content at 95%RH ($r = 0.88$), the methylene blue adsorption value ($r = 0.97$), the plasticity index ($r = 0.99$) and swelling strain measured on remoulded samples ($r = 0.97$). Significant correlations also exist between adsorption water at 95%RH, and porosity and dry density (respectively, $r = 0.89$ and $r = -0.92$).

It was found, on the basis of the correlations obtained and from SEM examination of the samples included in this lithological group, that the durability and strength of these materials are controlled by mineralogical composition, distribution of void space (including micro-discontinuities) and rock fabric.

The proportion of clay minerals, namely expandable clay minerals, and of quartz-feldspar fraction are the mineralogical features that affect more significantly the geotechnical properties of these rocks.

The development of microfractures in this lithological group is related to the fissility and lamination present. Such features provides access for water to the sites of reactive clays and also potential sites for air breakage to occur. The durability of these materials may also be controlled by the occurrence of different compositional layers. This fact is shown by the relationship between the quartz-feldspar fraction and the I_{45} values (which is higher than that obtained for I_{42}). Accordingly, the material retained at the end of the slake durability test was mainly from the laminae composed of quartz and feldspar grains, which are sometimes cemented by sparite (see Fig. 5.20C and D and Fig. 5.21D) while the material lost was from the laminae formed chiefly by clay minerals, micrite and organic matter.

The assessment of the potential durability of these rocks may be evaluated via the determination of the methylene blue adsorption value, dry density, and the PI, I_{42} and I_j indices.

8.2.5 - Assessment of siltstone and siltshale durability

The siltstones and laminated siltstones analysed comprised samples 112, 114, 334, 342, 431, OB1 and OB2. The correlation coefficient matrix is presented in Table 8.3. Strong correlations were found as follows:

- $I_{d2} : \varepsilon_z$ ($r = -0.84$), ΔV ($r = -0.90$);
- $I_{d5} : \varepsilon_z$ ($r = -0.91$), ΔV ($r = -0.96$);
- $I_j : w_{ad95}$ ($r = 0.86$), $CI_{(0.635)}$ ($r = -0.89$);
- $\varepsilon_s : MBA$ ($r = 0.83$), ε_z ($r = 0.83$);
- $\varepsilon_z : \varepsilon_s$ ($r = 0.83$), I_{d2} ($r = -0.84$), I_{d5} ($r = -0.91$);
- $\sigma_c : N$ ($r = -0.82$);
- $CI_{(0.23)} : \rho_d$ ($r = 0.86$), w_{ad95} ($r = -0.80$);
- $CI_{(0.635)} : Q+F$ ($r = 0.84$), w_{ad95} ($r = -0.83$), I_j ($r = -0.89$).

Plots of selected correlations are presented in Fig. 8.33 to 8.40.

Less strong correlations also exist between the methylene blue adsorption value, ultimate compressive stress ($r = -0.77$) and cone indenter numbers for a steel blade deflection of 0.23 mm ($r = -0.77$). A significant relationship exists between expandable clay mineral content and I_{d2} value ($r = -0.76$). The cone indenter results for steel blade deflections of 0.23 mm and 0.635 mm correlate respectively with porosity ($r = -0.77$) and dry density ($r = 0.77$).

The durability and strength characteristics of this lithological group are governed by texture and to a lesser extent by their mineralogy as is shown by the correlations presented. The development of microfractures is the main control on durability of siltstones and siltshales because they provide access for water to the sites of the reactive clays and also potential sites for air breakage to occur. The microfracture development could also be due to stress relief effects.

Table 8.3 - Correlation coefficient matrix between the main mineralogical, physical and geotechnical parameters determined for siltstones(shales).

	Q+F	Carb	TCM	TECM	LOI	% Clay	G _s	ρ _d	N	w _{ad95}	MBA	PI	ε _s	ε _z	ΔV	σ _c	CI _(0.23)	CI _(0.635)	I ₄₂	I ₄₅	I _j
Q+F	1.00	-0.61	-0.46	0.39	-0.68	-0.78	-0.93	0.65	-0.44	-0.47	-0.15	-0.22	-0.12	0.41	0.49	0.11	0.65	0.84	-0.68	-0.46	-0.70
Carb		1.00	-0.19	-0.09	0.52	0.48	0.77	-0.80	0.77	-0.01	0.15	-0.10	-0.28	-0.66	-0.63	-0.59	-0.48	-0.42	0.44	0.49	0.01
TCM			1.00	-0.54	-0.14	0.54	0.16	0.25	-0.42	0.02	-0.49	-0.07	-0.15	-0.31	-0.45	0.74	0.19	-0.21	0.72	0.57	0.49
TECM				1.00	-0.21	-0.46	-0.25	-0.18	0.20	-0.44	0.67	0.53	0.52	0.52	0.54	-0.06	-0.17	0.11	-0.76	-0.65	-0.26
LOI					1.00	0.45	0.72	-0.78	0.70	0.83	0.45	0.46	0.27	-0.09	-0.04	-0.47	-0.89	-0.87	0.19	-0.09	0.68
% Clay						1.00	0.62	-0.49	0.49	0.29	-0.01	0.13	-0.15	-0.55	-0.58	0.03	-0.44	-0.66	0.74	0.57	0.60
G _s							1.00	-0.74	0.57	0.39	0.31	0.15	0.17	-0.35	-0.41	-0.36	-0.71	-0.77	0.50	0.36	0.50
ρ _d								1.00	-0.92	-0.48	-0.55	-0.50	-0.16	0.30	0.25	0.78	0.86	0.77	-0.17	-0.05	-0.42
N									1.00	0.38	0.55	0.40	0.05	-0.30	-0.20	-0.82	-0.77	-0.61	0.06	0.00	0.24
w _{ad95}										1.00	0.51	0.73	0.57	0.31	0.34	-0.23	-0.80	-0.83	-0.05	-0.42	0.86
MBA											1.00	0.75	0.83	0.58	0.60	-0.77	-0.77	-0.51	-0.59	-0.69	0.29
PI												1.00	0.74	0.47	0.48	-0.46	-0.72	-0.66	-0.36	-0.61	0.66
ε _s													1.00	0.83	0.77	-0.33	-0.57	-0.43	-0.58	-0.76	0.45
ε _z														1.00	0.98	-0.10	-0.12	0.06	-0.84	-0.91	0.08
ΔV															1.00	-0.18	-0.14	0.08	-0.90	-0.96	0.03
σ _c																1.00	0.67	0.35	0.41	0.38	0.16
CI _(0.23)																	1.00	0.91	0.03	0.28	-0.68
CI _(0.635)																		1.00	-0.30	0.01	-0.89
I ₄₂																			1.00	0.92	0.32
I ₄₅																				1.00	-0.05
I _j																					1.00

Q+F - Sum of percentages of quartz plus feldspar; Carb - Percentage of carbonates; TCM - Total clay minerals content (%); TECM - Expandable clay minerals content (%); LOI - Loss on ignition (%); % Clay - Percentage of material < 2μm determined in slake durability test residue; G_s - Grain specific gravity; ρ_d - Dry density (Mg.m⁻³); N - Porosity (%); w_{ad95} - Water adsorption at 95%RH (%); MBA - Methylene blue adsorption value (g/100g fines); PI - Plasticity index (%); ε_s - Swelling strain measured on remoulded specimens (%); ε_z - Swelling strain measured on intact specimens perpendicular to stratification (%); ΔV - Volumetric strain (%); σ_c - Ultimate compressive stress (MPa); CI_(0.23) and CI_(0.635) - Cone indenter numbers measured for steel blade deflections, respectively, of 0.23 and 0.635 mm; I₄₂ and I₄₅ - Percentages of retained material in slake durability test, respectively, after 200, 400 and 1,000 rotations (%); I_j - Jar slake index.

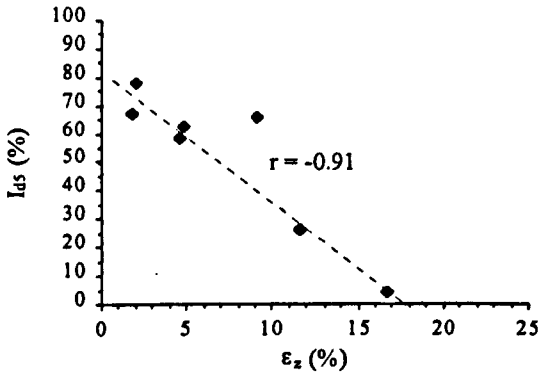


Fig. 8.33 - Plot of I_{d5} versus ϵ_x

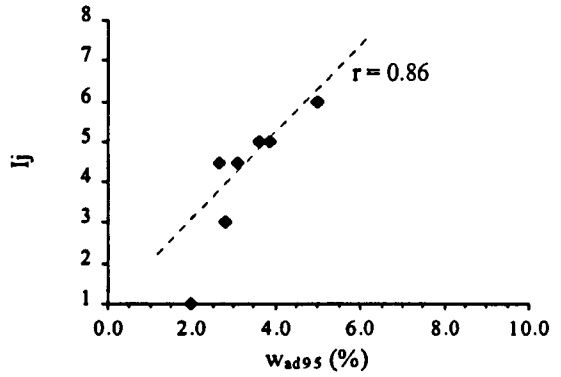


Fig. 8.34 - Plot of I_j versus w_{ad95}

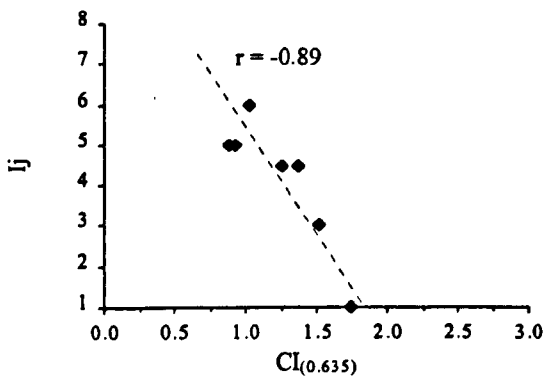


Fig. 8.35 - Plot of I_j versus $CI_{(0.635)}$

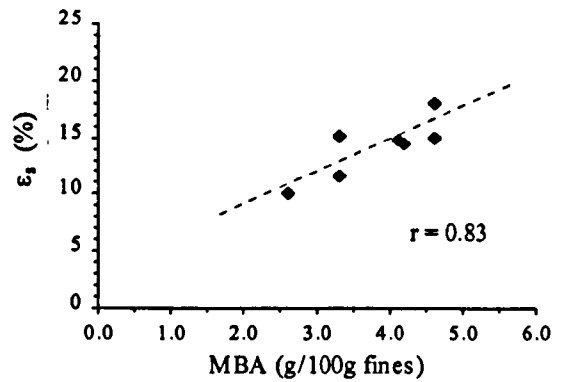


Fig. 8.36 - Plot of ϵ_s versus MBA.

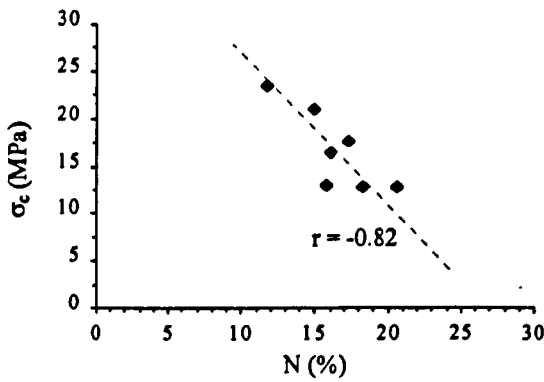


Fig. 8.37 - Plot of σ_c versus N .

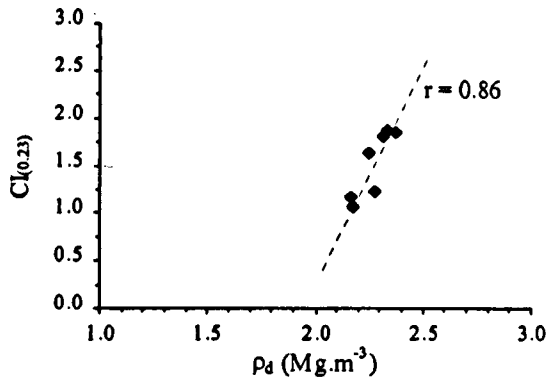


Fig. 8.38 - Plot of $CI_{(0.23)}$ versus ρ_d .

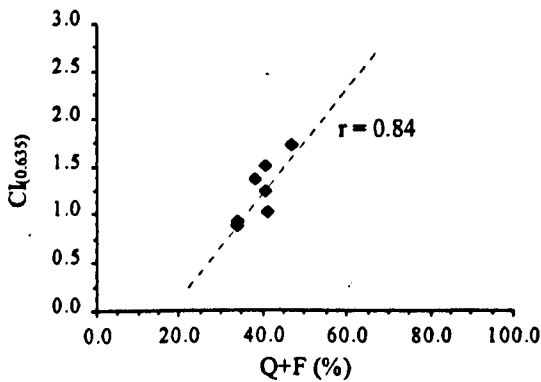


Fig. 8.39 - Plot of $CI_{(0.635)}$ versus $Q+F$ (%).

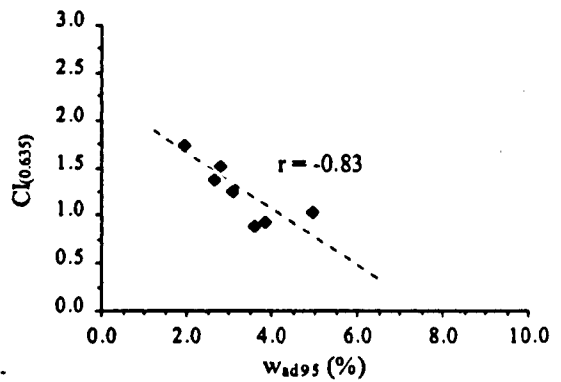


Fig. 8.40 - Plot of $CI_{(0.635)}$ versus w_{ad95} .

The assessment of the potential durability of these rocks may be evaluated via the determination of the methylene blue adsorption value, dry density, water adsorption at 95%RH and the, I_{d2} and I_j indices.

8.3 - Classification of the mudrocks studied

The geotechnical characterization of mudrocks present in important engineering works requires a study carried out in two different phases, which involve distinct laboratory resources.

In an initial phase, the study of mudrocks with reference to a specific application must include the lithological classification and detailed mineralogical, textural and geotechnical characterization of a set of representative samples of the various lithotypes present. During this phase the laboratory studies could involve time-consuming and costly analytical techniques, such as X-ray diffraction, scanning electron microscopy, wet chemical analyses and mercury porosimetry.

Lithological classification

The lithological classification of mudrocks should be carried out according to the scheme presented in Table 3.7. This differentiates the various lithotypes on the basis of the percentage of quartz plus feldspar present in the rocks (Spears, 1980, Grainger, 1984 and Taylor, 1988) and on the occurrence or absence of laminae in samples. The latter can be determined using a binocular microscope and thin sections under optical microscope).

Mineralogical characterization

The analyses to be conducted should enable the characterization of the following features: (a) determination of the quartz and feldspar concentrations so that the previous lithological classification can be used; (b) identification and quantitative determination of the clay mineralogy, especially the expandable clay

minerals content, cement phases *i.e.* carbonates and organic matter and minor potential reactive phases *e.g.* pyrite and gypsum.

Textural characterization

The textural characterization of mudrocks should be carried out according to the descriptive scheme of microtextural features presented in Table 5.9, using optical microscope and scanning electron microscope (SEM). Additional data on the development of microfractures can be obtained from the jar slake test results adopting the classification presented in Table 6.4.

Geotechnical characterization

The main geotechnical properties of mudrocks that should be determined are as follows: swelling potential, strength and slaking.

Swelling potential can be determined on rock samples simply along the direction perpendicular to bedding/lamination or obtained via triaxial swelling tests. In the case of rocks with a high susceptibility to slaking, the results of swelling potential can be under-estimated as the material degrades during the test. In this situation swelling potential can be evaluated on the basis of testing remoulded/powdered samples.

Strength can be evaluated directly through uniaxial compressive tests or estimated indirectly via point load or cone indenter tests. The advantage of the latter tests is that they use irregular samples and accordingly, minimum sample preparation is required. Point load tests can only be used on more indurated mudrocks, while cone indenter tests can be carried out on both strong and weak or weathered mudrocks.

Slaking potential can be evaluated based on both slake durability test and jar slake test. So far as the former is concerned, the durability classes defined for mudrocks are based on the values of the I_{42} (Gamble, 1971; Dick *et al.*, 1994) and I_{43} indices (Taylor, 1988) determined. Although, the jar slake test has a mainly descriptive character, it can also be used to evaluate the durability of

mudrocks as can be seen from the correlation between the parameters (I_j and I_{d2}) of each test presented in Fig. 6.34.

In the second phase of an investigation, the evaluation of mudrock durability and the classification of new samples may be based on the index tests which showed stronger correlations with the main mineralogical, textural and physical features that control the behaviour of the various lithological groups of mudrocks (see Section 8.2).

However, as has already been stated pre-construction detailed characterization of mudrocks involves mineralogical and textural determinations that are complex and costly to perform. Therefore, the adoption of the methodology proposed may not be feasible at the reconnaissance phase of projects, yet not taking into account the presence of potentially problematic materials can lead to greater construction and/or maintenance costs. The solution to this problem is to use simple index tests to distinguish between potentially problematic and non-problematic materials.

Mudrock durability assessment is usually based on the results of the slake durability test. However, as mentioned in Section 6.7, the durability of materials can be overestimated when test samples breakdown into fragments larger than 2 mm.

In previous works Rodrigues (1988) and Rodrigues & Jeremias (1990) showed that swelling strain and porosity were two fundamental parameters in the evaluation of the durability of carbonate and greywacke rocks, because they characterize two different features of the materials: the nature and amount of clay minerals and the amount and character of the void space. As it was found in the analysis carried out in Section 6.7, that these two parameters also control the behaviour of mudrocks.

On the other hand, it was noted from the correlation analysis presented in Section 8.2, that the various lithological groups which comprised the mudrock class can be characterized on the basis of a minimum set of index tests, which include dry density and methylene blue adsorption value. Thus, the development of a classification scheme for mudrocks, based on the assumptions mentioned before and using these index tests is justified because dry density is directly related to accessible porosity (see Fig. 8.41) and the methylene blue adsorption value evaluates the nature and quantity of clays. Since

slaking affects strongly the behaviour of mudrocks, the inclusion of a parameter that evaluates this property is necessary, and the slake durability test was accordingly adopted.

Fig. 8.41 presents the relationship between porosity and dry density (black markers) and the linear regression line obtained. In order to compare the results determined with those obtained by other researchers, Rodrigues's (1986) data for carbonate rocks as well as data for mudrocks quoted by Duncan *et al.* (1969), Czerewko (1997), Dick *et al.* (1994) and Sarman *et al.* (1994) are also plotted.

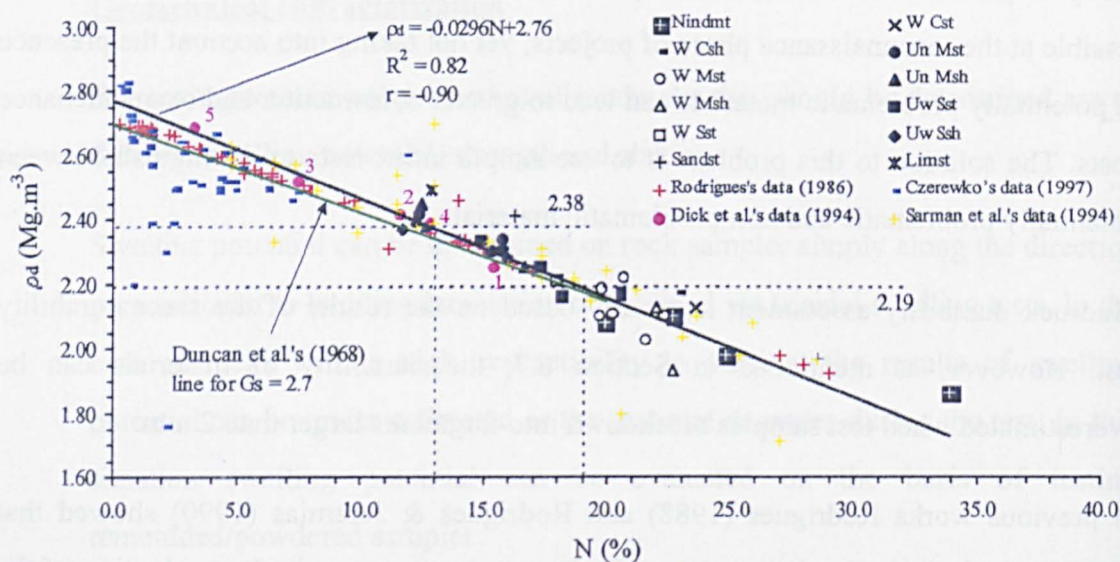


Fig. 8.41 - Relationship between porosity and dry density.

The data (red markers) from Rodrigues (1986) consist of a wide variety of Portuguese carbonate rocks ranging from pure limestones to argillaceous rich carbonate rocks. The rocks with porosity values higher than 10% have in general a more argillaceous composition and they fit well in the trend plotted for the mudrocks studied. The rocks with lower porosity values (< 10%) have mostly a carbonate composition and they also define a trend which is very close to the regression line plotted for the mudrocks studied.

From the testing of 70 mudrock samples covering a broad range of geological ages, Duncan *et al.* (1968) plotted dry density versus porosity average relationships for different values of grain specific gravity. These relationships were plotted for porosity values ranging between 0 to 20%. The green line plotted in Fig. 8.41 represents the dry

density - porosity relationship obtained by Duncan assuming an average grain specific gravity of 2.7. As it can be seen from the figure the two trends are very close and almost parallel.

Czerewko's (1997) data (blue markers) consisted of British mudrocks ranging from Cambrian slates to Carboniferous Coal Measures. These mudrocks have much lower porosity values than those studied in this work. The scatter of the data shows that they neither follow the trend defined for the mudrocks studied nor any other in particular. This result can probably be attributed to the presence in some of Czerewko's samples, of siderite.

The data (purple markers) from Dick *et al.* (1994) include 61 mudrocks ranging in age from Cambrian to Miocene, from different areas of the USA. The mean data plotted in Fig. 8.41 for 10 claystones (label 1), 22 mudstones (label 2), 17 samples of shales, including 7 siltshales (label 3), 13 samples of combined siltstones-siltshale (label 4) and 6 samples of argillites (label 5) also correlate well. In addition, the mean values show that even for the low porosity range, good agreement is found with the trend established for the mudrocks studied.

Sarman *et al.*'s (1994) data (yellow markers) consist of 42 USA mudrocks ranging also in age from Cambrian to Miocene and from different areas on USA. The data includes both mudrocks with low and high porosity values. Notwithstanding, some scatter of the data, Fig. 8.41 shows that in general the data fits well with the trend defined for mudrocks studied, including the ones on low porosity range.

The high correlation obtained between dry density and porosity values for the mudrocks studied makes it possible to conclude that dry density may be used to evaluate this textural feature of the materials. This has the advantage of avoiding the use of porosity which, although an obvious classification parameter, is difficult to determine (see Section 6.2.3). On the contrary dry density is determined using a easy and rapid method involving ordinary laboratory resources. Moreover, the results from other researchers, with exception of Czerewko's data, fit well in the trend defined for the rocks studied in this work. Provided that specific relationships can be established for each site (taking into account the grain specific gravity) the trend proposed seems to have wide

applicability for mudrocks whose composition do not give rise to unusual grain specific gravity values.

The methylene blue adsorption value evaluates mostly the presence and amount of potentially reactive clay minerals content (*i.e.* those with greater hydrophilic surface) *e.g.* mixed-layer clay minerals and smectites. Therefore, this index test makes it possible to characterize whether expandable clay content is a control on durability of the materials being analysed.

Because the slake durability test is widely used and provides a quantitative index, it is proposed to use it to evaluate the susceptibility to slaking of mudrocks. However, it should be noted that the I_j indices determined in the jar slake test can also be used as an alternative classification parameter to evaluate the susceptibility to slaking, adopting the classes presented in Fig. 6.34. This test would be particularly useful if slake durability test equipment is not available and also in the case of the test samples breakdown mostly into fragments larger than 2 mm (in the latter case the results of the slake durability test overestimate the durability of the materials).

Based on the results determined for each of the parameters selected classes were established, to which a ranking system has been applied (Czerewko, 1997). Although the intervals adopted for the classes defined for each parameter are arbitrary they seek to reflect some behavioural changes obtained within the samples studied

Using only the data from the mudrocks studied, the intervals adopted for dry density were determined on the basis of the relationship between this parameter and the porosity presented in Fig. 8.41. The classes were defined on the basis of the distribution of porosity values. Thus, based on the analysis of Fig. 8.41, three groups may be distinguished corresponding to mudrocks with relatively low ($N < 13\%$), medium ($13\% < N < 19\%$) and high ($N > 19\%$) porosity values. Accordingly, the limits adopted for dry density classes (2.38 and 2.19) were determined from the linear regression line plotted in Fig. 8.41.

The intervals selected for methylene blue adsorption value were obtained from the relationship presented in Fig. 8.42 between this parameter and expandable clay mineral

content. Despite the evident correlation between the two parameters, the scattering of the results affects the statistical value of the linear regression line. Accordingly a band was plotted which expresses the relationship between the parameters in question. Almost all the data fall inside this band. The higher limit of 4.1 was adopted based on the work of Taylor & Spears (1970), who found that materials with >22% expandable clay minerals content are more prone to slaking and swelling. The lower limit was defined by the intercept calculated for the best fit straight line plotted in Fig. 8.42. Values of MBA less than 2.8 correspond with mudrocks with low expandable clay mineral content, and therefore they do not have a significant control on the behaviour of these materials.

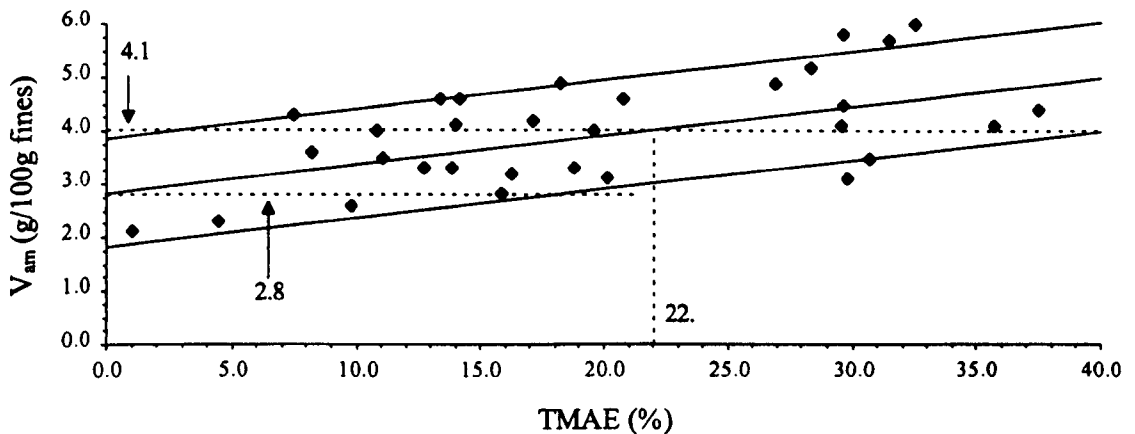


Fig. 8.42 - Relationship between the expansive clay minerals content and the methylene blue adsorption value.

The intervals adopted for I_{d2} index correspond to the classes defined by Dick *et al.* (1994). The intervals adopted in the definition of the classes of the various classification parameters, as well as the corresponding rank values attributed to each of those classes, are presented in Table 8.4.

It was decided that the highest rank value should be attributed to the class corresponding to the interval of values of the index test considered, which reflects a higher durability. Accordingly, for example, a I_{d2} value greater than 85% indicates a durable material and therefore a rank value of 3 has been attributed to this class. On the other hand, a methylene blue adsorption value in excess of 4.1 indicates a high expandable clay

minerals content and accordingly a material that is potentially less durable. Such a material has been attributed to class 1.

Table 8.4 - Intervals of values adopted for each index test selected as classification parameter and corresponding rank values.

Parameter A		Parameter B		Parameter C	
I_{d2} (%)	Rank value	ρ_d (Mg.m ⁻³)	Rank value	MBA (g/100g fines)	Rank value
<50	1	<2.19	1	≥4.1	1
50 - 85	2	2.19 - 2.38	2	2.8 - 4.1	2
>85	3	>2.38	3	<2.8	3

Based on this reasoning a durability index (DI) was defined, which corresponds to the sum of the rank values attributed to the various classification parameters. Table 8.5 provides an example of the determination of the DI index for sample 431.

Table 8.5 - Determination of the DI index for sample 431.

Value determined for parameter	Rank value
A ↔ $I_{d2} = 84.2$	$RV_{(A)} = 2$
B ↔ $\rho_d = 2.37$	$RV_{(B)} = 2$
C ↔ MBA = 3.3	$RV_{(C)} = 2$
	$DI = RV_{(A)} + RV_{(B)} + RV_{(C)} = 6$

The classification parameters matrix, which discriminates the durability class of the materials (low, medium or high) according to the DI values calculated are presented in Table 8.6. It was considered that DI values of less than 6 should be classed as non-durable materials, values between 6 and 7 should be classed as rocks with medium durability and values over 7, should be classed as durable materials. The application of this classification to the samples studied is presented in Table 8.6.

Table 8.6 - Classification of the samples according to the DI index proposed and the corresponding durability classes.

Samples	Parameter A		Parameter B		Parameter C		Durability Index - DI DI = (RV _(A)) + (RV _(B)) + (RV _(C))
	I _{d2} (%)	Rank value (RV _(A))	ρ _d (Mg.m ⁻³)	Rank value (RV _(B))	MBA (g/100g fines)	Rank value (RV _(C))	
51	11.3	1	1.86	1	3.6	2	4
52	14.7	1	1.93	1	6.0	1	3
81	8.3	1	2.19	2	4.1	1	4
83	96.3	3	2.41	3	2.3	3	9
111	38.3	1	1.98	1	4.5	1	3
112	85.6	3	2.25	2	3.3	2	7
114	90.6	3	2.33	2	2.6	3	8
151	17.1	1	2.08	1	4.4	1	3
152	18.5	1	2.17	1	3.5	2	4
153	42.8	1	2.13	1	3.1	2	4
154	74.5	2	2.25	2	2.8	2	6
156	84.0	2	2.38	2	3.1	2	6
162	49.5	1	2.10	1	4.3	1	3
163	68.7	2	2.18	1	4.0	2	5
283	48.5	1	2.11	1	4.6	1	3
285	59.2	2	2.22	2	4.1	1	5
286	92.3	3	2.39	3	4.0	2	8
294	2.5	1	2.13	1	5.7	1	3
296	49.1	1	2.03	1	5.2	1	3
332	23.8	1	2.10	1	4.9	1	3
333	4.1	1	2.10	1	4.9	1	3
334	44.2	1	2.28	2	4.6	1	4
336	42.3	1	2.30	2	5.8	1	4
342	34.3	1	2.31	2	4.2	1	4
345	74.5	2	2.49	3	2.1	3	8
431	84.2	2	2.37	2	3.3	2	6
436	90.7	3	2.38	2	3.5	2	7
441	79.7	2	2.40	3	3.3	2	7
445	92.7	3	2.45	3	3.2	2	8
OB1	81.3	2	2.16	1	4.1	1	4
OB2	83.1	2	2.17	1	4.6	1	4

 DI < 6 - Low durability
 6 ≤ DI ≤ 7 - Medium durability
 DI > 7 - High durability

It can be seen from Table 8.6 that all non-indurated materials and weathered samples, as well as the most problematic unweathered rocks, are included in the low durability class (red highlighted). Samples 112, 154, 156, 431, 436 and 441 are included in the medium durability class (blue highlighted). These latter samples correspond to materials that may exhibit potential loss of durability and therefore, would require further characterization testing. Samples 83, 114, 286, 345 and 445 are included in the high durability class and represent the stronger and apparently with lower susceptibility to slaking. As expected, samples 83 (calcareous sandstone) and 345 (oolitic limestone),

corresponding to stronger lithotypes, also fall within this latter class. However, it should be noted that samples 114 and 286 exhibit important deterioration at the end of the natural exposure tests due to the progressive dissolution of carbonate cement, thus they show a long-term susceptibility to breakdown. Therefore, the inclusion of these samples in the high durability class is not rigorous. Nevertheless, the fact that the behaviour described was not observed in sample 83 and this sample has a DI value higher than the previous samples (114, 286 and 445) may reflect the need to create another durability class. Applications of the proposed index on a larger data set of mudrocks will allowed legitimization of a durability class for rocks with a DI value equal to 9.

In order to evaluate the success of the classification proposed on characterization of mudrock durability the results obtained for the samples studied were compared with those determined applying the schemes developed by Gamble (1971) and Dick *et al.* (1994). The classification scheme proposed by Gamble (1971), with the samples plotted, is presented in Fig. 8.43. The durability classes proposed by Dick *et al.* (1994) are presented in Fig. 3.14.

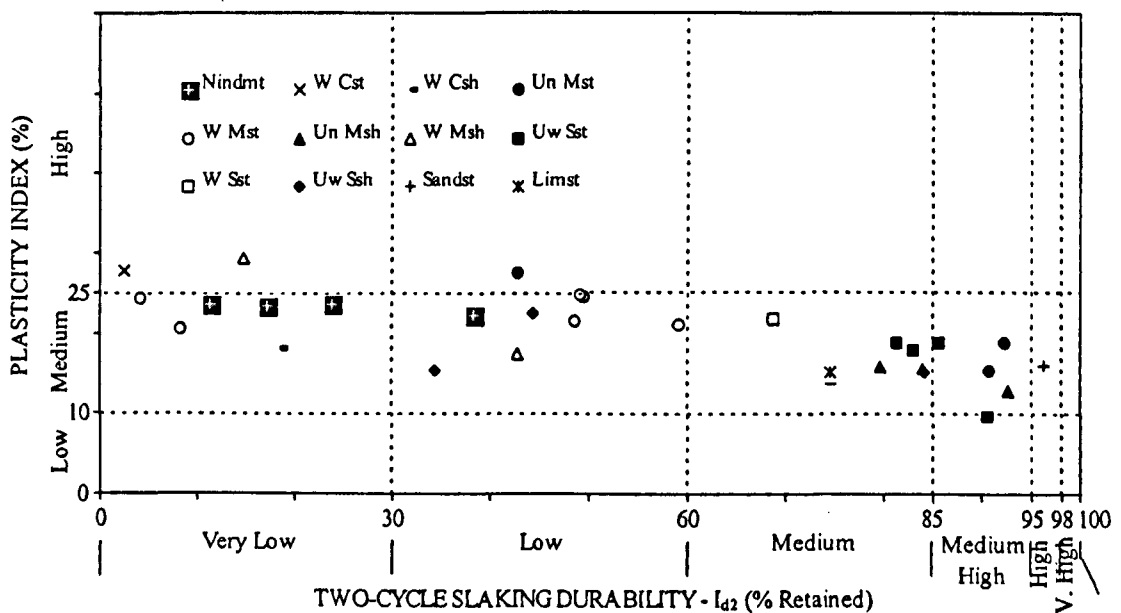


Fig. 8.43 - Classification of the samples studied using the durability-plasticity chart of Gamble (1971).

The durability classes adopted for each sample following the criteria of DI index and according to the classifications proposed by Gamble (1971) and Dick *et al.* (1994) are presented in Table 8.7.

Table 8.7 - Comparison of the durability classes adopted for the samples studied, applying various classification schemes.

Sample	Durability classification based on DI index	Durability classification proposed by Gamble (1971)	Durability classification proposed by Dick <i>et al.</i> (1994)	Sample	Durability classification based on DI index	Durability classification proposed by Gamble (1971)	Durability classification proposed by Dick <i>et al.</i> (1994)
51	Low	Very Low	Low	336	Low	Low	Low
52	Low	Very Low	Low	342	Low	Low	Low
81	Low	Very Low	Low	OB1	Low	Medium	Medium
111	Low	Low	Low	OB2	Low	Medium	Medium
151	Low	Very Low	Low	112	Medium	Medium High	High
152	Low	Very Low	Low	154	Medium	Medium	Medium
153	Low	Low	Low	156	Medium	Medium	Medium
162	Low	Low	Low	431	Medium	Medium	Medium
163	Low	Medium	Medium	436	Medium	Medium High	High
283	Low	Low	Low	441	Medium	Medium	Medium
285	Low	Low	Medium	83	High	High	High
294	Low	Very Low	Low	114	High	Medium High	High
296	Low	Low	Low	286	High	Medium High	High
332	Low	Very Low	Low	345	High	Medium	Medium
333	Low	Very Low	Low	445	High	Medium High	High
334	Low	Low	Low				

It was found from the analysis of Table 8.7 that the evaluation of durability according to the three criteria presented leads, in general, to similar results. Thus, the samples classed as having low durability according to the DI index, are included mostly in very low and low durability classes of Gamble and in the low durability class of Dick *et al.*. Samples 163, 285, OB1 and OB2 which are classified as non-durable according to the DI index, are included in medium durability classes of both Gamble (not including sample 285) and Dick *et al.*. However, it can be expected that they will have low durability, since the results of jar slake test show that these materials are very prone to slaking. The porosity values (between 18 and 21%) and the methylene blue adsorption values (between 4.0 and 4.6) determined for these samples suggest a potential durability behaviour of this type. Indeed, the methylene blue adsorption values reflect the occurrence of a reactive clay fraction, while the dry density values indicate that these mudrocks have significant void space. These two features complement each other, since a higher porosity allows easier water access to the interior of the materials, namely, to the sites of expansive components, which leads to the breakdown of the samples.

The samples classified as medium durability according to DI index are included in the medium durability classes of Gamble and Dick *et al.*, while high-durability samples are included in medium to high and high according to Gamble's classes and in high according to Dick *et al.*'s classification. The durability characterization of samples 112 and 436 based on the three classification schemes under discussion is the main difference recorded. Therefore, according to DI values, Gamble's and Dick *et al.*'s classifications these samples were included respectively, in medium, medium to high and high durability classes. As stated in Section 6.7, these samples are very prone to breakdown into fragments larger than 2 mm. In these conditions the slake durability test would overestimate the durability of the materials. Since Gamble and Dick *et al.*'s classifications are based solely on the results of this index test, in these cases their durability is not successfully evaluated.

The application of the DI index was also investigated using data from other mudrocks. For this purpose Czerewko's (1997) data concerning British mudrock samples ranging from Cambrian slates to Carboniferous Coal Measures in age were used. The values of the index tests adopted in DI index for Czerewko's mudrocks are present in Table 8.8.

It can be seen from this Table that several samples included in high durability class of the DI index are classified according to Czerewko's classification as non-durable (highlighted samples). This is probably due to the presence of large amounts of siderite and organic matter within these mudrocks (*e.g.* sample C161 had a siderite content of 37.5%; sample C92 had a organic content of 41.5%) which makes it difficult to obtain an accurate estimate of porosity from dry density values. Furthermore, Czerewko's mudrocks have much lower porosity values than those investigated in this work. The highest porosity value of Czerewko's mudrocks (sample C161 - 11.8%) is similar to the lowest porosity value of the mudrocks studied (sample 431 - 11.7%). Effective porosity of the materials may also be estimated using water absorption values. This index test has the advantage that it is not influenced by mineralogical composition of the materials. However, difficulties arise if the rock slakes when immersed in water, as the case of the mudrocks studied in this work.

Table 8.8 - Czerewko mudrock's data and comparison of the durability classes adopted for the samples applying the DI index and the Czerewko's classification.

Sample	ρ_d (Mg.m ⁻³)	MBA (g/100g)	I _{d2} (%)	Durability classification based on DI index	Czerewko's Classification (Czerewko, 1997)
Ca11	2.82	0.29	99.2	High	Extremely durable
Ca12	2.81	0.21	99.5	High	Extremely durable
Ca13	2.83	0.22	99.6	High	Extremely durable
O11	2.64	2.48	74.1	High	Non-durable
O12	2.61	2.42	48.9	Medium	Non-durable
O21	2.71	0.45	98.6	High	Extremely durable
O31	2.68	0.35	98.7	High	Extremely durable
S11	2.56	2.20	95.9	High	Durable
S31	2.67	0.86	99.2	High	Extremely durable
S32	2.73	0.61	98.7	High	Extremely durable
D11	2.62	0.75	96.5	High	Durable
D12	2.62	2.07	98.1	High	Durable
D21	2.59	0.81	98.8	High	Extremely durable
C1B1	2.20	1.85	98.2	High	Durable
C1B2	2.65	1.05	94.7	High	Durable
C1B4	2.66	1.18	98.0	High	Extremely durable
C1B5	2.61	1.49	89.6	High	Durable
C21	2.30	2.57	66.2	Medium	Non-durable
C31	2.66	1.15	98.0	High	Extremely durable
C41	2.50	2.35	84.6	High	Non-durable
C51	2.53	1.96	49.9	Medium	Non-durable
C52	2.46	1.54	65.1	High	Non-durable
C61	2.63	2.01	68.4	High	Non-durable
C71	2.52	1.78	90.7	High	Non-durable
C82	2.49	2.66	30.8	Medium	Non-durable
C83	2.48	2.00	89.1	High	Durable
C92	1.76	1.65	98.8	Medium	Extremely durable
C101	2.52	2.23	72.3	High	Non-durable
C111	2.49	3.09	64.1	Medium	Non-durable
C112	2.50	1.48	86.5	High	Durable
C121	2.57	1.75	79.7	High	Non-durable
C122	2.39	1.49	88.7	High	Durable
C131	2.39	1.49	49.8	Medium	Non-durable
C132	2.48	1.27	94.1	High	Durable
C133	2.49	1.85	13.0	Medium	Non-durable
C141	2.50	2.49	76.5	High	Non-durable
C151	2.51	2.20	79.5	High	Durable
C161	2.60	1.41	95.4	High	Non-durable
C171	2.59	2.06	94.0	High	Durable
C172	2.61	1.21	96.6	High	Durable
C181	2.52	1.47	93.9	High	Durable

In addition, the importance of clay fraction within the mudrocks was evaluated on the basis of methylene blue adsorption value. Although, this index test is included both in DI index and Czerewko's classification there are slight differences between the test procedures used in this work and those in Czerewko's study that could unduly affect the results and inhibit comparison of the results. Therefore, the classes defined for the MBA's values for both classifications are different. Moreover, clay mineral content, mainly those of expansive nature, is higher in the Portuguese mudrocks, which can bias the results as methylene blue adsorption test is especially sensitive to the amount of expandable clay minerals present.

In short Czerewko's mudrocks are rather different from the mudrocks studied in this work. They are more indurated, with lower porosity values and expandable clay mineral content as well as being rich in siderite and organic matter. The classification proposed was developed using a data set of soft mudrocks and it is not directly applicable to a suite of more indurated mudrocks (*e.g.* UK Carboniferous Coal Measures Mudrocks) without changes to the parameter classes. Further research on mudrocks collected from other formations including both soft and strong types is required to improve durability ranking scheme. However, based on the results obtained it is considered that the scheme proposed is a useful qualitative approach to durability assessment of soft mudrock, particularly during the reconnaissance phases of engineering schemes, when it is not feasible to perform a more detailed characterization of materials.

8.4 - Application of durability classification to mudrock behaviour in natural and cut slopes

The behaviour of mudrock formation in natural and cut slopes depends upon two types of factors: (a) lithological characteristics and engineering properties of rock mass; and (b) slope characteristics. In the former are included the aspects related to rock material (type and amount of clay minerals, rock fabric, structure, strength and slake durability) and the characteristics of discontinuities. The slope characteristics include ground-water seepage, slope vegetation, slope angle, topography, climate, previous failures, and other features. The approach adopted in this study only takes into consideration those factors

relating to the rock material characteristics, because the other aspects have different importance depending on the particular case.

Many instability problems associated with low durability mudrocks, such as the materials studied, are superficial type failures involving in general the upper part of rock masses, which are more weathered and loose (Franklin, 1981). The superficial types of failures most likely to occur in mudrocks are as follows:

- excessive erosion;
- slump failures;
- debris flow;
- undercutting.

Although, there is generally no safety hazard associated with the occurrence of these types of failures, they may require costly remediation and/or routine maintenance.

The knowledge of mudrock durability characteristics allows the prediction of long-term slope behaviour. Based on the work of Dick & Shakoor (1995) the types of failures most likely to occur according to the durability classes defined for DI index (see Section 8.3) are presented in Table 8.9.

Table 8.9 - Types of slope instability which according to mudrock durability are more probable to occur (adapted from Dick & Shakoor, 1995).

Durability classes defined on the basis of DI index	Types of slope instability			
	Excessive erosion	Slump	Debris flow	Undercutting
High - $DI > 7$	+	+	++	+++
Medium - $6 \leq DI \leq 7$	+	++	+++	+++
Low - $DI < 6$	+++	+++	+++	+++

Probability of occurrence: + low; ++ medium; +++ high.

The purpose of Table 8.9 is not to define criteria to be used in slope design, because the data have not been validated on the basis of study cases, but to point out the types of slope instability which potentially may occur associated with mudrocks included in the various durability classes.

Excessive erosion is a type of slope instability that is likely to occur in materials prone to slaking, characterized by high expandable clay minerals content and low degree of induration (low dry density values). The probability of occurrence of this type of slope instability is high for the materials classified as low durability ($DI < 6$) which includes in the samples used the non-indurated materials and all weathered mudrock samples. The remedial measures to be adopted in order to minimize excessive erosion should be focused in the surface runoff control (slope angle, vegetative cover and drainage measures).

Slump failures generally occur after prolonged wet periods in which the upper part of the slope fan tends to become saturated. This process leads to an increase of weight and pore-water pressures and to a decline of shear strength of the superficial zone of rock mass. These conditions can cause the failure of this superficial layer composed of saturated soils, which moves downslope forming a plastic mass of debris in which the matrix (mud) component predominates over the clastic fraction. The lithological characteristics of mudrocks that control this type of slope instability are the presence of expandable clay minerals and a relatively high frequency of microfractures (Dick & Shakoor, 1995). The probability of occurrence of this type of failure was considered to be high and medium respectively for low and medium durability mudrocks. Weathered mudrocks samples showed in the jar slake test high breakdown revealing a tendency for the occurrence of this type of failure in those materials. So far as the medium durability mudrocks are concerned, the natural exposure and simulated ageing tests conducted on some samples revealed that prolonged exposure gives rise to a very high state of breakdown, which are compatible with this type of slope instability. In addition to surface runoff control, the remedial measures to minimize the occurrence of slump failures must as usual include internal drainage of slopes.

Debris flow is a common form of mudrock slope instability and, as in the case of slump failures, tends to occur after prolonged periods of rain. However, it occurs mainly due to the state of breakdown of the rocks acted upon by gravity. The results of jar slake test and natural exposure weathering experiments show that even the more durable mudrocks exhibit some breakdown giving rise to millimetric and centimetric debris. Therefore, it is considered that this type of slope instability may occur in mudrocks of

all durability classes. The remedial measures to minimize debris flow failures would usually include flattening of the slope geometry to a lower angle and placement of anchored wire-mesh nets over the slope face.

Mudrocks usually occur in association with resistant lithotypes such as sandstones and limestones. This type of stratigraphy is particularly prone to differential weathering. Accordingly, when slopes are cut through such lithological sequence, exposure to weathering for long periods leads to erosion of the softer units such that more competent overlying formations become undercut. As undercutting proceeds the vertical support of the stronger overlying layers reduces, which leads to the formation of overhangs and to slope instability. Undercutting can induce a variety of slope movements such as rock falls and wedge failures. It is considered that undercutting is likely to occur in mudrocks of all DI classes defined in Table 8.9, although the rate of undercutting will be high in rocks of lower durability. Shakoor & Rodgers (1992) proposed that the rate of undercutting may be predicted based on slake durability index (I_{d2}). Although, this will depend on climatic conditions prevailing elsewhere, for USA mudrocks these researchers showed that high, medium and low durability materials are expected to have undercutting rates respectively of 2 to 3, 3 to 5 and 5 to 10 cm per year. The remedial measures to be adopted to minimize undercutting-induced failures can be of two types (Shakoor, 1995):

- a) those that retard the rate of undercutting and prevent the initiation of overhang formation;
- b) those that minimize the effects of potential slope movements induced by differential weathering.

Remedial measures of the first type includes the protection of slope face with shotcrete, gabions walls and masonry, and of the second type the stabilization of unstable wedges and rock blocks involve using active or passive supporting structures such as anchorages and rock bolts.

8.5 - Characterizing studied mudrocks behaviour in fills as construction material

Construction with mudrock fills requires an adequate laboratory characterization of these materials, including the determination of their plasticity, swell potential, strength and durability. However, DiMillio & Strohm (1981) indicate that the latter property (durability) is a major factor that controls the behaviour of fills. Accordingly, this section is concerned with only the influence of rock material durability on the behaviour of fills constructed with mudrocks. Other aspects, such as foundations and drainage conditions, which are also important in the stability of fills, are not considered because they are beyond the scope of this work.

Maranha das Neves (1993) defined three possible typical situations from a grain size point of view for soft soil and weak rocks materials used as fills, these are illustrated diagrammatically in Fig. 8.44.

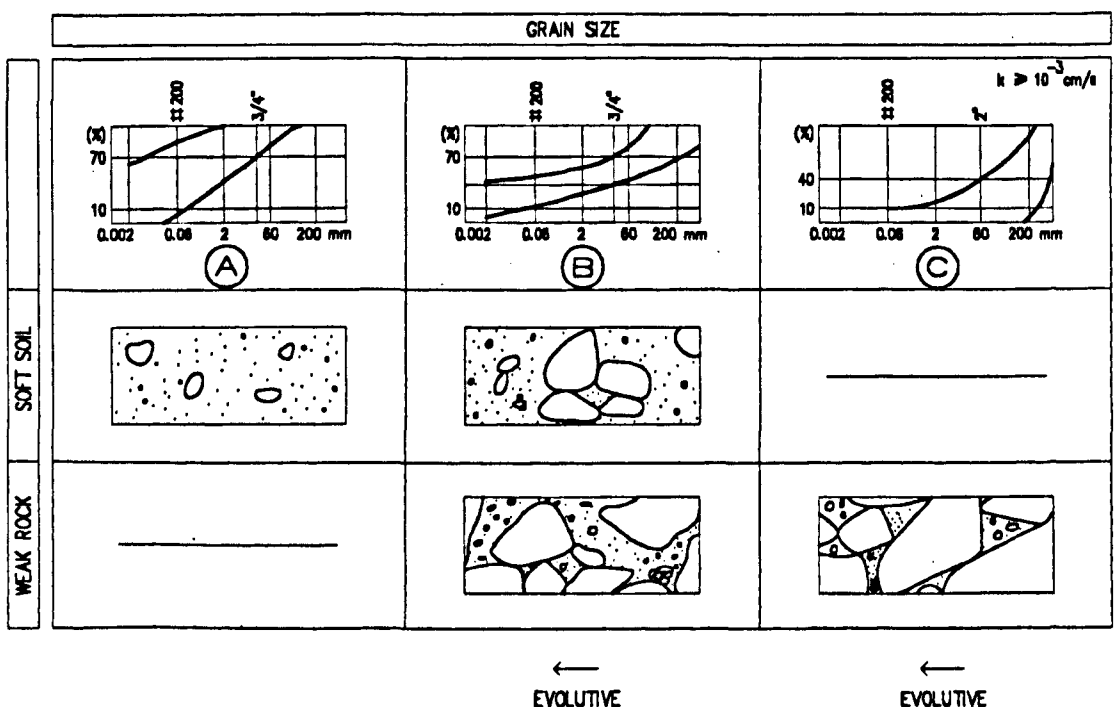


Fig. 8.44 - Typical grain size distributions and materials structure for soil, soil and rockfill mixture and rockfill (after Maranhã das Neves, 1993).

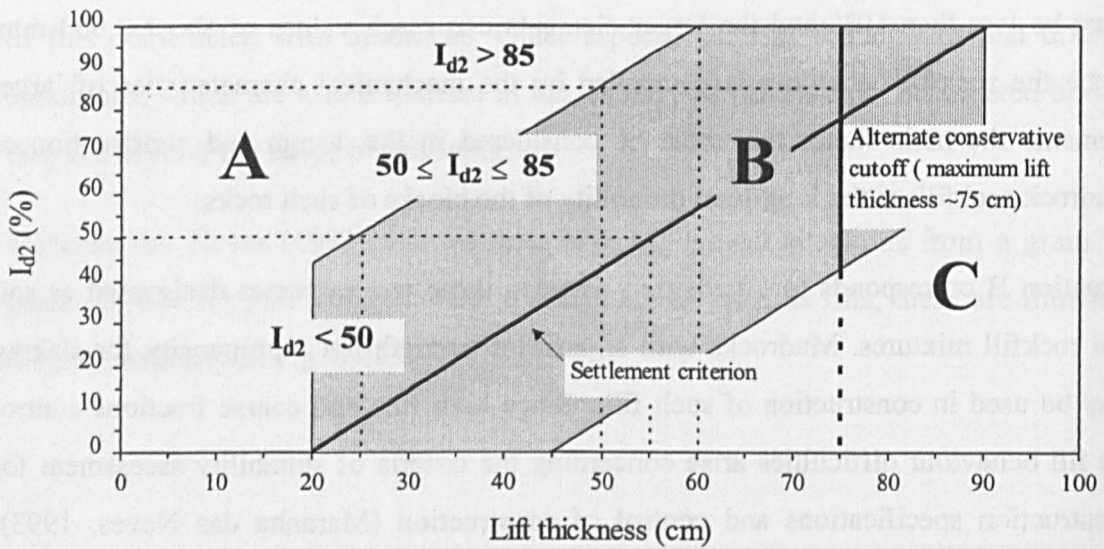
Situation A corresponds to soil fills which may be formed from weak and weathered mudrocks with low durability. These materials should be disaggregated and compacted like soils in thin lifts. The mechanical and permeability properties in these fills are controlled by the fine fraction and elements coarser than 19 mm can not exceed 30% in weight. The compaction properties (maximum dry density and optimum moisture content) can be specified from the results of Proctor compaction tests.

Situation C corresponds to rockfills in which mudrocks classified as mechanically resistant and durable can be used. The percentage of the fraction finer than 0.075 mm must be less than 10% and the larger elements can reach values of about 2,000 mm. Since the rockfill behaviour is controlled by the mechanical characteristics of larger elements the main factor that must be considered in the design and construction of mudrock rockfills is the long-term durability of the blocks of such rocks.

Situation B corresponds to a transition between these two extremes designated as soil and rockfill mixtures. Mudrocks with significant strength but a propensity for slaking may be used in construction of such fills. Since both fine and coarse fractions control the fill behaviour difficulties arise concerning the criteria of suitability assessment for construction specifications and control of construction (Maranha das Neves, 1993). Therefore, in order to achieve adequate compaction and reduce the settlement potential it may be necessary to use heavy compaction equipment capable of breaking oversized mudrock pieces. The excavation procedures (ripping and blasting) should be adjusted to achieve the grading required for compaction in relatively thin lifts. Furthermore, durable and non-durable materials should be identified during excavation operations to prevent mixing rocks with quite different durability characteristics.

Since mudrock durability is the major control on the behaviour of fills constructed with these rocks, several researchers have adopted the results of jar slake and slake durability tests (slaking behaviour of materials) as criteria to define the maximum lift thickness (Lutton, 1977; Strohm *et al.*, 1978; Franklin, 1981). Based on information on construction practice and performance of representative existing fills, Lutton (*id.*) found that the main cause of excessive settlements in road embankments resulted from the low durability of mudrock materials used in fills. In order to predict these type of instability Lutton (*ibid.*) developed a classification chart (Fig. 8.45) which indicates the maximum

lift thickness of the layer on the basis of I_{d2} values determined. The durability index service criterion (line) presented in Fig. 8.45 is expressed as a band in which different lift thicknesses can be considered for the same durability value, depending on the type and importance of the fill. Accordingly in the case of fills in which only minor settlements can be tolerated (e.g. bridge approach fills) the conservative limit (left side line) of the criterion band could be considered for evaluating the maximum lift thickness. In the case of fills in which minor settlements may be acceptable lifts could be adopted of greater thickness.



- A - No major problems, few minor problems.
- B - Few major problems, many minor problems.
- C - Major problems.

Fig. 8.45 - Criteria for evaluating embankment construction based on mudrock durability classes defined for I_{d2} values (adapted from Lutton, 1977).

The lift thickness intervals which correspond to the I_{d2} index intervals adopted in this work are presented in Fig. 8.45. Only the figures for the settlement criterion line and for the conservative limit (left side line) were taken into consideration. However, it was found that the lift thicknesses obtained according to the first criterion appear to be too high given the slaking behaviour of the rocks studied. Although, the natural exposure weathering tests had not been carried out on all the materials studied, they indicate that mudrocks, including samples with I_{d2} values greater than 90% (114 and 286), show significant degradations with breakdown of the initial test samples. The long-term

slaking behaviour of these materials resulting from the progressive dissolution of carbonate cements (see Chapter 7), which was not identified in the slake durability or jar slake tests, prevents the use of mudrocks with $I_{d2} > 85\%$ in lifts with thickness greater than 60 cm, *i.e.* as rockfill.

Accordingly, the use of the mudrocks studied as construction material in fills, requires the breakdown of larger particles and blocks through proper excavation procedures, watering of materials during placement and spreading phases or crushing. Therefore, for non-durable (soil-like) materials the adoption of the conservative limit (left side line of the band presented in Fig. 8.45) leads generically to a lift thickness between 20 and 25 cm. For mudrocks with $I_{d2} > 50\%$ the adoption of the conservative limit allows the use of these materials as soil and rockfill mixtures in maximum 60 cm lift thicknesses.

The compaction tests (Section 6.6.1) showed that the compaction characteristics are better in mixtures containing durable mudrocks and with mudrocks having a predominantly silt size particle composition. These tests also revealed that the use of weathered mudrocks (mixture SA1) as construction material on soil fills is viable.

Penetration tests using a CBR plunger showed that compacted samples with a water content in the range of 2% higher than the optimum moisture content, exhibit higher strength values after soaking. This fact shows the advantages of using water during the construction of mudrock fills and, therefore, it must be stressed that the materials should be compacted with a water content higher than the optimum moisture content (wet side of compaction curve). The purpose of this procedure is to prevent the harmful effects of saturation of fill materials, for example hydrocompaction, after construction.

9 - CONCLUSIONS AND SUGGESTIONS FOR FUTURE RESEARCH

9.1 - General conclusions

9.1.1 - Overview

The objective of the research was to determine the geological controls on the engineering properties of mudrocks in the north Lisbon area. The choice of this research theme was justified basically by the following reasons: (a) the relatively small number of studies on the characterization of fine-grained sedimentary rocks (mudrocks) that have been carried out by the Portuguese technical community; (b) the increasing involvement of these materials in planned or under construction engineering works particularly infrastructure projects in Portugal; (c) opportunity to extend existing research on durability of mudrocks into a suite of calcareous mudrocks; (d) examine the best means of characterizing the durability behaviour of a suite of mudrocks and select indicative index parameters.

This work contributes to the existing body of research on the classification of mudrocks which are the predominant lithologies in some regions of Portugal and to present the laboratory techniques to be used in their mineralogical, textural and geotechnical characterization. Accordingly, the characterization of geological and geotechnical properties of these rocks is a fundamental task, *e.g.* in road works, to evaluate the

stability of cut slopes and in the use (for economic and environmental reasons) of excavated material in construction of fills. Although these research topics are addressed in this work, they are far from being exhausted, given their multidisciplinary nature and the fact that the methodologies proposed need to be tested and adjusted according to experience gained from their use in practice. Therefore, it is expected that further research work will lead to new developments in these fields.

The most important aspects developed in this work and the main conclusions reached in the laboratory study performed are presented in the following sections. Based on this work, some suggestions for future research are outlined in Section 9.2.

9.1.2 - Classification and description of mudrocks

The terminology of fine-grained detrital sedimentary rocks (mudrocks) and the geological and geotechnical classifications most widely used to describe and classify these materials were reviewed in Chapter 3.

From the geological point of view, it was considered that the various lithotypes which comprise mudrocks should be distinguished on the basis of texture and structure. The first of these properties is characterised by the particle size of the components of mudrocks and it should not be determined by grain size analysis (sieving and sedimentation). Due to the difficulties arising from the disaggregation of more indurated mudrocks, the grain size composition of mudrocks is best obtained on the basis of mineralogy (Spears, 1980). Although, requiring specialized equipment and expertise, X-ray diffractometry and/or chemical dissolution methods provide an indication of the percentage of the resistate fraction (quartz plus feldspars). In the field the various lithotypes can be distinguished using certain simple identification techniques, which allow a rough evaluation of the grain size of the constituents of the rock. Such techniques are discussed in Section 2.2.3.

Structure in mudrocks is a feature mainly related to the presence and thickness of stratification and fissility. Beds and laminae are distinguished on the basis of an arbitrary thickness limit of 10 mm (Ingram, 1954; Potter *et al.*, 1980). This criterion was

adopted to classify mudrocks as massive or laminated. The presence of lamination and/or fissility in these rocks is accordingly indicated by the use of the suffix *-shale* after the name of the lithotype defined according to the grain size of the rock. It was also suggested in the case of mudrocks with a carbonate minerals content in excess of 10%, determined by wet chemical analysis, that the rock name should also include the term calcareous (Stow, 1981). Based on the parameters described and other geological and geotechnical parameters [strength, colour, stratification thickness, rock name, discontinuity spacing, other characteristics (when applicable) and weathering state] a classification for mudrocks is presented in Section 3.4. This classification was applied to describe and classify the samples collected and used in the research.

9.1.3 - Mineralogical studies

The mineralogical and textural characterization of mudrocks was of fundamental importance in the work carried out, given the importance of these aspects in the durability behaviour of these materials.

The proportions of the various constituents present in mudrocks were determined on the basis of various techniques, including X-ray diffraction, X-ray fluorescence and wet chemical analysis. The results made it possible to calculate the mineralogical composition of a suite of rocks which were chiefly composed of quartz, feldspars (K-feldspar and plagioclase), carbonate minerals (calcite and dolomite), pyrite, organic matter and clay minerals (see Section 5.2.4.2).

The non-clay constituents, with the exception of feldspars*, including quartz, carbonates, pyrite and organic matter were determined by wet chemical analysis techniques. These techniques proved, in general, to be appropriate providing a good level of reproducibility.

* The concentrations of feldspars were determined by X-ray diffraction while those of apatite and rutile were calculated directly from the data obtained from X-ray fluorescence.

The clay minerals identified in the samples comprised kaolinite, illite, chlorite, smectite and mixed-layer illite-smectite. Given the weak orientation of clay minerals and the dilution of the clay mineral peaks on the XRD traces due to the presence of quartz and calcite in the whole rock smear mounts, clay mineral quantification was carried out on the less than 2 μm fraction. The relative proportions were determined using the semi-quantitative method proposed by Schultz (1964). The relative percentages of clay minerals determined in the less than 2 μm fraction were considered to be more representative of the concentrations in which they occur in rock. It was also assumed that the total percentage of clay minerals present in the rocks corresponded to the difference between 100% and the non-clay constituents (essentially determined by wet chemical analysis techniques). Although, this approach is not without problems it is considered to be more suitable in clay mineral quantification than whole rock determinations.

9.1.4 - Textural characterization

The examination of the samples by optical microscopy and with scanning electron microscope made it possible to study the microtextural features of mudrocks and to complement information about some aspects of the mineralogy of the samples. Both SEM and EDS analysis were used to determine the mode of occurrence of the different mineral phases present in mudrocks. Accordingly, in Section 5.3.3 it was shown that the matrix of the mudrocks studied is mainly composed of clay minerals enabling the identification of areas with a predominantly kaolinitic composition and others with a composition close to illite-smectite. The relative proportions of non-clay minerals could also be studied.

In order to systematize the optical and scanning electron microscope observations the samples were described on the basis of microtextural parameters defined for the purpose: particle orientation, grain to grain relations, clay fabric and carbonate occurrence mode. Such parameters are discussed in Section 5.3.2 and applied in Section 5.3.3 on description of the mudrocks studied.

As particle orientation is concerned, the samples were differentiated between lithotypes with and without microlamination, the latter were distinguished according to whether they did or did not show preferred orientation of the rock forming constituents.

It was noted from the examinations carried out that quartz and feldspar (K-feldspar and plagioclase) constitute the coarser detrital fraction of the rocks studied and may occur as floating grains spread in the matrix or form a granular skeleton by grain-to-grain contacts and cementation bonds. It was also noted that grain-to-grain contacts predominated in siltstones, while in more fine-grained materials, such as claystones, the grains were mostly spread through the clay matrix. Obviously such observations are of fundamental importance to the performance of the materials in durability and strength tests.

The clay fabric was described on the basis of the clay particle association mode. From the samples collected, it was found that in weathered mudrocks clay particles were arranged in a predominantly EE and/or EF contacts giving rise to an open and loose structure (high porosity). On the contrary more indurated unweathered mudrocks had a dense structure with a relatively low porosity in which the arrangement of particles is essentially of the low angle EF and FF type.

Of the carbonates, calcite predominated and was sometimes the only constituent with sometimes dolomite also present. Calcite was identified in all samples, occurring as micrite, in medium and fine silt-sized grains and as sparite cement (mostly between coarser detrital grains of quartz and feldspar).

9.1.5 - Geotechnical characterization

The geotechnical characterization of mudrocks was undertaken on the basis of various laboratory tests by which were determined the physical parameters and geotechnical properties with most influence on engineering performance of the materials. The compaction characteristics of various mixtures of crushed rocks were also determined in order to evaluate the use of these rocks as fills.

The mudrocks studied are very prone to slaking when immersed in water which prevented the determination of porosity using vacuum saturation and buoyancy techniques. For this reason porosity was determined using a mercury porosimeter. However, the determination of porosity by the latter technique has some disadvantages because it requires specific equipment and is costly. Given the fact that mudrocks, possess particularly those studied relatively similar grain specific gravity values, the determination of dry density, the procedure for which involves the use of commonly available laboratory equipment, may constitute an attractive alternative method. The good correlation between porosity and dry density values that was found in the rocks studied shows that the latter parameter can be used to estimate the importance of void space in mudrocks (see Section 8.3). Therefore, in routine applications when the use of a mercury porosimeter is not feasible, the importance of void space can be evaluated in relative terms by determining the dry density. However, care would be required to ensure that the material does not include large amounts of siderite or organic matter.

The range of results obtained for porosity reflects the clay fabric (typified on the basis of SEM examination) and the weathering state of mudrocks. Accordingly, non-indurated materials exhibiting a loose packed mineral structure and weathered mudrocks (for which porosity may result from the dissolution of carbonate cements) have higher porosity values. Unweathered mudrocks having a more closely packed mineral structure usually show porosity values of less than 15%.

The geotechnical characterization of the clay fraction was of particular interest in this work. It is considered that the methylene blue adsorption test is especially suited to evaluate the potential for breakdown. The test is very sensitive to potential reactive clay minerals (see Section 6.7) and is easy and rapid to perform.

Uniaxial compression and cone indenter tests were employed to assess the strength of the suite of mudrocks. The correlations obtained in Section 6.7 between uniaxial compressive strength and the cone indenter numbers measured according to the standard ($CI_{(0.635)}$) and soft rock ($CI_{(0.23)}$) versions (with R^2 values higher than 0.86) confirmed that, given the easy and speed of testing as well as the fact that irregular samples can be used this determination is a useful alternative method of assessment of the strength of soft mudrocks. It was also concluded from the test results that strength characteristics of

these materials are controlled mainly by the porosity and mineralogical composition, namely by the amount and type of clay minerals. In this respect, an increase of porosity or of the clay fraction leads to a decrease in the strength values as determined by both uniaxial compressive and cone indenter tests.

Swelling tests on radially confined remoulded specimens and unconfined triaxial free swelling tests were employed to assess to the swelling potential of the suite of mudrocks. These tests characterized the influence of the mineralogical, structural and textural aspects of mudrocks on the determination of this property. It was shown in Section 6.7 that, although the swelling of mudrocks resulted from the hydration of clays, textural and structural characteristics, *e.g.* preferential orientation of clay minerals and the occurrence of lamination, have an important influence on this property. These textural and structural effects explain the anisotropic behaviour and the extremely high values of swelling determined for laminated lithotypes. The slaking of samples during triaxial tests, especially of the weathered materials, probably affected the swelling strain values obtained, which prevented the use of this property in the evaluation of the engineering performance of the mudrocks studied.

The assessment of mudrock slaking durability was based on slake durability and jar slake tests. Concerning the slake durability test, it was shown in Section 6.7 that an increase in test time (a further cycle of 600 rotations) made it possible to distinguish clearly between the weathered and unweathered materials. Particle size analysis carried out on the fraction smaller than 2 mm and the description of the material retained in the drum mesh are useful complements to the characterization of tested materials. This latter aspect is of particular importance as one of the main limitations of this test is to overestimate slake durability when the test fragments break down into fragments larger than 2 mm. Since the jar slake test reflects the development of microfractures, as was pointed out by Czerewko (1997), it is suited to the characterization of the slake durability of materials in such cases. Therefore, it is recommended, given the ease of testing, that the jar slake test be used together with slake durability test in the evaluation of mudrock slaking durability.

9.1.6 - Natural exposure and simulated ageing tests

The objective of the natural exposure and simulated ageing tests was to predict the long-term durability behaviour of the rocks studied, mainly in order to investigate their suitability as construction fill materials. With the exception of tests performed in the environmental chamber with relative humidity/temperature control, the weathering experiments gave rise to significant breakdown of mudrock materials. The mineralogical and geochemical characterization undertaken at the end of the tests, and presented in Sections 7.3.2 and 7.3.3, showed that the changes in composition were minor and mostly related to the dissolution of carbonates [in the case of materials subjected to acid (H_2SO_4) treatment this process led to the formation of gypsum]. Therefore, it is concluded that the breakdown of mudrocks, as shown by intense fragmentation of test samples, was controlled mainly by physical weathering processes.

To summarise, it was possible to distinguish the long-term durability behaviour of the various samples based on their mineralogical and lithological characteristics, despite the fact that the mudrocks exhibited at the end of tests a relative homogeneity in terms of level of breakdown (see Section 7.4). Thus, clayey mudrocks showed a rapid slaking rate, while highly calcareous mudrocks (carbonates in excess of 10%) exhibited a moderately slow progressive rate of breakdown controlled by the gradual dissolution of carbonate cements. This process allows water access into voids and discontinuities and to the sites of expandable clays, leading to secondary physico-chemical breakdown caused by clay mineral expansion and air breakage*. As a consequence, the level of breakdown of highly calcareous mudrocks will be underestimated on the basis of the jar slake test because, although this test has proved to be sensitive to physical weathering mechanisms, the 24 h period adopted for testing is insufficient to allow the dissolution of the carbonate cement. Therefore, the jar slake test alone is insufficient to predict the long-term durability of highly calcareous mudrocks under exposure to natural weathering conditions.

* The lowest $CI_{(0.23)}$ values determined for the samples subjected to acid (H_2SO_4) treatment proved the importance of the dissolution of carbonate cements in the breakdown of highly calcareous mudrocks, since this process is greatly enhanced by the addition of this acid.

9.1.7 - Assessment of mudrock durability

Using linear correlation analysis between the various mineralogical, physical and geotechnical parameters determined on the mudrocks it was possible to identify the major geological controls on durability. This analysis showed that durability cannot be based upon a single characteristic property. On the other hand, it was found from the laboratory characterization programme that certain index tests correlate strongly with mineralogical, textural and geotechnical properties which control the durability of the various mudrock lithotypes (see Sections 8.2.1 to 8.2.5).

The selection of the most suitable index tests for assessment of mudrock durability should be done on a case by case basis through the analysis of data obtained from detailed laboratory characterization of some representative samples. However, it was considered that this approach is not always feasible because is costly and involves complex laboratory resources. Therefore, it was concluded that dry density, methylene blue adsorption value and the percentage of material retained in the second cycle of the slake durability test are the minimum set of parameters recommended for the evaluation of mudrock durability in the reconnaissance phase of design studies. These parameters were integrated in a form of a ranking index - DI - defined in Section 8.3, which seemed to be suitable to predict durability of soft mudrock, namely to distinguish between potential problematic and non-problematic materials.

Superficial slope instability problems associated with mudrocks occurring in natural and cut slopes are discussed on the basis of the durability of such rocks in Section 8.4. Accordingly, it was investigated which types of slope instability were more likely to occur involving the materials included in each of durability classes defined for DI index. This approach neither included any factor linked to the slope characteristics nor was it validated with case studies and therefore is based only on the rock material intrinsic factors that control the mudrock durability.

Durability is the property of mudrocks that has a more effective control on the behaviour of fills constructed with these materials. The applicability to the mudrocks studied of the settlement criterion proposed by Lutton (1977) to define the maximum lift thickness to be used in the construction of fills was analysed in Section 8.5. Based on

long-term durability behaviour of the mudrocks only the lift thicknesses given by the conservative limit (left side line in Fig. 8.45) of the criterion band were considered. Accordingly, in the case of non-durable mudrocks ($I_{d2} < 50\%$) the adoption of the conservative limit of the criterion band gives to lift thicknesses of between 20 and 25 cm. In the case of mudrocks with $I_{d2} > 50\%$ the adoption of the conservative limit implies that these materials can be used as soil and rockfill mixtures with up to 60 cm lift thickness. On the other hand, the results of the compaction tests and the penetration tests using a CBR plunger showed that the use of weathered mudrocks as construction material is viable as well as that the fills should be compacted with a water content higher than the optimum moisture content.

9.2 - Suggestions for future research

Finally it should be stressed that it is fundamental to the continuation of research in this area that future studies be linked to the construction and monitoring of engineering schemes. Some suggestions for future research are identified as follows:

- a) laboratory characterization of a larger suite of samples collected from other mudrock formations, namely very fine-grained (claystones) and more indurated mudrocks, in order to validate the classification presented for assessment of mudrock durability; the application to other mudrocks of the DI index proposed could lead, in particular, to the adjustment of the intervals adopted for the classification parameters;
- b) work on case studies associated with engineering works (roads, man-made excavations, etc.) where the mudrocks present have demonstrated different long-term engineering behaviour; this would enable the approach defined in this study for assessment of mudrock durability to be tested;
- c) to investigate the degradability of stronger mudrocks when subjected to various types of processing [disaggregation of the material using a Los Angeles machine (ASTM C131, 1996; ASTM C535, 1996), drying and slaking cycles, etc.] and to different compactive energies (using Proctor type tests) in order to predict based on

laboratory results the change of grading that these materials undergo when used on fills;

- d) to develop studies which allow correlation between mudrock durability and measurements from periodic monitoring of road cuts profiles on mudrock formations, in order to establish appropriate design criteria and/or remedial measures intended to predict and minimize the occurrence of superficial failures in such works;
- e) to investigate through the construction of trial embankments the compactive characteristics of mudrocks varying lithological composition, durability, grain size range of the materials used, field compaction and volume of water added during placement and compare with those obtained in laboratory in order to improve the specifications used in the construction and control of compacted mudrock fills.

REFERENCES

- AASHTO T224, 1982 - Standard specifications for transportation materials and methods of sampling and testing. Part II, American Association of State Highway and Transportation Officials, Washington D. C.
- Andrews, D. E.; Withiam, J. L.; Perry, E. F. & Crouse, H. L., 1980 - Environmental effects of slaking of surface mine spoils: Eastern and Central United States. Bureau of Mines, U.S. Department of Interior, Denver, CO, Final Report, 247p.
- Anon., 1969 - New device for measuring rock strength. Mining and Minerals Engineering, March, p.59.
- Anon., 1970 - Working party report on the logging of rock cores for engineering purposes. Quarterly Journal of Engineering Geology, 3, 1-24.
- Anon., 1977 - The description of rock masses for engineering purposes. Quarterly Journal of Engineering Geology, 10, 355-388.
- Anon., 1995 - The description and classification of weathered rocks for engineering. Quarterly Journal of Engineering Geology, 28, 207-242.
- ASTM C131, 1996 - Test method for resistance to degradation of small-size coarse aggregate by abrasion and impact in the Los Angeles machine. 1999 Annual Book of ASTM Standards. Concrete and concrete aggregates, Section 4, Volume 04.02.
- ASTM C535, 1996 - Test method for resistance to degradation of large-size coarse aggregate by abrasion and impact in the Los Angeles machine. 1999 Annual Book of ASTM Standards. Concrete and concrete aggregates, Section 4, Volume 04.02.

ASTM D422, 1998 - Test method for particle size analysis of soils. 1999 Annual Book of ASTM Standards. Soil and Rock; Geosynthetics, Section 4, Volume 04.08.

ASTM D698, 1998 - Test method for laboratory compaction characteristics of soil using standard effort [12,400 ft-lbt/ft³ (600 kN.m/m³)]. 1999 Annual Book of ASTM Standards. Soil and Rock; Geosynthetics, Section 4, Volume 04.08.

ASTM D854, 1992 - Test method for specific gravity of soils. 1999 Annual Book of ASTM Standards. Soil and Rock; Geosynthetics, Section 4, Volume 04.08.

ASTM D1557, 1998 - Test method for laboratory compaction characteristics of soil using modified effort [56,000 ft-lbt/ft³ (2700 kN.m/m³)]. 1999 Annual Book of ASTM Standards. Soil and Rock; Geosynthetics, Section 4, Volume 04.08.

ASTM D1883, 1994 - Test method for CBR (California Bearing Ratio) of laboratory-compacted soils. 1999 Annual Book of ASTM Standards. Soil and Rock; Geosynthetics, Section 4, Volume 04.08.

ASTM D2216, 1998 - Test method for laboratory determination of water (moisture) content of soil and rock. 1999 Annual Book of ASTM Standards. Soil and Rock; Geosynthetics, Section 4, Volume 04.08.

ASTM D2217, 1998 - Practice for wet preparation of soil samples for particle size analysis and determination of soil constants. 1999 Annual Book of ASTM Standards. Soil and Rock; Geosynthetics, Section 4, Volume 04.08.

ASTM D2487, 1998 - Test method for classification of soils for engineering purposes (Unified Soil Classification System). 1999 Annual Book of ASTM Standards. Soil and Rock; Geosynthetics, Section 4, Volume 04.08.

ASTM D4254, 1996 - Test method for minimum index density and unit weight of soils and calculation of relative density. 1999 Annual Book of ASTM Standards. Soil and Rock; Geosynthetics, Section 4, Volume 04.08.

ASTM D4318, 1998 - Test method for liquid limit, plastic limit, and plasticity index of soils. 1999 Annual Book of ASTM Standards. Soil and Rock; Geosynthetics, Section 4, Volume 04.08.

ASTM D4404, 1992 - Test method for determination of pore volume and pore volume distribution of soil and rock by mercury intrusion porosimetry. 1999 Annual Book of ASTM Standards. Soil and Rock; Geosynthetics, Section 4, Volume 04.08.

ASTM D4644, 1992 - Test method for slake durability of shales and similar weak rocks. 1999 Annual Book of ASTM Standards. Soil and Rock; Geosynthetics, Section 4, Volume 04.08.

- ASTM D4718, 1994 - Practice for correction of unit weight and water content for soils containing oversize particles. 1999 Annual Book of ASTM Standards. Soil and Rock; Geosynthetics, Section 4, Volume 04.08.
- Aufmuth, R. E., 1974 - A systematic determination of engineering criteria for rock. *Bulletin of the Association of Engineering Geologists*, **11**, 235-245.
- Badger, C. W.; Cummings, A. D. & Whitmore, R. L., 1956 - The disintegration of shales in water. *Journal of the Institute of Fuel*, **29**, 417-423.
- Barton, N.; Lien, R. & Lunde, J., 1974 - Engineering classification of rock masses for the design of tunnel support. *Rock Mechanics*, **6**, 189-236.
- Bayliss, P., 1986 - Quantitative analysis of sedimentary minerals by powder X-ray diffraction. *Powder Diffraction*, **1**, 37-39.
- Bell, F. G., 1992 - Laboratory testing of rocks. In: Bell, F.G. (Ed.) *Engineering in rock masses*, Butterworth Heinmann Ltd., 151-171.
- Bell F. G.; Cripps, J. C.; Culshaw, M. G. & Entwisle, D., 1993 - Volume changes in weak rocks: Prediction and measurement. In: Anagnostopoulos, A. *et al.* (Eds.) *Geotechnical engineering of hard soils-soft rocks*, Balkema, Rotterdam, 925-932.
- Bell, F. G.; Entwisle, D. C. & Culshaw, M. G., 1997 - A geotechnical survey of some British Coal Measures mudstones with particular emphasis on durability. *Engineering Geology*, **46**, 115-129.
- Bennett, H. & Oliver, G., 1992 - XRF analysis of ceramics, minerals and allied materials. John Wiley & Sons, 298p.
- Bennett, R. H.; Bryant, W. R. & Keller, G. H., 1981 - Clay fabric of selected submarine sediments: Fundamental properties and models. *Journal of Sedimentary Petrology*, **51**, 217-232.
- Bennett, R. H. & O'Brien, N. R., 1991 - Determinants of clay and shale microfabrics signatures: Processes and mechanisms. In: Bennett, R. H.; Bryant, W. R.; Hulbert, M. H. (Eds.) *Microstructure of fine-grained sediments from mud to shale*, Springer-Verlag, 5-32.
- Berkovitch, I.; Manackerman, M. & Potter, N. M., 1959 - The Shale breakdown problem in coal washing: Part I - Assessing the breakdown of shales in water. *Journal of the Institute of Fuel*, **32**, 579-589.
- Bieniawski, Z. T., 1973 - Engineering classifications of jointed rock masses. *Transactions of South Africa Institute of Civil Engineers*, **15**, 335-344.

-
- Bieniawski, Z. T., 1975 - The point-load test in geotechnical practice. *Engineering Geology*, **9**, 1-11.
- Biscaye, P. E., 1965 - Mineralogy and sedimentation of recent deep sea clay in the Atlantic ocean and adjacent seas and oceans. *Geological Society of America Bulletin*, **76**, 803-832.
- Bjerrum, L., 1967 - Progressive failure in slopes of overconsolidated plastic clay and clay shales. *Journal of the Soil Mechanics and Foundations Division, ASCE*, **93**, 1-49.
- Blatt, H. 1982 - *Sedimentary petrology*. Freeman, New York.
- Blatt, H.; Jones, R. L. & Charles, R. G., 1982 - Separation of quartz and feldspars from mudrocks. *Journal of Sedimentary Petrology*, **52**, 660-662.
- Blatt, H.; Middleton, G. V. & Murray, R. C., 1980 - *Origin of sedimentary rocks*. 2nd Ed. Prentice-Hall, New Jersey, 782p.
- Broch E. & Franklin, J. A., 1972 - The point-load strength test. *International Journal of Rock Mechanics and Mining Science*, **9**, 669-697.
- Bromhead, E. N., 1979 - A simple ring shear apparatus. *Ground Engineering*, **12**, 40-44.
- Brook, N., 1980 - Size corrections for point load testing. Technical Note. *International Journal of Rock Mechanics and Mining Science & Geomechanics Abstracts*, **17**, 231-235.
- Brown, G. & Brindley, G. W., 1980 - X-ray diffraction procedures for clay mineral identification. In: Brindley, G. W. & Brown, G. (Eds.) *Crystal structure of clay minerals and their X-ray identification*. Mineralogical Society, Monograph N°5, London, 305-359.
- BS 812, 1990 - Testing aggregates. Part 112: Methods for determination of aggregate impact value (AIV).
- BS 1377, 1990 - Methods of test for soils for civil engineering purposes.
- BS 5930, 1981 - Code of practice for site investigations.
- Burnett, A. D., 1974 - The modification of the quantitative X-ray diffraction method of Schultz (1964) to the mineralogical study of London Clay samples. *Journal of Soil Science*, **25**, 179-188.
- Byers, C. W., 1974 - Shale fissility: Relation to bioturbation. *Sedimentology*, **21**, 479-484.

- Campbell, C. V., 1967 - Lamina, laminaset, bed and bedset. *Sedimentology*, **8**, 7-26.
- Campbell, I., 1993 - Engineering properties of kimmerdgian clays. Unpublished PhD Thesis, Sheffield University, 290p.
- Carter, P. G. & Mills, D. A., 1976 - Engineering geological investigations for the Kielder tunnels. *Quarterly Journal of Engineering Geology*, **9**, 125-141.
- Carter, P. G. & Sneddon, M., 1977 - Comparison of Schmidt hammer, point load and unconfined compression tests in carboniferous strata. In: Attewell, P. B. (Ed.) *Rock Engineering*. British Geotechnical Society, Newcastle-upon-Tyne, 197-220.
- Chandler, R. J., 1969 - The effect of weathering on the shear strength properties of Keuper Marl. *Géotechnique*, **19**, 321-334.
- Chandler, R. J., 1974 - Lias clay: The long-term stability of cutting slopes. *Géotechnique*, **24**, 21-38.
- Chandler, R. J.; Pachakis, M.; Mercer, J. & Wrightman, J., 1973 - Four long-term failures of embankments found on areas of landslip. *Quarterly Journal of Engineering Geology*, **6**, 405-422.
- Chandler, R. J. & Skempton, A. W., 1974 - The design of permanent cutting slopes in stiff fissured clays. *Géotechnique*, **24**, 457-466.
- Chapman, D. R.; Wood, L. E.; Lovell, C. W. & Sisiliano, W. J., 1976 - A comparative study of shale classification tests and systems. *Bulletin of the Association of Engineering Geologists*, **13**, 247-266.
- Chapman, S. L.; Syers, J. K. & Jackson, M. L., 1969 - Quantitative determination of quartz in soils, sediments and rocks by pyrosulfate fusion and hydrofluosilicic acid treatment. *Soil Science*, **107**, 348-355.
- Clark, A. R. & Walker, B. F., 1977 - A proposed scheme for the classification and nomenclature for use in the engineering description of Middle Eastern sedimentary rocks. *Geotechnique*, **27**, 93-99.
- Coelho, A. G., 1979 - Engineering geological evaluation of slope stability for urban planning and construction. *Bulletin of the International Association of Engineering Geology*, **19**, 75-78.
- Collins, K. & McGown, A., 1974 - The form and function features in a variety of natural soils. *Géotechnique*, **24**, 223-254.

-
- Collis, L. & Fox, R. A., 1985 - Aggregates: sand, gravel and crushed rock aggregates for construction purposes. Engineering Geology Special Publication N°1, Geological Society of London, London, 220p.
- Cripps, J. C. & Taylor, R. K., 1981 - The engineering properties of mudrocks. Quarterly Journal of Engineering Geology, **14**, 325-346.
- Czerewko, M. A., 1997 - Diagenesis of mudrocks, illite 'crystallinity' and the effects on engineering properties. Unpublished PhD Thesis, Sheffield University, 305p.
- Deen, R. C., 1981 - The need for a scheme for the classification of transitional (Shale) materials. Geotechnical Testing Journal, GTJODJ, **4**, 3-10.
- Deere, D. U. & Miller, R. P., 1966 - Engineering classification and index properties for intact rock., Air force Weapons Laboratory, Kirtland Air Base, New Mexico, Technical Report N° AFWL-TR-65-116.
- Denis, A.; Tourenq, C. & Lan, T. N., 1980 - Capacite d'adsorption d'eau des sols et des roches. Bulletin of the International Association of Engineering Geology, **22**, 201-205.
- Deo, P.; Wood, L. E. & Lovell, C. W., 1974 - Use of shale in embankments. National Research Council, Transportation Research Board, Special Report, **148**, 87-96.
- Dick, J. C., 1992 - Relationships between durability and lithological characteristics of mudrocks. Unpublished PhD thesis, Kent State University, 235p.
- Dick, J. C. & Shakoor, A., 1992 - Lithologic controls of mudrock durability. Quarterly Journal of Engineering Geology, **25**, 31-46.
- Dick, J. C. & Shakoor, A., 1995 - Characterizing durability of mudrocks for slope stability purposes. Geological Society of America, Reviews in Engineering Geology, **X**, 121-130.
- Dick, J. C.; Shakoor, A. & Wells, N., 1994 - A geological approach toward developing a mudrock-durability classification system. Canadian Geotechnical Journal, **31**, 17-27.
- DiMillio, A. F. & Strohm, W. E., 1981 - Technical guidelines for the design and construction of shale embankments. Transportation Research Record, **790**, 12-18.
- Dunbar, C. O. & Rodgers, J., 1957 - Principles of stratigraphy. John Wiley & Sons, New York, 356p.
- Duncan, N.; Dunne, M. H. & Petty, S., 1968 - Swelling characteristics of rocks. Water Power, **May**, 185-192.

- Dunoyer De Segonzac, G., 1970 - The transformation of clay minerals during diagenesis and low grade metamorphism: A review. *Sedimentology*, **15**, 281-346.
- Dusseault, M. B.; Cimolini, P.; Soderberg, H. & Scafe, D. W., 1983 - Rapid index tests for transitional materials. *Geotechnical Testing Journal*, GTJODJ, **6**, 64-72.
- Fairchild, I.; Hendry, G.; Quest, M. & Tucker, M. E., 1988 - Chemical analysis of sedimentary rocks. In: Tucker, M. E. (Ed.) *Techniques in sedimentology*, Blackwell, 275-354.
- Felix, C., 1987 - Essais et critères de choix pour des grès (molasses) de substitution lors de travaux de restauration. *Chantiers/Suisse*, **18**, 419-423.
- Fellows, P. M. & Spears, D. A., 1978 - The determination of feldspars in mudrocks using an X-ray powder diffraction method. *Clays and Clay Minerals*, **26**, 231-236.
- Fleming, R. W.; Spencer, G. S.; Banks, D. C., 1970 - Empirical study of behaviour of clay shale slopes. US Army Engineer Nuclear Cratering Group (NCG), Technical Report, N°15, **1**, 93p.
- Folk, R. L., 1968 - Petrology of sedimentary rocks. Hemphill's, Austin, 170p.
- Franklin, J. A., 1981 - A shale rating system and tentative applications to shale performance. *Transportation Research Record*, **790**, 2-12.
- Franklin, J. A., 1984 - A ring swell test for measuring swelling and shrinkage characteristics of rock. *International Journal of Rock Mechanics and Mining Science & Geomechanics Abstracts*, **21**, 113-121.
- Franklin, J. A.; Broch, E. & Walton, G., 1971 - Logging the mechanical character of rock. *Transactions/Section A of the Institution of Mining and Metallurgy*, **80**, A1-A9.
- Franklin, J. A. & Chandra, R., 1972 - The slake-durability test. *International Journal of Rock Mechanics and Mining Science*, **9**, 325-341.
- Fürsich, F. T. & Werner, W., 1987 - The upper Jurassic Bivalvia of Portugal. Part I. Palaeotaxodonta and Pteriomorphia (Arcoida and Mytiloidea). *Comunicações dos Serviços Geológicos de Portugal*, **73**, 103-144.
- Gamble, J. C., 1971 - Durability-plastic classification of shales and other argillaceous rocks. PhD Thesis, University of Illinois at Urbana-Champaign, 161p.
- Geological Society of America, 1991 - Rock colour chart. The Geological Society of America, 8th printing, USA, 1995.

-
- Gibbs, R. J., 1965 - Error due to segregation in quantitative clay mineral X-ray diffraction mounting techniques. *The American Mineralogist*, **50**, 741-751.
- Gillott, J. E., 1987 - *Clay in engineering geology*. Elsevier, Amsterdam, 468p.
- Grainger, P., 1984 - The classification of mudrocks for engineering purposes. *Quarterly Journal of Engineering Geology*, **17**, 381-387.
- Guifu, X. & Hong, L., 1986 - On the statistical analysis of data and strength expression in the rock point load tests. *Proceedings of the 5th Congress of the International Association of Engineering Geology*, Buenos Aires, 383-394.
- Hale, B. C.; Lovell, C. W. & Wood, L. E., 1981 - Development of a laboratory compaction-degradation test for shales. *Transportation Research Record*, **790**, 45-52.
- Hardy, R. G. & Tucker, M. E., 1988 - X-ray powder diffraction of sediments. In: Tucker, M. E. (Ed.) *Techniques in sedimentology*, Blackwell, 191-228.
- Hawkes, I. & Mellor, M., 1970 - Uniaxial testing in rock mechanics laboratories. *Engineering Geology*, **4**, 177-284.
- Hawkins, A. B. & Pinches, G. M., 1992 - Engineering description of mudrocks. *Quarterly Journal of Engineering Geology*, **25**, 17-30.
- Heley, W. & MacIver, B. N., 1971 - Engineering properties of clay shales. Development of classifications indexes for clay shales. Technical Report N° S-71-6, 1, US Army Engineer Waterways Experiment Station, Vicksburg, Mississippi, 89p.
- Hencher, S. R., 1993 - Conference summary. In: Cripps, J. C. *et al.* (Eds.) *The engineering geology of weak rock*, Balkema, Rotterdam, 499-504.
- Hongxi, L., 1993 - Physico-chemical properties of swelling soft rocks. In: Anagnostopoulos, A. *et al.* (Eds.) *Geotechnical engineering of hard soils-soft rocks*, Balkema, Rotterdam, 665-670.
- Hooton, D. H. & Giorgetta, N. E., 1977 - Quantitative X-ray diffraction analysis by a direct calculation method. *X-ray Spectrometry*, **6**, 2-5.
- Hopkins, T. C. & Deen, R. C., 1984 - Identification of shales. *Geotechnical Testing Journal*, GTJODJ, **7**, 10-18.
- Houston, S. & Walsh, K., 1993 - Comparison of rock correction methods for compaction of clayey soils. *Journal of Geotechnical Engineering*, ASCE, **119**, 763-778.

- Hudec, P. P., 1982 - Statistical analysis of shale durability factors. *Transportation Research Record*, **873**, 28-35.
- Hurlbut, C. S. & Klein, C., 1977 - *Manual of mineralogy* (after James D. Dana) 19th Ed. John Wiley & Sons, New York, 532p.
- IAEG, 1979 - Classification of rocks and soils for engineering geological mapping. Part I: Rock and soil materials. *Bulletin of the International Association of Engineering Geology*, **19**, 364-371.
- IAEG, 1981 - Rock and soil description and classification for engineering geological mapping. *Bulletin of the International Association of Engineering Geology*, **24**, 235-274.
- Ingram, R. L., 1953 - Fissility of mudrocks. *Bulletin of the Geological Society of America*, **64**, 869-878.
- Ingram, R. L., 1954 - Terminology for the thickness of stratification and parting units in sedimentary rocks. *Bulletin of the Geological Society of America*, **65**, 937-938.
- ISRM, 1972 - Suggested method for determining the point load strength index. Committee on Field Tests, Document N°1.
- ISRM, 1974 - Suggested method for determining shear strength. Final Draft. ISRM Commission on Standardization of Laboratory and Field Tests, Document N°1.
- ISRM, 1978a - Suggested method for determining hardness and abrasiveness of rocks. *International Journal of Rock Mechanics and Mining Science & Geomechanics Abstracts*, **15**, 89-97.
- ISRM, 1978b - Suggested method for determining the uniaxial tensile strength of rock materials. *International Journal of Rock Mechanics and Mining Science & Geomechanics Abstracts*, **15**, 99-103.
- ISRM, 1979a - Suggested method for determining the uniaxial compressive strength and deformability of rock materials. *International Journal of Rock Mechanics and Mining Science & Geomechanics Abstracts*, **16**, 135-140.
- ISRM, 1979b - Suggested method for determining water content, porosity, density, absorption and related properties and swelling and slake-durability index properties. *International Journal of Rock Mechanics and Mining Science & Geomechanics Abstracts*, **16**, 141-156.
- ISRM, 1981 - Basic geotechnical description of rock masses. *International Journal of Rock Mechanics and Mining Science & Geomechanics Abstracts*, **18**, 85-110.

-
- ISRM, 1983 - Characterization of swelling rock. Pergamon Press, Oxford.
- ISRM, 1985 - Suggested method for determining point load strength. *International Journal of Rock Mechanics and Mining Science & Geomechanics Abstracts*, **22**, 51-60.
- ISRM, 1989 - Suggested methods for laboratory testing of argillaceous swelling rocks. *International Journal of Rock Mechanics and Mining Science & Geomechanics Abstracts*, **26**, 415-426.
- ISRM, 1994 - Suggested methods for rapid field identification of swelling and slaking rocks. *International Journal of Rock Mechanics and Mining Science & Geomechanics Abstracts*, **31**, 547-550.
- ISSMFE., 1993 - Testing methods of indurated soils and soft rocks - Suggestions and Recommendations. Koichi, A. (Ed.), Japanese Society of Soil Mechanics and Foundation Engineering.
- Kiely, P. V. & Jackson, M. L., 1965 - Quartz, feldspar and mica determination for soil by sodium pyrosulfate fusion. *Soil Science Society Proceedings*, 159-163.
- Klug, H. P. & Alexander, L. E., 1974 - X-ray diffraction procedures. 2nd Ed. John Wiley & Sons, New York, 966p.
- Kojima, K.; Saito, Y. & Yokokura, M., 1981 - Quantitative estimation of swelling and slaking characteristics for soft rockmass. *Proceedings of the International Symposium on Weak Rock*, Tokyo, 219-223
- Krinsley, D. H.; Pye, K. & Kearsley, A. T., 1983 - Application of backscattered electron microscopy in shale petrology. *Geological Magazine*, **120**, 109-118.
- Krinsley, D. H.; Nagy, B.; Dypvik, H. & Rigali, M., 1993 - Microtextures in mudrocks as revealed by backscattered electron imaging. *Precambrian Research*, **61**, 191-207.
- Jackson, J. O. & Fookes, P. G., 1974 - The relationship of the estimated former burial depth of the Lower Oxford Clay to some soil properties. *Quarterly Journal of Engineering Geology*, **7**, 137-179.
- JCPDS, 1974 - Powder diffraction file. Joint Committee on Powder Diffraction Standards, Pennsylvania, USA.
- Jeremias, F. T., 1991 - Importância da expansibilidade na durabilidade dos materiais rochosos e técnicas laboratoriais para a sua avaliação. Unpublished Msc Thesis, UNL, Lisboa, 220p.

- Jeremias, F. T., 1993 - Determinação das pressões de expansão em rochas argilosas. *Geotecnia*, **68**, 81-88.
- Lan, T. N., 1981 - Utilisation de l'essai au bleu de méthylène en terrassement routier. *Bulletin de Liaison des Laboratoires des Ponts et Chaussées*, **111**, 5-16.
- Lan, T. N. & Millon-Devigne, P., 1984 - L'essai au bleu de méthylène turbidimétrique. *Bulletin of the International Association of Engineering Geology*, **29**, 453-456.
- Lewan, M., 1978 - Laboratory classification of very fine grained sedimentary rocks. *Geology*, **6**, 745-748.
- LNEC, 1967a - Solos. Análise granulométrica. LNEC Standard Nº 196, LNEC, Lisboa.
- LNEC, 1967b - Solos. Ensaio de compactação. LNEC Standard Nº 197, LNEC, Lisboa.
- LNEC, 1967c - Solos. Determinação do CBR. LNEC Standard Nº 198, LNEC, Lisboa.
- LNEC, 1967d - Solos. Ensaio de expansibilidade. LNEC Standard Nº 200, LNEC, Lisboa.
- LNEC, 1967e - Solos. Determinação do teor em matéria orgânica. LNEC Standard Nº 201, LNEC, Lisboa.
- LNEC, 1971 - Solos. Análise granulométrica por peneiração húmida. LNEC Standard Nº 239, LNEC, Lisboa.
- LNEC, 1996 - Ensaio de determinação da porometria de mercúrio. Laboratorial Procedure LERO PE-15, LNEC, Lisboa.
- Lo, K. Y.; Wai, R. S. C. & Palmer, J. H. L.; Quigley, R. M., 1978 - Time-dependent deformation of shaly rocks in southern Ontario. *Canadian Geotechnical Journal*, **15**, 537-547.
- Lowell, S. & Shields, J. E., 1991 - Powder surface area and porosity. 3rd Ed. Chapman & Hall, London, 250p.
- Lundegard, P. D. & Samuels, N. D., 1980 - Field classification of fine-grained sedimentary rocks. *Journal of Sedimentary Petrology*, **50**, 781-786.
- Lutton, R. J., 1977 - Design and construction of compacted shales embankments. Volume 3 - Slaking Indexes for Design. Federal Highway Administration, US Department of Transportation, Report Nº FHWA-RD-77-1, 94p.

-
- Macquaker, J. H. S., 1994 - A lithofacies study of the Peterborough Member, Oxford clay formation (Jurassic), UK: An example of sediment bypass in a mudstone succession. *Journal of the Geological Society, London*, **151**, 161-172.
- Macquaker, J. H. S. & Gawthorpe, R. L., 1993 - Mudstone lithofacies in the kimmeridge clay formation, Wessex Basin, Southern England: Implications for the origin and controls of the distribution of mudstones. *Journal of Sedimentary Petrology*, **63**, 1129-1143.
- Magnan, J. P. & Youssefian, G., 1989 - Essai au bleu de méthylène et classification géotechnique des sols. *Bulletin de Liaison des Laboratoires des Ponts et Chaussées*, **159**, 93-104.
- Maranha das Neves, E., 1993 - General report session 5: Fills and embankments. In: Anagnostopoulos, A. *et al.* (Eds.) *Geotechnical engineering of hard soils-soft rocks*, Balkema, Rotterdam, 2023-2037.
- Maxwell, J. A., 1981 - Rock and Mineral analysis. *Chemical Analysis*, **27**, Interscience, New York.
- McKee, E. D. & Weir, G. W., 1953 - Terminology for stratification and cross-stratification in sedimentary rocks. *Bulletin of the Geological Society of America*, **64**, 381-389.
- Mead, W. J., 1936 - Engineering geology of dam sites. *Transactions of 2nd International Congress on Large Dams, Washington, D. C.*, **4**, 183-198.
- Mesri, G. & Cepeda-Diaz, A. F., 1986 - Residual shear strength of clays and shales. *Géotechnique*, **36**, 269-274.
- Monahan, E. J., 1986 - Construction of and on compacted fills. John Wiley & Sons, New York, 200p.
- Moon, C. F. & Hurst, C. W., 1984 - Fabric of muds and shales: An overview. In: Stow, D. A. V. & Piper, D. J. W. (Eds.) *Fine-grained sediments: Deep water processes and facies*, Oxford, Blackwell, 579-593.
- Moore, D. M. & Reynolds, R. C., 1989 - X-ray diffraction and the identification and analysis of clay minerals. Oxford University Press, 332p.
- Morgenstern, N. R. & Eigenbrod, K. D., 1974 - Classification of argillaceous soils and rocks. *Journal of Geotechnical Engineering, ASCE*, **100**, 1137-1157.
- Mugrider, S. & Young, H. R., 1983 - Disintegration of shale by cyclic wetting and drying and frost action. *Canadian Journal of Earth Sciences*, **20**, 568-576.

- Nascimento, U; Oliveira, R. & Graça, R., 1968 - Rock swelling tests. Proceedings of the International Symposium on Rock Mechanics, Madrid, 363- 365.
- National Coal Board, 1977 - NCB cone indenter. Mining Research and Development Establishment Handbook N°5, London, England, 12p.
- Norrish, K. & Hutton, J. T., 1969 - An accurate X-ray spectrographic method for the analysis of a wide range of geological samples. *Geochimica et Cosmochimica Acta*, **33**, 431-453.
- Norrish, K. & Chappell, B. W., 1977 - X-ray fluorescence spectrometry. In: Zussman, J. (Ed.) *Physical methods in determinative mineralogy*, Academic Press, London, 201-272.
- NP-83, 1965 - Solos. Determinação da densidade das partículas. Portuguese Standard N°83, Lisboa, Portugal.
- NP-84, 1965 - Solos. Determinação do teor em água. Portuguese Standard N°84, Lisboa, Portugal.
- NP-143, 1969 - Solos. Determinação dos limites de consistência. Portuguese Standard N°143, Lisboa, Portugal.
- O'Brien, N. R., 1970 - The fabric of a shale - an electron microscope study. *Sedimentology*, **15**, 229-246.
- Oakland, M. W. & Lovell, C. W., 1982 - Standardized tests for compacted shale highway embankments. *Transportation Research Record*, **873**, 15-21.
- Odom, I. E., 1967 - Clay fabric and its relation to structural properties in mid-continental Pennsylvanian sediments. *Journal of Sedimentary Petrology* **37**, 610-623.
- Okagbue, C.O., 1984 - The geotechnical characteristics and stability of a spoil heap at a southwestern Pennsylvania coal mine USA. *Engineering Geology*, **20**, 325-341.
- Okamoto, R.; Sugahara, H. & Hirano, I., 1981 - Slaking and swelling properties of mudstone. Proceedings of the International Symposium on Weak Rock, Tokyo, 213-218.
- Oliveira, R., 1993 - Weak rock materials. In: Cripps *et al.* (Eds.) *The engineering geology of weak rock*, Balkema, Rotterdam, 5-15.
- Olivier, H. J., 1976 - Importance of rock durability in the engineering classification of Karoo rock masses for tunnelling. Proceedings of the Symposium on Exploration for Rock Engineering, Johannesburg, Balkema, 137-144.

-
- Olivier, H. J., 1979 - A new engineering-geological rock durability classification. *Engineering Geology*, **14**, 255-279.
- Ordaz, J. & Argandoña, V., 1981 - Swelling characteristics of some mudrocks from Asturias (Spain). *Proceedings of the International Symposium on Weak Rock*, Tokyo, 231-235.
- Penner, E.; Eden, W. J. & Gillott, J. E., 1973 - Floor heave due to biochemical weathering of shale. *Proceedings of the 8th International Conference on Soil Mechanics and Foundation Engineering*, Moscow, 151-158.
- Perry, E. F. & Andrews, D. E., 1982 - Slaking modes of geologic materials and their impact on embankment stabilization. *Transportation Research Record*, **873**, 22-28.
- Pettijohn, F. J., 1975 - *Sedimentary rocks*. New York, Harper and Row, 628p.
- Picard, M. D., 1971 - Classification of fine-grained sedimentary rocks. *Journal of Sedimentary Petrology*, **41**, 179-195.
- Pike, S., 1989 - Mineral matter in coal and its influence on ash combustion. Unpublished PhD Thesis, University of Sheffield.
- Potter, P. E.; Maynard, J. B. & Pryor, W. A., 1980 - *The sedimentology of shale: A study guide and reference source*. New York, Springer-Verlag, 306p.
- Potts, P. J., 1987 - *A handbook of silicate rock analysis*. Chapman and Hall, New York, 621p.
- Pye, K. & Krinsley, D. H., 1986 - Microfabric, mineralogy and early diagenetic history of the Whitby Mudstone Formation (Toarcian), Cleveland Basin, UK. *Geological Magazine*, **123**, 191-203.
- Reynolds, S. & Gorsline, D. S., 1992 - Clay microfabric of deep-sea, detrital mud(stone)s, California continental borderland. *Journal of Sedimentary Petrology*, **62**, 41-53.
- Rocha, M., 1977 - Alguns problemas relativos à mecânica das rochas dos materiais de baixa resistência. Memory N°491, LNEC, Lisboa.
- Rocha, M., 1981 - *Mecânica das rochas*. LNEC, Lisboa, 445p.
- Rodrigues, J. D., 1986 - Contribuição para o estudo das rochas carbonatadas e para a sua classificação geotécnica. Internal Report 104/86-NP, LNEC, Lisboa.

- Rodrigues, J. D., 1988 - Proposed geotechnical classification of carbonate rocks based on Portuguese and Algerian examples. *Engineering Geology*, **25**, 33-43.
- Rodrigues, J. D. & Jeremias, F. T., 1989 - Contribuição para o estudo das rochas grauvacóides e para a avaliação da sua durabilidade. Internal Report 101/89-NP, LNEC, Lisboa.
- Rodrigues, J. D. & Jeremias, F. T., 1990 - Assessment of rock durability through index properties. Proceedings of the 6th Congress of the International Association of Engineering Geology, Amsterdam, 3055-3060.
- Russell, D. J., 1982 - Controls on shale durability: The response of two ordovician shales in the slake durability test. *Canadian Geotechnical Journal*, **19**, 1-13.
- Sá, C. P. M., 1993 - A microscopia electrónica de varrimento (SEM) e a microanálise por raios X (EPMA) na caracterização de materiais. In: *Técnicas microanalíticas em geologia suas aplicações industriais*, IGM, Porto, 1-66.
- Sarman, R. & Shakoor, A., 1990 - Prediction of volumetric increase of selected mudrocks. Proceedings of the 6th Congress of the International Association of Engineering Geology, Amsterdam, 459-465.
- Sarman R.; Shakoor, A. & Palmer, D. F., 1994 - A multiple regression approach to predict swelling in mudrocks. *Bulletin of the Association of Engineering Geologists*, **31**, 107-121.
- Sasaki, T.; Kinoshita, S. & Ishijima, Y., 1981 - A study on water-sensitivity of argillaceous rock. Proceedings of the International Symposium on Weak Rock, Tokyo, 149-154.
- Schultz, L. G., 1960 - Quantitative X-ray determinations of some aluminous clay minerals in rocks. In: Swineford, Ada (Ed.) *Clays and clay minerals*, New York, Pergamon Press, 216-224.
- Schultz, L. G., 1964 - Quantitative interpretation of mineralogical composition from X-ray and chemical data for the Pierre Shale. US Geological Survey Professional Paper 391-C, 31p.
- Seedsman, R., 1986 - The behaviour of clays shales in water. *Canadian Geotechnical Journal*, **23**, 18-22.
- Shakoor, A., 1995 - Slope stability considerations in differentially weathered mudrocks. Geological Society of America, *Reviews in Engineering Geology*, **X**, 131-138.

-
- Shakoor, A. & Brock, D., 1987 - Relationship between fissility, composition and engineering properties of selected shales from northeast Ohio. *Bulletin of the Association of Engineering Geologists*, **24**, 363-379.
- Shakoor, A. & Rodgers, J., 1992 - Predicting the rate of shale undercutting along highway cuts. *Bulletin of the Association of Engineering Geologists*, **29**, 61-75.
- Shakoor, A. & Scholer, C. F., 1985 - Comparison of aggregate pore characteristics as measured by mercury intrusion porosimeter and Iowa pore index tests. *ACI Journal*, **82-83**, 453-458.
- Shakoor, A. & Weber, M. W., 1988 - Role of shale undercutting in promoting rock falls and wedge failures along Interstate 77. *Bulletin of the Association of Engineering Geologists*, **25**, 219-234.
- Shamburger, J. H.; Patrick, D. M. & Lutton, R. I., 1975 - Design and construction of compacted shale embankments. Volume 1 - Survey of problem areas and current practices. Federal Highway Administration, US Department of Transportation, Report N°FHWA-RD-75-61.
- Shaw, D. B. & Weaver, C. E., 1965 - The mineralogical composition of shales. *Journal of Sedimentary Petrology*, **35**, 213-222.
- Skempton, A. W., 1964 - Long-term stability of clay slopes. *Géotechnique*, **14**, 77-101.
- Spears, D. A., 1976 - The fissility of some carboniferous shales. *Sedimentology*, **23**, 721-725.
- Spears, D. A., 1980 - Towards a classification of shales. *Journal of the Geological Society, London*, **137**, 125-130.
- Spears, D. A. & Taylor, R. K., 1972 - The influence of weathering on the composition and engineering properties of *in situ* Coal Measures rocks. *International Journal of Rock Mechanics and Mining Science*, **9**, 729-756.
- Spink, T. W. & Norbury, D. R., 1993 - The engineering geological description of weak rocks and overconsolidated soils. In: Cripps *et al.* (Eds.) *The engineering geology of weak rock*, Balkema, Rotterdam, 289-301.
- Stacey, T. R.; Heerden, W. L. & Vogler, U. W., 1987 - Properties of intact rock. In: Bell, F. G. (Ed.) *Ground engineer's reference book*, Butterworths, London, 4/1-4/28.
- Starkey, R. J.; Blackmon, P. D. & Hauff, P. L., 1984 - The routine mineralogical analysis of clay-bearing samples. US Geological Survey, Bulletin 1563.

- Steward, H. E. & Cripps, J. C., 1983 - Some engineering implications of chemical weathering of pyritic shale. *Quarterly Journal of Engineering Geology*, **16**, 281-289.
- Stimpson, B. & Acott, C. P., 1983 - Application of the NCB cone indenter to strength index of sedimentary rock from western Canada. *Canadian Geotechnical Journal*, **20**, 532-535.
- Stow, D. A., 1981 - Fine-grained sediments: Terminology. *Quarterly Journal of Engineering Geology*, **14**, 243-244.
- Strohm, W. E.; Bragg, G. H. & Ziegler, T. W., 1978 - Design and construction of compacted shale embankments: Volume 5 - Technical guidelines. Federal Highway Administration, US Department of Transportation, Report N° FHWA-RD-78-141.
- Surendra, M.; Lovell, C. W. & Wood, L. E., 1981 - Laboratory studies of the stabilization of non-durable shales. *Transportation Research Record*, **790**, 33-41.
- Swan, A. R. H. & Sandilands, M., 1995 - Introduction to geological data analysis. Blackwell, 446p.
- Taylor, R. K., 1988 - Coal Measures mudrocks: Composition classification and weathering processes. *Quarterly Journal of Engineering Geology*, **21**, 85-99.
- Taylor, R. K. & Cripps, J. C., 1984 - Mineralogical controls on volume change. In: Attewell, P. B. & Taylor, R. K. (Eds.) *Ground movements and their effects on structures*, Surrey University Press/Blackie Group, Glasgow, 268-302.
- Taylor, R. K. & Cripps, J. C., 1987 - Weathering effects: Slopes in mudrocks and over-consolidated clays. In: Anderson, M. G. & Richards, K. S. (Eds.) *Slope Stability*, John Wiley & Sons, 405-445.
- Taylor, R. K. & Smith, T. J., 1986 - The engineering geology of clay minerals: Swelling, shrinking and mudrock breakdown. *Clay Minerals*, **21**, 235-260.
- Taylor, R. K. & Spears, D. A., 1970 - The breakdown of British Coal Measure Rocks. *International Journal of Rock Mechanics and Mining Science*, **7**, 481-501.
- Taylor, R. K. & Spears, D. A., 1981 - Laboratory investigation of mudrocks. *Quarterly Journal of Engineering Geology*, **14**, 291-309.
- Till, R. & Spears, D. A., 1969 - The determination of quartz in sedimentary rocks using an X-ray diffraction method. *Clays and Clay Minerals*, **17**, 323-327.
- Tourtlot, H. A., 1960 - Origin and use of the word "shale". *American Journal of Science*, **258-A**, 335-343.

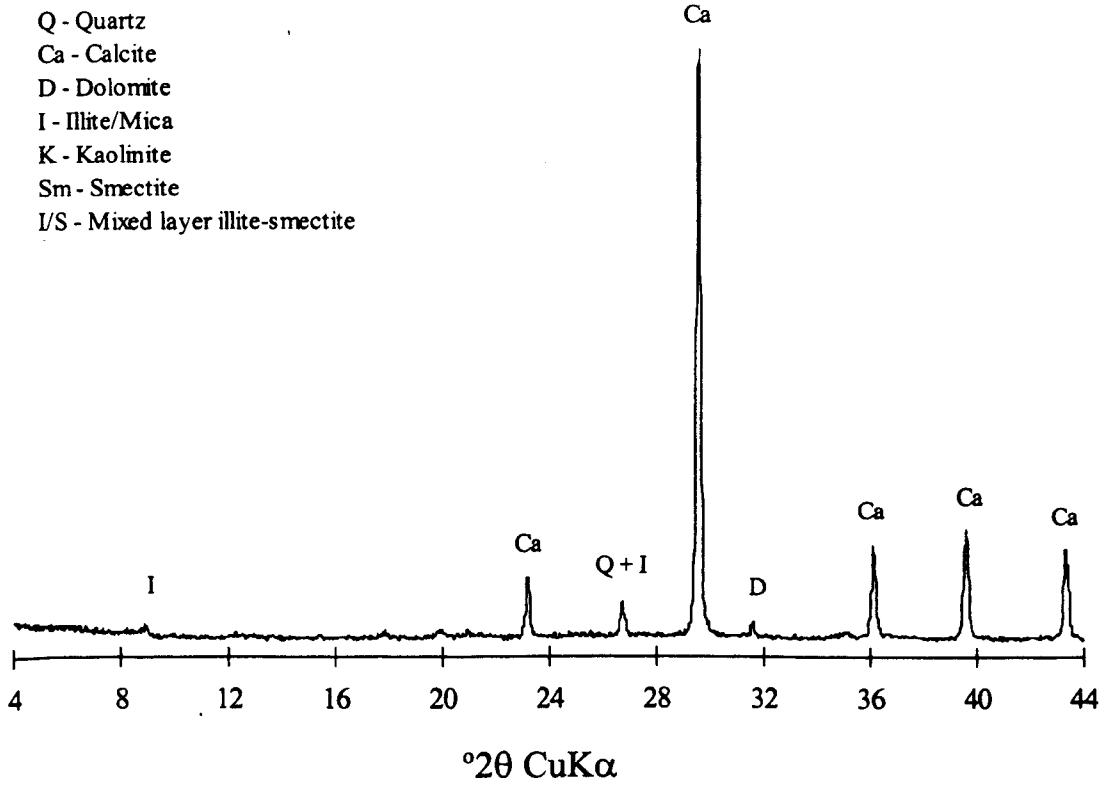
-
- Towe, K. M., 1974 - Quantitative clay petrology: The trees but not the forest ? *Clays and Clay Minerals*, **22**, 375-378.
- Trewin, N. H., 1988 - Use of the scanning electron microscope in sedimentology. In: Tucker, M. E. (Ed.) *Techniques in sedimentology*, Blackwell, 229-273.
- Trostel, L. J. & Wynne, D. J., 1940 - Determination of quartz (free silica) in refractory clays. *Journal of the American Ceramic Society*, **23**, 18-22.
- Tsige, M.; Vallejo, L. G.; Doval, M.; Barba, C.; Oteo, C., 1994 - Microfabric of Guadalquivir 'Blue Marls' and its engineering geological significance. *Proceedings of the 7th Congress of the International Association of Engineering Geology, Lisboa*, 659- 665.
- Tucker, M. E., 1994 - *Sedimentary petrology*. 2nd Ed. Blackwell, Oxford, 260p.
- Tucker, M. E., 1995 - *Sedimentary rocks in the field*. 2nd Ed. John Wiley & Sons, 153p.
- Underwood, L. B., 1967 - Classification and identification of shales. *Journal of the Soil Mechanics and Foundations Division, ASCE*, **93**, 97-116.
- Venter, J. P., 1980 - An investigation of the slake durability test for mudrocks used in road construction. *Proceedings of the 7th Regional Conference for Africa on Soil Mechanics and Foundation Engineering*, 201-207.
- Venter, J. P., 1998 - An overview of the engineering properties and the use of mudrock in road construction in South Africa. *Proceedings of the 8th Congress of the International Association of Engineering Geology, Amsterdam*, 2785-2796.
- Volger, U. W., 1985 - Laboratory techniques for assisting in the characterization of non-durable rock masses. *Proceedings of the Symposium on Rock Mass Characterization, Randburg, South Africa*, 99-105.
- Weaver, C. E., 1980 - Fine-grained rocks: Shale or physilites. *Sedimentary Geology*, **27**, 301-313.
- Weaver, C. E., 1989 - *Clays, muds, and shales. Developments in sedimentology* 44. Elsevier, Amsterdam, 819p.
- Weir, A. H.; Ormerod, E. C.; El-Mansey, I. M. I., 1975 - Clay mineralogy of sediments of the western Nile delta. *Clay Minerals*, **10**, 369-386.
- Wentworth, C. K., 1922 - A scale of grade and class terms for clastic sediments. *Journal of Geology*, **30**, 377-392.

- White, S. H.; Shaw, H. F.; Huggett, J. M., 1984 - The use of back-scattered electron imaging for the petrographic study of sandstones and shales. *Journal of Sedimentary Petrology*, **54**, 487-494.
- Wickham, G. E.; Tiedemann, H. R.; Skinner, E. H., 1972 - Support determinations based on geological predictions. *Proceedings of the 1st North America Rapid Excavations and Tunnelling Conference*, 43-64.
- Wilson, M. J., 1987 - X-ray powder diffraction methods. In: Wilson, M. J. (Ed.) *A handbook of determinative methods in clay mineralogy*, Glasgow, Blackie, 26-98.
- Wilson, R. C., 1979 - A reconnaissance study of upper Jurassic sediments of the Lusitanian Basin. *Ciências da Terra*, **5**, 53-84.
- Wood, L. E. & Deo, P., 1975 - A suggested system for classifying shale materials for embankments. *Bulletin of the Association of Engineering Geologists*, **12**, 39-55.
- Yaalon, D. H., 1962 - Mineral composition of average shale. *Clay Minerals Bulletin*, **5**, 31-36.
- Zbyszewski, G. & Assunção, C. T., 1965 - *Notícia explicativa da Folha 30D, Alenquer. Serviços Geológicos de Portugal, Lisboa, 104p.*
- Zbyszewski, G. & Moitinho de Almeida, F., 1960 - *Notícia explicativa da Folha 26D, Caldas da Rainha. Serviços Geológicos de Portugal, Lisboa, 56p.*

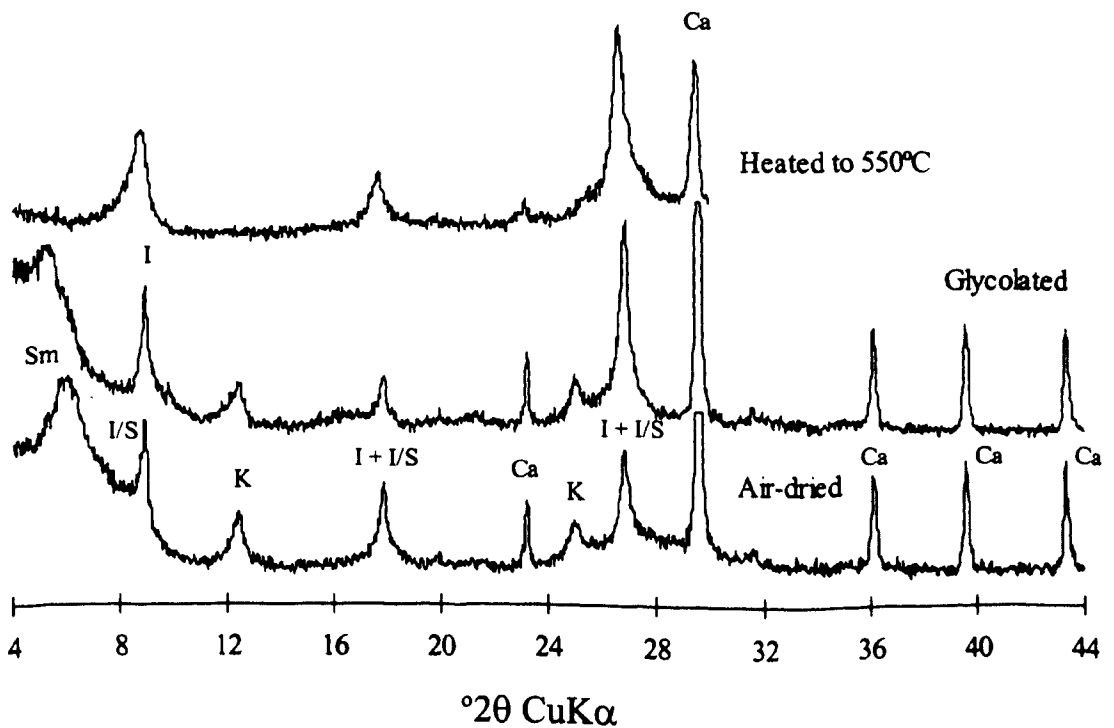
**APPENDIX I - MINERALOGY AND
GEOCHEMISTRY**

Appendix I.1 - Whole rock and less than 2 μm fraction XRD scans

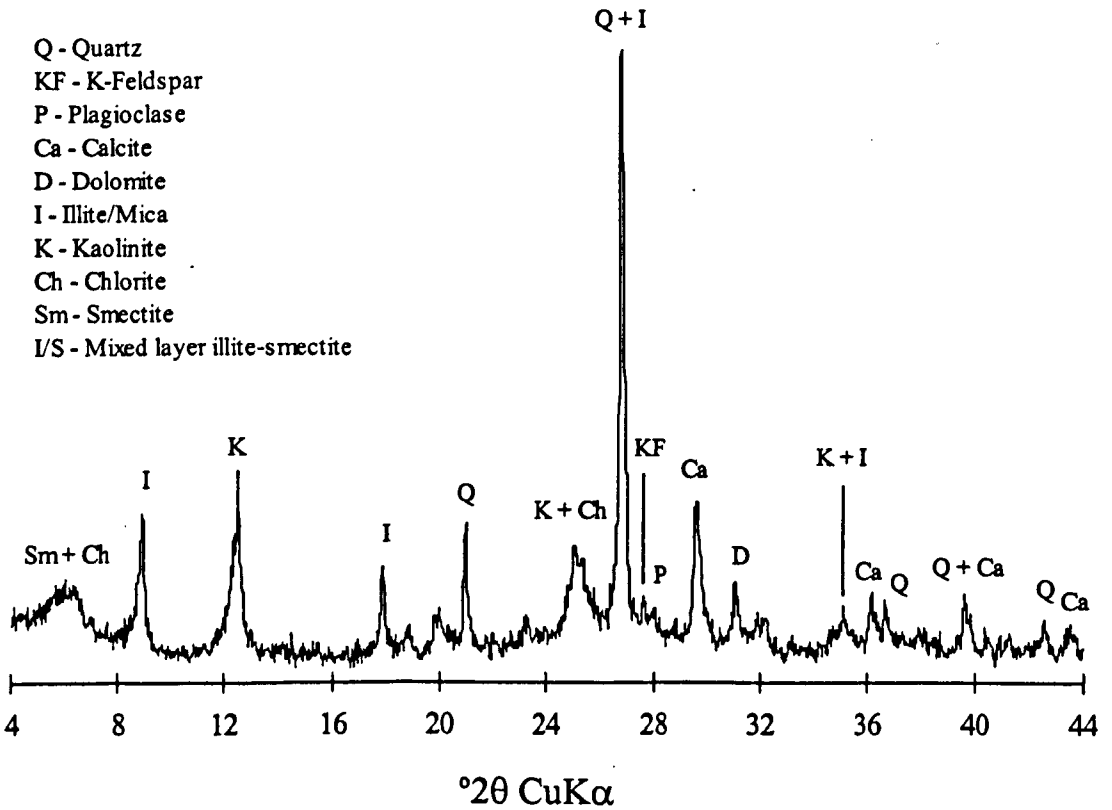
Sample 51 whole rock scan



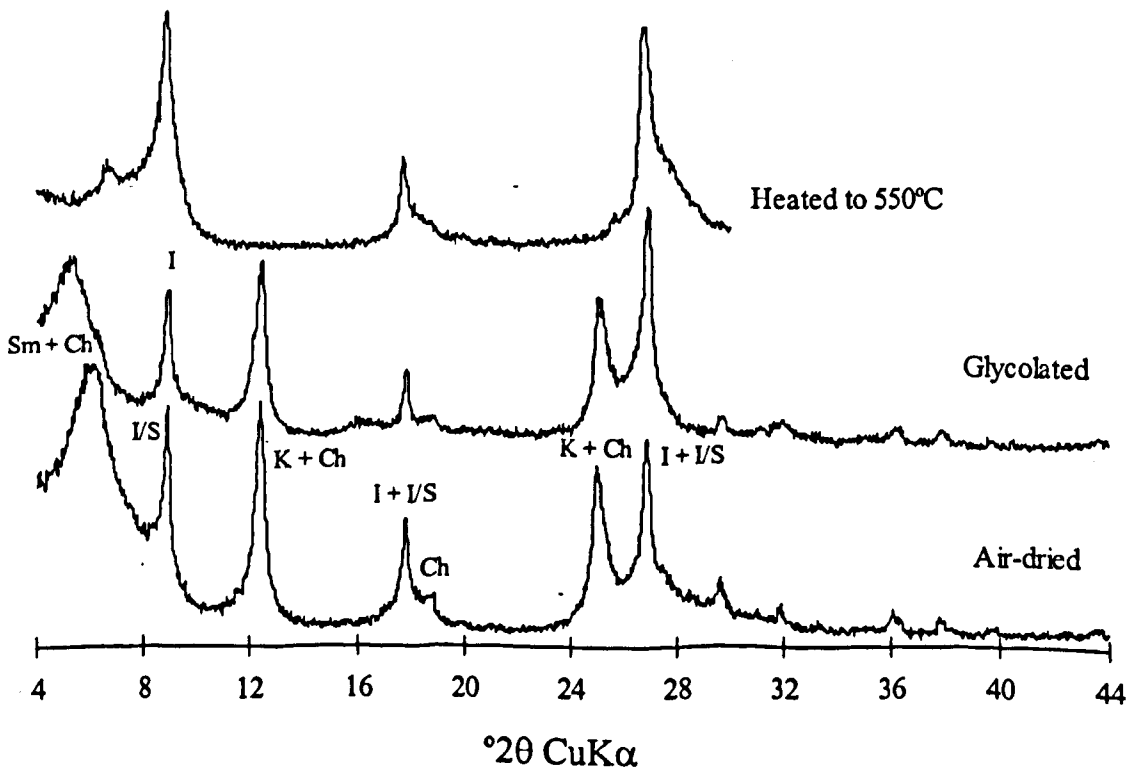
Sample 51 less than 2 μm fraction scan



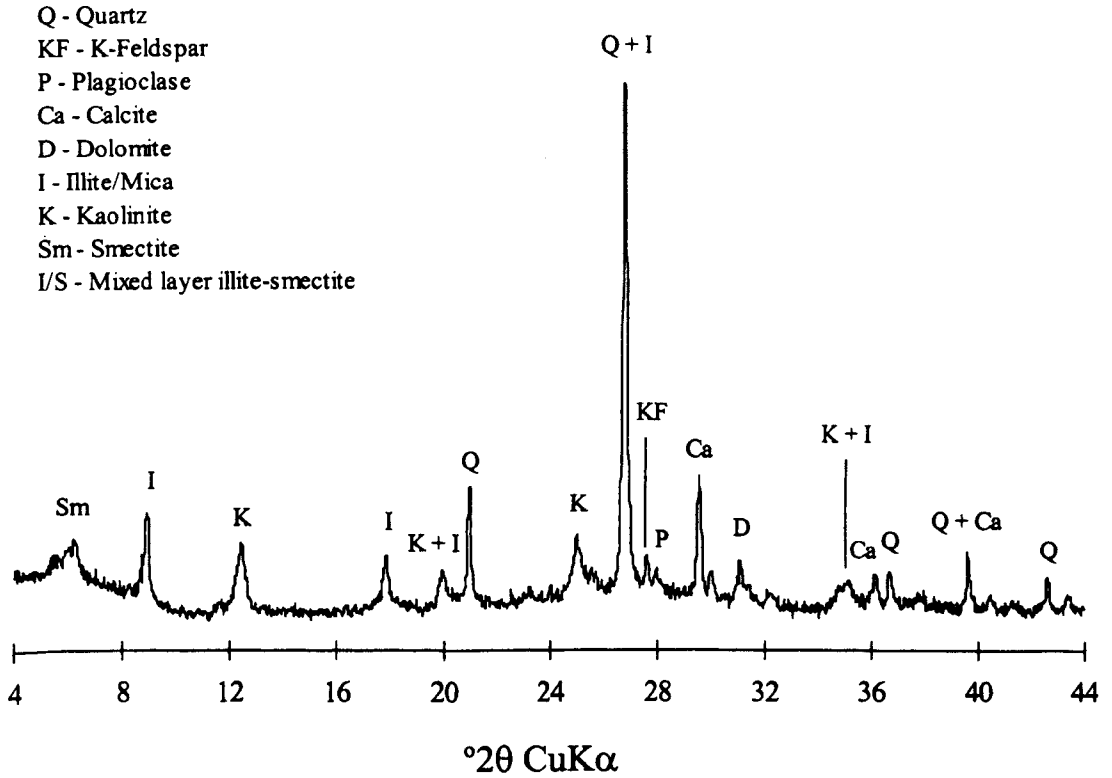
Sample 52 whole rock scan



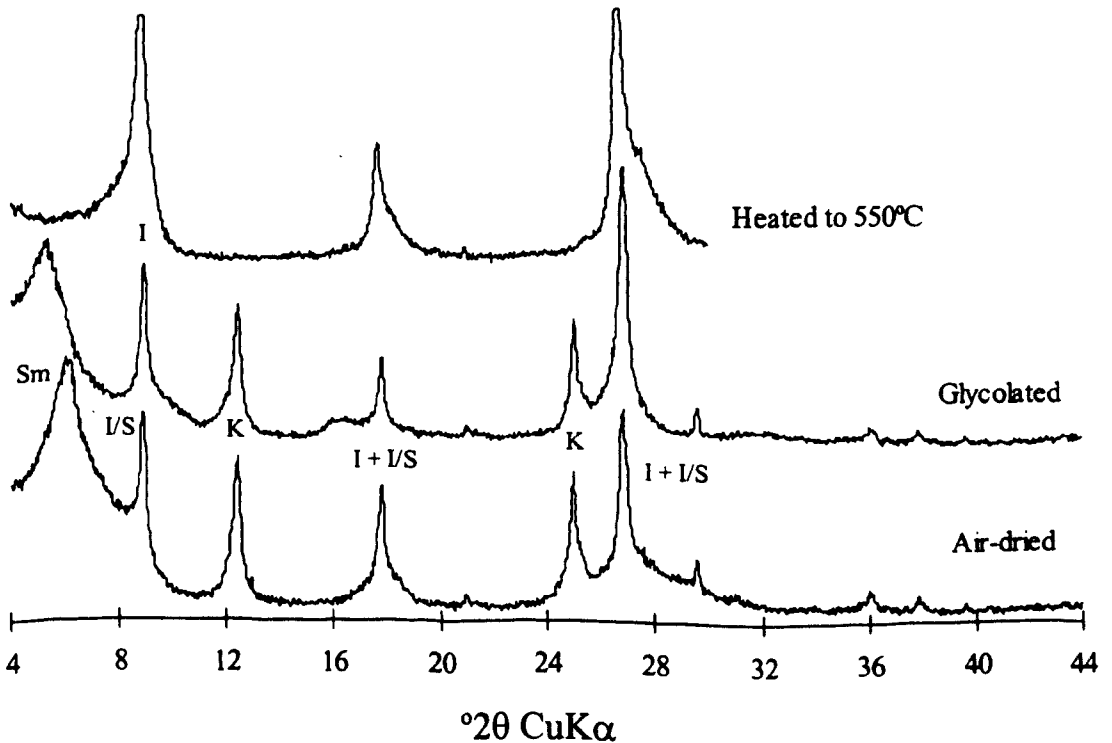
Sample 52 less than 2 μm fraction scan



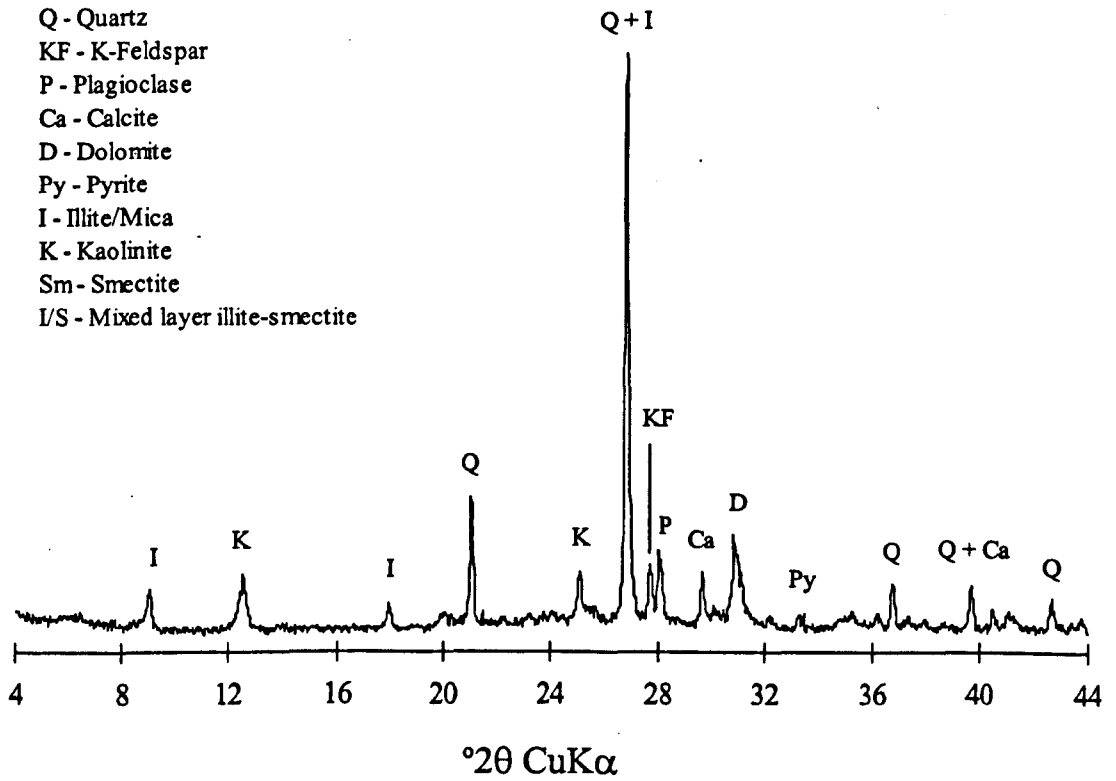
Sample 81 whole rock scan



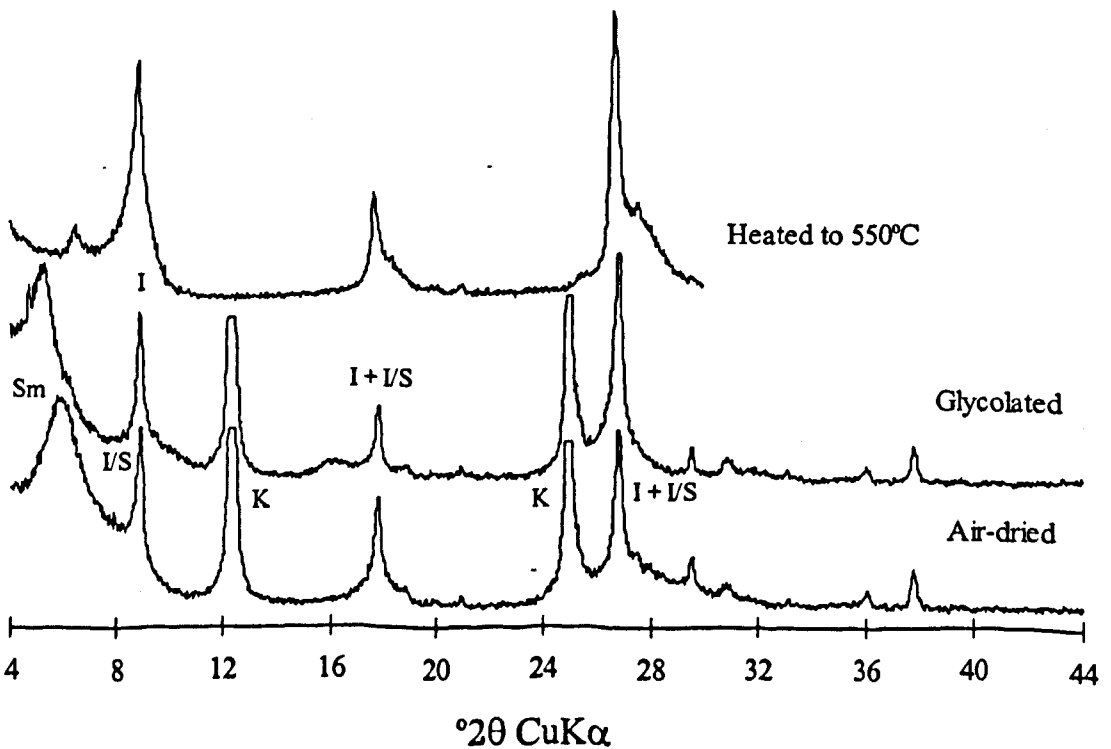
Sample 81 less than 2 μm fraction scan



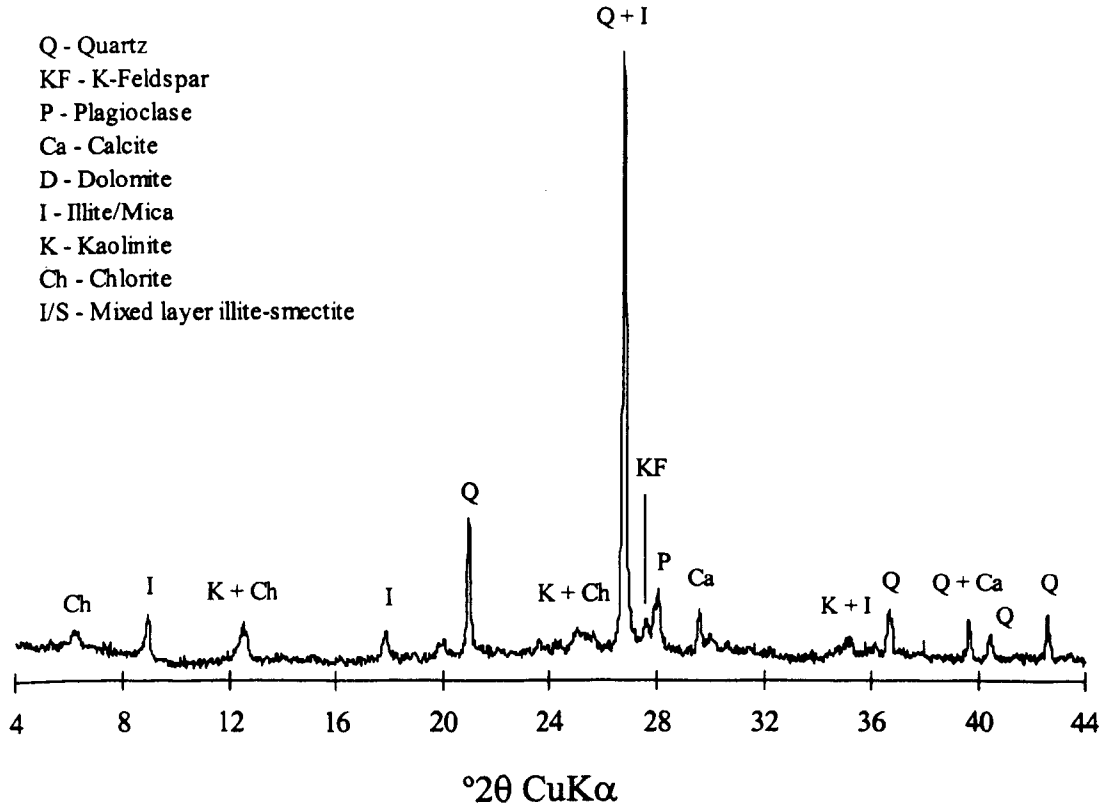
Sample 83 whole rock scan



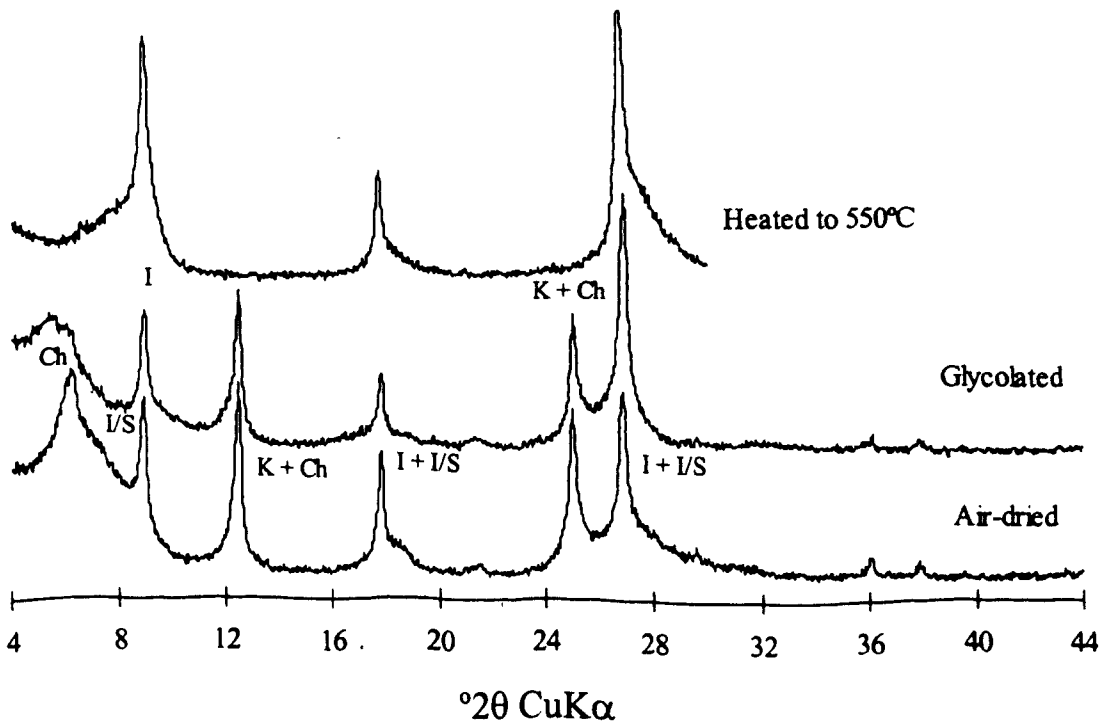
Sample 83 less than 2 μm fraction scan



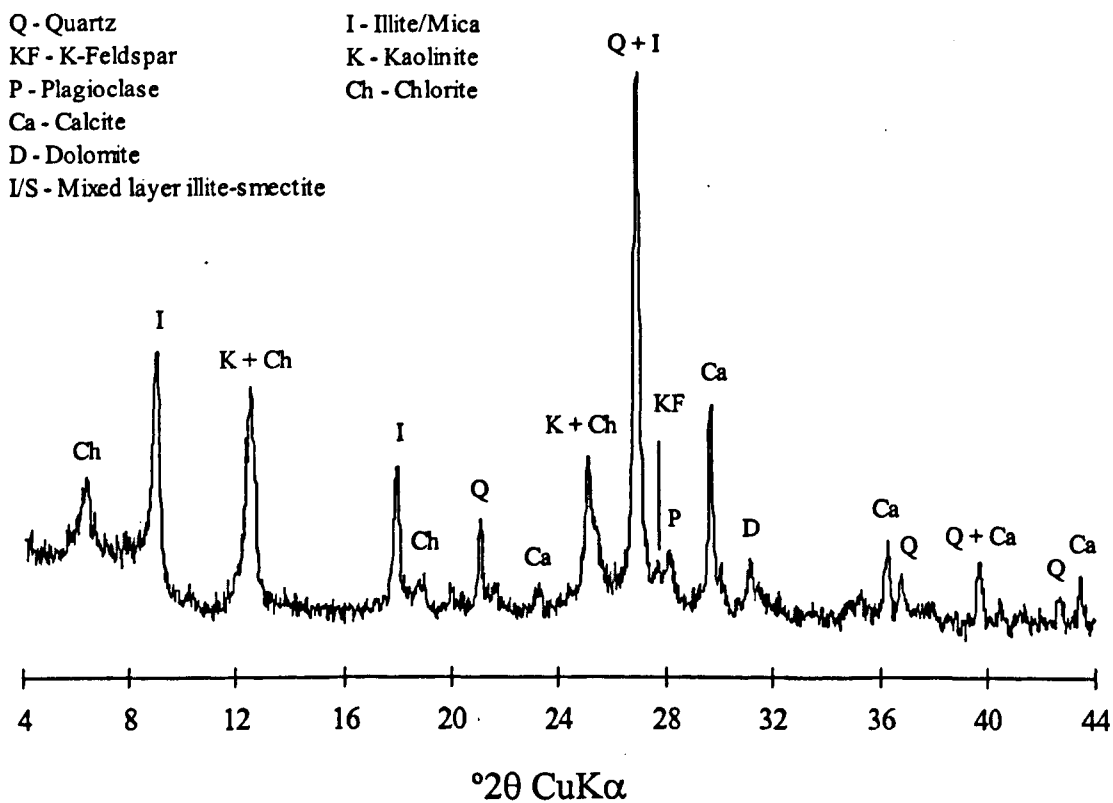
Sample 111 whole rock scan



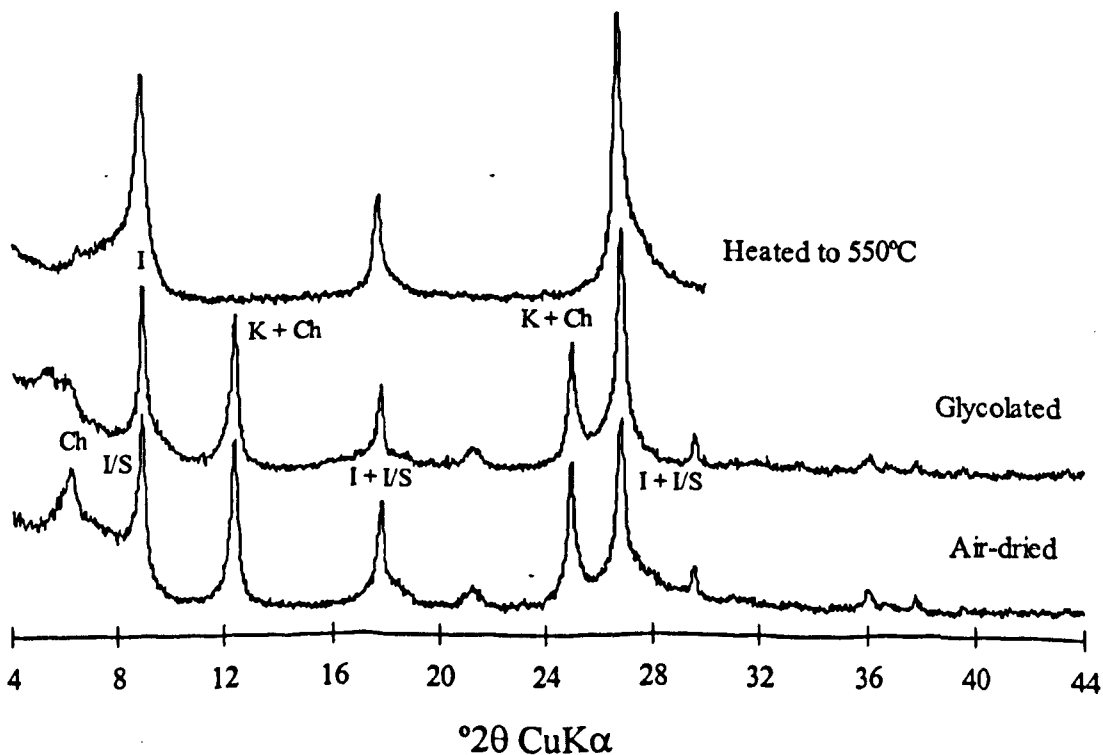
Sample 111 less than 2 μm fraction scan



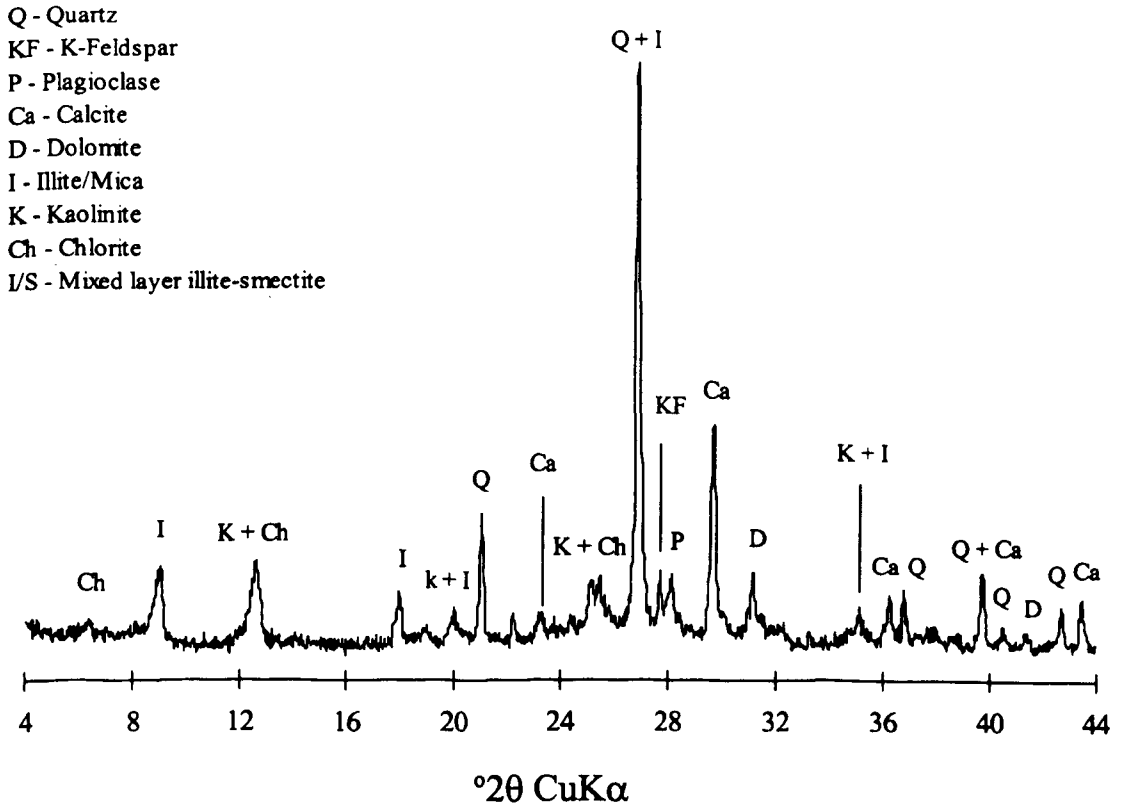
Sample 112 whole rock scan



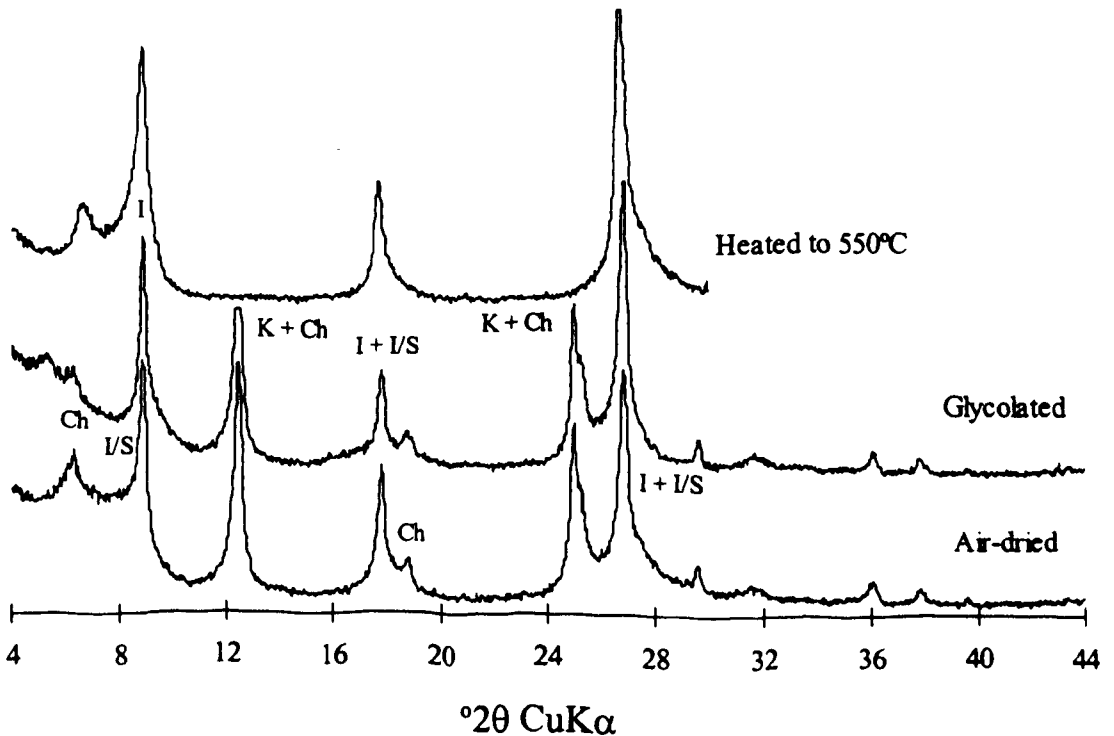
Sample 112 less than 2 μ m fraction scan



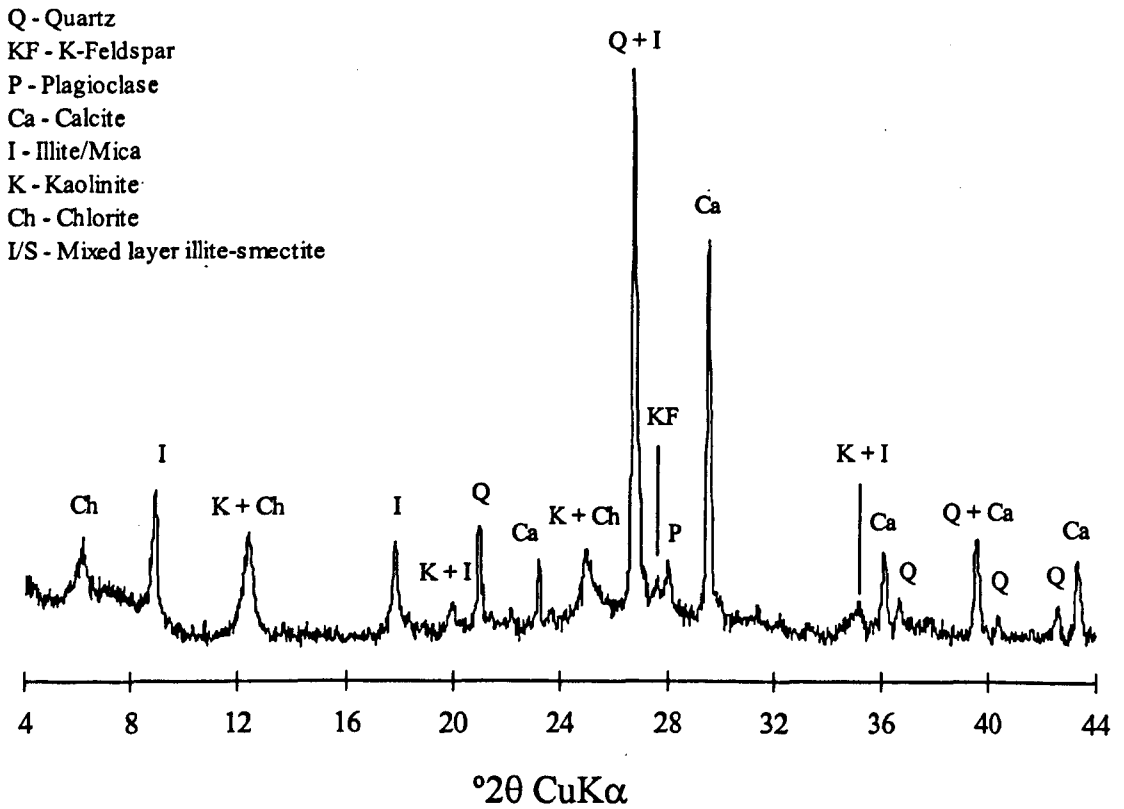
Sample 114 whole rock scan



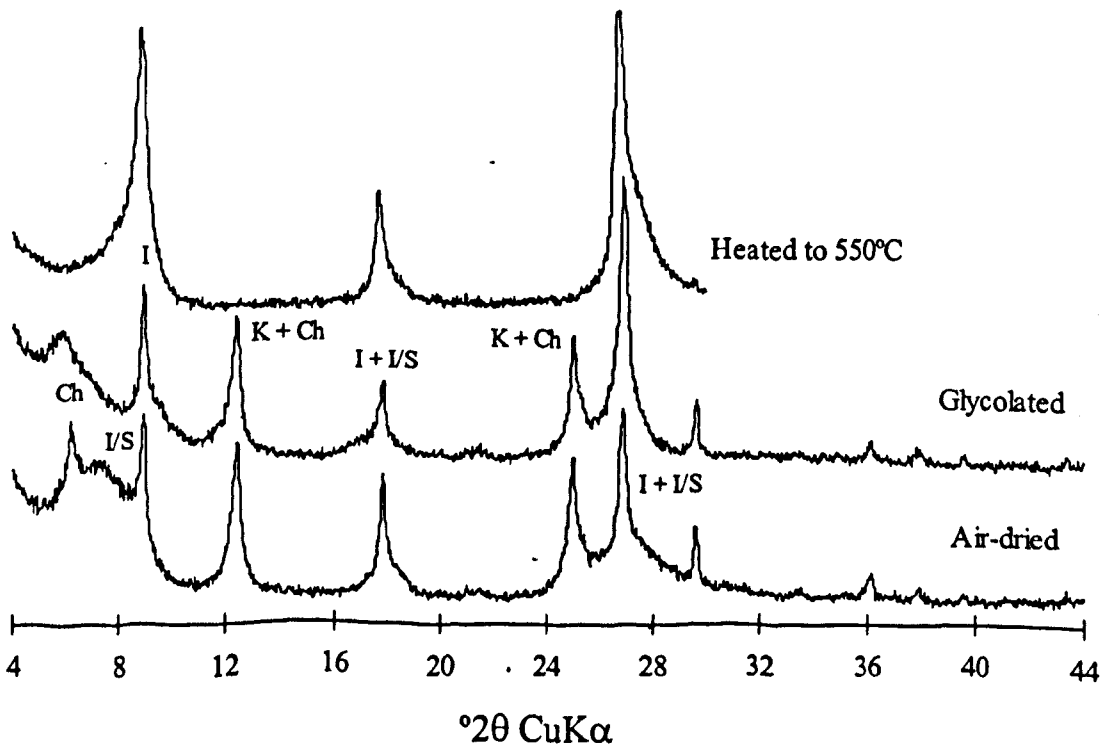
Sample 114 less than 2 μ m fraction scan



Sample 151 whole rock scan

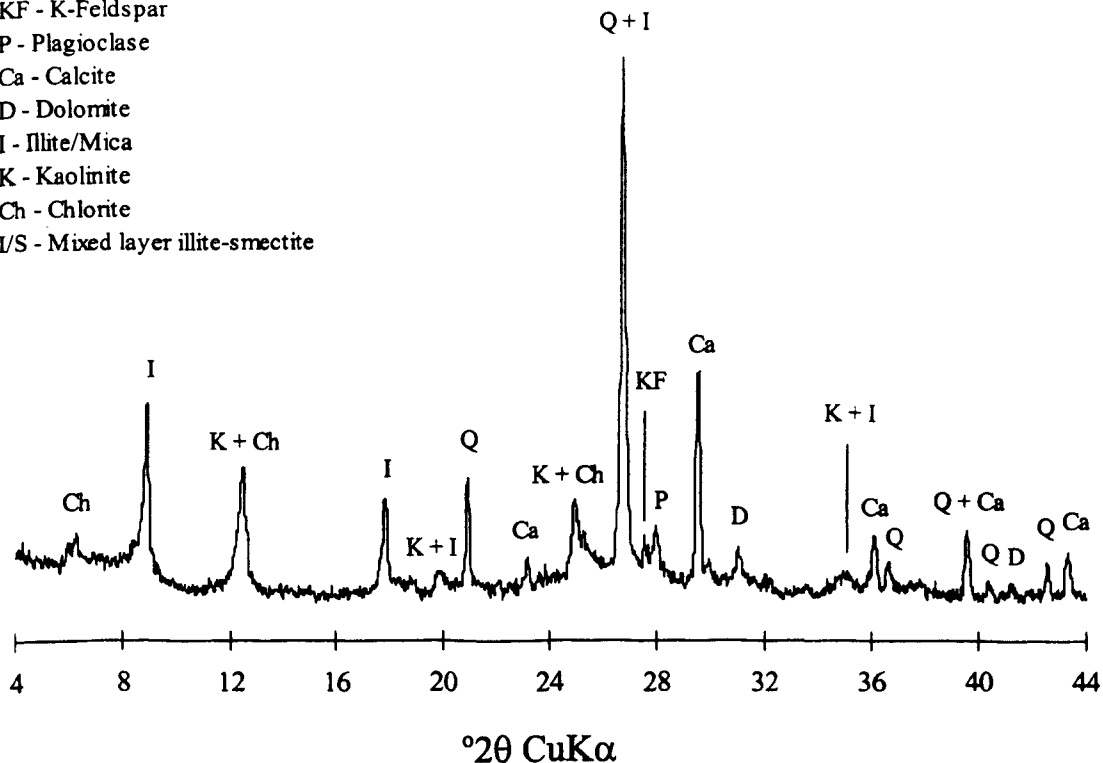


Sample 151 less than 2 μ m fraction scan

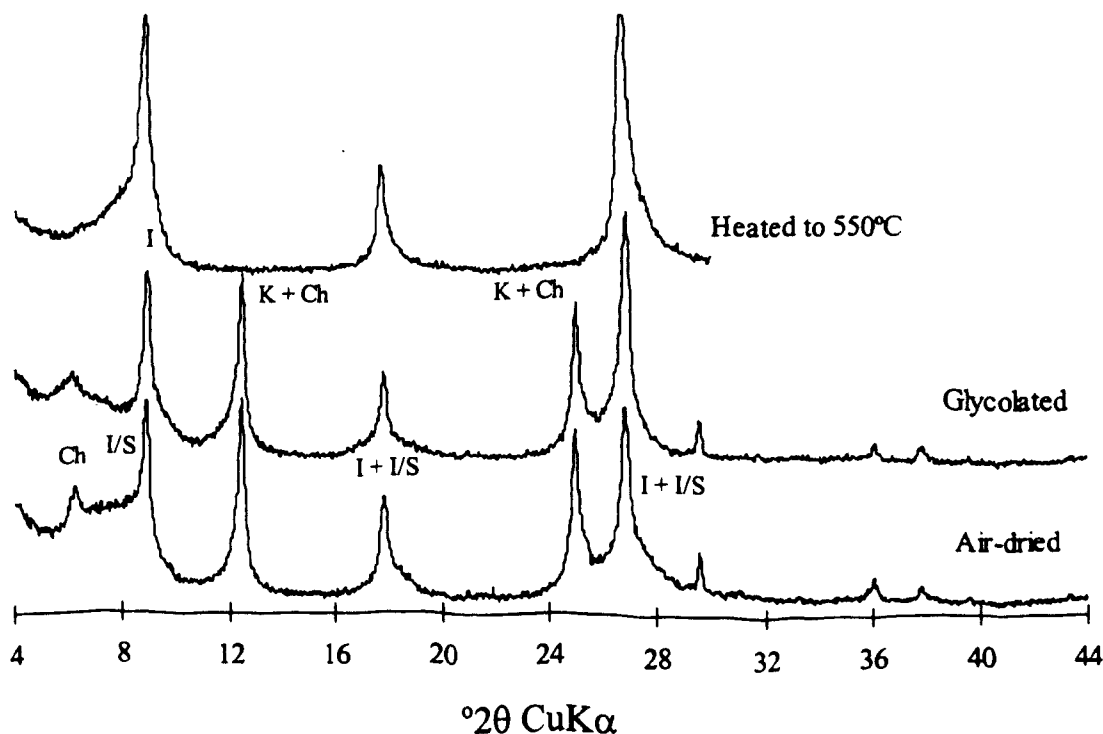


Sample 152 whole rock scan

- Q - Quartz
- KF - K-Feldspar
- P - Plagioclase
- Ca - Calcite
- D - Dolomite
- I - Illite/Mica
- K - Kaolinite
- Ch - Chlorite
- I/S - Mixed layer illite-smectite



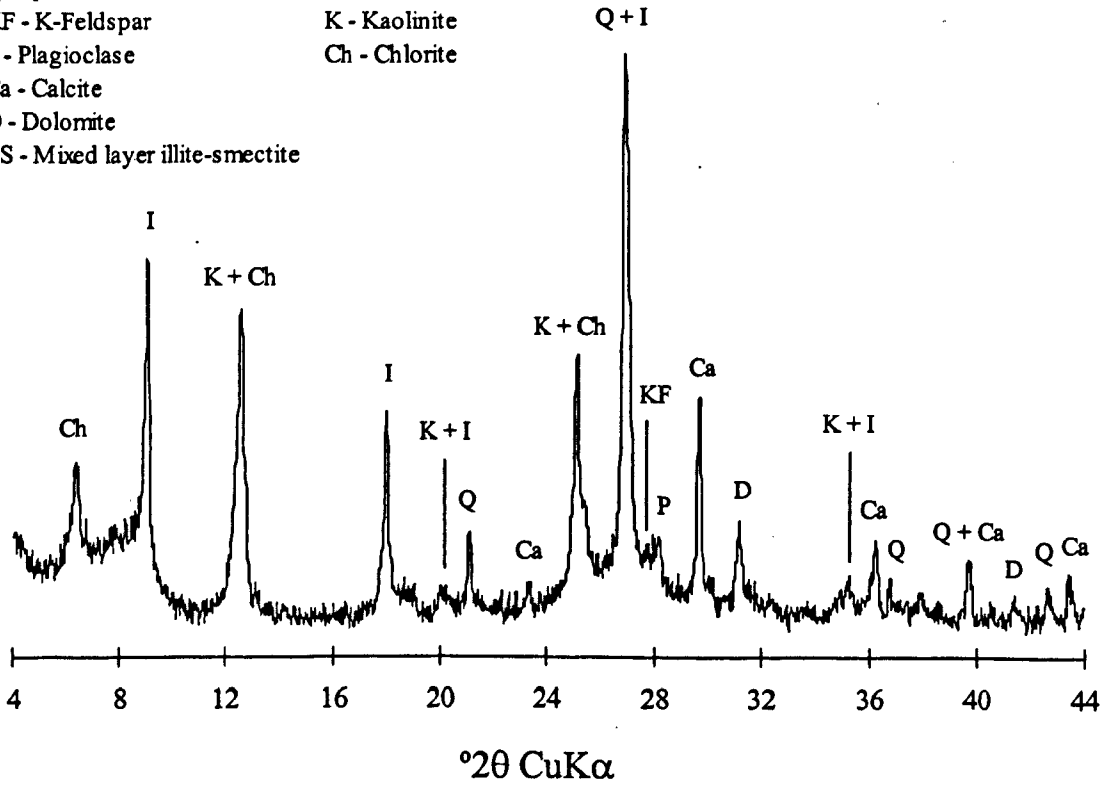
Sample 152 less than 2 μm fraction scan



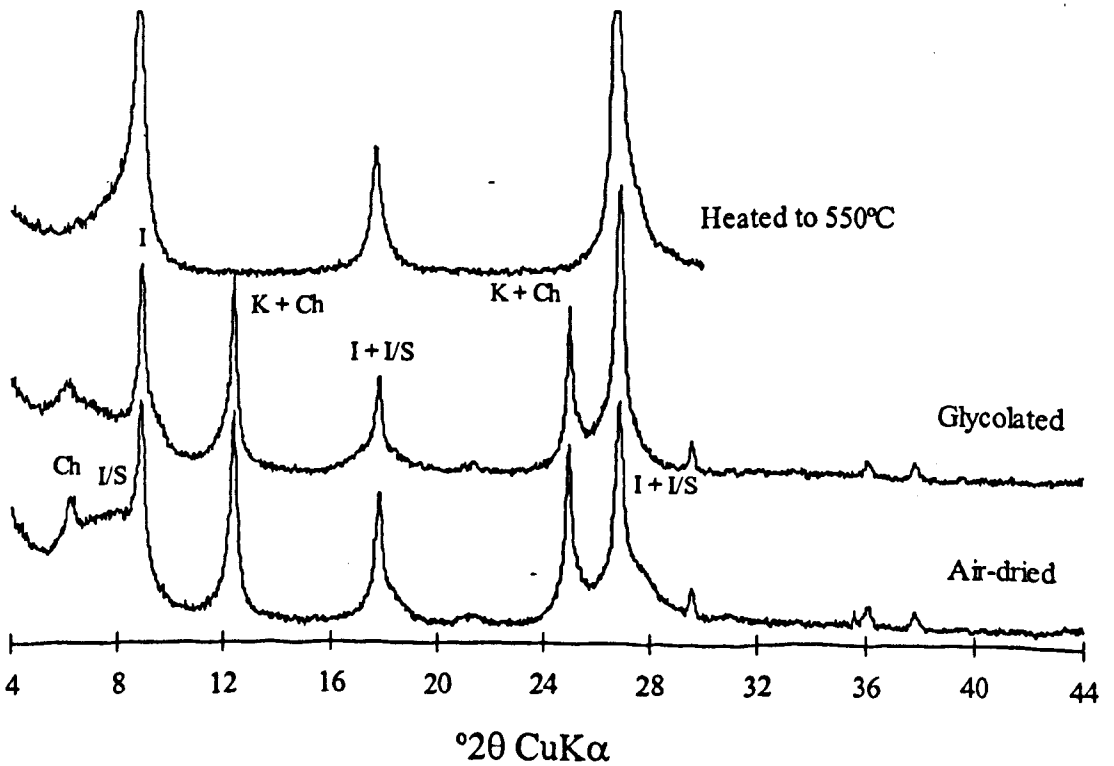
Sample 153 whole rock scan

Q - Quartz
 KF - K-Feldspar
 P - Plagioclase
 Ca - Calcite
 D - Dolomite
 I/S - Mixed layer illite-smectite

I - Illite/Mica
 K - Kaolinite
 Ch - Chlorite



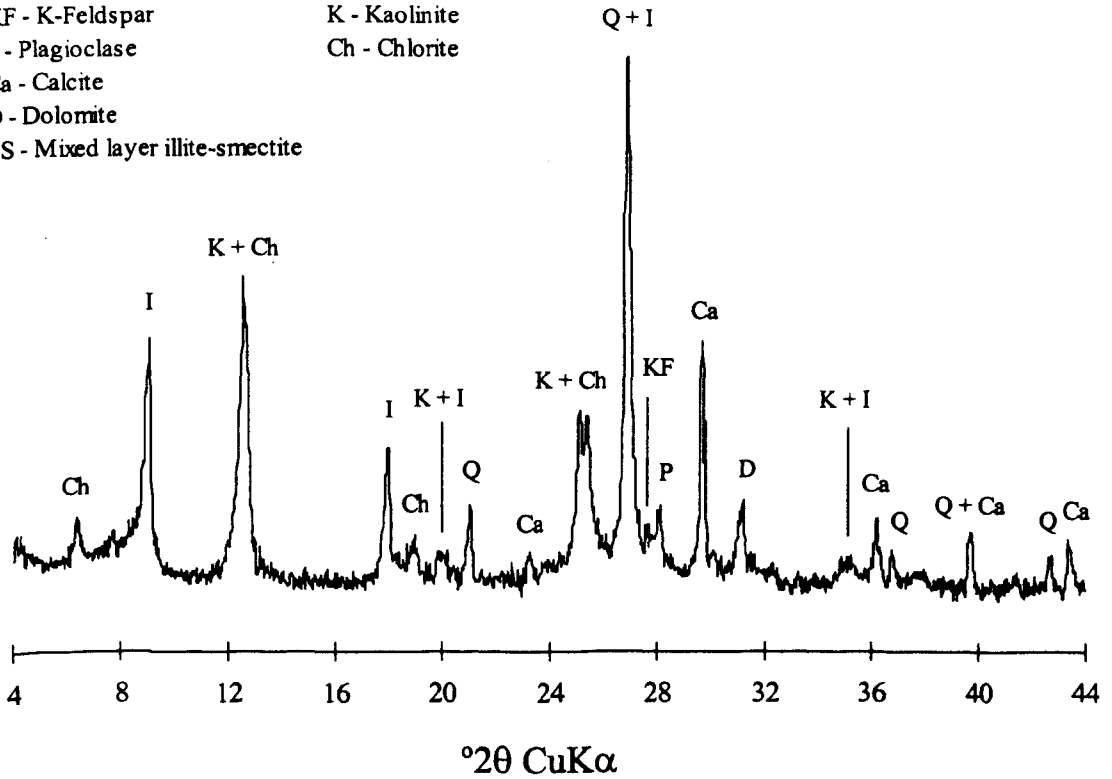
Sample 153 less than 2 μm fraction scan



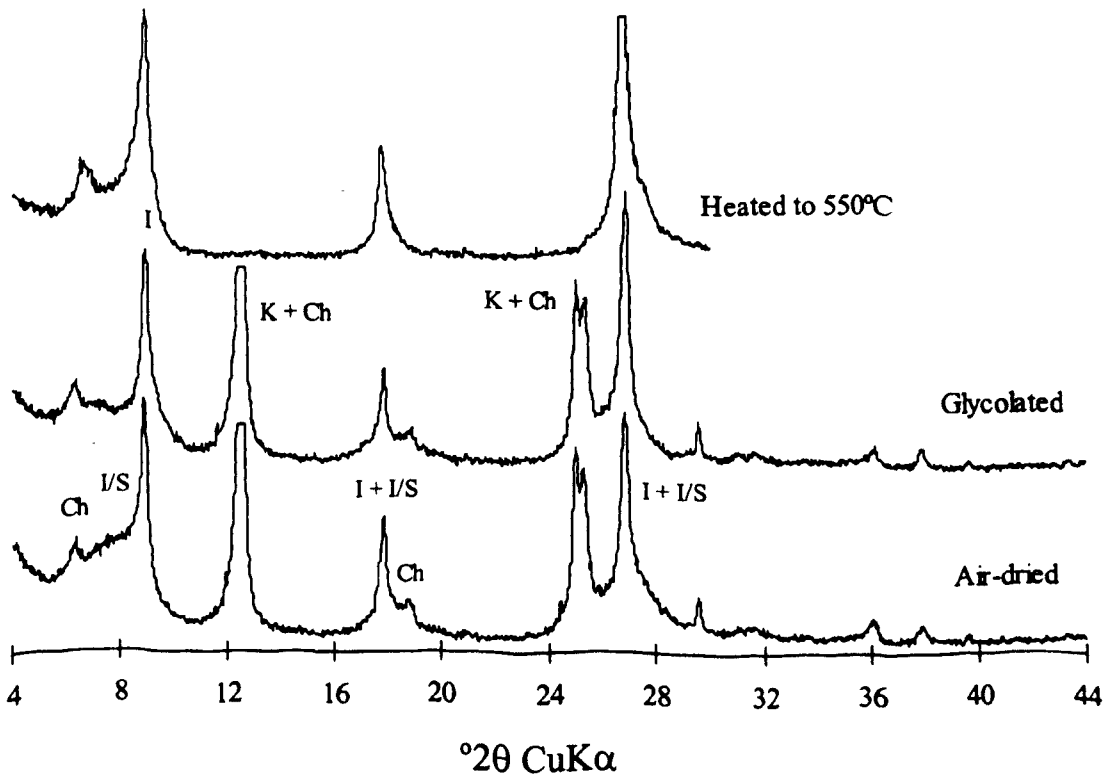
Sample 154 whole rock scan

- Q - Quartz
- KF - K-Feldspar
- P - Plagioclase
- Ca - Calcite
- D - Dolomite
- I/S - Mixed layer illite-smectite

- I - Illite/Mica
- K - Kaolinite
- Ch - Chlorite

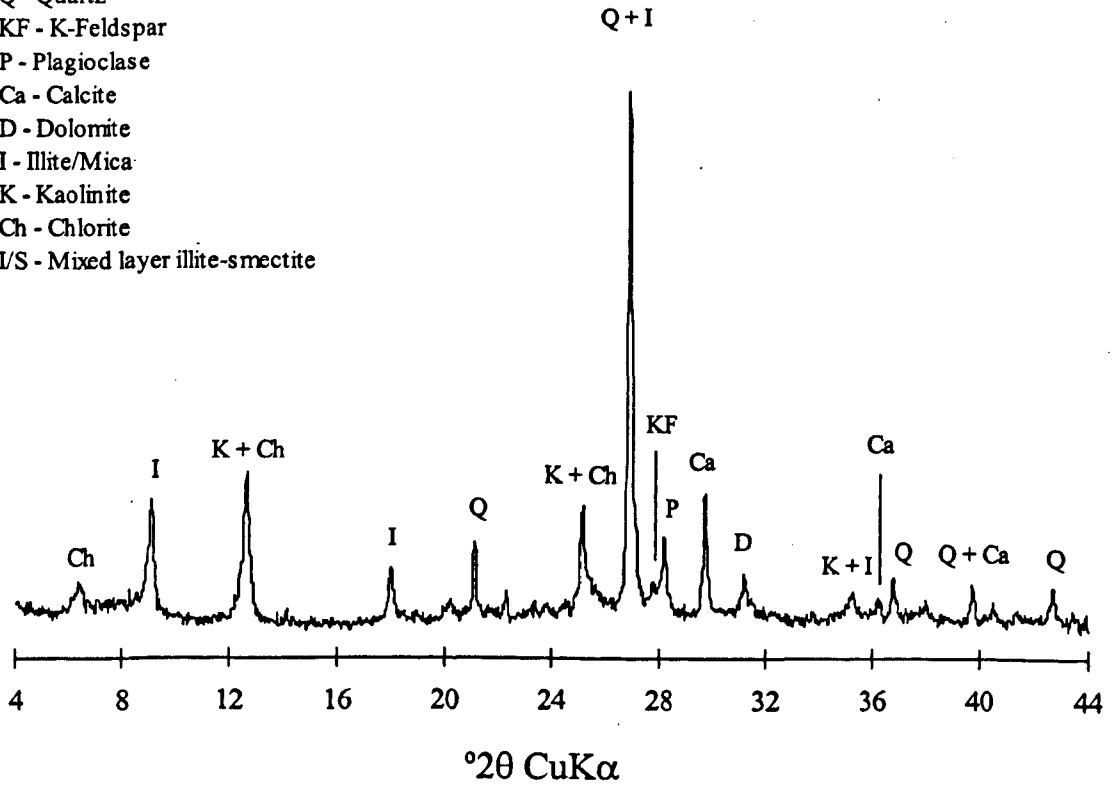


Sample 154 less than 2 μm fraction scan

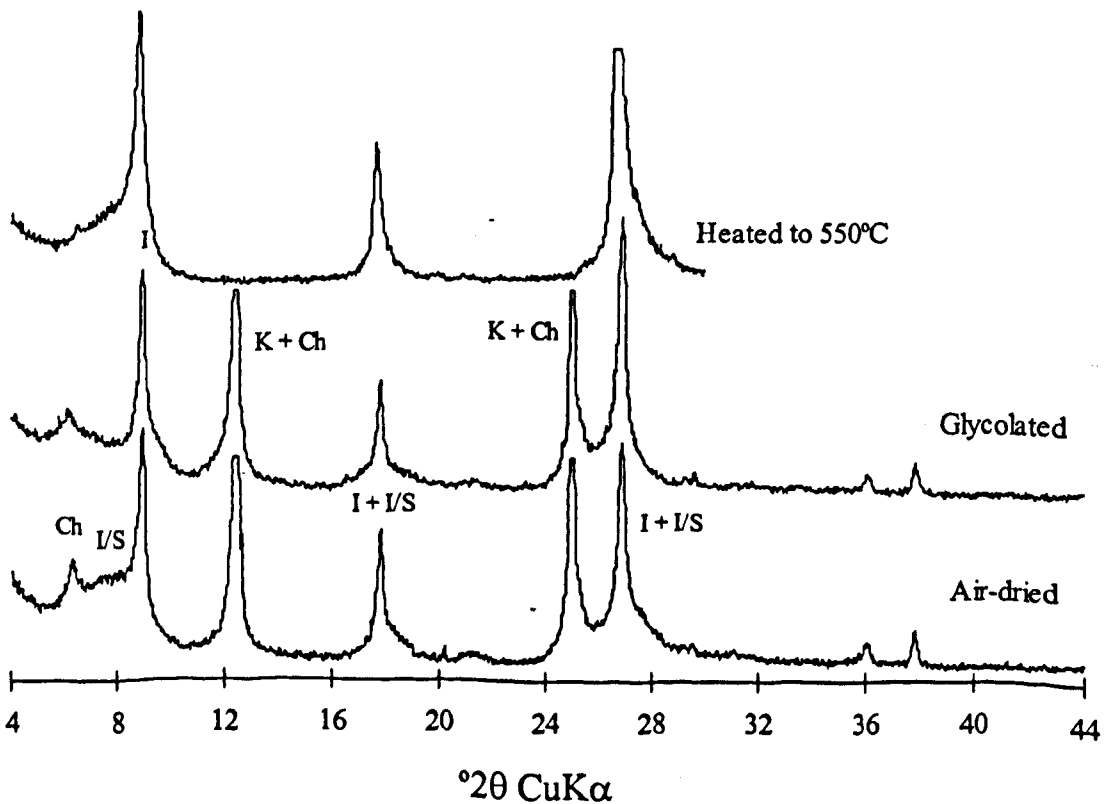


Sample 156 whole rock scan

- Q - Quartz
- KF - K-Feldspar
- P - Plagioclase
- Ca - Calcite
- D - Dolomite
- I - Illite/Mica
- K - Kaolinite
- Ch - Chlorite
- I/S - Mixed layer illite-smectite



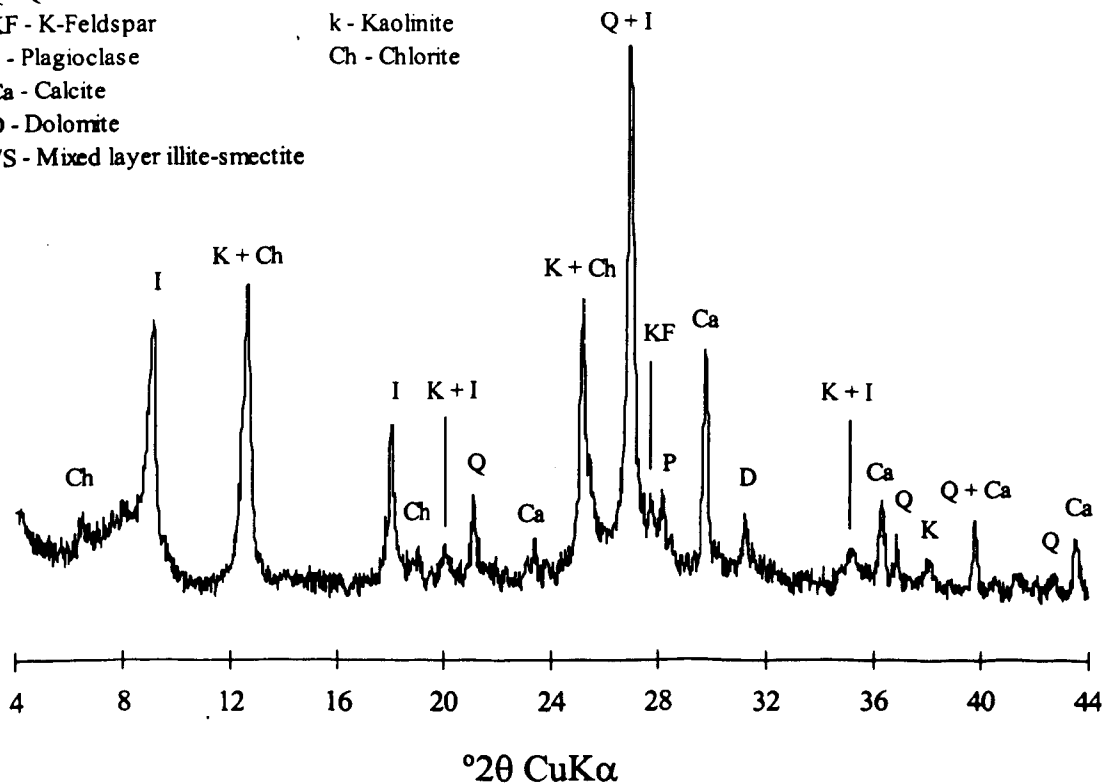
Sample 156 less than 2 μm fraction scan



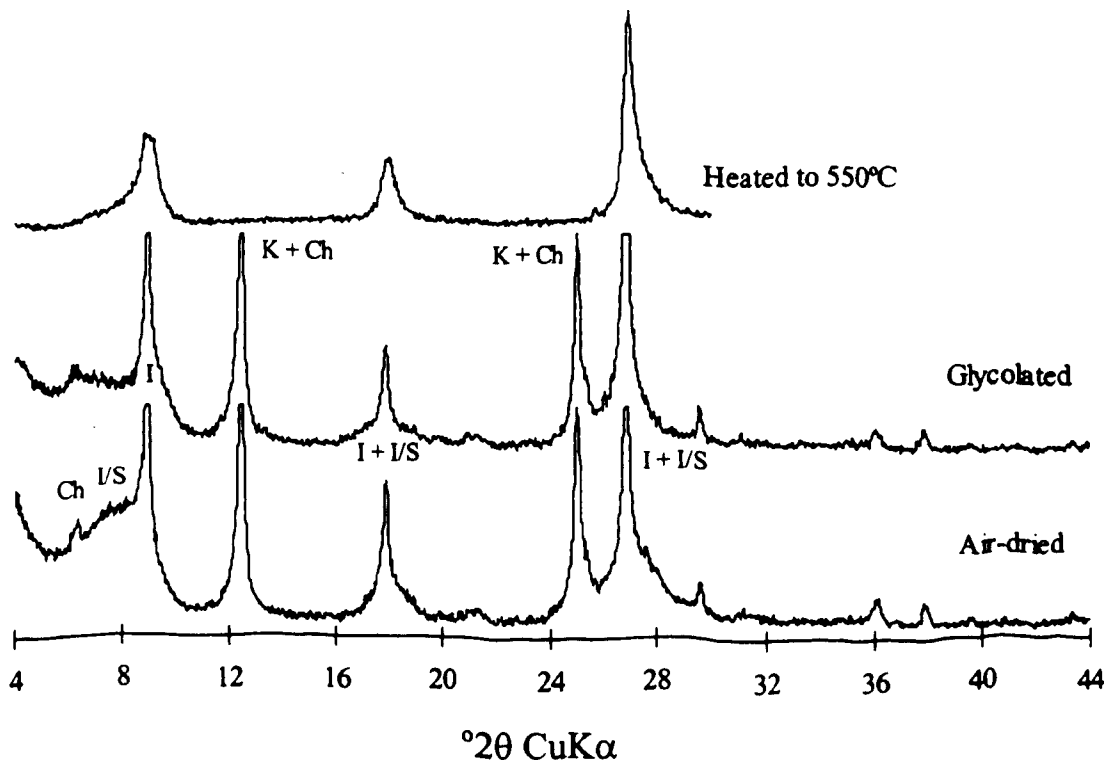
Sample 162 whole rock scan

- Q - Quartz
- KF - K-Feldspar
- P - Plagioclase
- Ca - Calcite
- D - Dolomite
- I/S - Mixed layer illite-smectite

- I - Illite/Mica
- k - Kaolinite
- Ch - Chlorite

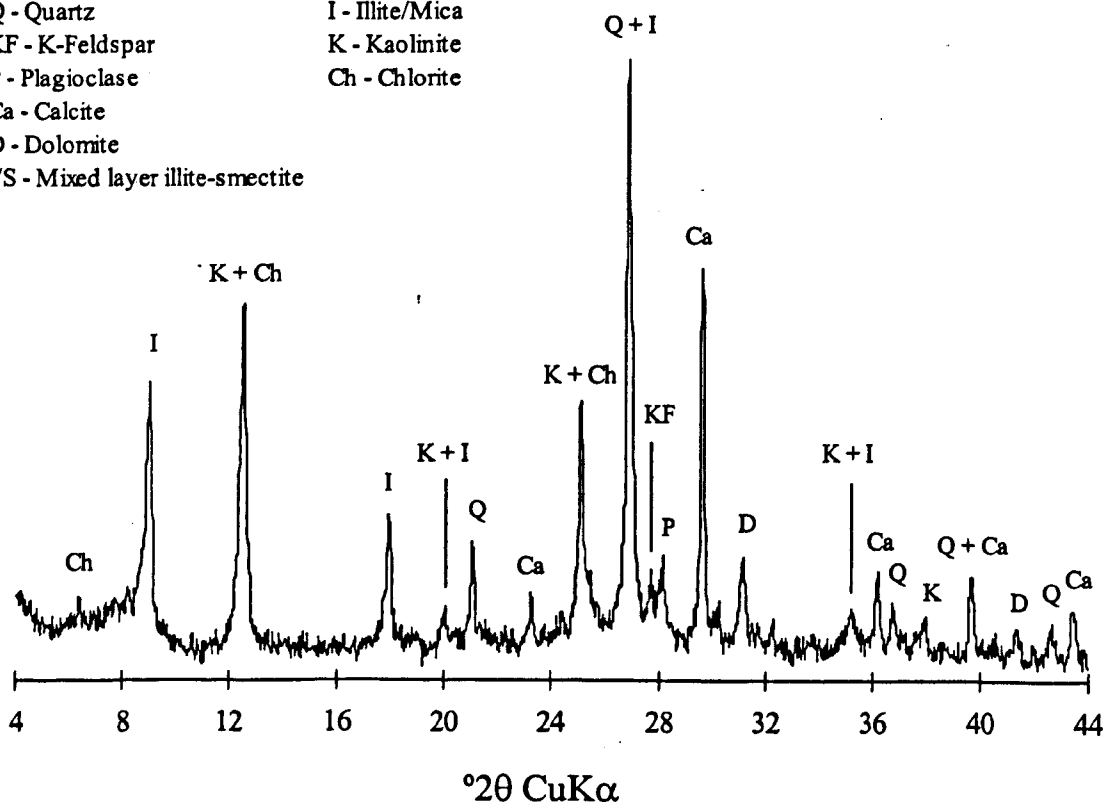


Sample 162 less than 2 μm fraction scan

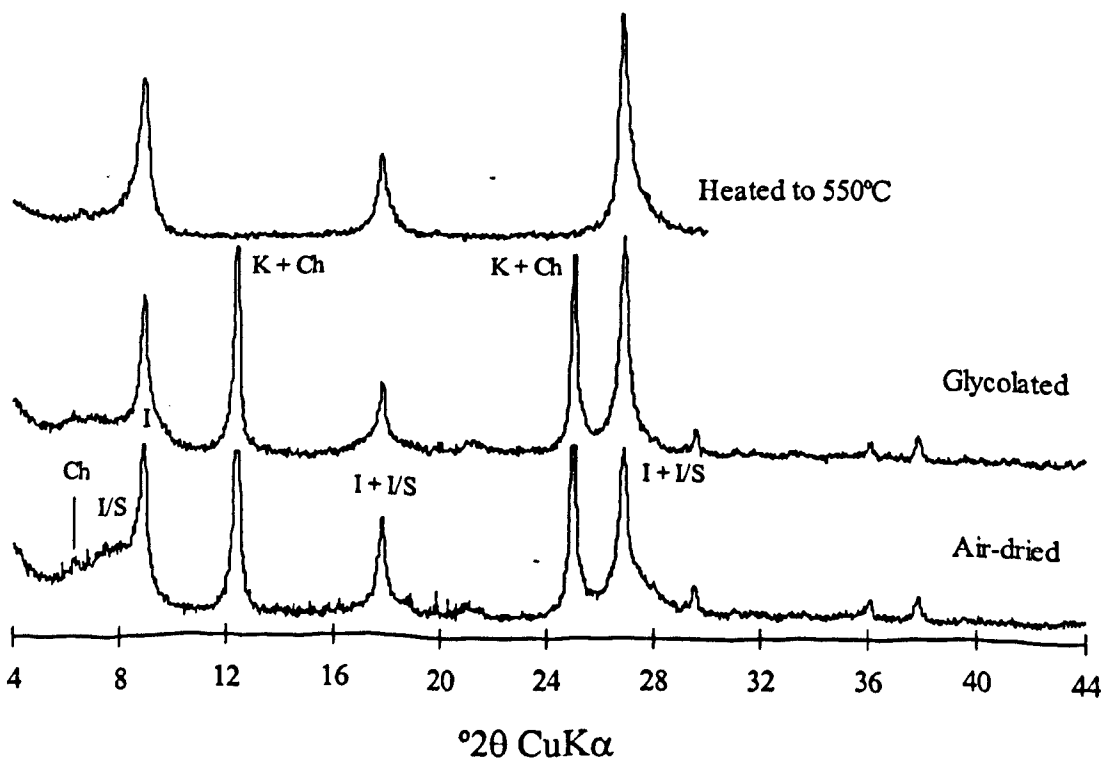


Sample 163 whole rock scan

- Q - Quartz
- KF - K-Feldspar
- P - Plagioclase
- Ca - Calcite
- D - Dolomite
- I/S - Mixed layer illite-smectite
- I - Illite/Mica
- K - Kaolinite
- Ch - Chlorite

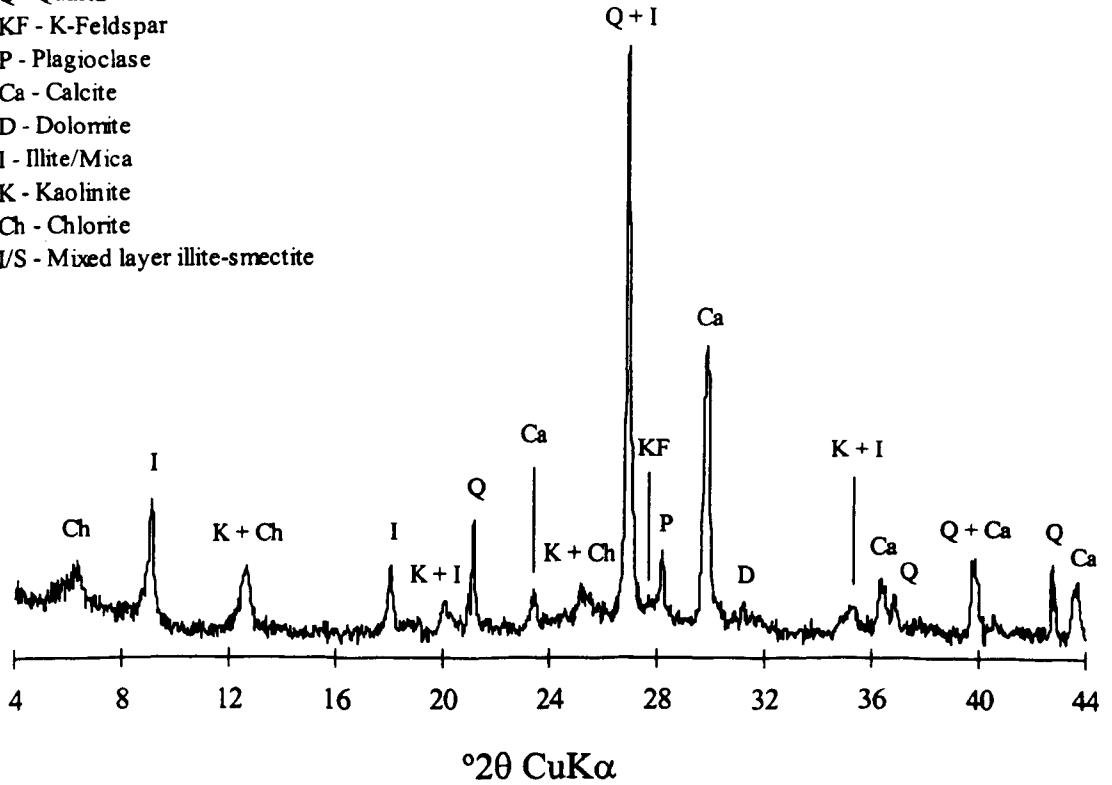


Sample 163 less than 2 μm fraction scan

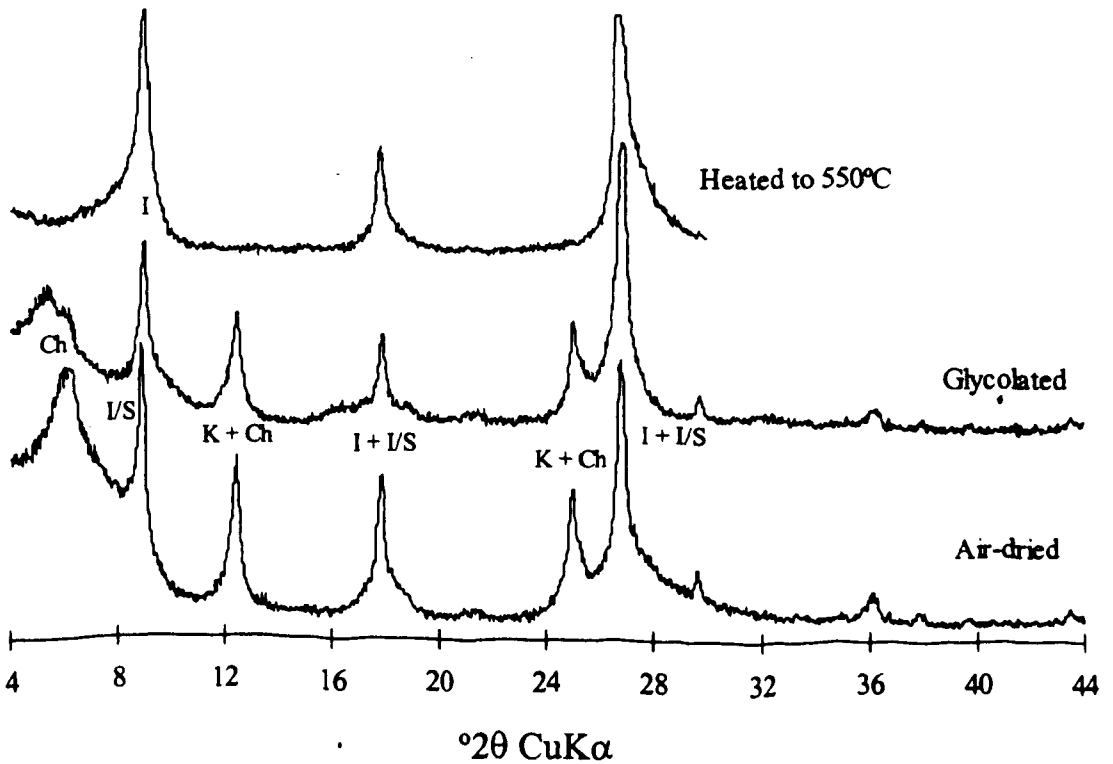


Sample 283 whole rock scan

- Q - Quartz
- KF - K-Feldspar
- P - Plagioclase
- Ca - Calcite
- D - Dolomite
- I - Illite/Mica
- K - Kaolinite
- Ch - Chlorite
- I/S - Mixed layer illite-smectite



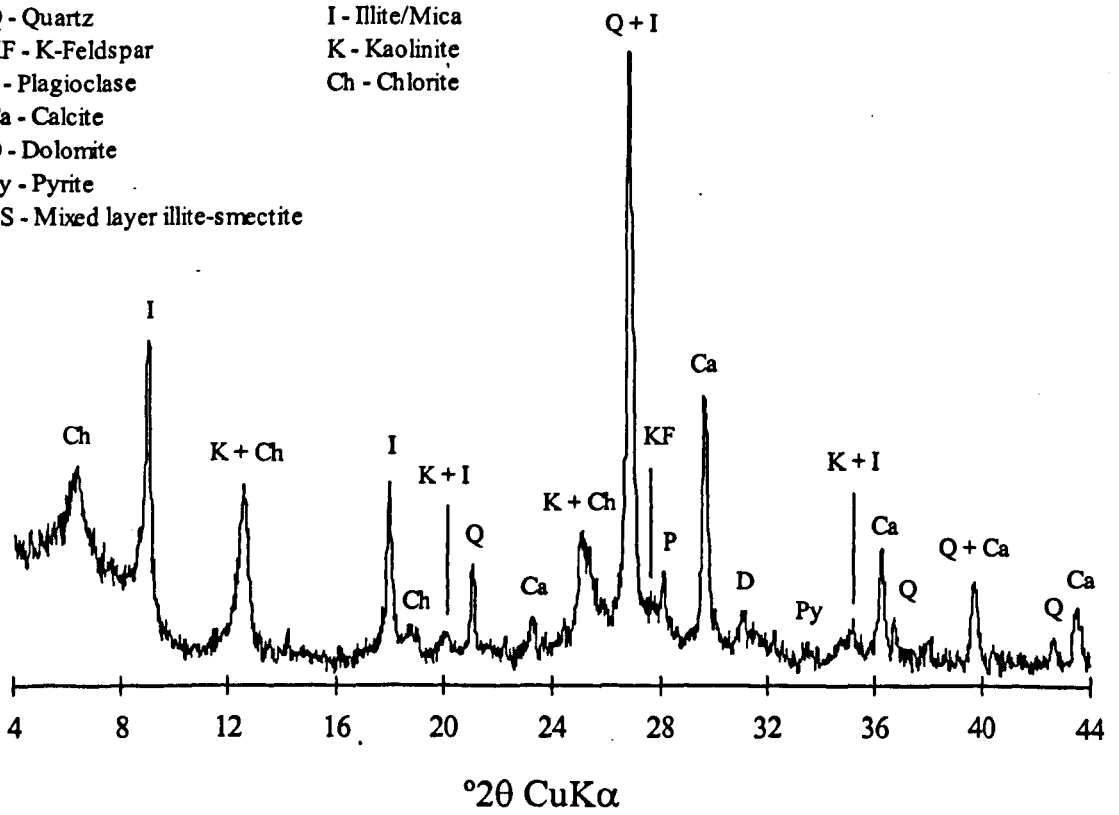
Sample 283 less than 2 μm fraction scan



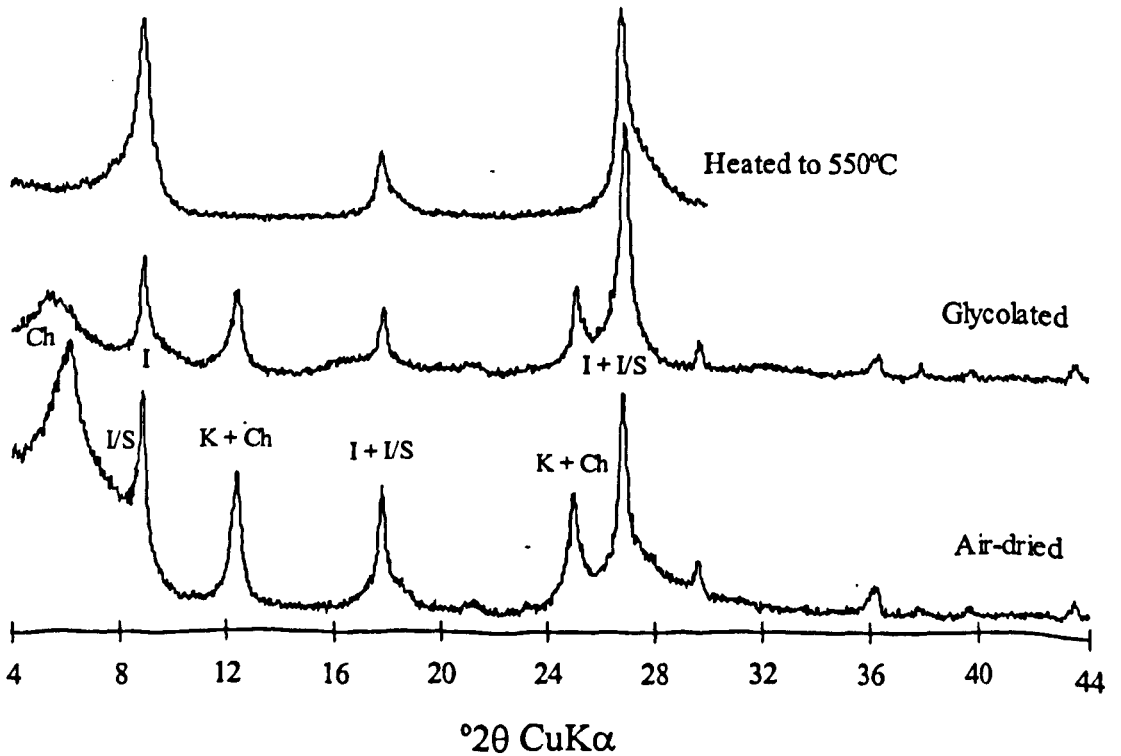
Sample 285 whole rock scan

- Q - Quartz
- KF - K-Feldspar
- P - Plagioclase
- Ca - Calcite
- D - Dolomite
- Py - Pyrite
- I/S - Mixed layer illite-smectite

- I - Illite/Mica
- K - Kaolinite
- Ch - Chlorite



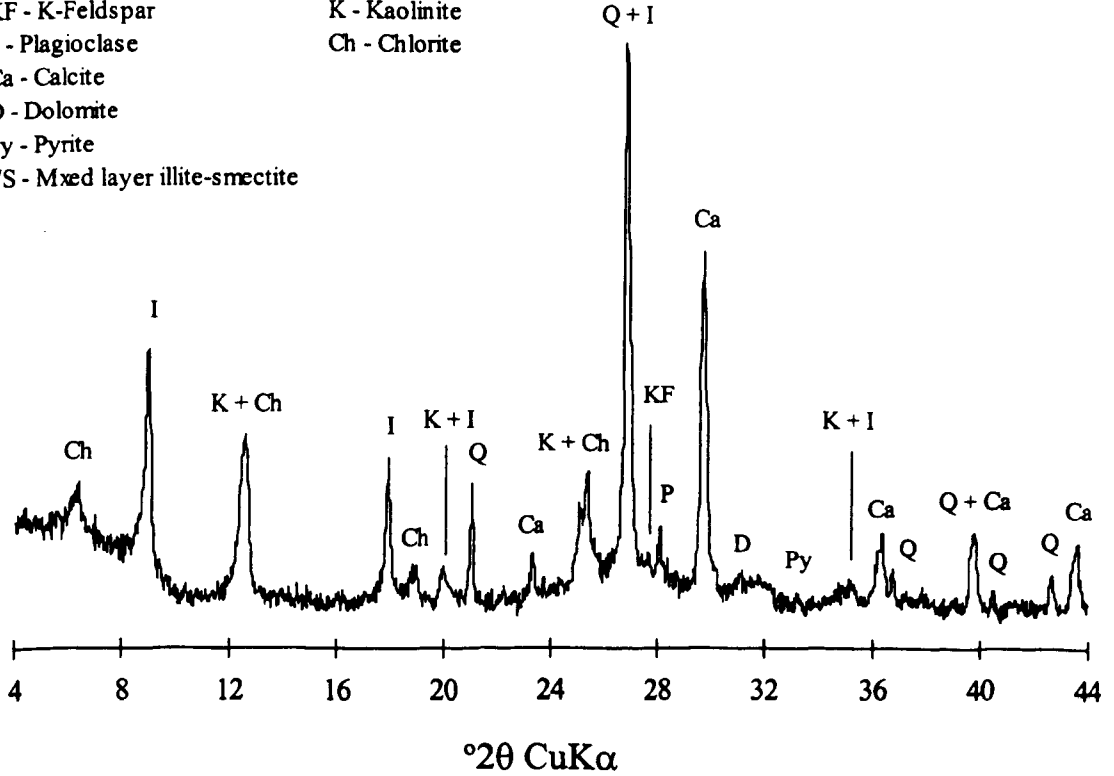
Sample 285 less than 2 μm fraction scan



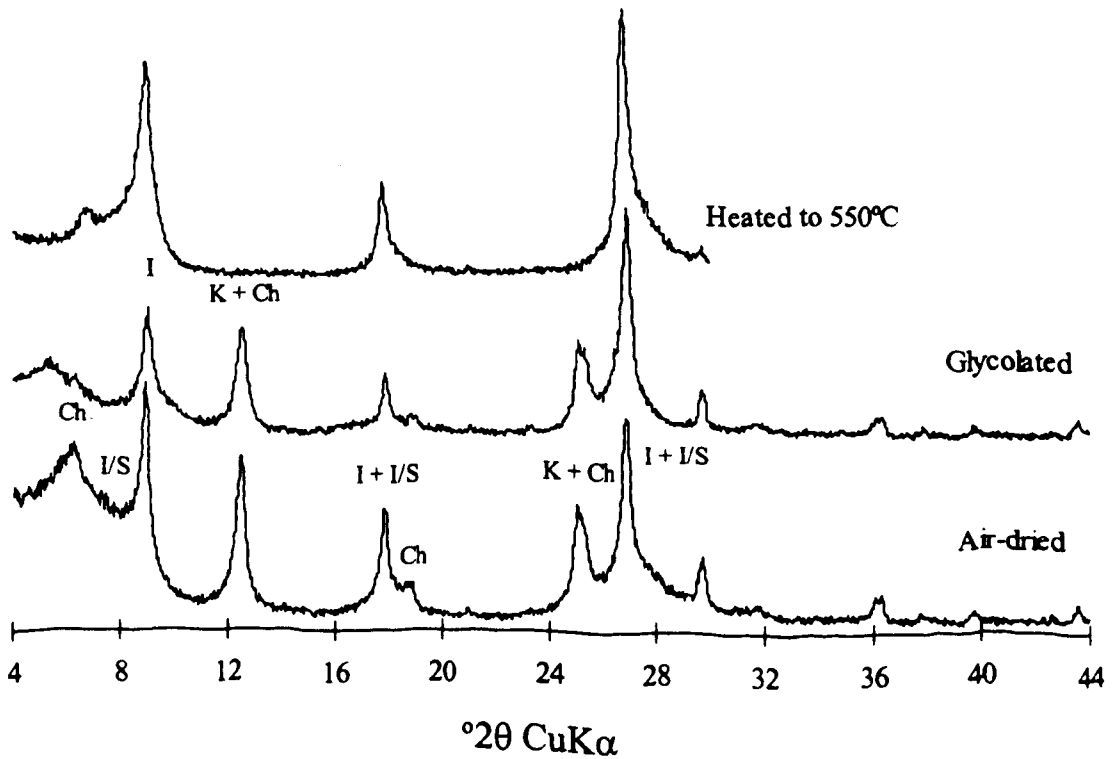
Sample 286 whole rock scan

- Q - Quartz
- KF - K-Feldspar
- P - Plagioclase
- Ca - Calcite
- D - Dolomite
- Py - Pyrite
- I/S - Mixed layer illite-smectite

- I - Illite/Mica
- K - Kaolinite
- Ch - Chlorite

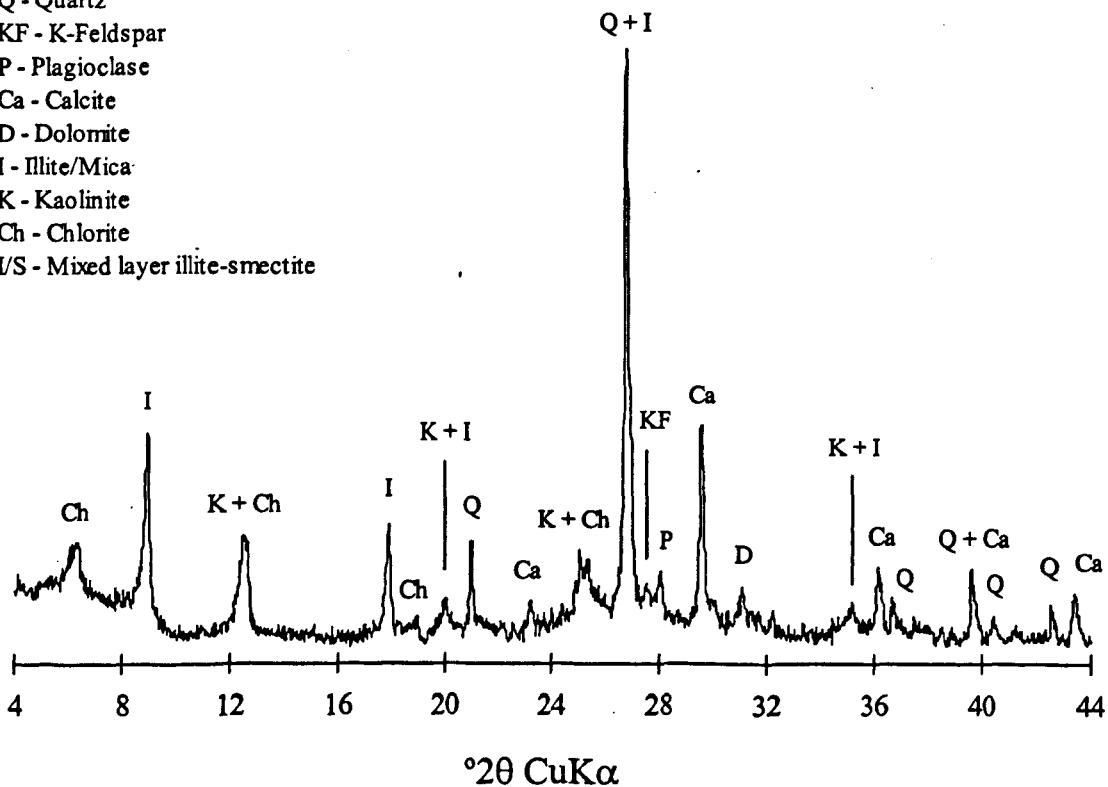


Sample 286 less than 2 μm fraction scan

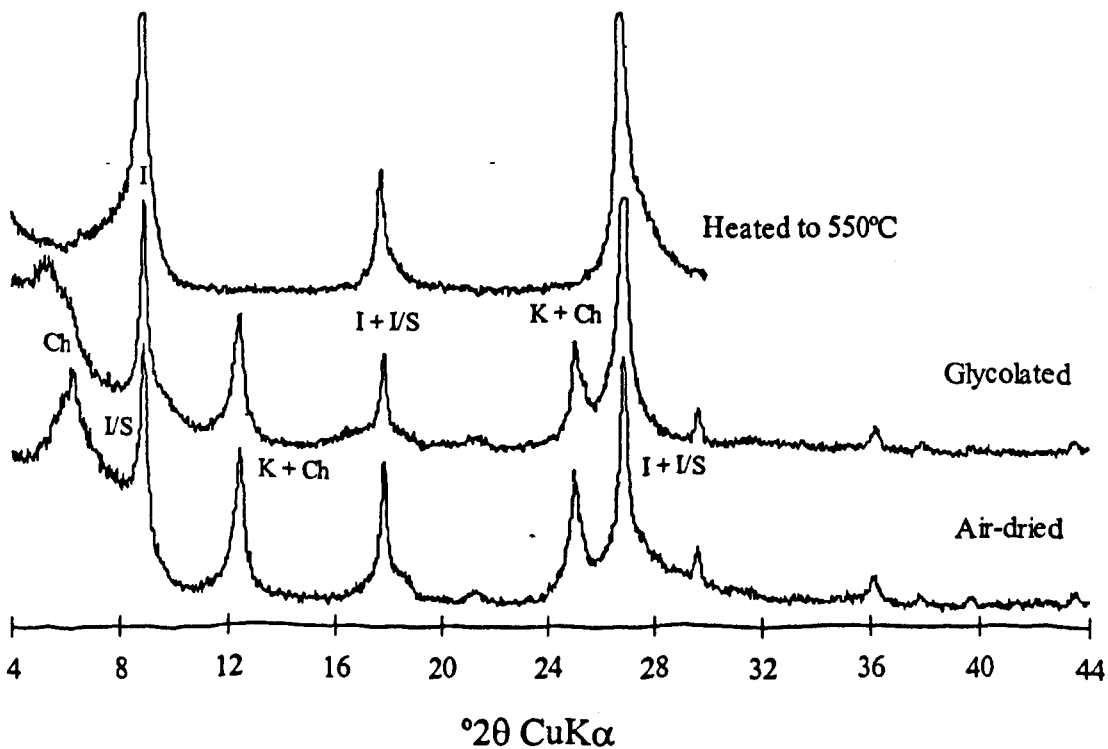


Sample 294 whole rock scan

- Q - Quartz
- KF - K-Feldspar
- P - Plagioclase
- Ca - Calcite
- D - Dolomite
- I - Illite/Mica
- K - Kaolinite
- Ch - Chlorite
- I/S - Mixed layer illite-smectite



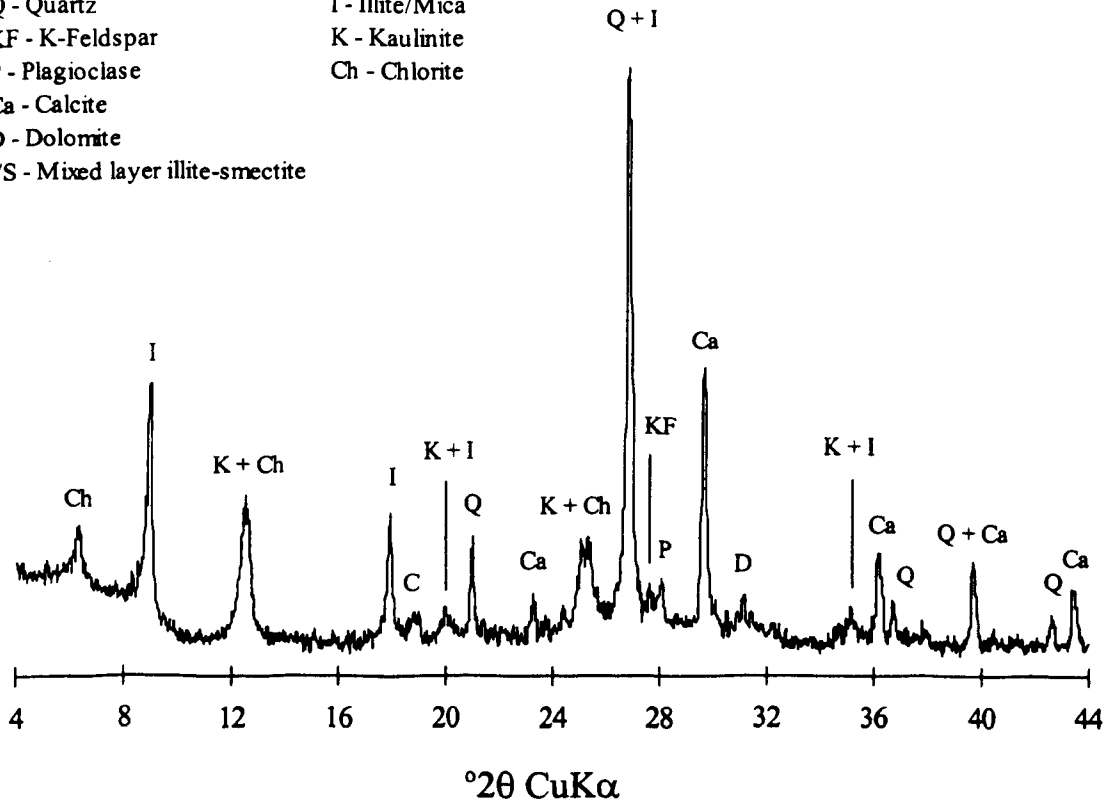
Sample 294 less than 2 μm fraction scan



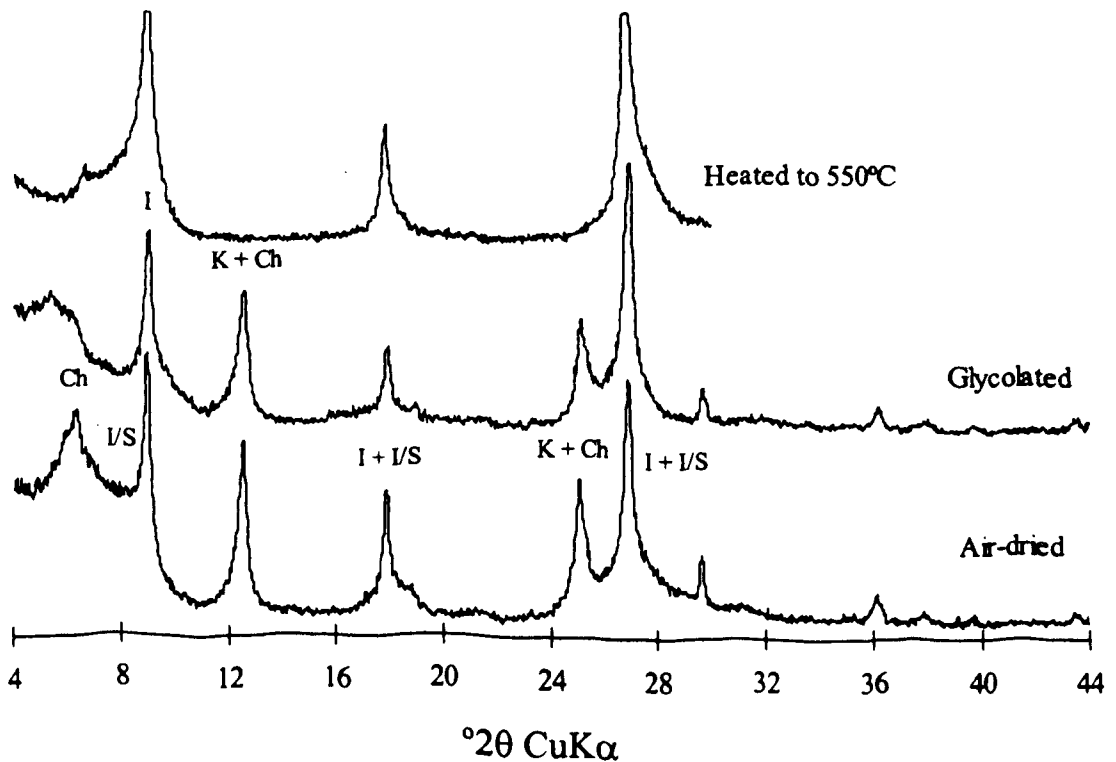
Sample 296 whole rock scan

Q - Quartz
 KF - K-Feldspar
 P - Plagioclase
 Ca - Calcite
 D - Dolomite
 I/S - Mixed layer illite-smectite

I - Illite/Mica
 K - Kaulinite
 Ch - Chlorite

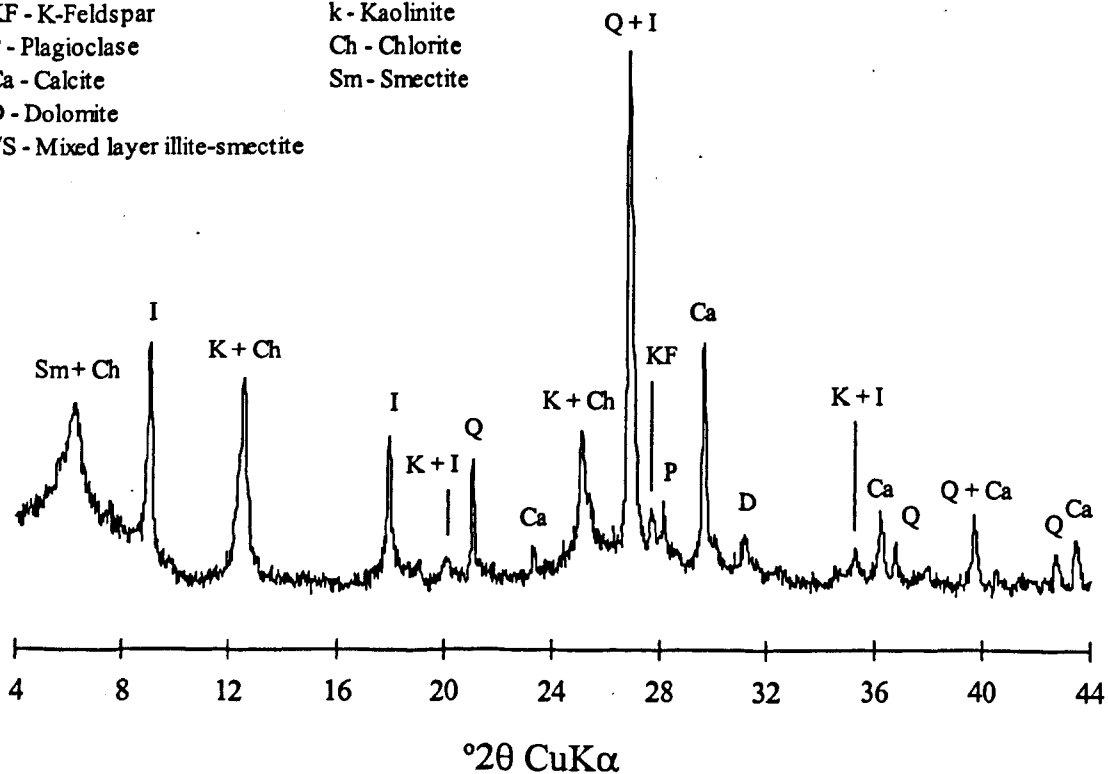


Sample 296 less than 2 μm fraction scan

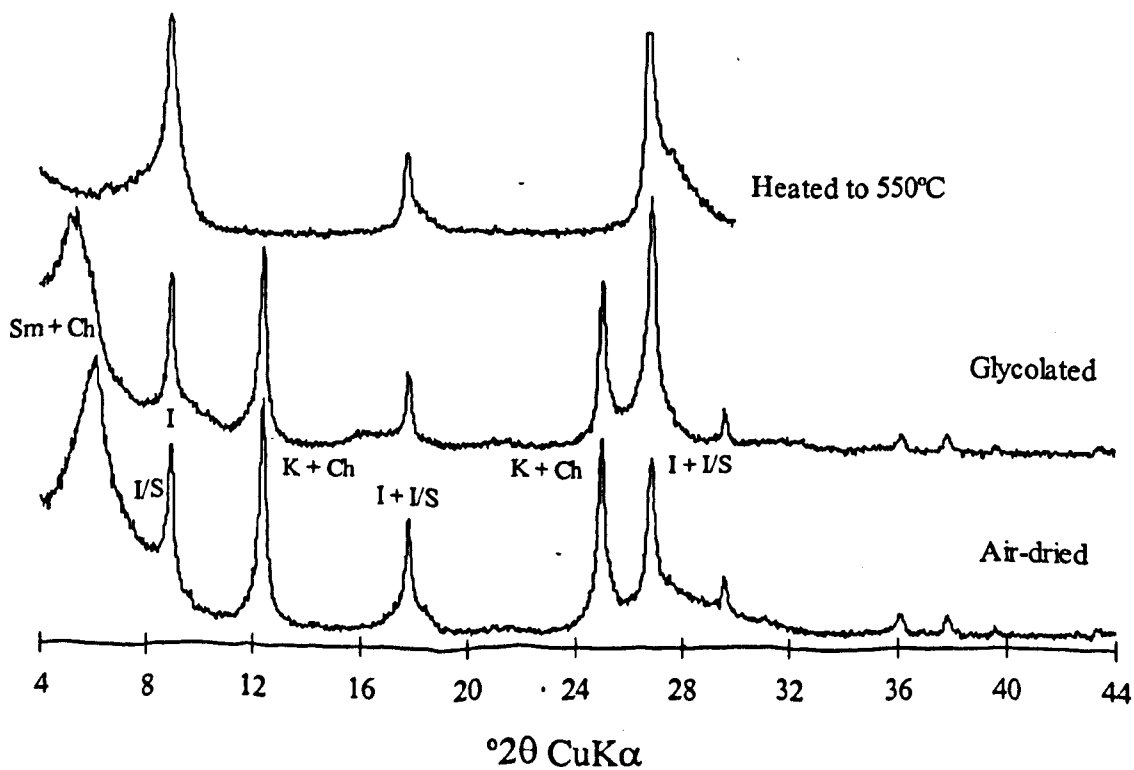


Sample 332 whole rock scan

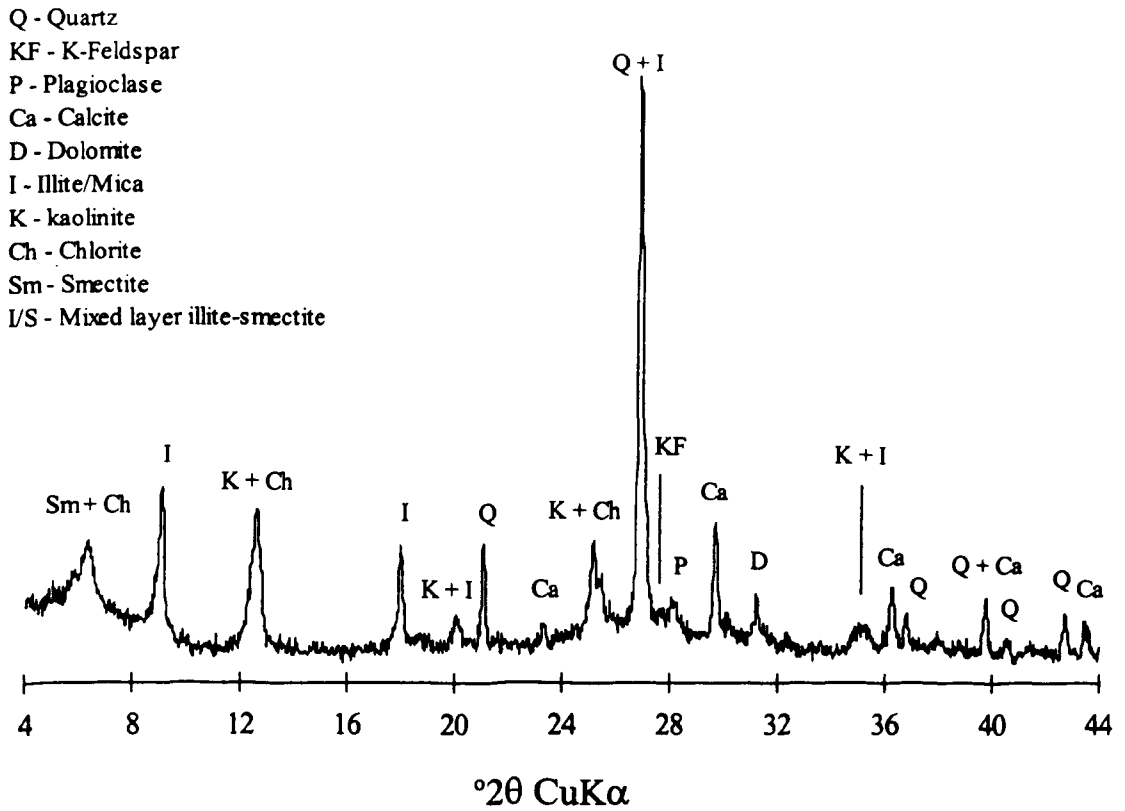
- Q - Quartz
- KF - K-Feldspar
- P - Plagioclase
- Ca - Calcite
- D - Dolomite
- I/S - Mixed layer illite-smectite
- I - Illite/Mica
- k - Kaolinite
- Ch - Chlorite
- Sm - Smectite



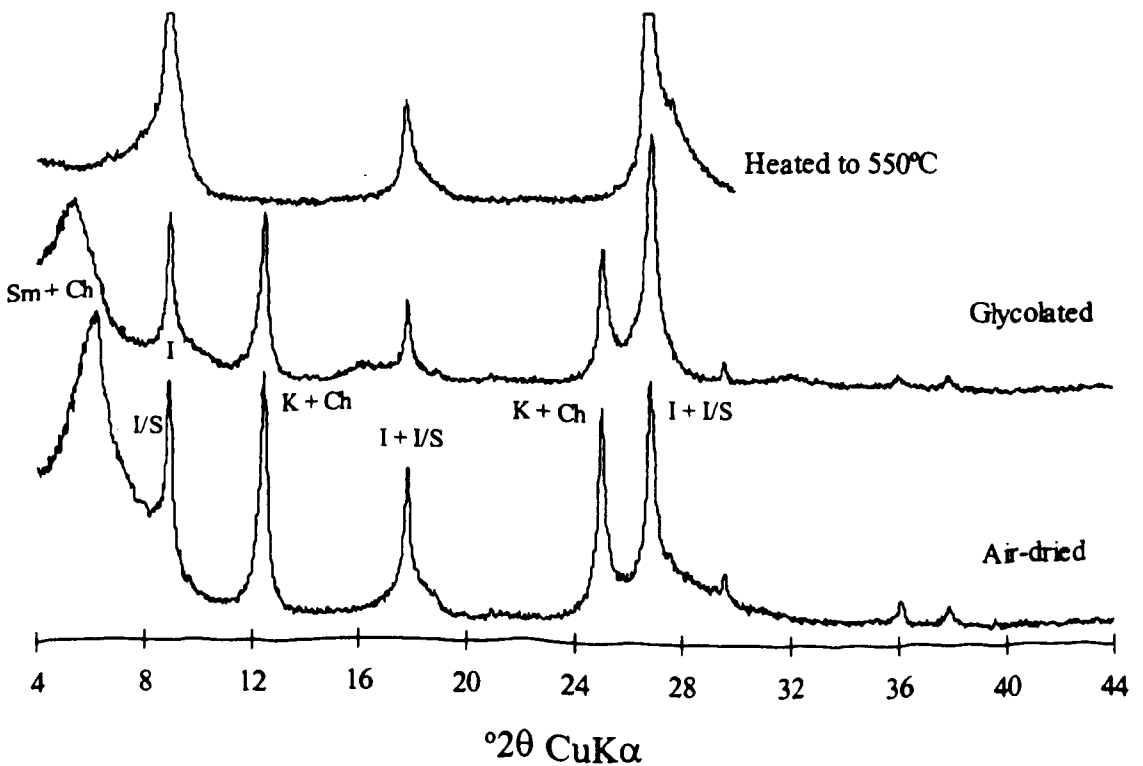
Sample 332 less than 2 μm fraction scan



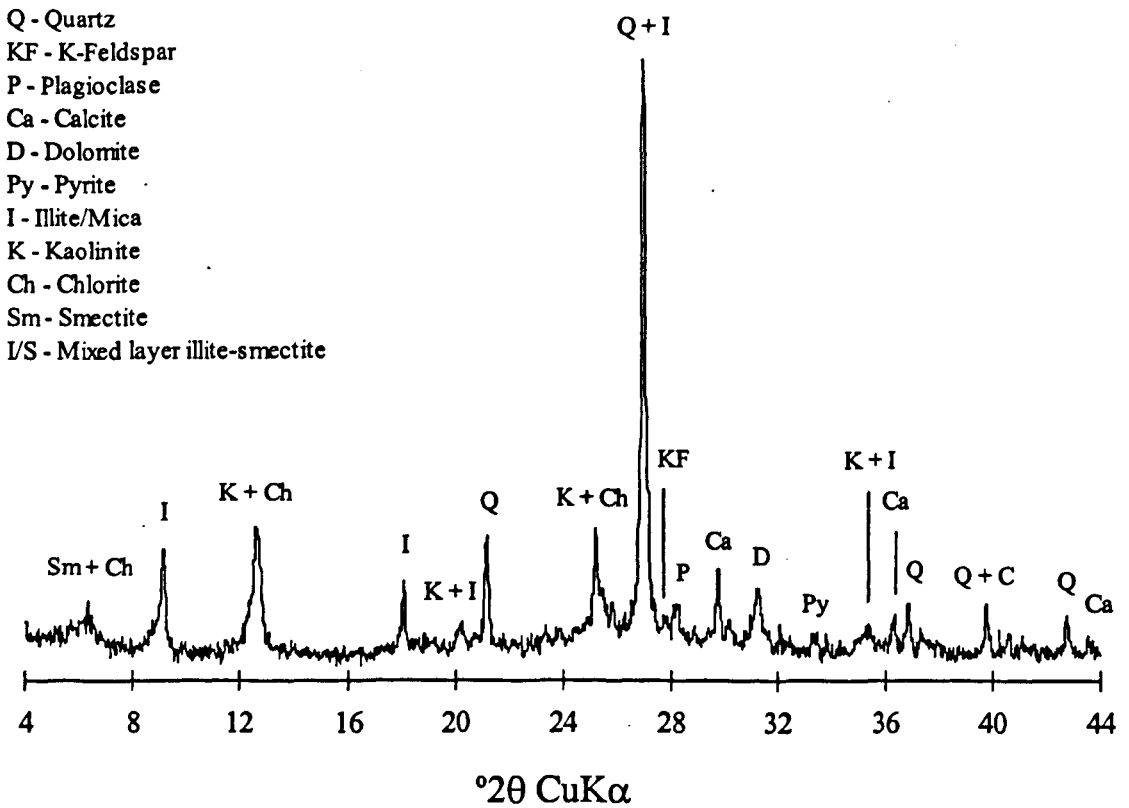
Sample 333 whole rock scan



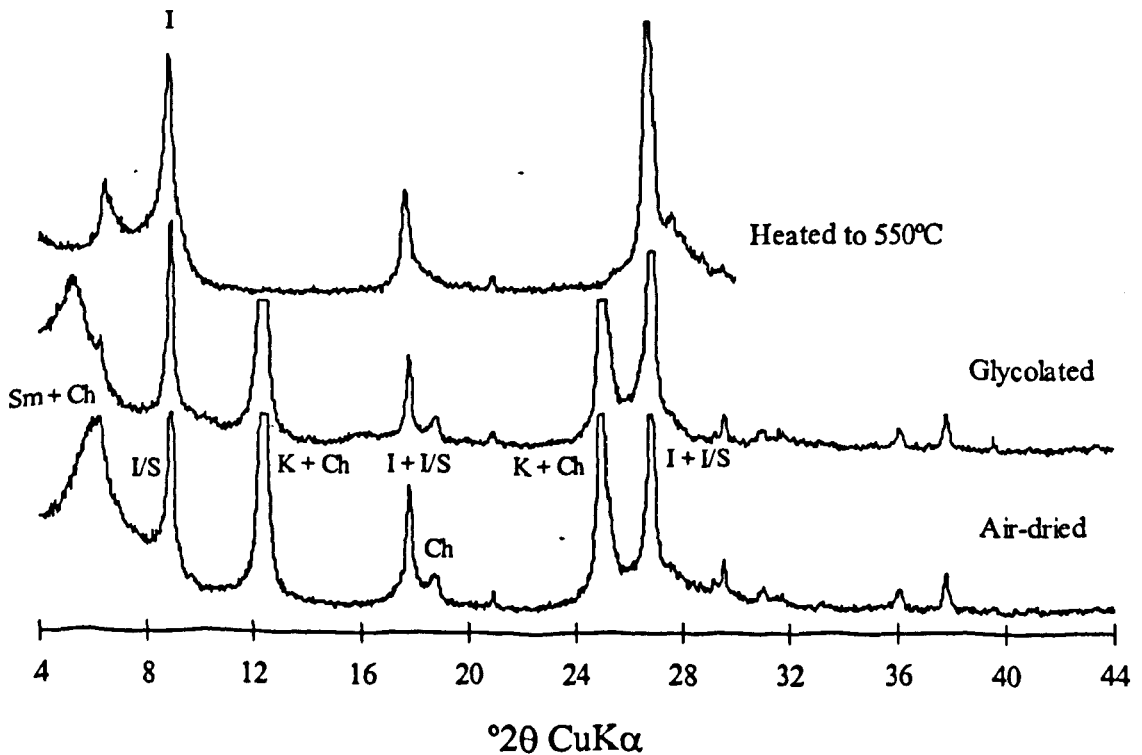
Sample 333 less than 2 μ m fraction scan



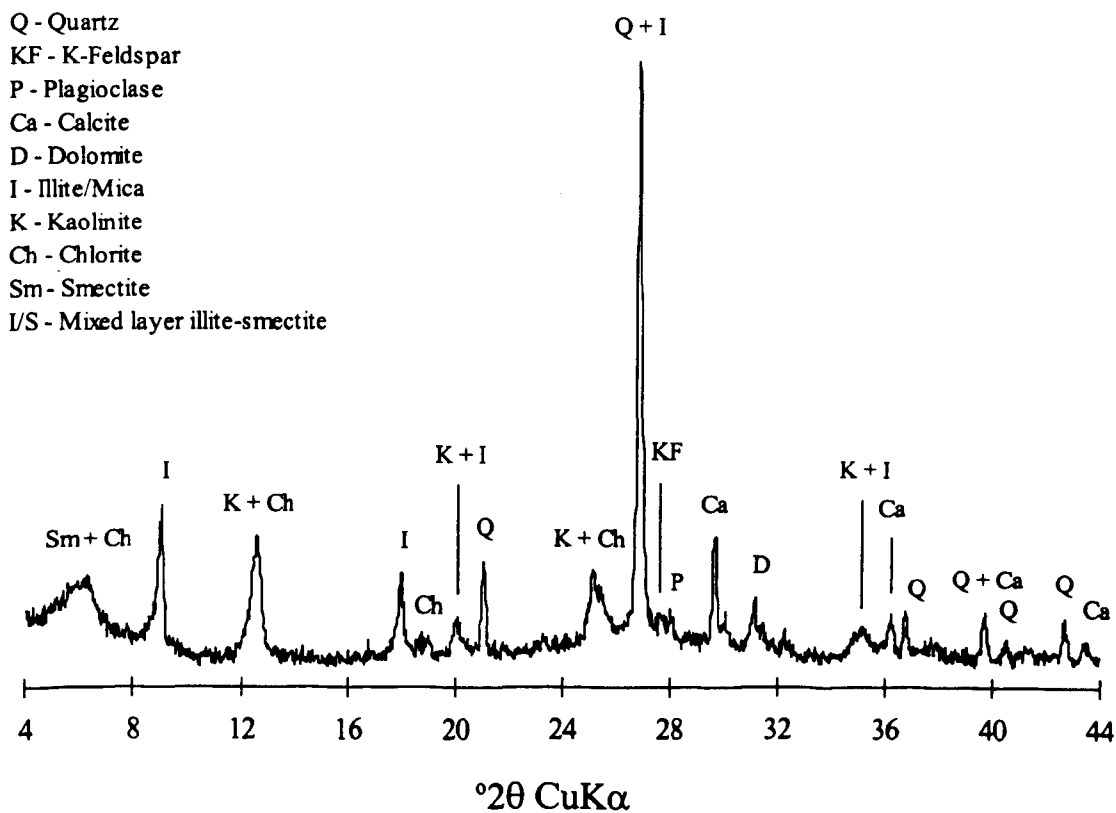
Sample 334 whole rock scan



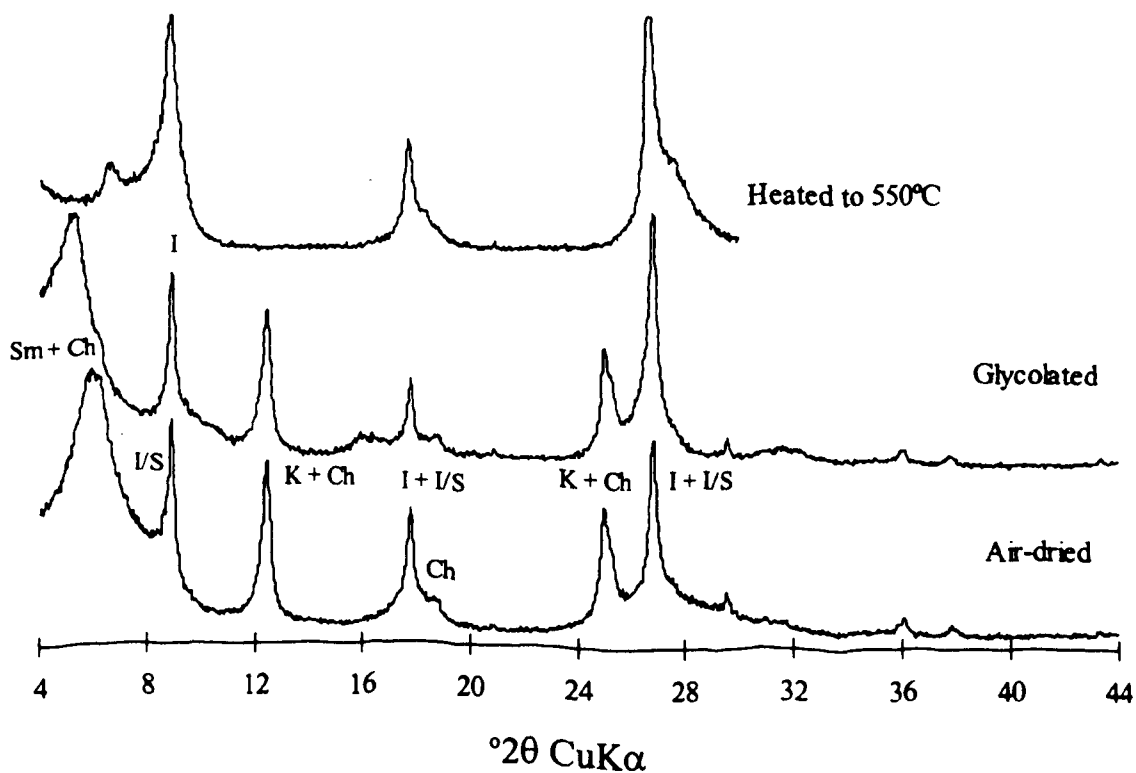
Sample 334 less than 2 μ m fraction scan



Sample 336 whole rock scan

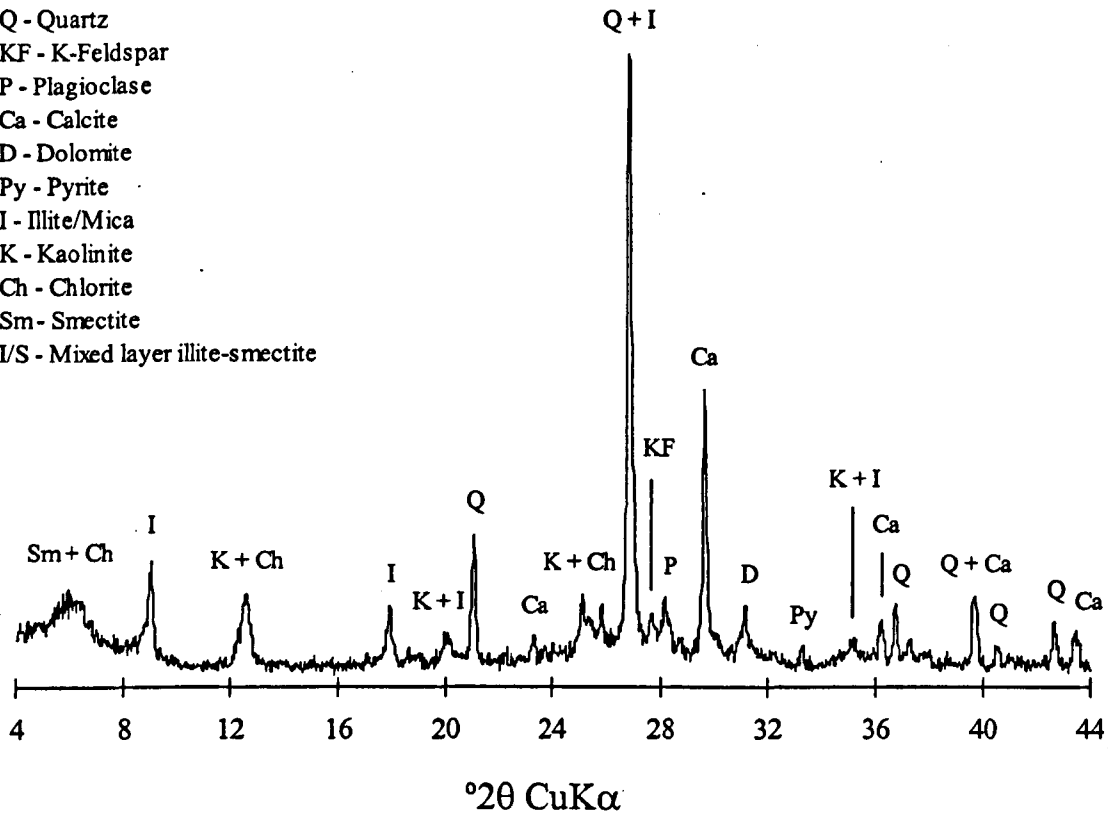


Sample 336 less than 2 μ m fraction scan

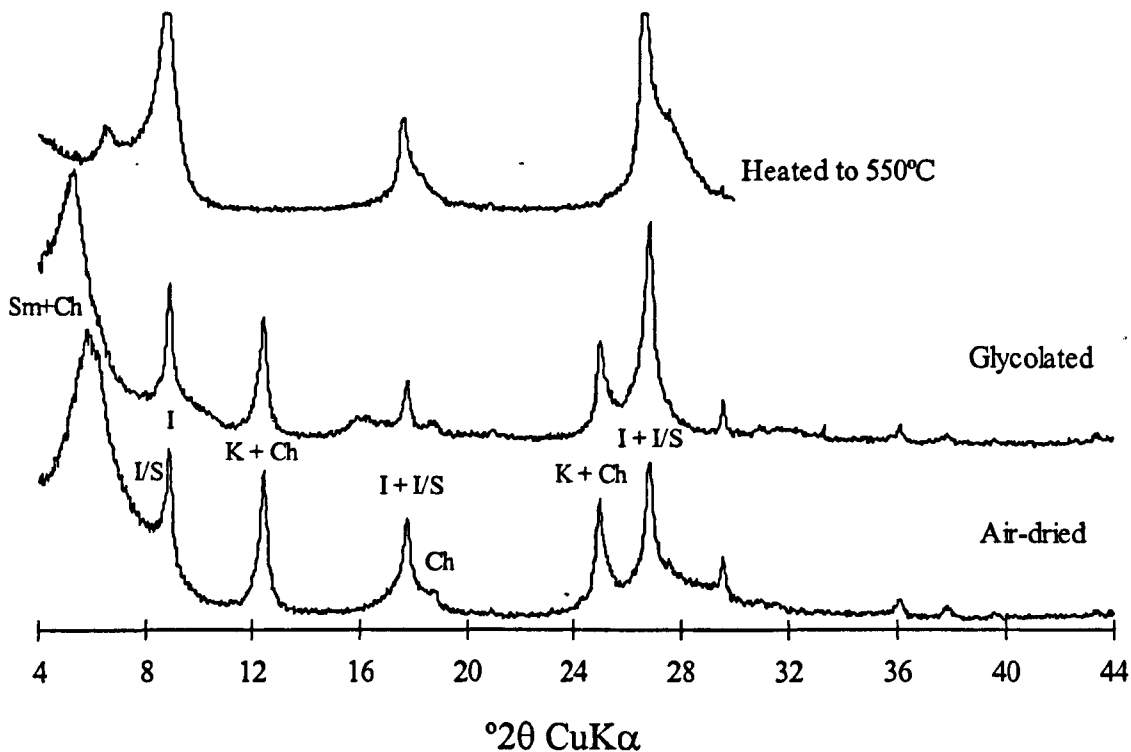


Sample 342 whole rock scan

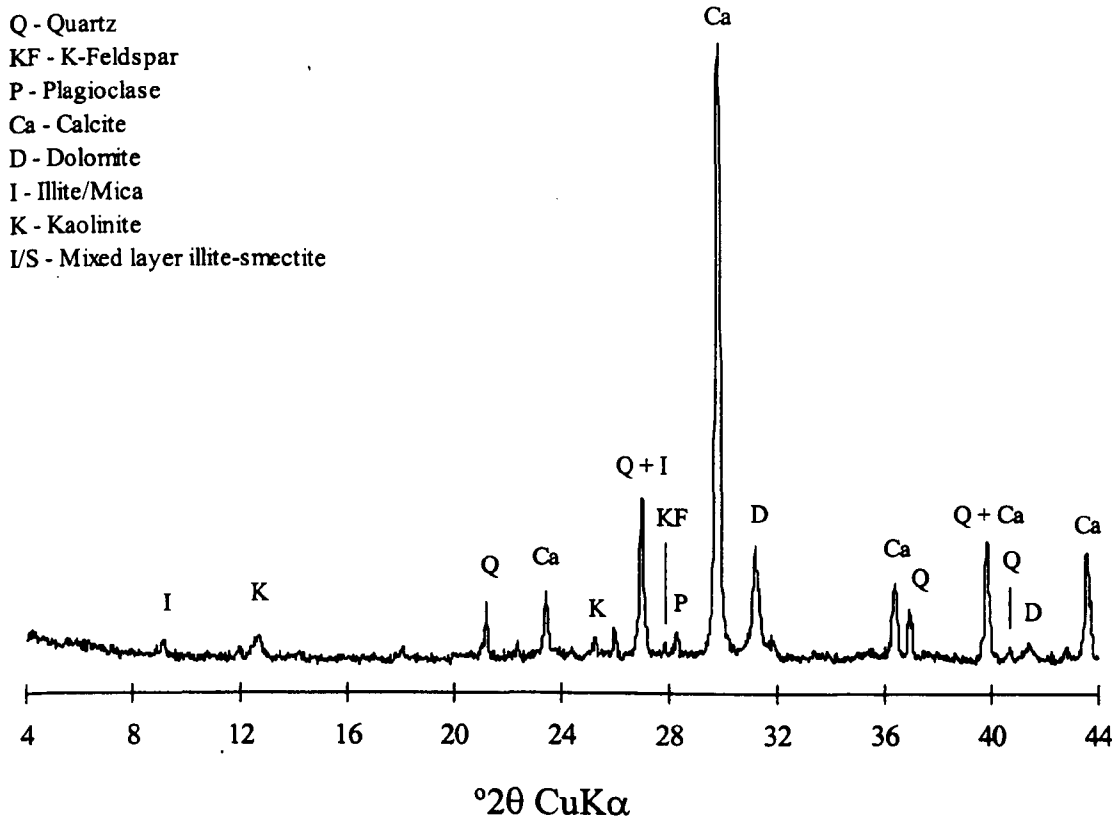
- Q - Quartz
- KF - K-Feldspar
- P - Plagioclase
- Ca - Calcite
- D - Dolomite
- Py - Pyrite
- I - Illite/Mica
- K - Kaolinite
- Ch - Chlorite
- Sm - Smectite
- I/S - Mixed layer illite-smectite



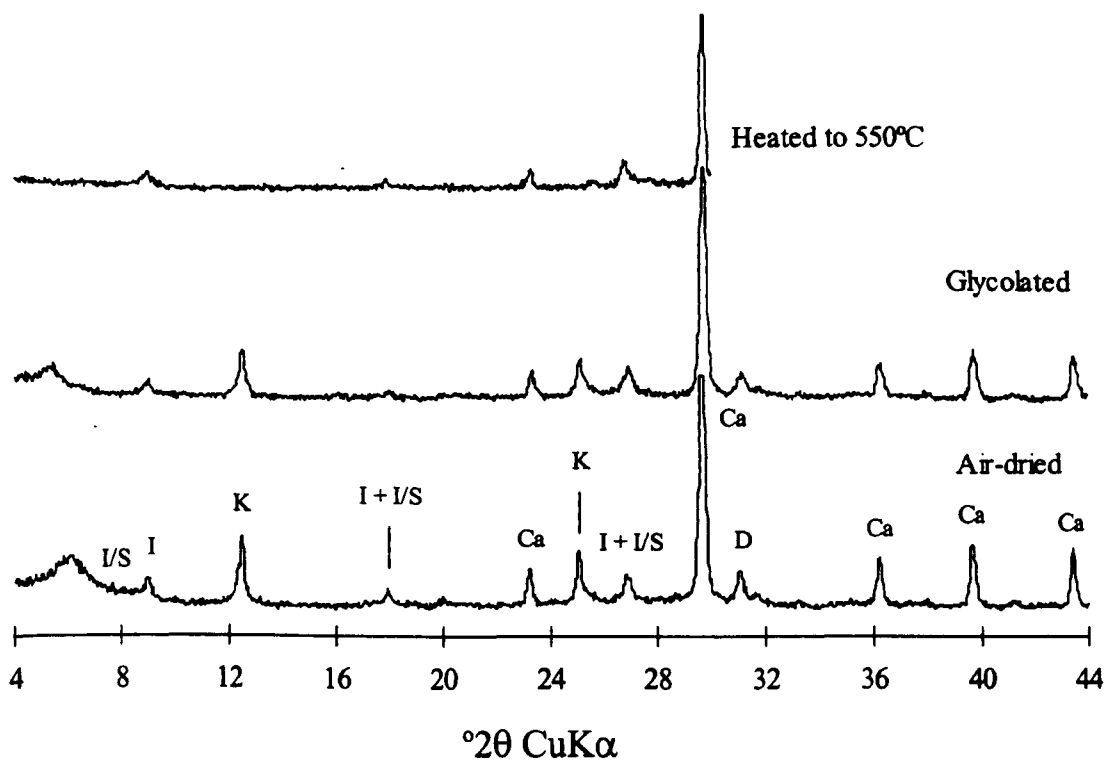
Sample 342 less than 2 μ m fraction scan



Sample 345 whole rock scan

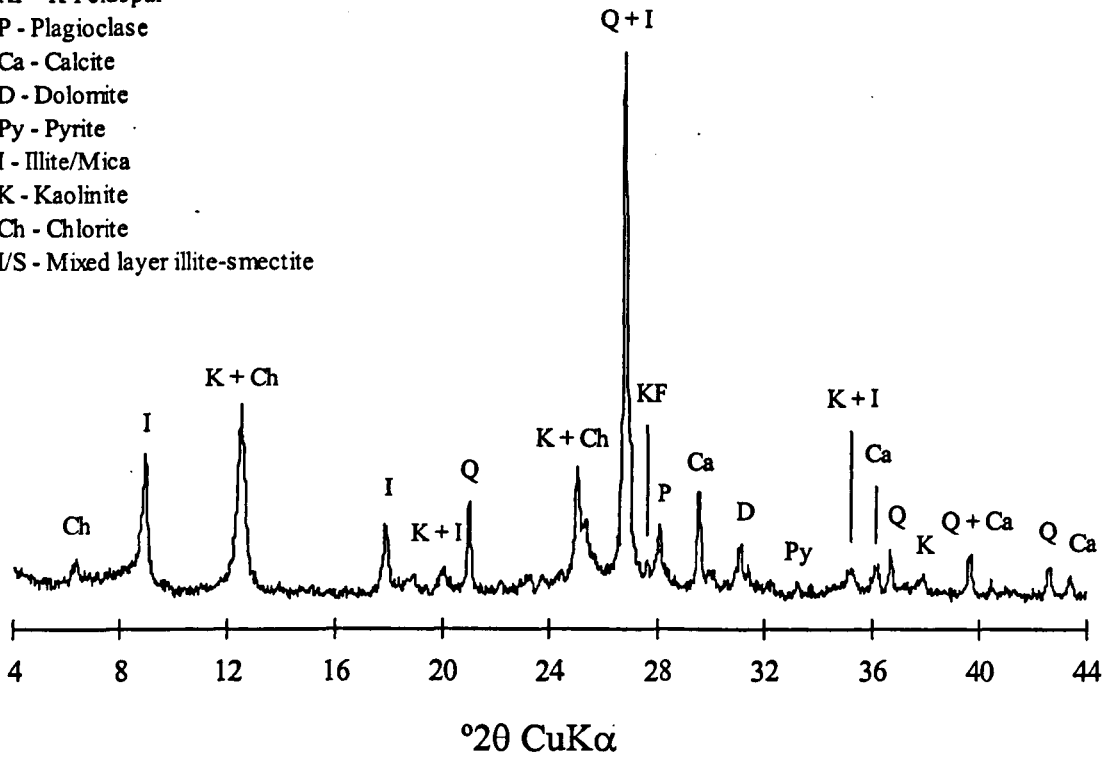


Sample 345 less than 2 μ m fraction scan

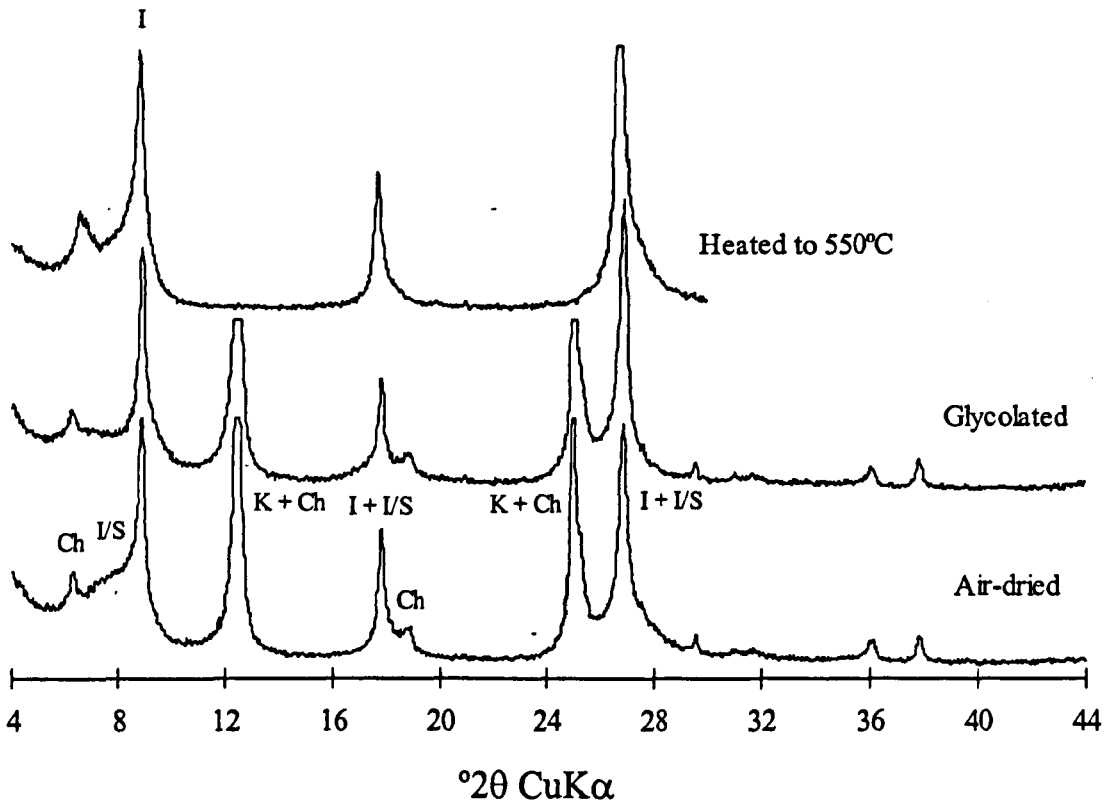


Sample 431 whole rock scan

- Q - Quartz
- KF - K-Feldspar
- P - Plagioclase
- Ca - Calcite
- D - Dolomite
- Py - Pyrite
- I - Illite/Mica
- K - Kaolinite
- Ch - Chlorite
- I/S - Mixed layer illite-smectite

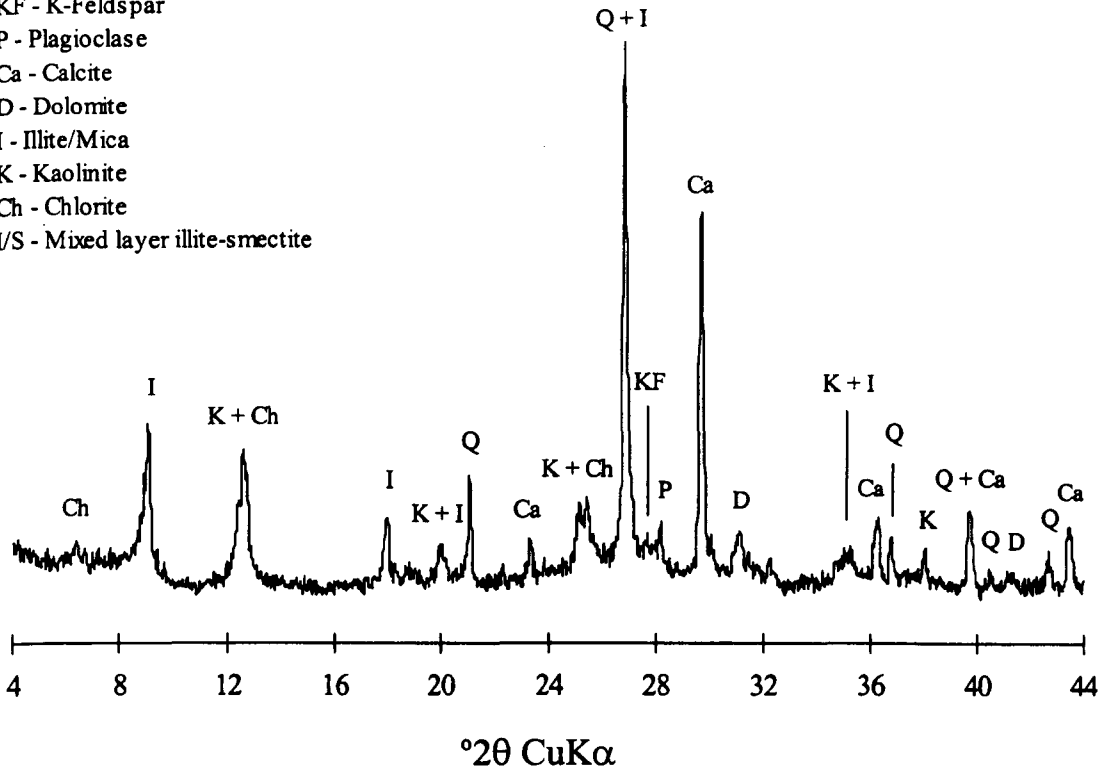


Sample 431 less than 2 μ m fraction scan

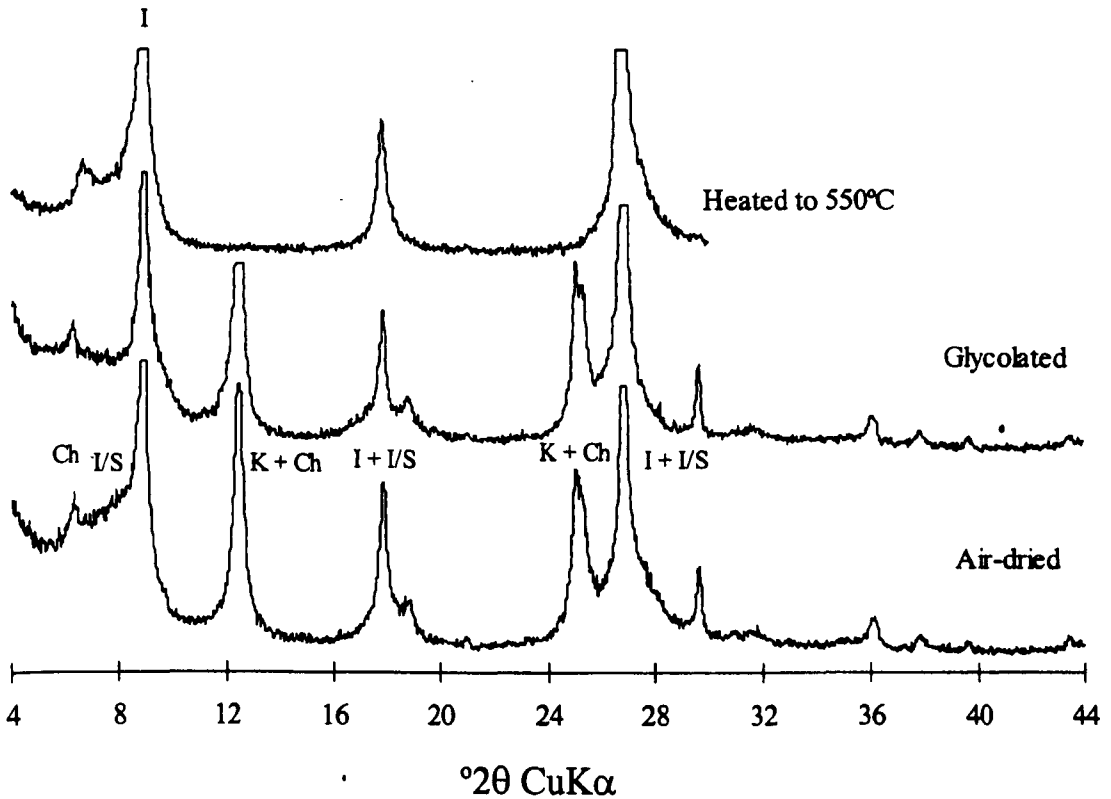


Sample 436 whole rock scan

- Q - Quartz
- KF - K-Feldspar
- P - Plagioclase
- Ca - Calcite
- D - Dolomite
- I - Illite/Mica
- K - Kaolinite
- Ch - Chlorite
- I/S - Mixed layer illite-smectite



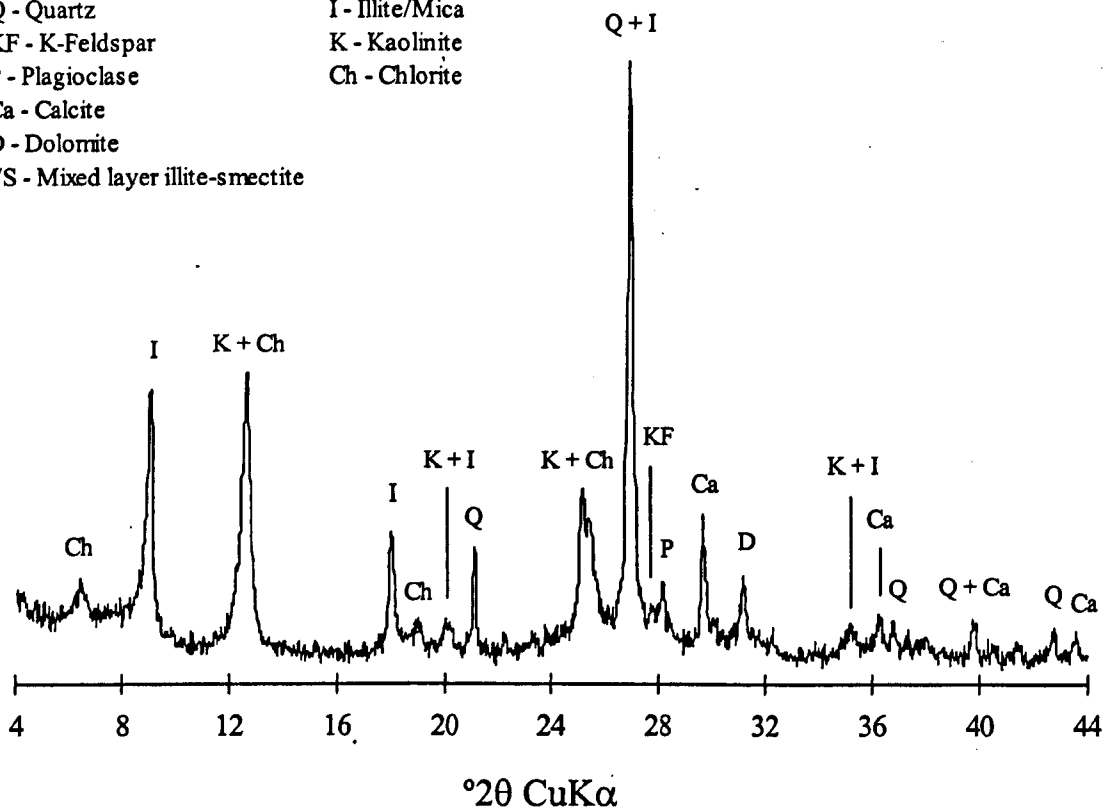
Sample 436 less than 2 μm fraction scan



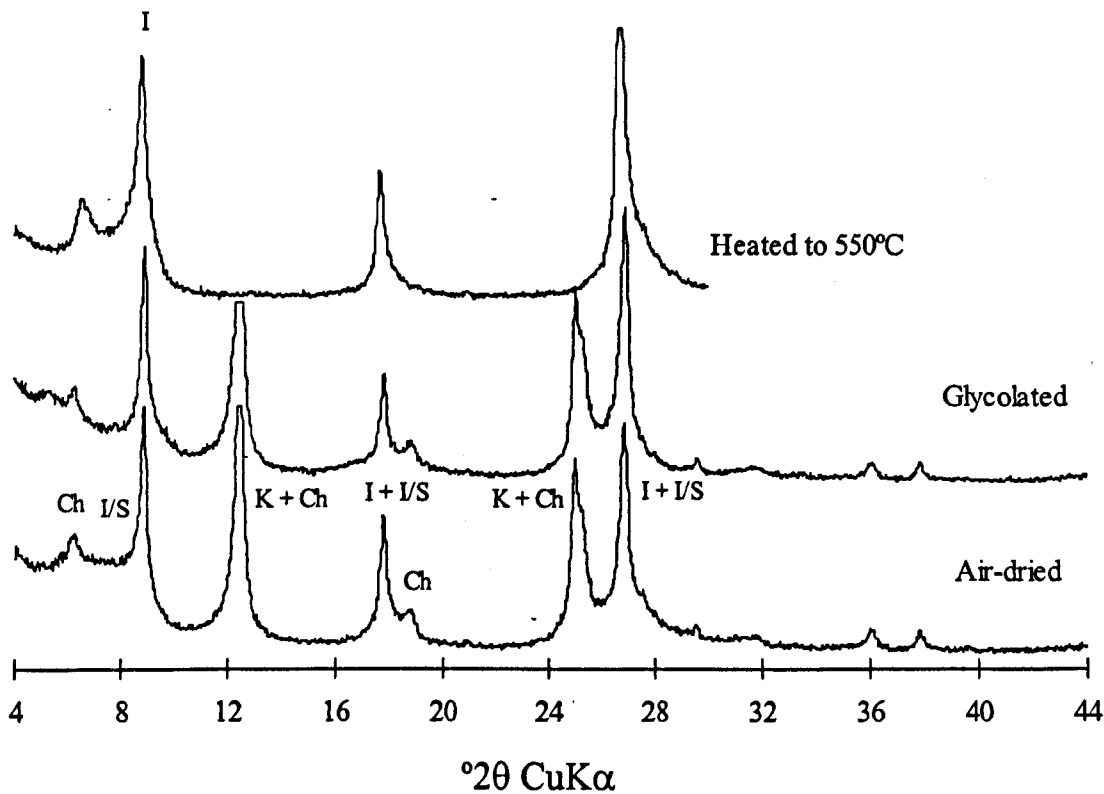
Sample 441 whole rock scan

Q - Quartz
 KF - K-Feldspar
 P - Plagioclase
 Ca - Calcite
 D - Dolomite
 I/S - Mixed layer illite-smectite

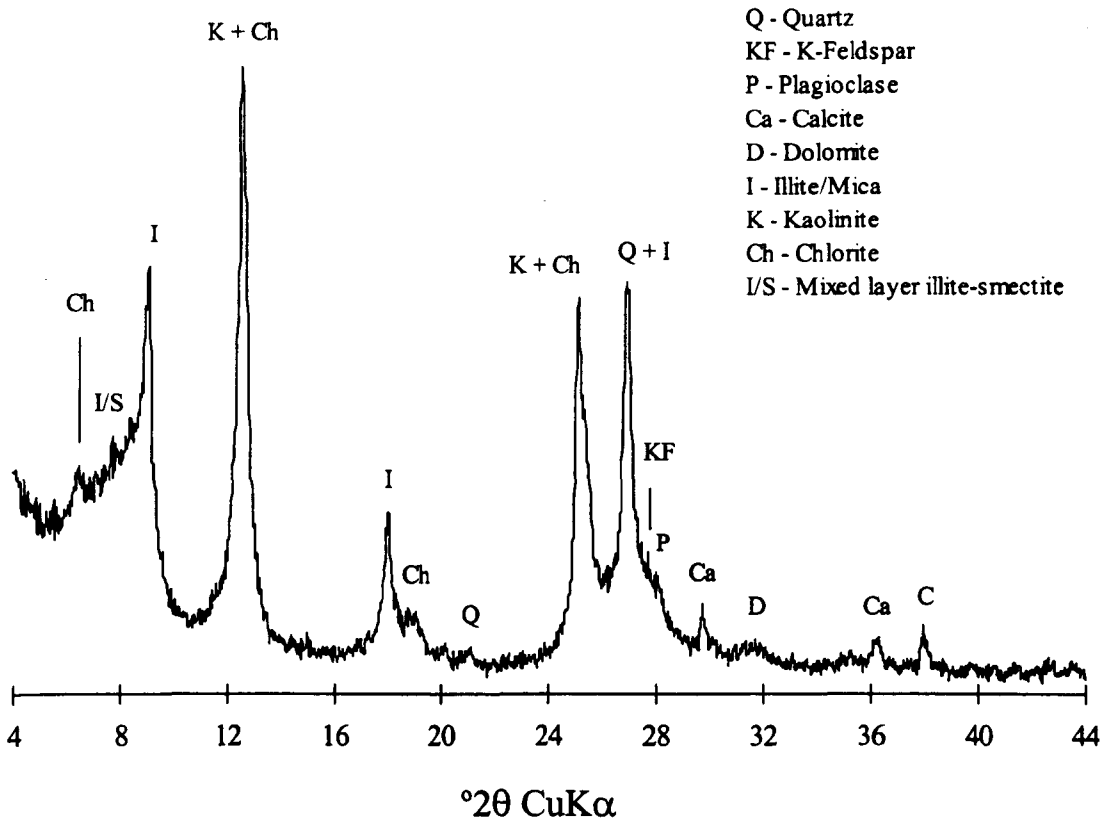
I - Illite/Mica
 K - Kaolinite
 Ch - Chlorite



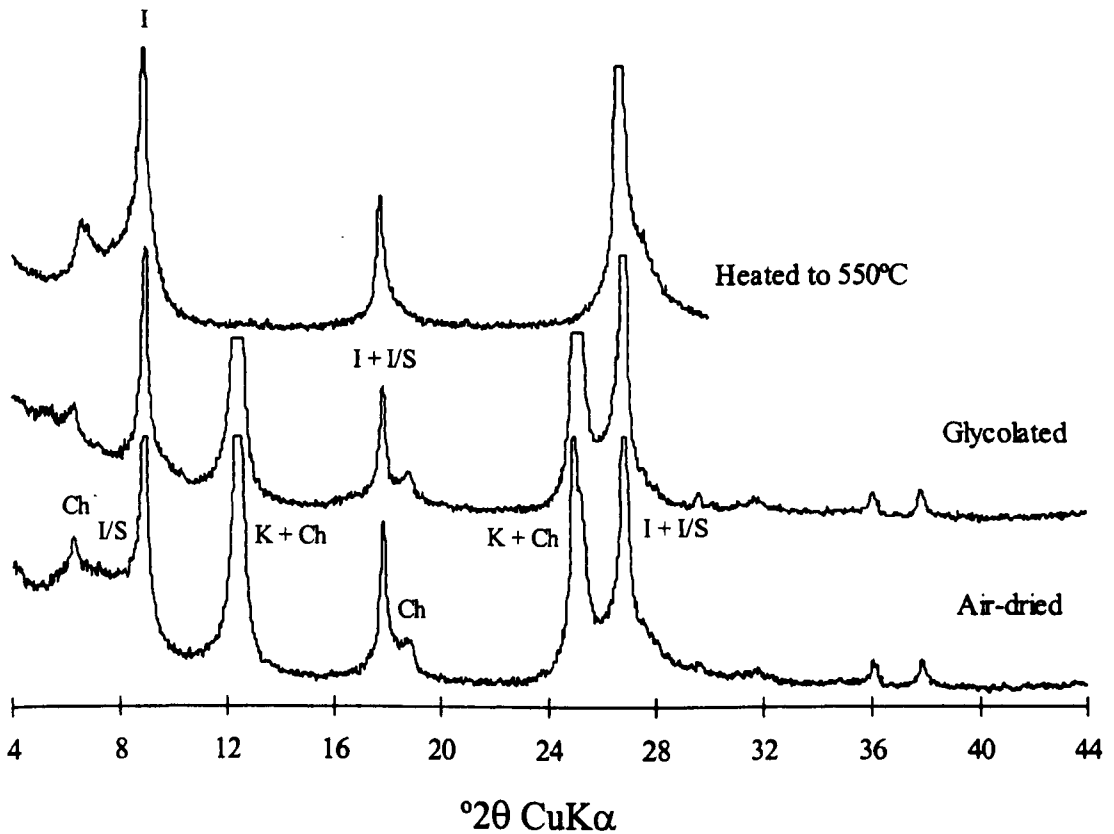
Sample 441 less than 2 μm fraction scan



Sample 445 whole rock scan

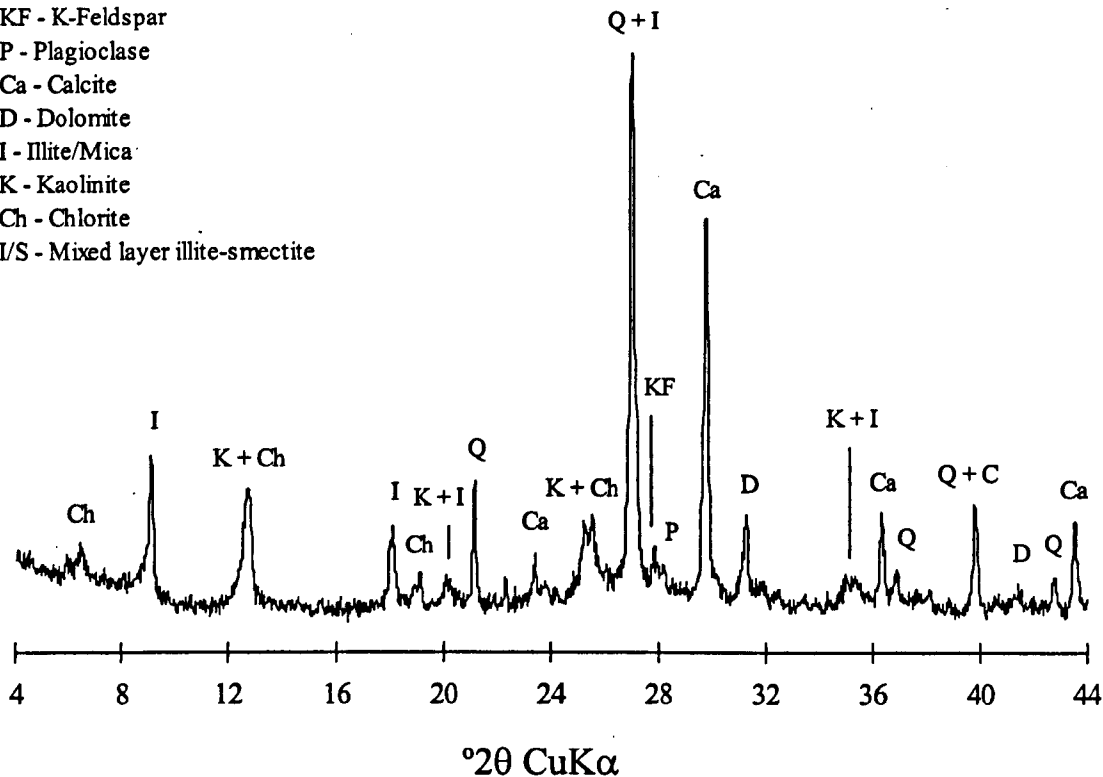


Sample 445 less than 2 μm fraction scan

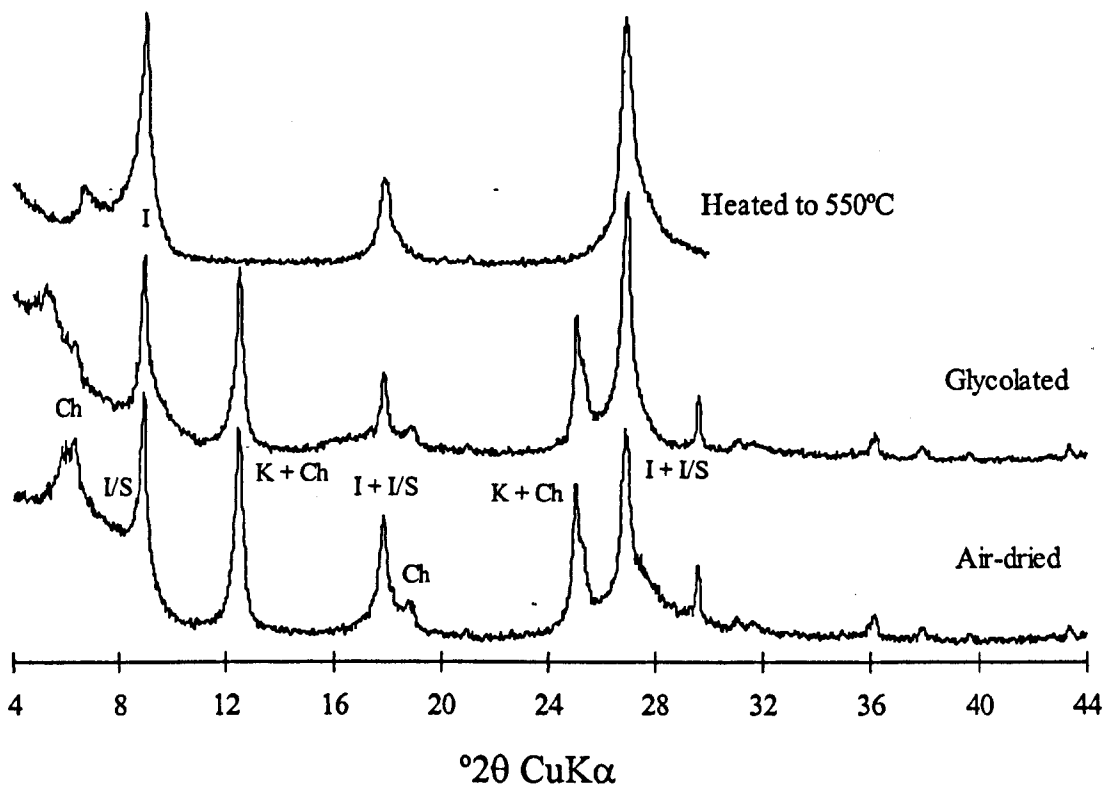


Sample OB1 whole rock scan

- Q - Quartz
- KF - K-Feldspar
- P - Plagioclase
- Ca - Calcite
- D - Dolomite
- I - Illite/Mica
- K - Kaolinite
- Ch - Chlorite
- I/S - Mixed layer illite-smectite

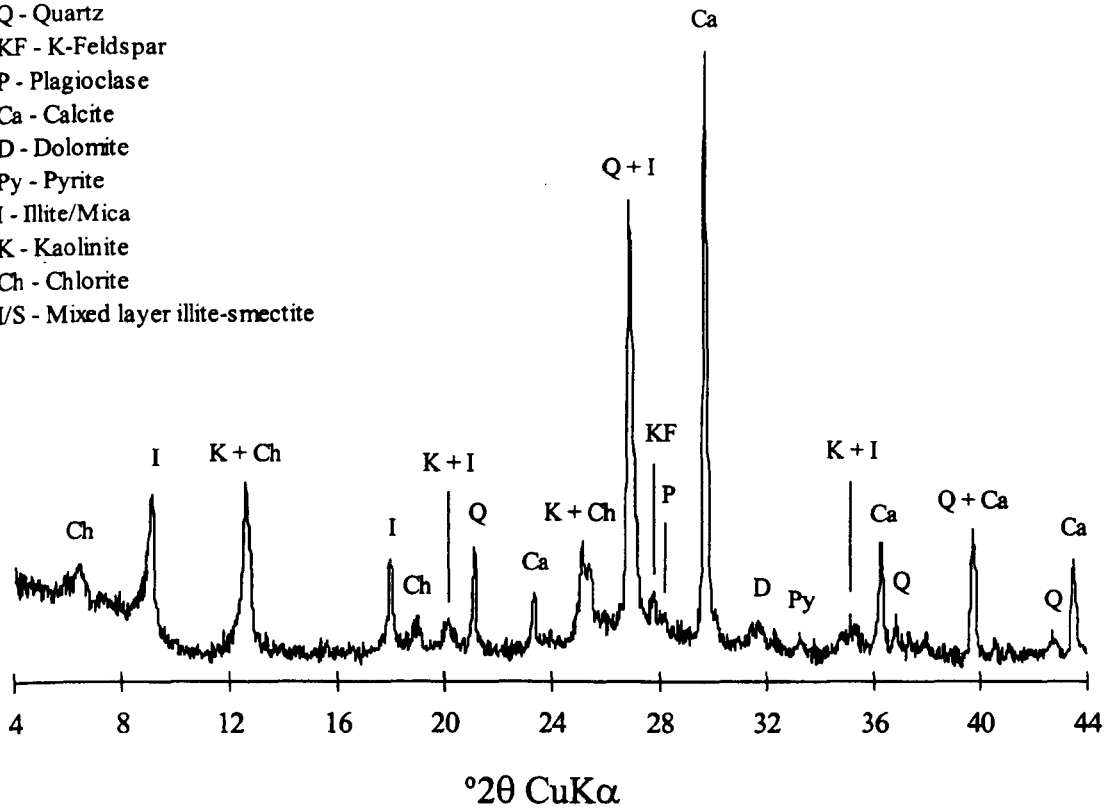


Sample OB1 less than 2 μm fraction scan

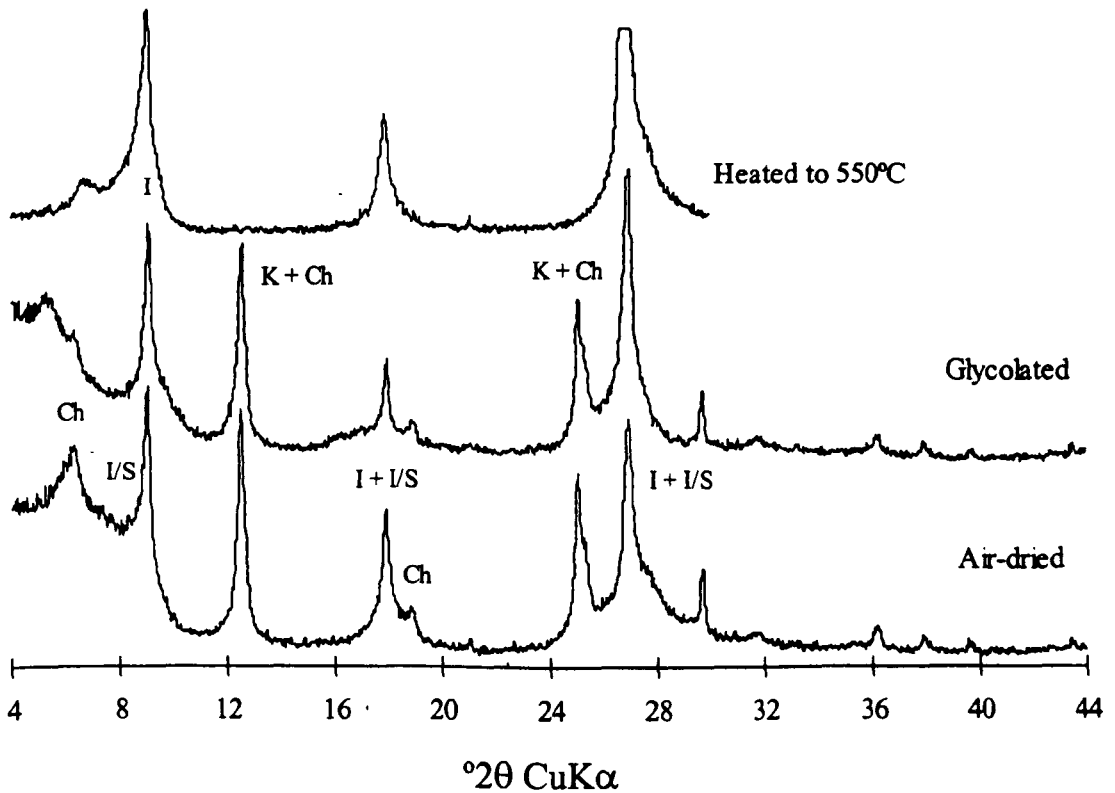


Sample OB2 whole rock scan

- Q - Quartz
- KF - K-Feldspar
- P - Plagioclase
- Ca - Calcite
- D - Dolomite
- Py - Pyrite
- I - Illite/Mica
- K - Kaolinite
- Ch - Chlorite
- I/S - Mixed layer illite-smectite



Sample OB2 less than 2 μ m fraction scan



Appendix I.2 - XRF raw data

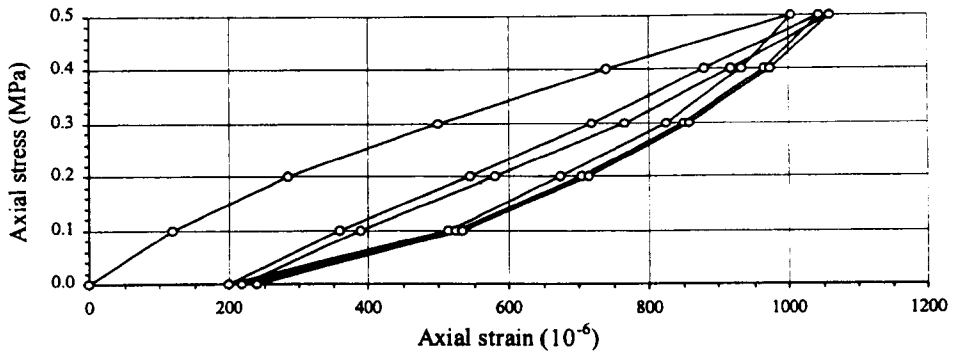
Raw XRF data in percent for the mudrocks studied

Sample	SiO ₂	TiO ₂	Al ₂ O ₃	Fe ₂ O ₃	MnO	MgO	CaO	Na ₂ O	K ₂ O	P ₂ O ₅	SO ₃	Total
51	18.23	0.31	7.80	3.69	0.05	1.83	67.57	0.10	0.05	0.20	0.39	100.22
52	52.29	1.02	20.29	8.11	0.07	3.77	9.66	0.46	3.71	0.12	0.08	99.58
81	56.18	0.90	20.34	5.41	0.03	2.78	6.25	0.19	3.94	0.10	0.16	96.28
83	64.01	0.82	14.38	4.24	0.04	3.29	8.49	1.11	3.20	0.10	0.31	99.99
111	64.20	1.11	17.48	6.80	0.11	1.83	3.47	1.71	3.10	0.06	0.08	99.95
112	56.10	0.86	16.95	7.12	0.07	2.98	10.64	0.89	3.27	0.18	0.08	99.14
114	56.56	0.88	17.09	5.75	0.07	3.05	11.27	0.89	3.34	0.14	0.14	99.18
151	49.06	0.86	19.64	7.80	0.07	1.99	16.16	0.61	3.58	0.12	0.18	100.07
152	52.64	0.94	20.26	6.19	0.07	2.70	11.61	0.70	3.94	0.10	0.06	99.21
153	53.48	0.95	20.60	7.08	0.05	3.00	9.41	0.82	4.01	0.14	0.06	99.60
154	53.58	0.94	19.73	6.12	0.05	3.22	9.53	1.07	3.83	0.15	0.26	98.48
156	58.89	1.08	20.66	6.00	0.05	2.79	4.79	0.79	3.87	0.10	0.09	99.11
162	53.22	0.92	21.25	5.78	0.04	2.59	9.95	0.90	4.50	0.08	0.06	99.29
163	57.04	0.82	17.17	5.74	0.04	2.66	11.22	1.02	3.71	0.14	0.16	99.72
283	51.49	0.82	15.71	5.55	0.09	2.73	19.21	0.82	3.11	0.13	0.27	99.93
285	52.56	0.87	18.01	6.45	0.07	3.28	13.30	0.72	3.58	0.11	0.20	99.15
286	51.44	0.77	15.80	6.04	0.09	2.96	17.71	0.93	3.17	0.14	0.25	99.30
294	51.52	0.87	19.59	7.76	0.08	3.10	11.00	0.31	3.77	0.16	0.46	98.62
296	51.49	0.85	18.60	6.51	0.09	3.25	13.82	0.81	3.62	0.12	0.29	99.45
332	60.77	1.04	16.34	4.22	0.04	2.34	9.92	0.93	3.46	0.09	0.13	99.28
333	59.70	0.92	18.97	5.46	0.03	2.57	6.56	0.77	3.94	0.12	0.24	99.28
334	59.43	0.91	18.11	6.81	0.04	3.12	5.43	1.11	3.81	0.12	0.62	99.51
336	56.28	0.95	21.52	5.80	0.04	3.61	6.33	0.27	4.13	0.10	0.06	99.09
342	60.52	0.92	15.74	4.90	0.04	2.82	9.44	0.89	3.39	0.10	0.59	99.35
345	32.23	0.33	6.79	2.06	0.08	3.49	45.03	2.18	1.52	0.11	0.55	94.37
431	57.50	1.07	20.98	5.56	0.03	2.89	5.70	1.05	3.79	0.11	0.21	98.89
436	49.98	0.85	19.80	6.46	0.06	3.26	13.53	0.62	4.01	0.10	0.16	98.83
441	54.21	0.96	21.64	6.65	0.07	3.68	6.91	0.90	3.86	0.08	0.05	99.01
445	56.11	1.08	22.16	6.53	0.05	2.93	4.78	1.05	3.75	0.10	0.10	98.64
OB1	53.27	0.74	16.04	5.14	0.06	3.38	15.69	0.17	3.88	0.13	0.51	99.01
OB2	52.87	0.74	16.33	4.83	0.05	1.98	17.14	0.42	3.93	0.14	0.47	98.90

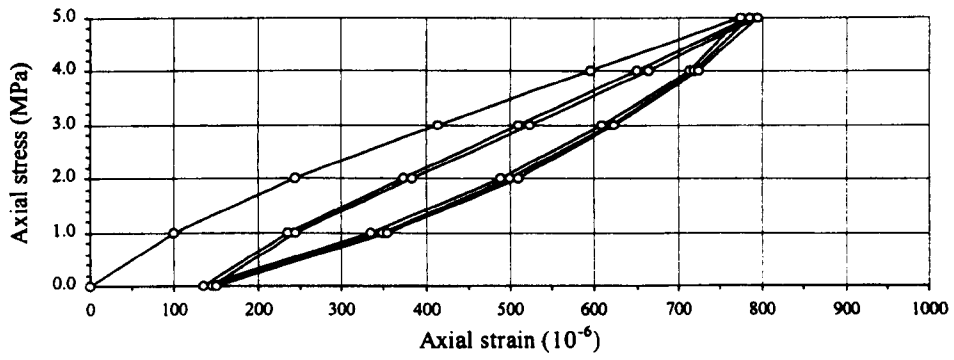
**APPENDIX II - GEOTECHNICAL
CHARACTERIZATION TESTS**

Appendix II.1 - Uniaxial compressive strength test plots

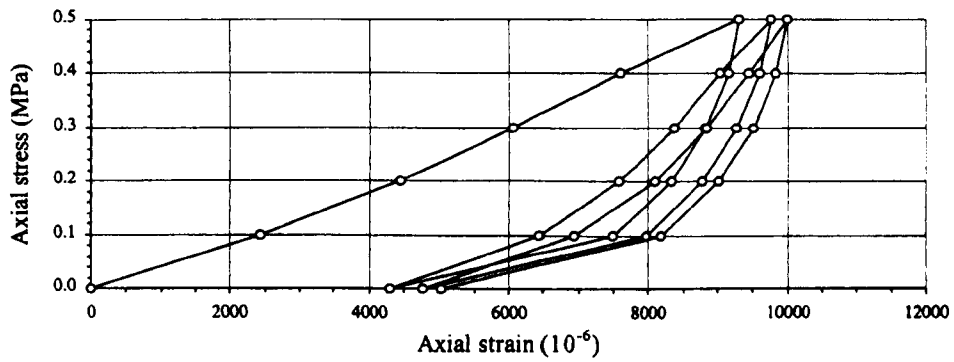
Sample 81



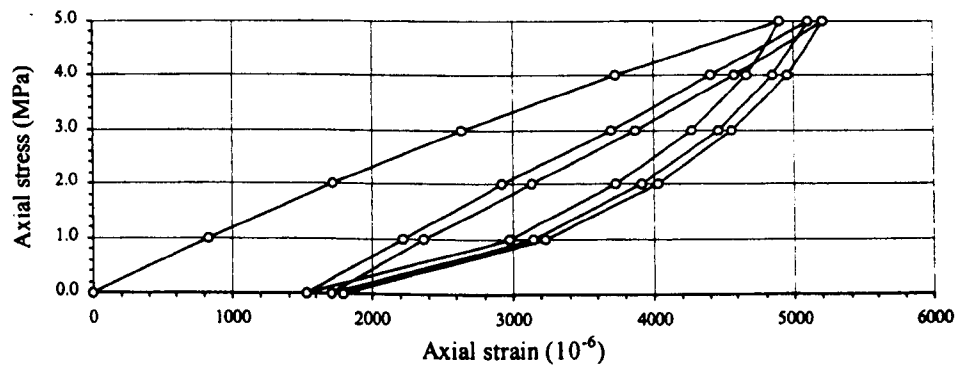
Sample 83



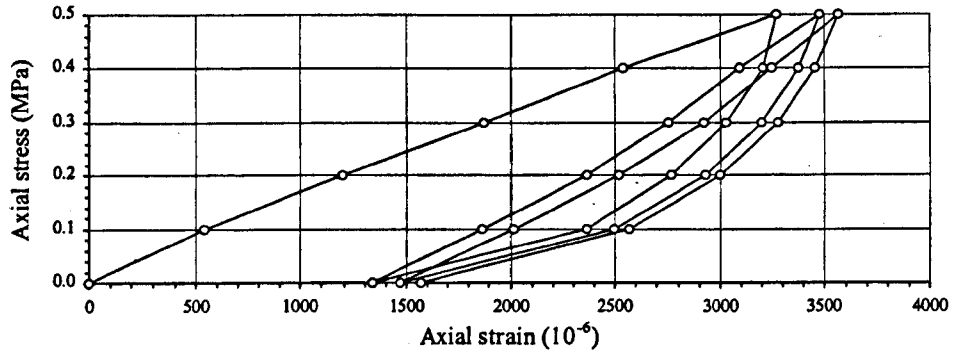
Sample 283



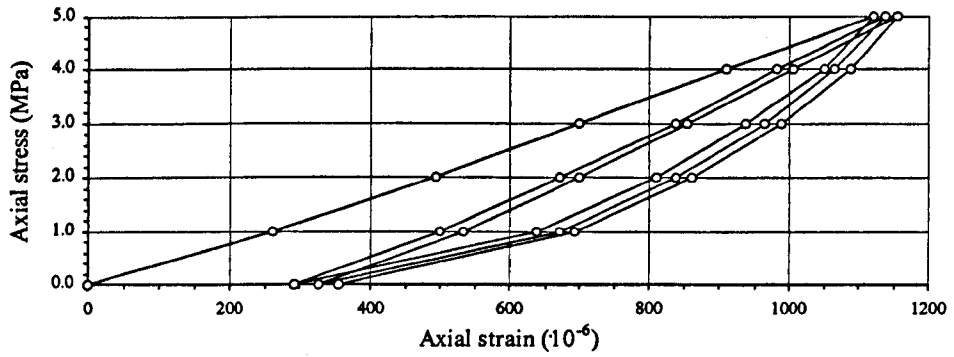
Sample 286



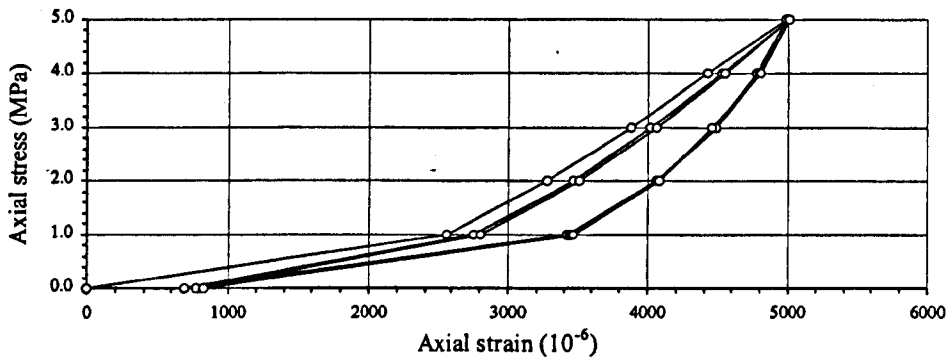
Sample 332



Sample 345

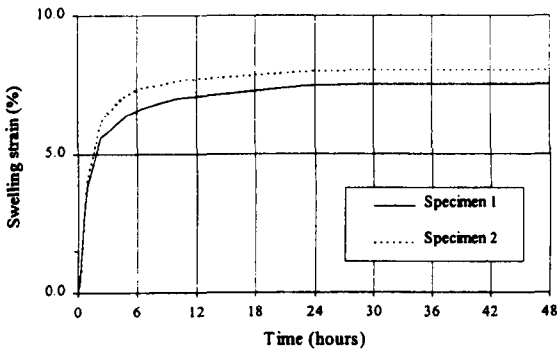


Sample 431

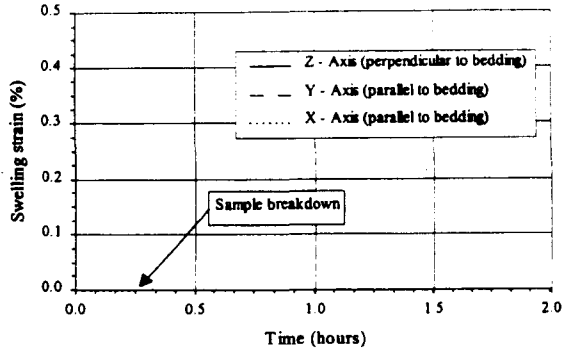


Appendix II.2 - Swelling tests plots

Sample 51

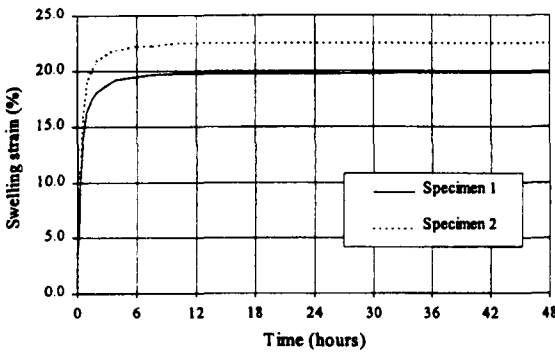


Plot of swelling test on remoulded specimens

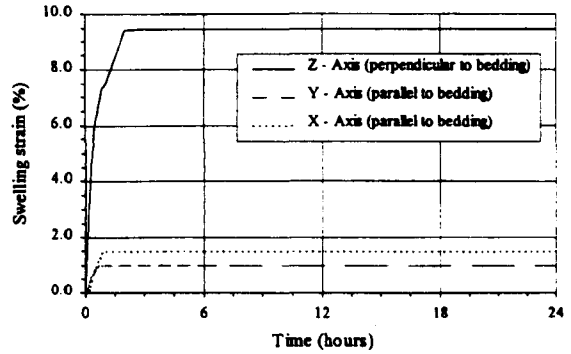


Triaxial swelling test plot

Sample 52

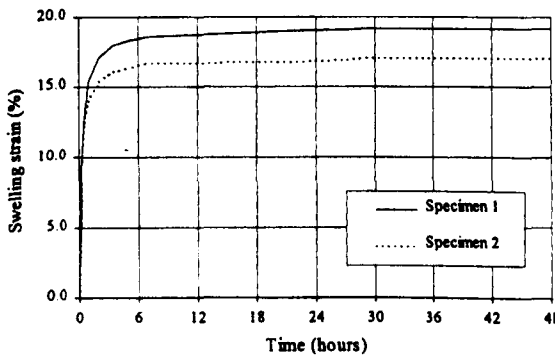


Plot of swelling test on remoulded specimens

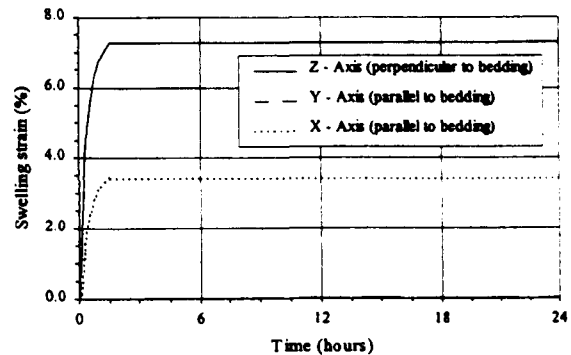


Triaxial swelling test plot

Sample 81

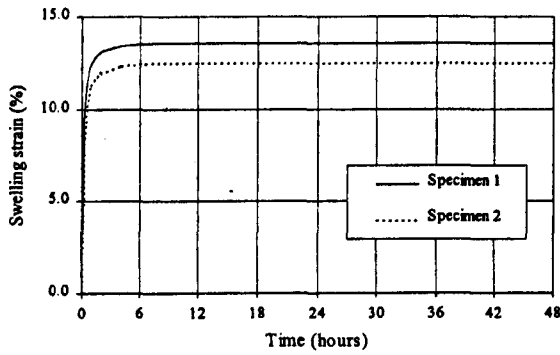


Plot of swelling test on remoulded specimens

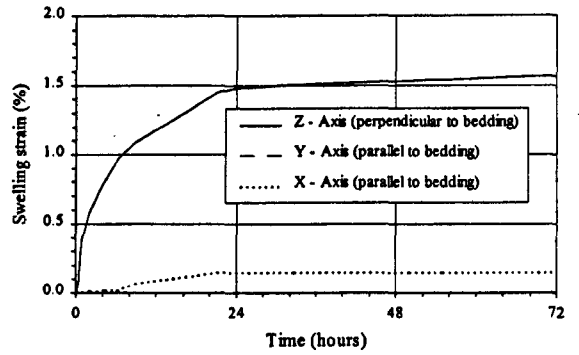


Triaxial swelling test plot

Sample 83

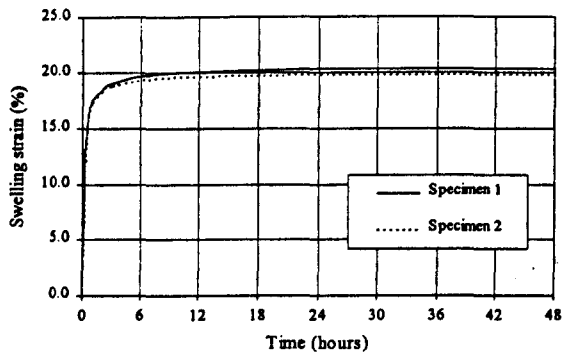


Plot of swelling test on remoulded specimens

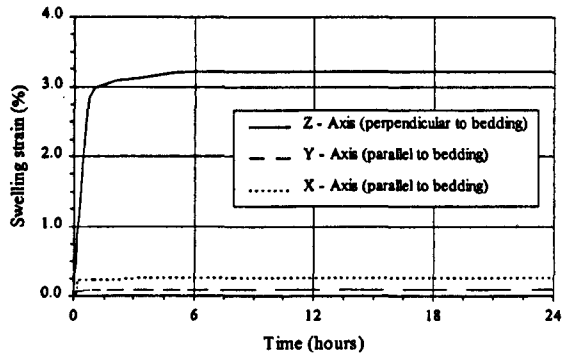


Triaxial swelling test plot

Sample 111

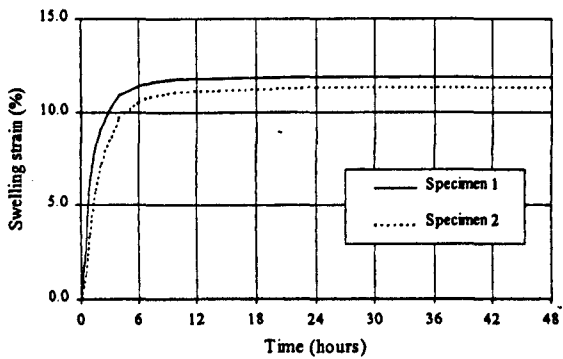


Plot of swelling test on remoulded specimens

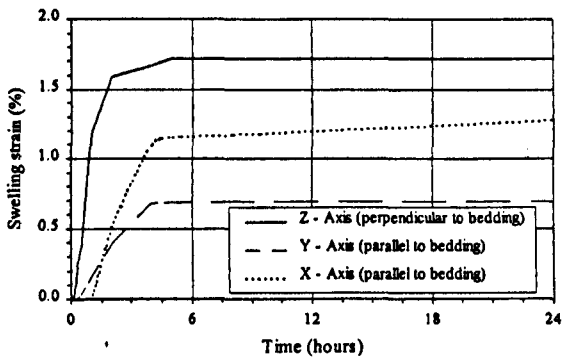


Triaxial swelling test plot

Sample 112

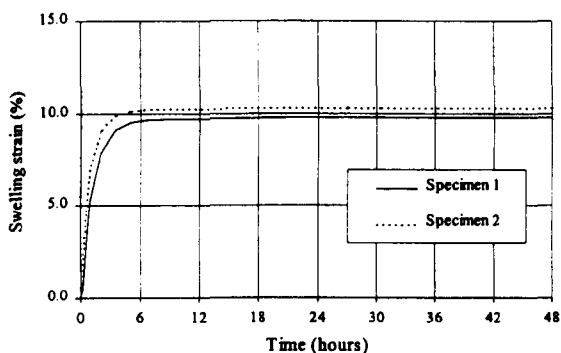


Plot of swelling test on remoulded specimens

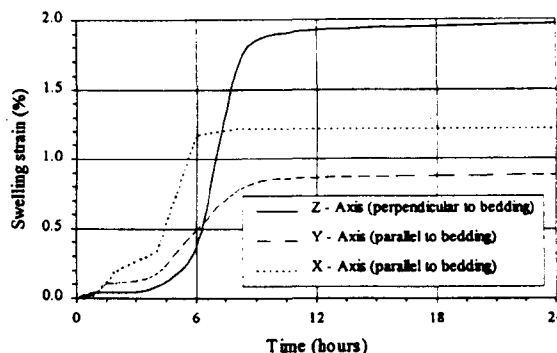


Triaxial swelling test plot

Sample 114

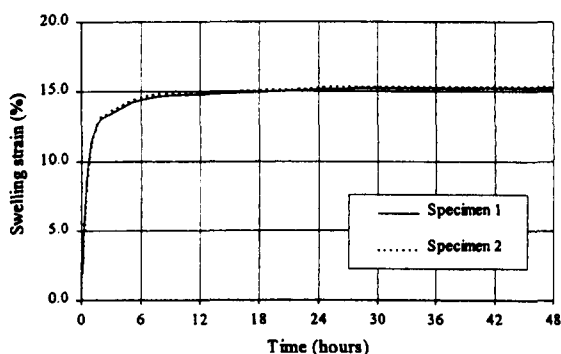


Plot of swelling test on remoulded specimens

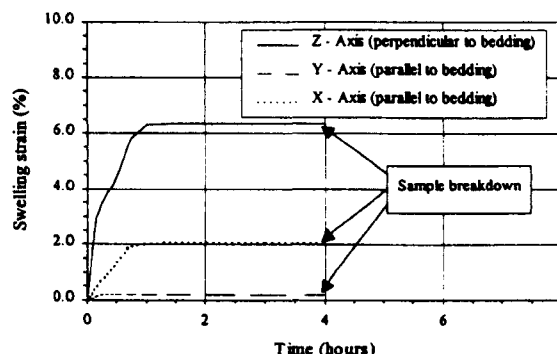


Triaxial swelling test plot

Sample 151

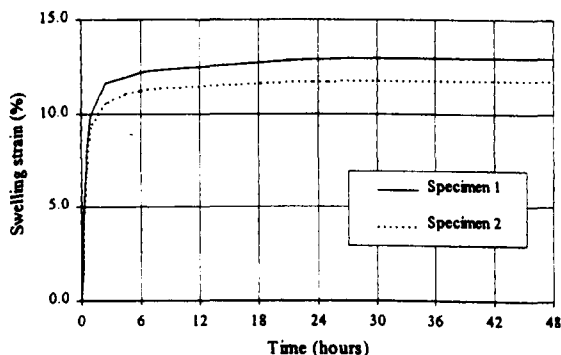


Plot of swelling test on remoulded specimens

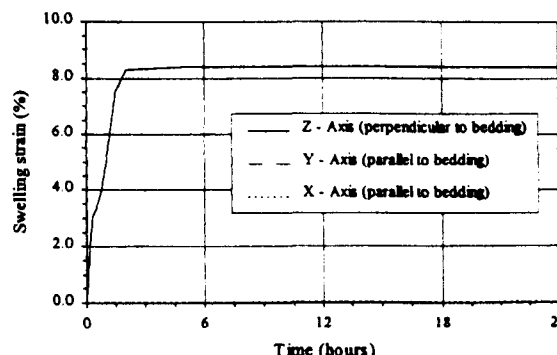


Triaxial swelling test plot

Sample 152

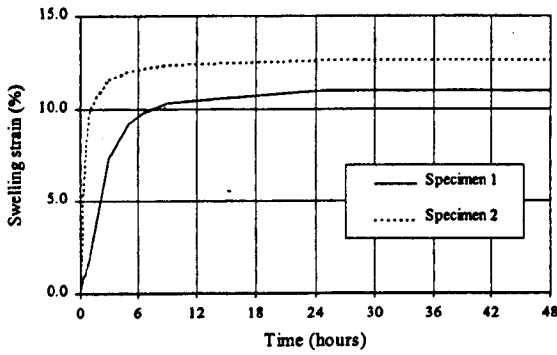


Plot of swelling test on remoulded specimens

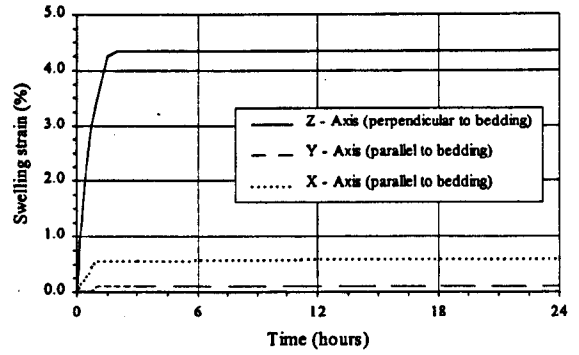


Triaxial swelling test plot

Sample 153

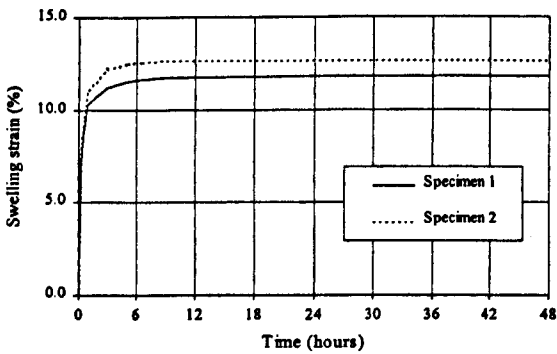


Plot of swelling test on remoulded specimens

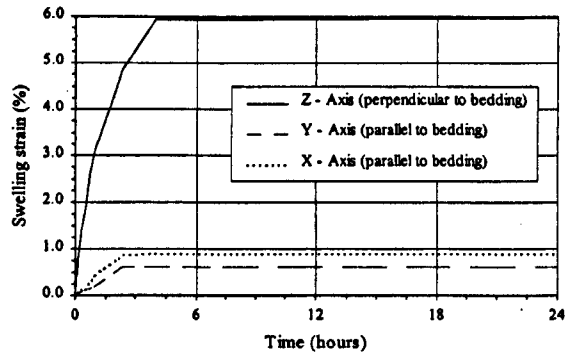


Triaxial swelling test plot

Sample 154

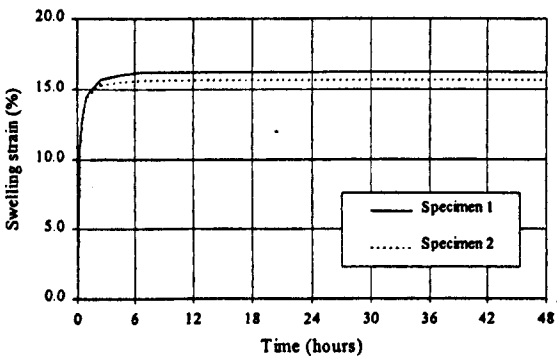


Plot of swelling test on remoulded specimens

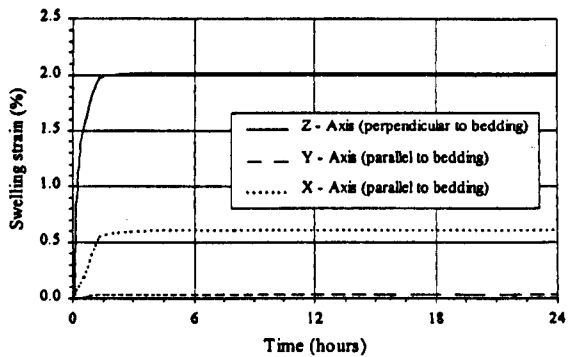


Triaxial swelling test plot

Sample 156

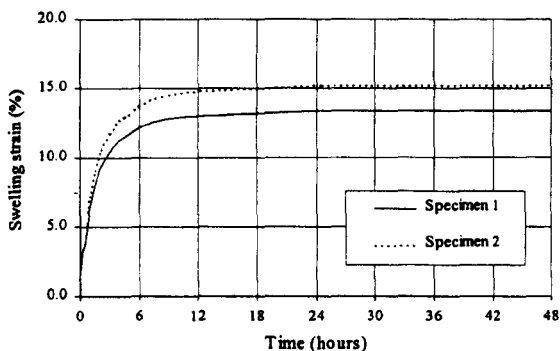


Plot of swelling test on remoulded specimens

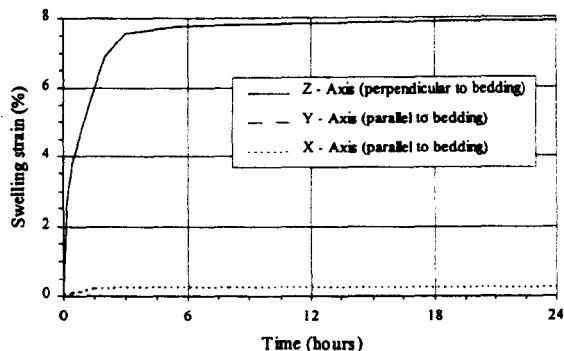


Triaxial swelling test plot

Sample 162

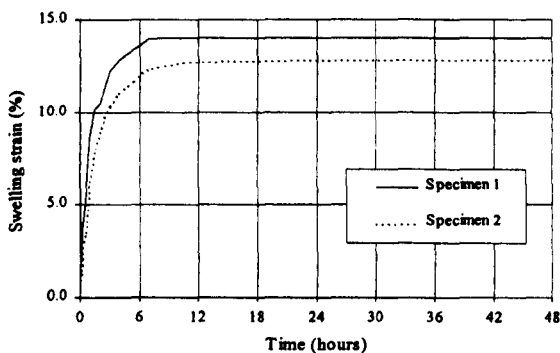


Plot of swelling test on remoulded specimens

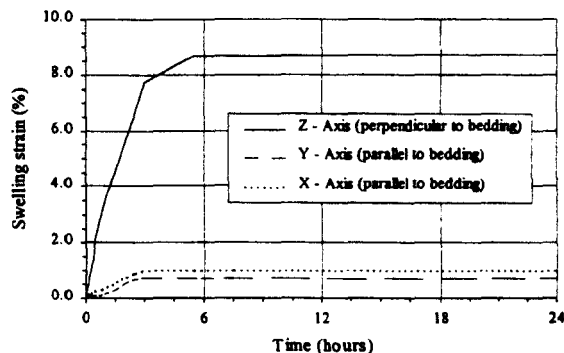


Triaxial swelling test plot

Sample 163

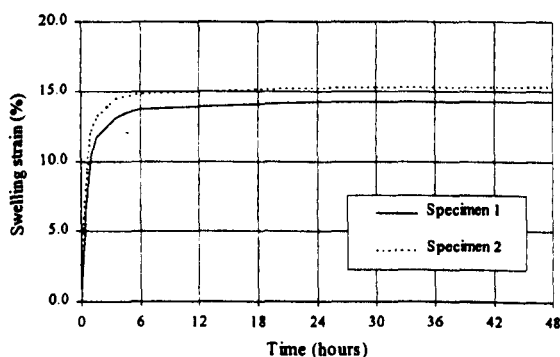


Plot of swelling test on remoulded specimens

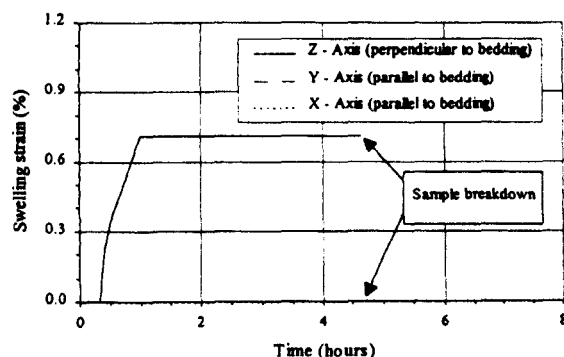


Triaxial swelling test plot

Sample 283

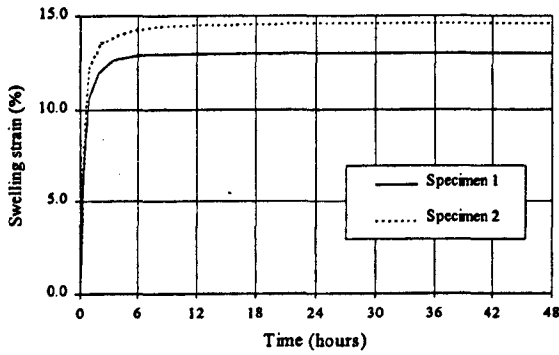


Plot of swelling test on remoulded specimens

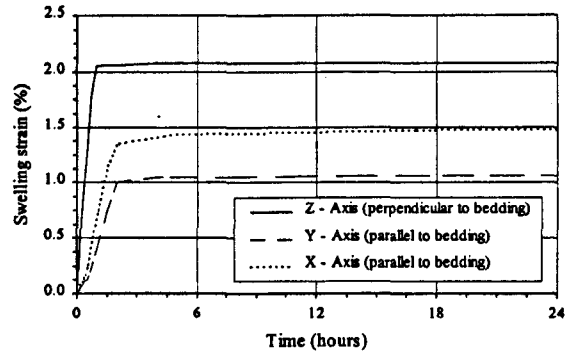


Triaxial swelling test plot

Sample 285

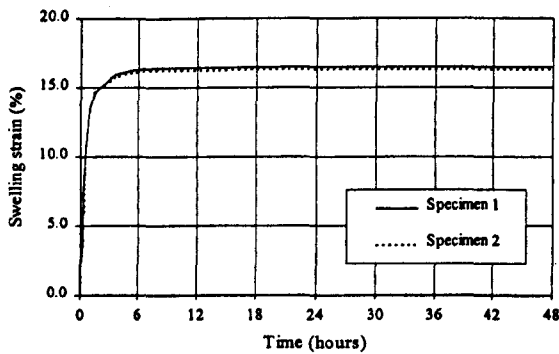


Plot of swelling test on remoulded specimens

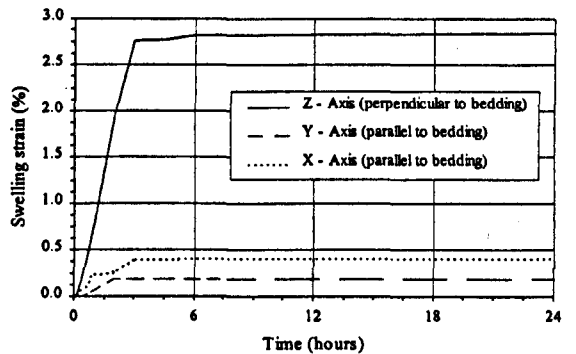


Triaxial swelling test plot

Sample 286

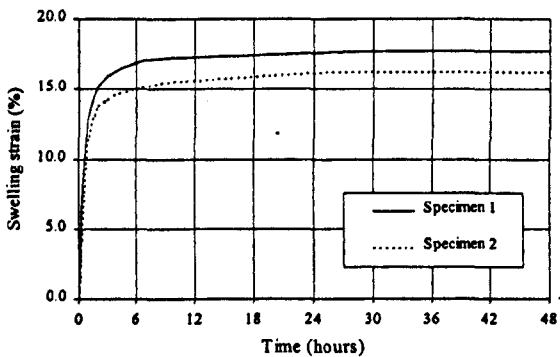


Plot of swelling test on remoulded specimens

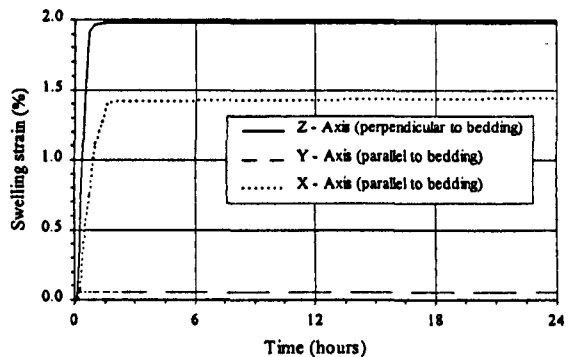


Triaxial swelling test plot

Sample 294

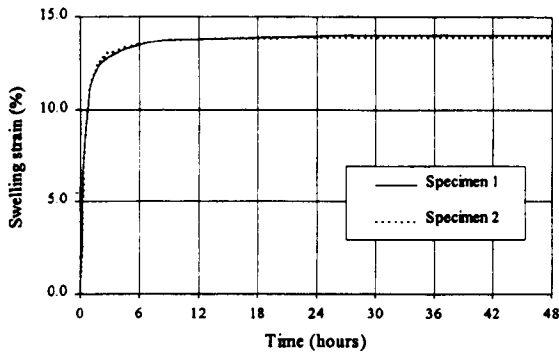


Plot of swelling test on remoulded specimens

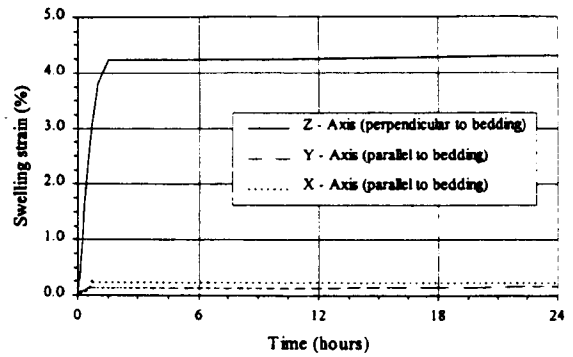


Triaxial swelling test plot

Sample 296

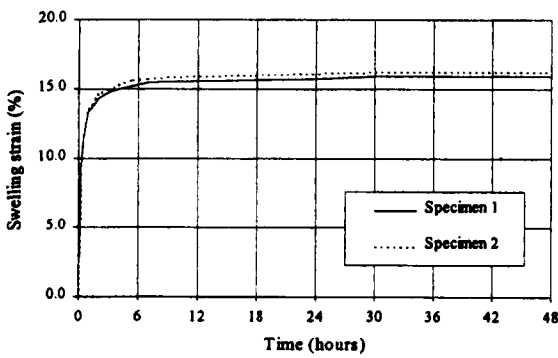


Plot of swelling test on remoulded specimens

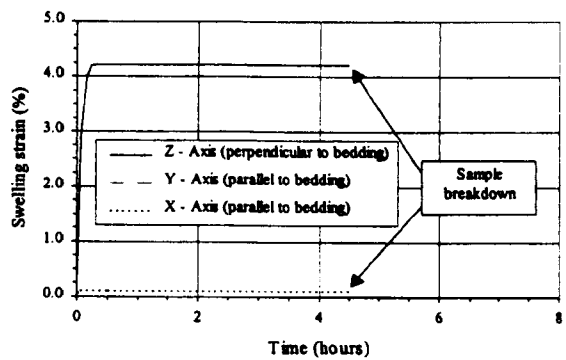


Triaxial swelling test plot

Sample 332

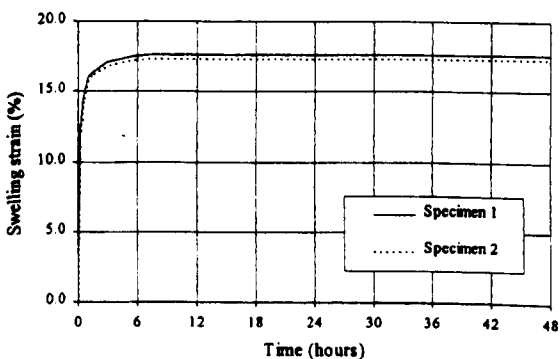


Plot of swelling test on remoulded specimens

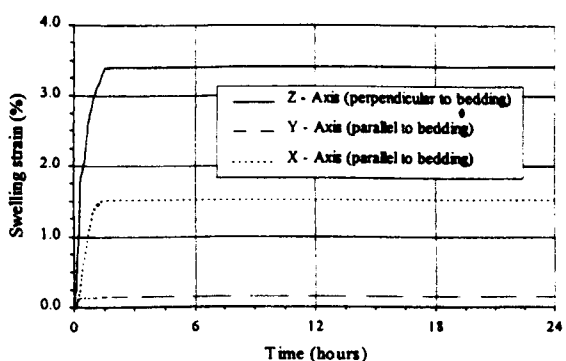


Triaxial swelling test plot

Sample 333

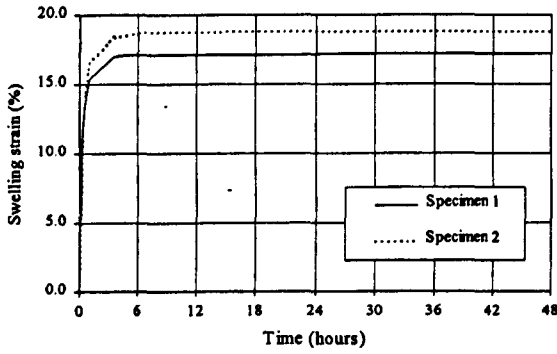


Plot of swelling test on remoulded specimens

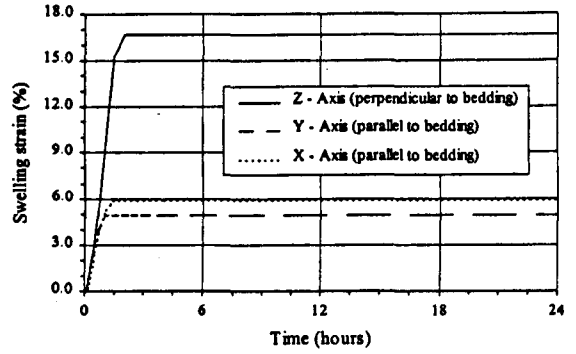


Triaxial swelling test plot

Sample 334

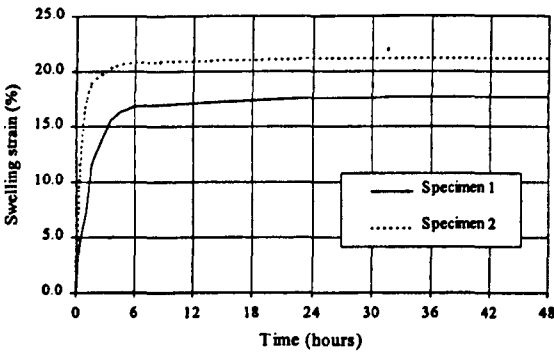


Plot of swelling test on remoulded specimens

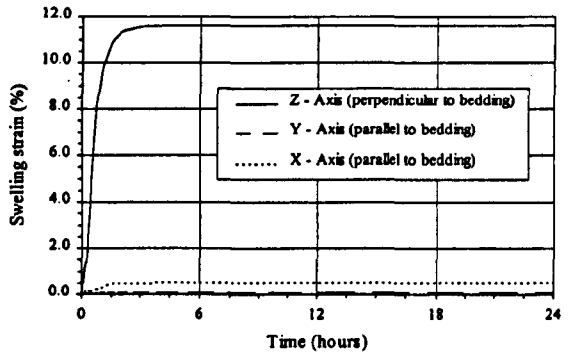


Triaxial swelling test plot

Sample 336

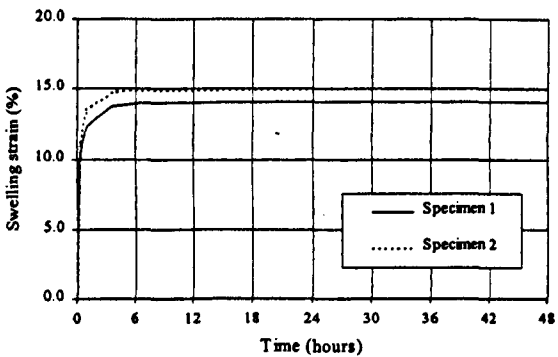


Plot of swelling test on remoulded specimens

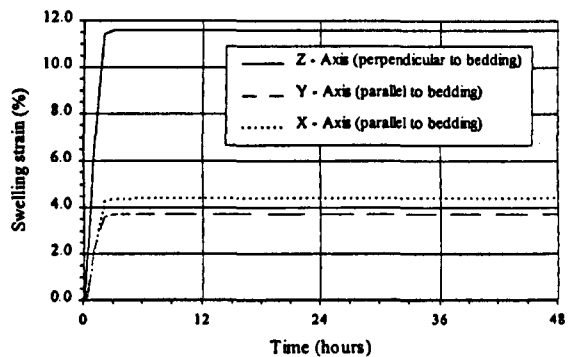


Triaxial swelling test plot

Sample 342

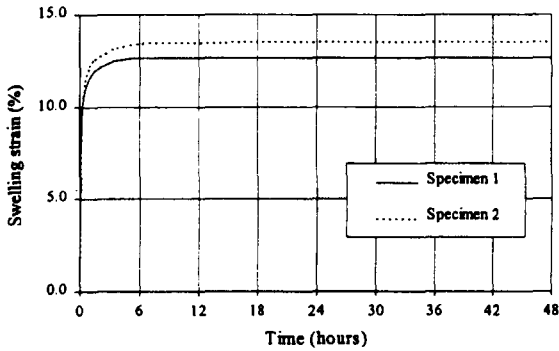


Plot of swelling test on remoulded specimens

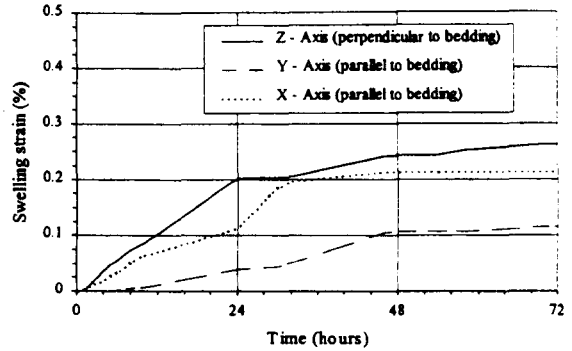


Triaxial swelling test plot

Sample 345

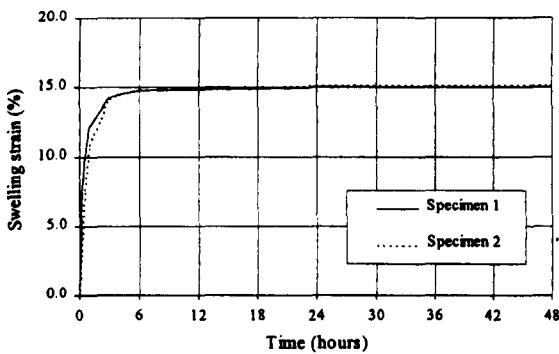


Plot of swelling test on remoulded specimens

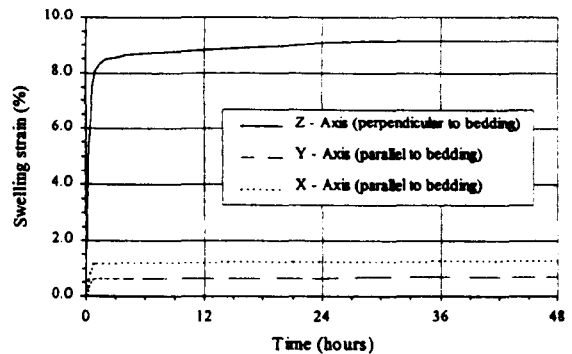


Triaxial swelling test plot

Sample 431

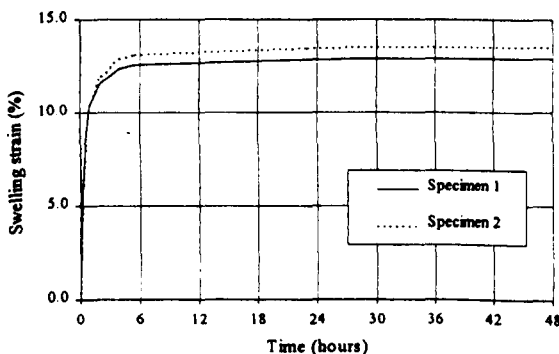


Plot of swelling test on remoulded specimens

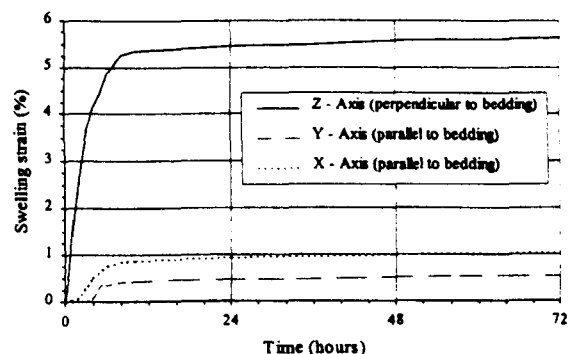


Triaxial swelling test plot

Sample 436

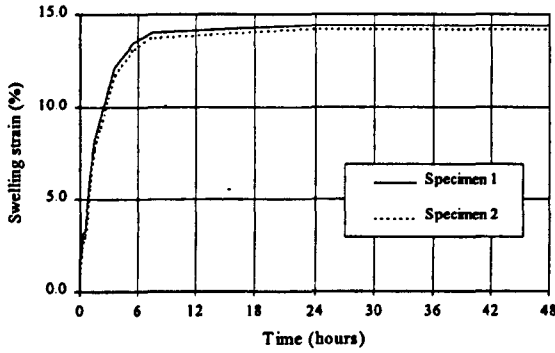


Plot of swelling test on remoulded specimens

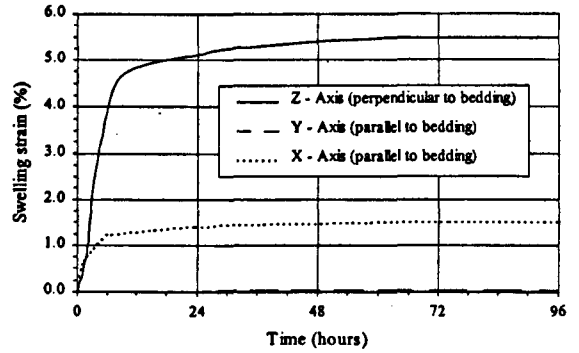


Triaxial swelling test plot

Sample 441

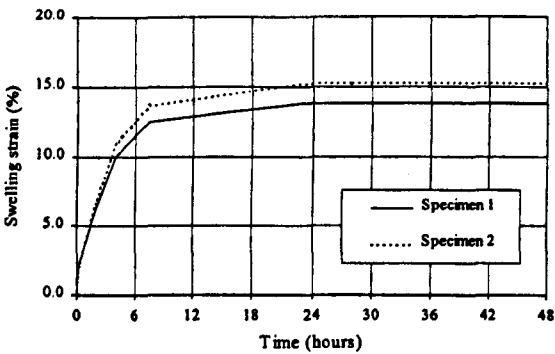


Plot of swelling test on remoulded specimens

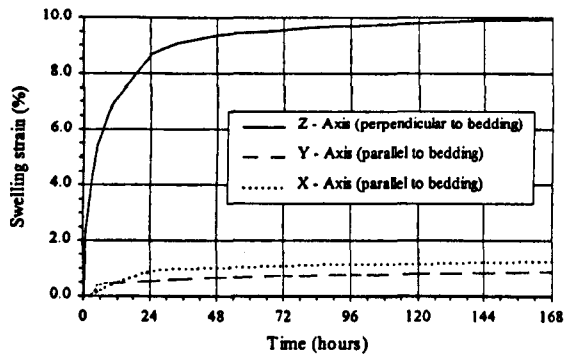


Triaxial swelling test plot

Sample 445

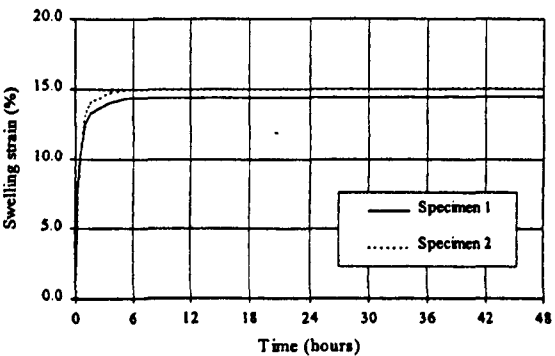


Plot of swelling test on remoulded specimens

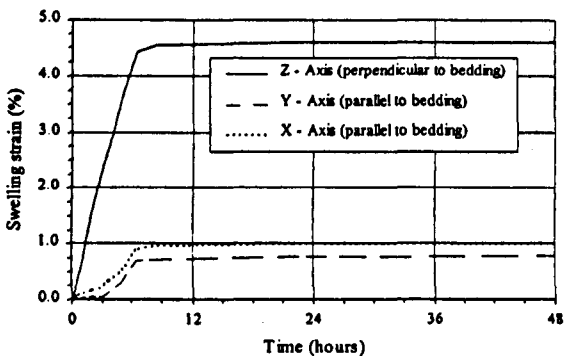


Triaxial swelling test plot

Sample OB1

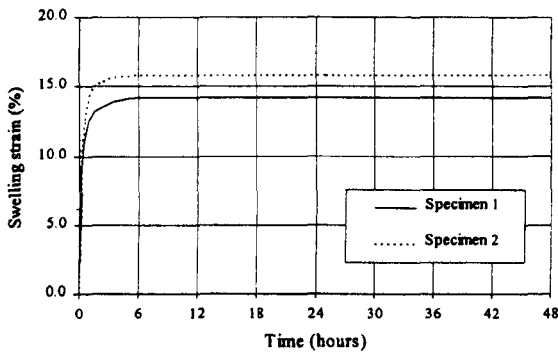


Plot of swelling test on remoulded specimens

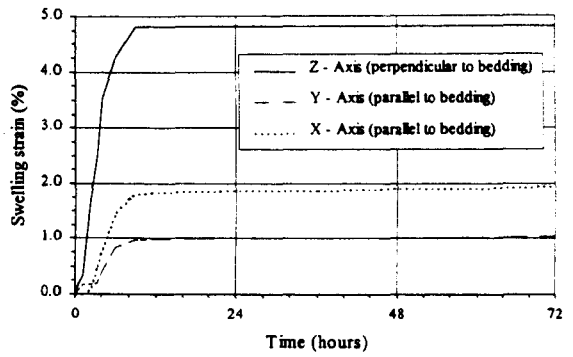


Triaxial swelling test plot

Sample OB2



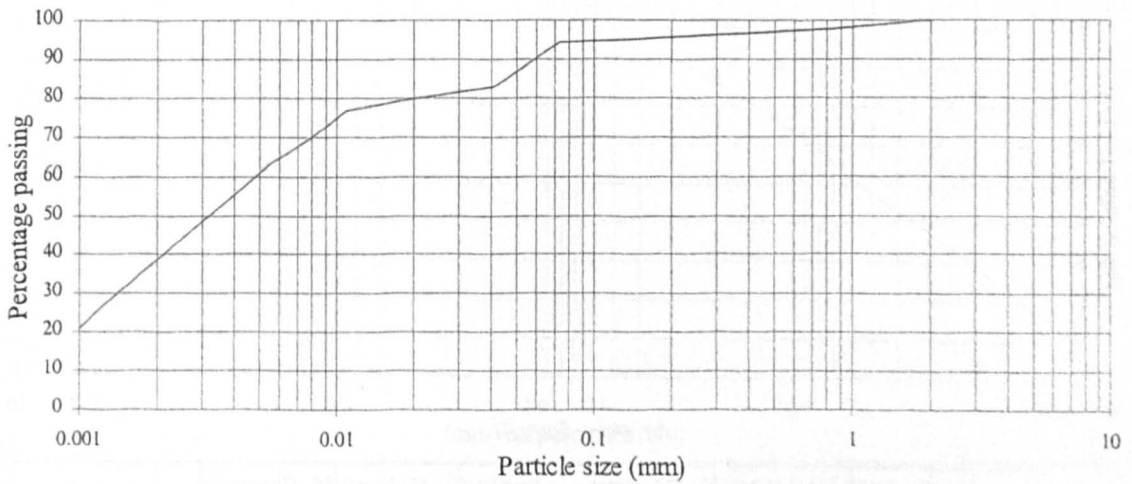
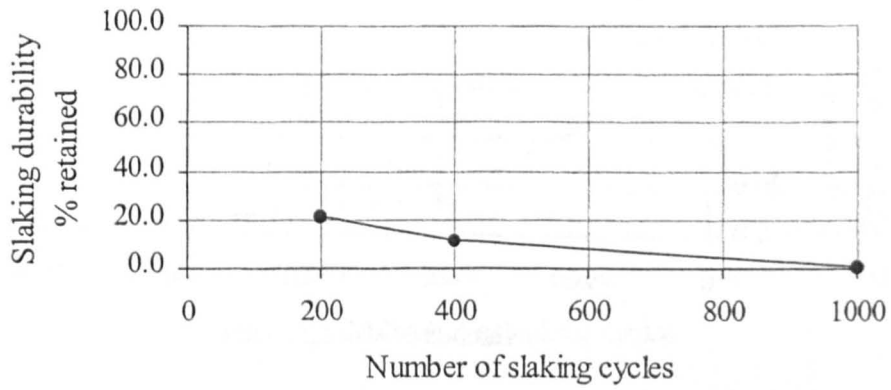
Plot of swelling test on remoulded specimens



Triaxial swelling test plot

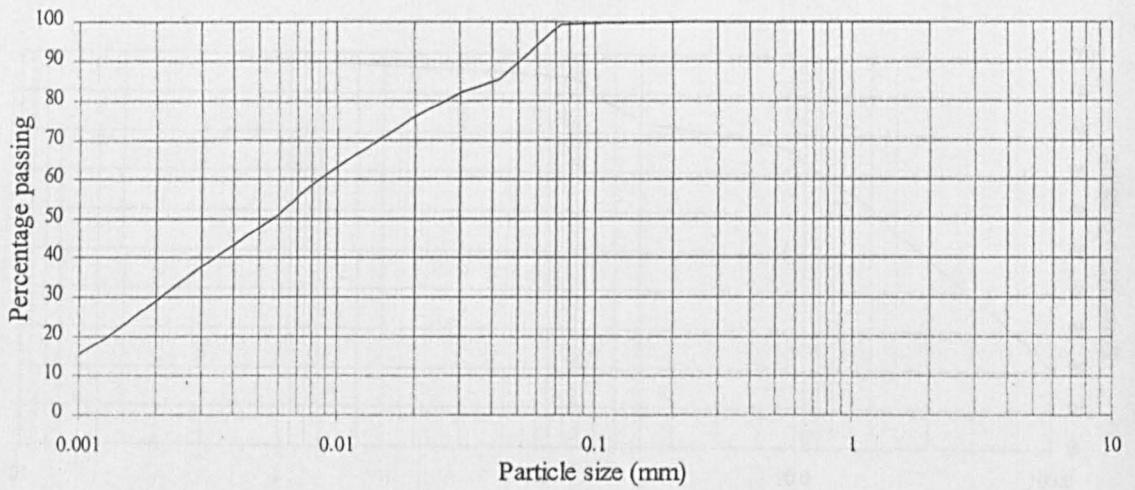
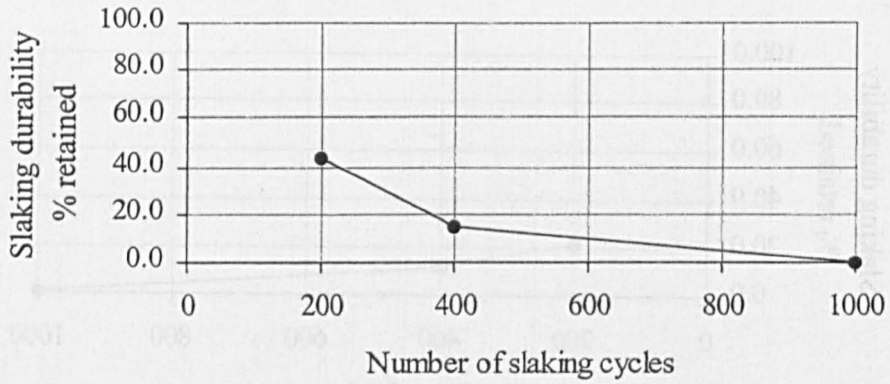
Appendix II.3 - Results for the slake durability tests - Particle size distribution plots and photographic record of the fragments retained in the drum

Sample 51

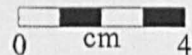


CLAY	Fine	Medium	Coarse	Fine	Medium	Coarse	GRAVEL
	SILT			SAND			

Sample 52

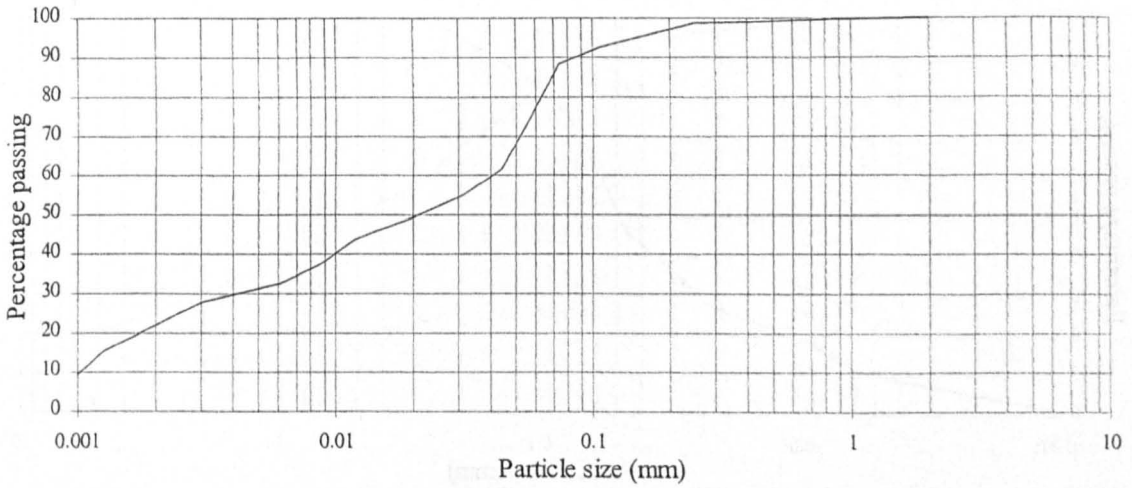
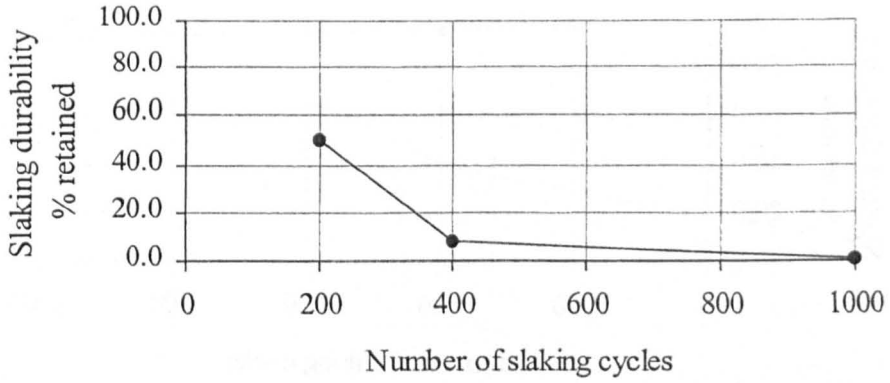


CLAY	Fine	Medium	Coarse	Fine	Medium	Coarse	GRAVEL
	SILT			SAND			



Remainder from slake durability testing after 1,000 rotations.

Sample 81

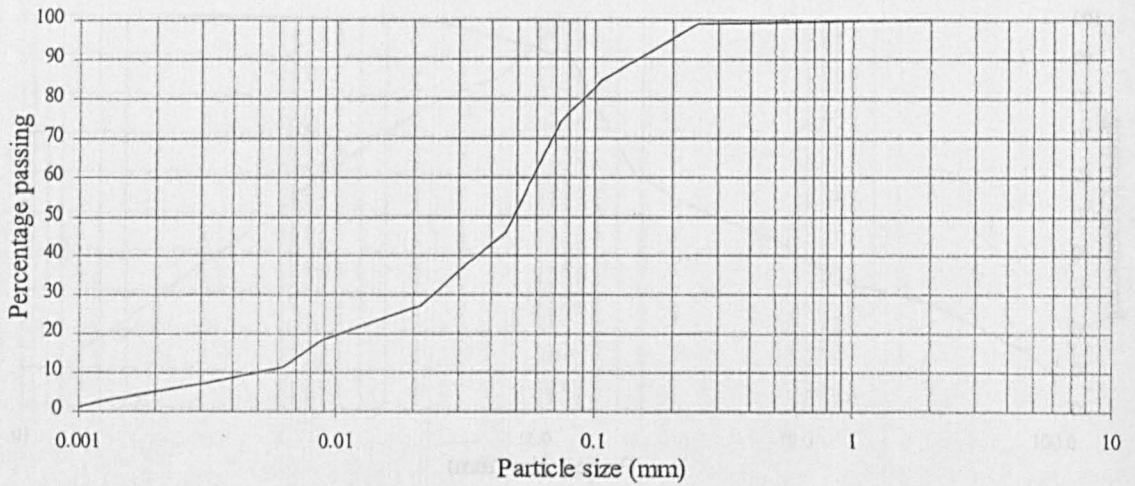
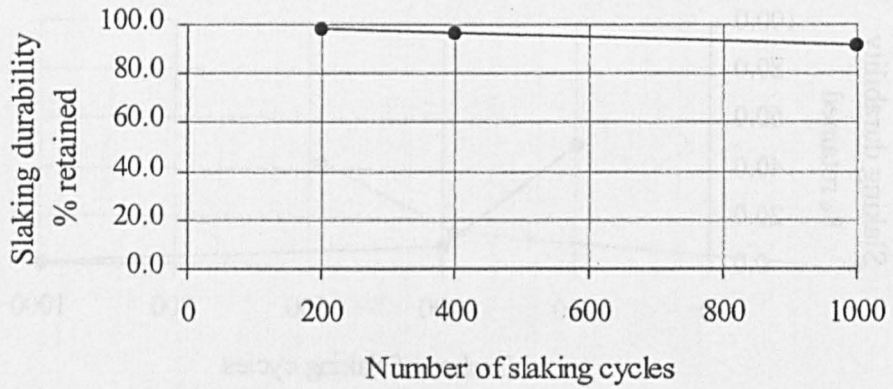


CLAY	Fine	Medium	Coarse	Fine	Medium	Coarse	GRAVEL
	SILT			SAND			



Remainder from slake durability testing after 1,000 rotations.

Sample 83

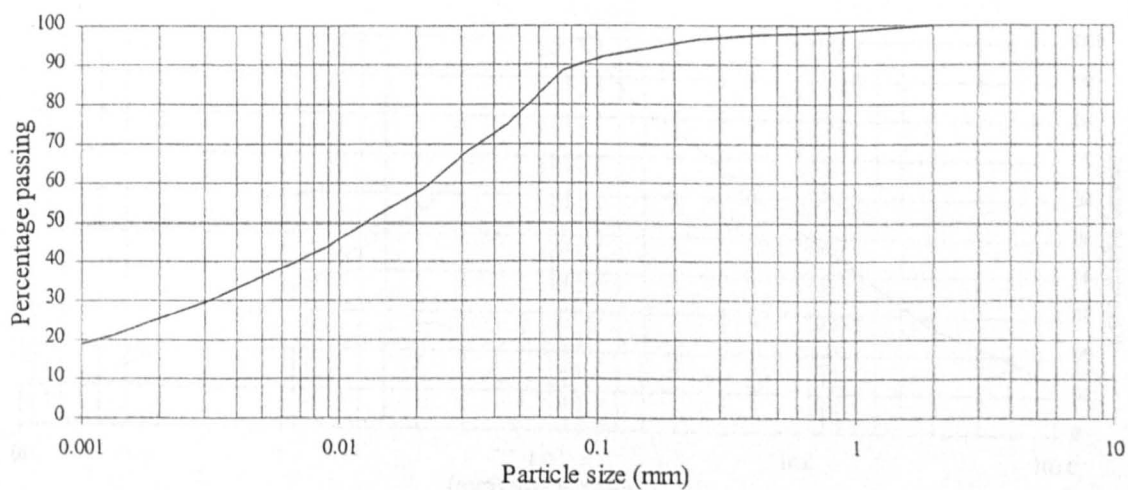
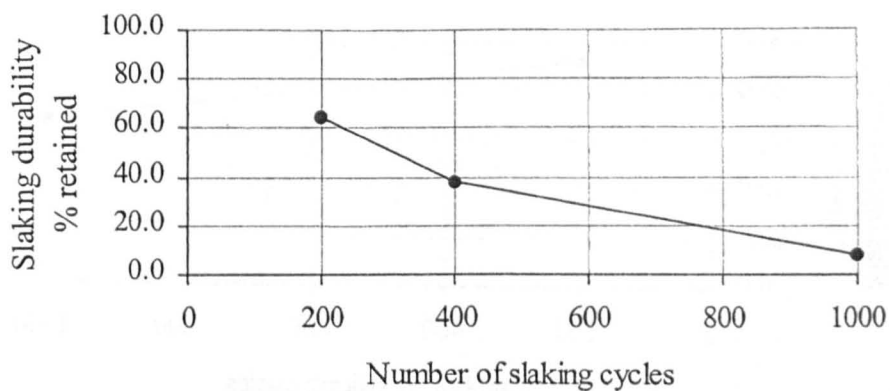


CLAY	Fine	Medium	Coarse	Fine	Medium	Coarse	GRAVEL
	SILT			SAND			

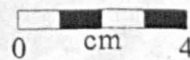


Remainder from slake durability testing after 1,000 rotations.

Sample 111

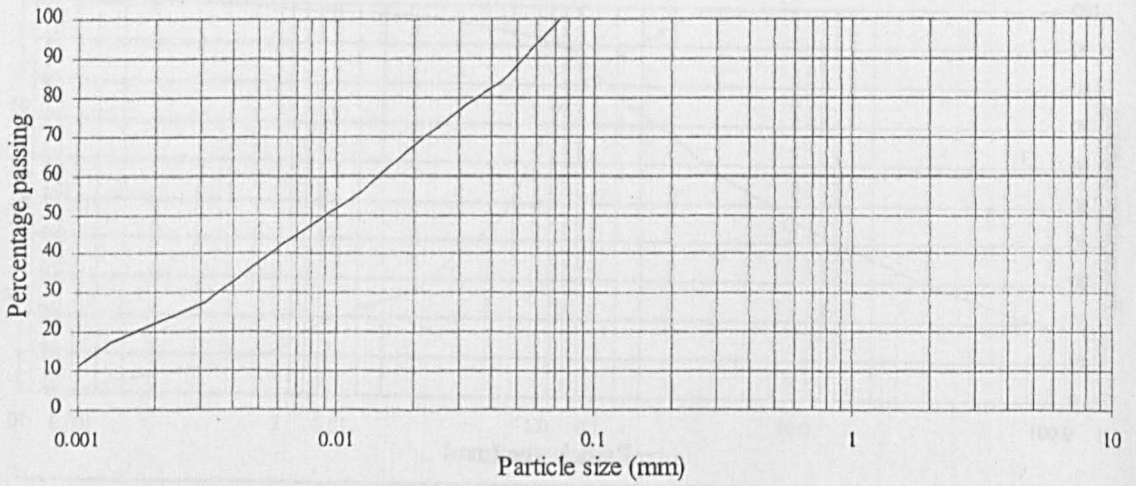
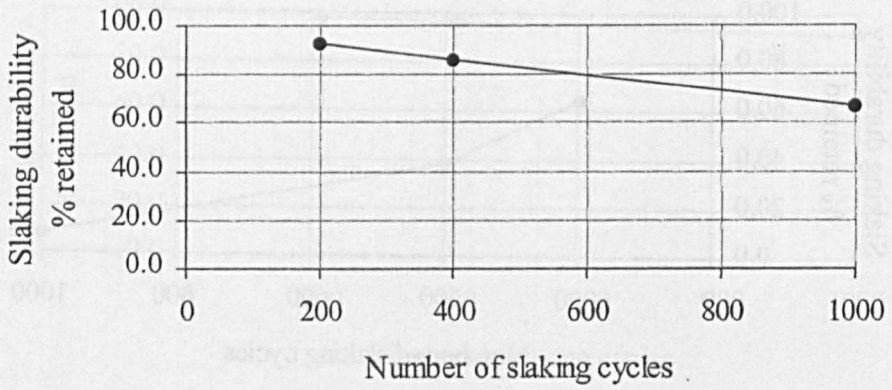


CLAY	Fine	Medium	Coarse	Fine	Medium	Coarse	GRAVEL
	SILT			SAND			



Remainder from slake durability testing after 1,000 rotations.

Sample 112

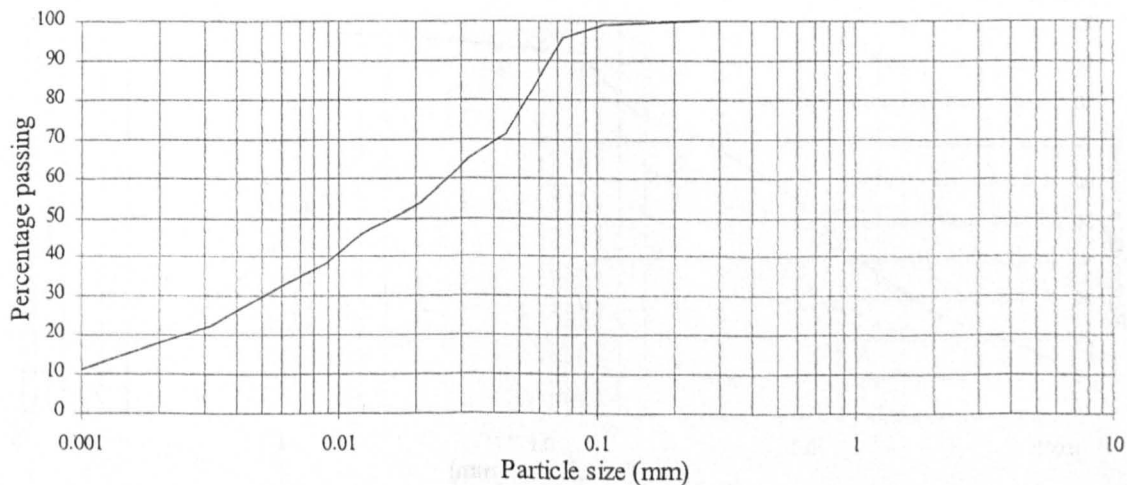
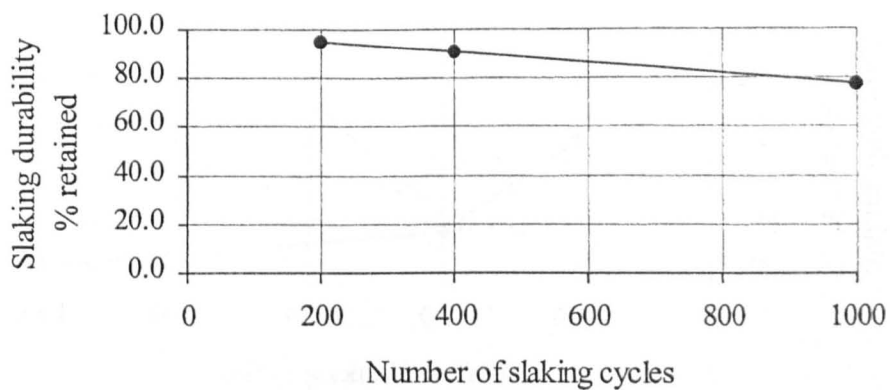


CLAY	Fine	Medium	Coarse	Fine	Medium	Coarse	GRAVEL
	SILT			SAND			



Remainder from slake durability testing after 1,000 rotations.

Sample 114

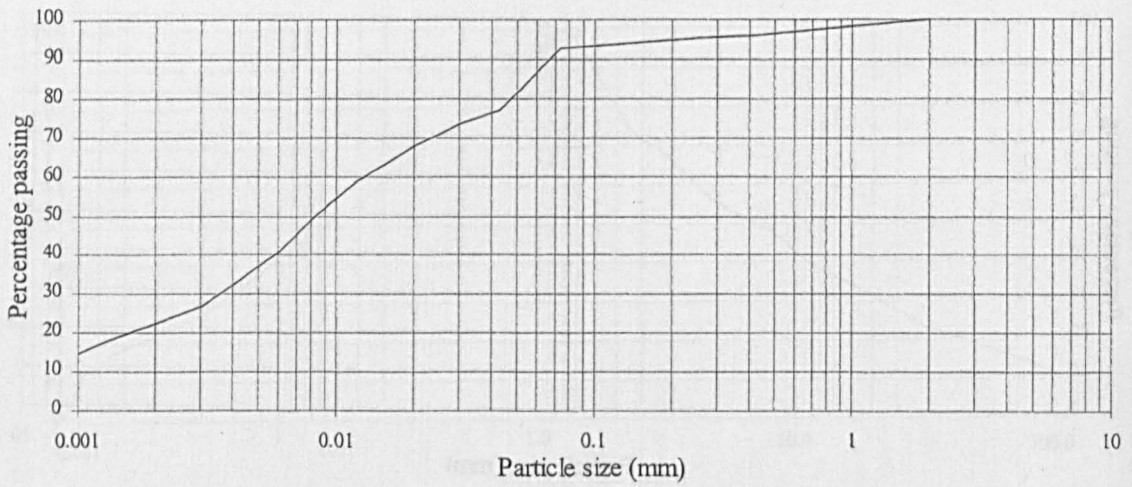
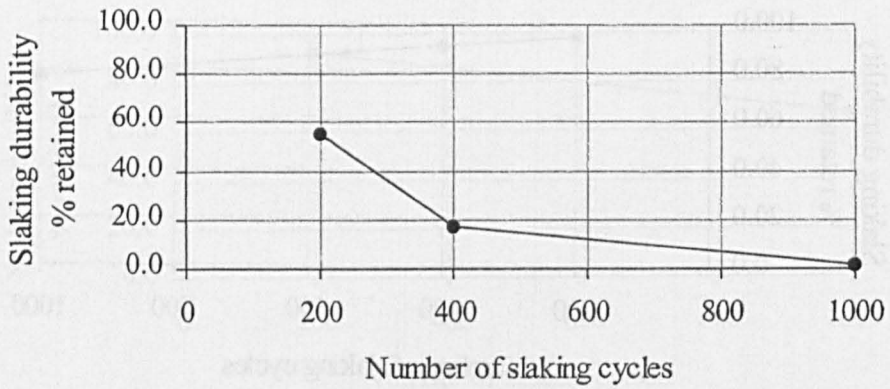


CLAY	Fine	Medium	Coarse	Fine	Medium	Coarse	GRAVEL
	SILT			SAND			

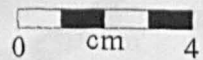
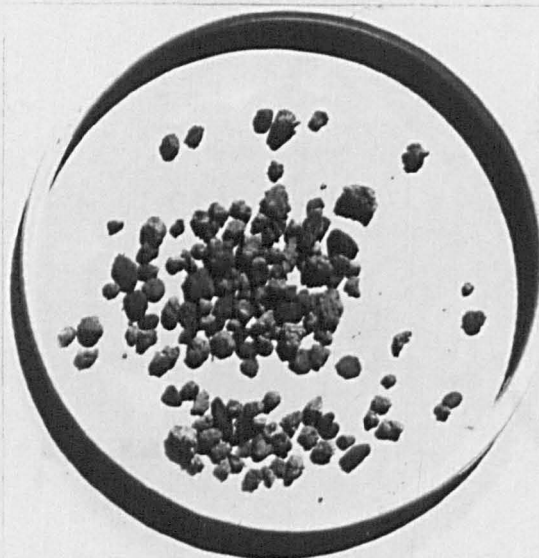


Remainder from slake durability testing after 1,000 rotations.

Sample 151

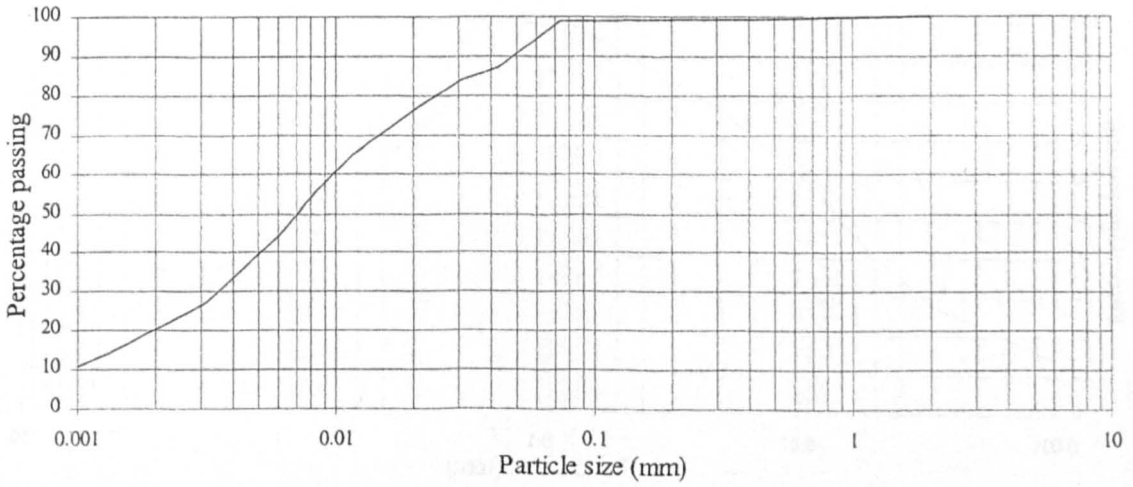
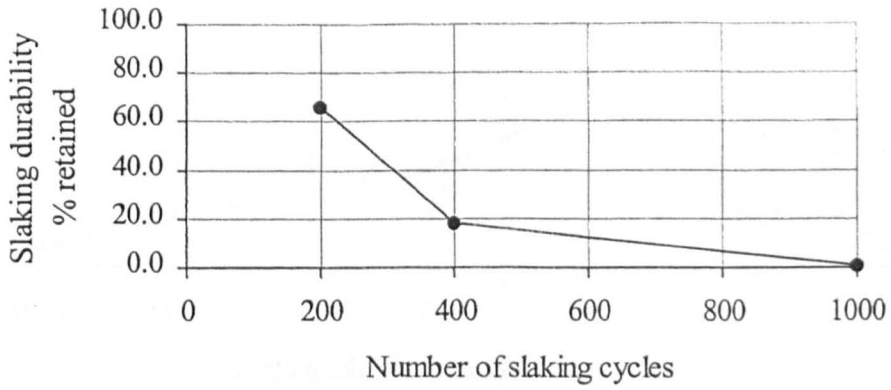


CLAY	Fine	Medium	Coarse	Fine	Medium	Coarse	GRAVEL
	SILT			SAND			

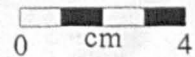
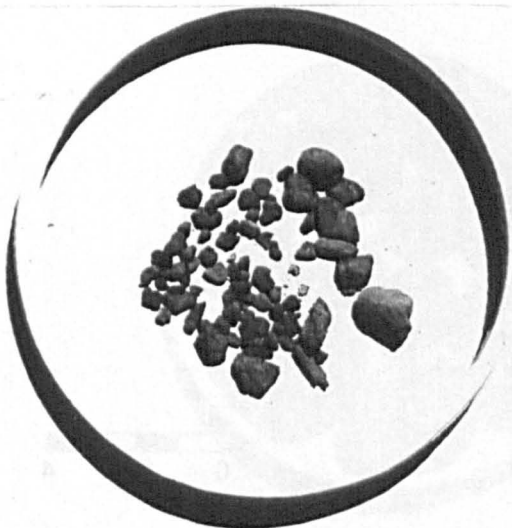


Remainder from slake durability testing after 1,000 rotations.

Sample 152

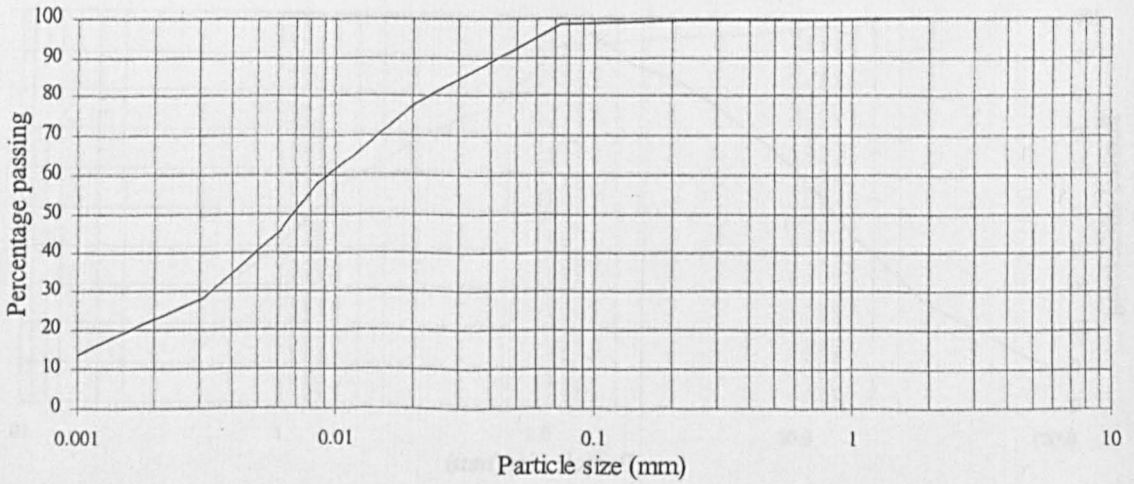
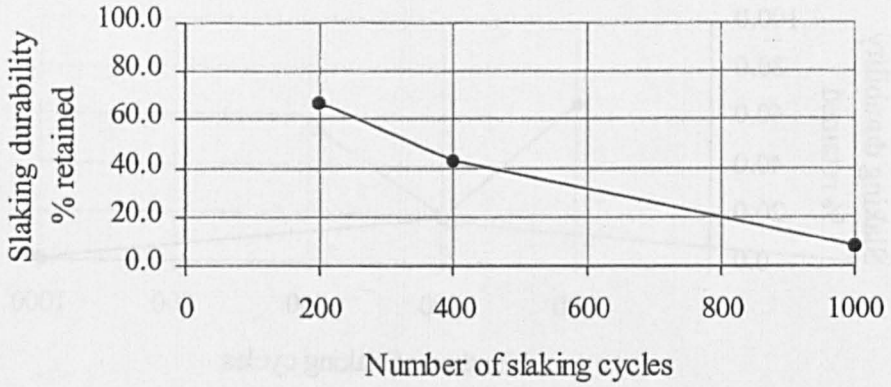


CLAY	Fine	Medium	Coarse	Fine	Medium	Coarse	GRAVEL
	SILT			SAND			

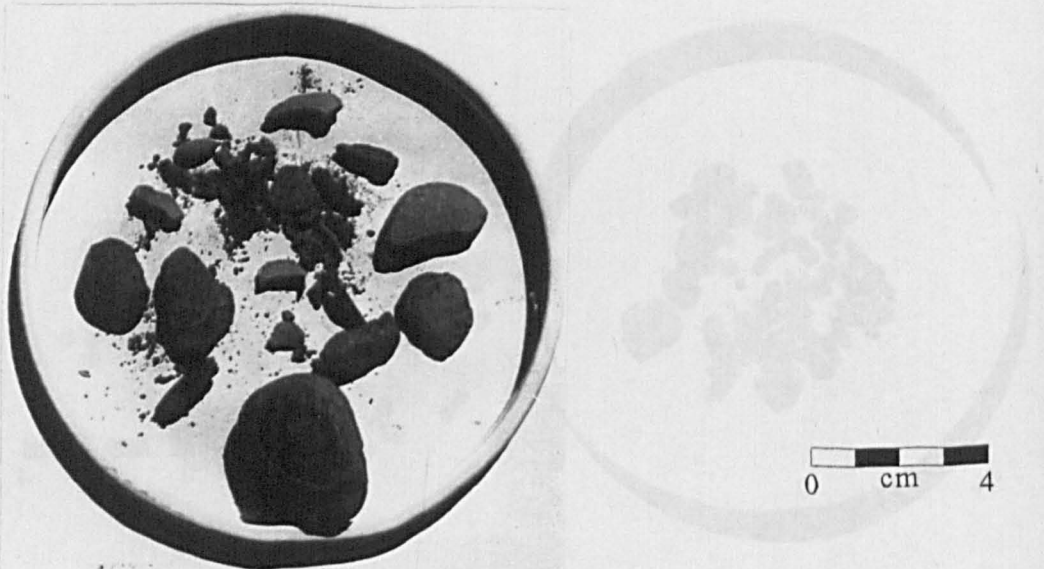


Remainder from slake durability testing after 1,000 rotations.

Sample 153

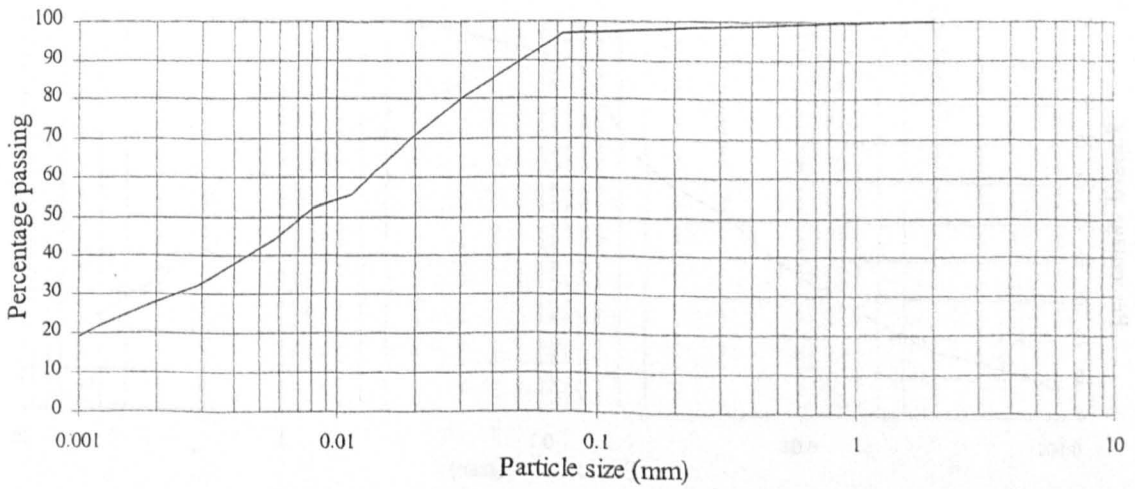
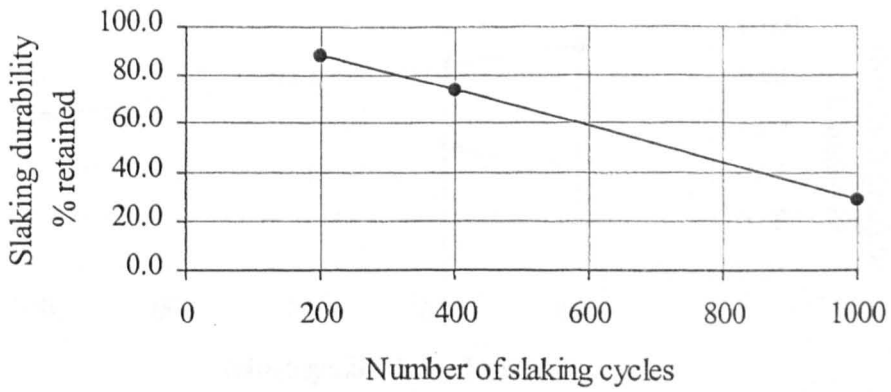


CLAY	Fine	Medium	Coarse	Fine	Medium	Coarse	GRAVEL
	SILT			SAND			

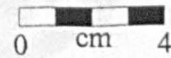
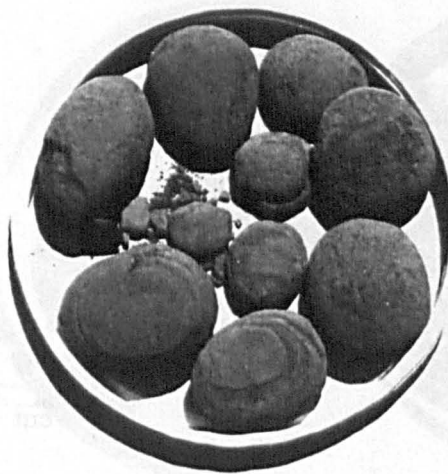


Remainder from slake durability testing after 1,000 rotations.

Sample 154

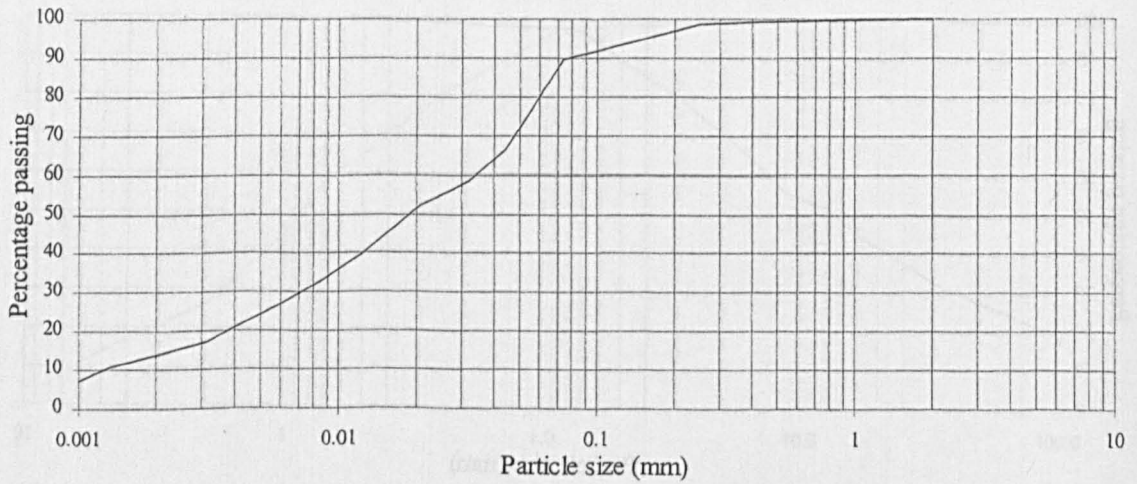
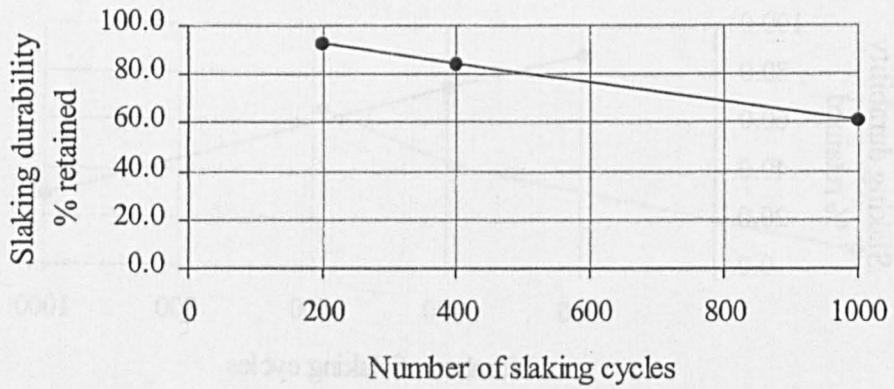


CLAY	Fine	Medium	Coarse	Fine	Medium	Coarse	GRAVEL
	SILT			SAND			

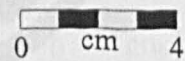
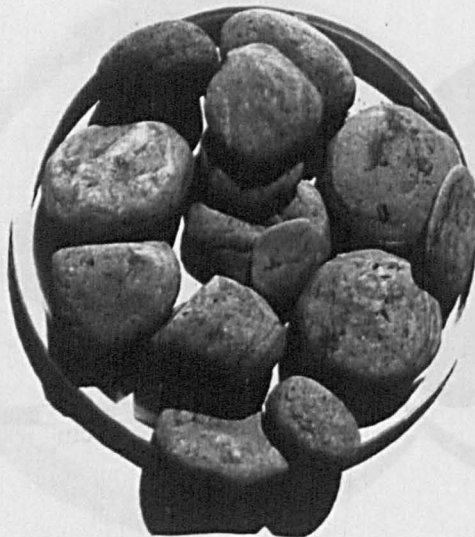


Remainder from slake durability testing after 1,000 rotations.

Sample 156

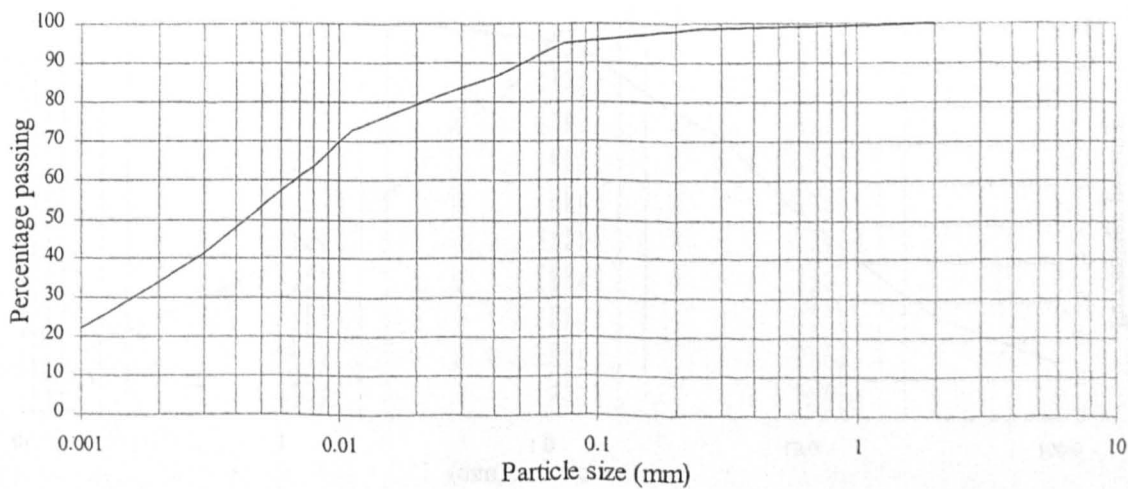
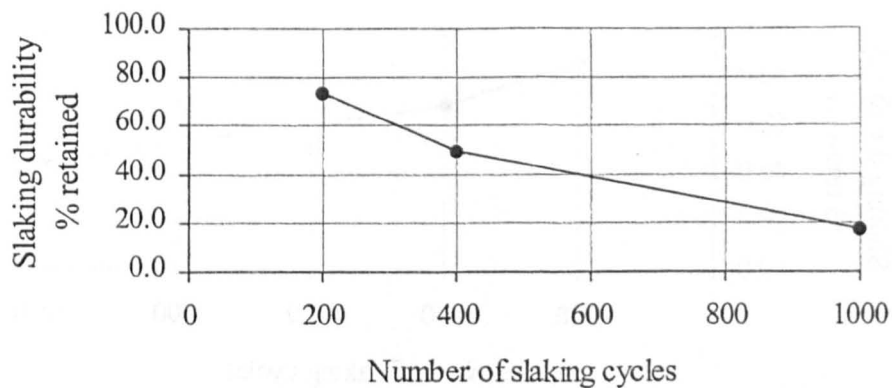


CLAY	Fine	Medium	Coarse	Fine	Medium	Coarse	GRAVEL
	SILT			SAND			

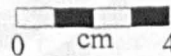


Remainder from slake durability testing after 1,000 rotations.

Sample 162

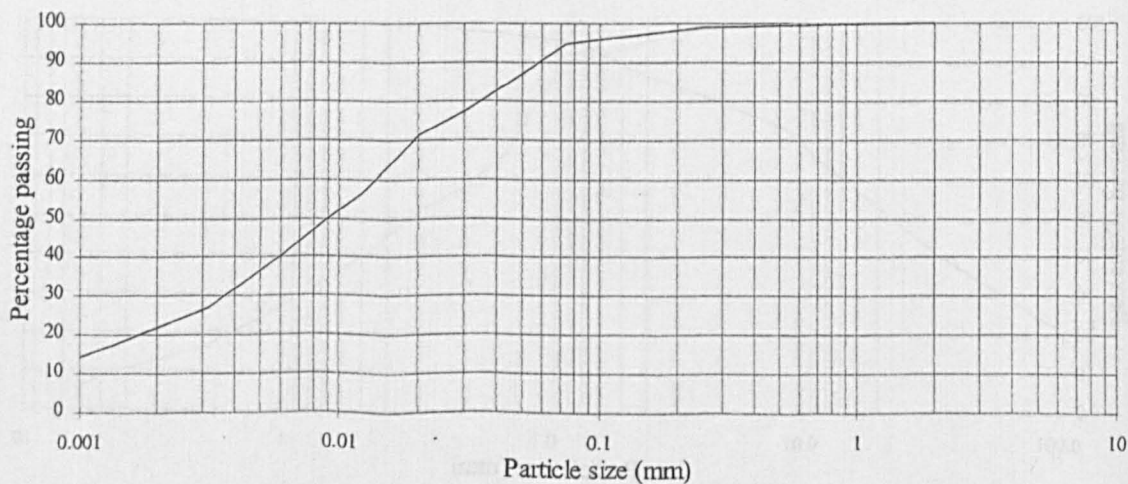
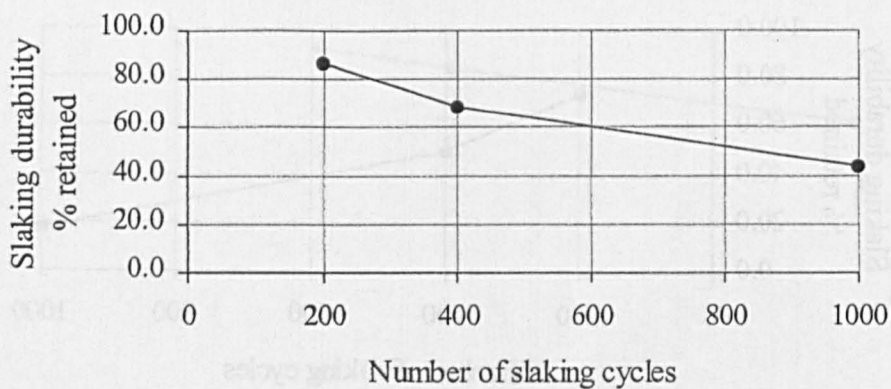


CLAY	Fine	Medium	Coarse	Fine	Medium	Coarse	GRAVEL
	SILT			SAND			

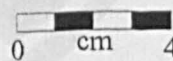
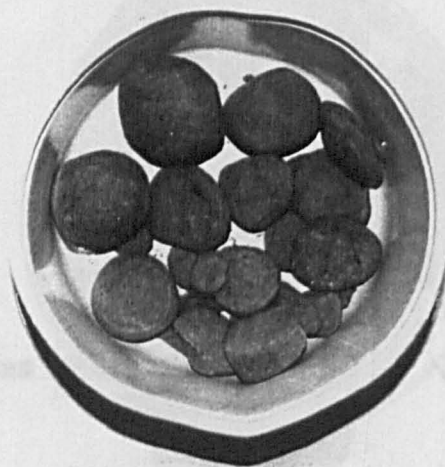


Remainder from slake durability testing after 1,000 rotations.

Sample 163

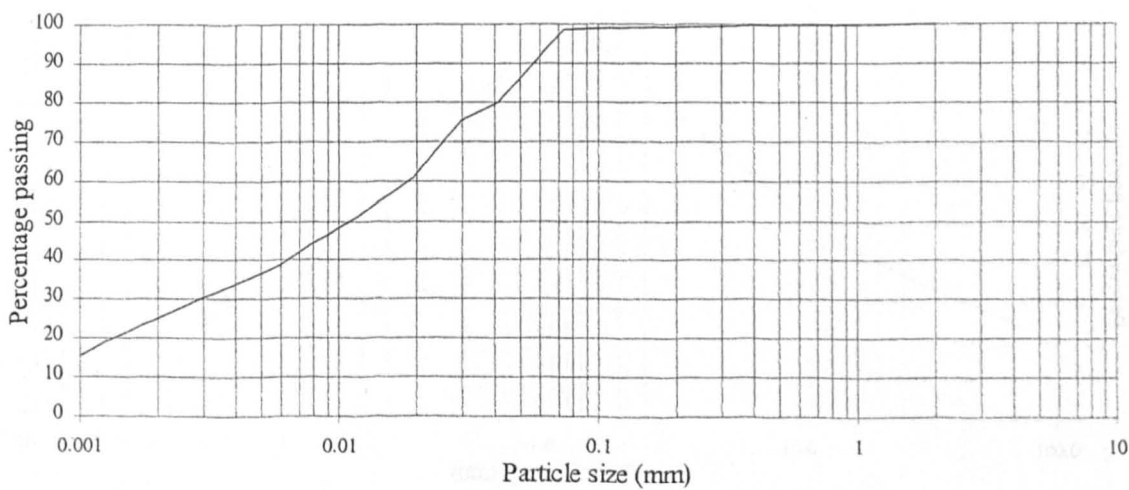
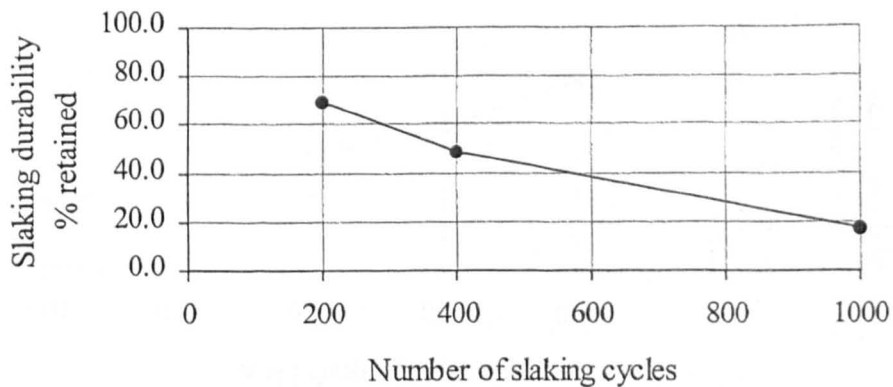


CLAY	Fine	Medium	Coarse	Fine	Medium	Coarse	GRAVEL
	SILT			SAND			

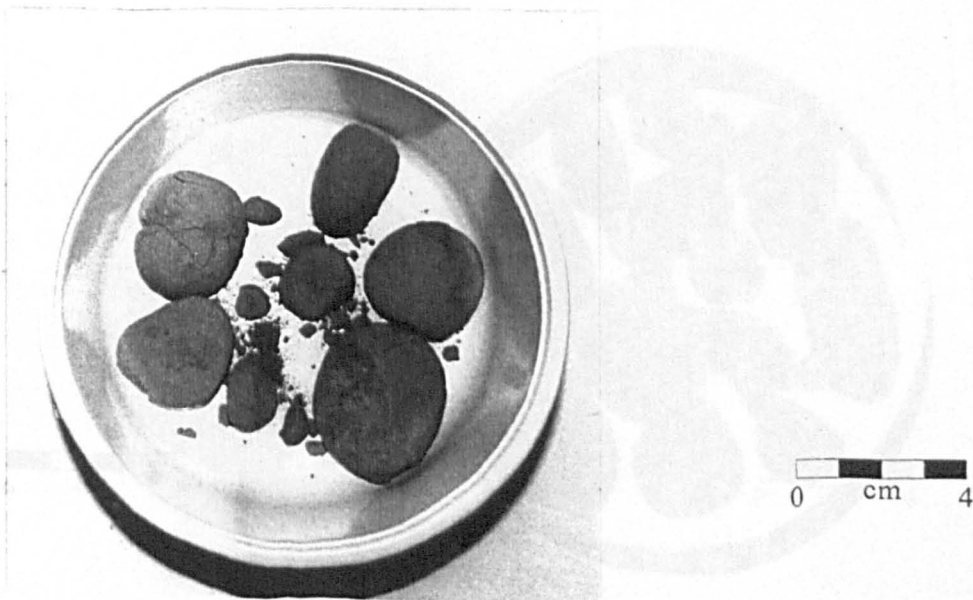


Remainder from slake durability testing after 1,000 rotations.

Sample 283

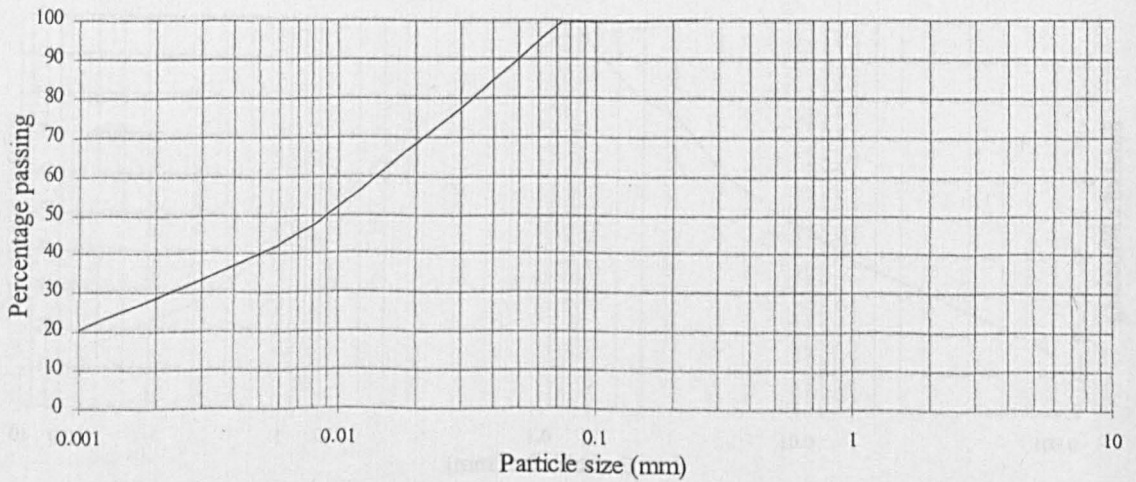
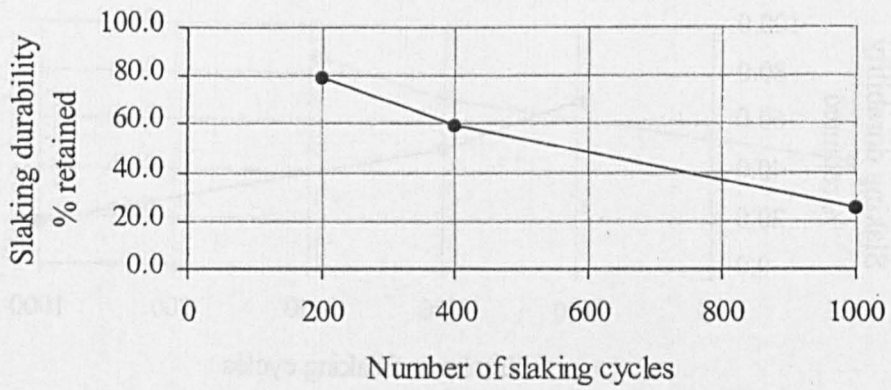


CLAY	Fine	Medium	Coarse	Fine	Medium	Coarse	GRAVEL
	SILT			SAND			

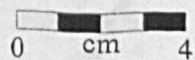
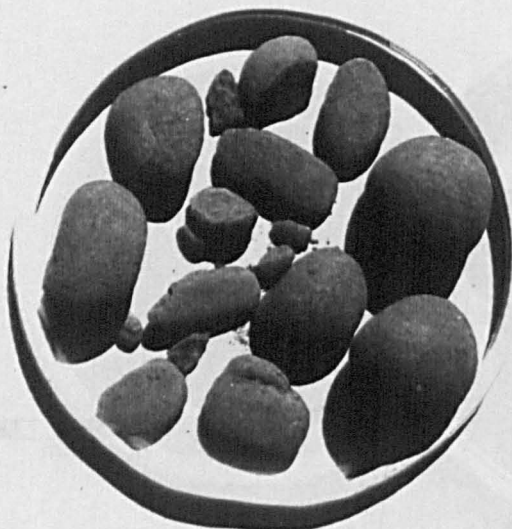


Remainder from slake durability testing after 1,000 rotations.

Sample 285

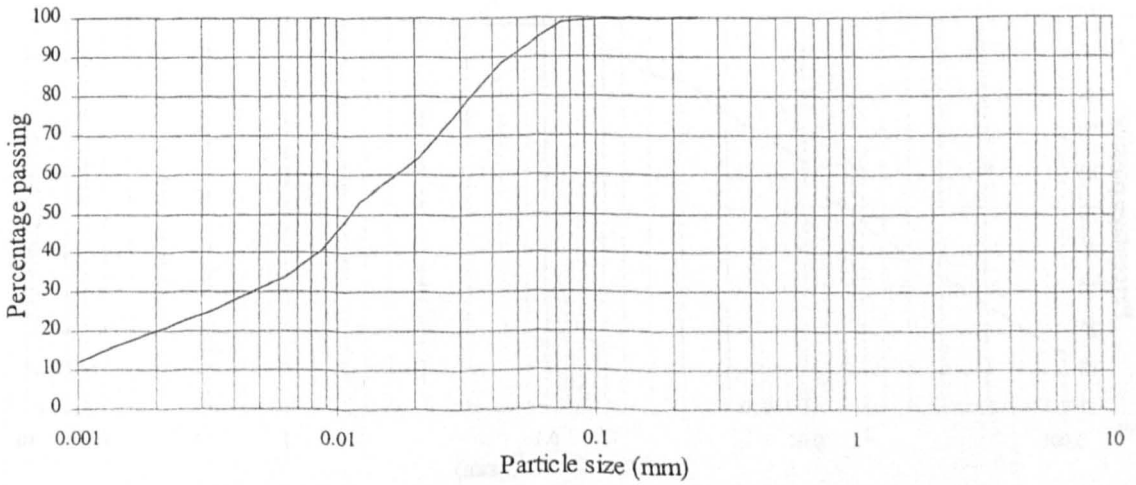
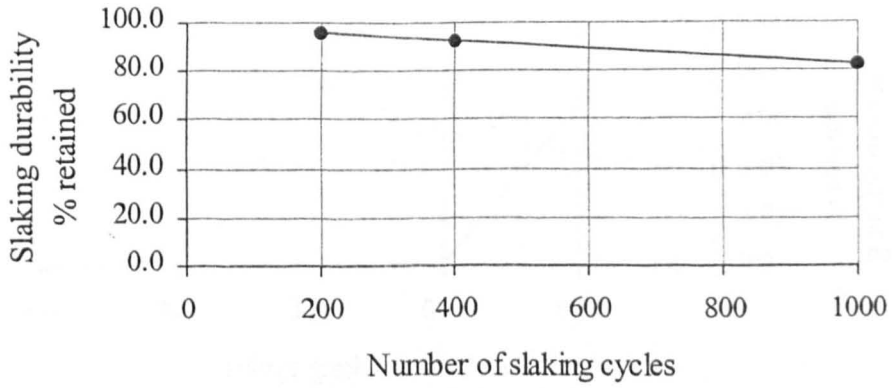


CLAY	Fine	Medium	Coarse	Fine	Medium	Coarse	GRAVEL
	SILT			SAND			

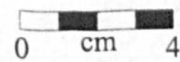


Remainder from slake durability testing after 1,000 rotations.

Sample 286

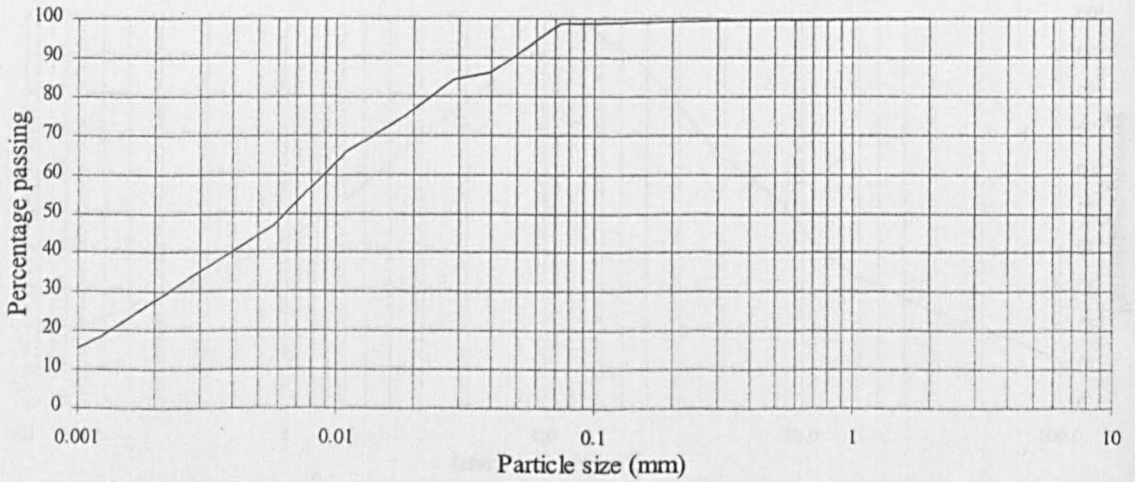
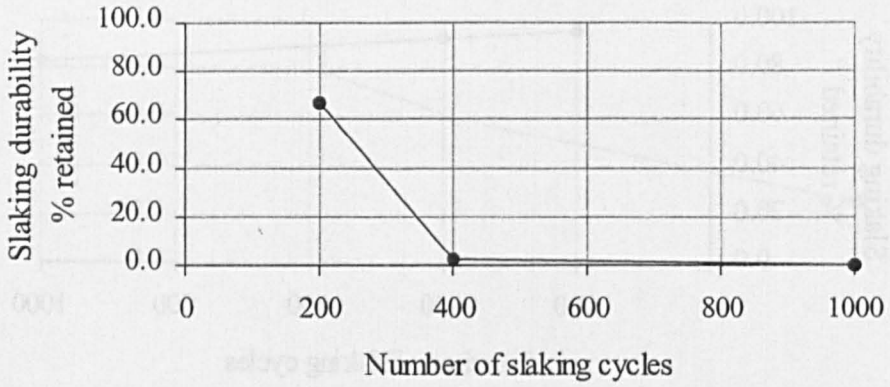


CLAY	Fine	Medium	Coarse	Fine	Medium	Coarse	GRAVEL
	SILT			SAND			



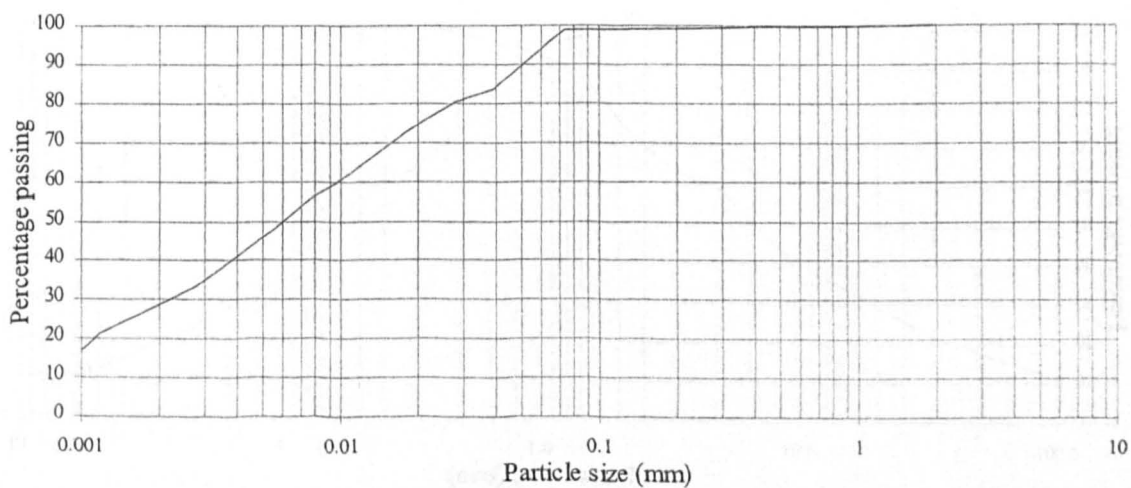
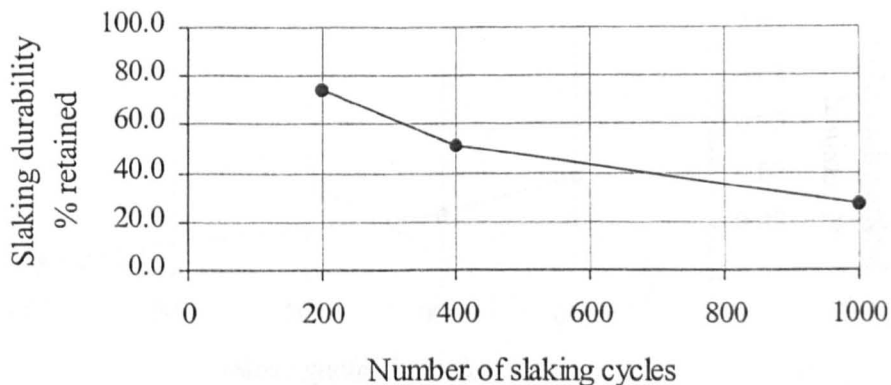
Remainder from slake durability testing after 1,000 rotations.

Sample 294

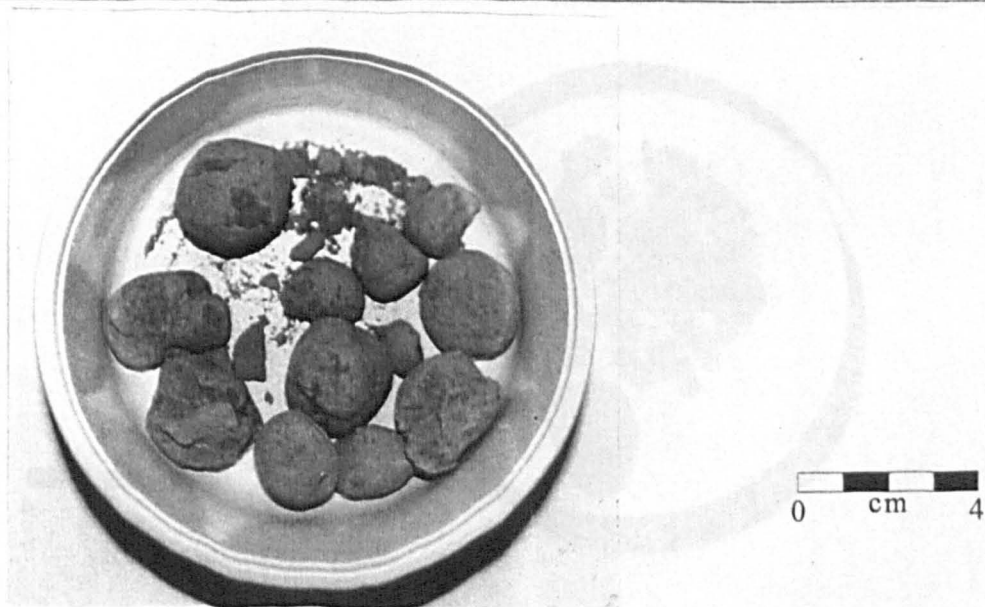


CLAY	Fine	Medium	Coarse	Fine	Medium	Coarse	GRAVEL
	SILT			SAND			

Sample 296

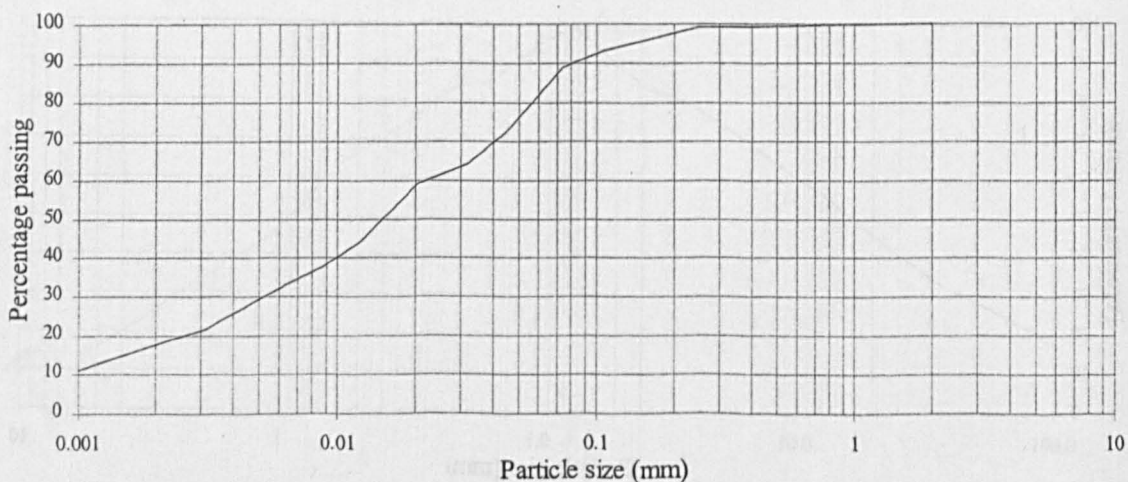
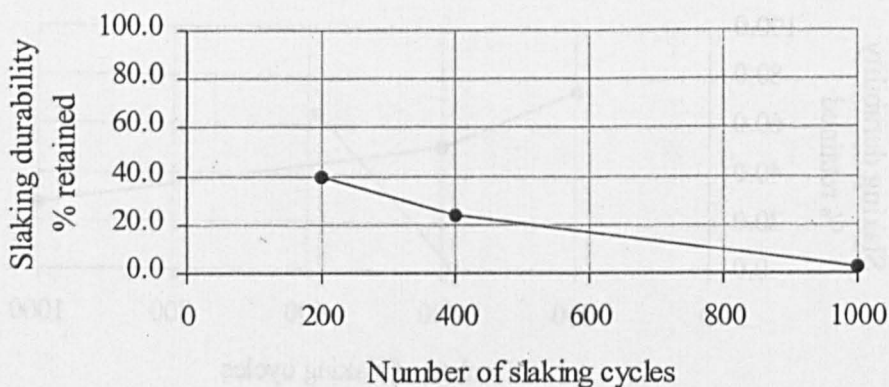


CLAY	Fine	Medium	Coarse	Fine	Medium	Coarse	GRAVEL
	SILT			SAND			

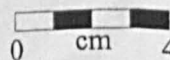
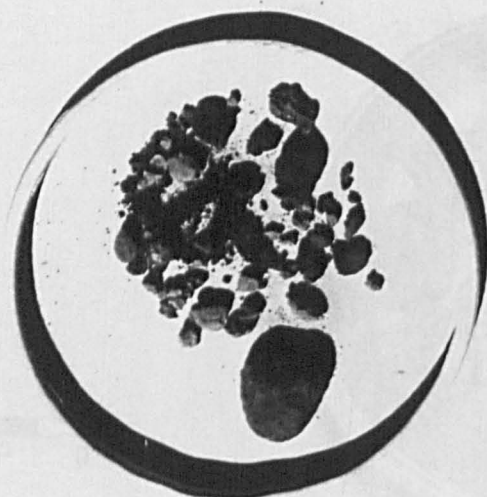


Remainder from slake durability testing after 1,000 rotations.

Sample 332

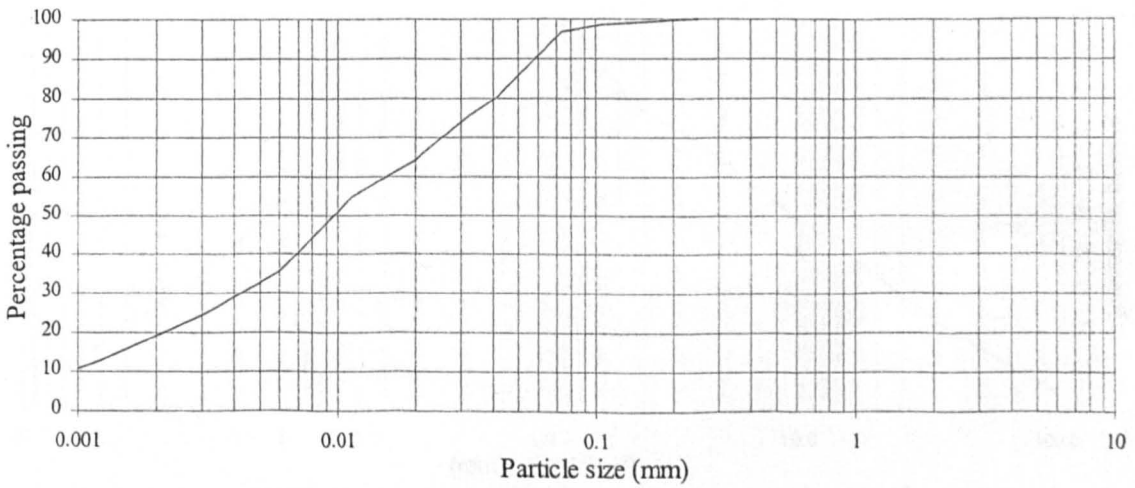
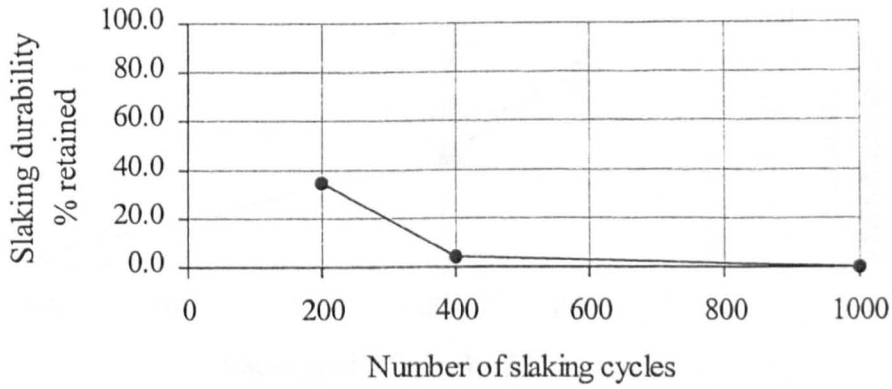


CLAY	Fine	Medium	Coarse	Fine	Medium	Coarse	GRAVEL
	SILT			SAND			



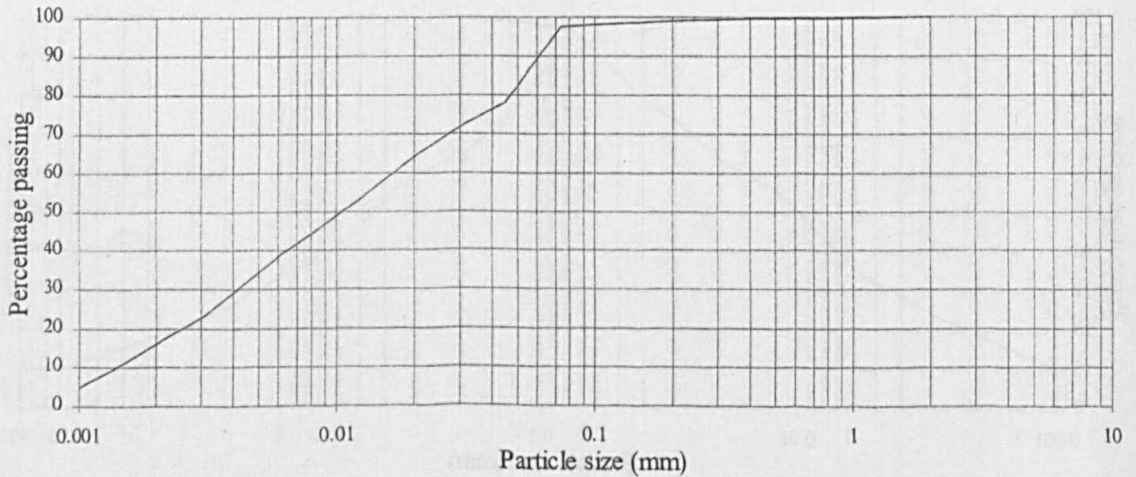
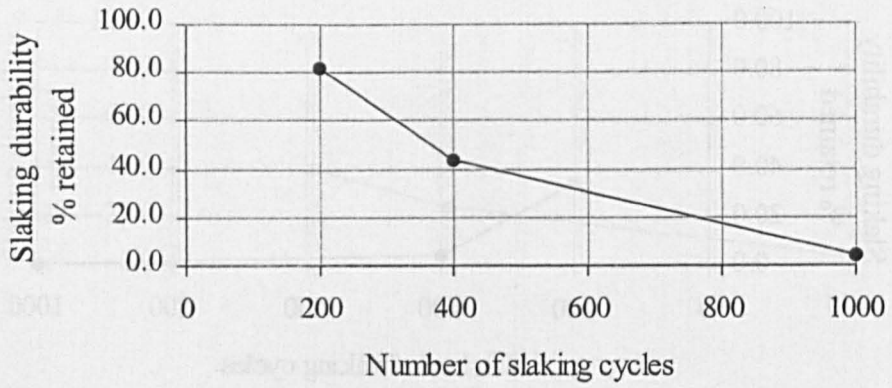
Remainder from slake durability testing after 1,000 rotations.

Sample 333

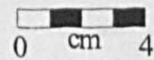
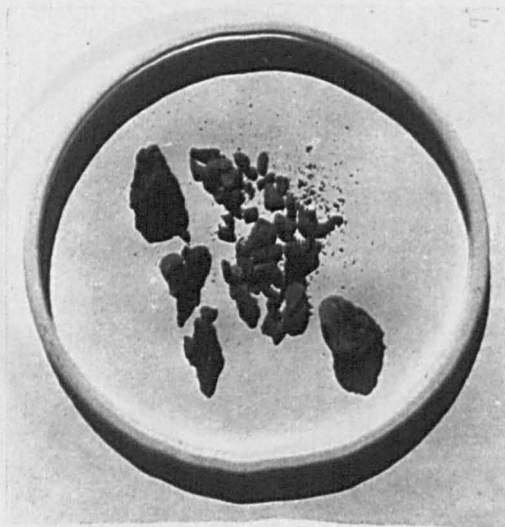


CLAY	Fine	Medium	Coarse	Fine	Medium	Coarse	GRAVEL
	SILT			SAND			

Sample 334

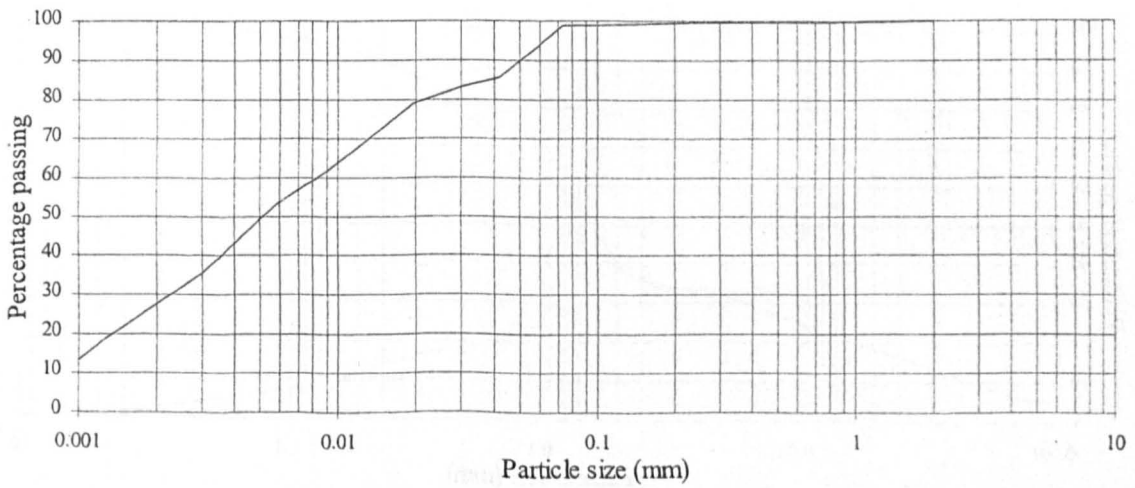
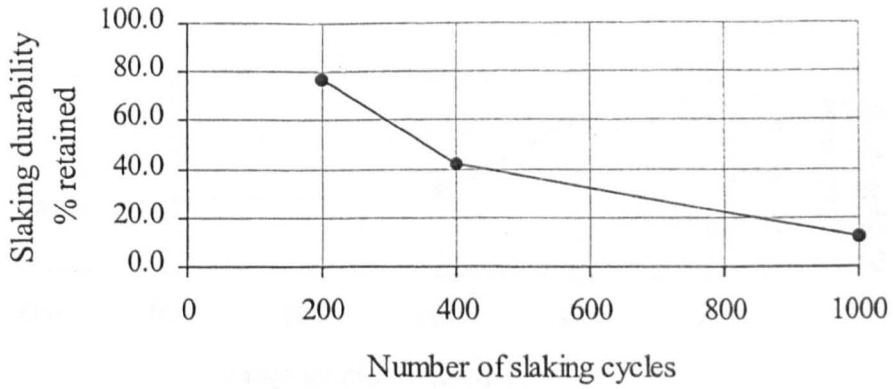


CLAY	Fine	Medium	Coarse	Fine	Medium	Coarse	GRAVEL
	SILT			SAND			

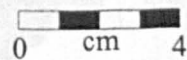
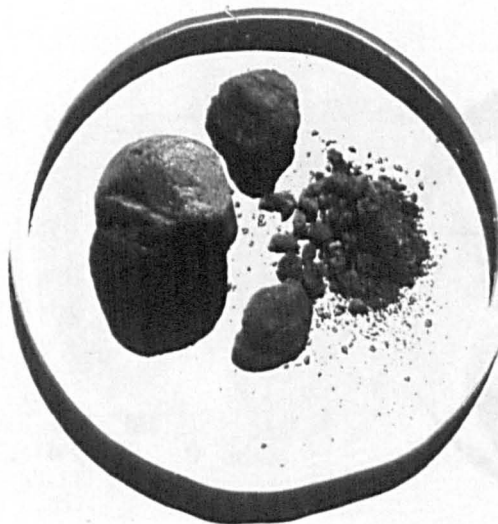


Remainder from slake durability testing after 1,000 rotations.

Sample 336

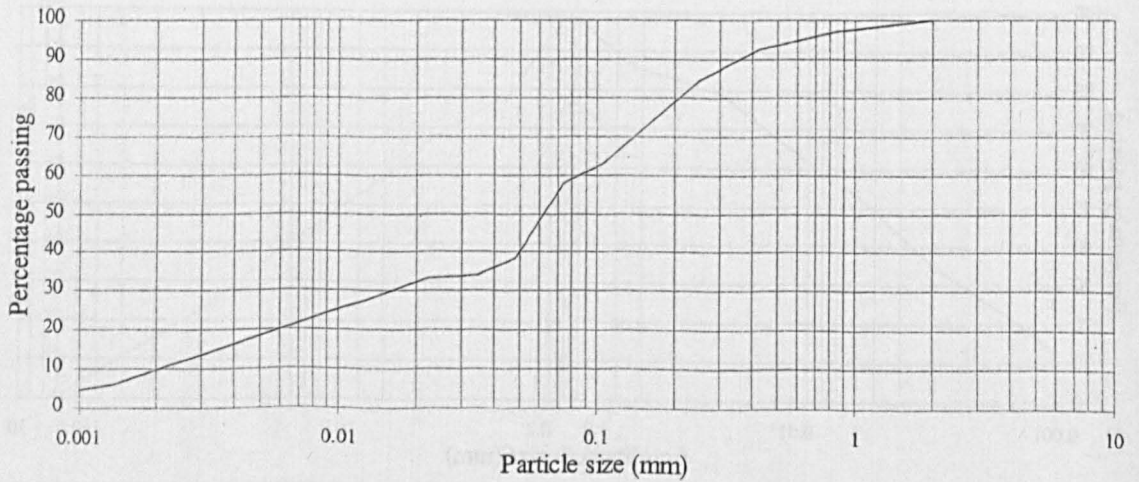
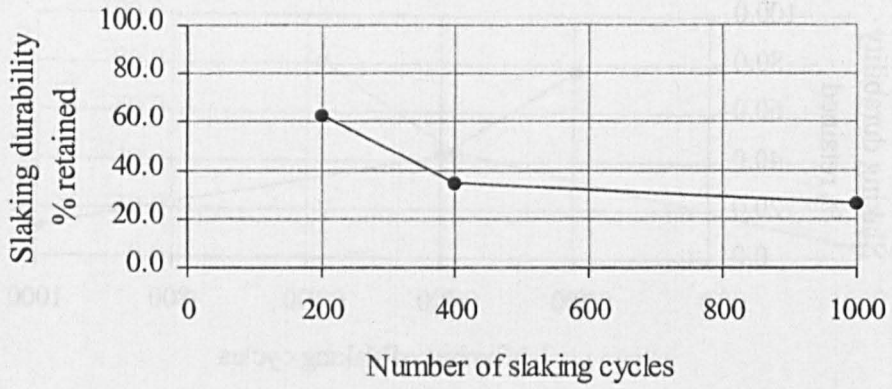


CLAY	Fine	Medium	Coarse	Fine	Medium	Coarse	GRAVEL
	SILT			SAND			

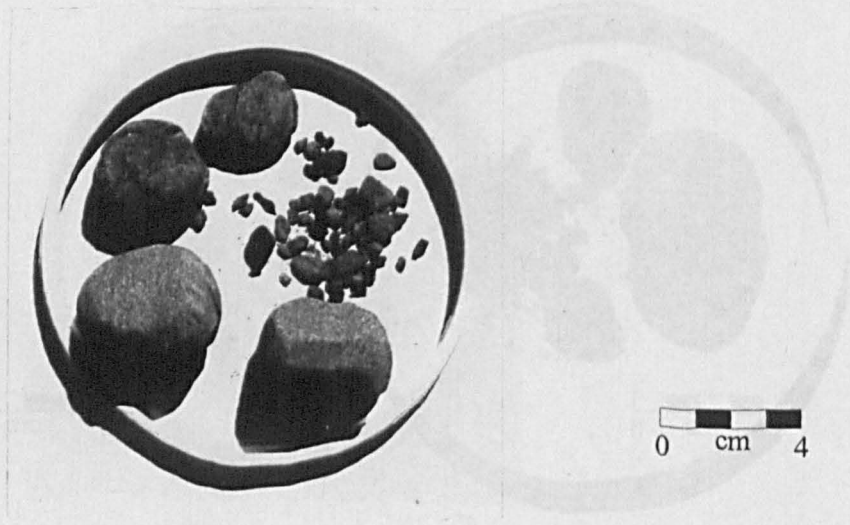


Remainder from slake durability testing after 1,000 rotations.

Sample 342

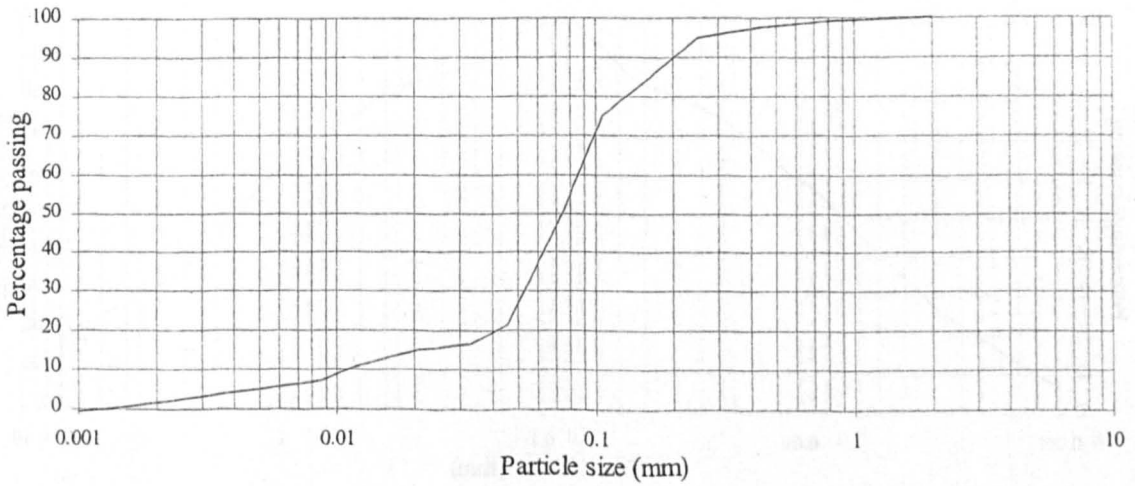
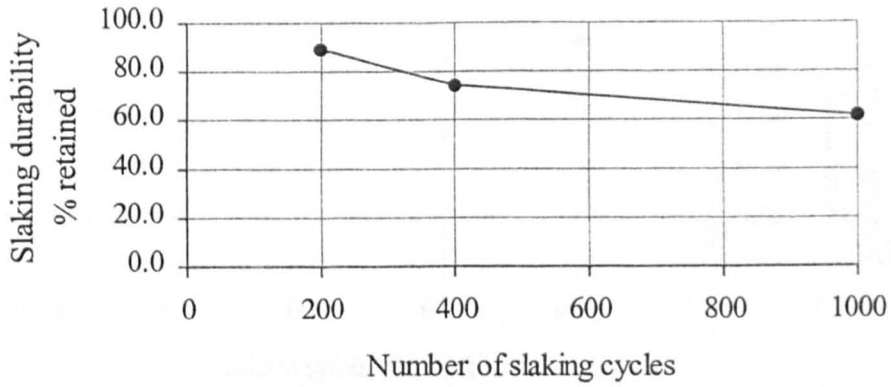


CLAY	Fine	Medium	Coarse	Fine	Medium	Coarse	GRAVEL
	SILT			SAND			

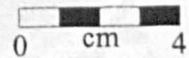


Remainder from slake durability testing after 1,000 rotations.

Sample 345

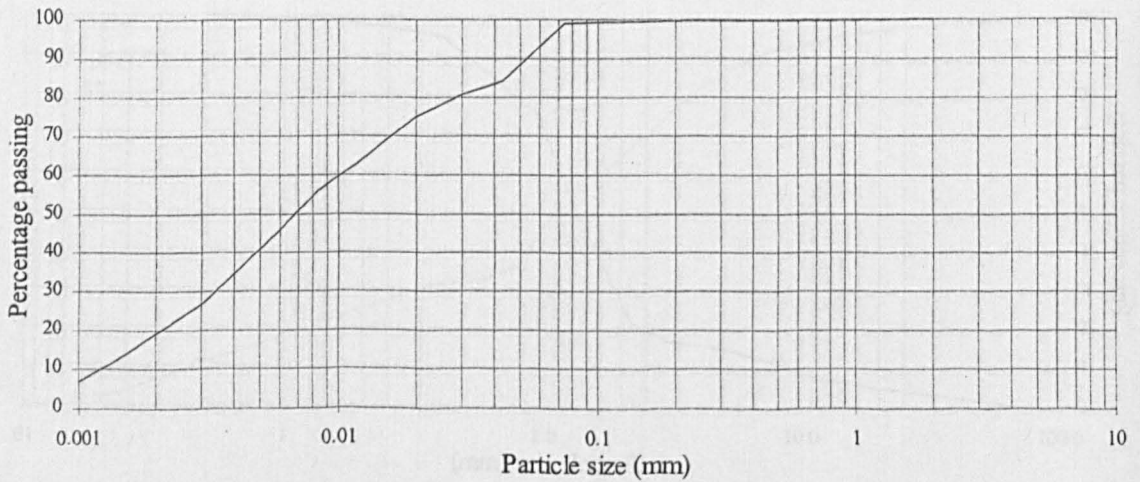
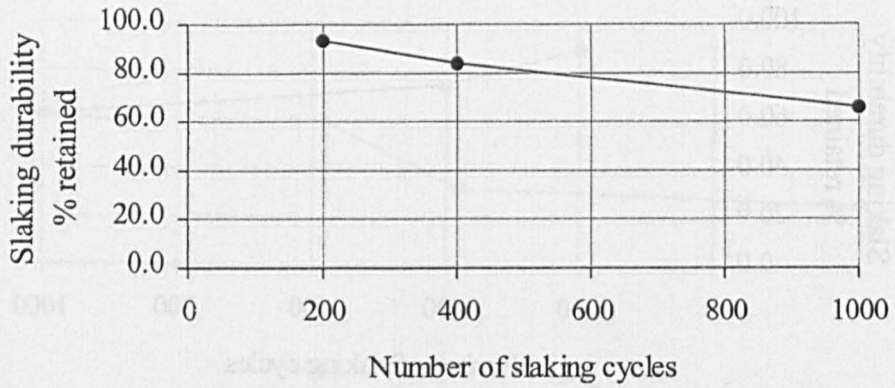


CLAY	Fine	Medium	Coarse	Fine	Medium	Coarse	GRAVEL
	SILT			SAND			

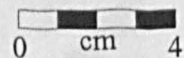


Remainder from slake durability testing after 1,000 rotations.

Sample 431

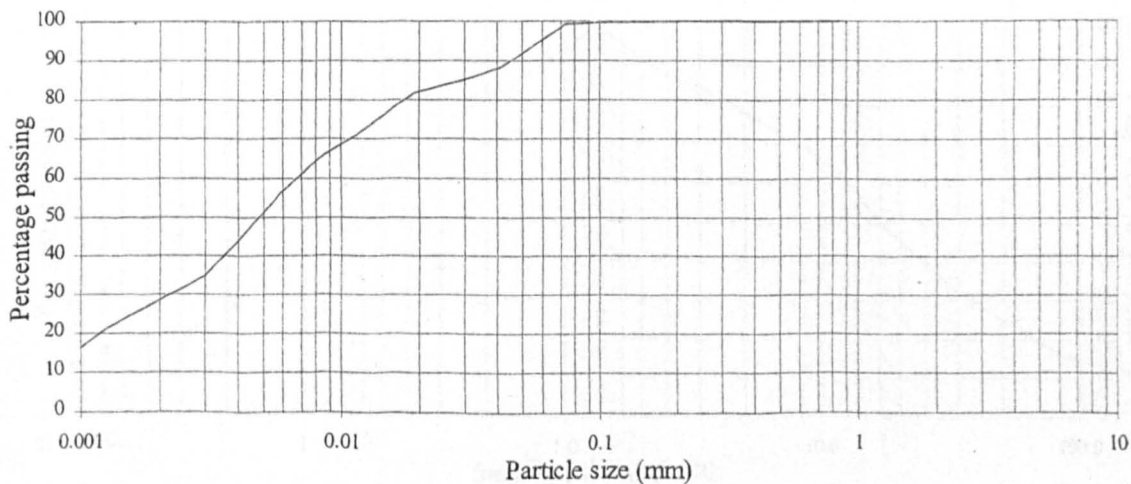
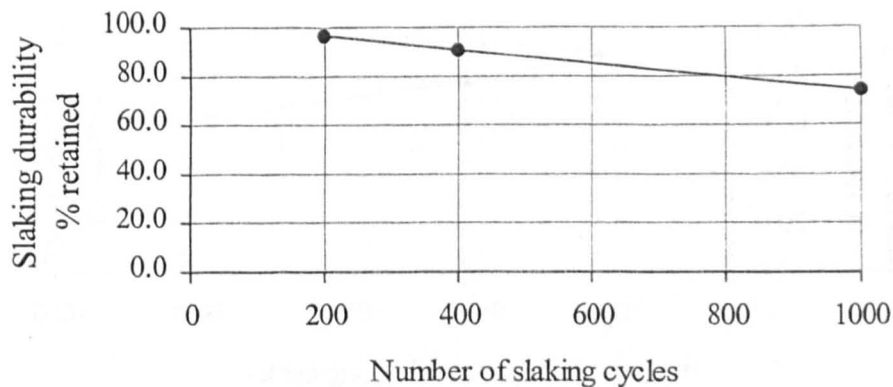


CLAY	Fine	Medium	Coarse	Fine	Medium	Coarse	GRAVEL
	SILT			SAND			



Remainder from slake durability testing after 1,000 rotations.

Sample 436

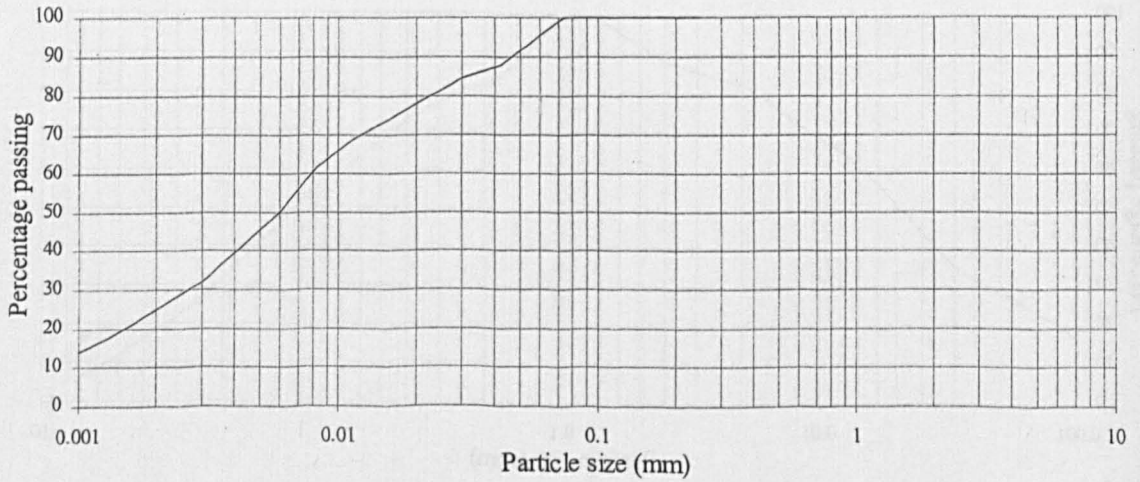
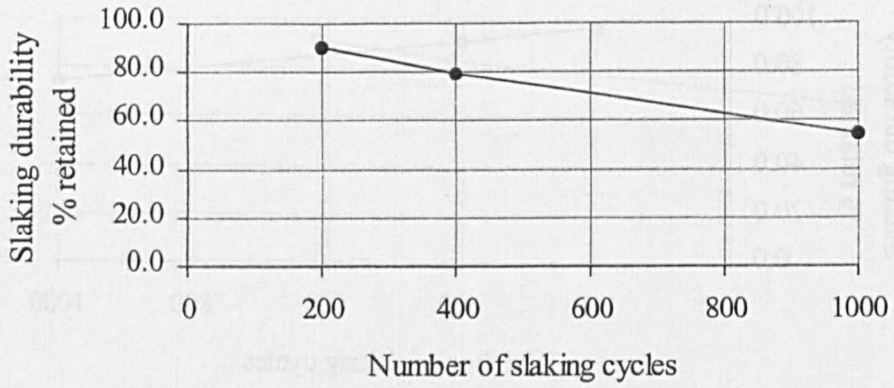


CLAY	Fine	Medium	Coarse	Fine	Medium	Coarse	GRAVEL
	SILT			SAND			



Remainder from slake durability testing after 1,000 rotations.

Sample 441

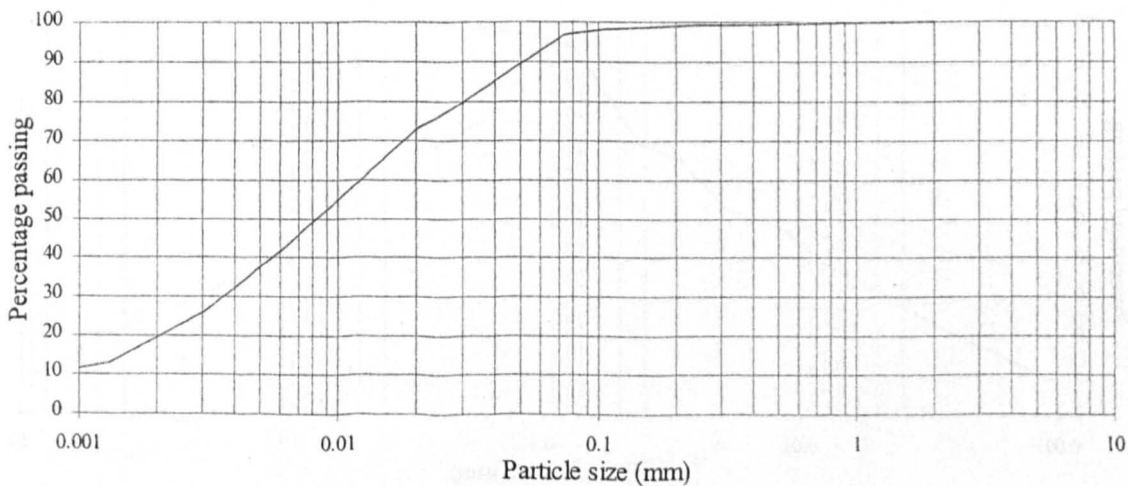
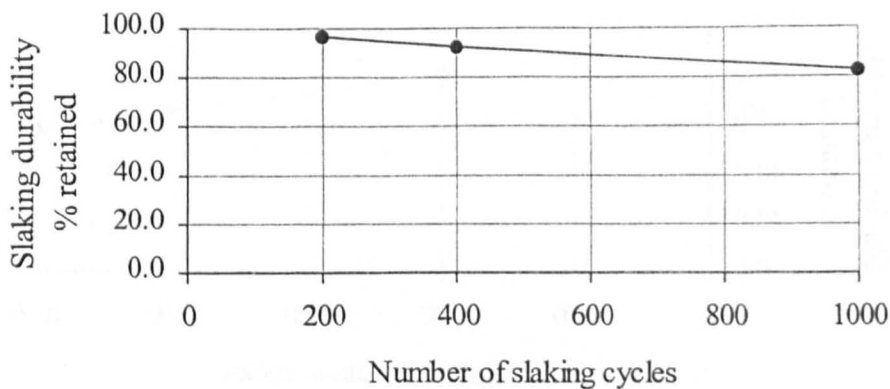


CLAY	Fine	Medium	Coarse	Fine	Medium	Coarse	GRAVEL
	SILT			SAND			

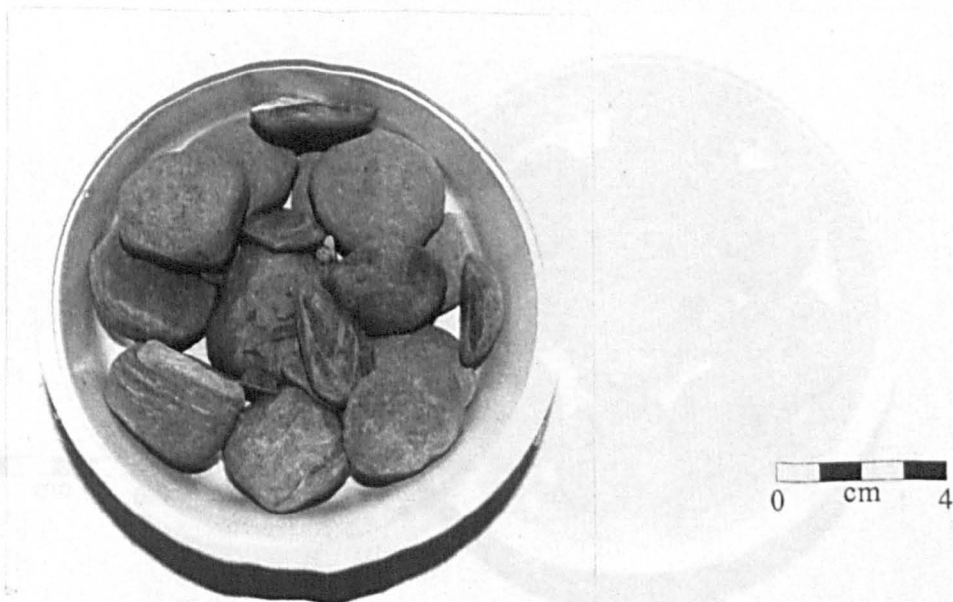


Remainder from slake durability testing after 1,000 rotations.

Sample 445

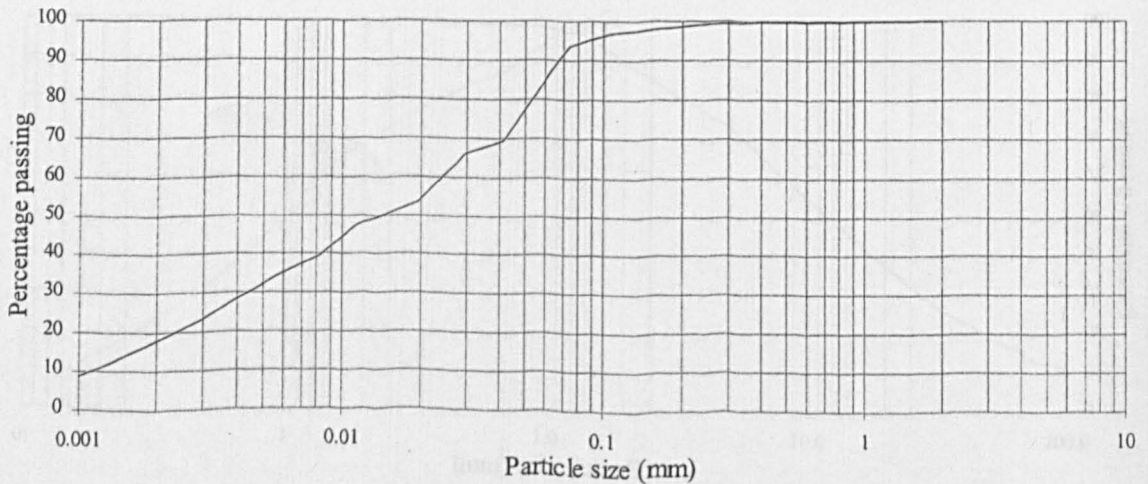
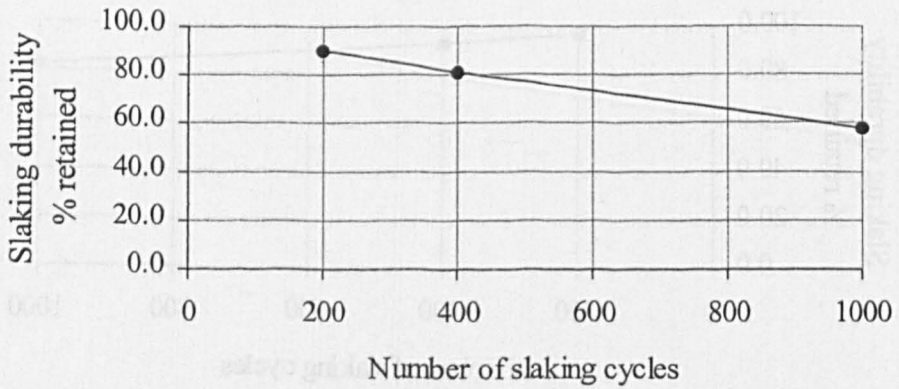


CLAY	Fine	Medium	Coarse	Fine	Medium	Coarse	GRAVEL
	SILT			SAND			

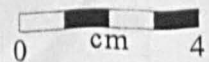


Remainder from slake durability testing after 1,000 rotations.

Sample OB1

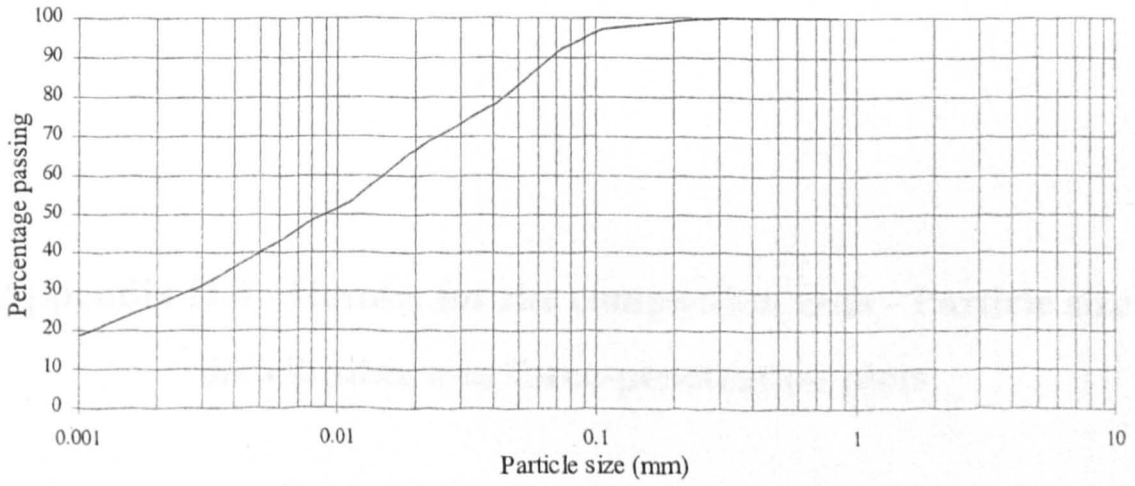
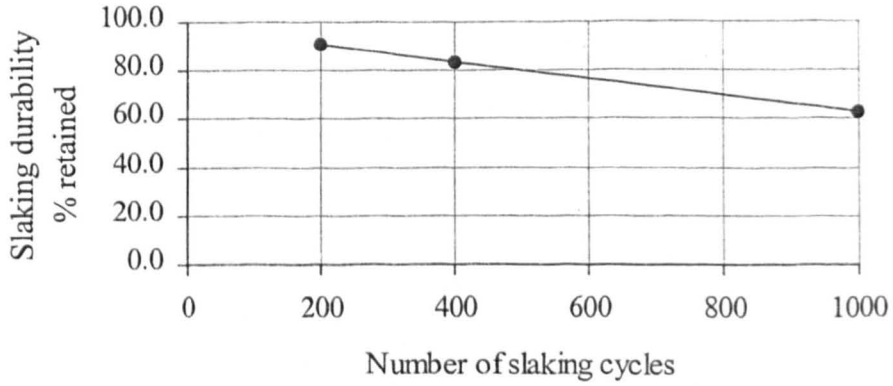


CLAY	Fine	Medium	Coarse	Fine	Medium	Coarse	GRAVEL
	SILT			SAND			

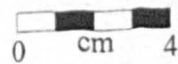


Remainder from slake durability testing after 1,000 rotations.

Sample OB2



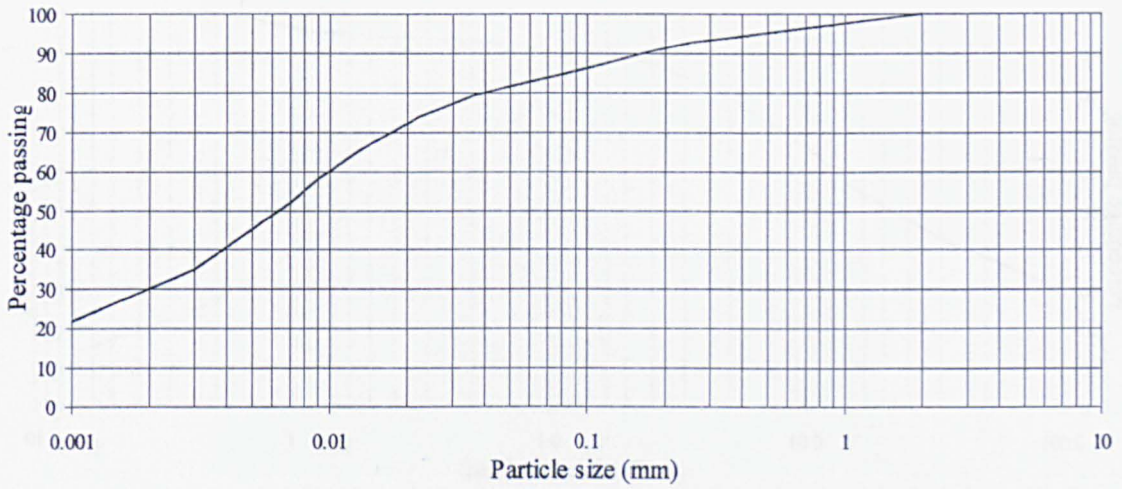
CLAY	Fine	Medium	Coarse	Fine	Medium	Coarse	GRAVEL
	SILT			SAND			



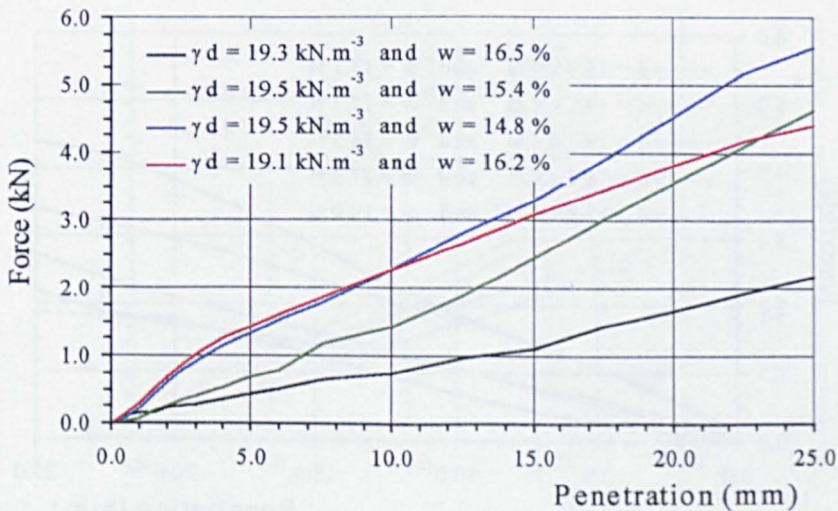
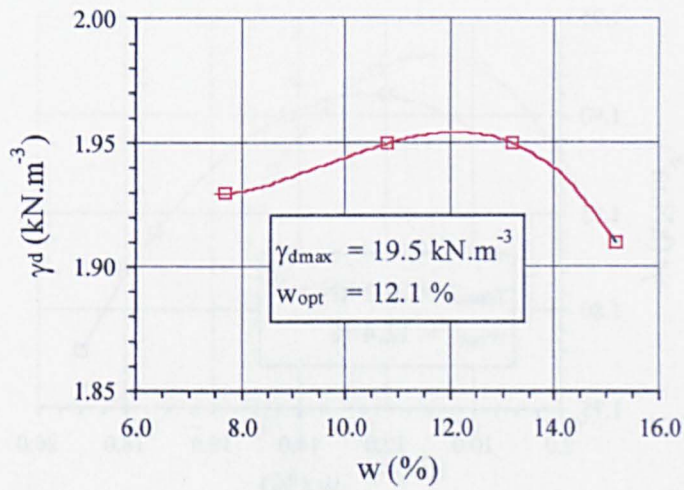
Remainder from slake durability testing after 1,000 rotations.

**Appendix II.4 - Results for the compaction tests - Particle size
distribution and force-penetration plots**

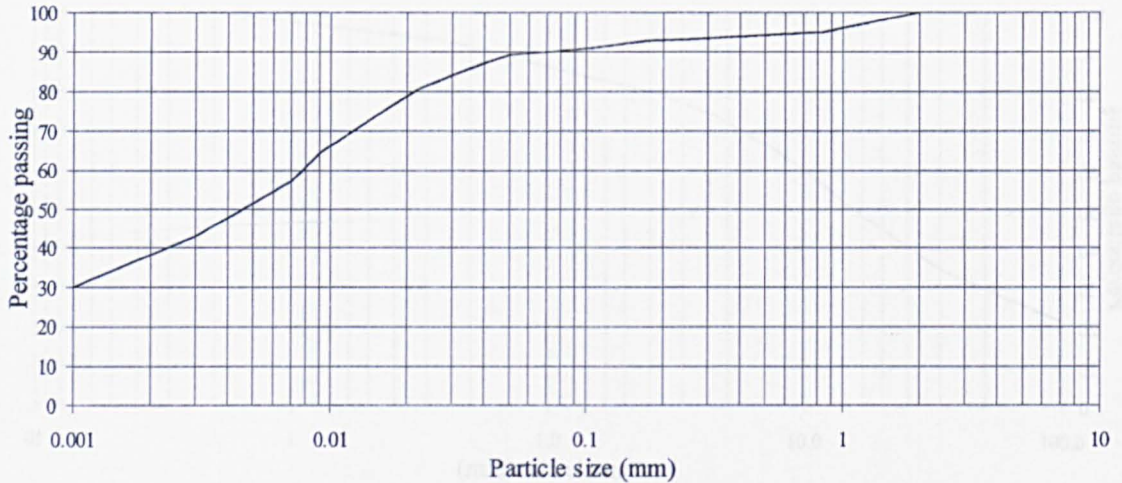
Mixture S1



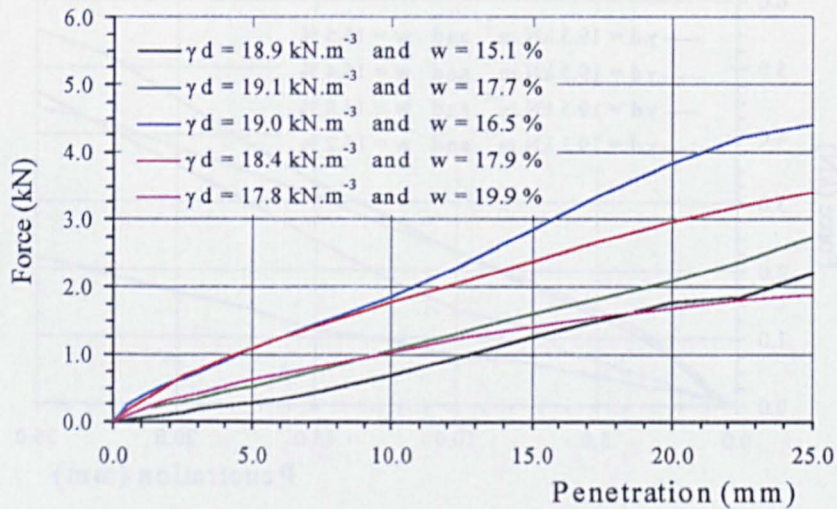
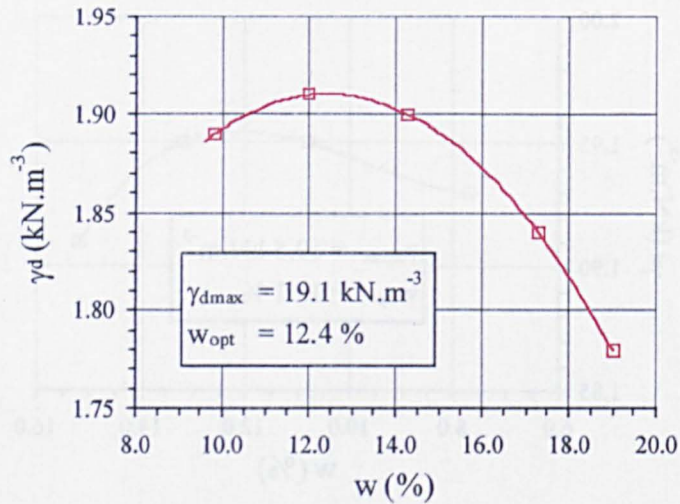
CLAY	Fine	Medium	Coarse	Fine	Medium	Coarse	GRAVEL
	SILT			SAND			



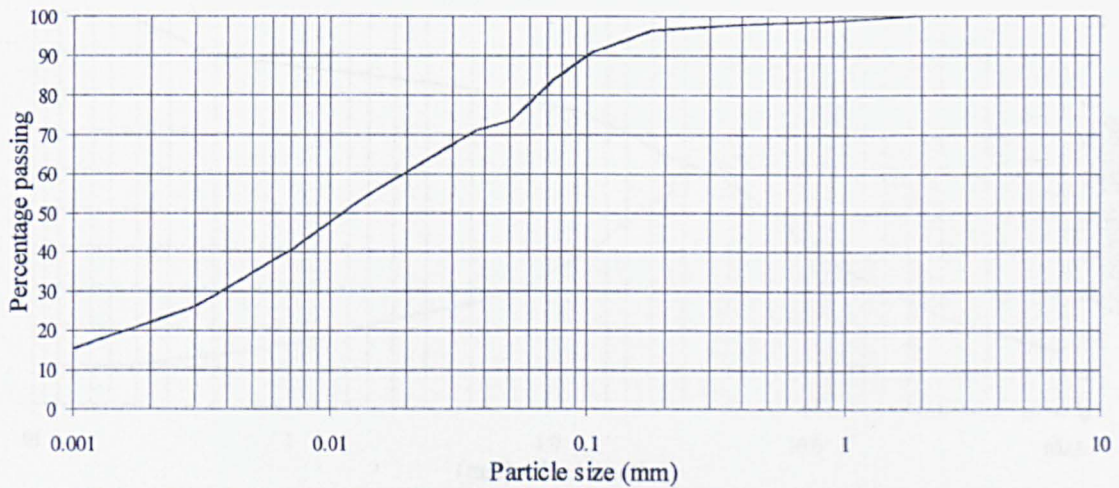
Mixture SA1



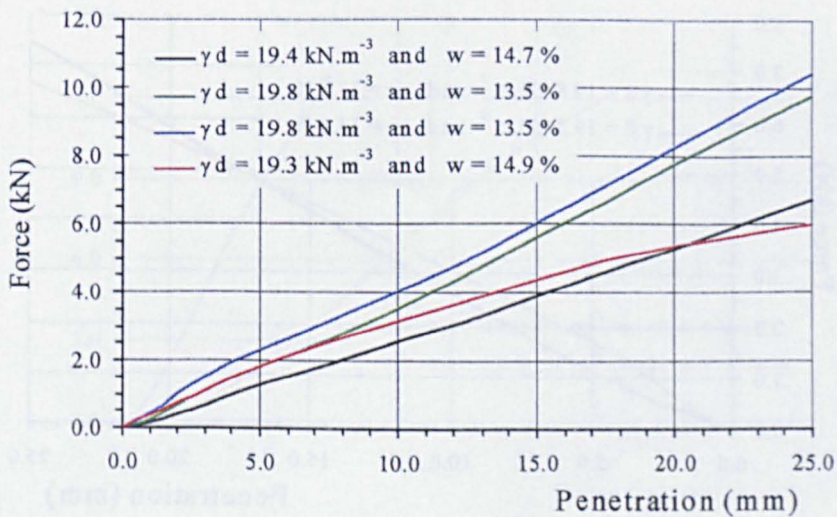
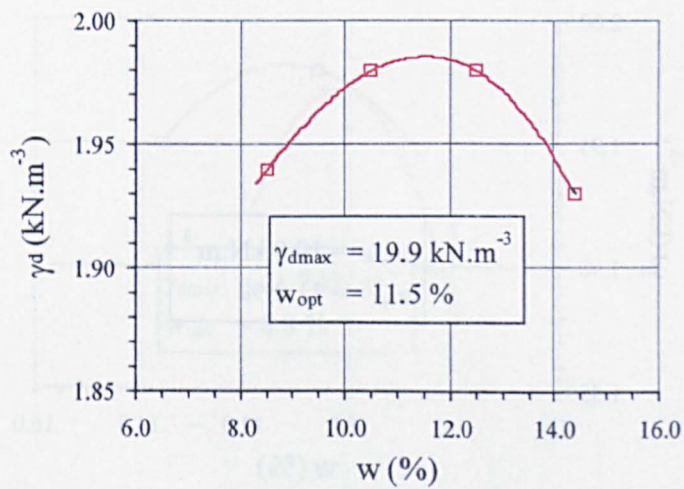
CLAY	Fine	Medium	Coarse	Fine	Medium	Coarse	GRAVEL
	SILT			SAND			



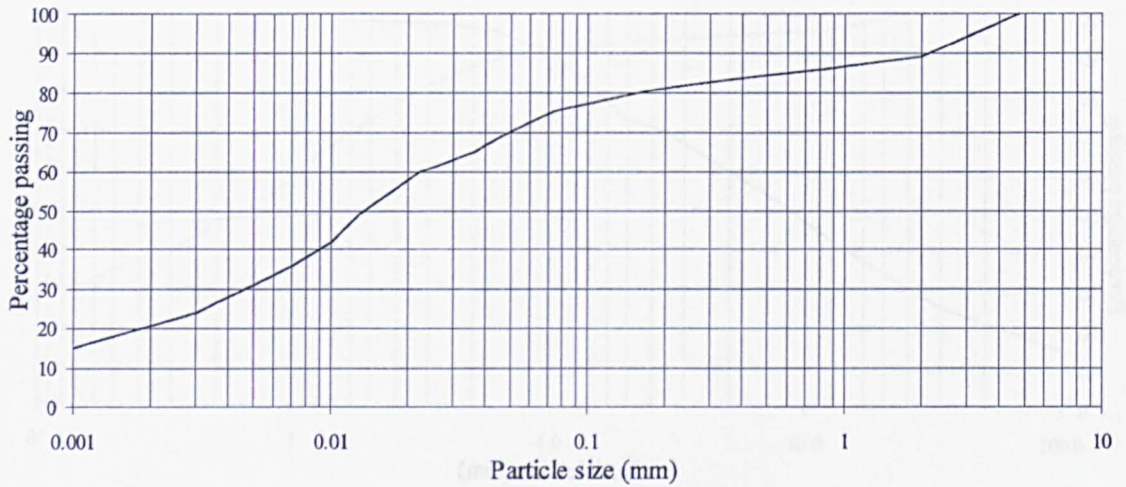
Mixture S2



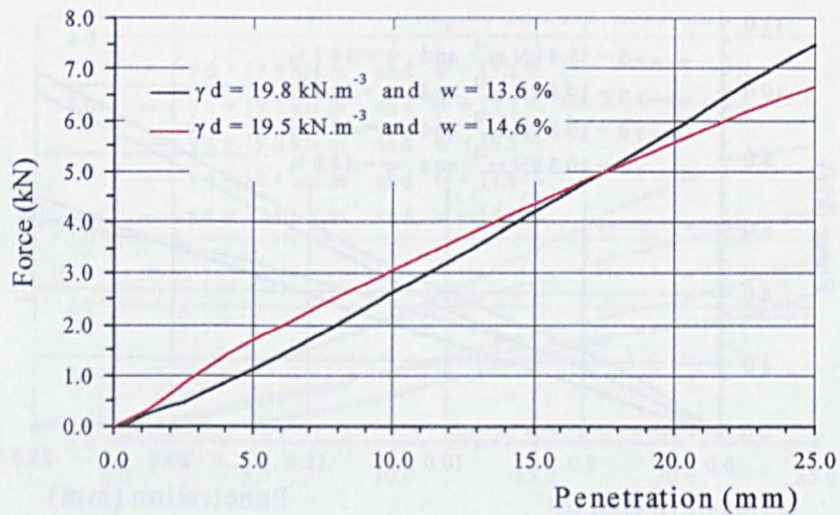
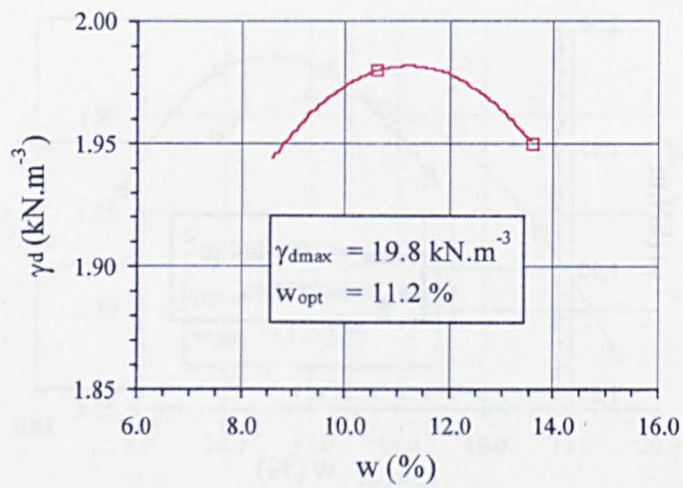
CLAY	Fine	Medium	Coarse	Fine	Medium	Coarse	GRAVEL
	SILT			SAND			



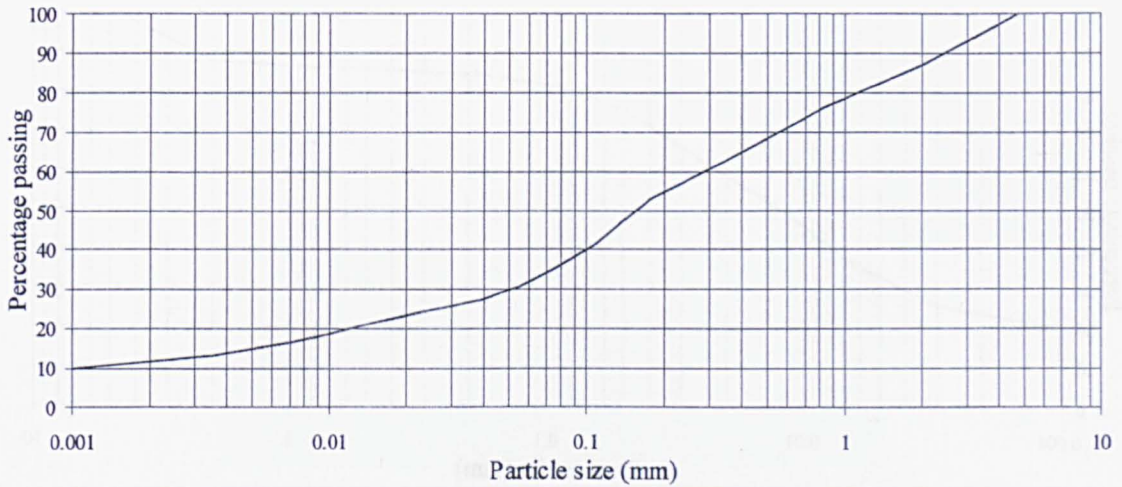
Mixture SA2



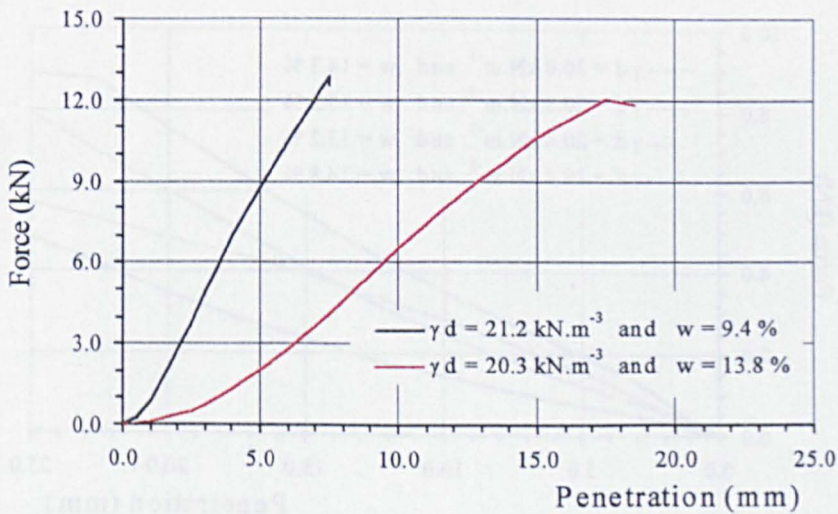
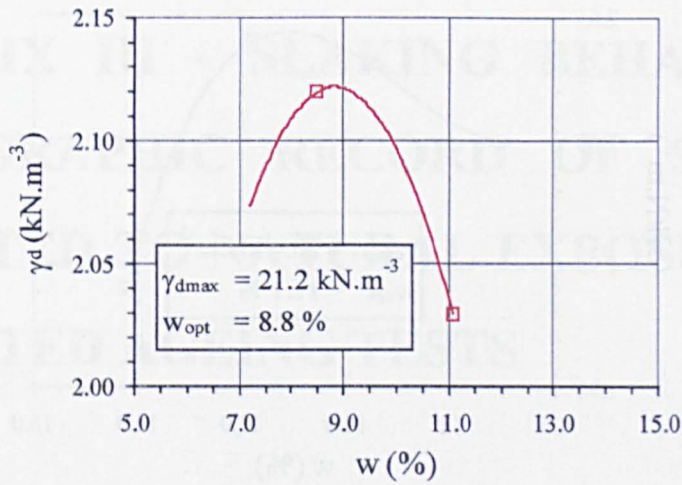
CLAY	Fine	Medium	Coarse	Fine	Medium	Coarse	GRAVEL
	SILT			SAND			



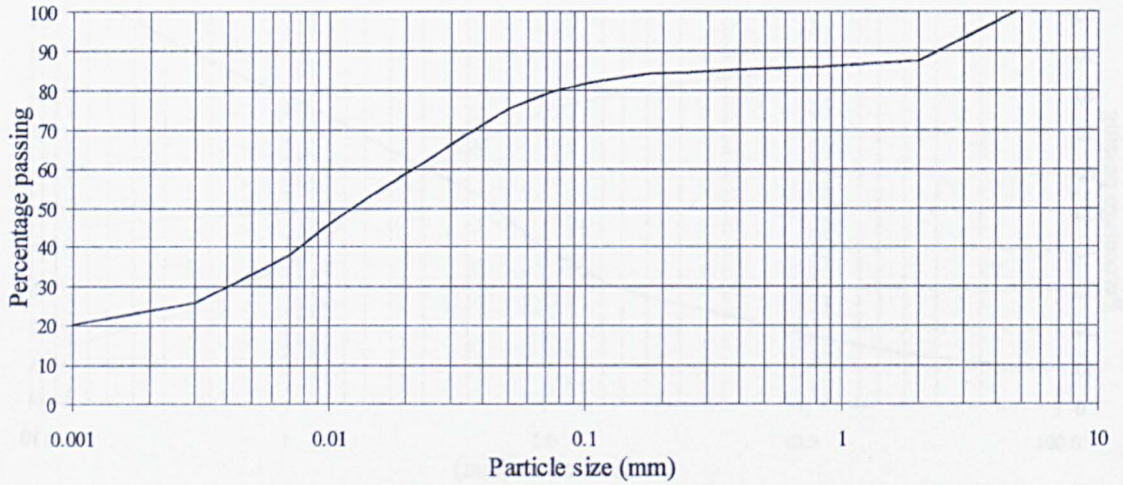
Mixture A1



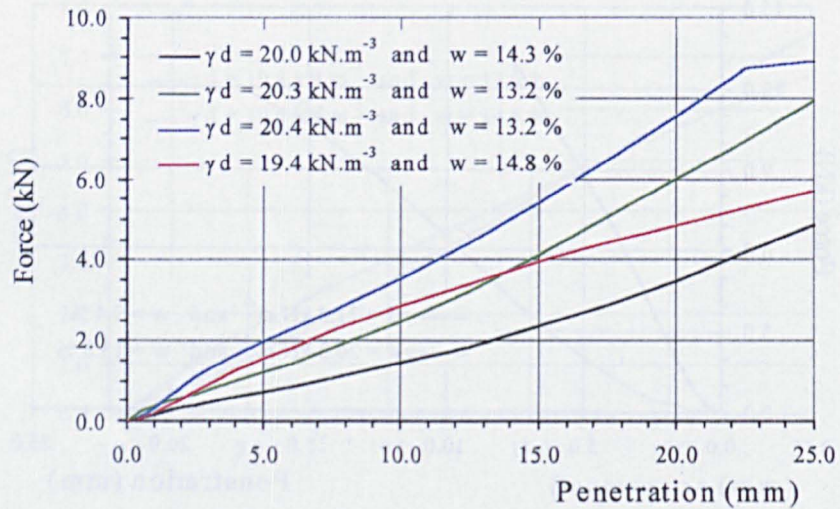
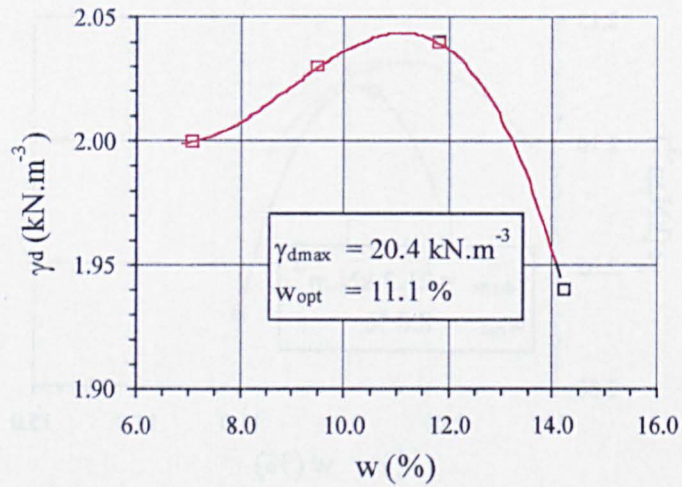
CLAY	Fine	Medium	Coarse	Fine	Medium	Coarse	GRAVEL
	SILT			SAND			



Mixture SA3



CLAY	Fine	Medium	Coarse	Fine	Medium	Coarse	GRAVEL
	SILT			SAND			



**APPENDIX III - SLAKING BEHAVIOUR -
PHOTOGRAPHIC RECORD OF SAMPLES
SUBJECTED TO NATURAL EXPOSURE AND
SIMULATED AGEING TESTS**



A

B



C

D



Fig. AIII.1 - Natural exposure test (N): (A) initial breakdown state of sample 83; (B) final breakdown state of sample 83; (C) initial breakdown state of sample 114; (D) final breakdown state of sample 114.

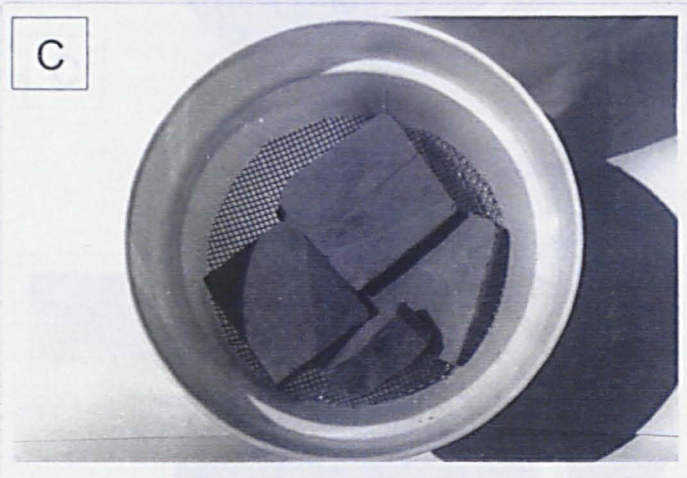
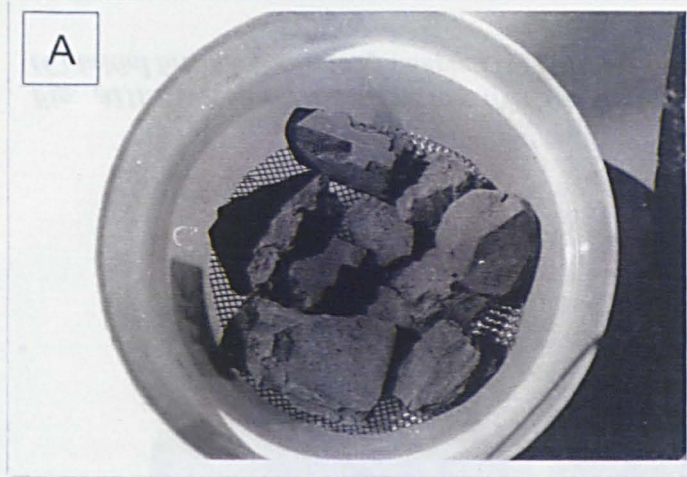


Fig. AIII.2 - Natural exposure test (N): (A) initial breakdown state of sample 283; (B) final breakdown state of sample 283; (C) initial breakdown state of sample 286; (D) final breakdown state of sample 286.

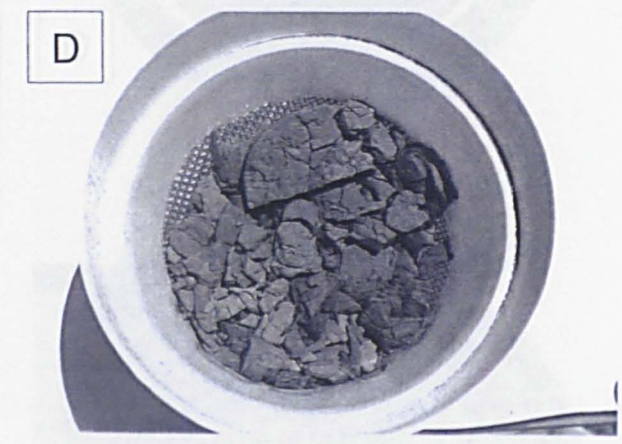
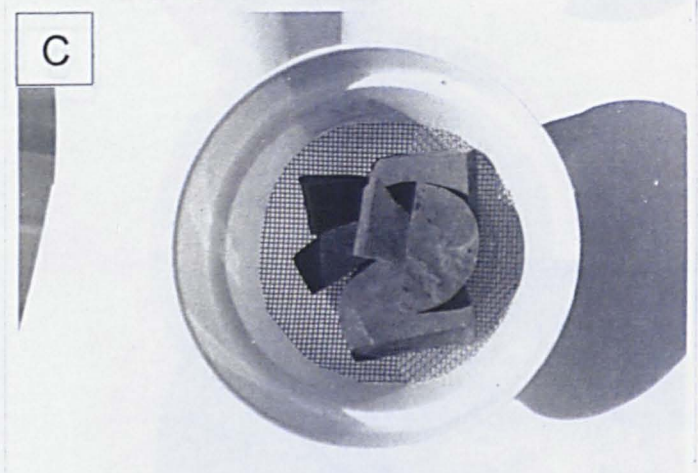


Fig. AIII.3 - Natural exposure test (N): (A) initial breakdown state of sample 333; (B) final breakdown state of sample 333; (C) initial breakdown state of sample 336; (D) final breakdown state of sample 336.

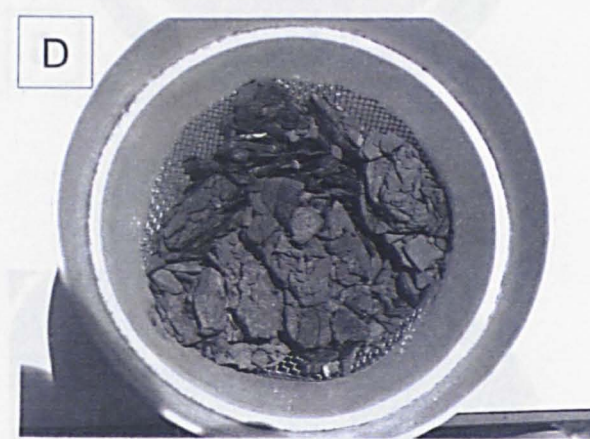
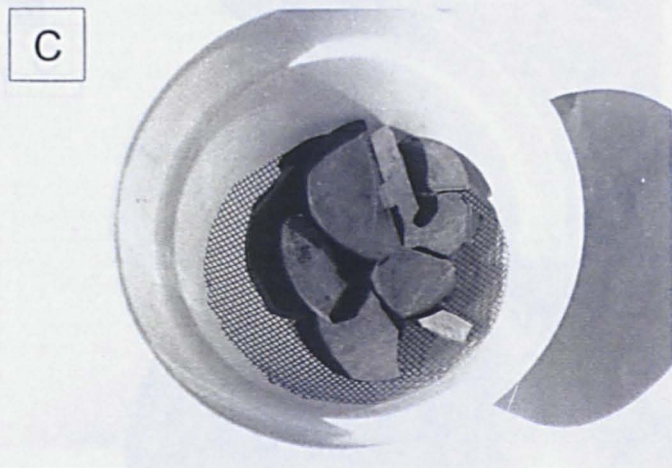
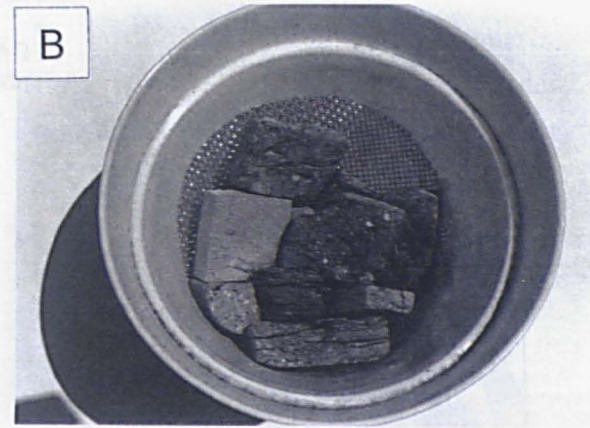
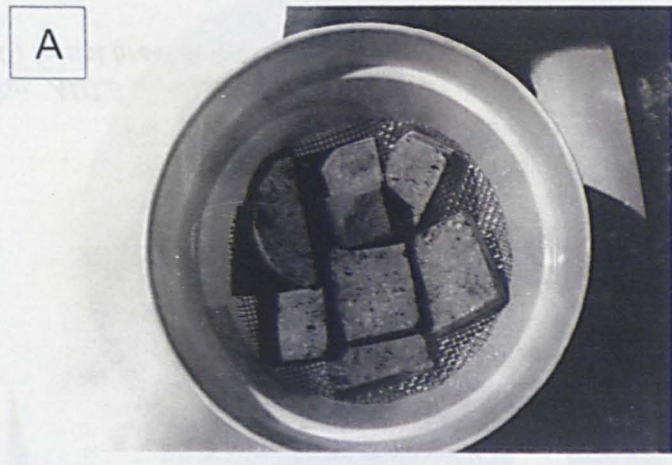


Fig. AIII.4 - Natural exposure test (N): (A) initial breakdown state of sample 342; (B) final breakdown state of sample 342; (C) initial breakdown state of sample 431; (D) final breakdown state of sample 431.

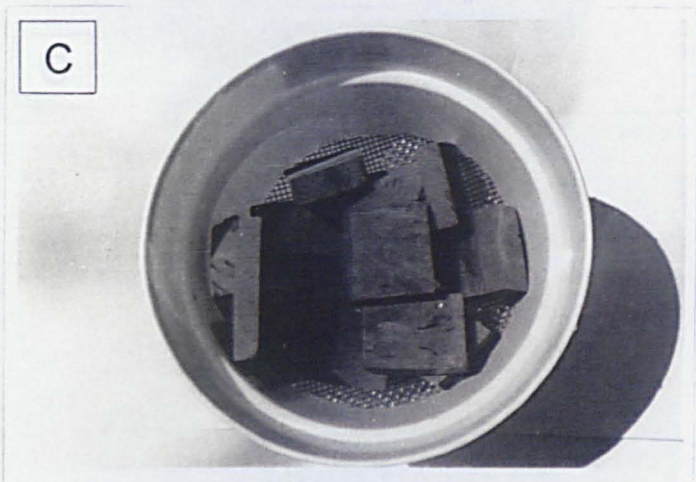
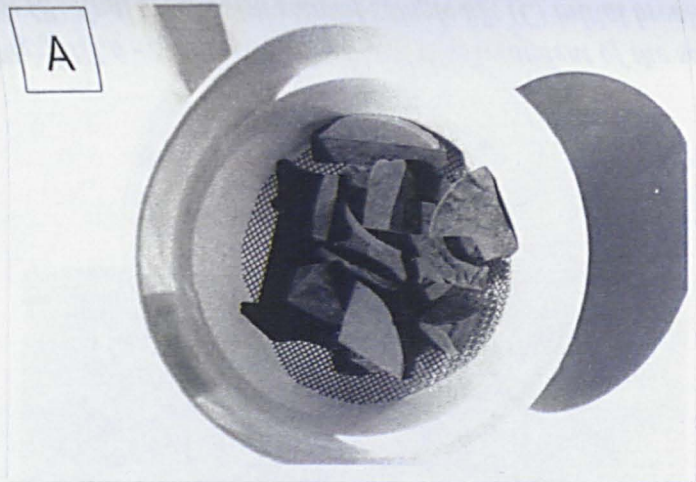


Fig. AIII.5 - Natural exposure test (N): (A) initial breakdown state of sample 441; (B) final breakdown state of sample 441; (C) initial breakdown state of sample OB2; (D) final breakdown state of sample OB2.

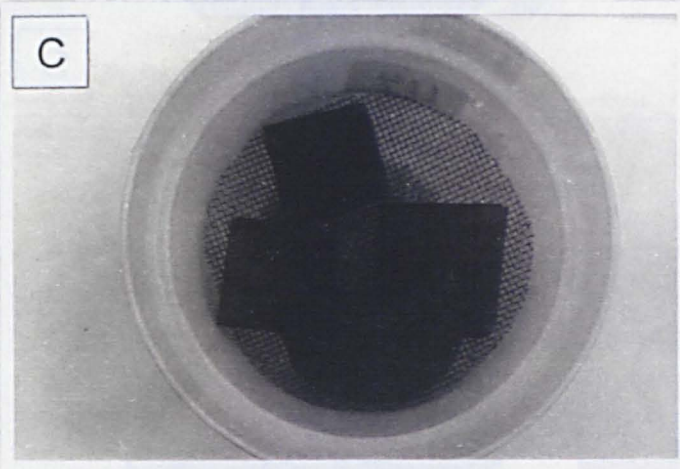


Fig. AIII.6 - Simulated ageing test with treatment of the samples with a acid solution (HS): (A) initial breakdown state of sample 83; (B) final breakdown state of sample 83; (C) initial breakdown state of sample 114; (D) final breakdown state of sample 114.

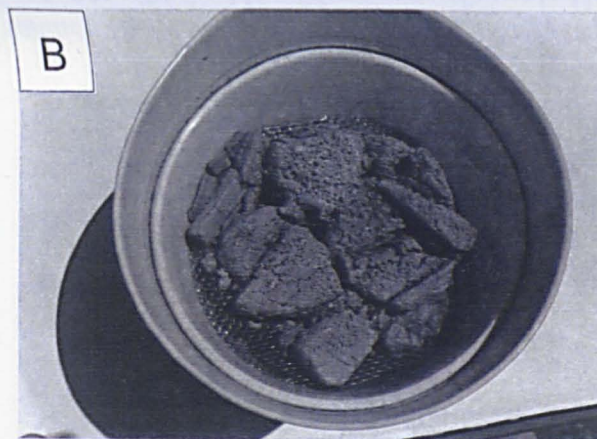


Fig. AIII.7 - Simulated ageing test with treatment of the samples with a acid solution (HS): (A) initial breakdown state of sample 283; (B) final breakdown state of sample 283; (C) initial breakdown state of sample 286; (D) final breakdown state of sample 286.

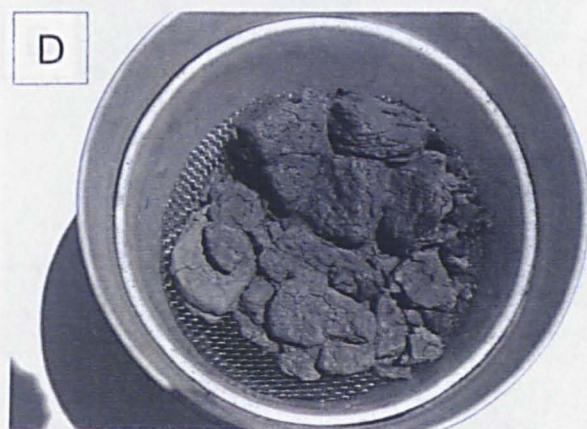
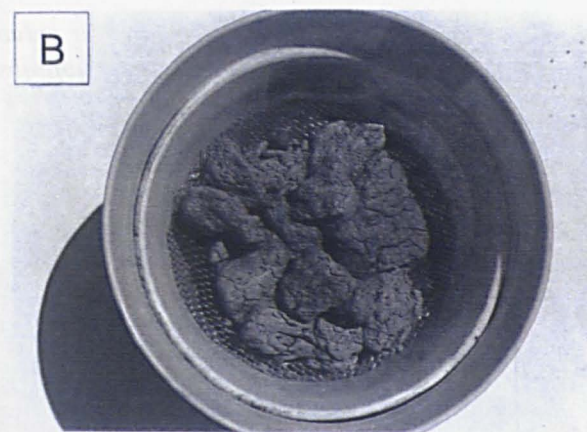


Fig. AIII.8 - Simulated ageing test with treatment of the samples with a acid solution (HS): (A) initial breakdown state of sample 333; (B) final breakdown state of sample 333; (C) initial breakdown state of sample 336; (D) final breakdown state of sample 336.

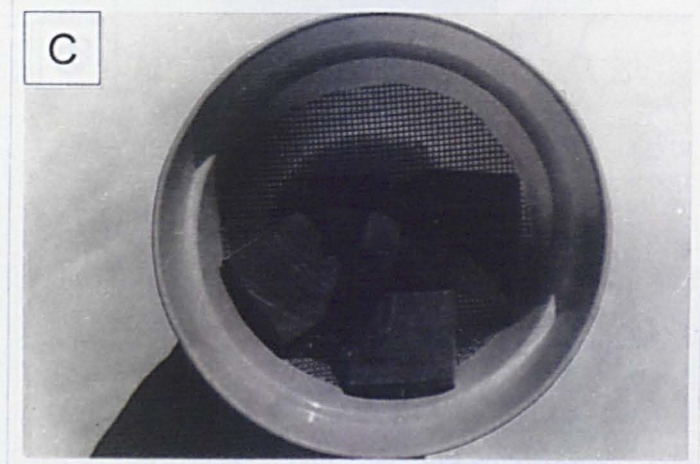
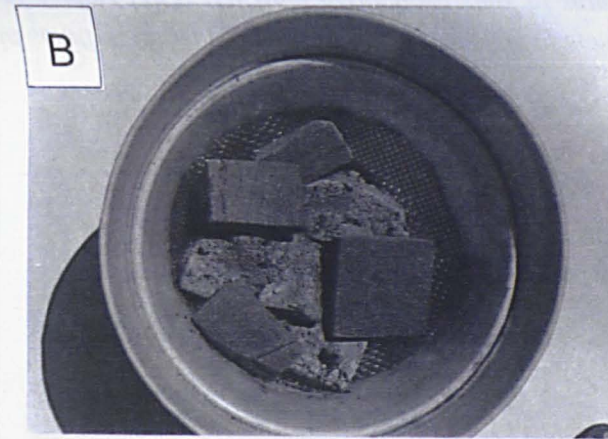


Fig. AIII.9 - Simulated ageing test with treatment of the samples with a acid solution (HS): (A) initial breakdown state of sample 342; (B) final breakdown state of sample 342; (C) initial breakdown state of sample 431; (D) final breakdown state of sample 431.

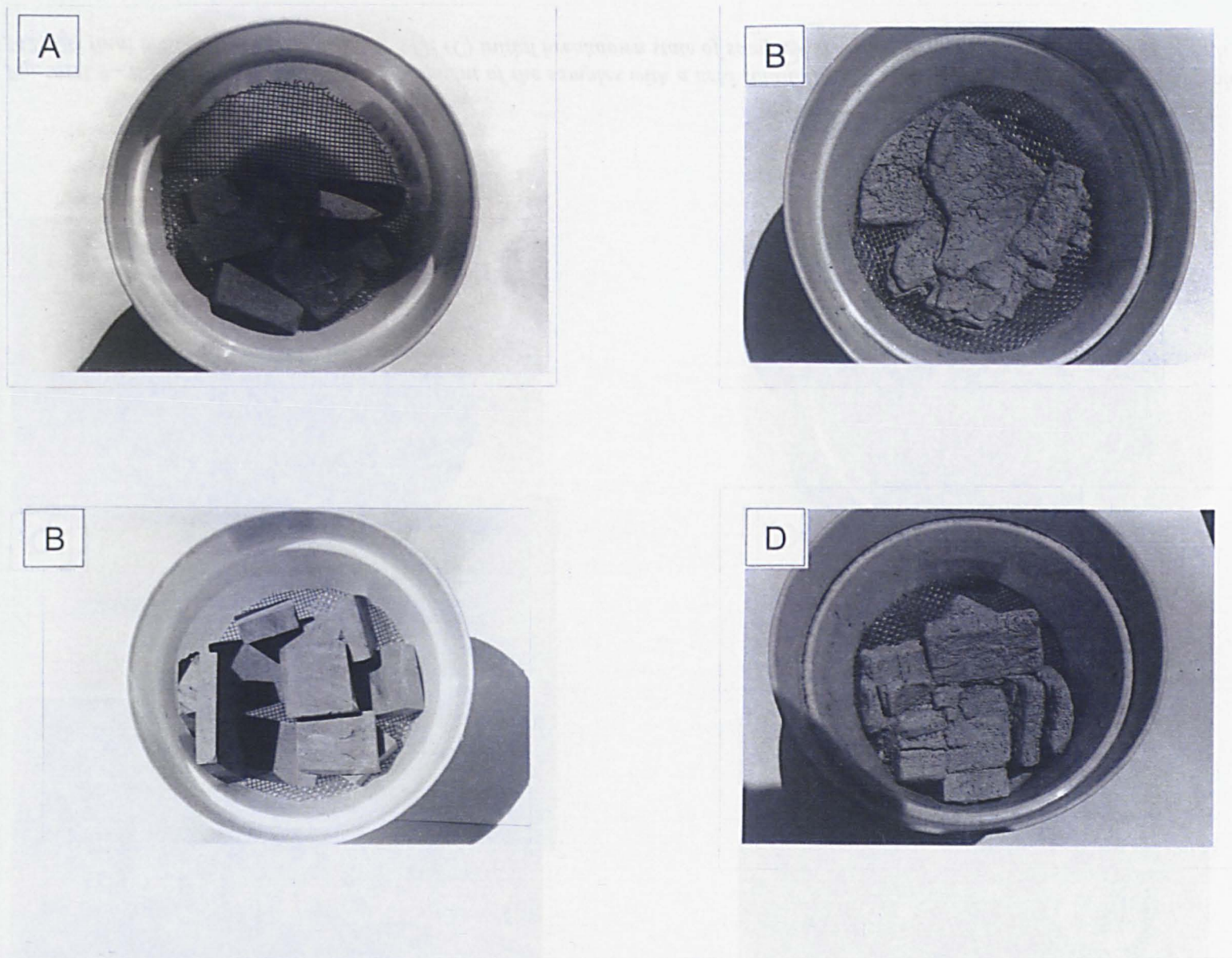


Fig. AIII.10 - Simulated ageing test with treatment of the samples with a acid solution (HS): (A) initial breakdown state of sample 441; (B) final breakdown state of sample 441; (C) initial breakdown state of sample OB2; (D) final breakdown state of sample OB2.

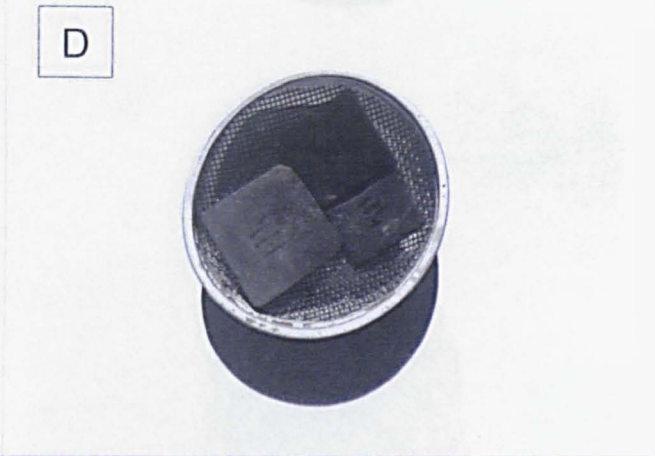
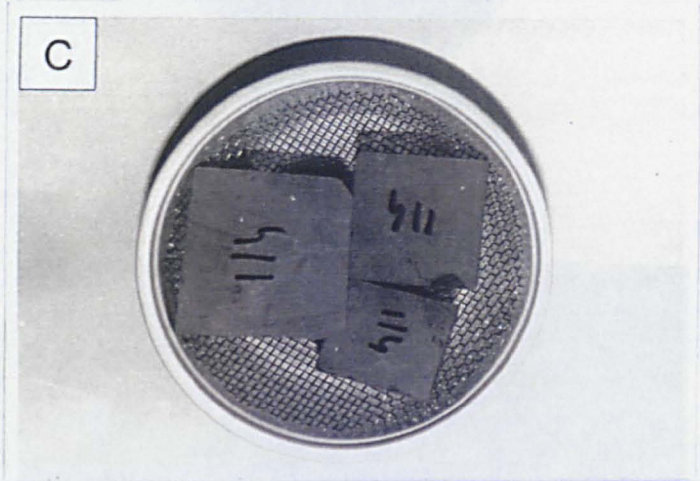
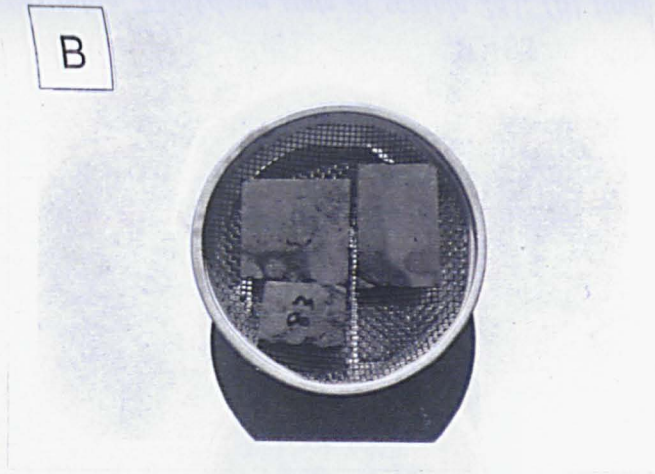
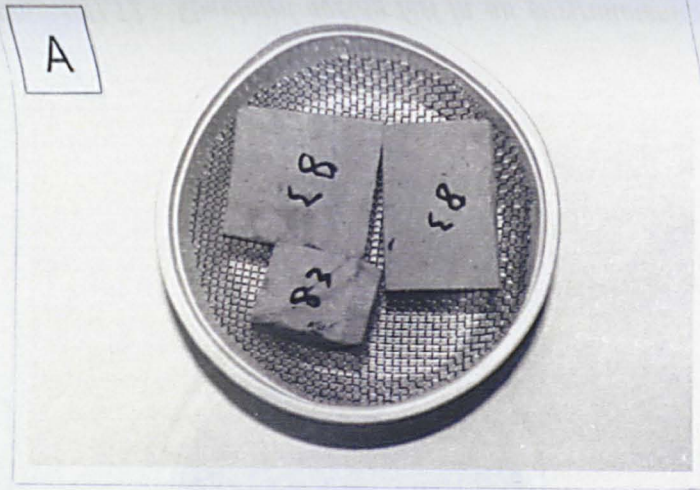


Fig. AIII.11 - Simulated ageing test in an environmental chamber (HT): (A) initial breakdown state of sample 83; (B) final breakdown state of sample 83; (C) initial breakdown state of sample 114; (D) final breakdown state of sample 114.

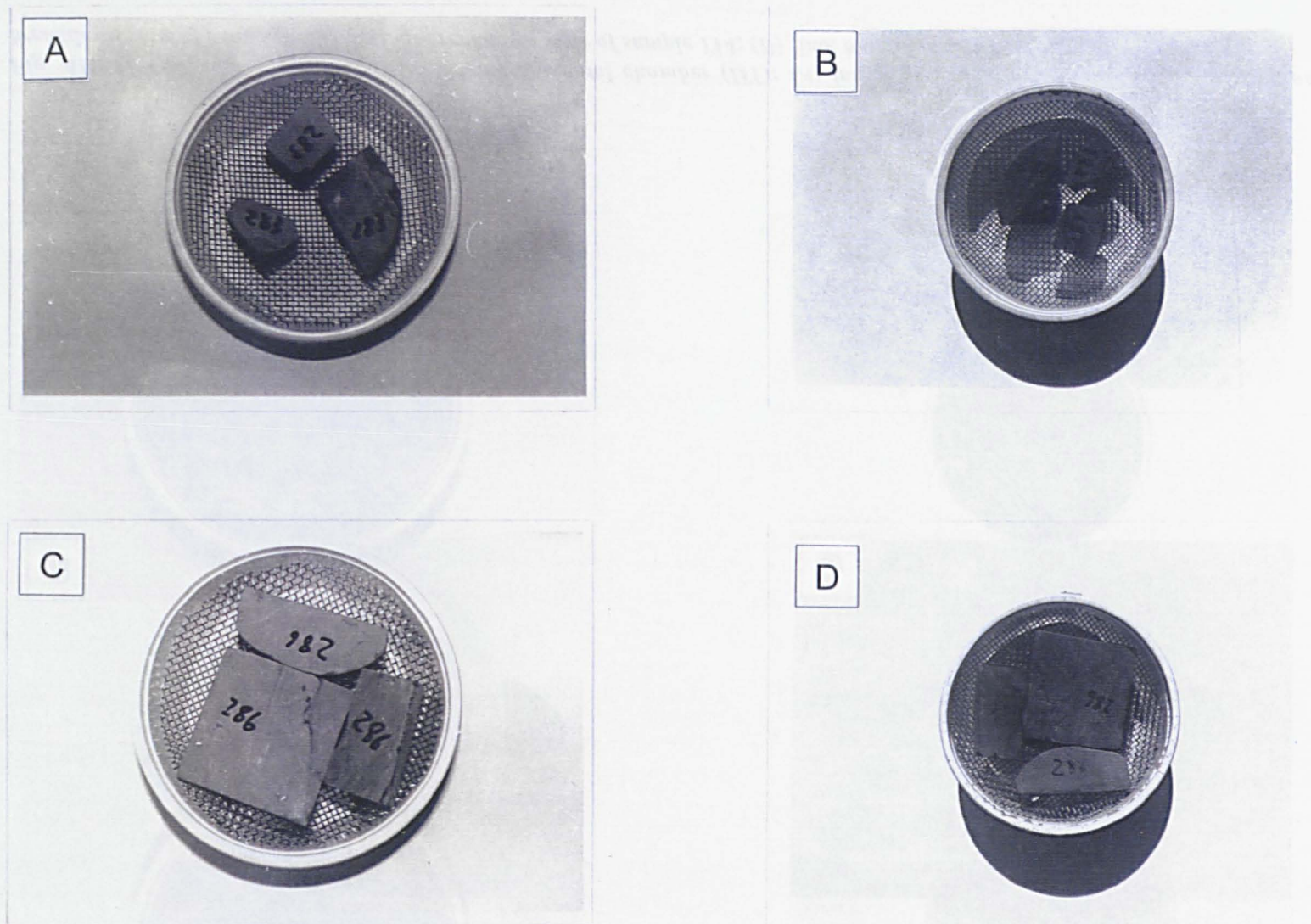


Fig. AIII.12 - Simulated ageing test in an environmental chamber (HT): (A) initial breakdown state of sample 283; (B) final breakdown state of sample 283; (C) initial breakdown state of sample 286; (D) final breakdown state of sample 286.

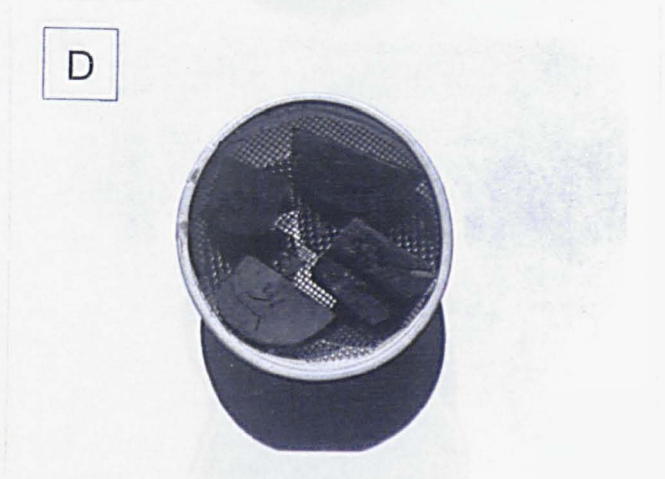
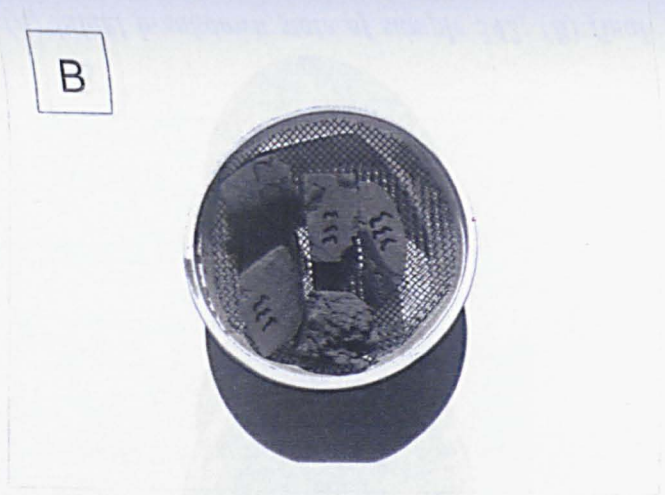


Fig. AIII.13 - Simulated ageing test in an environmental chamber (HT): (A) initial breakdown state of sample 333; (B) final breakdown state of sample 333; (C) initial breakdown state of sample 336; (D) final breakdown state of sample 336.

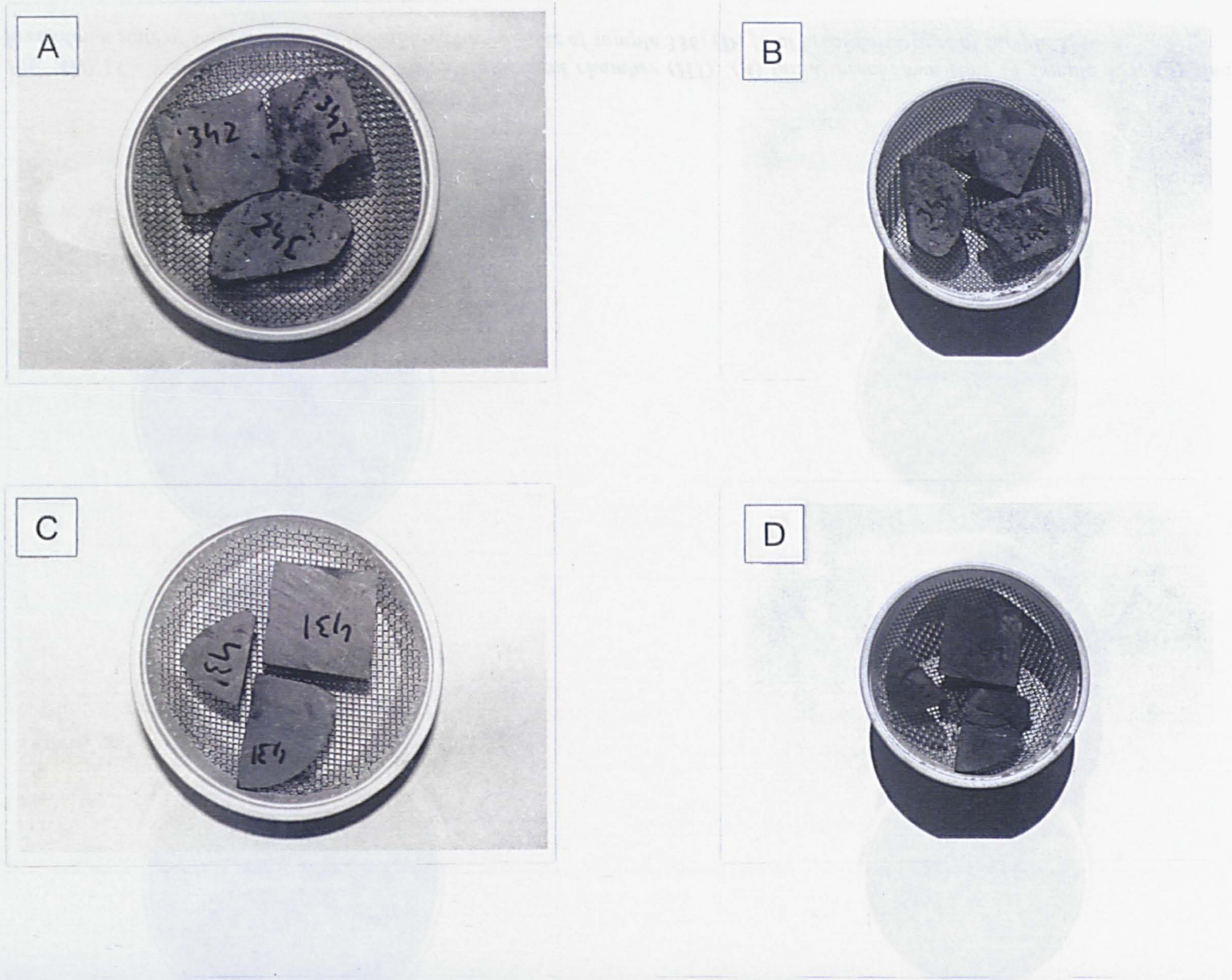


Fig. AIII.14 - Simulated ageing test in an environmental chamber (HT): (A) initial breakdown state of sample 342; (B) final breakdown state of sample 342; (C) initial breakdown state of sample 431; (D) final breakdown state of sample 431.

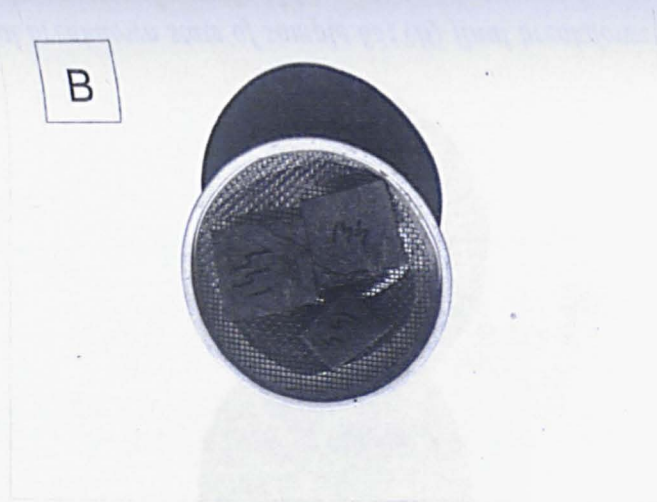
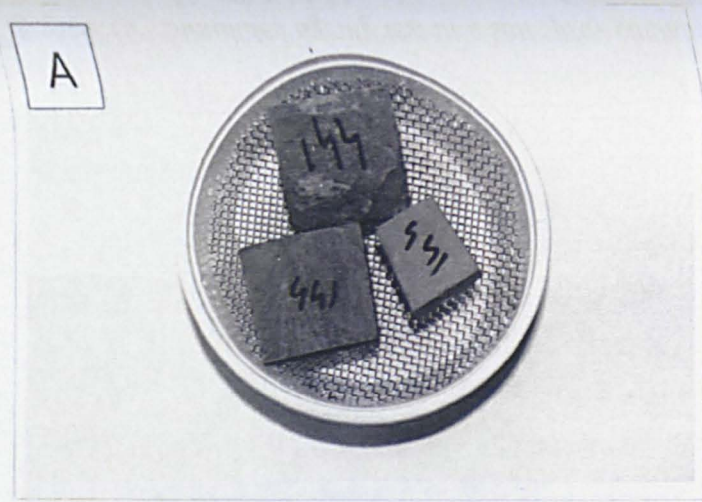


Fig. AIII.15 - Simulated ageing test in an environmental chamber (HT): (A) initial breakdown state of sample 441; (B) final breakdown state of sample 441; (C) initial breakdown state of sample OB2; (D) final breakdown state of sample OB2.

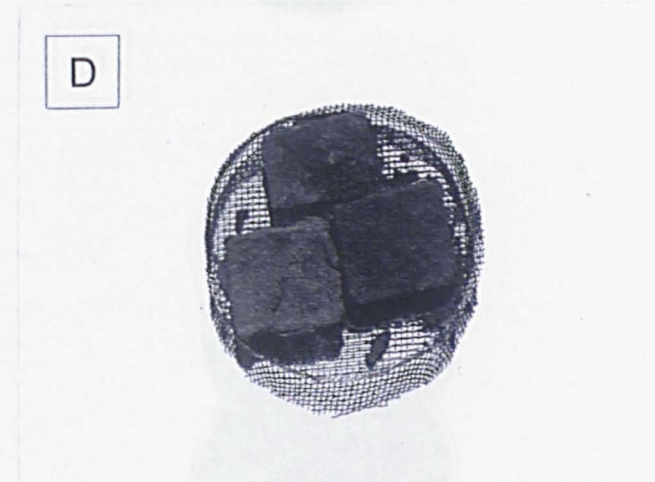
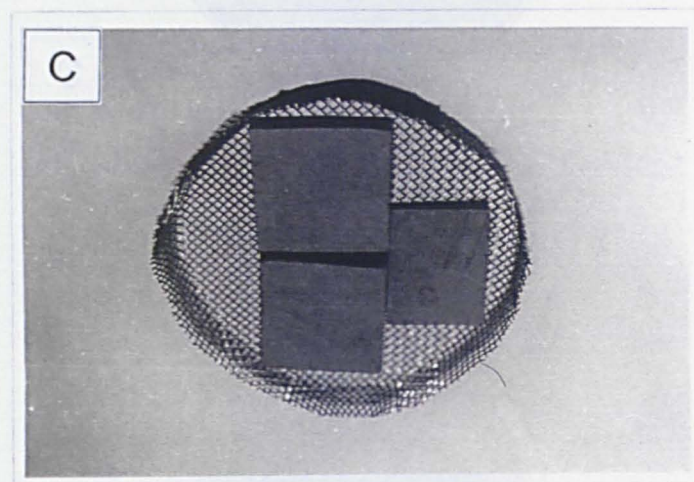
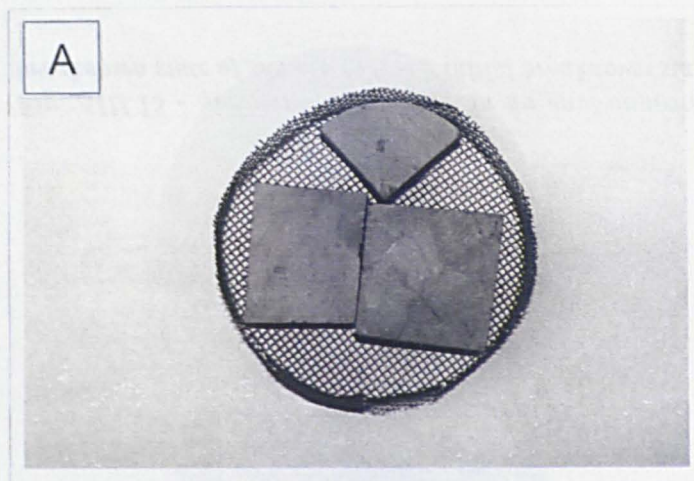


Fig. AIII.16 - Simulated ageing test in a salt spray chamber (SC): (A) initial breakdown state of sample 83; (B) final breakdown state of sample 83; (C) initial breakdown state of sample 114; (D) final breakdown state of sample 114.

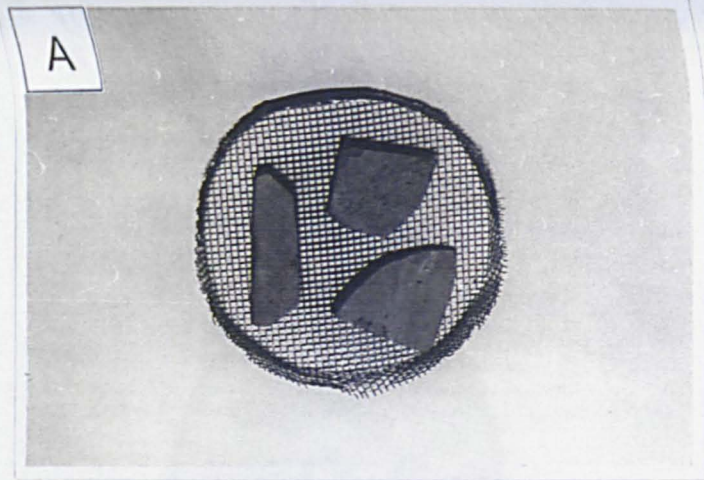


Fig. AIII.17 - Simulated ageing test in a salt spray chamber (SC): (A) initial breakdown state of sample 283; (B) final breakdown state of sample 283; (C) initial breakdown state of sample 286; (D) final breakdown state of sample 286.

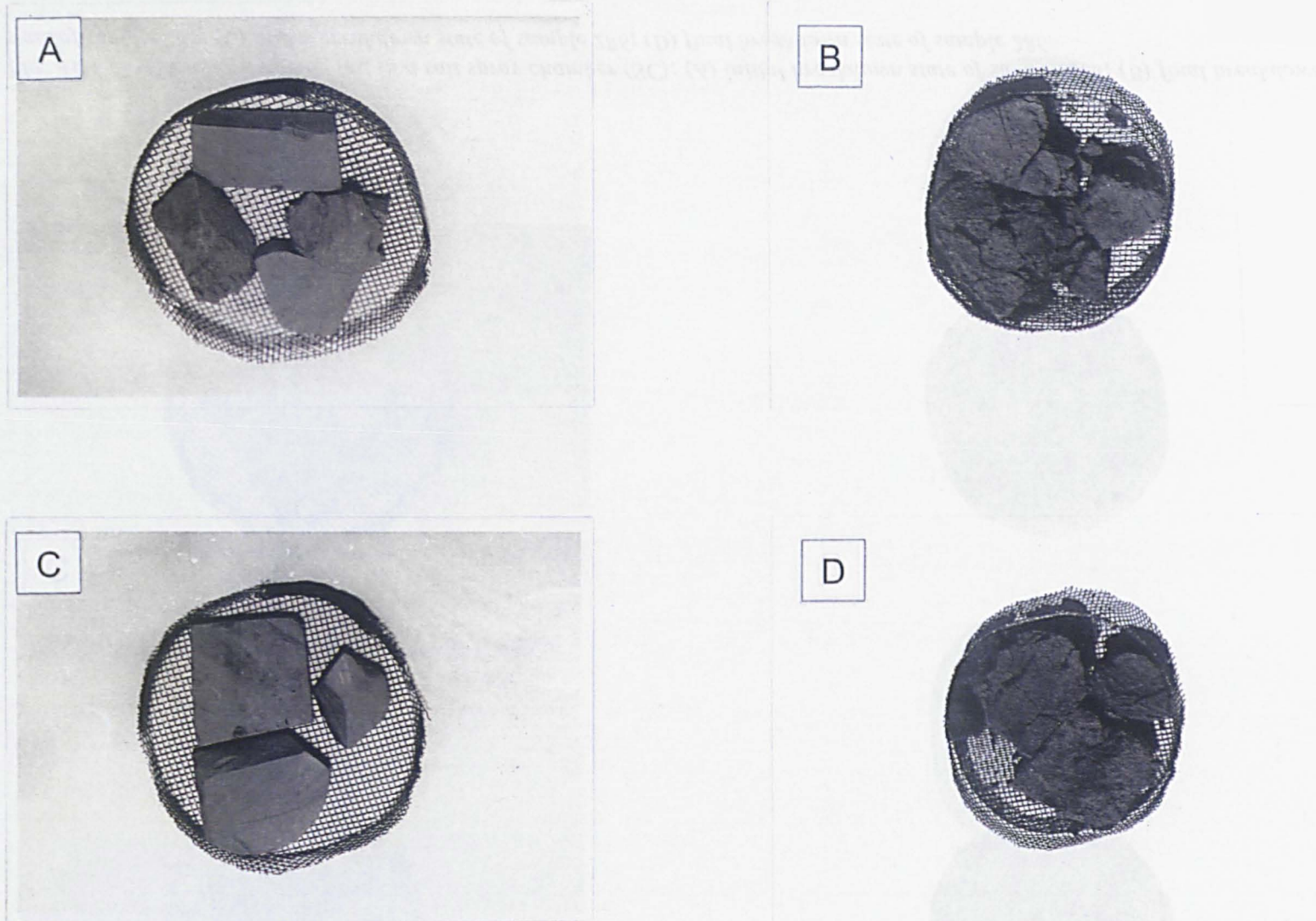


Fig. AIII.18 - Simulated ageing test in a salt spray chamber (SC): (A) initial breakdown state of sample 333; (B) final breakdown state of sample 333; (C) initial breakdown state of sample 336; (D) final breakdown state of sample 336.

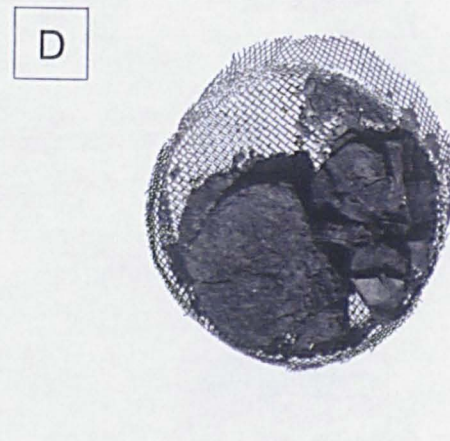
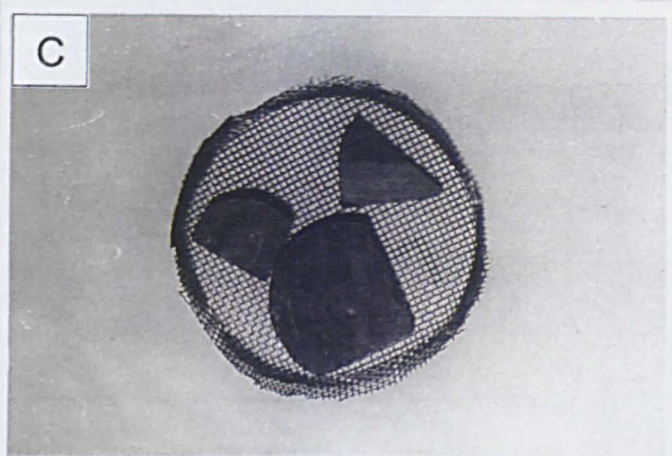
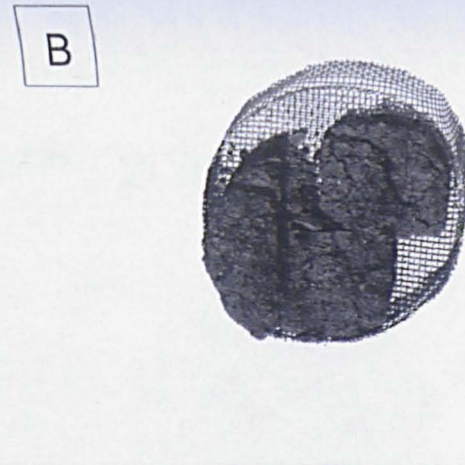
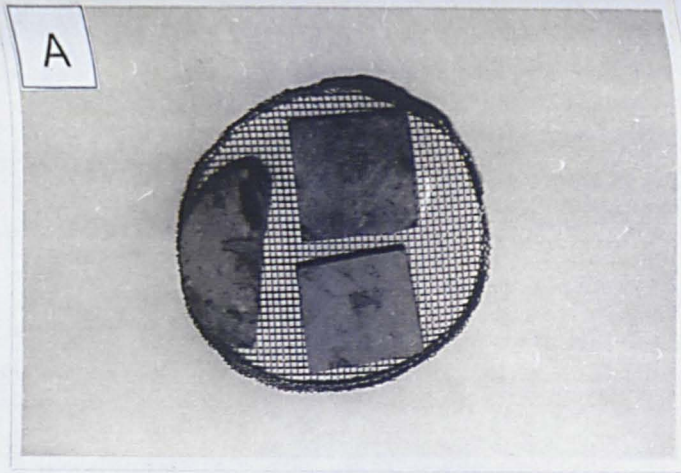


Fig. AIII.19 - Simulated ageing test in a salt spray chamber (SC): (A) initial breakdown state of sample 342; (B) final breakdown state of sample 342; (C) initial breakdown state of sample 431; (D) final breakdown state of sample 431.

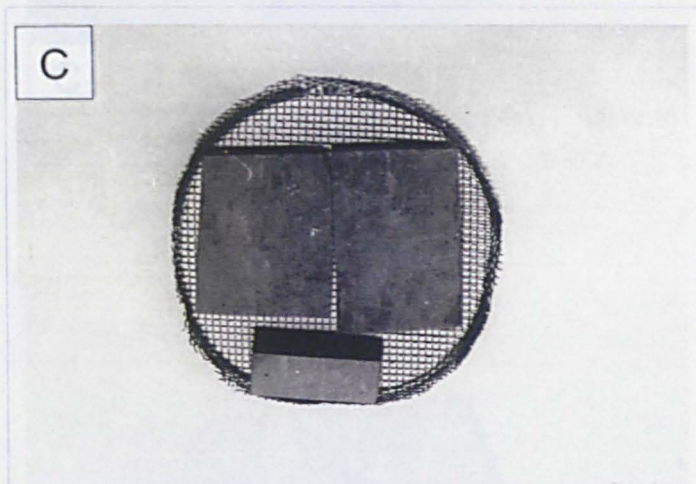
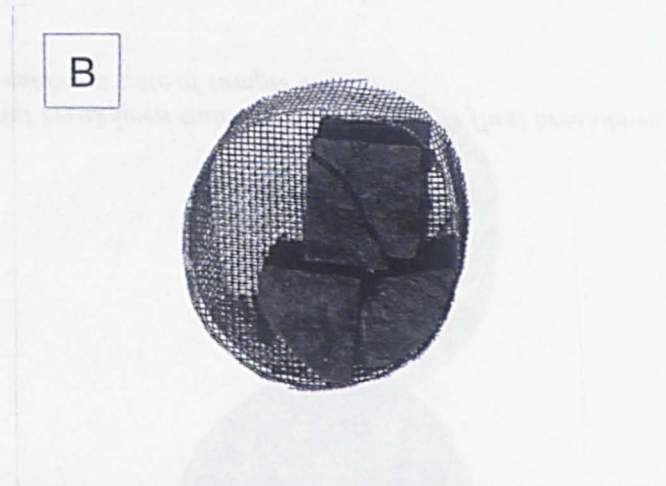
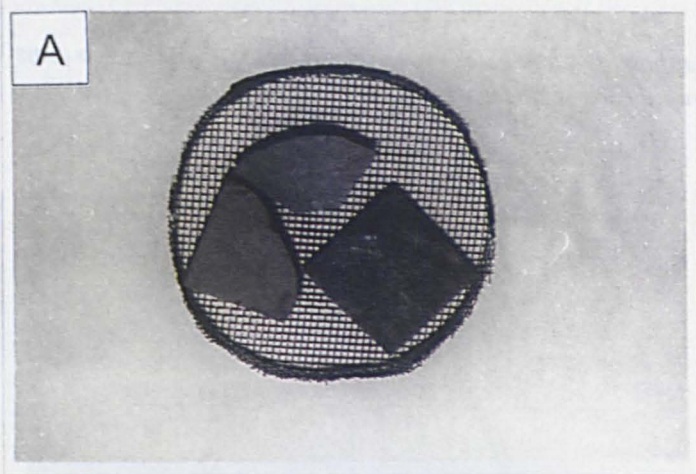


Fig. AIII.20 - Simulated ageing test in a salt spray chamber (SC): (A) initial breakdown state of sample 441; (B) final breakdown state of sample 441; (C) initial breakdown state of sample OB2; (D) final breakdown state of sample OB2.